

Fugro - Earth Mechanics
A JOINT VENTURE

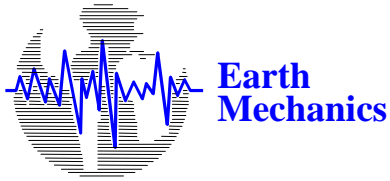
AXIAL PILE DESIGN AND DRIVABILITY MAIN SPAN-EAST PIER & SKYWAY STRUCTURES

SAN FRANCISCO-OAKLAND BAY BRIDGE EAST SPAN SEISMIC SAFETY PROJECT



**Prepared for
CALIFORNIA DEPARTMENT OF TRANSPORTATION**

March 2001



**Earth
Mechanics**



Fugro - Earth Mechanics
A JOINT VENTURE

March 5, 2001
Project No. 98-42-0054

California Department of Transportation
Engineering Service Center
Office of Structural Foundations
5900 Folsom Boulevard
Sacramento, California 95819-0128

7700 Edgewater Drive, Suite 848
Oakland, California 94621
Tel: (510) 633-5100
Fax: (510) 633-5101

Attention: Mr. Mark Willian
Contract Manager

**Final Axial Pile Design and Drivability
Main Span-East Pier and Skyway Structures
SFOBB East Span Seismic Safety Project**

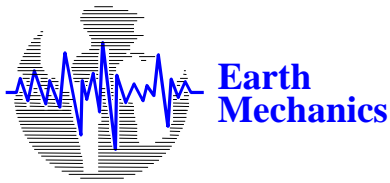
Dear Mr. Willian:

The geologic and geotechnical studies for the San Francisco-Oakland Bay Bridge (SFOBB) East Span Seismic Safety Project are being conducted by Fugro-Earth Mechanics (a joint venture of Fugro West, Inc., and Earth Mechanics, Inc.) under California Department of Transportation (Caltrans) Contract 59A0053. The work scope authorized by Task Order No. 5 includes the geotechnical components of the final foundation design studies.

The current report provides the final axial pile capacity, axial load-deformation, and pile drivability analyses for the driven piles that will support the Main Span-East Pier and Skyway structures. Final lateral load analyses are provided in a separate report. The design analyses reported herein are based on structure information as defined by the 65-percent submittal (and preliminary footing layouts from the 85-percent submittal) for the Main Span, and the draft 100-percent submittal for the Skyway Structure submitted by TY Lin/Moffatt & Nichol (TY Lin/M&N). The subsurface conditions that form the basis for these analyses are as described in the Final Marine Geotechnical Site Characterization report (Fugro-EM, 2001e).

In August 1999, a draft version of this report was submitted that was based on the 65-percent design submittal. Subsequent to the draft report submittal: 1) several design modifications were made by TY Lin/M&N to both the Skyway and Main Span structure foundations; 2) additional subsurface explorations (Phase 3 site investigation) were performed to refine shallow stratigraphy at many of the piers; 3) additional evaluations were performed to assist with the development of the Skyway Special Provisions; and 4) the Pile Installation Demonstration Project (PIDP) was successfully completed. As a part of finalizing this report, the design analyses and recommendations presented in the draft report were modified to reflect those design modifications and the additional data collected.

This report includes text that summarizes the subsurface conditions that control axial pile design and installation, and describes the design issues relative to axial capacity, load-deformation, setup, and pile drivability. The report includes general illustrations that support the text. In addition, the pier-specific design analyses results are provided on a series of illustrations in Appendix A, whose numbering corresponds to the pier numbers designated on the TY Lin/M&N drawings. Further description of the analyses methods are included in Appendix B.



Fugro - Earth Mechanics
A JOINT VENTURE

California Department of Transportation
March 5, 2001 (98-42-0054)

On behalf of the project team, we appreciate the opportunity to contribute to Caltrans' design of the new bridge to replace the existing SFOBB East Span. Please call if we can answer any questions relative to the information presented in the enclosed report.

Sincerely,

FUGRO-EARTH MECHANICS, A Joint Venture



M. Jacob Chacko, P.E.
Project Engineer



Roger Howard, Jr., P.E.
Project Engineer

Robert Stevens, Ph D., P.E.
Senior Technical Consultant

Thomas W. McNeilan, C.E., G.E.
Vice President



Attachment

Copies submitted:

- Mr. Mark Willian, Caltrans
- Mr. Saba Mohan, Caltrans
- Mr. Robert Price, Caltrans
- Dr. Brian Maroney, Caltrans
- Ms. Sharon Naramore, Caltrans
- Mr. Gerry Houlahan, TY Lin/M&N
- Mr. Sajid Abbas, TY Lin/M&N
- Mr. Al Ely, TY Lin/M&N

**SAN FRANCISCO-OAKLAND BAY BRIDGE
EAST SPAN SEISMIC SAFETY PROJECT
CALTRANS CONTRACT 59A0053**

**AXIAL PILE DESIGN AND DRIVABILITY
MAIN SPAN-EAST PIER & SKYWAY STRUCTURES**

MARCH 2001

Prepared For:

CALIFORNIA DEPARTMENT OF TRANSPORTATION
Engineering Service Center
Office of Structural Foundations
5900 Folsom Boulevard
Sacramento, California 95819-0128

Prepared By:

FUGRO-EARTH MECHANICS
A Joint Venture
7700 Edgewater Drive, Suite 848
Oakland, California 94621

CONTENTS

	Page
EXECUTIVE SUMMARY	ES-1
1.0 INTRODUCTION.....	1-1
1.1 Background	1-1
1.1.1 SFOBB East Span Seismic Safety Project	1-1
1.1.2 Caltrans Contract for Geotechnical and Geological Investigations for the Project.....	1-2
1.2 N6 Main Span and Skyway.....	1-3
1.2.1 N6 Alignment Description	1-3
1.2.2 Signature Structure Spans and Pier Locations	1-4
1.2.3 Skyway Structure	1-5
1.3 Foundation Description.....	1-5
1.3.1 Pile Type, Size, and Section.....	1-5
1.3.2 Pier Footings (Pile Caps) and Number of Piles.....	1-5
1.4 Project Datum.....	1-6
1.5 Basis of Characterization	1-6
1.5.1 Site Investigations	1-6
1.5.2 Integrated Approach and GIS Database.....	1-7
1.5.3 Report Organization	1-8
1.6 Related Project Reports Prepared by Fugro-Earth Mechanics.....	1-8
2.0 GENERALIZED SUBSURFACE CONDITIONS AND SUBSURFACE STRATIGRAPHIC MODEL.....	2-1
2.1 San Francisco Bay Bathymetry	2-1
2.2 Geologic Features and Subsurface Stratigraphy	2-2
2.2.1 Principal Features and Formations.....	2-2
2.2.2 Structural Contour and Isopach Thickness Maps.....	2-3
2.2.3 Subsurface Cross Sections	2-4
2.3 Description of Geologic Features.....	2-4
2.3.1 Easterly Sloping Bedrock of the Franciscan Formation.....	2-4
2.3.2 Holocene- and Pleistocene-Age Marine and Alluvial Sediments	2-5
2.3.3 Channeling	2-6
2.3.4 Gassy Sediments	2-7
2.3.5 Definition of Areas With Common Geologic Structure	2-7
2.4 Formation Description.....	2-8
2.4.1 Young Bay Mud (YBM).....	2-9
2.4.2 Merritt-Posey-San Antonio (MPSA) Formations	2-9
2.4.3 Old Bay Mud/Upper Alameda (Primarily) Marine (OBM/UAM) Sediments	2-10
2.4.4 Lower Alameda (Primarily) Alluvial (LAA) Sediments.....	2-11



CONTENTS -- CONTINUED

	Page
2.5 Upper Alameda Marine Paleochannel (El. -70 Meters) Sand at Main Span-East Pier.....	2-13
2.5.1 Extent and Thickness of Upper Alameda Marine Paleochannel Sand....	2-13
2.5.2 Characteristics of Upper Alameda Marine Paleochannel Sands.....	2-13
2.6 Characteristics of the Lower Alameda Alluvium.....	2-13
2.6.1 Lithology.....	2-14
2.6.2 Implications of Lower Alameda Alluvium Variations for Design and Construction.....	2-15
2.6.3 Soil Properties.....	2-15
3.0 AXIAL PILE DESIGN OVERVIEW.....	3-1
3.1 Design, Construction, And Performance Issues.....	3-1
3.1.1 Channeling.....	3-1
3.1.2 End-Bearing Stratum Variations.....	3-1
3.1.3 Load-Transfer Considerations.....	3-2
3.1.4 Post-Installation Setup of Axial Capacity.....	3-2
3.1.5 Cyclic Degradation and Strain Rate Effects During Earthquake Loading.....	3-3
3.2 Preliminary Design And Seismic Design Philosophy.....	3-3
3.3 Pier-Specific Design Information.....	3-4
3.4 Pile Tip Elevations.....	3-5
3.4.1 Preliminary Pile Tip Elevations.....	3-5
3.4.2 Structural Analyses And Results.....	3-5
3.4.3 Design Modifications.....	3-6
3.4.4 Revised Pile Tip Elevations For Skyway Structure Piers.....	3-6
3.4.5 Additional Considerations For Piers E3 Through E5.....	3-7
3.5 Skyway Temporary Towers.....	3-8
4.0 AXIAL PILE DESIGN METHODOLOGY AND DATA.....	4-1
4.1 Design Basis.....	4-1
4.1.1 Boring-Specific Design Data.....	4-1
4.1.2 "Synthetic" Boring Design Data.....	4-2
4.1.3 General Pier-Specific Information.....	4-2
4.2 Design Methodology.....	4-3
4.3 Ultimate Static Axial Pile Capacity.....	4-4
4.3.1 Side Shear (Skin Friction).....	4-4
4.3.2 End Bearing.....	4-6
4.4 Axial Load-Deformation Relationships.....	4-8
4.4.1 t-z Curves.....	4-8
4.4.2 q-z Curves.....	4-9
4.5 Axial Pile Head Load-Deformation Curves.....	4-10



CONTENTS -- CONTINUED

	Page
4.6 Earthquake Loading Effects	4-10
4.6.1 Cyclic Degradation of Pile Capacity	4-10
4.6.2 Strain Rate Effects	4-11
4.6.3 Example Calculations of Earthquake Loading Effects	4-12
4.6.4 Recommendations for Design	4-13
5.0 PILE SETUP	5-1
5.1 Introduction	5-1
5.2 Prediction of Pile Setup	5-1
5.2.1 Preliminary Predictions of Pile Setup in Clay	5-2
5.2.2 Revised Setup Predictions Based on Soderberg (1962)	5-3
5.2.3 Discussion of Prediction of Pile Setup in Clay	5-3
5.2.4 Setup In Sand	5-4
5.3 Impact of Pile Setup on Construction Schedule	5-4
5.3.1 Preliminary Evaluations	5-4
5.3.2 Findings From the Pile Installation Demonstration Project	5-5
6.0 PILE DRIVABILITY CONSIDERATIONS	6-1
6.1 Introduction	6-1
6.2 Drivability Analyses	6-1
6.2.1 Analytical Process	6-1
6.2.2 Soil Resistance to Driving	6-2
6.2.3 Wave Equation Analyses	6-5
6.2.4 Evaluation of Pile Drivability	6-6
6.3 Results of Preliminary Drivability Analyses	6-7
6.3.1 Computed Soil Resistance to Driving	6-7
6.3.2 Pile Run	6-8
6.3.3 Blow Counts	6-8
6.3.4 Driving Stresses	6-10
6.4 Analysis of Drivability Into The Franciscan Formation Bedrock	6-11
6.4.1 Introduction	6-11
6.4.2 Analyses	6-11
6.4.3 Results and Discussion	6-12
6.5 Findings From the Pile Installation Demonstration Project	6-13
6.5.1 Introduction	6-13
6.5.2 Summary of Drivability-Related Findings	6-13
7.0 PILE INSTALLATION CONSIDERATIONS AND RECOMMENDATIONS	7-1
7.1 Introduction	7-1
7.2 Driving System Submittal	7-1
7.3 Pile Tip Elevations	7-2



CONTENTS -- CONTINUED

	Page
7.4 Pile Schedule	7-3
7.5 Delays and Redriving	7-3
7.6 Dynamic Monitoring	7-4
7.6.1 Preparation of Piles To Be Monitored	7-4
7.6.2 Mounting Instrumentation on the Pile	7-4
7.6.3 Removal of Instrumentation	7-5
7.7 Acceptable Hammer Types	7-5
7.7.1 Primary Hammer	7-6
7.7.2 Secondary Hammers	7-6
7.8 Refusal Blow Count Criteria	7-6
7.9 Allowable Driving Stress Criteria	7-7
7.10 Minimum Blow Count Criteria (If Needed)	7-7
7.11 Pile Acceptance Criteria	7-8
7.12 Remedial Installation Procedures	7-9
7.13 Pile Clean Out	7-10
7.13.1 Placement of Structural Concrete	7-10
7.13.2 Installation of Seismic Monitoring Instruments	7-10
7.14 Pile Setup and Construction Schedule	7-10
8.0 REFERENCES	8-1

PLATES

	Plate
Bathymetry and N6 Alignment	1.1
Main Span Alignment	1.2
Skyway Structure Alignment	1.3
Main Span East Pier and Skyway Footing Geometry	1.4
Marine Exploration Location Map	1.5
Final Fugro-EM Reports	1.6
Delineation of Areas Addressed by Fugro-EMI Reports	1.7
Structural Contours	
Base of Young Bay Mud	2.1
Top of Upper Alameda Marine Paleochannel Sand	2.2
Base of Upper Alameda Marine Paleochannel Sand	2.3
Top of Lower Alameda Alluvial Sand	2.4
Regional, Top of Franciscan Formation	2.5
Isopach (Thickness) of:	
Young Bay Mud	2.6
Upper Alameda Marine Paleochannel Sand	2.7
Sediment Section Above Lower Alameda Alluvial Sand	2.8



CONTENTS -- CONTINUED

PLATES -- CONTINUED

	Plate
Conceptual East-West Soil Profile Outside (South) of Recent Paleochannel, Proposed N6 Alignment Skyway	2.9
Conceptual Section at South Edge of (East-West) Recent Paleochannel	2.10
Subsurface Cross Sections Along N6 Alignment, Yerba Buena Island to Oakland Mole, Pier E1 to E8.....	2.11a
Pier E9 to E20.....	2.11b
Interpreted Variations at Edge of Recent Paleochannel	2.12
Example Detail of LAA Stratigraphy	2.13
Expected Variation of Top of LAA Sand	2.14
LAA-Clay Interbed Thickness, 1998 Marine Borings	2.15
Distribution of LAA-Clay Interbed Thickness	2.16
Percent LAA-Clay Interbeds Within LAA Sand	2.17
Distribution of LAA-Clay Interbeds With Elevation	2.18
Distribution of LAA-Clay Interbeds With Depth	2.19
Static Axial Loads and Recommended Pile Tip Elevations, Skyway Structure Piers	3.1
Variation of Pile Length and Tip Elevation Along N6 Alignment, Skyway Structure Piers	3.2
Estimated Factors of Safety Against Static Loads, Skyway Structure Piers.....	3.3
Predicted Setup of Skin Friction in Clay, 2.5-Meter-Diameter Steel Pipe Piles	5.1
Estimated CAPWAP Skin Friction Capacity and Anticipated Construction Pile Loads, Pile Capacity from Pile Installation Demonstration Project.....	5.2
Schematic Illustration of Pile Drivability Analysis.....	6.1
Comparison of Calculated Soil Resistance to Driving Profiles, Pier E7-Eastbound (Boring 98-49).....	6.2
Summary of Wave Equation Parameters	6.3
Wall Thickness Schedule Used in Preliminary Drivability Analyses, 2.5-Meter-Diameter Pipe Pile Composite Profile	6.4
Summary of Preliminary Drivability Analyses.....	6.5
Comparison of Predicted Coring Case Blow Counts, Pier E7-Eastbound (Boring 98-49), Menck MHU-170, 2.5-Meter-Diameter Driven Pipe Piles	6.6
Drivability of Piles Tipped in Franciscan Formation Bedrock, Piers E3 through E5, Eastbound and Westbound	6.7
PDA-Measured and Predicted Soil Resistance to Driving, Pile No. 2, Pile Installation Demonstration Project	6.8
Observed and Predicted Blow Counts, Pile No. 2, Pile Installation Demonstration Project	6.9



CONTENTS -- CONTINUED

APPENDICES

APPENDIX A: PIER-SPECIFIC DESIGN PLATES

Pier and Boring Location Plan,	
Frame 1	A-1
Frame 2	A-2
Frames 3 and 4	A-3
Pier-Boring Correlation Table	A-4
Key to Terms and Symbols Used on Axial Pile Design Parameters and Results	A-5
Summary of Preliminary Axial Pile Capacity, Piers E2 through E16	A-6

*For a guide to pier-specific design plates in Appendix A,
please refer to the chart on the following page.*

APPENDIX B: VERIFICATION OF AXIAL PILE DESIGN METHODS

Static Compression Load Test	B-1
Statnamic Test Results	B-2
Drive Simulation,	
Compression Test	B-3
Statnamic Load Test	B-4
Load Tests	B-5
Original and Simplified Soil Reactions	B-6
Axial Pile Load-Settlement Behavior	B-7
Load-Settlement Behavior With Self-Weight	B-8
Degradation Parameters From Model Tests	B-9
Load-Time History at the Mudline	B-10
Pile Head Displacement-Time History	B-11
Pile Tip Displacement-Time History	B-12
Effects of Earthquake on Residual Loads	B-13
Effects of Earthquake on Displacements	B-14
Static and Degraded Soil Reactions	B-15





CONTENTS -- CONTINUED

PIER-SPECIFIC DESIGN PLATE NUMBERING GUIDE

	Pier Number																								
	E2-EB	E2-WB	E3-EB	E3-WB	E4-EB	E4-WB	E5-EB	E5-WB	E6-EB	E6-WB	E7-EB	E7-WB	E8-EB	E8-WB	E9-EB&WB	E10-EB	E10-WB	E11-EB	E11-WB	E12-EB&WB	E13-EB	E13-WB	E14-EB&WB	E15-EB&WB	E16-EB&WB
Axial Pile Design Parameters and Results	1	1	1	1	1	1	1	1	1	1	1	1	1	1	1	1	1	1	1	1	1	1	1	1	1
Axial Pile Load Transfer-Displacement Curve	2a-b	2a-b	2	2	2	2	2	2	2	2	2	2	2	2	2	2	2	2	2	2	2	2	2	2	2
Tabulated Axial Pile Load Transfer Data	3a-b	3a-b	3	3	3	3	3	3	3	3	3	3	3	3	3	3	3	3	3	3	3	3	3	3	3
Static Pile Head Load-Deformation Curve	4a-b	4a-b	4	4	4	4	4	4	4	4	4	4	4	4	4	4	4	4	4	4	4	4	4	4	4
Soil Resistance to Driving	5	5	5							5	5	5				5			5		5		5	5	
Predicted Blow Counts, Menck MHU-500T	6a	6a	6a							6a	6a	6a				6a			6a		6a		6a	6a	
Predicted Blow Counts, Menck MHU-1000	6b	6b	6b							6b	6b	6b				6b			6b		6b		6b	6b	
Predicted Blow Counts, Menck MHU-1700	6c	6c	6c							6c	6c	6c				6c			6c		6c		6c	6c	

 Analyses performed

 No analyses performed

EXECUTIVE SUMMARY

PROJECT BACKGROUND AND STUDY DESCRIPTION

The geologic and geotechnical studies for the San Francisco-Oakland Bay Bridge (SFOBB) East Span Seismic Safety Project are being conducted by Fugro-Earth Mechanics (a joint venture of Fugro West, Inc., and Earth Mechanics, Inc.) under California Department of Transportation (Caltrans) Contract 59A0053. The "Phase 2 (Final) Site Exploration and Characterization" activities were authorized by the July 30, 1998, notice to proceed for Task Order No. 5. That task order included provisions for the final design-phase subsurface exploration, the final site characterization, and the final geotechnical foundation design recommendations.

REPORT DESCRIPTION AND INTENT

This report provides the axial pile design and pile drivability analyses for the driven piles that will support the Main Span-East Pier and Skyway structures. The information includes:

- Representative soil profiles at each pier,
- Estimates of ultimate axial pile capacity,
- Axial load-deformation data,
- Predictions of pile setup,
- Results of pile drivability analyses, and
- Pile installation considerations and recommendations for the preparation of the project specifications.

Final lateral load analyses are provided in a separate report (Fugro-EM, 2001a). Information for the two Main Span piers founded in rock is provided under separate cover, as are the design information for the Oakland Shore Approach structures.

The design analyses reported herein are based on structure information as defined by the draft 100-percent submittal for the Skyway and preliminary drawings from the 85-percent submittal for the Main Span-East Pier developed by TY Lin/Moffatt & Nichol (TY Lin/M&N). The subsurface conditions that form the basis for our analyses are as described in the Final Marine Geotechnical Site Characterization Reports (Fugro-EM, 2000e).

The design analyses results are presented for each of the individual piers (Bridge Piers E2 through E16). The pier-specific design analyses results are provided on a series of illustrations whose numbering corresponds to the pier number as designated on the Project drawings



OVERVIEW OF SUBSURFACE CONDITIONS

The bathymetry underlying the Main Span-East Pier and Skyway structures slopes downward to the west and varies from a minimum of elevation (El.) -3 meters (re: mean sea level [MSL] datum) at Bridge Pier E16 down to El. -13 meters at the Main Span-East Pier.

The subsurface conditions underlying the Main Span-East Pier and Skyway portions of the SFOBB East Span are influenced by the following geologic features:

- Shallow, easterly sloping bedrock of the Franciscan Formation offshore eastern Yerba Buena Island.
- Holocene- and Pleistocene-age marine and alluvial sediments that unconformably overlay the Franciscan Formation bedrock. In general, the marine sediments (deposited during sea level high stands) are more prevalent and are primarily clay. In contrast, the alluvial sediments (deposited during sea level low stands) are more commonly sand.
- The Holocene- and Pleistocene-age sequence has been eroded (and complicated) by various episodes of channeling. In many locations, the channels have subsequently been filled with comparatively softer sediments. The geologically Recent channeling includes: 1) an east-west-trending paleochannel sequence to the north of and subparallel to the existing East Span bridge alignment, and 2) north-south-oriented subsidiary channels that cross under the bridge alignments and flow into the east-west channel(s). A somewhat deeper (and older) nested series of north-south-oriented paleochannels were imaged in the western portion of the bridge alignment offshore from the eastern end of Yerba Buena Island.

The primary geologic formations that underlie the Skyway alignment (or portions of the alignment) are listed below in descending sequence. While the formation designations are useful, the subsurface conditions are described primarily in terms of undrained shear strength (of cohesive soils) and relative density or measured cone tip resistance (of granular soils). That choice was made based on the extensive test data from the 1998 Fugro borings and the direct applicability of the test data to foundation design. The typical soil designations for the formations are included in the following table:

Formation Designation	Typical Soil Designation
Young Bay Mud	Very Soft to Soft or Soft to Firm Clay
Merritt-Posey-San Antonio Formations (also referred to as Merritt Sand)	Dense to Very Dense Sand with Stiff to Very Stiff Clay Layers
Old Bay Mud	Very Stiff to Hard Clay with Dense Sand Layers
Upper Alameda Sediments	Very Stiff to Hard Clay with Dense Sand Layers
Lower Alameda Sediments	Dense to Very Dense Sand and Hard Clay



The proposed N6 alignment is underlain by variable subsurface conditions that are intrinsic to any replacement bridge alignment to the north of the existing bridge. Whereas the Main Span-Pylon structure will be sited on shallow, sloping bedrock, the remainder of the marine structures will be founded on a significant thickness of sediment. Many details of the stratigraphy and characteristics of the subsurface sediments vary continuously along the alignment.

MAIN SPAN-EAST PIER AND SKYWAY FOUNDATIONS

The Marine Geotechnical Site Characterization studies (Fugro-EM, 2001e) recognized that the variability of the subsurface conditions will significantly affect the site response and the axial and lateral load deflection response of the foundation. From a geotechnical standpoint, a foundation design that reduces the sensitivity of the foundation (and superstructure) response to those inevitable variations across and along the Skyway was recommended. The choice (made by TY Lin/M&N) of battered, large-diameter, driven steel pipe piles is considered appropriate relative to that goal.

Large-diameter, driven steel pipe piles are considered to be an appropriate and desirable foundation type for the Main Span-East Pier and Skyway. The piles will be driven open ended and will subsequently be partially filled with concrete. Large-diameter pipe piles provide a number of advantages:

- Comparatively high axial and lateral load capacity per pile can be used to reduce the number of piles, pile group effects, and the pile cap size.
- Piles can be designed to provide elastic behavior during extreme seismic loading per Caltrans design criteria.
- The pile wall thickness can be designed to provide desired pile stiffness, accommodate an appropriate-sized pile hammer, and facilitate driving.
- Axial load-carrying capacity under service loads will be largely developed by skin friction at relatively small pile deflections. Additional axial capacity in end bearing can be mobilized (albeit at larger pile deflections) when piles are subjected to extreme loads.
- Construction experience including the recently completed Pile Installation Demonstration Project (Fugro-EM, 2001f) suggests that the piles can be driven and that add-ons can be restarted with an appropriately sized, large offshore pile hammer.

On the basis of information provided by TY Lin/M&N, the Main Span-East Pier and the Skyway piers will be supported on 2.5-meter-diameter steel pipe piles. The upper sections of the piles will be filled with reinforced concrete to form a composite structural member denoted by Caltrans as a cast-in-steel shell (CISS) pile. The Skyway piles will extend down to between El. -93 and El. -108 meters with structural concrete fill to between approximately El. -63 and

El. -71 meters. Alternate pile tip elevations of El. -75 and El. -95 meters are being considered for the Main Span-East Pier. The piles are currently being designed to include a variable wall thickness schedule, which TY Lin/M&N indicates will vary from 76 millimeters (mm) at the pile cap to 51 mm near the pile tip.

The foundation layouts provided in the TY Lin/M&N design drawings indicate that the Main Span-East Pier will be supported by 16 piles. These piles will be arranged in two groups of eight piles each that are centered beneath the westbound and eastbound bridge alignments. For the Skyway Piers E3 through E14, the eastbound and westbound piers are to be supported by a group of six battered piles. Eastbound and Westbound piers for Skyway Piers E15 and E16 are to be supported by groups of four battered piles. The area circumscribed by the loci of the pile tips for each Skyway pier is on the same order of magnitude as a football field.

TARGET PILE TIP STRATUM

Skyway

Recommended tip elevations for the piers supporting the Skyway structures were developed on the basis of the geotechnical properties of the underlying sediments and the service load/seismic performance information provided by TY Lin/M&N. Piles supporting Piers E3 through E5 are the most heavily loaded of the Skyway piles. To reduce the potential for excessive deformations, tip elevations for those piers were selected slightly below the interpreted bedrock elevation. Tip elevations for the remaining piers were selected so as to maximize the probability of piles being tipped in a predominantly sand sequence in the Lower Alameda Alluvium (LAA-sand).

Both the variation of the top elevation of the LAA-sand and the local presence or absence of LAA-clay interbeds within the underlying LAA-sand are intrinsic variations of the deposit. Because these are local variations, it is impractical to expect to predict how those variations occur over the football-field-sized area circumscribed by the loci of the pile tips at each set of piers. Thus, the pile design and construction will need to accommodate these variations. From a design standpoint, the primary implication was to formulate predictions of the range of pile end-bearing capacity and stiffness with recognition of the variations that could be logically expected to occur.

Main Span-East Pier

The stratigraphy at the Main Span-East Pier varies somewhat from the typical stratigraphy encountered beneath the Skyway alignment. The proposed Main Span-East Pier location is within the area directly affected by geologically Recent channeling. Above about El. -70 meters, the stratigraphy includes relatively thick and soft paleochannel clays. At about El. -70 meters, an approximately 15-meter-thick, dense, sand-filled paleochannel is encountered at the top of the Upper Alameda Marine sequence.

Driving steel pipe piles through that 15-meter-thick sand layer (Upper Alameda Marine Paleochannel Sand) may be problematic. In addition, the Main Span-East Pier corresponds to the location where the Lower Alameda Alluvium onlaps the Franciscan Formation, and only a thin layer of Lower Alameda Alluvium is present. Thus, rock may be encountered at about the pile tip elevation if that elevation is to be the same as those used for the Skyway piers.

Pile design data are provided for both piles tipped in the Upper Alameda Marine Paleochannel Sand and piles driven deeper into the thin Lower Alameda Alluvium layer. Careful consideration should be given to the choice of pile length at the Main Span-East Pier location.

AXIAL PILE DESIGN ANALYSES AND RESULTS

The large-diameter steel pipe piles and soil conditions are similar to those used/encountered in many offshore structures. Thus, the design methods used are based on site-specific modifications to the procedures recommended by API RP 2A Guidelines for the Design of Fixed Offshore Structures (API, 1993a,b), rather than the conventional Caltrans procedures that have been formulated and used for the design of much smaller piles. The design methods were developed with the intent of providing the soil parameters necessary for the assessment of pile performance under static and dynamic loading.

Due to the economic importance of the SFOBB and the consequences of catastrophic failure in both economic and human terms, the design and analysis of the pile foundations supporting the bridge explicitly consider a number of aspects of pile-soil behavior that are normally ignored. These aspects include: 1) the effects of consolidation and setup, 2) the behavior under dynamic loading, 3) the losses of resistance under cyclic loading, and 4) the load-settlement behavior of the piles under severe cyclic loading conditions. Since the treatment of complex aspects of pile foundation behavior is not codified in any guiding documents, several project-specific methods were developed for design and analysis of the foundation piles.

Information provided by TY Lin/M&N indicates that the piles will experience their maximum loads during the design earthquake. Calculated seismic loads on the Skyway piles varied as a function of the pile stiffness and damping assumed in the analyses. For the Safety Evaluation Earthquake, tension loads of up to approximately 80 to 90 MN and compression loads of up to approximately 120 to 140 MN were calculated. Structural analyses and design of the Main Span structure are ongoing, and the results of those analyses were unavailable at the time this report was being prepared.

The design seismic loading conditions produce: a) temporary losses in the axial capacity due to cyclic degradation, and b) transient increases in the capacity due to rate of loading effects. Because of those phenomena, evaluation of relative safety factors based on calculated static axial capacities are not meaningful for seismic design. Furthermore, the magnitude of seismic loads imposed on the piles is dependent upon the stiffness of the foundation response. In general, for

the typical range of structure periods considered, the stiffer the foundation (frequently due to increased pile capacity), the higher the loads imposed on it. Therefore, a range of anticipated foundation parameters was used to evaluate the load-deformation behavior of the piles and to estimate the stresses imposed on the structure.

The results of our static axial capacity and axial load-deformation analyses are presented on a series of illustrations for each pier. The analyses results and the plate numbering nomenclature are as follows:

- Axial Pile Design Parameters and Results, including:
soil stratigraphy, interpreted design strength and submerged
unit weight profiles, unit skin friction and unit end-bearing
curves, static axial pile capacity, recommended tip elevation Plate EX-YB.1
- Axial Pile Load Transfer-Displacement Curves Plate EX-YB.2
- Tabulated Axial Pile Load Transfer Data Plate EX-YB.3
- Static Pile Head Load-Deformation Curves..... Plate EX-YB.4

In the above nomenclature, "X" corresponds to the pier number and "Y" corresponds to either an eastbound or westbound pier designation. For example, Plate E3-WB.2 presents the axial pile load transfer-displacement curve for westbound Pier E3.

PILE DRIVABILITY ANALYSES

An evaluation of pile drivability was conducted for the Main Span-East Pier and representative Skyway piers. The analyses were conducted for the anticipated pile wall schedules shown in the 45-percent drawings (TY Lin/M&N, 1999). Three large offshore hammers were considered: 1) a 550-kilojoule (kJ) Menck MHU-500T, 2) a 1,000 kJ Menck MHU 1000, and 3) a 1,700 kJ Menck MHU-1700.

When drivability analyses were performed for a pier, the results are provided with the pier-specific axial design results and include:

- Soil Resistance to Driving..... Plate EX-YB.5
- Predicted Blow Counts, Menck MHU 500T Plate EX-YB.6a
- Predicted Blow Counts, Menck MHU 1000 Plate EX-YB.6b
- Predicted Blow Counts, Menck MHU 1700 Plate EX-YB.6c

In general, the drivability analyses suggest that the MHU 500T hammer will be inadequate for driving piles to the recommended tip elevations. The data suggest that the MHU 1000 hammer has the minimum energy capable of driving the Skyway foundation piles at Piers E7 through E16 to the proposed tip elevations. However, that hammer is likely to encounter



refusal above the proposed pile tip elevations at Piers E3 through E5, where the piles are to be tipped in rock, or at a number of other pier locations if the pile plugs. With few exceptions, it generally should be possible to restart driving within the LAA-sand with the Menck MHU 1700 hammer even if delays occur during driving within that layer.

The results for the Main Span-East Pier show that the smaller MHU 500T hammer will be inadequate to drive the piles through the Upper Alameda Marine Paleochannel Sand encountered at about El. -70 meters. Hard driving should be expected even when using the larger MHU 1700, and contingencies should be provided in the specifications for refusal above the specified tip elevations.



**SECTION 1.0
INTRODUCTION**

1.0 INTRODUCTION

1.1 BACKGROUND

This Axial Pile Design Report has been prepared to provide final design recommendations for large-diameter steel pipe piles that will be driven to support the Main Span-East Pier and Skyway structures. These piles are planned to be 2.5 meters in diameter, about 100 meters long, and penetrate between about 70 and 95 meters into the soils underlying this portion of the alignment. This report is being provided to assist the California Department of Transportation (Caltrans) and its design team during the final design of the Main Span (East Pier) and Skyway structures of the San Francisco-Oakland Bay Bridge (SFOBB) East Span Seismic Safety Project.

1.1.1 SFOBB East Span Seismic Safety Project

Bridge and Route Description. The SFOBB carries 10 lanes of Interstate 80 traffic, 5 eastbound and 5 westbound, across San Francisco Bay. The bridge is bisected longitudinally by Yerba Buena Island, with the West Span(s) extending from San Francisco to Yerba Buena Island and the East Span(s) extending from Yerba Buena Island to Oakland. The existing bridge is a double-decked structure that was constructed in the 1930s.

Earthquake Damage and Retrofit Evaluation. During the 1989 Loma Prieta earthquake, the East Span(s) of the bridge suffered considerable damage, including the collapse of one span. Recognizing the vulnerability of the structure to future earthquake shaking, Caltrans embarked on a seismic retrofit program to upgrade the bridge. In the summer of 1995, Caltrans presented their retrofit strategy for the SFOBB East Span to the Seismic Advisory Board, who suggested replacement in lieu of retrofit.

Subsequently, Caltrans developed a 30-percent design of a continuous viaduct replacement structure. In 1996, that 30-percent design was presented to the Bay Bridge Design Task Force, who had been appointed by the Metropolitan Transportation Commission (MTC) to select a bridge type for the East Span replacement structure. The MTC and their task force then formed an Engineering and Design Advisory Panel (EDAP), who advised against Caltrans' proposed replacement bridge type.

Replacement Bridge. Following those recommendations, Caltrans contracted with a joint venture between TY Lin International and Moffatt & Nichol Engineers (TY Lin/M&N) to develop 30-percent designs for two alternative bridge types (Phase 1 design). The two bridge-type alternatives included a cable-supported Main Span offshore from Yerba Buena Island and a Skyway structure farther to the east, as well as the associated Yerba Buena Island transition structure(s) and Oakland Mole Shore Approach structure(s). The locations of the various components of the chosen N6 alignment are shown on Plate 1.1 and large-scale maps of the areas



discussed in this report are shown on Plates 1.2 and 1.3. The alternative cable-supported main structures that were considered included single-tower or dual-tower, cable-stayed and self-anchored suspension bridge structures. The timing for the design project required that Caltrans and TY Lin/M&N submit 30-percent design-level schedule and cost estimates to EDAP and MTC by May 29, 1998.

In June 1998, EDAP and MTC selected the single-tower, self-anchored suspension bridge structures and haunched, concrete Skyway structures for final design. Final design of the chosen structure types and alignment was begun by the TY Lin/M&N team in late Fall 1998. The following table summarizes submission dates for various design submittals that have since been prepared. The most recent submittal for each component of the replacement bridge (see tabulation below) provides the basis for descriptions of structures presented in this report.

Design Submittal	Main Span	Skyway	Oakland Shore Approach
45 percent	January 1999	January 1999	January 1999
65 percent	August 1999	July 1999	August 1999
85 percent		February 2000	August 2000 (Long Structure) September 2000 (Short Structure)
100 percent		November 2000 (Draft)	

1.1.2 Caltrans Contract for Geotechnical and Geological Investigations for the Project

To support their design efforts, Caltrans also has contracted with Fugro-Earth Mechanics (a joint venture between Fugro West, Inc., and Earth Mechanics, Inc.) to conduct geotechnical and geological investigations and studies for the replacement bridge. Caltrans Contract 59A0053, dated August 27, 1997, authorized those studies.

To date, six task orders have been issued under Contract 59A0053:

- Task Order No. 1 - Initial Site Characterization-Geophysical Surveys phase with a Notice to Proceed issued January 6, 1998.
- Task Order No. 2 - Project Management and Coordination with a Notice to Proceed issued January 26, 1998.
- Task Order No. 3 - Preliminary Site Exploration and Testing with a Notice to Proceed issued January 26, 1998.
- Task Order No. 4 - Probabilistic Seismic Hazard Analysis Update and Preliminary Site Response Analysis with a Notice to Proceed issued May 19, 1998.
- Task Order No. 5 - Phase 2 and Phase 3 Site Exploration and Characterization with a Notice to Proceed issued July 23, 1998.



- Task Order No. 6 - Pile Installation Demonstration Project Engineering/Monitoring with a Notice to Proceed issued December 23, 1998.

Task Order No. 5 Work Scope. The Task Order No. 5 work scope included provisions for the final design phase of site exploration, testing, and characterization for the chosen bridge alignment and structures. The task order authorized the extensive marine exploration as well as the land exploration programs on Yerba Buena Island and the Oakland Mole. The task order also provided authorization for the final geotechnical foundation design analyses and recommendations. This report was prepared as a part of the work scope authorized by Task Order No. 5.

1.2 N6 MAIN SPAN AND SKYWAY

The following descriptions of the N6 alignment, Main Span and Skyway structures, and pile groups are based on the information contained in the 65-percent Main Span design plans and the draft 100-percent Skyway design plans that were submitted by TY Lin/M&N in August 1999 and November 2000, respectively. Additional footing layout data for the Main Span East Pier were provided in TY Lin (2001b).

1.2.1 N6 Alignment Description

The N6 alignment, as received from TY Lin/M&N (2001a), is shown on Plate 1.1, and various Main Span and Skyway portions of the alignment are shown on Plates 1.2 and 1.3, respectively. The proposed N6 alignment lies to the north of the existing alignment generally as follows:

- The proposed N6 alignment transitions from a double-decked structure at the tunnel portal on Yerba Buena Island to two, parallel, side-by-side structures north of the existing bridge.
- The maximum deviation between the alignments is to the east of existing Bridge Pier E4. At that point, the centerline of the N6 alignment is about 220 meters to the north of the centerline of the existing bridge alignment.
- From its point of curvature, the new alignment extends easterly to the Oakland Mole. The proposed alignment centerline is about 80 meters north of the existing bridge centerline at the point of curvature of the existing bridge at Pier E10.
- At the western end of the Oakland Mole, the proposed new alignment centerline is about 55 meters to the north of the existing bridge centerline.
- At its easternmost end, the N6 alignment is coincident with the existing at-grade SFOBB approach to the west of the toll plaza.



The N6 alignment structure is understood to include the following features:

- Twin bridge structures carrying separate east- and westbound traffic.
- A total width of the corridor for the new structures of about 70 meters. The replacement bridge provides for 5 lanes of traffic in either direction, and a bike path along the eastbound structure.
- An approximately 410-meter-long transition structure extending from the Yerba Buena Island Tunnel to the eastern tip of Yerba Buena Island.
- An approximately 565-meter-long, single-tower, self-anchored suspension cable, main-span signature structure extending offshore from the tip of Yerba Buena Island.
- An approximately 2.1-kilometer-long, four-frame Skyway structure extending from the signature structure eastward to the Oakland Shore Approach.
- An Oakland Shore Approach structure extending about 700 meters from the Skyway structure to the north side of the Oakland Mole.
- An earthen fill transition from the Oakland Shore Approach structure to the roadways leading to and from the existing bridge.

1.2.2 Signature Structure Spans and Pier Locations

The Main Span signature structure (Plate 1.2) will be an asymmetrical structure with a longer East Span and shorter West Span. The signature structure will be supported on three piers. The West Pier will be located on the eastern end of Yerba Buena Island, as shown on Plate 1.2.

The shorter West Span will be 180 meters long. The main tower (or pylon) will be 35 meters to the west and upslope of the tower location that was originally planned during the initial Phase 1 studies. As shown on Plate 1.2, this location is about 65 meters offshore from the east end of Yerba Buena Island. At this location, the Bay floor slopes to the southeast and the mudline elevation varies between about elevation (El.) -13 to -20 meters, relative to mean sea level (MSL) datum, beneath the pylon centerline.

The East Span of the main structure is expected to have a length of 385 meters. The East Pier location is thus about 75 meters farther to the east than the East Pier location originally planned during the initial Phase 1 studies. The East Pier will be located about 75 meters east of the location proposed in the initial Phase 1 study and about 190 meters north of existing Bridge Pier E3.



1.2.3 Skyway Structure

The approximately 2.1-kilometer-long Skyway structure (Plate 1.3) will extend from the Main Span-East Pier to the Oakland Mole. The Skyway will include separate, parallel eastbound and westbound structures. Each structure will include four structural frames that are numbered 1 through 4 from west to east.

Frames 1 through 3 (which will comprise about 90 percent of the total Skyway length) will each be supported by four piers, and Frame 4 will be supported by two. Pier spacings for Frames 1 and 2 are 160 meters. As the Skyway approaches the Oakland Mole, pier height progressively decreases with water depth. Pier spacing of Frames 3 and 4 also will decrease from 160 meters to 96 meters as the Skyway nears the Oakland Shore Approach structure.

1.3 FOUNDATION DESCRIPTION

1.3.1 Pile Type, Size, and Section

On the basis of information provided by TY Lin/M&N, the Main Span-East Pier and the Skyway piers will be supported on 2.5-meter-diameter steel pipe piles. The upper sections of the piles will be filled with reinforced concrete to form a composite structural member denoted by Caltrans as a cast-in-steel shell (CISS) pile. The piles will be about 70 to 95 meters long, and extend down to between El. -93 and El. -108 meters with structural concrete fill to between approximately El. -63 and El. -71 meters. The piles are currently being designed to include a variable wall thickness schedule provided by TY Lin/M&N that varies from 76 millimeters (mm) at the pile cap to 51 mm near the pile tip.

1.3.2 Pier Footings (Pile Caps) and Number of Piles

The pile caps for the Skyway Structure and Main Span are structural steel frames that are encased in concrete. The pile cap forms a footing for concrete box section piers. Footing layouts for the Main Span-East Pier (TY Lin/M&N, 2001b) and Skyway piers (TY-Lin/M&N, 2000b) are shown on Plate 1.4.

Main Span East Pier. The Main Span-East Pier footings are connected octagonal units that are 25.3 meters in the transverse direction by 24.5 meters in the longitudinal direction. The Main Span-East Pier footings are connected octagonal units that are 25.3 meters in the transverse direction by 24.5 meters in the longitudinal direction. The Main Span-East Piers are each approximately 6 meters by 5.4 meters.

As shown on Plate 1.4, the Main Span-East Pier will be supported on 16 piles. The piles will consist of two groups of eight vertical piles centered on the piers supporting the eastbound and westbound bridge alignments, respectively.



Skyway Structure Piers. The Skyway footings for Piers E3 through E14 are octagonal while the footings for Piers E15 and E16 are roughly rectangular. The footings are 20.8 meters in the transverse direction, and 18.4 meters (Piers E3 through E14) or 14.3 meters (Piers E15 and E16) in the longitudinal direction. The Skyway piers are 8.5 meters wide, in the transverse direction, and vary from 6.5 meters to 5.5 meters in the longitudinal direction.

As shown on Plate 1.4, Skyway Piers E3 through E14 are each supported on six batter piles. The piles at the four corners of the footing have a batter of 1:8 while the piles that are located along the longitudinal axis of the alignment have a batter of 1:12. Skyway Piers E15 and E16 are supported on four batter piles that have a batter of 1:8.

During the development of the 85-percent design submittal, a design modification performed to increase the flexibility of the piers (and thereby reduce the loads induced on the foundation) resulted in the lengthening of the piers supporting Frames 2 through 4. The lengthening of the piers resulted in the lowering of the pier footing to between 6 and 13 meters below the existing Bay floor. To allow for inspection/maintenance, an approximately 11.5- to 2.5-meter-diameter access casing is provided around each of those piers.

1.4 PROJECT DATUM

The horizontal and vertical datum specified by Caltrans (1997b) for use on this project were as follows:

- Horizontal Datum: California Coordinate System Zone 3, NAD 1983 (meters)
- Vertical Datum: Mean Sea Level (MSL) Datum of 1929

Locations and elevations presented in this report are in reference to this project datum. The NGVD 29 datum is generally close to MSL datum. Caltrans (1997b) specified that MSL (or NGVD) was 0.942 meter above mean lower low water (MLLW) datum (e.g., to convert MLLW elevations to MSL/NGVD elevations, *subtract* 0.94 meter from the MLLW elevation values).

1.5 BASIS OF CHARACTERIZATION

1.5.1 Site Investigations

Our interpretation of the subsurface conditions is based primarily on the Phase 1, 2, and 3 marine site investigation activities conducted in January through April 1998, September through November 1998, and September through October 2000, respectively. The marine investigation activities included:

- Phase 1:
 - 14 regional marine borings with extensive in situ and laboratory testing
 - 2-D and 3-D marine geophysical surveys



- Phase 2:
 - 30 pier-specific marine borings with extensive in situ and laboratory testing
 - 49 tethered Seascout cone penetration test (CPT) soundings
- Phase 3:
 - 77 wheeldrive Seacalf CPT soundings
 - 2-D marine geophysical survey around Yerba Buena Island

The marine explorations were completed using offshore equipment and included extensive in situ testing and strength testing. The methods used for the various Fugro-EM site investigations are described in and the collected data presented in the Final Marine Geotechnical Site Characterization Report (Fugro-EM, 2001e), respectively. The locations of the borings are shown on Plate 1.5.

In addition to the Fugro-EM site investigation data, the following were also considered:

- Various previous borings completed in 1994 through 1996 for the Caltrans' retrofit studies, and
- Other historic drilling information.

1.5.2 Integrated Approach and GIS Database

For the interpretations presented in this report, primary emphasis was placed on the site-specific conditions encountered in the 1998 borings, 2000 CPTs, and the subsurface geometry imaged by the 1998 and 2000 marine geophysical surveys. The 1998 borings include extensive in situ and laboratory test data (on relatively undisturbed push samples), whereas the older borings include variable (and often limited) quantities of test data (on comparatively disturbed driven samples). Testing on samples recovered from the 1998 borings together with the 1998 and 2000 in situ test data are the principal basis for the interpretations described herein. Other older data have generally been used to supplement the stratigraphic information provided in that new data.

The stratigraphy in the borings and CPTs has been compared and integrated with the interpreted stratigraphic relationships as imaged by the geophysical surveys (Fugro-EM, 2001d). That integrated effort has been used to prepare surface contour and isopach (thickness) contour maps for various stratigraphic horizons and units that underlie the site.

All of the new and past drilling data have been input into a Geographic Information System (GIS) to allow synthesis, comparison, analyses, and output of the data.



1.5.3 Report Organization

Main Text. The main text of this Axial Pile Design and Drivability report includes the following sections:

- Section 1.0 - Introduction
- Section 2.0 - Generalized Subsurface Conditions and Stratigraphic Model
- Section 3.0 - Axial Pile Design Overview
- Section 4.0 - Axial Pile Design Methodology and Data
- Section 5.0 - Pile Setup
- Section 6.0 - Pile Drivability Considerations
- Section 7.0 - Pile Installation Considerations and Recommendations
- Section 8.0 - References

Various list and graphical information are provided on tables and illustrations that follow each section of the main text.

Appendix A - Pier-Specific Design Data. The axial pile design data are provided as pier-specific groups of plates for the Main Span-East Pier and each of the Skyway piers. The pier-specific plates include:

- Axial Pile Design Parameters and Results,
- Axial Pile Load Transfer-Displacement Curves,
- Tabulated Axial Pile Load Transfer Data, and
- Static Pile Head Load-Deformation Curves.

When drivability analyses were performed for a pier, the following plates also are included with the pier-specific plate group:

- Soil Resistance to Driving
- Predicted Blow Counts, Menck MHU 500T
- Predicted Blow Counts, Menck MHU 1000
- Predicted Blow Counts, Menck MHU 1700

Appendix B - Verification of Pile Design Methods. This appendix documents several of the data sources and example analyses that were performed to verify the methods described in Section 4.0 of the main text.

1.6 RELATED PROJECT REPORTS PREPARED BY FUGRO-EARTH MECHANICS

The flowchart presented on Plate 1.6 has been prepared to clarify and delineate the areas and issues addressed (or to be addressed) by the primary reports prepared (or to be prepared) for the project by Fugro-Earth Mechanics (Fugro-EM, 2001a-h). As shown on Plate 1.6, the project



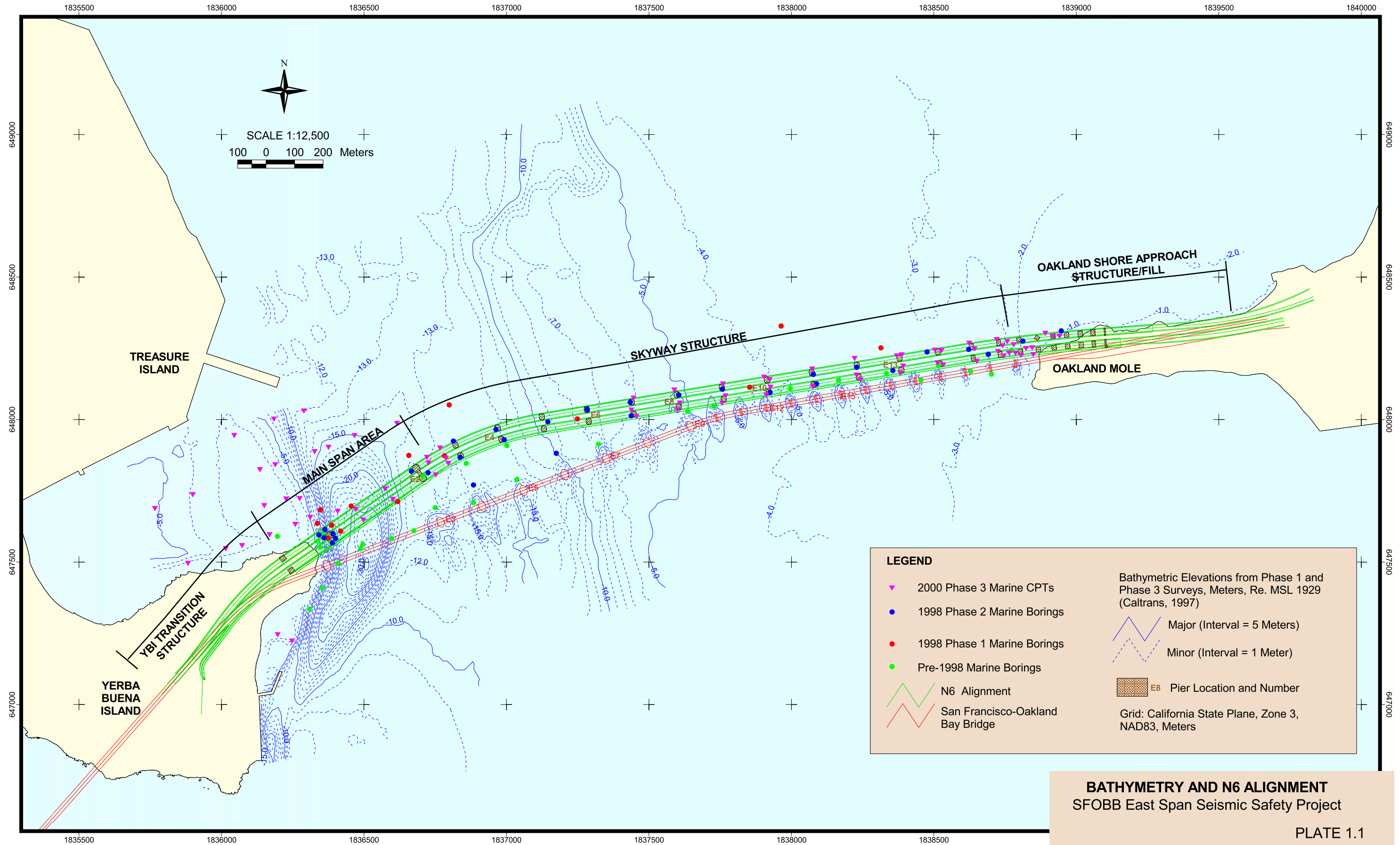
submittals have generally been divided into: a) geotechnical site characterization reports, and b) foundation design reports.

Site characterization report submittals consist of: a) marine, b) Oakland Shore Approach, and c) Yerba Buena Island. Final foundation reports will be prepared to address: a) Yerba Buena Island transition structures and Main Span-West Pier and Main Span-Pylon, b) Main Span-East Pier and Skyway Piers (E3 through E16), and c) Oakland Shore Approach structures to the east of Pier E16. In general, foundation design recommendations and results are developed interactively and iteratively with the structural engineers. Since the design loads and foundation layouts are still being modified, all but the Skyway structure foundation reports are either in draft or in preparation. Design recommendations are typically being provided to the design team via memoranda and will be included in the final foundation reports.

Areas addressed by various site characterization and foundation reports are shown on Plate 1.7. As shown on Plate 1.7, delineation of these areas is generally based on the site investigation techniques used. In contrast, the areas addressed by the final foundation reports are based on: a) the subsurface conditions (as defined in the geotechnical site characterization reports), and b) the requirements of the various bridge and structural engineering teams. Consequently, the division of areas addressed in each of the foundation reports is somewhat different from the division of areas addressed in each of the site characterization reports.

As shown on Plate 1.6, the final reports for the foundation design of the Main Span-East Pier and Skyway structures include: 1) this Axial Pile Design and Drivability report, 2) a companion Lateral Pile Design report, and 3) a Temporary Towers report.





LEGEND

- ▼ 2000 Phase 3 Marine CPTs
- 1998 Phase 2 Marine Borings
- 1998 Phase 1 Marine Borings
- Pre-1998 Marine Borings
- N6 Alignment
- San Francisco-Oakland Bay Bridge

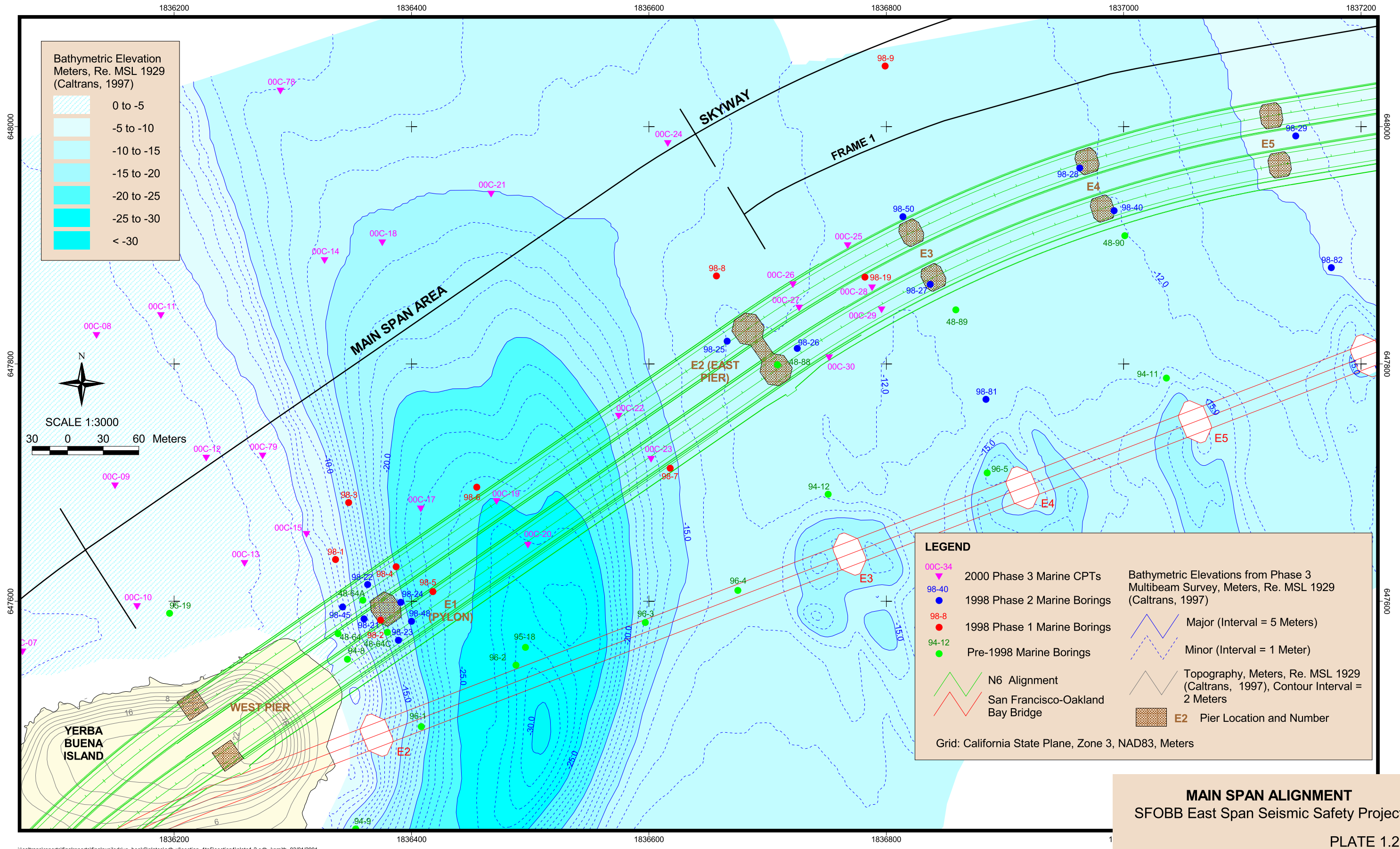
Bathymetric Elevations from Phase 1 and Phase 3 Surveys, Meters, Re. MSL 1929 (Caltrans, 1997)

- Major (Interval = 5 Meters)
- Minor (Interval = 1 Meter)
- E8 Pier Location and Number

Grid: California State Plane, Zone 3, NAD83, Meters

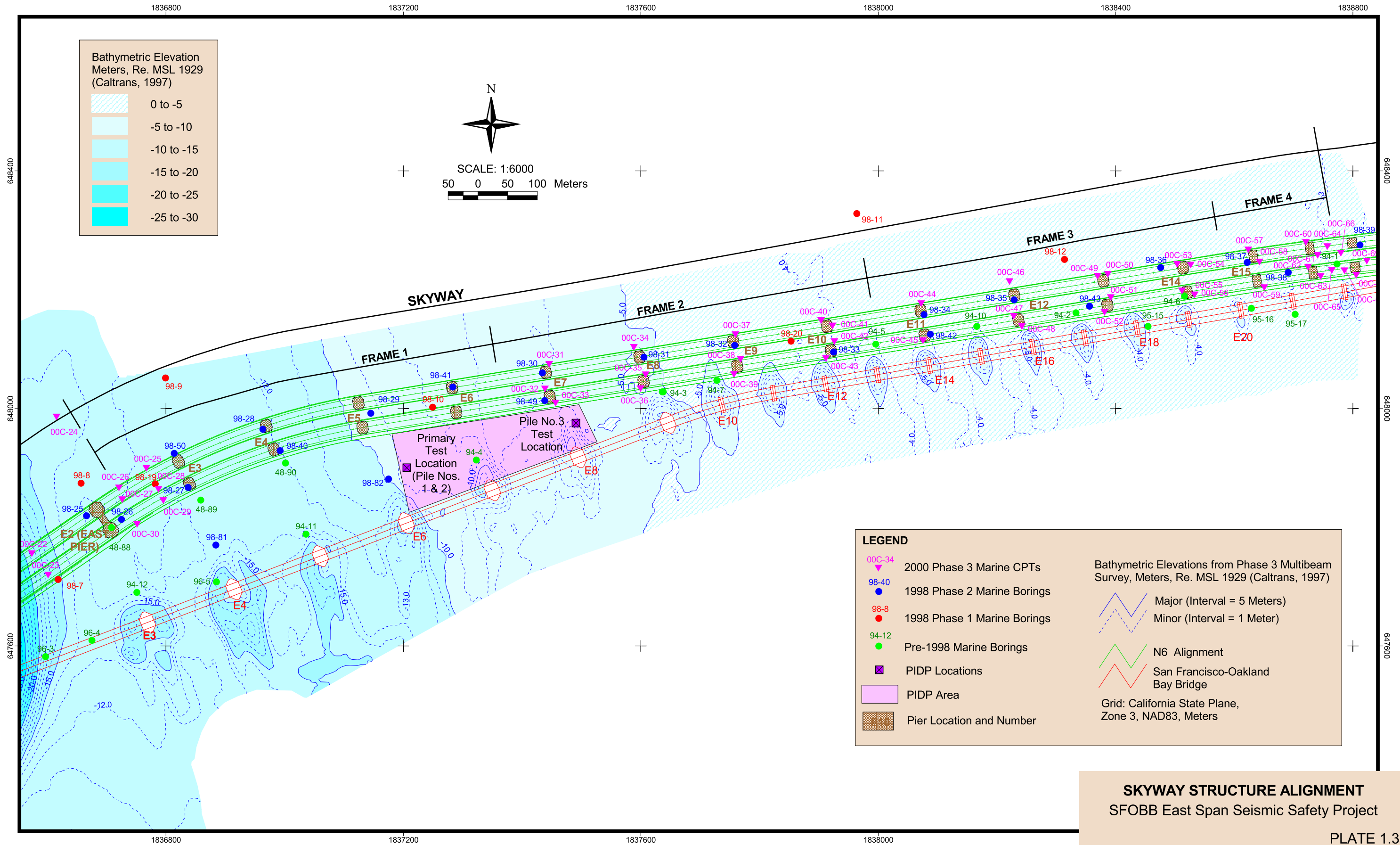
BATHYMETRY AND N6 ALIGNMENT
SFOBB East Span Seismic Safety Project
PLATE 1.1

j:\caltrans\reports\finalreports\final\appliedrive_book6\plates\odb-xf\section_1to5\section1\plate1-1.odb, ksmith, 03/01/2001



MAIN SPAN ALIGNMENT
SFOBB East Span Seismic Safety Project
PLATE 1.2

J:\caltrans\reports\finalreports\final\expil\drive_book\plates\odp-x\lsection_1\to5\section1\plate1-2.odp, ksmith, 03/01/2001



Bathymetric Elevation
Meters, Re. MSL 1929
(Caltrans, 1997)

0 to -5
-5 to -10
-10 to -15
-15 to -20
-20 to -25
-25 to -30

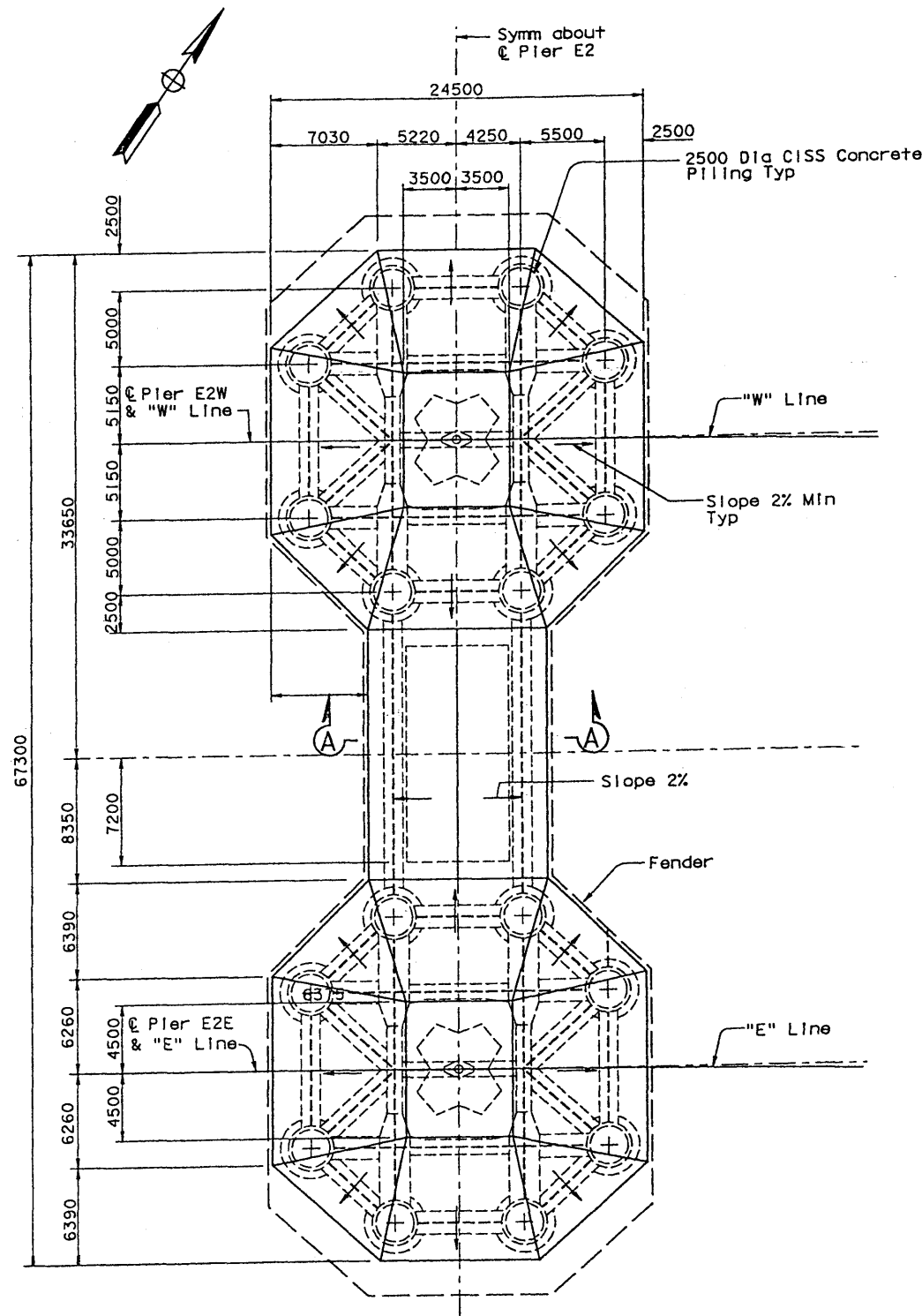
N

SCALE: 1:6000
50 0 50 100 Meters

LEGEND

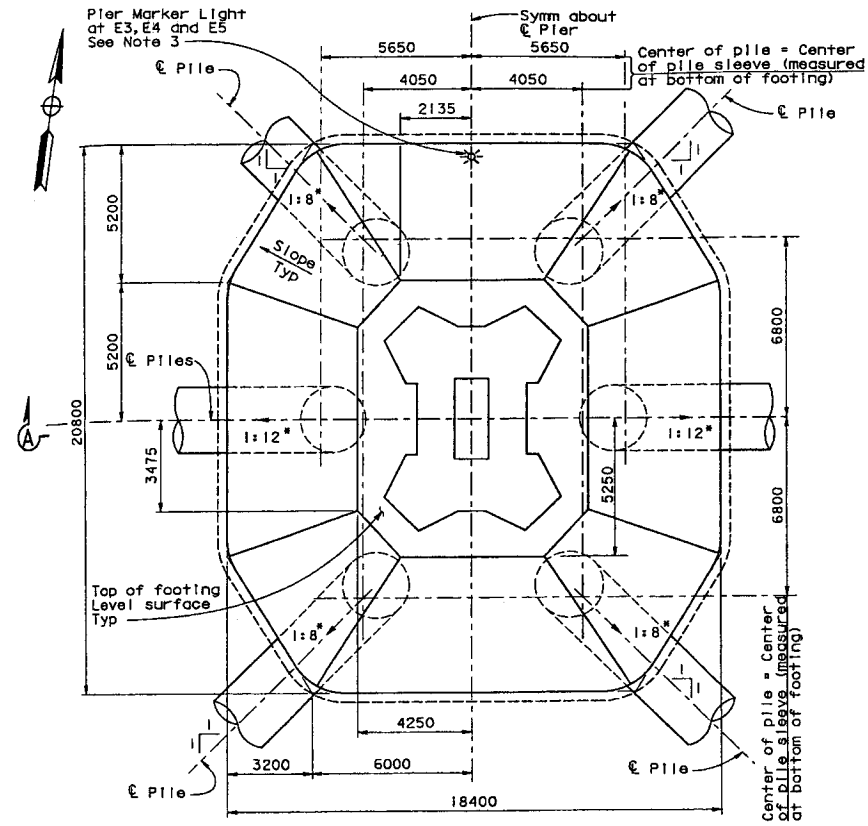
00C-34	2000 Phase 3 Marine CPTs	Bathymetric Elevations from Phase 3 Multibeam Survey, Meters, Re. MSL 1929 (Caltrans, 1997)
98-40	1998 Phase 2 Marine Borings	Major (Interval = 5 Meters)
98-8	1998 Phase 1 Marine Borings	Minor (Interval = 1 Meter)
94-12	Pre-1998 Marine Borings	N6 Alignment
⊠	PIDP Locations	San Francisco-Oakland Bay Bridge
■	PIDP Area	Grid: California State Plane, Zone 3, NAD83, Meters
⊠	Pier Location and Number	

SKYWAY STRUCTURE ALIGNMENT
SFOBB East Span Seismic Safety Project
PLATE 1.3

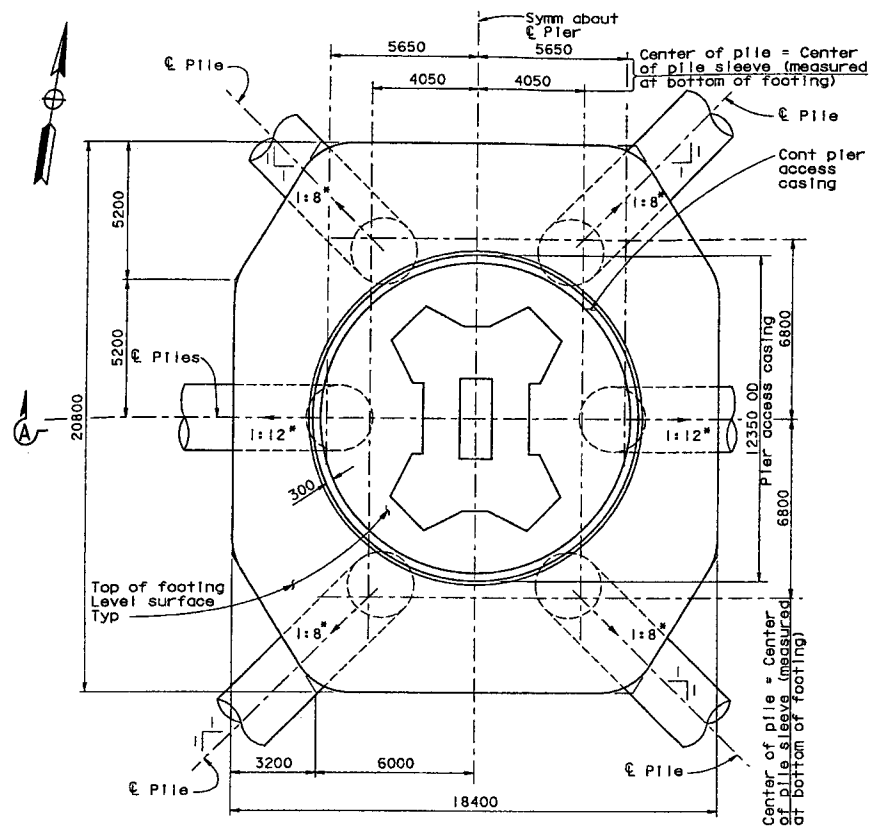


MAIN SPAN EAST PIER

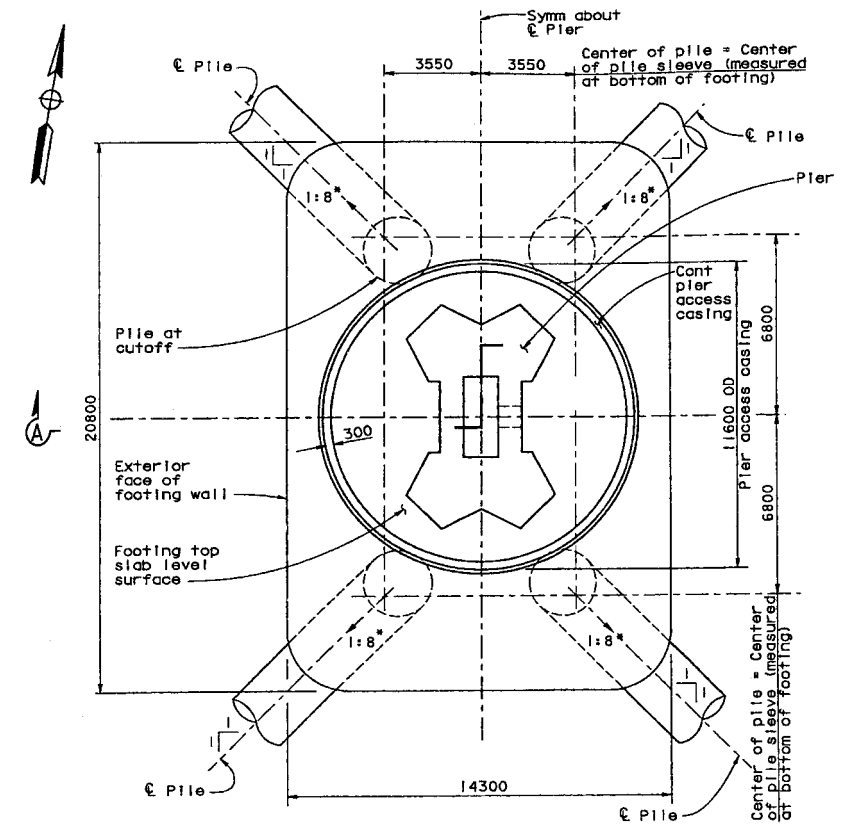
NOTES: 1) Footing layout from TY Lin-Moffat & Nichol drawings.
2) Dimensions shown on plans are in millimeters.



SKYWAY PIER E3 THROUGH E6



SKYWAY PIER E7 THROUGH E14

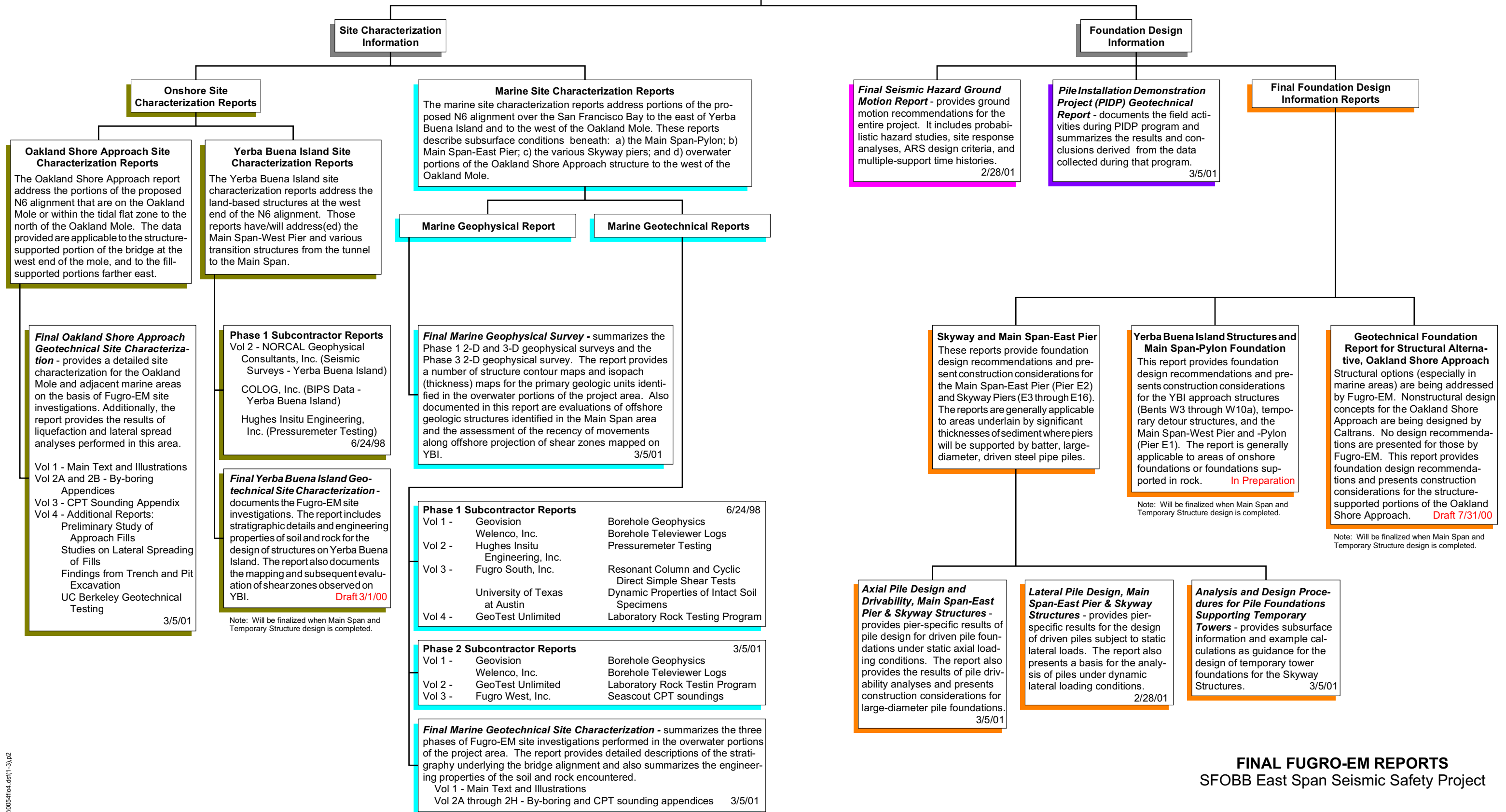


SKYWAY PIER E15 THROUGH E16

**MAIN SPAN EAST PIER AND
SKYWAY FOOTING GEOMETRY**
SFOBB East Span Seismic Safety Project

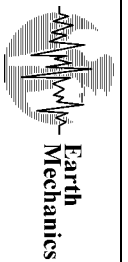
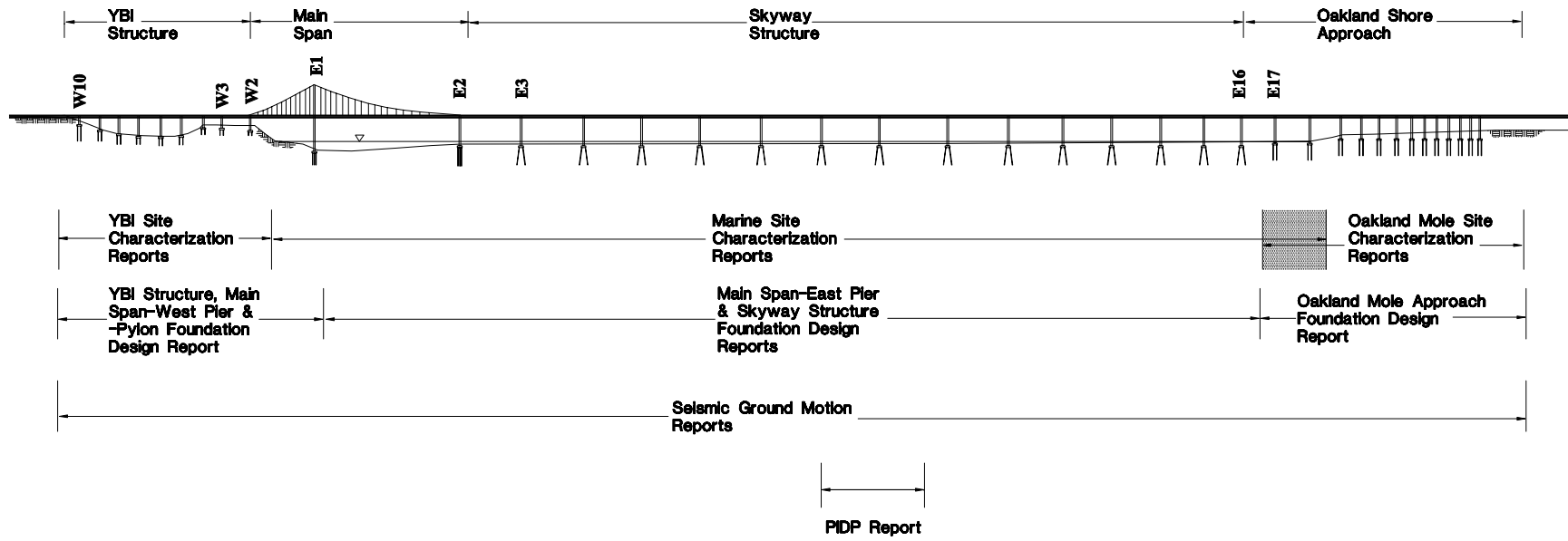


**FUGRO-EM
GEOTECHNICAL STUDY**



9842/0054/04.dsf(1-3).p2





DELINEATION OF AREAS ADDRESSED BY FUGRO-EMI REPORTS
SFOBB East Span Seismic Safety Project

**SECTION 2.0
GENERALIZED SUBSURFACE CONDITIONS AND
SUBSURFACE STRATIGRAPHIC MODEL**

2.0 GENERALIZED SUBSURFACE CONDITIONS AND SUBSURFACE STRATIGRAPHIC MODEL

The following discussion summarizes the subsurface stratigraphy and subsurface conditions underlying the Main Span-East Pier and Skyway of the N6 alignment. This summary is a synopsis of the more detailed description contained in the Final Marine Geotechnical Site Characterization report (Fugro-EM, 2001e). The following discussion is limited to the conditions underlying the approximately 70-meter-wide N6 alignment corridor. The discussion also is limited to the stratigraphic section within the depth penetrated by and immediately underlying the Main Span-East Pier and Skyway pile foundations (i.e., this discussion is limited to the sediment section above about El. -110 meters). The Final Marine Geotechnical Site Characterization report (Fugro-EM, 2001e) should be referred to for information relative to: 1) the shallow, easterly sloping rock offshore Yerba Buena Island, 2) the regional stratigraphic conditions beyond the alignment corridor, or 3) the deeper sediment and rock stratigraphy below the depth of interest for pile design.

2.1 SAN FRANCISCO BAY BATHYMETRY

Contours of Bay floor elevation in the project area are presented on Plates 1.1 through 1.3. The bathymetric data are from: 1) a multibeam bathymetric survey (May 2000) along most of the existing bridge and N6 alignments; and 2) fathometer measurements taken during the 2-D and 3-D geophysical surveys (January to April 1998). Details of the various bathymetric surveys are presented in the Final Marine Geophysical Survey report (Fugro-EM, 2001d).

As shown on Plates 1.1 through 1.3, the Bay floor within the survey areas generally slopes east to west from between 0.15 to 2 percent to within about 300 meters offshore Yerba Buena Island. Offshore Yerba Buena Island, the surface slopes more steeply to the east. The lowest elevation in the survey area is about El. -30 meters (re: MSL datum) in the deep scour depression offshore the eastern tip of Yerba Buena Island.

A north-south-trending channel is located to the east of Yerba Buena Island. Along the channel axis, the nominal elevation of the channel base is El. -15 meters. Between the existing Bridge Piers E2 and E3, however, the channel reaches a depth of El. -30 meters. This scour hole measures about 700 by 300 meters and is elongated in a north-southwest direction. It is more than 15 meters deep relative to its outlet to the southwest. The east- and west-facing slopes of the depression, which underlie the area between the Main Span pylon and East Pier, are as steep as about 10 to 30 percent while the north- and south-facing slopes are more typically about 3 to 4 percent.

In addition to the prominent scour hole between existing Bridge Piers E2 and E3, there are scour depressions adjacent to a number of the bridge piers. The scour holes are typically 3 to



5 meters deep. Around the piers, scour hole sizes generally increase to the west. While the scour holes around existing Bridge Pier E22 measure approximately 30 to 50 meters in length, they elongate to 200+ meters around existing Bridge Pier E3. To the west of existing Bridge Pier E6, the scour holes extend largely to the south of the piers.

Beneath the Main Span-East Pier and Skyway, the bathymetry slopes to the west. The bathymetric features to the west of the Oakland Mole are described below:

- Beneath the Oakland Shore Approach and immediately to the west of the Oakland Mole, the Bay floor slopes easterly from about El. -1 meter down to El. -3 meters. The majority of that slope difference occurs beneath the western two-thirds of the Oakland Shore Approach.
- Beneath Skyway Frames 3 and 4, the Bay floor consists of a broad, approximately 700-meter-wide, nearly flat-bottomed shallow area. In this area, the Bay floor slopes westerly from about El. -3 meters down to about El. -3.75 meters at a slope of less than 0.15 percent.
- A slightly steeper slope is present beneath Skyway Frame 2. In that area, the Bay floor slopes from about El. -3.5 to El. -7 meters at an average slope of about 0.8 percent.
- A north-south-trending, approximately 5-meter-high slope is present below the eastern half of Skyway Frame 1. In this area, the Bay floor deepens from about El. -7 to El. -12 meters over a horizontal distance of about 300 meters. The Bay floor is locally as steep as about 2 percent in this area of steeper bay bottom.
- Beneath the western half of Skyway Frame 1 and the area of the Main Span-East Pier, the slope flattens to about 0.3 to 0.4 percent and the Bay floor decreases from about El. -12 to El. -13 meters.

A variety of cultural features were observed on the side scan sonar data in the survey area. These features include several utility cables and pipelines as well as: a) debris; b) scour depressions; c) changes in sediment density; d) small linear anomalies from anchor chains, buoys, pipelines, and cables; e) bridge piers, dolphins, signs, platforms, and other obstructions with a positive relief; and f) unidentifiable features of unknown origin. The features are shown on a 1:5,000-scale map in the Final Marine Geophysical Survey report (Fugro-EM, 2001d).

2.2 GEOLOGIC FEATURES AND SUBSURFACE STRATIGRAPHY

2.2.1 Principal Features and Formations

The geologic structure underlying the N6 alignment includes the following general features:



- Easterly sloping bedrock of the Franciscan Formation
- A westerly thinning sequence of Holocene- and Pleistocene-age marine and alluvial sediments
- Extensive channeling within the Holocene- and Pleistocene-age sediments

The primary geologic formations that underlie the N6 alignment (or portions of the alignment) are listed in descending sequence:

- Young Bay Mud (YBM)
- Merritt-Posey-San Antonio (MPSA) Formations (sometimes simplified as Merritt Sand)
- Old (Yerba Buena) Bay Mud (OBM)
- Upper Alameda (primarily) Marine (UAM) Sediments
- Lower Alameda (primarily) Alluvial (LAA) Sediments
- Franciscan Formation (FF) Bedrock

Descriptions of the sediments in each of those units are provided subsequently.

2.2.2 Structural Contour and Isopach Thickness Maps

Interpreted structural contour and isopach (thickness) maps of the various geologic formations that underlie the site are presented in the Final Marine Geophysical Survey report (Fugro-EM, 2001d). Reduced page-size versions (typically at a scale of 1:10,000) of some of the interpretive maps presented in that report are provided on Plates 2.1 through 2.8. The reduced-scale maps provided in this report are:

- Structural Contours, Base of Young Bay Mud - Plate 2.1
- Structural Contours, Top of Upper Alameda Marine Paleochannel Sand - Plate 2.2
- Structural Contours, Base of Upper Alameda Marine Paleochannel Sand - Plate 2.3
- Structural Contours, Top of Lower Alameda Alluvial Sand - Plate 2.4
- Structural Contours, Top of Franciscan Formation - Plate 2.5
- Isopach (Thickness) of Young Bay Mud - Plate 2.6
- Isopach (Thickness) of Upper Alameda Paleochannel Sand - Plate 2.7
- Isopach (Thickness) of Sediment Section Above Lower Alameda Alluvial Sand - Plate 2.8



2.2.3 Subsurface Cross Sections

The geologic structure and stratigraphic relationships underlying the SFOBB East Span Skyway are illustrated on two simplified, conceptual, subsurface cross sections:

- Plate 2.9 - Conceptual east-west cross section to the south of the east-west-oriented paleochannel
- Plate 2.10 - Conceptual north-south cross section at the south edge of the east-west paleochannel

The soil lithologies encountered in the borings, data from the borings, and the interpreted stratigraphic contacts, as imaged on the marine geophysical records, are shown on a series of three cross sections that span Plates 2.11a and 2.11b. The cross sections presented on those plates were generated along: 1) the centerline of the N6 alignment; 2) the centerline of the westbound lanes; and 3) the centerline of the eastbound lanes. The cross sections include the measured undrained shear strength data and CPT tip resistance (q_c).

Additional cross sections are presented in the Final Marine Geotechnical Site Characterization report (Fugro-EM, 2001e) and the Skyway Temporary Towers report (Fugro-EM, 2001c). Transverse cross sections presented in Fugro-EM (2001e) illustrate: 1) the subsurface conditions down to bedrock in the area around Piers E2, E3, and E11; and 2) the shallow stratigraphic conditions (down to El. -80 meters) at the locations of buried Skyway pier footings (Piers E7 through E16). The cross sections presented in Fugro-EM (2001c) provide stratigraphic details and material properties at the anticipated locations of temporary towers to support the ends of the Skyway structures during construction.

2.3 DESCRIPTION OF GEOLOGIC FEATURES

2.3.1 Easterly Sloping Bedrock of the Franciscan Formation

The eastern San Francisco Bay is underlain by Franciscan Formation bedrock that slopes to the east from Yerba Buena Island.

Bedrock Surface Contours. As shown on Plate 2.5, a prominent bedrock high or nose extends to the northeast of Yerba Buena Island. Offshore, the bedrock slopes down (at an inclination of between about 2.5 horizontal to 1 vertical [2.5H:1V] to 3.5H:1V [approximately 15 to 22 degrees]) to the north, east, and southeast from the edge of the island out to about El. -70 meters on the north and El. -95 meters on the east and southeast. In this area, the inclination of the bedrock surface is generally consistent with the dip of the bedrock strata observed in our marine borings, suggesting that the easterly-facing slope is a dip-slope.

The bedrock slope flattens farther to the east. Along the N6 alignment, that change of bedrock slope occurs about 70 meters to the west of the Main Span-East Pier. From that point,



the bedrock surface continues to slope to the east, but at a flatter average slope of about 1.5 to 2 percent (approximately 0.8 to 1.2 degrees), and reaches about El. -135 meters near the tip of the Oakland Mole. The bedrock surface between the toe of the steeper slope and the Oakland Mole decreases in several 5- to 10-meter-high steps separated by several-hundred-meter-wide areas of relatively flatter slope.

Bedrock Lithology. The bedrock beneath the Skyway portion of the N6 alignment consists of nearly equal amounts of thinly to thickly interbedded sandstone (graywacke) and fine-grained siltstone and claystone. In most areas, the upper approximately 6 to 9 meters of bedrock is typically intensely to moderately weathered. In the weathered zone, the recovered cores were intensely to very intensely fractured into pieces ranging from about 25 to 75 mm long. The Rock Quality Designation (RQD) of the weathered zone generally is less than about 25. The weathered zone is underlain by a relatively thin, 1.5- to 3-meter-thick layer of slightly weathered rock with up to 12 mm of light brown moderately weathered rock on each side of the fractures and joints.

The thinly to thickly bedded siltstone and claystone interbeds are dark gray to black, moderately hard, and normally intensely to very intensely fractured into pieces generally less than about 100 mm long. The siltstone/claystone rock in the cores generally broke along smooth, polished, bedding-plane partings, the majority of which were inclined at about 20 to 40 degrees. The siltstone/claystone beds typically range from about 0.1 to 0.3 meter thick, although several thickly bedded zones of fine-grained rock up to 3 meters thick were encountered.

Below the weathered zone, the fresh rock is typically moderately to slightly fractured, with zones of intensely fractured rock up to about 1.5 to 1.8 meters thick in several borings. RQD values for fresh rock typically range from about 40 to 70. Within the slightly to intensely fractured rock, at least three primary fracture inclinations were observed in the rock cores: a) 40 to 50 degrees, b) 60 degrees, and c) 70 to 90 degrees.

2.3.2 Holocene- and Pleistocene-Age Marine and Alluvial Sediments

A westerly-thinning sequence (Plates 2.9 and 2.10) of Holocene- and Pleistocene-age marine and alluvial sediments unconformably overlay the Franciscan Formation bedrock along the N6 alignment. In general, the marine sediments (deposited during sea level high stands) are primarily clays and silts. In contrast, the alluvial sediments (deposited during sea level low stands) are more commonly sands. In some depth zones, sequences that are composed of primarily fine-grained marine clays contain interbedded layers of sand. In addition, the primarily granular alluvial sequences often contain significant quantities of fine-grained layers.

Except where eroded and then backfilled by past sequences of channeling, the bedding inclination of the marine and alluvial sediments is slight and, for practical purposes, the bedding can be considered to be near horizontal. The Holocene- and Pleistocene-age marine and alluvial sediments, however, are frequently interfingered and interlayered. Thus, although the



stratigraphic sequence generally can be extrapolated between borings (and geophysical tracklines), the lithologic and geotechnical properties of the soils can vary significantly over limited horizontal distances.

2.3.3 Channeling

The SFOBB East Span project area contains a series of nested, shallow, buried paleochannels. Paleochannels that are infilled with geologically Recent Holocene-age sediments (referred to subsequently as Recent channels or paleochannels) are shown on Plate 2.2 and include: a) east-west-trending channeling to the north of the existing SFOBB alignment (consistent with the channeling mapped by Trask and Rolston [1951]), and b) tributary south-to-north channels associated with the east-west channeling. In general, the marine clays are thicker and the alluvial sands are thinner, deeper, or absent within the limits of the Recent paleochannels.

The geophysical records and their integration with the boring data document the presence of the east-west-trending paleochannel to the north of the existing bridge. The approximate limits and thalweg of that channel are shown on Plate 2.1. Borings 98-11 and 98-9, drilled near the thalweg of the paleochannel, penetrated approximately 25 meters of very soft to firm clay (Young Bay Mud). The thalweg of the paleochannel is interpreted to slope to the west (Plate 2.1), although the gradient of the thalweg is minimal. As shown on Plate 2.1, the southern edge of the paleochannel meanders across both the existing and proposed N6 bridge alignments. The width of the east-west paleochannel is variable. To the north of existing Bridge Piers E5 through E7, the paleochannel is only about 600 meters. Farther to the east, however, the width of the paleochannel exceeds 1,000 meters. The narrow portion of the paleochannel (to the north of Bridge Piers E5 through E7) coincides with the area of steeper bathymetry.

Most previous interpretations (Trask and Rolston, 1951; Goldman, 1969; Rogers and Figures, 1991) of widely spaced borings have suggested that the east-west-trending geologically Recent channel deflects to the southwest and passes around the southern tip of Yerba Buena Island. However, other interpretations of regional geology (Lee and Praszker, 1969) suggest that a Recent paleochannel also extends northward along what is now the eastern edge of Treasure Island. As shown on Plate 2.1, the available geotechnical and geophysical data show that the outlet to the east-west-trending Recent paleochannel is to the north.

In addition to the geologically Recent channels described above, the site also is underlain by a number of deeper and older channels. In general, the records suggest that as the channel system evolved, successive channels eroded into, along, across, and through older, deeper channels. As described subsequently, geophysical data for areas underlain by the east-west-trending Recent paleochannel are of limited quality due to the pervasive presence of biogenic gas within the channel infill. Consequently, it was relatively difficult to map deeper paleochannels beneath the Recent east-west-trending paleochannel. The boring and CPT data, however, show



one such series of nested paleochannels beneath a north-south-trending tributary to the primary east-west-trending Recent channel in the vicinity of proposed Bridge Pier E7. That series of nested paleochannels is illustrated on the cross sections presented on Plate 2.11a.

A somewhat deeper (and older) nested series of north-south-oriented channels were clearly imaged in the western one-third of the survey area. The east-west- and north-south-trending paleochannels merge in the area below the Main Span-East Pier and the western one-half of Skyway Frame 1. Two north-south-trending paleochannels are shown on the cross-sections presented on Plate 2.11a. The upper channel is within the Old Bay Mud unit and is infilled with very stiff clay. The lower channel is a predominantly sand-filled channel that was eroded into the top of the Upper Alameda Marine Formation. The base of the sand-filled channel that eroded into the Upper Alameda Marine was mapped as part of the integrated study and the resultant structural contours are shown on Plate 2.3.

2.3.4 Gassy Sediments

Much of the region surveyed for this project has shallow gas in the sediments. This gas is assumed to be biogenic in origin and is dissolved in the interstitial fluid in the sediment. The gas appears to be derived from both the paleochannel sediments as well as the surface of the underlying paleochannel bank into which the paleochannels have been cut. The gassy characteristics of the paleochannel sediments are observed in the boring suspension logs where very low primary wave velocities (V_p) were measured in the geologically Recent paleochannel sediments.

2.3.5 Definition of Areas With Common Geologic Structure

The stratigraphic conditions beneath the overwater portion of the proposed N6 alignment of the SFOBB East Span replacement bridge can be divided into three segments.

Shallow Bedrock Area Offshore From Yerba Buena Island. This portion of the alignment is defined as the area shoreward (to the west) of the El. -40-meter structural contour on top of the Franciscan Formation as presented on Plate 2.5. The area extends about 150 meters offshore from the eastern tip of Yerba Buena Island (or about 30 percent of the distance from the proposed Main Span-Pylon to the Main Span-East Pier of the proposed N6 alignment. The Main Span-Pylon structure will be founded in this area on shallow, sloping Franciscan Formation bedrock. However, the Pylon foundation is not addressed within the current report.

Channel Intersection Area Beneath Western One-Third of N6 Alignment. Beyond the Shallow Bedrock Area, the approximately western one-third of the N6 alignment is underlain by complex stratigraphy created by the intersection (or merging) of the east-west and north-south sets of nested paleochannels. The western area extends eastward to beyond the apex of the N6 alignment, in the middle of Skyway Frame 1. This eastern limit approximately coincides with the location where the Bay floor slope steepens to about 2 percent between the El. -8-meter and



El. -12-meter contours. This area includes the Main Span-East Pier and most of Skyway Frame 1.

Paleochannel Margin Area Beneath Eastern Two-Thirds of N6 Alignment. The eastern two-thirds of the N6 alignment extend eastward of the apex of the N6 alignment to the Oakland Mole. The subsurface geometry underlying the eastern two-thirds of the bridge has significant north-south variation in the upper 30 meters due to the presence of the incised east-west-aligned paleochannel sequence to the north of the bridge. Because the edge of channeling meanders along the bridge alignment (Plate 2.12) and tributary channels cross the proposed N6 alignment, there also is significant east-west variation beneath much of the alignment. The deeper stratigraphy also varies in the east-west direction due to the easterly sloping surface of the Franciscan Formation and the westerly thinning wedges of deeper sediment that overlie the Franciscan basement. This area includes the eastern limit of Skyway Frame 1 as well as Skyway Frames 2 through 4.

2.4 FORMATION DESCRIPTION

The geologic formations (as defined by Caltrans, 1997a) that underlie the N6 alignment (or portions of the alignment) include, in descending sequence:

- Young Bay Mud (YBM)
- Merritt-Posey-San Antonio (MPSA) Formations (sometimes simplified as Merritt Sand)
- Old (Yerba Buena) Bay Mud (OBM)
- Upper Alameda (primarily) Marine (UAM) Sediments
- Lower Alameda (primarily) Alluvial (LAA) Sediments
- Franciscan Formation (FF) Bedrock

While the formation designations are useful, the subsurface conditions are described primarily in terms of undrained shear strength (of cohesive soils) and relative density or measured cone tip resistance (of granular soils). That choice was made based on the extensive strength data from the Fugro-EM borings and CPT soundings and the direct applicability of the strength data to foundation design.





The typical soil designations for the formations are as follows:

Formation Designation	Typical Soil Designation
Young Bay Mud	Very Soft to Soft or Soft to Firm Clay
Merritt-Posey-San Antonio Formations (also referred to as Merritt Sand)	Dense to Very Dense Sand with Stiff to Very Stiff Clay Layers
Old Bay Mud and Upper Alameda Marine Sediments	Very Stiff to Hard Clay
Lower Alameda Alluvial Sediments	Dense to Very Dense Sand (or Very Dense Sand) and Hard Clay

The general relative relationships of these soil strata and formations are illustrated on Plates 2.9 through 2.11. The following paragraphs provide an overview of each formation.

2.4.1 Young Bay Mud (YBM)

The Young Bay Mud is a marine clay deposited since the end of the last sea level low stand (circa 11,000 years ago). The YBM occurs as a blanket of sediments that cover the majority of the Bay floor between Yerba Buena Island and the Oakland Mole and as infill in the geologically Recent paleochannels (Plates 2.1 and 2.6).

As much as 29 meters of Young Bay Mud were encountered within the center of the east-west paleochannel to the north of the N6 alignment. Outside of the paleochannel, this surface clay consists of a westerly thinning wedge of sediments that thins from about 8 to 10 meters thick to the east of Pier E8. To the west of the steeper Bay floor bathymetry (beneath the eastern portion of Skyway Frame 1), the surface clay layer is between 3 and 5 meters thick. The base of the deposit is typically at about El. -12 to El. -18 meters.

The Young Bay Mud typically is composed of fat clay. The YBM within the paleochannel is very soft to firm and its undrained shear strength increases with depth. The YBM paleochannel fill includes sand layers and/or seams within several depth intervals. The surface blanket of YBM is typically soft outside of the paleochannels.

The Young Bay Mud provides only a relatively small percentage of the axial skin friction capacity of the piles. For earthquake-loading conditions, the undrained shear strength will degrade. The variable thickness of the YBM, however, has a more significant impact on the lateral response of the piles during seismic loading.

2.4.2 Merritt-Posey-San Antonio (MPSA) Formations

Beneath the Young Bay Mud, a layered sequence of sands and clays is present (Plate 2.12) over portions of the eastern San Francisco Bay. The terminology Merritt-Posey-San Antonio Formations is preferred over the more simplified designation of Merritt Sand in recognition of the layered and interbedded characteristics of the sequence. The geophysical reflections in the MPSA Formations are generally discontinuous and suggest that individual



layers are often of limited lateral extent. Borings and CPT soundings along the proposed N6 bridge alignments suggest that the MPSA Formation sequence generally is no more than 5 to 10 meters thick.

The MPSA Formations include dense to very dense sand with layers of stiff to very stiff sandy clay and clay. In some areas, such as beneath the Oakland Shore Approach (Piers E17 through E22), the sequence includes a distinct 3- to 4.5-meter-thick, very dense sand (Merritt) layer. This sand layer is often overlain by a limited thickness of clayey sand (or sandy clay) and is underlain by variable amounts of stiff to very stiff clay and sandy clay with sand layers. The lowest layer in the MPSA Formations is often a stiff to very stiff clay layer. Beneath much of the Main Span and at certain locations beneath the Skyway (such as in the vicinity of Pier E16), the borings suggest that little or no sand is present within the MPSA Formations. At those locations, the sequence is entirely composed of stiff to very stiff clay.

The geophysical records suggest that the elevation of the top of the sequence varies due to erosion and channeling. Although the base elevation of the sequence is less variable, the bottom of the sequence locally extends down into erosional channels that are cut into the underlying Old Bay Mud.

The variability of the presence or absence of MPSA along the N6 alignment is illustrated on Plate 2.12, which shows the relative amount of dense sand encountered in the soil borings and CPT soundings relative to the mapped limits of the geologically Recent paleochannel edge. Also shown on Plate 2.12 is an indication as to whether the sand layers are relatively deep (below approximately El. -25 meters) or shallow (above approximately El. -25 meters). Outside of the Recent paleochannels, the mapped thickness of the layered sand-and-clay sequence is approximately 5 to 10 meters, and the sand layers are typically shallow. As shown on Plate 2.11, along the flanks of the Recent paleochannels, the thickness of the shallow sand layers in the MPSA Formations are often reduced due to partial erosion. Several explorations along the N6 alignment encountered relatively thick layers of deeper sand within the MPSA Formations. At those locations, the MPSA is present along the flank of the Recent paleochannel and/or at the base of the paleochannel. Since the Recent paleochannel sometimes may not have eroded the MPSA Formations as deeply as the MPSA-infilled channel eroded the underlying strata, the thickness of the MPSA Formations (as shown on Plate 2.12) along those portions of the paleochannel flank may exceed its thickness outside of the paleochannel areas.

2.4.3 Old Bay Mud/Upper Alameda (Primarily) Marine (OBM/UAM) Sediments

The Old Bay Mud and Upper Alameda Marine sediments both consist primarily of very stiff to hard fat clay. Because the composition and geotechnical properties of the two units are similar, the two formations have been mapped and are discussed as one combined sequence of sediments. Except where eroded by channeling, the top of the sequence typically is present from about El. -17 to El. -25 meters. The Old Bay Mud and Upper Alameda Marine sediments,



although somewhat stiffer, are also similar in composition and geotechnical properties to the clay layers that are frequently present near the base of the Merritt-Posey-San Antonio (MPSA) Formations. In many instances, the demarcation between the MPSA and the OBM/UAM sequences is tenuous and subject to interpretation.

Borings show that the combined generally 60-meter thickness of the two formations typically includes multiple crust layers with locally higher strength. Geophysical reflectors within the sequence are generally flat-lying, frequently discontinuous, and often show evidence of channeling (particularly in the western portion of the alignment). At any given elevation, the sediments in the sequence within the western portion of the site are inferred to be generally younger than those at the same elevation farther to the east. This is due to the presence of the nested set of north-south channels that underlie the site to the west of the apex of the N6 alignment.

The majority of the axial pile capacity due to skin friction is derived in the Old Bay Mud and Upper Alameda Marine sediments. The marine clays that comprise the OBM and UAM sequences are generally very stiff to hard fat clays with shear strengths increasing from approximately 125 to 175 kilopascals (kPa) at the top of the sequence to about 150 to 250 kPa at the base of the sequence. The sequence also includes numerous crust layers where the undrained shear strengths are at least 25 to 50 kPa higher than the adjacent layers. In the western one-third of the site, the OBM/UAM sequence was subject to various episodes of channeling and redeposition, and the sediments are commonly somewhat younger than the sediments at equivalent elevations along the eastern two-thirds of the alignment. Consequently, below the heavily overconsolidated top of the OBM, the undrained shear strengths within the OBM/UAM sequence in the western one-third of the site are commonly 25 to 40 kPa less than at equivalent elevations to the east.

Although composed primarily of clay, the sequence includes some sand layers that tend to become more prevalent below about El. -65 meters. Sand layers below that depth are more common at the western end of the area. The relative prevalence of sand near the base of the OBM/UAM sequence in the western portion of the area is interpreted to reflect the presence of a sand-filled paleochannel overlying the toe of the steep bedrock slope to the west. The presence of Upper Alameda Marine Paleochannel Sand at about El. -70 meters is of significant consequence to the design and installation of the piles for the Main Span-East Pier. That local condition is described subsequently.

2.4.4 Lower Alameda (Primarily) Alluvial (LAA) Sediments

The sediments present below about El. -80 to El. -85 meters are interpreted to be the Lower Alameda (primarily granular) Alluvial sediments. These primarily dense, granular sediments onlap the lower portion of the bedrock slope in the western portion of the site and



overlie the Franciscan Formation bedrock to the east of the toe of the steep bedrock slope (Plate 2.11a).

The geophysical reflector mapped as the top of Lower Alameda Alluvial sediments is a strong, generally continuous, flat-lying reflector. The reflector depth correlates to a distinct increase in primary and shear wave velocities (V_p and V_s , respectively) measured in the borings. The interpreted top of LAA is generally relatively horizontal over most of the N6 alignment. To the east beneath Skyway Frames 3 and 4, however, the top of LAA is interpreted to slope upward to the east (Plate 2.11b).

Although the Lower Alameda Alluvial Formation is composed of primarily granular sediments, the reflector interpreted to correlate to the top of the formation generally correlates to the top of a lean clay layer, subsequently referred to as the LAA-clay cap. This clay layer is distinctly different in composition than the overlying clays of the Upper Alameda. This reflector is typically 5 to 10 meters above the top of the first dense sand layer, subsequently referred to as the LAA-sand, which is present at about El. -90 to El. -92 meters (see Plate 2.4).

The draft 100-percent design submittal for the Skyway structures (TY Lin/M&N, 2000b) shows that the Skyway pile foundations will consist of piles driven to tip at about one to two pile diameters into the first significant sand stratum within the Lower Alameda Alluvial sediments or down to bedrock. Since the bedrock surface dips to the east, piles designed to be tipped in bedrock are limited to the western part of Skyway Frame 1 (Piers E3 through E5) with anticipated bedrock elevations ranging from approximately El. -103 to El. -105 meters. Farther to the east, the piles are designed to be tipped below the top of the LAA-sand. Thus, the pile tip elevation for Piers E6 through E16 is expected to be at about El. -94 meters (± 4 meters).

The geophysical data suggest local variation of the LAA-sand and the borings show that the primarily alluvial sediments include an appreciable quantity of clay layers. It should also be noted that the top of the LAA-sand shown on Plate 2.4 generally correlates to the top of a relatively continuous layer of medium- to coarse-grained granular sediments. This surface, however, does not always correlate to the first significant sand stratum within the Lower Alameda Alluvial sediments. In a few of the borings drilled in the Skyway area (e.g., Boring 98-43), significant fine-grained sand layers were encountered above the surface of the LAA-sand.

The variability of the Lower Alameda Alluvial Formation is critical to the choice of pile tip elevation and the definition of pile end bearing and pile tip stiffness. Those variations are described and discussed subsequently.



2.5 UPPER ALAMEDA MARINE PALEOCHANNEL (EL. -70 METERS) SAND AT MAIN SPAN-EAST PIER

As described above, with the exception of the dense sand layers within the Merritt-Posey-San Antonio (MPSA) sequence, most of the sediments above the LAA-bearing stratum are clay soils with variable, but generally relatively limited, quantities of sand layers. An exception to this generality occurs at the top of the Upper Alameda Marine (UAM) sequence in the area of the Main Span-East Pier. At this location, the top of the UAM is encountered at about El. -70 meters and consists of a very dense, fine to medium sand, which is subsequently defined as the Upper Alameda Marine Paleochannel Sand.

2.5.1 Extent and Thickness of Upper Alameda Marine Paleochannel Sand

The Upper Alameda Marine (UAM) Paleochannel Sand appears to infill a north-south-oriented paleochannel that is incised into the top of the UAM in the western one-third of the N6 alignment. The relatively flat surface of the top of the UAM Paleochannel Sand is present at about El. -70 meters. On the west, the UAM Paleochannel Sand appears to onlap onto the eastwardly dipping Franciscan Formation. To the east, the UAM Paleochannel Sand extends to about the location of Skyway Frame 1, Pier E3; however, in that area, the UAM Paleochannel Sand thins rapidly at the edge of the paleochannel. At the location of the Main Span-East Pier, the UAM Paleochannel Sand is about 15 meters thick, and extends down to the top of the underlying Lower Alameda Alluvium. The extent and geometry of the UAM Paleochannel Sand are shown on Plates 2.2, 2.3, and 2.7.

2.5.2 Characteristics of Upper Alameda Marine Paleochannel Sands

The UAM Paleochannel Sand is typically fine to medium sand with about 5 to 10 percent fines and a mean grain size of between about 0.15 and 0.6 mm. The sand frequently includes layers of sandy silt. A submerged unit weight of about 10.5 kilonewtons per cubic meter (kN/m^3) is representative of the UAM Paleochannel Sand.

The measured cone tip resistance in the UAM Paleochannel Sand typically ranges from about 20 to 50 megapascals (MPa). An angle of internal friction of between 38 and 42 degrees is considered to be representative of fine to medium sand.

2.6 CHARACTERISTICS OF THE LOWER ALAMEDA ALLUVIUM

The steel pipe piles planned to support the Skyway (and possibly the Main Span-East Pier) are to be driven down into the Lower Alameda Alluvium (LAA). The following description is intended to be a synopsis of the characteristics of the LAA. This synopsis is to provide input into the evaluation of the pile tip elevation, end-bearing capacity, and end-bearing stiffness. A more detailed description is provided in the Final Marine Geotechnical Site Characterization report (Fugro-EM, 2001e)



2.6.1 Lithology

Principal Materials. The Lower Alameda Alluvium (LAA) includes a cap layer of very stiff to hard lean clay (LAA-clay cap) underlain by a sequence of primarily very dense granular alluvial sediments (LAA-sand). The LAA-sand consists of a wide range of granular sediments that include poorly graded silty fine sand, fine to coarse sand (or clayey fine to coarse sand) with gravel, and gravel with sand and silt. The poorly graded silty fine sand typically has 10 to 42 percent finer than a No. 200 sieve, and a median grain size of 0.1 to 0.35 mm. The fine to coarse sand and gravel typically have 3 to 12 percent finer than a No. 200 sieve, and a median grain size of about 1.5 to 8.5 mm. Interbedded within the LAA-sand are layers of hard lean and fat clay (LAA-clay interbeds). Plate 2.13 provides an example of the layering and the relationships of the three components of the LAA. The representative undrained shear strength of the LAA-clay cap is about 250 kPa. In contrast, the representative undrained shear strength of the LAA-clay interbeds is more typically about 350 to 400 kPa.

The LAA-clay cap is typically about 3 to 10 meters thick. Globally, the LAA-clay cap includes about 15 percent sand layers. The sand layers are typically less than about 1 meter thick, although layers as much as 2.5 meters thick were occasionally encountered. The top of the underlying LAA-sand is typically encountered at between about El. -89 and El. -92 meters. Plate 2.14 provides a cross section showing the elevation of the top of the LAA-sand as encountered in the borings. As shown, the top of the LAA-sand appears to vary locally by about ± 5 meters. The borings suggest that the local variation across the alignment at a set of piers (i.e., adjacent eastbound and westbound piers) may be as much as the variation between a set of adjacent piers.

LAA-Clay Interbeds. The thickness of the individual clay interbeds encountered in the twenty-six (26) 1998 marine borings underlying the Skyway is shown on Plate 2.15. In addition, Plate 2.16 shows the cumulative frequency distribution of the clay interbed thickness for different distances below the top of the LAA-sand. As shown on those two illustrations, more than 50 percent of the individual clay interbeds are less than 0.65 meter thick, and only about 10 to 15 percent of the interbeds are more than 2.5 meters thick.

Plate 2.17 shows the total thickness of the clay interbeds (encountered in the 1998 borings) as a percentage of the total thickness of sediments below the top of the first significant sand in the Lower Alameda Alluvium (defined as the top of the LAA-sand). The data from the borings suggest that total thickness of clay interbeds is less than about 5 percent of the total thickness of sediments in the first 4 meters below the interpreted top of the LAA-sand. Globally, however, the clay interbeds account for about 20 to 30 percent of the total thickness of the LAA deposit in the next 10 to 15 meters below the top of the LAA-sand.

Distribution of Clay Interbeds with Depth, Elevation, and Location. The distribution of LAA-clay interbeds with elevation and depth below the top of the LAA-sand are shown on



Plates 2.18 and 2.19, respectively. This analysis examined the occurrence or non-occurrence of clay interbeds within each 0.2-meter depth or elevation increment.

As shown, the frequency of clay interbeds varies with depth below the top of the LAA-sand and elevation. In general, the data show that less than about 5 percent of the borings included clay interbeds within any depth or elevation interval in the top 3 to 4 meters of the LAA-sand. The frequency of clay interbeds increases to about 30 percent of the borings within the depth interval between about 5 to 8 meters below the top of the LAA-sand, and then decreases to about 10 to 15 percent of the locations within the depth interval between about 9 to 11 meters below the top of the LAA-sand. Within the depth interval about 12 to 15 meters below the top of the LAA-sand, the frequency of clay interbeds again increases.

2.6.2 Implications of Lower Alameda Alluvium Variations for Design and Construction

Both the variation of the top elevation of the LAA-sand and the local presence or absence of LAA-clay interbeds within the underlying LAA-sand are intrinsic variations of the deposit. Because these are local variations, it is impractical to expect to predict how those variations occur over the football-field-sized area circumscribed by the loci of the pile tips at each set of piers. Thus, the pile design and construction will need to accommodate these variations.

From a design standpoint, the primary implication is prediction of the range of pile end-bearing capacity and stiffness that can be logically expected to occur. If the pile tip elevations are to be pre-established, the implications of those variations for construction include: 1) establishment of the maximum depth to which the piles can be driven below the top of the LAA-sand and the minimum pile hammer required to accomplish that, 2) the practical under- and over-drive allowances that the prefabricated pile head connection can accommodate, and 3) the required length of sacrificial pile length above the pile head connection.

2.6.3 Soil Properties

Undrained Shear Strength. The interpreted representative undrained shear strength of the LAA-clay cap is about 250 kPa. In contrast, the representative undrained shear strength of the LAA-clay interbeds is more typically about 400 kPa.

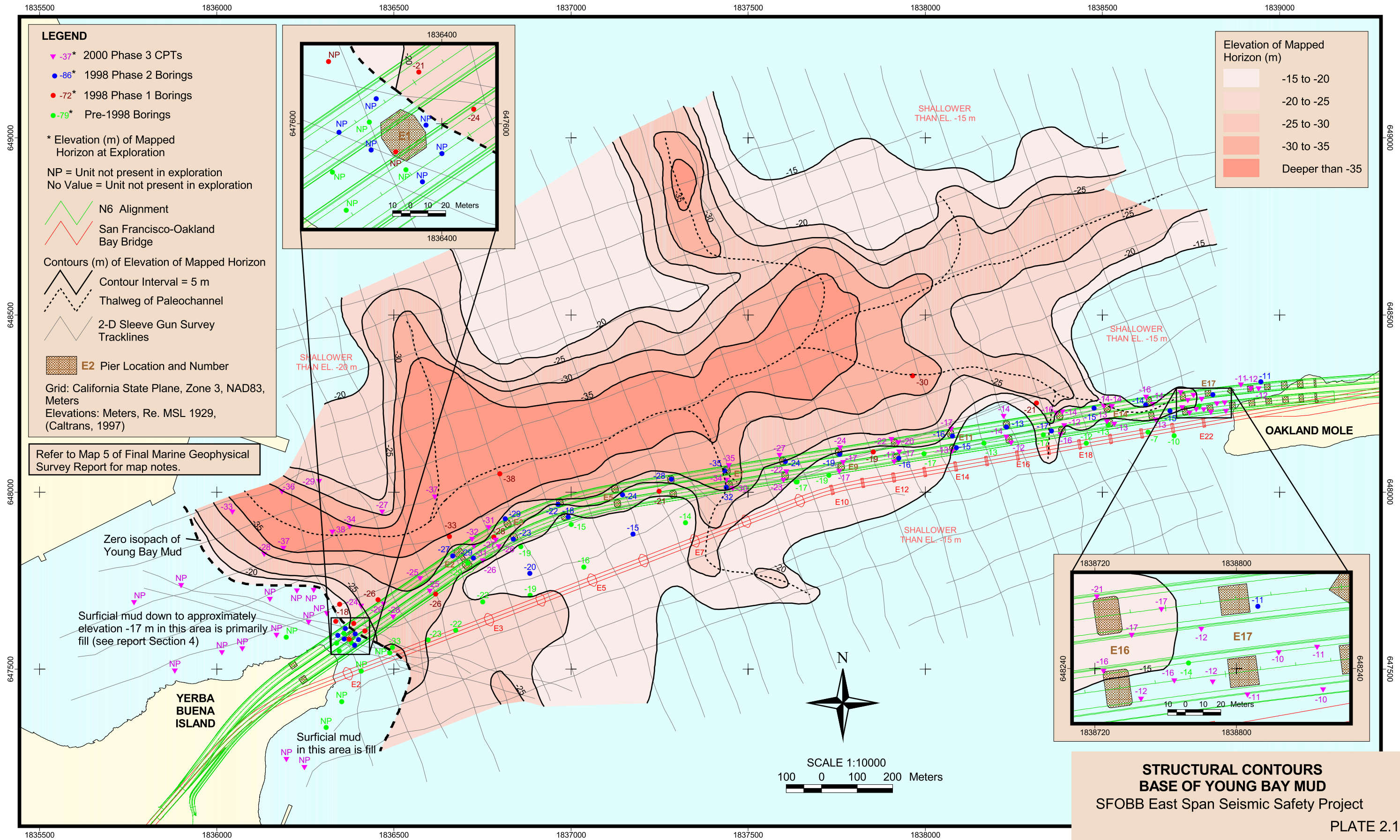
Drained Strength of LAA-Sand. The data show that the Lower Alameda Alluvial sediments are generally dense to very dense with relative densities in excess of 80 percent. The standard penetration test (SPT) N-values exceed 50 and commonly greater than 50/15 centimeters (cm). The measured cone tip resistances are greater than 30 MPa. Friction angles estimated from in situ CPT data generally range from about 38 to 43 degrees.

State of Consolidation. Consolidation test results and empirical indices show that the clay cap and clay interbeds within the Lower Alameda Alluvium are overconsolidated. The data suggest a preconsolidation pressure of about 1,000 to 1,300 kPa in the LAA-clay cap and about

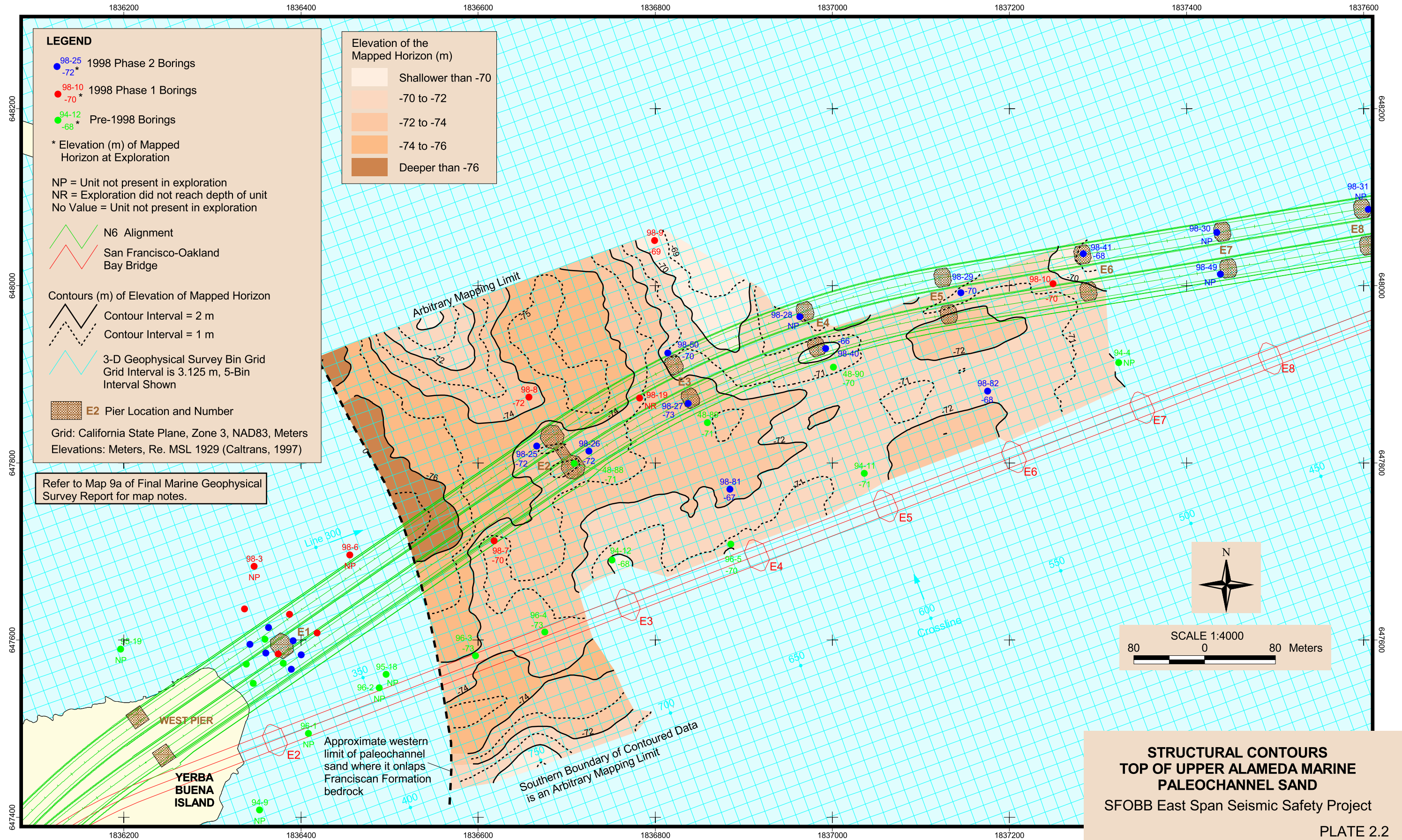


1,500 kPa in the LAA-clay interbeds. Those values correspond to an overconsolidation ratio (OCR) of about 1.5 with a typical range of about 1.3 to 1.8 for the LAA-clay cap, and an OCR of between 1.5 and 2 for the LAA-clay interbeds. The relatively low OCRs at greater depths are not indicative of light overconsolidation, since the interpreted maximum past pressures are on the order of 300 to 800 kPa higher than the estimated overburden stresses.

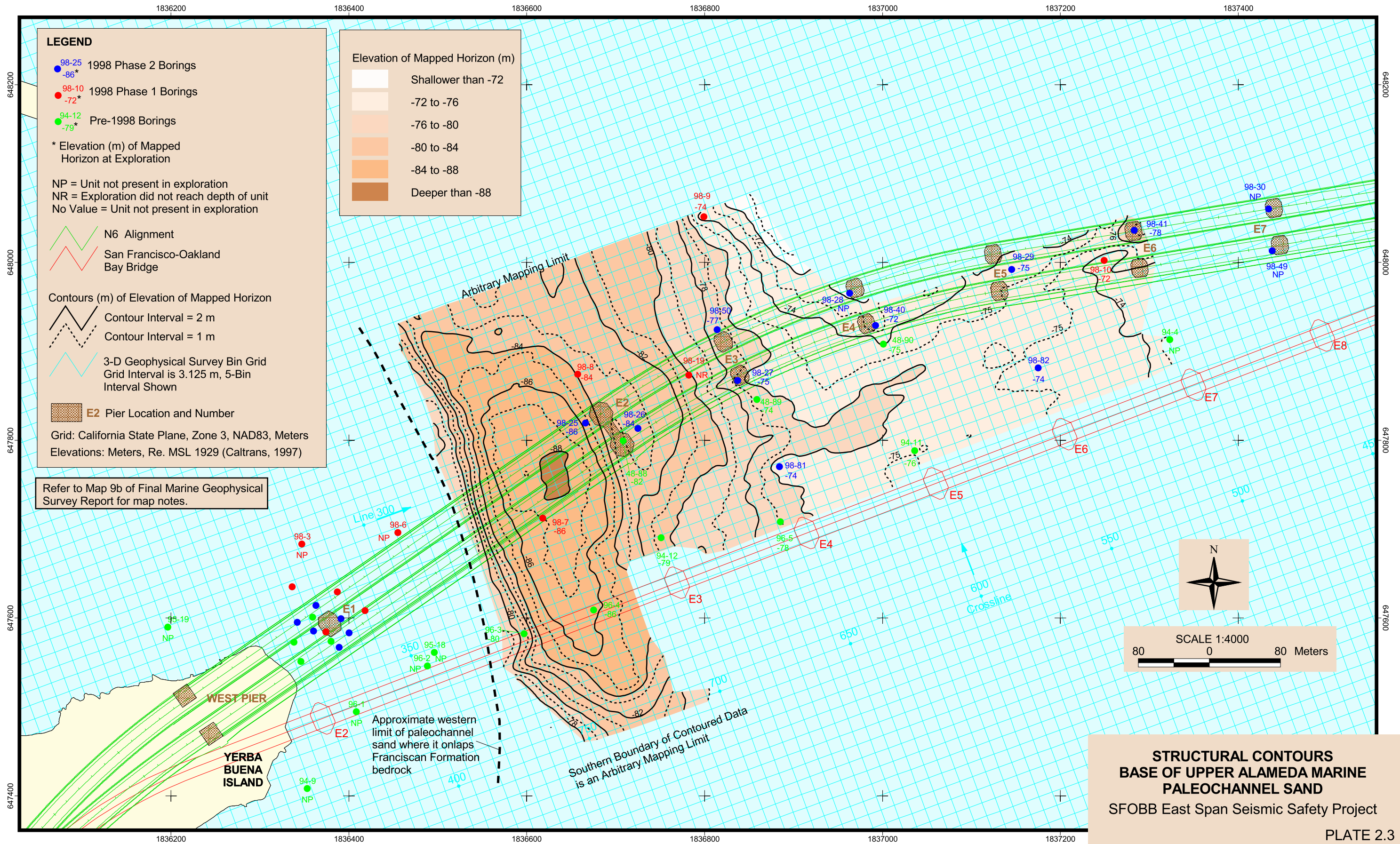




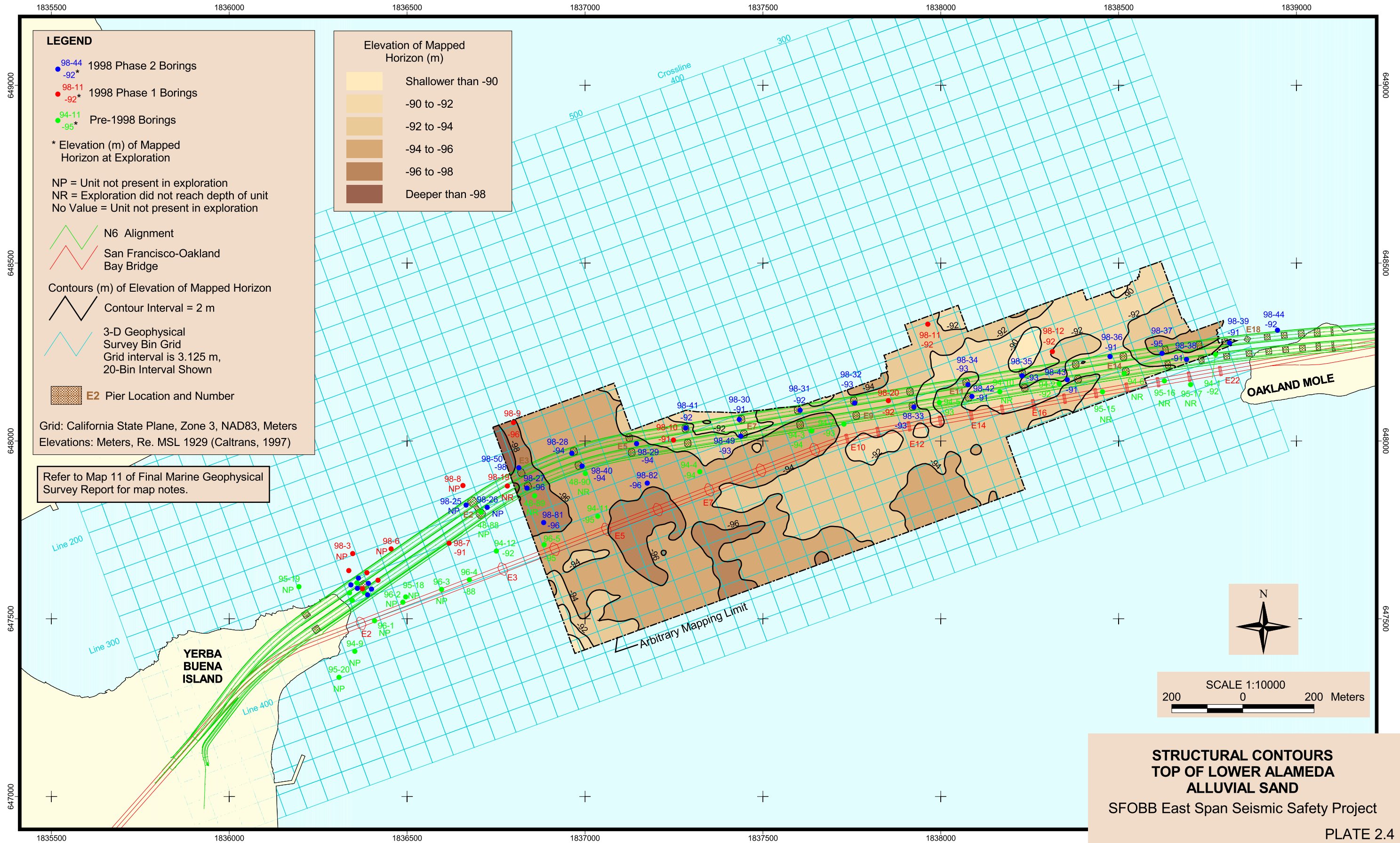
**STRUCTURAL CONTOURS
BASE OF YOUNG BAY MUD**
SFOBB East Span Seismic Safety Project
PLATE 2.1



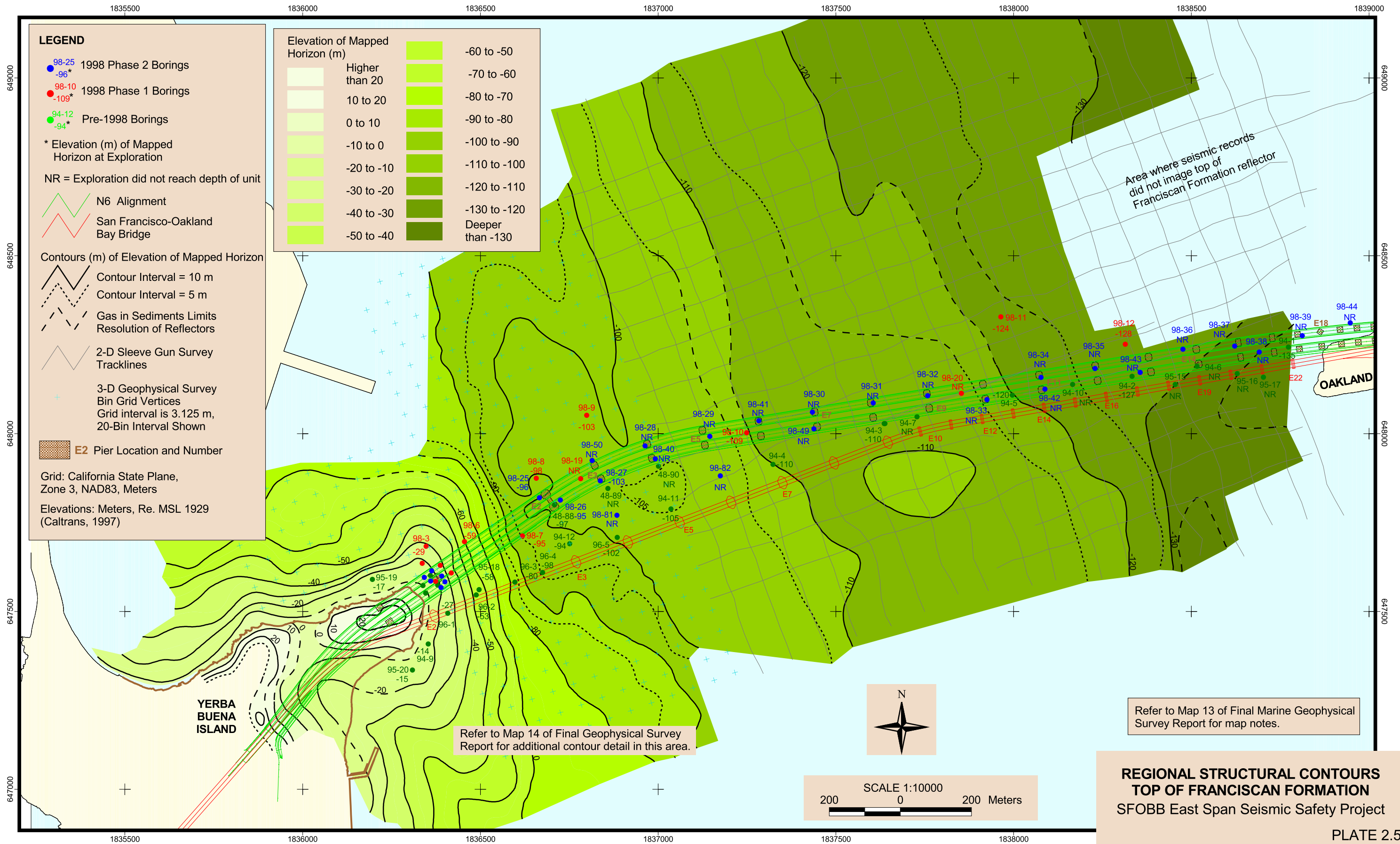
**STRUCTURAL CONTOURS
TOP OF UPPER ALAMEDA MARINE
PALEOCHANNEL SAND**
SFOBB East Span Seismic Safety Project
PLATE 2.2

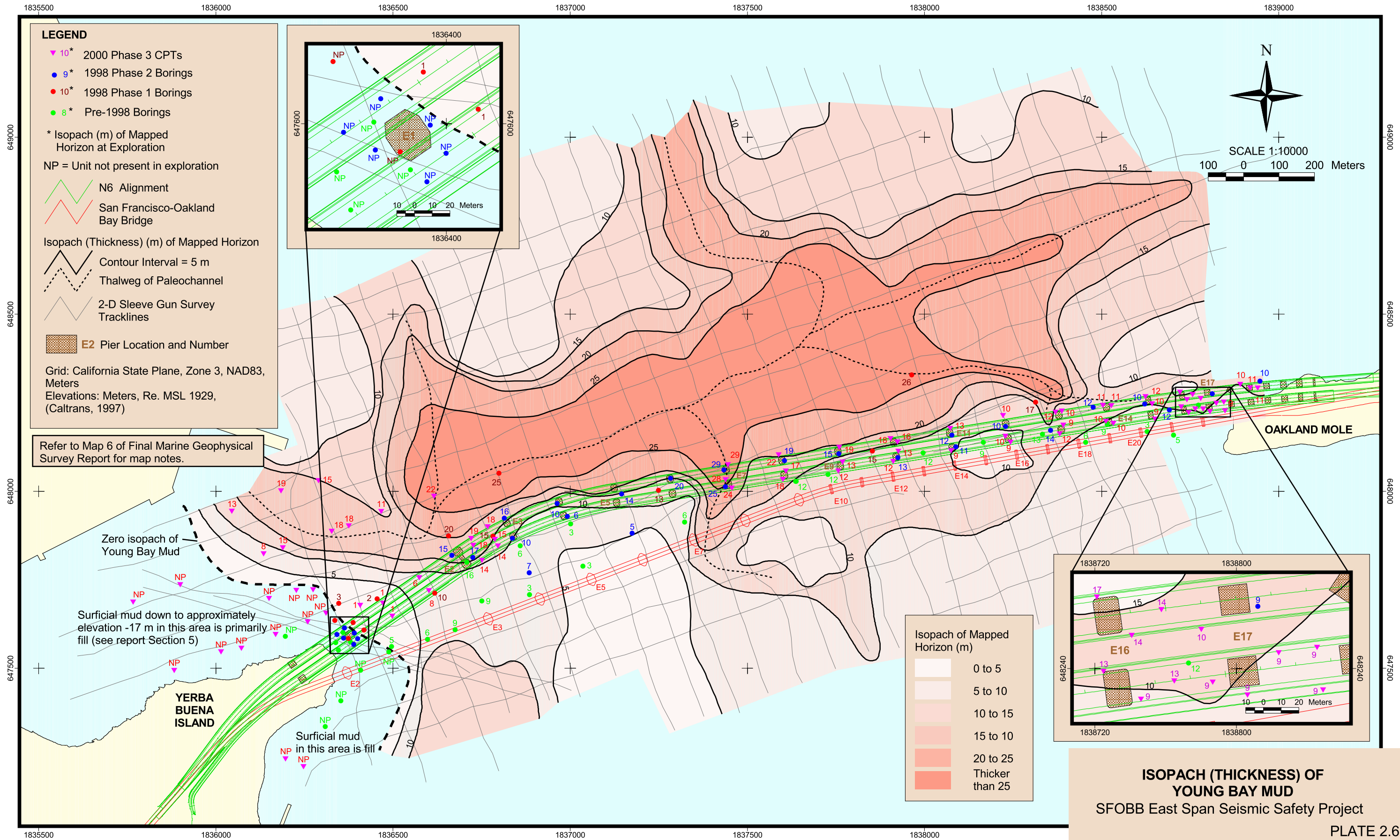


**STRUCTURAL CONTOURS
BASE OF UPPER ALAMEDA MARINE
PALEOCHANNEL SAND**
SFOBB East Span Seismic Safety Project
PLATE 2.3



**STRUCTURAL CONTOURS
TOP OF LOWER ALAMEDA
ALLUVIAL SAND**
SFOBB East Span Seismic Safety Project
PLATE 2.4





LEGEND

- ▼ 10* 2000 Phase 3 CPTs
- 9* 1998 Phase 2 Borings
- 10* 1998 Phase 1 Borings
- 8* Pre-1998 Borings

* Isopach (m) of Mapped Horizon at Exploration

NP = Unit not present in exploration

- N6 Alignment
- San Francisco-Oakland Bay Bridge

Isopach (Thickness) (m) of Mapped Horizon

- Contour Interval = 5 m
- - - Thalweg of Paleochannel
- 2-D Sleeve Gun Survey Tracklines

■ E2 Pier Location and Number

Grid: California State Plane, Zone 3, NAD83, Meters
Elevations: Meters, Re. MSL 1929, (Caltrans, 1997)

Refer to Map 6 of Final Marine Geophysical Survey Report for map notes.

Zero isopach of Young Bay Mud

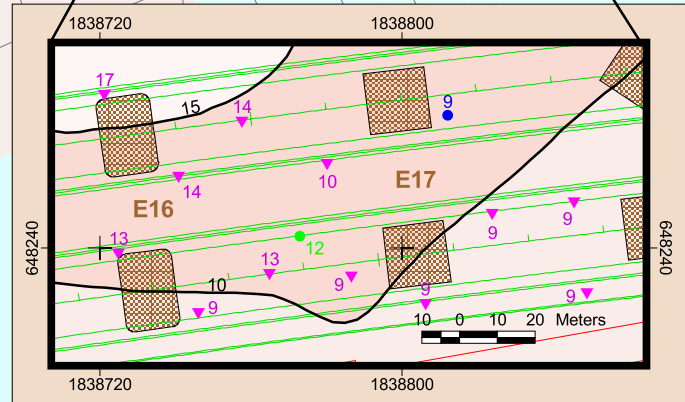
Surficial mud down to approximately elevation -17 m in this area is primarily fill (see report Section 5)

YERBA BUENA ISLAND

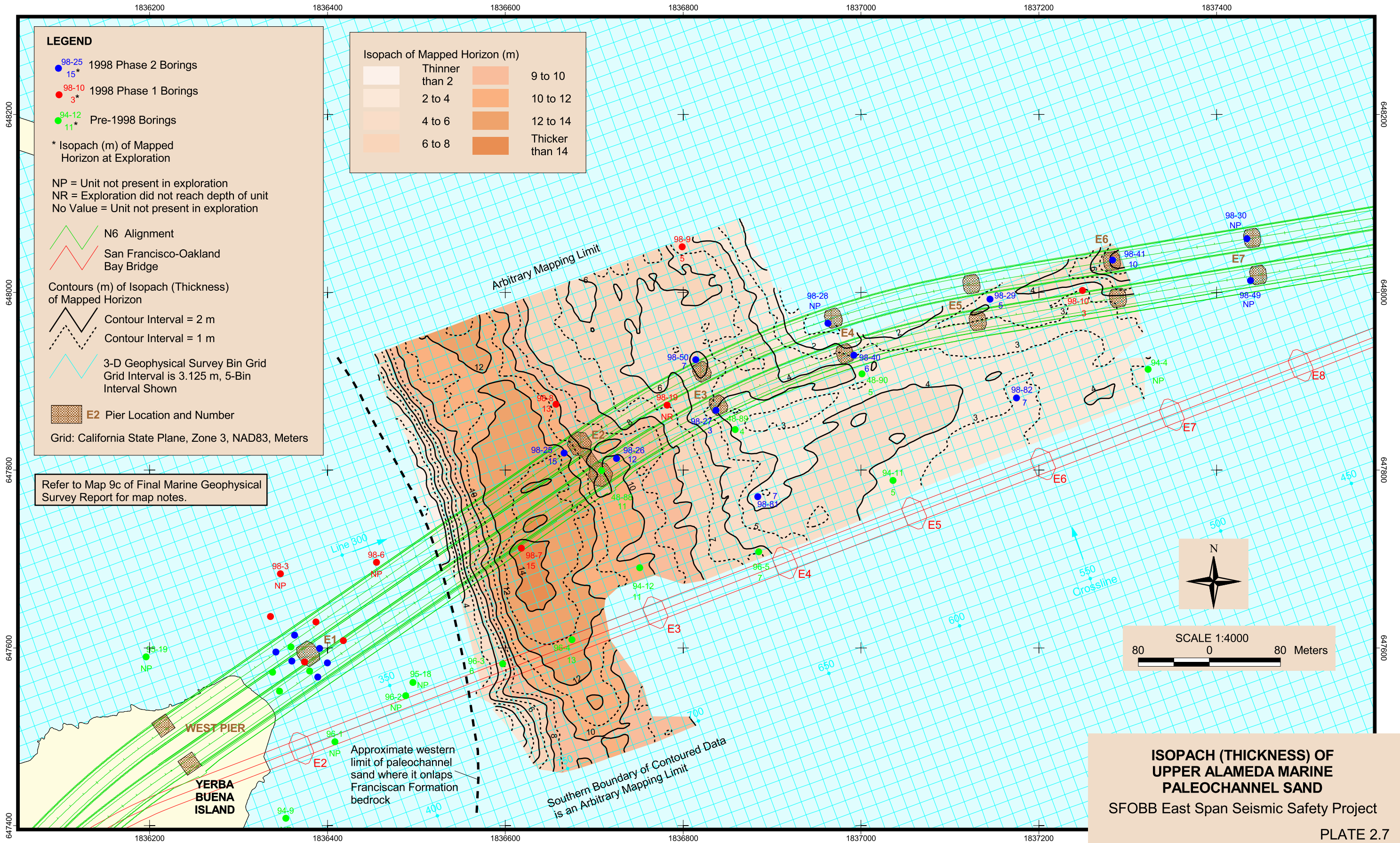
Surficial mud in this area is fill

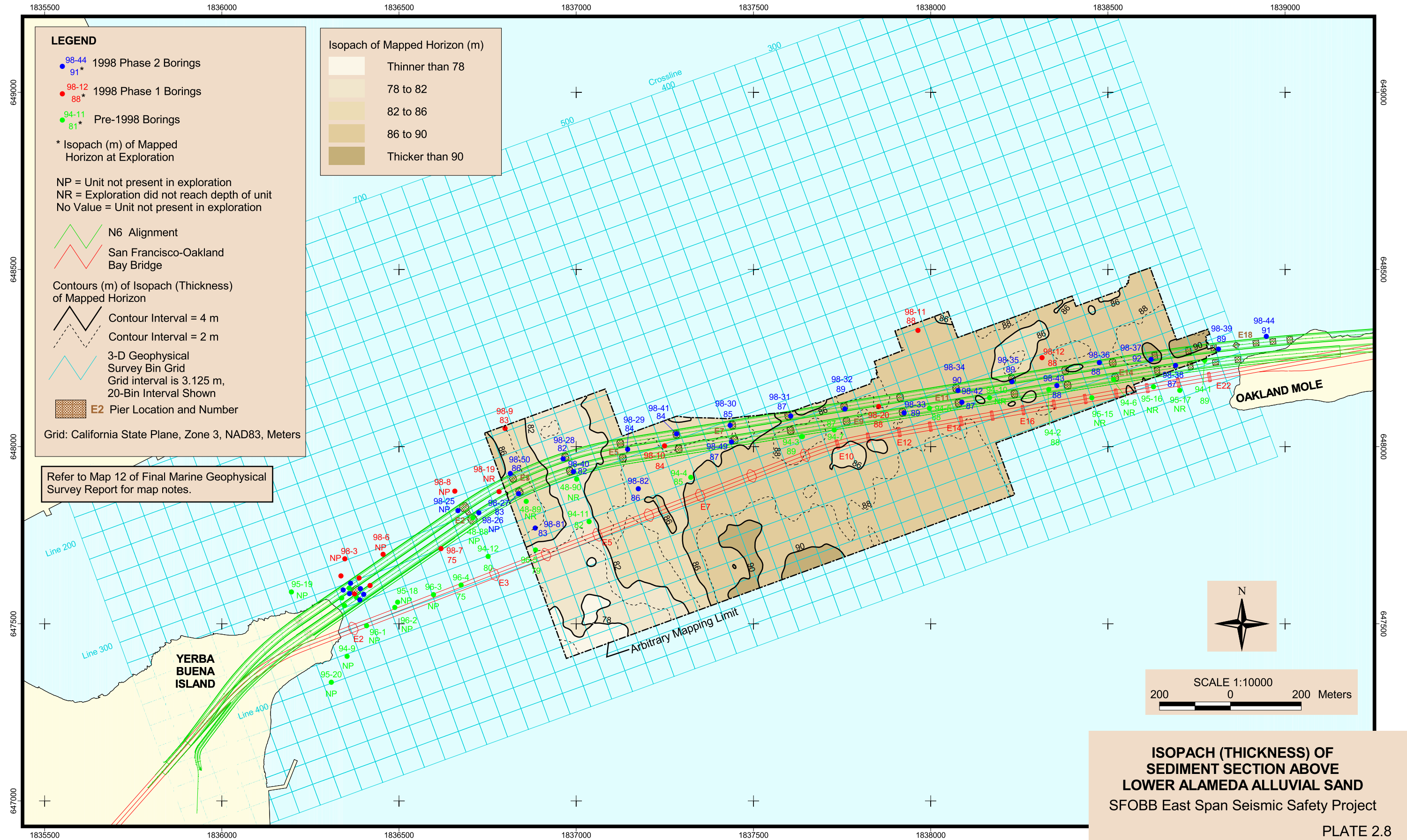
Isopach of Mapped Horizon (m)

0 to 5
5 to 10
10 to 15
15 to 20
20 to 25
Thicker than 25

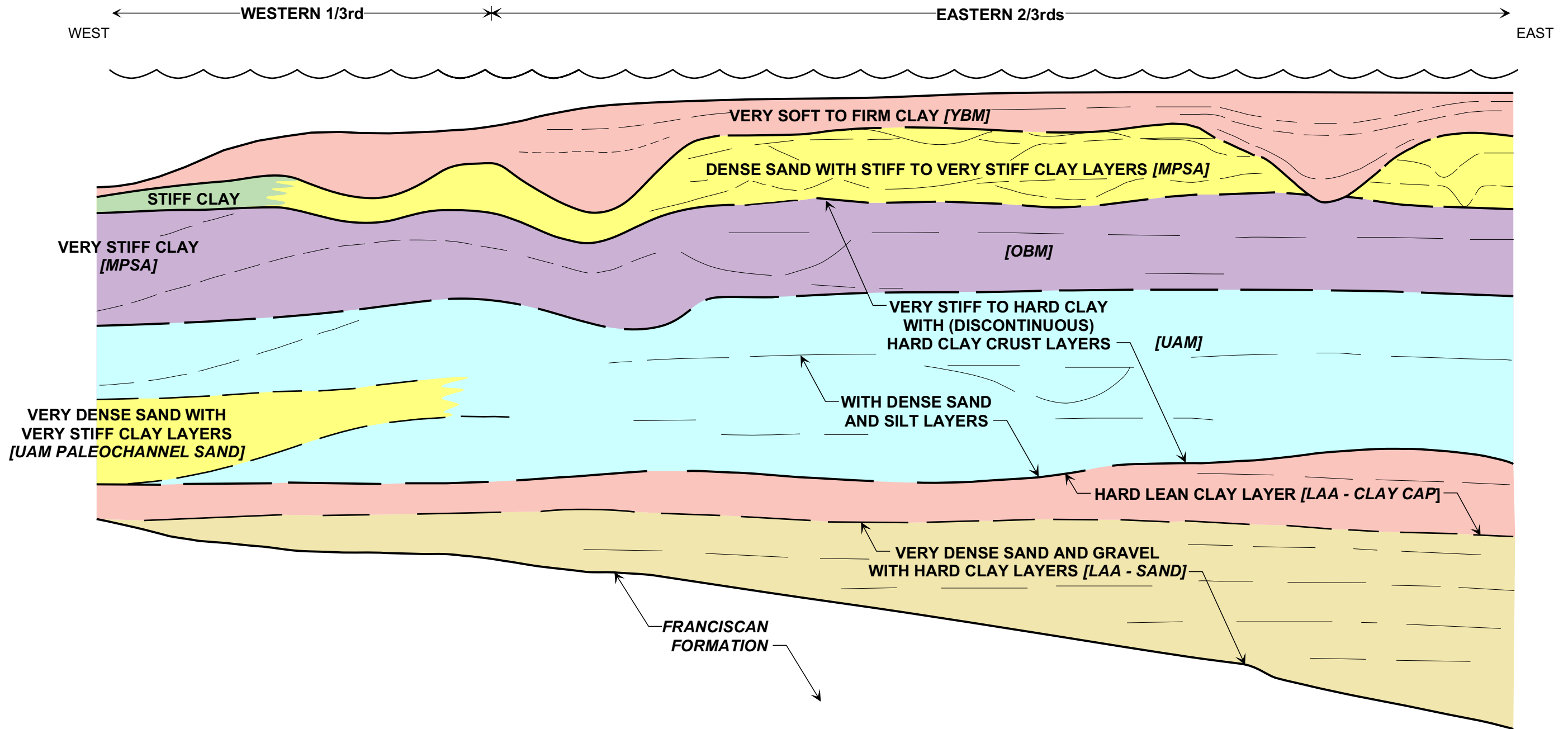


ISOPACH (THICKNESS) OF YOUNG BAY MUD
SFOBB East Span Seismic Safety Project
PLATE 2.6





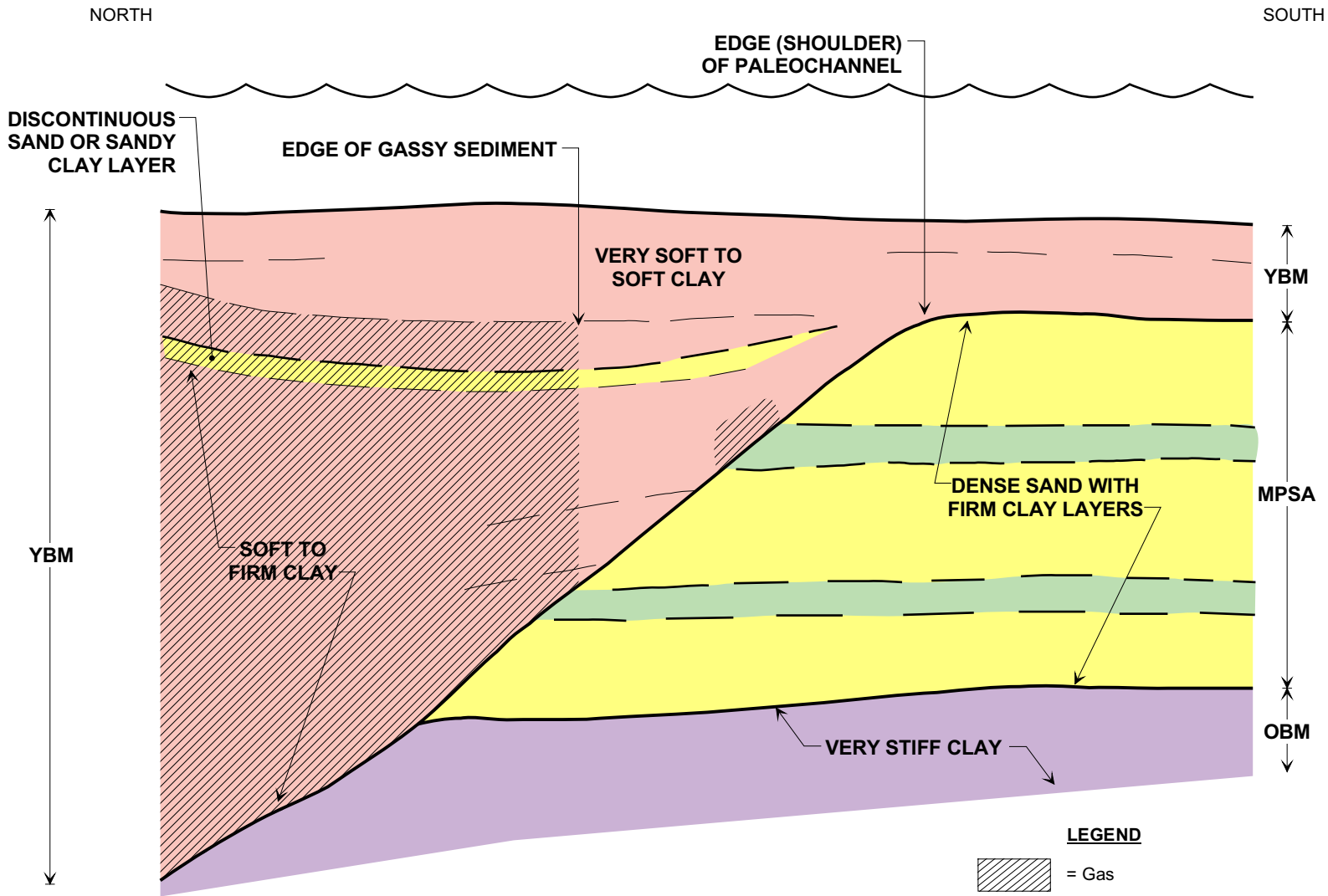
**ISOPACH (THICKNESS) OF
SEDIMENT SECTION ABOVE
LOWER ALAMEDA ALLUVIAL SAND**
SFOBB East Span Seismic Safety Project
PLATE 2.8



NOTE: Not to scale, profile is vertically exaggerated.

CONCEPTUAL EAST-WEST SOIL PROFILE
OUTSIDE (SOUTH) OF RECENT PALEOCHANNEL
Proposed N6 Alignment Skyway
SFOBB East Span Seismic Safety Project



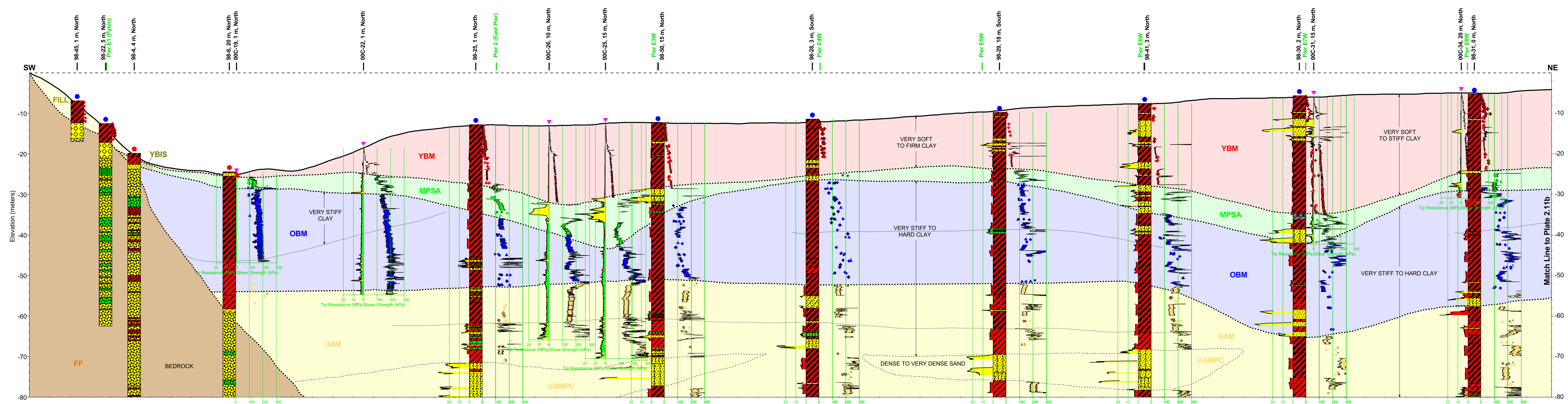


NOTE: Not to scale,
Profile is vertically exaggerated.

- LEGEND**
- = Gas
 - YBM** = Young Bay Mud
 - MPSA** = Merritt-Posey-San Antonio Formations
(Also may be referred to as Merritt Sand)
 - OBM** = Old Bay Mud

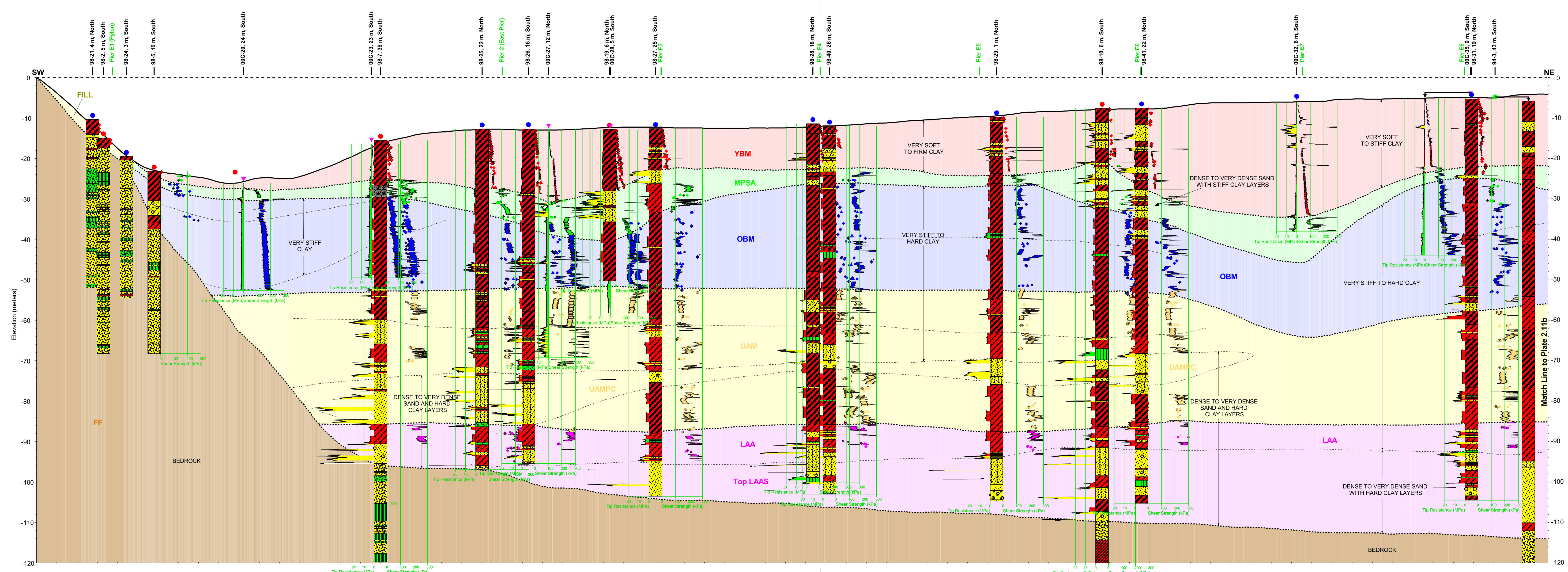
**CONCEPTUAL SECTION AT SOUTH EDGE
OF (EAST-WEST) RECENT PALEOCHANNEL**
SFOBB East Span Seismic Safety Project

CENTERLINE OF WESTBOUND STRUCTURES



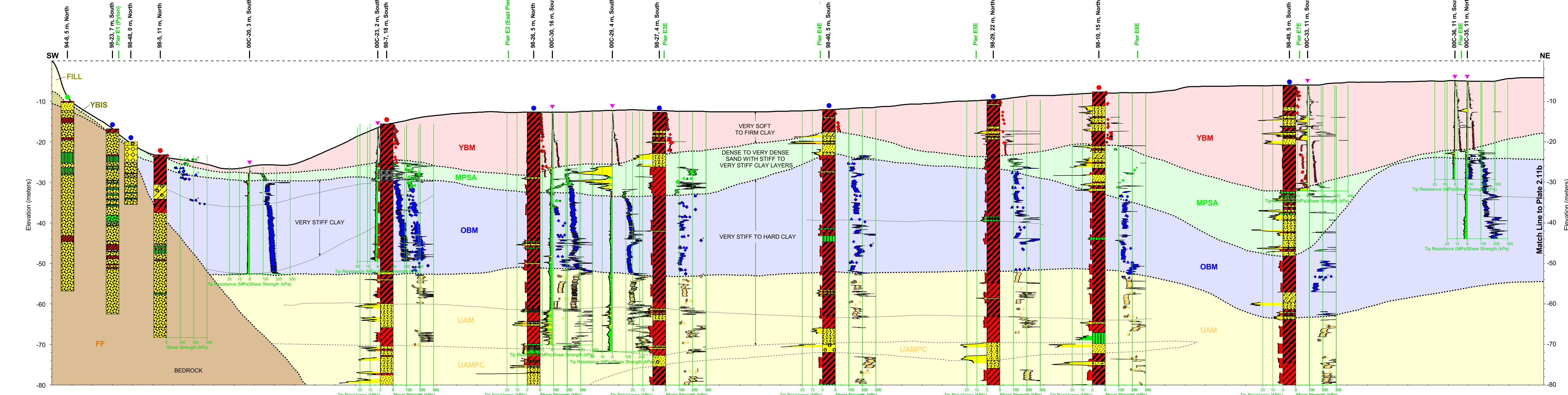
Horizontal Alignment of Sections is on Pier E4 Centerline

CENTERLINE OF N6 ALIGNMENT



Horizontal Alignment of Sections is on Pier E4 Centerline

CENTERLINE OF EASTBOUND STRUCTURES



KEY TO GEOLOGIC UNITS

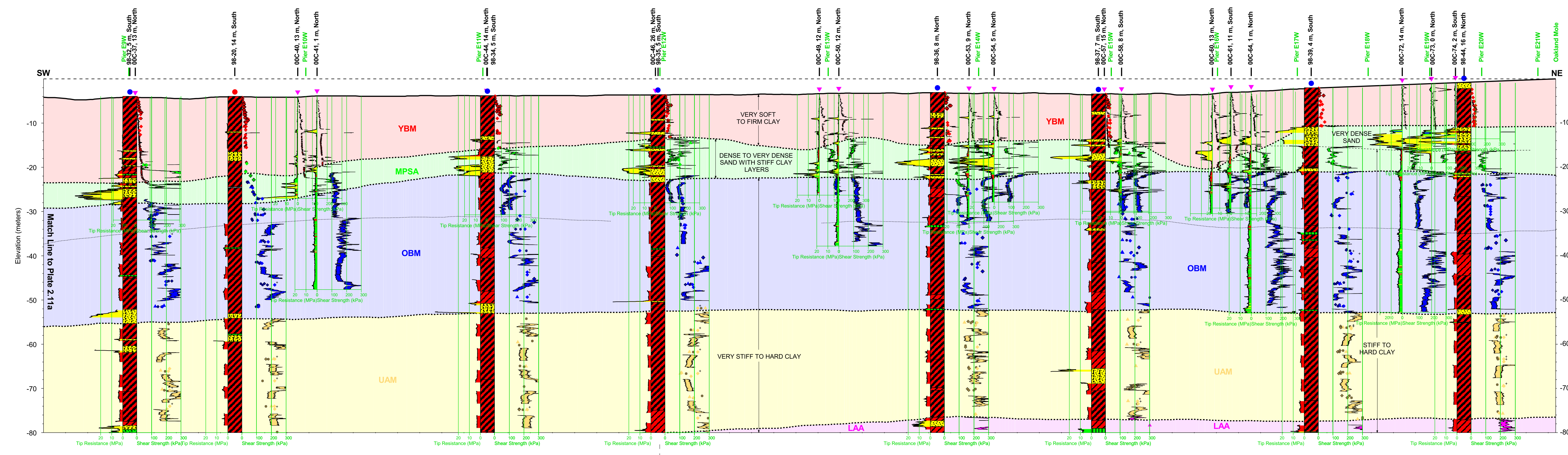
FILL	Upper Alameda Marine
YBIS	Upper Alameda Marine Paleochannel Sand
YBM	Young Bay Mud
MPSA	Merritt-Posey-San Antonio Formations
OBM	Old Bay Mud
UAM	Lower Alameda Alluvial
UAMPC	Lower Alameda Sand
LAA	Franciscan Formation

SHEAR STRENGTH SYMBOLS

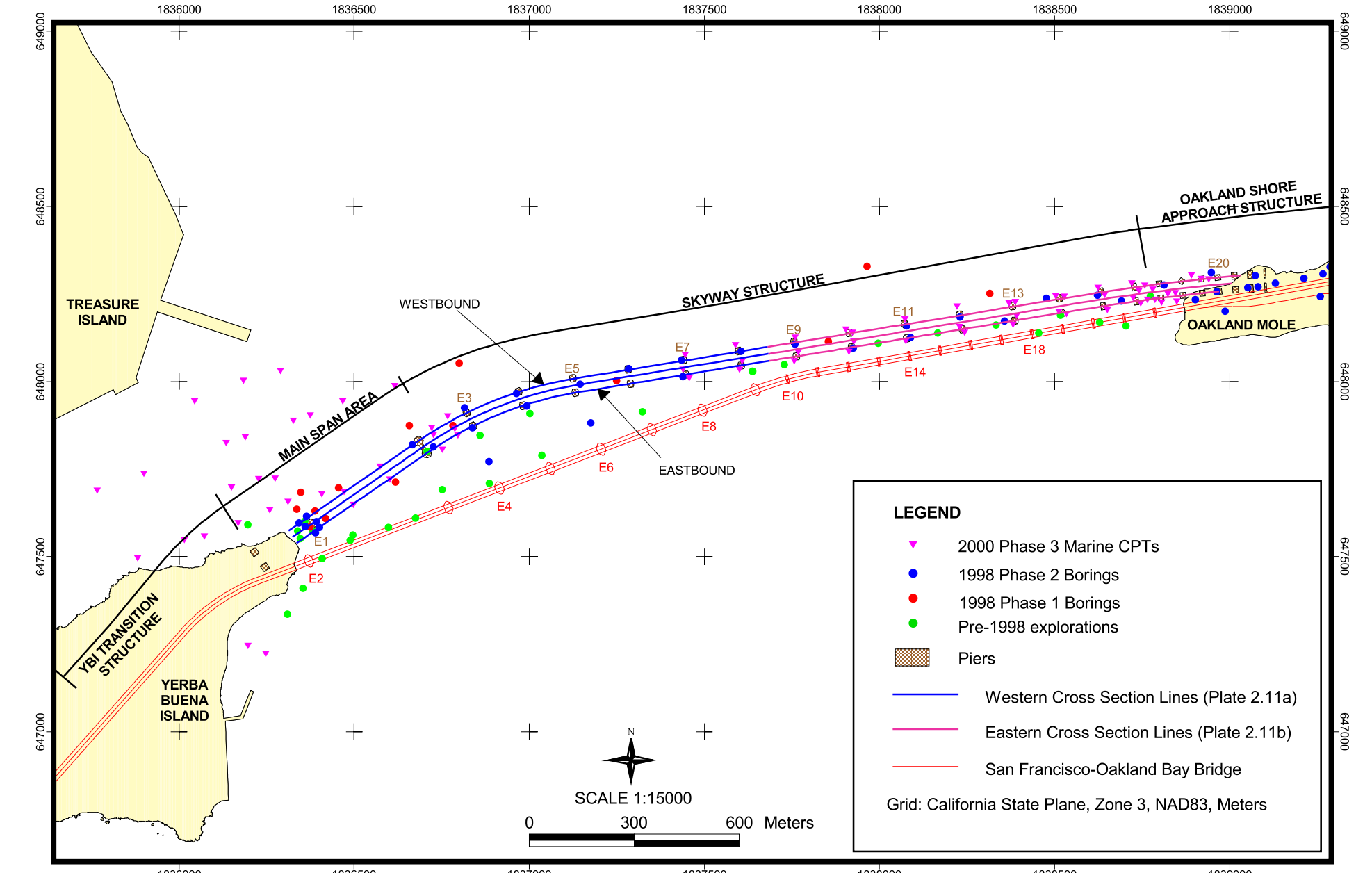
▲	Unconsolidated Undrained (UU)
□	Unconfined Compression (UC)
●	Pocket Penetrometer (PP)
○	Torsional (TV)
●	Miniature Vane (MV)
○	Remolded Vane (RV)
*	Strength Exceeds Capacity of Measuring Device

- Notes:**
- 1) Stratigraphic contacts are approximate and are interpreted from CPT soundings, borings, and seismic reflection survey data. Conditions vary both along and perpendicular to the section line.
 - 2) Boring and CPT sounding logs are projected onto the lines of the cross sections. Therefore stratigraphic contacts may not exactly correspond to the contact indications (lithology, shear strength, etc.) in the logs.
 - 3) Shear strengths are calculated from CPT tip resistances and measurements made on samples from borings.
 - 4) Horizon geometry between borings based on correlations with seismic reflection data.
 - 5) Lithology from pre-1998 borings are in some instances modified from those shown on the Caltrans Log of Test Boring sheets. Modifications were made based on subsequent laboratory test results and extrapolation from adjacent 1998 borings.
 - 6) Horizontal datum is California Coordinate System Zone 3, NAD83, in meters. Vertical datum is MSL, 1929, in meters (0.942 meters above MLLW; Caltrans, 1997).
 - 7) Refer to Plate 2.11a for Cross Section Location Map and Key to Data Shown on Borings and CPT Soundings.

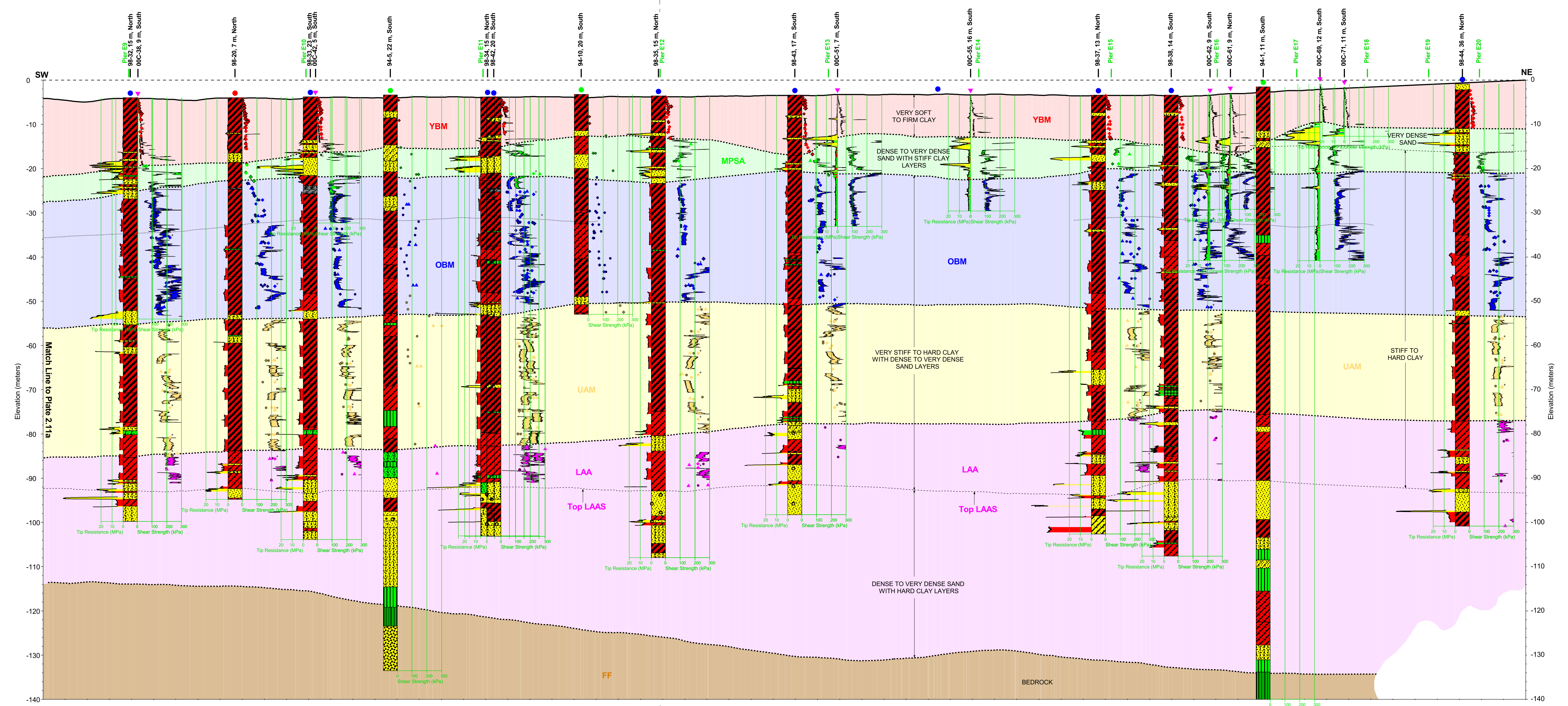
CENTERLINE OF WESTBOUND STRUCTURES



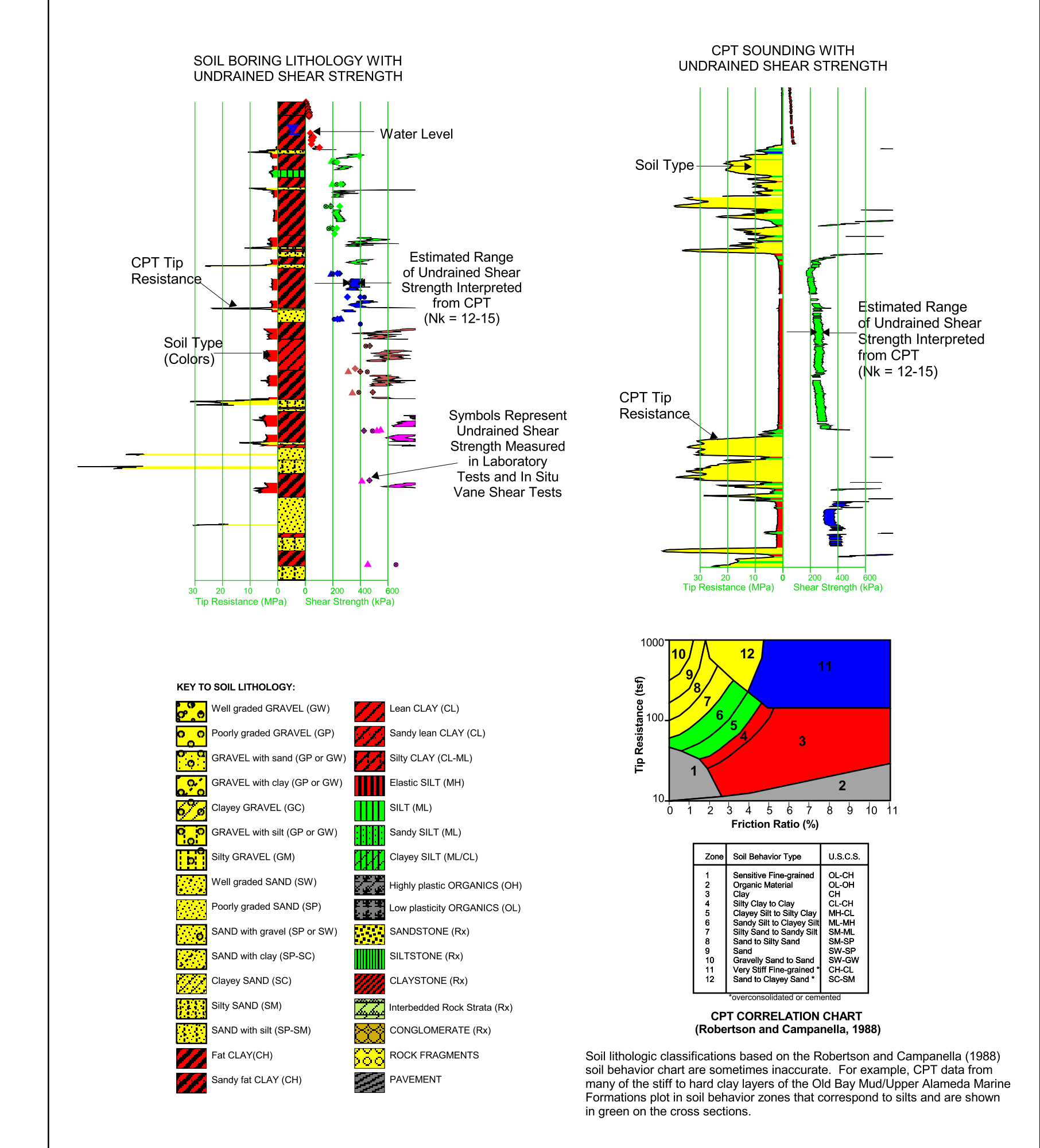
CROSS SECTION LOCATION MAP



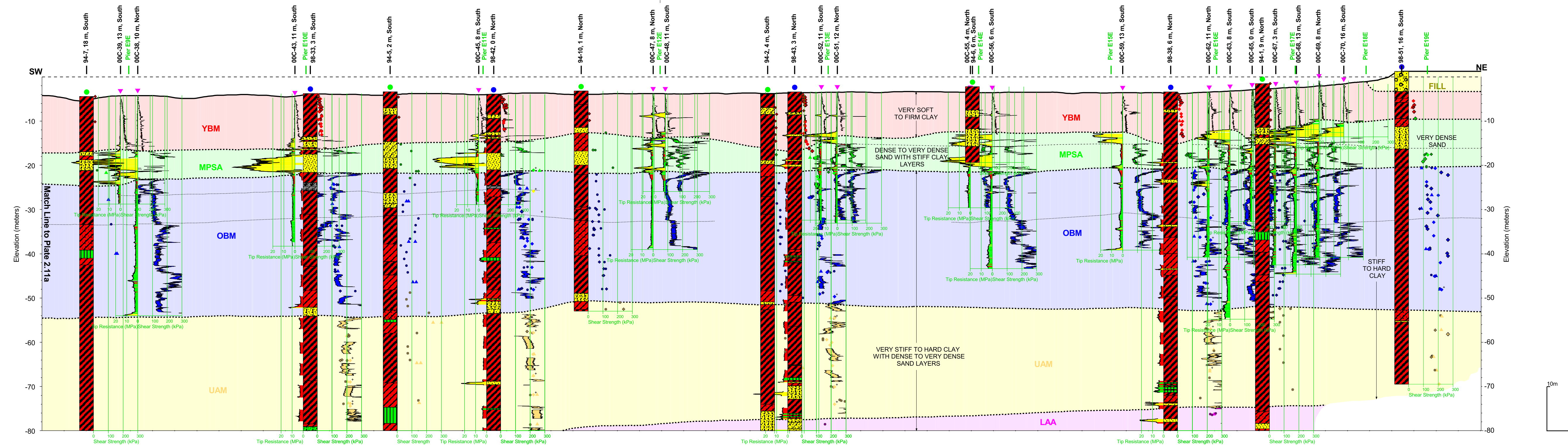
CENTERLINE OF N6 ALIGNMENT



KEY TO BORING LOGS AND CPT SOUNDINGS ON CROSS SECTIONS

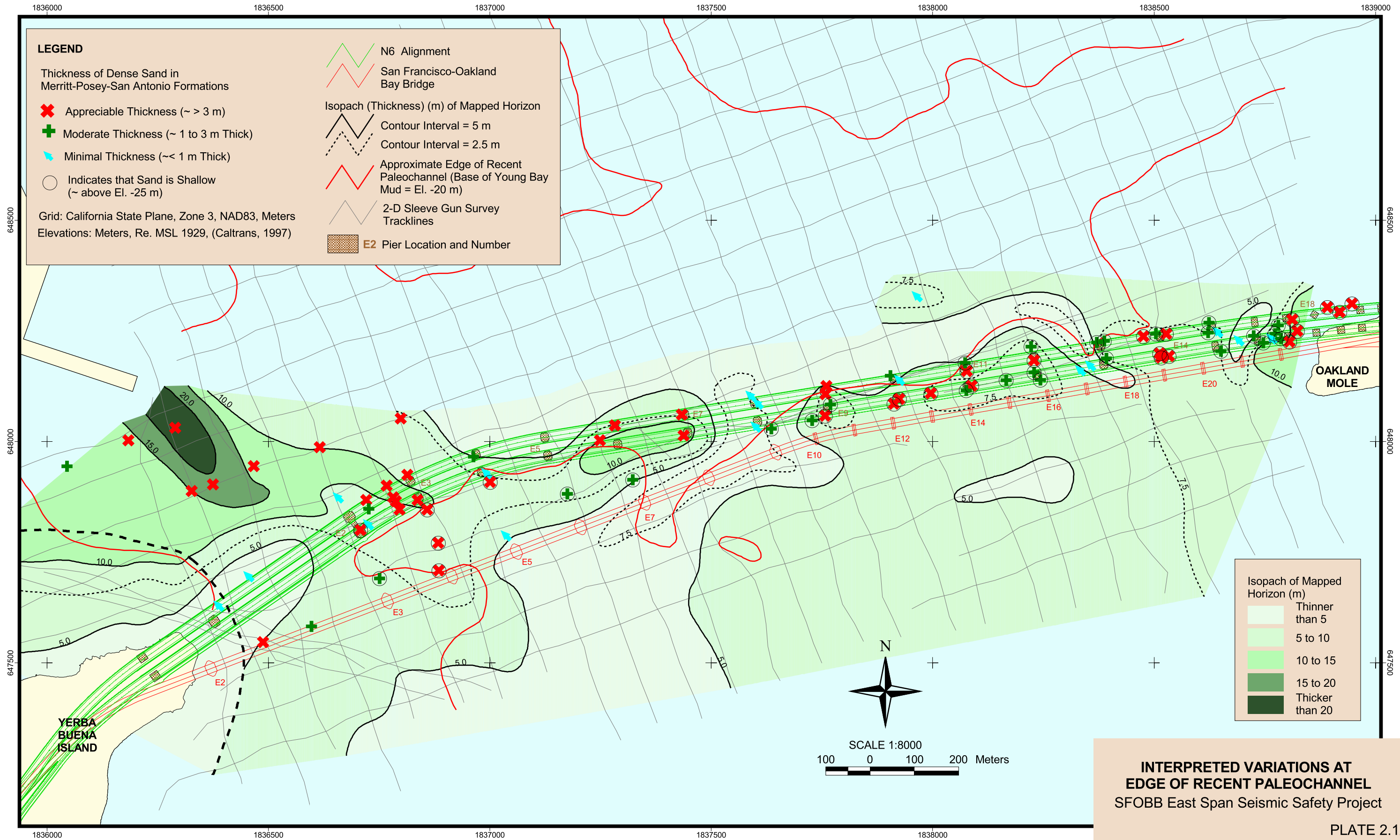


CENTERLINE OF EASTBOUND STRUCTURES



Notes:
 1) Stratigraphic contacts are approximate and are interpreted from CPT soundings, borings, and seismic reflection survey data. Conditions vary both along and perpendicular to the section line.
 2) Boring and CPT sounding logs are projected onto the lines of the cross sections. Therefore stratigraphic contacts may not exactly correspond to the contact indications (lithology, shear strength, etc.) in the logs.
 3) Shear strengths are calculated from CPT tip resistances and measurements made on samples from borings.
 4) Horizon geometry between borings based on correlations with seismic reflection data.
 5) Lithology from pre-1998 borings are in some instances modified from those shown on the Caltrans Log of Test Boring sheets. Modifications were made based on subsequent laboratory test results and extrapolation from relevant 1998 borings.
 6) Horizontal datum is California Coordinate System Zone 3, NAD83, in meters. Vertical datum is MSL, 1929, in meters (0.942 meters above MLLV; Caltrans, 1997).

SUBSURFACE CROSS SECTIONS ALONG N6 ALIGNMENT
YERBA BUENA ISLAND TO OAKLAND MOLE
PIER E9 TO PIER E20
SFOBB East Span Seismic Safety Project



LEGEND

Thickness of Dense Sand in Merritt-Posey-San Antonio Formations

- ✕ Appreciable Thickness (~ > 3 m)
- ⊕ Moderate Thickness (~ 1 to 3 m Thick)
- ↗ Minimal Thickness (~ < 1 m Thick)
- Indicates that Sand is Shallow (~ above El. -25 m)

Grid: California State Plane, Zone 3, NAD83, Meters
Elevations: Meters, Re. MSL 1929, (Caltrans, 1997)

- N6 Alignment
- San Francisco-Oakland Bay Bridge
- Isopach (Thickness) (m) of Mapped Horizon
 - Contour Interval = 5 m
 - - - Contour Interval = 2.5 m
- Approximate Edge of Recent Paleochannel (Base of Young Bay Mud = El. -20 m)
- 2-D Sleeve Gun Survey Tracklines
- E2 Pier Location and Number

Isopach of Mapped Horizon (m)

- Thinner than 5
- 5 to 10
- 10 to 15
- 15 to 20
- Thicker than 20

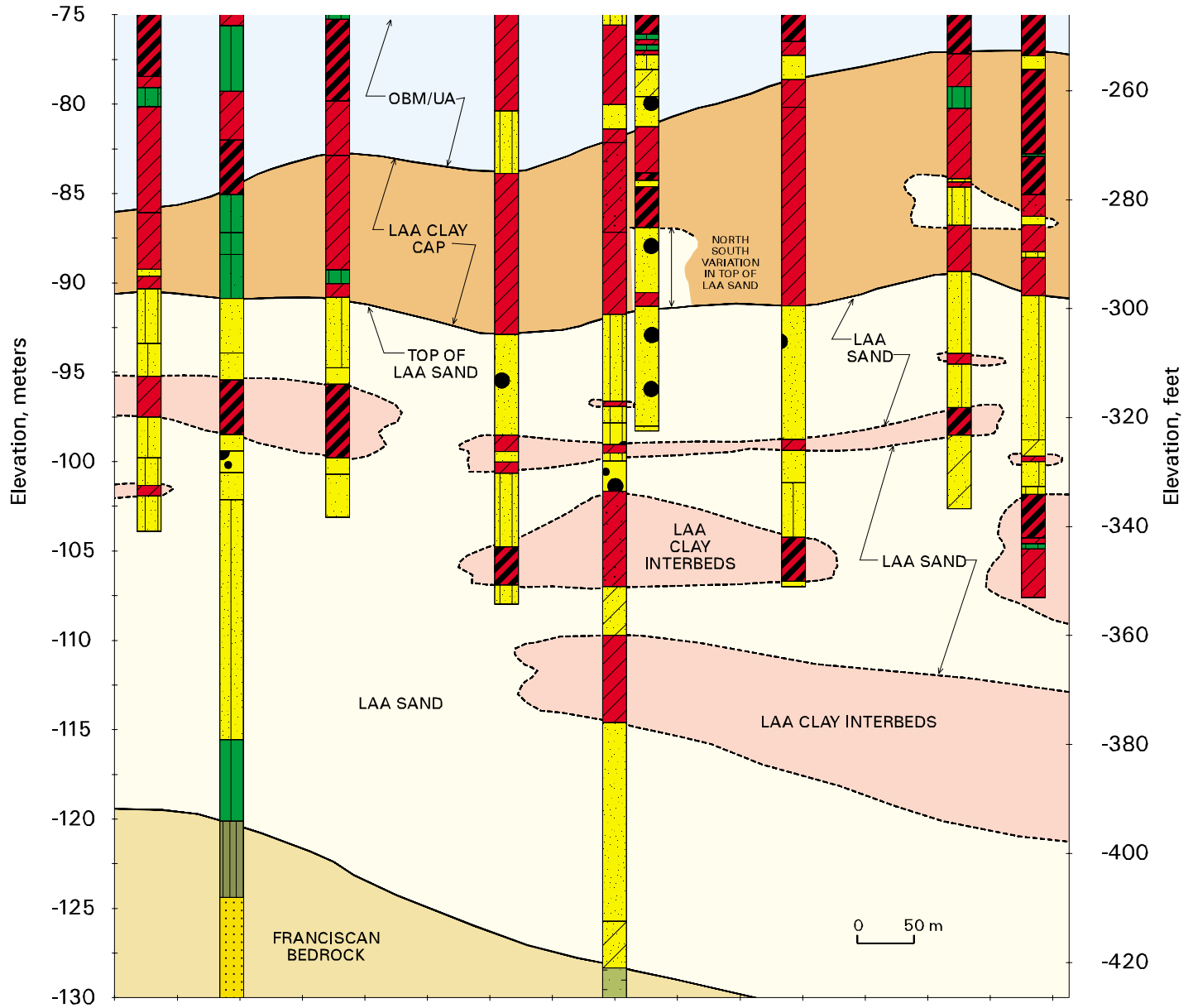
N

SCALE 1:8000

100 0 100 200 Meters

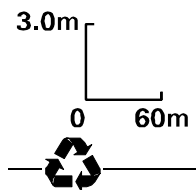
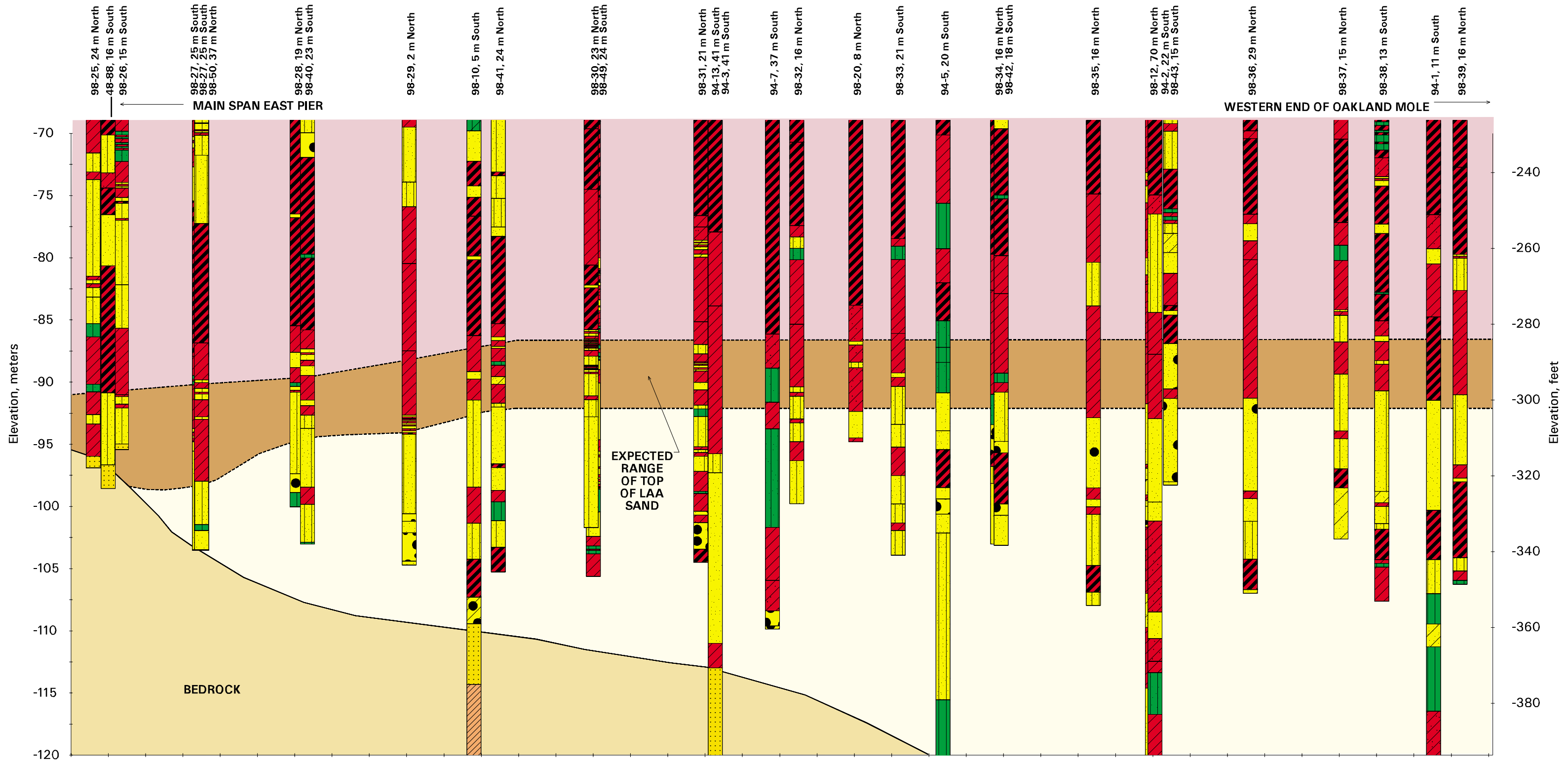
**INTERPRETED VARIATIONS AT
EDGE OF RECENT PALEOCHANNEL**
SFOBB East Span Seismic Safety Project

PLATE 2.12

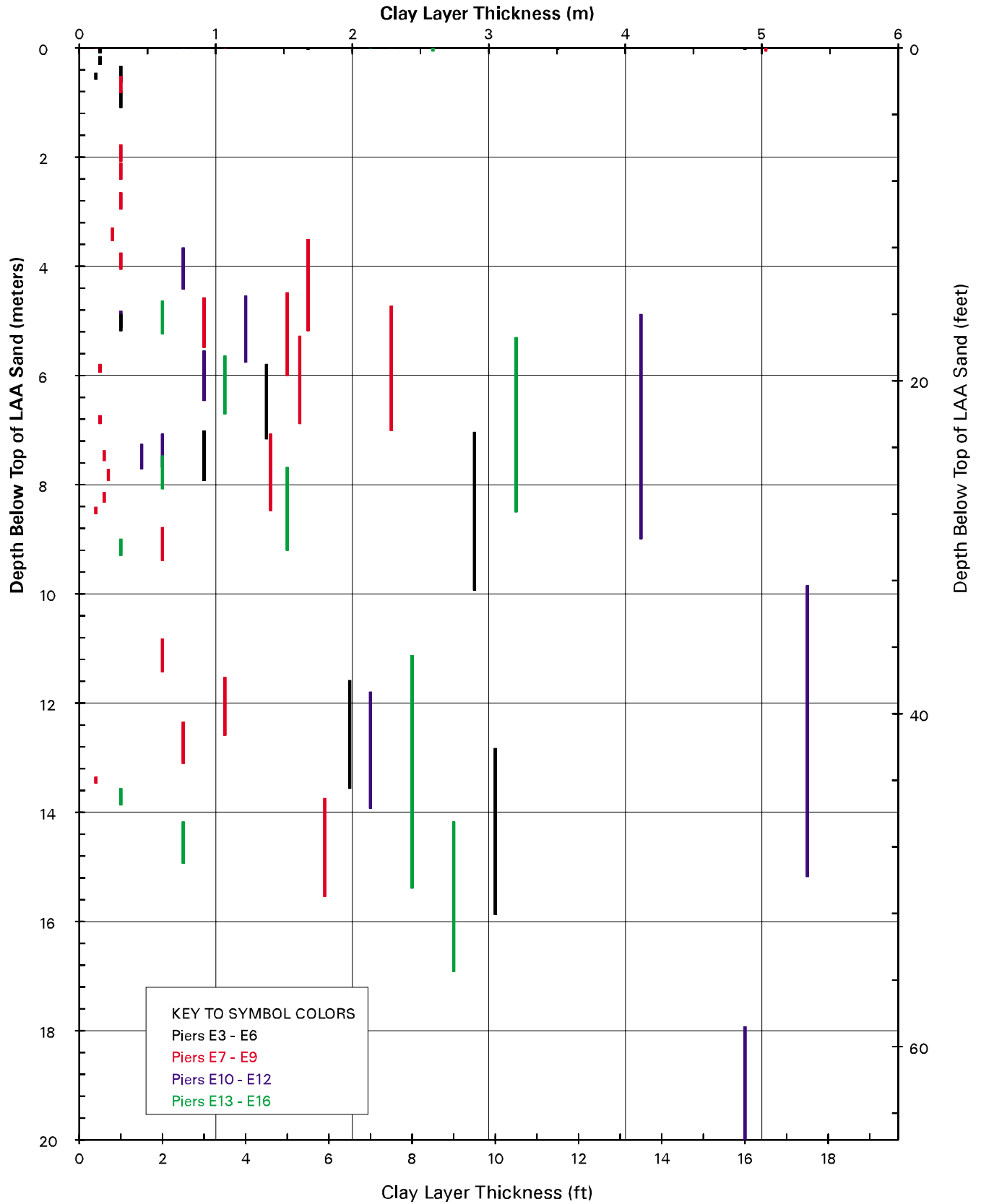


EXAMPLE DETAIL OF LAA STRATIGRAPHY
SFOBB East Span Seismic Safety Project



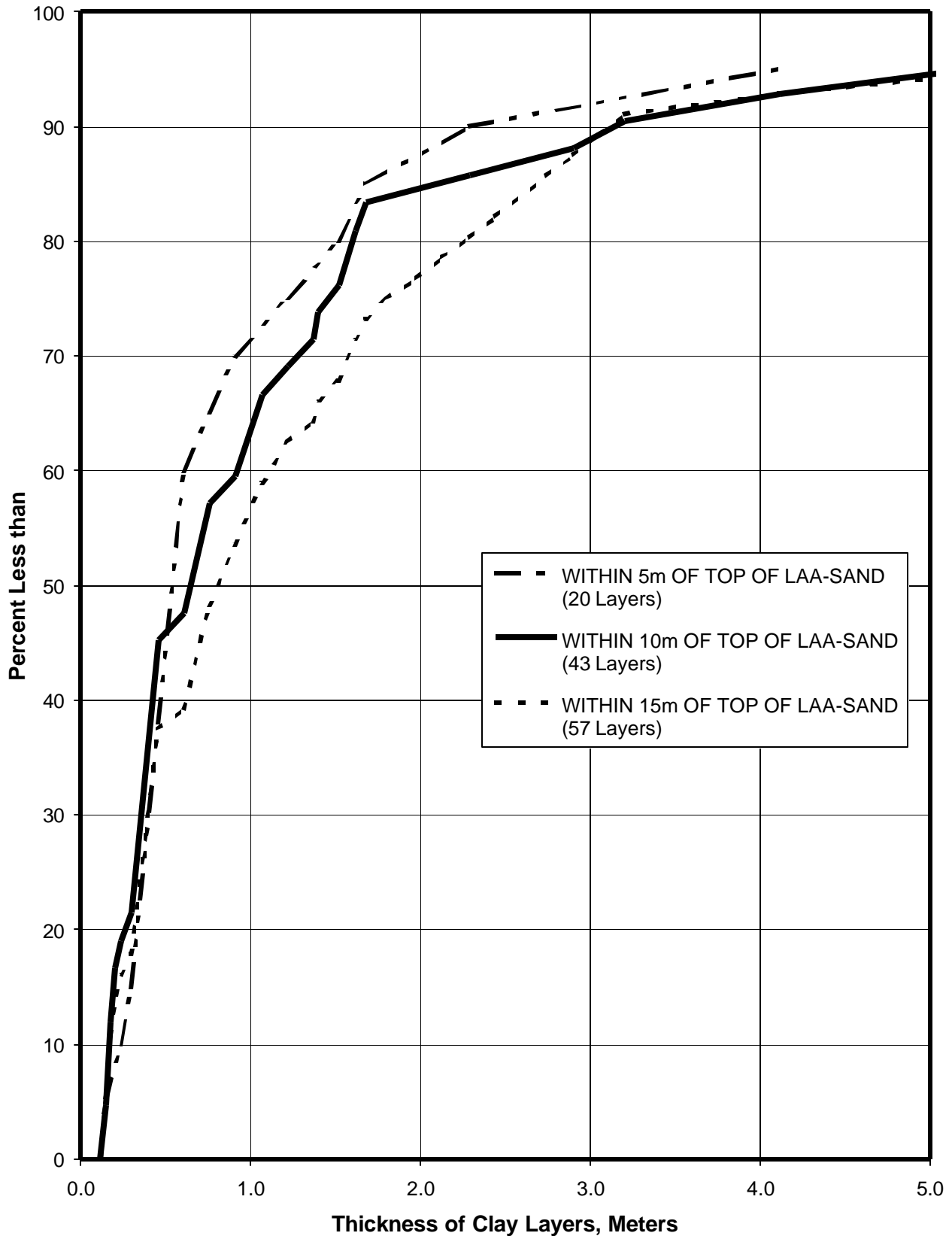


EXPECTED VARIATION OF TOP OF LAA SAND
SFOBB East Span Seismic Safety Project



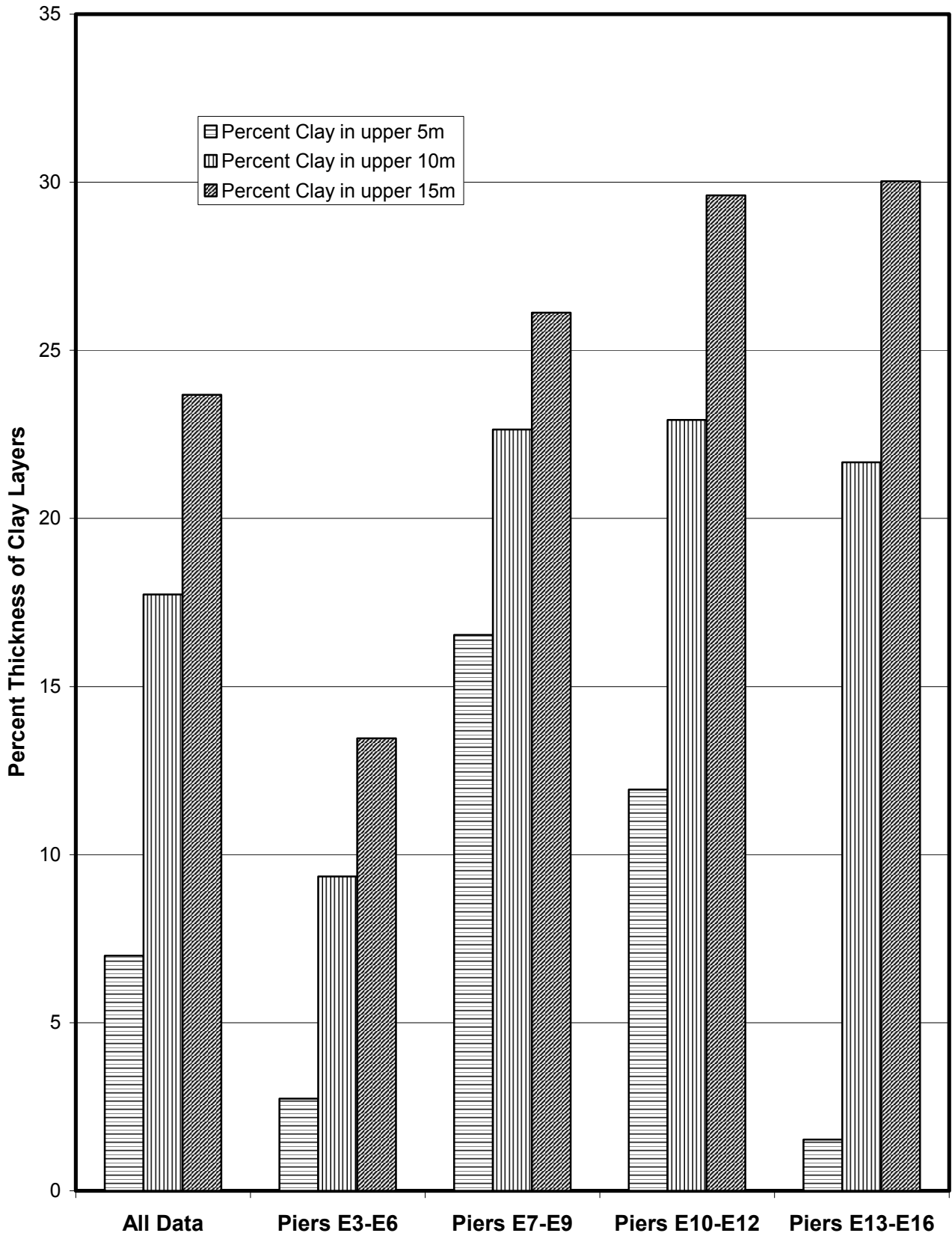
LAA- CLAY INTERBED THICKNESS
1998 Marine Borings
 SFOBB East Span Seismic Safety Project





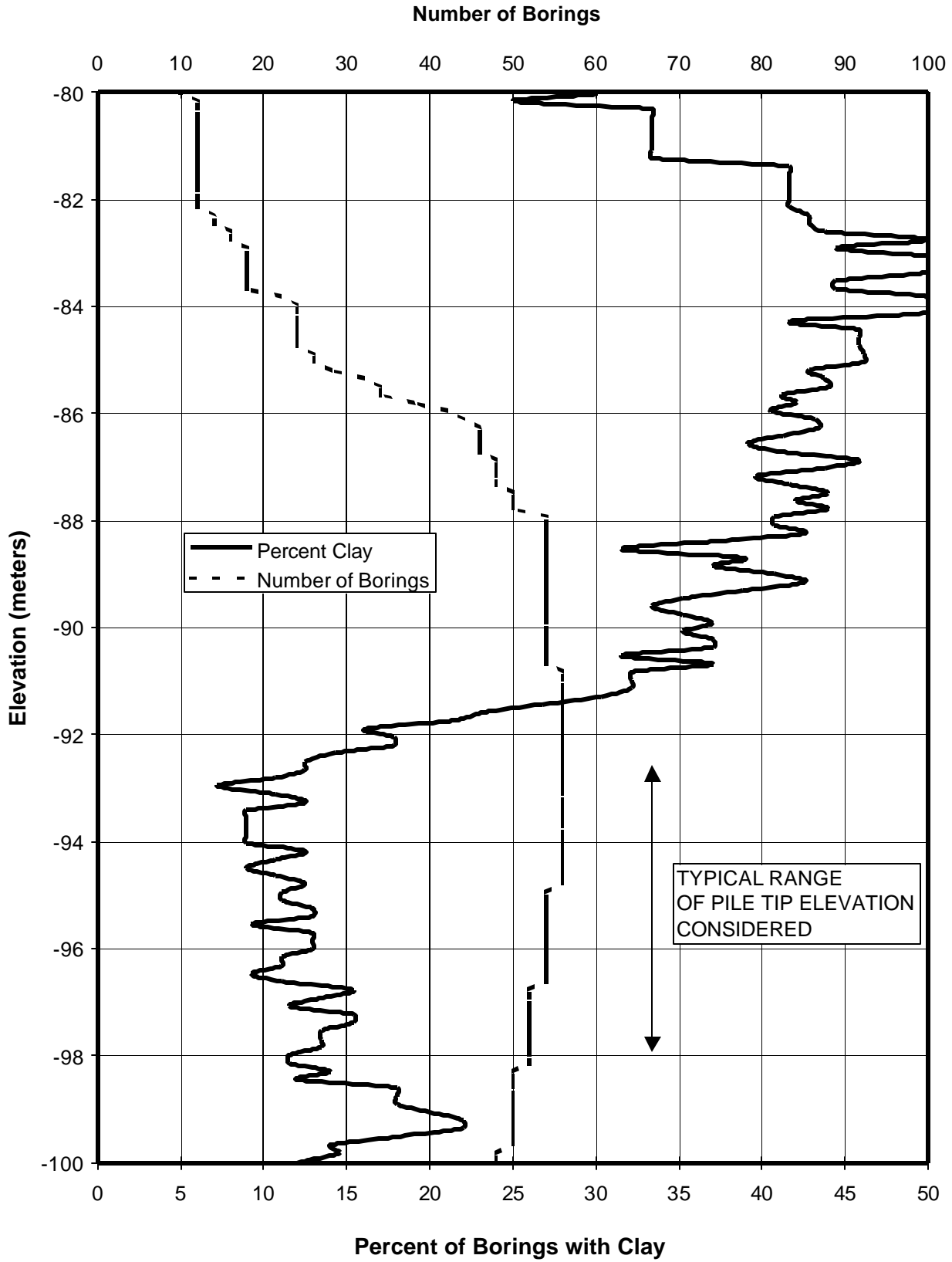
DISTRIBUTION OF LAA-CLAY INTERBED THICKNESS
 SFOBB East Span Seismic Safety Project





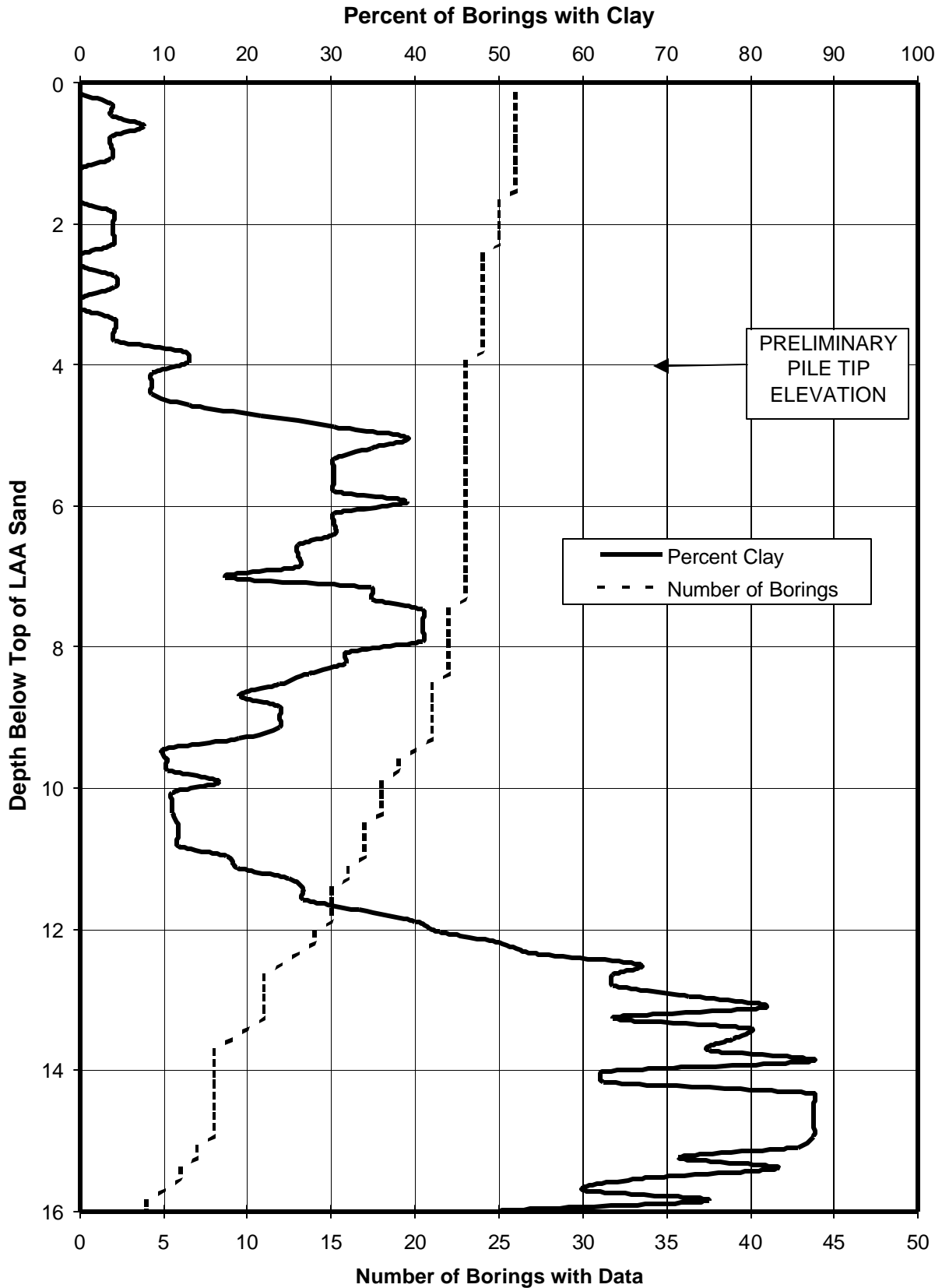
PERCENT LAA-CLAY INTERBEDS WITHIN LAA SAND
SFOBB East Span Seismic Safety Project





DISTRIBUTION OF LAA-CLAY INTERBEDS WITH ELEVATION
SFOBB East Span Seismic Safety Project





DISTRIBUTION OF LAA-CLAY INTERBEDS WITH DEPTH
SFOBB East Span Seismic Safety Project



**SECTION 3.0
AXIAL PILE DESIGN OVERVIEW**

SECTION 3.0

3.0 AXIAL PILE DESIGN OVERVIEW

3.1 DESIGN, CONSTRUCTION, AND PERFORMANCE ISSUES

3.1.1 Channeling

Main Span-East Pier. The proposed location for the Main Span-East Pier is in the area where an east-west and a north-south paleochannel sequence intersect or merge. The pier will be located along the southeastern bank of the paleochannel intersection where the thickness of very soft to firm geologically Recent paleochannel clays will vary across the width of the foundation. Due to those non-uniform conditions, the lateral pile load-deformation response will vary across the width of the pier and with the direction of loading. The load-deformation response of piles located along the northern limit of the alignment will be comparatively soft relative to those located along the southern limit of the alignment.

Skyway. The Skyway alignment overlies and straddles the meandering edge of the east-west geologically Recent paleochannel (Plate 2.12). Local near-surface variations relative to the thickness of surficial very soft to soft clay and the presence or absence of near-surface sand layers are inevitable beneath the Skyway alignment. Those variations, which occur continuously along the alignment, may occur across the width of an individual pier, between adjacent piers, and/or between adjacent Skyway frames. In general, the thickness of soft paleochannel clay beneath the alignment will increase, and the presence and thickness of sand layers will decrease to the north of the proposed alignment.

This variability of subsurface conditions will affect the lateral load deflection characteristics of the foundation. From a geotechnical standpoint, a foundation design that reduces the sensitivity of the foundation (and superstructure) response to those inevitable variations across and along the Skyway is desirable. Because the geologically Recent paleochannel is a near-surface feature, axial pile capacities are comparatively less sensitive to the variability of the near-surface sediments along the proposed N6 alignment. The batter piles that are proposed for the Main Span-East Pier and Skyway piers provide for additional lateral stiffness as well as reduce the sensitivity of the foundations to the intrinsic variations in the soil conditions by transferring lateral loads from the structure as axial loads on the pile.

3.1.2 End-Bearing Stratum Variations

The geophysical data and the borings drilled along the alignment suggest as much as 3 to 5 meters of local variation in the top elevation of the erosional surface of the LAA-sand end-bearing stratum. Furthermore, the borings show that the primarily alluvial sediment sequence includes an appreciable quantity of clay layers. Both the variation of the top elevation of the LAA-sand and the local presence or absence of LAA-clay interbeds within the underlying LAA-sand are intrinsic variations of the deposit. Because these are local variations, it is impossible to



predict how the variations occur over the football-field-sized area circumscribed by the loci of the pile tips at each set of piers. Thus, the pile design needed to accommodate these variations.

From a design standpoint, the primary implication of the variation in the end-bearing stratum is in prediction of the range of pile end bearing capacity and stiffness that logically can be expected to occur. Since the pile tip elevations are to be pre-established:

- It appears likely that at some pier locations not all piles of a given pier may be tipped in LAA-sand. The design process should include sensitivity analyses to evaluate the influence of such conditions on the performance of the structure;
- It is recommended that an adequate pile driving hammer that can advance the pile through a greater thickness of LAA-sand than suggested by the borings should be specified; and
- The design of the pile wall thickness schedule and the pile head connection detail should allow for an appropriate underdrive allowance.

3.1.3 Load-Transfer Considerations

In addition to load capacity, the design of long, large-diameter, driven pipe piles should consider axial load-deflection characteristics. Because the pile deflection required to mobilize the end-bearing component of pile capacity is significantly greater than the deflections required to mobilize the skin friction component of pile capacity, it has long been recognized (in offshore platform design) that the component of pile capacity due to end bearing is largely in reserve for piles driven through primarily clay soils and designed for normal factors of safety. In other words, the percentage of the total capacity in skin friction typically exceeds the applied load (i.e., the ultimate load divided by the factor of safety). Thus, the majority of the applied service load is mobilized in skin friction along the pile shaft at levels of deflection much smaller than those required to mobilize significant components of the end bearing.

For structures that are designed for both: a) gravity loads, live loads, and normal cyclic loads, and b) extreme infrequent dynamic loads (i.e., extreme earthquake loads), it is common to consider either a lower factor of safety for the extreme load or the use of a higher value of end bearing for calculating the capacity under extreme, infrequent loads. In either case, this potentially allows more load to be transferred to end bearing with a resulting increase in pile deflection.

3.1.4 Post-Installation Setup of Axial Capacity

The process of driving large-diameter pipe piles into plastic clays results in a high degree of disturbance in the soil adjacent to the pile and the creation of excess pore water pressures in the surrounding soil. One consequence of this disturbance is a significant decrease in the as-driven capacity and a subsequent increase in the capacity with time as the excess pore



pressures dissipate. The reduced as-driven pile capacities will need to be considered during the construction process. The recently completed Pile Installation Demonstration Project (PIDP) (Fugro-EM, 2001f) provides insight into the setup of large-diameter pipe piles in Bay soils. .

3.1.5 Cyclic Degradation and Strain Rate Effects During Earthquake Loading

There are two characteristics of pile-soil interaction that affect the axial pile capacity during earthquake loading. The first is the potential for cyclic degradation of the skin friction along the pile due to multiple cycles of reversal of the axial loads together with the combined interaction of cyclic axial and lateral loading. This effect tends to reduce (due to cyclic soil strength degradation) or eliminate (due to gapping) the axial pile capacity provided by the surficial soils, and axial pile loads are transferred farther down the pile shaft. Additional soil resistance to those loads are mobilized by increased relative pile-soil movement, and this results in increased pile settlement.

The second effect that occurs during the earthquake loading is an increase in soil resistance relative to static values due to rate-of-loading effects. Because earthquake loads occur rapidly, the soil undrained shear strength that can be mobilized will exceed the measured values from in situ and laboratory tests used for computation of the static axial capacity. This increase in capacity opposes and tends to compensate for the loss of strength due to cyclic degradation.

For the subsurface conditions underlying the N6 alignment, losses of resistance due to cyclic degradation in the relatively soft and relatively sensitive Young Bay Mud are estimated to be greater than the increases in resistance due to strain rate effects. However, for the relatively stiff underlying clays of the Old Bay Mud and Upper Alameda Marine sediments, the increase in soil resistance due to strain rate effects is estimated to exceed the loss in capacity due to degradation effects in the lower clays. Since a larger percentage of the axial capacity of the pile is mobilized within the relatively stiff underlying clay layers, the net result is estimated to be a higher axial capacity during earthquake loading when compared to the static axial capacity. However, because of degradation in the upper Young Bay Mud, load is redistributed down the pile and may result in additional pile settlement.

3.2 PRELIMINARY DESIGN AND SEISMIC DESIGN PHILOSOPHY

Foundation design parameters and recommendations for the development of the 30-percent submittal were provided in a Preliminary Foundation Design Report (Fugro-EM, 1998). Those recommendations were based on the Preliminary Phase 1 site investigations and provided design parameters for four representative areas along the Main Span-East Pier and Skyway alignments. Additional preliminary recommendations for the seismic foundation design were provided in Fugro-EM (1999). Those data were used to guide preliminary pile type and layout selection.



The preliminary analyses performed (using those data) by TY Lin/M&N suggested that the piles experience their maximum loads during the design earthquake event, which is denoted as the Safety Evaluation Earthquake. During this event, the peak loads (which are typically experienced for less than 1 second) were estimated by TY Lin/M&N to be on the order of 120 MN in compression and 80 MN in tension. In contrast, the static (gravity loads) on the piers were estimated to be on the order of 35 MN.

Since the earthquake loads were significantly higher than the static loads, the performance of piles under dynamic loading is of primary concern. Of particular interest are the evaluation of the expected permanent settlement and the potential temporary loss of static capacity resulting from the cyclic degradation of the soil shear strengths during the earthquake.

Since the design loading conditions result in temporary losses in the axial capacity due to cyclic degradation and transient increases in the capacity due to rate of loading effects, evaluation of relative safety factors based on calculated static axial capacities are not meaningful for seismic design. Furthermore, the magnitude of seismic loads imposed on the piles is dependent upon the stiffness of the foundation response. In general, for the typical range of structure periods considered, the stiffer the foundation (frequently due to increased pile capacity), the higher the loads imposed on it. The evaluation of the seismic performance of the foundation piles is therefore based on the estimated load-deformation behavior of the piles (and the associated stresses imposed on them) during the earthquake for an anticipated range of foundation support parameters.

3.3 PIER-SPECIFIC DESIGN INFORMATION

Subsequent to the performance of the Phase 2 (design level) geotechnical site investigations, pier-specific axial foundation design parameters were developed based on the geotechnical characteristics of the underlying strata and the approximate axial load values described above. The axial pile design data for the Main Span-East Pier and each Skyway pier were provided to TY Lin/M&N and are reproduced in Appendix A of this report. In many cases, separate data are provided for eastbound and westbound piers. The pier-specific axial pile design information provided includes:

- Representative soil profiles, soil properties, and axial pile capacity estimates;
- Discretized axial pile load transfer-displacement curves; and
- Preliminary static pile head load-deformation curves.

The methodology used to develop the axial pile design data and a discussion of the recommended pile design parameters are presented in Section 4.0.



3.4 PILE TIP ELEVATIONS

3.4.1 Preliminary Pile Tip Elevations

Since little pier-specific pile loading information had been provided to Fugro-Earth Mechanics, the preliminary pile tip elevations used to generate the load-deformation data presented in Appendix A were selected on the basis of the geotechnical characteristics of the underlying strata and the approximate axial load values provided by the design team.

When those tip elevations were selected, the pile-head connection design details would require that piles be driven to a specified elevation and there was to be little, if any, underdrive allowance. Consequently, the preliminary pile tip elevations were selected so as to: 1) have the highest probability of bearing in the sand layers of the Lower Alameda Alluvial Formation, and 2) have a low likelihood of encountering refusal within sand layers above the specified tip elevation. In general, those pile tip elevations were typically about 4 meters below the elevations where dense sand layers were anticipated at or near the surface of the Lower Alameda Alluvial (LAA) Formation. As noted in Section 2.0, the first relatively thick sand layer in the LAA (denoted as the top of the LAA-sand) is at about El. -90 meters (± 3 to 5 meters). The preliminary pile tip elevations are provided on Plate A-6 of Appendix A.

As discussed in Section 2.0, a significant thickness of sand (denoted as the Upper Alameda Marine [UAM] Paleochannel Sand) was encountered at approximately El. -70 meters in borings drilled in the vicinity of the Main Span-East Pier. Estimates of the static pile capacity show that the ultimate compression and tension capacity for piles tipped in the Franciscan Formation bedrock are approximately 125 MN and 65 MN, respectively. The estimated ultimate compression and tension capacity for piles tipped in the UAM Paleochannel Sand are approximately 80 MN and 47 MN, respectively. Depending on the foundation capacity requirements at the Main Span-East Pier, it also may be feasible to tip the piles in the UAM Paleochannel Sand.

3.4.2 Structural Analyses and Results

The axial design parameters presented in Appendix A and the lateral pile design parameters (provided in Fugro-EM, 2001a) were used by TY Lin/M&N in combination with the pier-specific, multiple-support free field motions (Fugro-EM, 2001b) to perform non-linear service load (static) and time history (earthquake) structural analyses for the Skyway. The discretized support springs used to model the pile in those analyses were linearized to relevant load levels. Estimates of permanent pier settlement and foundation loads for static and design seismic events were developed from those analyses.

The estimated static loads on the most loaded pile for each Skyway pier are provided on Plate 3.1. Calculated seismic loads on the Skyway piles varied as a function of the pile stiffness and damping assumed in the analyses. For the Safety Evaluation Earthquake, tension loads of up



to approximately 80 to 90 MN and compression loads of up to approximately 120 to 140 MN were calculated. Structural analyses and design of the Main Span structure are ongoing, and the results of those analyses were unavailable at the time this report is being prepared.

The structural analyses for the Skyway structure suggested that permanent settlement of the piers occurs during seismic events. The mechanism by which that deformation occurs has been described as a “ratcheting” or “scissoring” mechanism. During the earthquake, the piles at the corners of the piers are subject to cycles of compression and tension loads with downward movements of the pile during compressions phases. The alternating downward movement of opposing piles results in a net settlement at the center of the pier footing.

In general, the magnitude of the pier settlements varied as a function of the pile design parameters used in the analyses and ranged from approximately 40 to 50 mm at the most loaded piers. The piers with the highest predicted settlement typically were the ones with the lowest estimated factors of safety against static loads ($FS = 1.8$ to 2.0) when using static skin friction axial capacity (equivalent to tension capacity) only.

3.4.3 Design Modifications

Subsequent to the performance of structural analyses and during the development of the 85-percent design submittal, the design team made modifications to the pier and pile cap design. Those modifications provided additional flexibility to accommodate potential variations in both the horizontal alignment and penetration achieved during the installation of piles. The pile details were modified to allow for up to 5 meters of underdrive.

3.4.4 Revised Pile Tip Elevations for Skyway Structure Piers

The preliminary pile tip elevations were reviewed relative to the design modifications and the analyses performed by TY Lin/M&N. TY Lin/M&N stated that, in their opinion, the predicted range of pier settlements under extreme seismic loads was somewhat excessive at the most loaded Skyway piers. Consequently, the piles supporting the most loaded Skyway piers were lengthened.

The most heavily loaded piers were typically within the western portion of Skyway Frame 1. Since bedrock is interpreted to be relatively close to the preliminary pile tip elevation, those piles were extended to tip in bedrock. The additional end-bearing resistance provided by rock at the pile tip will likely reduce the potential for “ratcheting” settlements to impact the performance of the portion of the structure supported by those piers.

Additionally, the inclusion of a minimum 5-meter underdrive allowance allowed for refinements of the pile tip elevations at several other piers. Those modifications generally resulted in deeper pile tip elevations. The deeper tip elevations are intended to:



- Provide additional skin friction/tension capacity at other relatively heavily loaded piers; and
- Increase the probability of piles for Piers E6 through E16 being tipped in the sand layers of the Lower Alameda Alluvium.

Plate 3.1 provides a summary of the static axial pile loads and the revised recommendations for pile tip elevations at each Skyway pier. The tabulated pile loads are the average loads on the most loaded piles at each pier. The estimated ultimate static axial (tension and compression) capacity for piles driven to the recommended tip elevations are shown on the Axial Pile Design Parameters and Results plates for each pier in Appendix A. Those estimated capacities for each Skyway pier also are tabulated on Plate 3.1. The revised pile tip elevations are plotted along with the Bay floor or base of footing elevation on Plate 3.2. It should be noted, however, that although the revised tip elevations and associated static capacities are shown on the Axial Design Parameters and Results plates in Appendix A, the load-deformation analyses (which, with the exception of the piles tipped in bedrock, should be relatively insensitive to the small changes) were not updated to match the revised tip elevations.

Estimated factors of safety against the static loads are plotted on Plate 3.3. As shown on Plate 3.3, the estimated factors of safety for skin friction capacity generally increase with increasing pier numbers (i.e., to the east). Consideration was given to raising the pile tip elevations by a few meters for those piers with relatively high estimated factors of safety against static loads (and relatively low pier settlement). However, discussions among Caltrans, the design team, the seismic peer review panel, and Fugro-EM concluded that the pile tip elevations should not be changed. That conclusion was based on the judgement that the additional redundancy (in terms of end-bearing capacity from piles tipped in dense sand layers of the Lower Alameda Alluvium) for extreme seismic events outweighed the potential savings in cost that would be generated by shortening the piles.

3.4.5 Additional Considerations for Piers E3 through E5

The revised tip elevations for Piers E3 through E5 are to provide for the piles supporting those piers to be tipped in bedrock. Since there is some variability in the estimated bedrock elevation at those locations, the recommended tip elevations are approximately 3 meters below the estimated bedrock elevation. Consequently, it is considered likely that piles for Piers E3 through E5 will encounter bedrock above the recommended pile tip elevation. Since sudden increases in the toe stresses are likely to be observed when the bedrock surface is encountered, analyses were performed to evaluate the potential for damage to the driving shoe and to develop refusal criteria for those piles. Those analyses are discussed in Section 6.0. Pile installation considerations are presented in Section 7.0.



3.5 SKYWAY TEMPORARY TOWERS

The design drawings for the Skyway structure indicate that temporary towers are required for support of the peripheral deck sections during construction. The design of temporary tower foundations is the responsibility of the contractor. However, as requested by Caltrans, a summary of subsurface conditions in the temporary tower areas, criteria for the design of temporary tower foundations, and example calculations are provided under separate cover in Fugro-EM (2001c).





[EB = Eastbound; WB = Westbound; MN = meganewton; m = meter; MSL = mean sea level]

Pier	Static ^a Axial Load (MN)	Bay Floor/Base of Footing ^b Elevation (m, re MSL)	Recommended Pile Tip Elevation (m, re MSL)	Estimated Ultimate Static Tension Capacity (MN)	Estimated Ultimate Compression Capacity (MN)
Pier E3-EB	45.0	-13.0	-106 ^c	82	132+
Pier E3-WB	44.9	-12.0	-106 ^c	79	129+
Pier E4-EB	39.8	-12.0	-107 ^c	85	135+
Pier E4-WB	40.5	-11.0	-107 ^c	80	130+
Pier E5-EB	45.3	-10.0	-108 ^c	86	136+
Pier E5-WB	44.4	-10.0	-108 ^c	86	136+
Pier E6-EB	40.1	-8.0	-96	80	130
Pier E6-WB	38.6	-8.0	-96	80	130
Pier E7-EB	39.8	-12.5	-98	78	121
Pier E7-WB	38.3	-12.5	-98	78	121
Pier E8-EB	37.7	-11.3	-97	82	125
Pier E8-WB	36.5	-11.3	-97	82	125
Pier E9-EB	37.1	-10.9	-96	85	128
Pier E9-WB	35.8	-10.9	-96	85	128
Pier E10-EB	38.6	-11.75	-97	90	132
Pier E10-WB	35.2	-11.75	-97	89	132
Pier E11-EB	38.3	-9.6	-95	94	140
Pier E11-WB	36.7	-9.6	-95	91	137
Pier E12-EB	36.7	-12.6	-97	92	138
Pier E12-WB	34.7	-12.6	-97	92	138
Pier E13-EB	32.9	-14.5	-96	83	129
Pier E13-WB	30.9	-14.5	-96	86	132
Pier E14-EB	29.7	-16.0	-96	98	143
Pier E14-WB	28.5	-16.0	-96	98	143
Pier E15-EB	36.3	-10.5	-93	89	137
Pier E15-WB	35.2	-10.5	-93	89	137
Pier E16-EB	29.8	-11.0	-95	93	141
Pier E16-WB	28.2	-11.0	-95	93	141

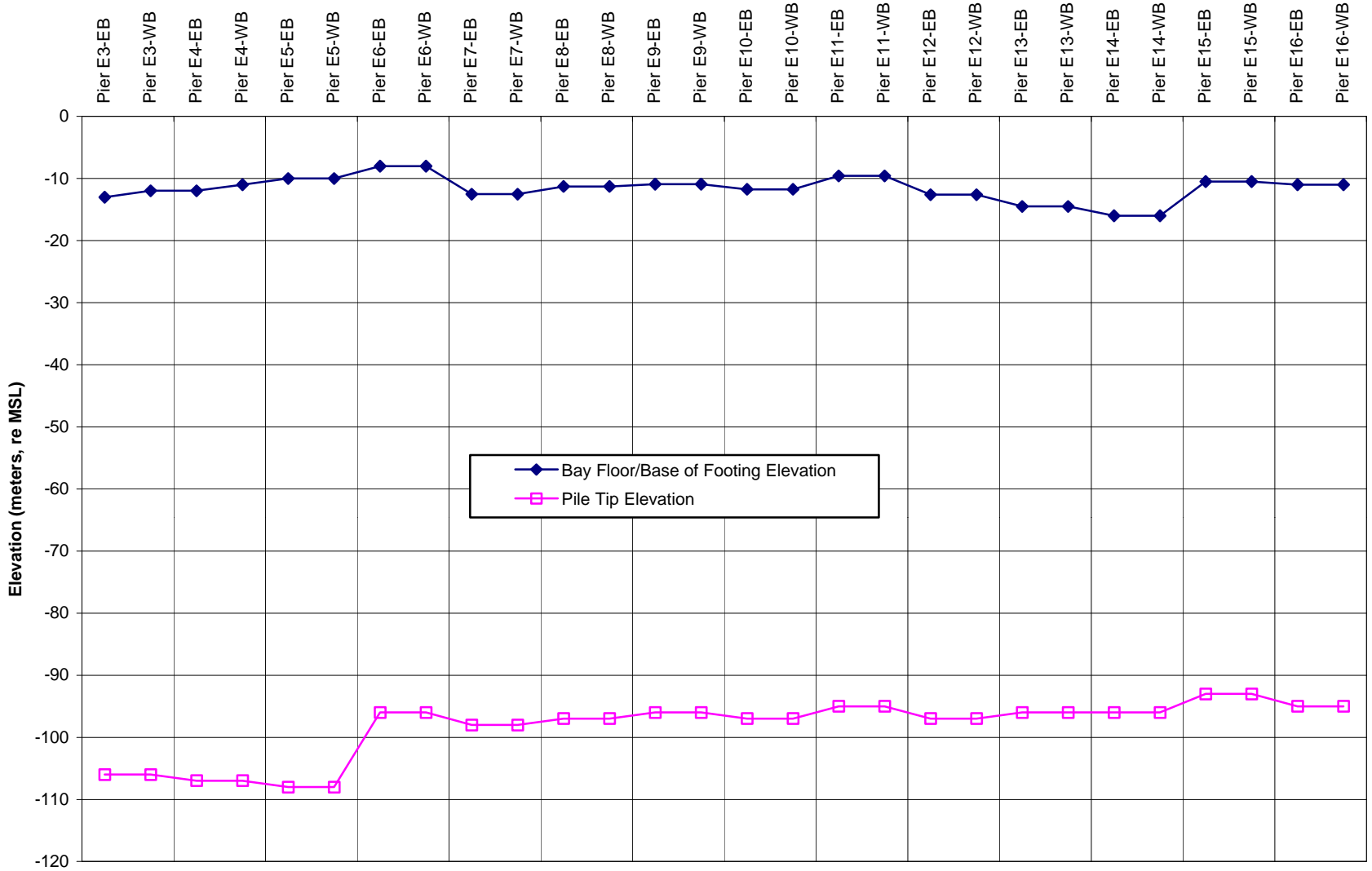
^a Static axial load values were provided by TY Lin/M&N.

^b Values listed are estimated mudline elevations for Piers E3 through E6 and planned base of footing elevations for Piers E7 through E16. They represent the elevation below which piles will derive soil support.

^c Pile tip elevations are for piles tipped in bedrock.

STATIC AXIAL LOADS AND RECOMMENDED PILE TIP ELEVATIONS
Skyway Structure Piers
SFOBB East Span Seismic Safety Project

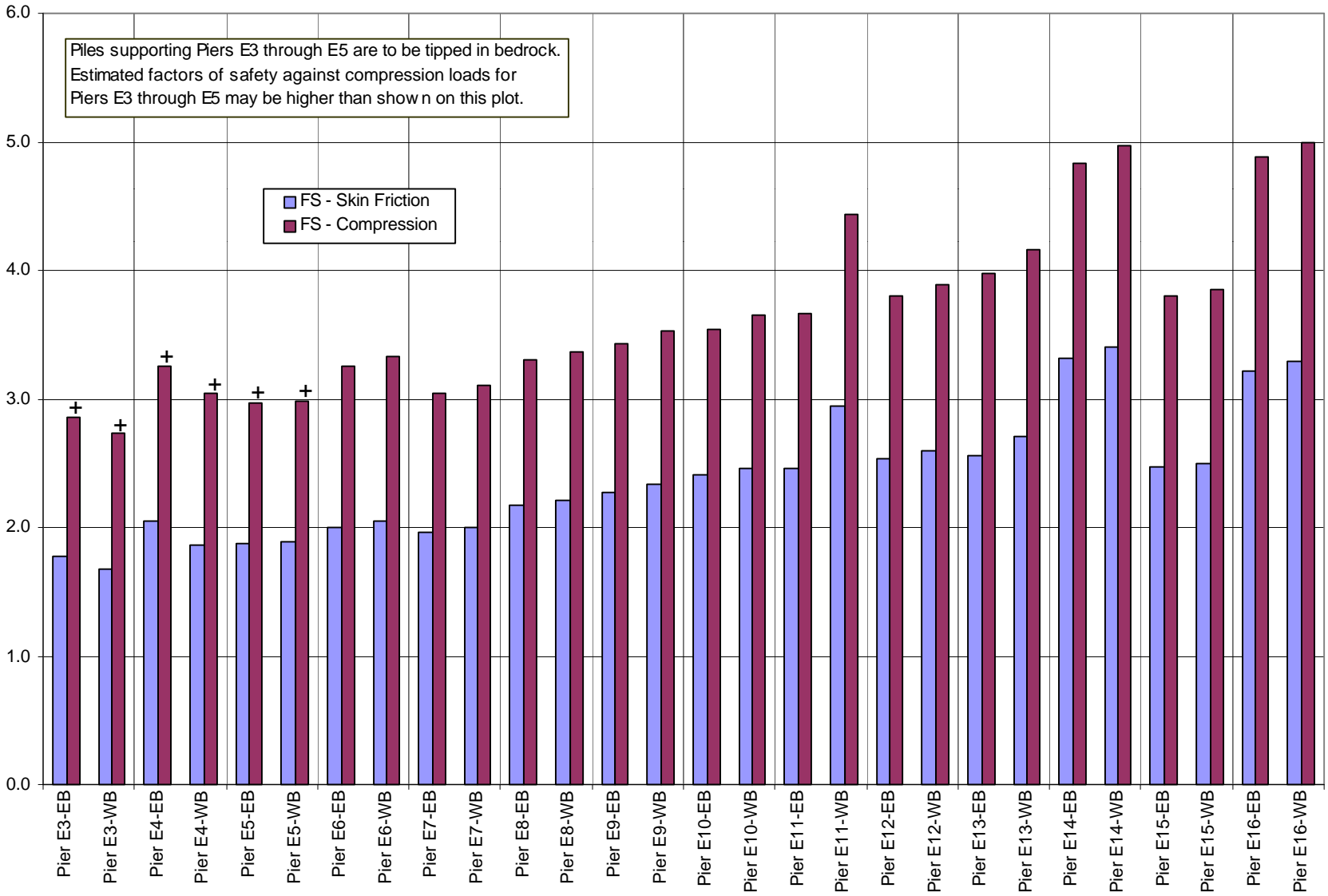




VARIATION OF PILE LENGTH AND TIP ELEVATION ALONG N6 ALIGNMENT

Skyway Structure Piers

SFOBB East Span Seismic Safety Project



ESTIMATED FACTORS OF SAFETY AGAINST STATIC LOADS
Skyway Structure Piers
 SFOBB East Span Seismic Safety Project

SECTION 4.0
AXIAL PILE DESIGN METHODOLOGY AND DATA

4.0 AXIAL PILE DESIGN METHODOLOGY AND DATA

Due to the economic importance of the San Francisco-Oakland Bay Bridge (SFOBB) and the consequences of catastrophic failure, in both economic and human terms, the design and analysis of the pile foundations supporting the bridge explicitly consider a number of aspects of pile-soil behavior that are normally ignored. These aspects include: 1) the effects of consolidation and setup, 2) the behavior under dynamic loading, 3) the losses of resistance under cyclic loading, and 4) the load-settlement behavior of the piles under severe cyclic loading conditions. Since the treatment of complex aspects of pile foundation behavior is not codified in any guiding documents, several project-specific methods were developed for design and analysis of the foundation piles.

4.1 DESIGN BASIS

The geologic conditions underlying the Main Span-East Pier and Skyway portions of the N6 alignment are relatively consistent. However, the thickness and presence or absence of the individual strata and layers, as well as the representative soil properties of the strata, are variable along the alignment. Therefore, pier-specific pile capacities are provided for the Main Span-East Pier and each of the Skyway piers. For these interpretations, primary emphasis was placed on the site-specific conditions encountered in the 1998 borings (which were drilled using offshore drilling equipment and wire-line sampling, in situ testing, and downhole tools) that included extensive in situ and laboratory test data (on relatively undisturbed push samples), the 2000 CPT soundings, and the subsurface geometry imaged by the marine 2-D and 3-D geophysical surveys.

4.1.1 Boring-Specific Design Data

A total of 44 borings were drilled during the Phase 1 and Phase 2 marine investigations. An additional 77 CPT soundings were performed during Phase 3. As shown on Plate 1.5, 27 of the marine soil borings were located within 40 meters of the N6 alignment to the east of the Main Span-East Pier. From the west end of Skyway Frame 1 through the middle pier of Skyway Frame 3 (Pier E12), there was at least one boring drilled under the anticipated location of the pier for either the eastbound or westbound alignment. In addition, 41 of the 77 CPT soundings performed during Phase 3 were along the Skyway alignment.

When a marine boring was located within the area circumscribed by the loci of the pile tips for the pier, the stratigraphy and interpreted soil parameters for that specific boring were used to develop the pier-specific pile design data. As discussed previously, at each pair of Skyway piers (E3 through E14) the area circumscribed by the loci of the pile tips will be about 30 by 25 meters. Therefore, there will be intrinsic variations in the subsurface within the area penetrated by the piles for each pier. The pier-specific borings should be recognized as



representative of the interpreted conditions underlying each pier, but not explicitly representative of the stratigraphy and conditions that will be penetrated by each of the individual piles beneath the pier.

4.1.2 "Synthetic" Boring Design Data

As noted in Section 2.0, the subsurface conditions vary both along and perpendicular to the N6 alignment. Because the drilling program was not scoped to include borings under both the eastbound and westbound piers, it is necessary to extrapolate the conditions from the boring under the adjacent westbound or eastbound pier to anticipate the conditions under the complementary pier without a boring.

To develop the design soil stratigraphy at those locations, the subsurface geometry imaged by the marine geophysical survey was used to help develop the expected soil stratigraphy at the pier locations that did not have borings. The data from the boring beneath the adjacent complementary pier and the next piers to the east and west were then used to estimate the soil properties at that location. The combined stratigraphy interpreted from the geophysical data and the soil properties interpolated from the adjacent borings thus were used to develop "synthetic" borings for the piers where marine borings were not drilled.

A similar procedure to that described above was used at the eastern end of the alignment beneath Skyway Frames 3 and 4. The pier spacing is reduced at that end of the alignment as compared to the typical 160-meter spacing beneath Skyway Frames 1 and 2. Because of the reduced pier spacing beneath those eastern Skyway frames, borings were not drilled under each set of piers.

4.1.3 General Pier-Specific Information

Pier-specific data are provided in groups of pier-specific plates in Appendix A. Pier and boring location plans for the Main Span-East Pier and the various Skyway frames are provided on Plates A-1 through A-3. A pier-boring correlation is shown on Plate A-4.

For each pier, the axial design data are presented on a series of four illustrations within the appropriate pier-specific plate group. For example, the plates for Skyway Frame 1, Eastbound Pier 3 (of the East Span) are numbered Plates E3-EB.1, E3-EB.2, E3-EB.3, etc. Similarly, the design data for Skyway Frame 1, Westbound Pier 3 are numbered Plates E3-WB.1, E3-WB.2, E3-WB.3, etc., and the design data for Skyway Frame 1, Eastbound Pier 4 are numbered Plates E4-EB.1, E4-EB.2, E4-EB.3, etc. An additional set of load-deformation analyses was performed for the borings located at the Main Span-East Pier (Borings 98-25 and 98-26). In the additional analyses, the load deformation-behavior was analyzed with the piles tipped in the middle of the Upper Alameda Marine sand layer. These plates are numbered E2-WB.2b, E2-WB.3b, E2-WB.4b, E2-EB.2b, E2-EB.3b, and E2-EB.4b.





The pile design data provided for each pier are as follows:

- Axial Pile Design Parameters and Results, including: soil stratigraphy, interpreted design strength and submerged unit weight profiles, unit skin friction and end-bearing curves, and static axial pile capacity Plate EX-YB.1
- Axial Pile Load Transfer-Displacement Curves Plate EX-YB.2
- Tabulated Axial Pile Load Transfer Data..... Plate EX-YB.3
- Static Pile Head Load-Deformation Curves Plate EX-YB.4

Plate A-5 provides a key to the legend for the Axial Pile Design Parameters and Results plates numbered as EX-YB.1.

The preliminary pile tip elevations used in developing the load-deformation data presented in Appendix A are shown on Plate A-6. As discussed in Section 3.0, those tip elevations were subsequently revised on the basis of subsequent structural analyses by TY Lin/M&N. The revised tip elevations are shown on Plate 3.1. The following sections summarize the design methodology used to develop the information provided on the pier-specific plates in Appendix A.

4.2 DESIGN METHODOLOGY

The piles supporting Piers E2 through E16 of the replacement bridge are proposed to be 2.5-meter-diameter pipe piles measuring approximately 100 meters in length that are driven to depths ranging from 70 to 95 meters below the Bay floor. Since these piles are outside the range of normal onshore experience, design methods generally used by Caltrans were considered to be inappropriate. Therefore, the methods used for design were adapted from the American Petroleum Institute (API) recommendations provided in the API RP 2A Guidelines for Design of Fixed Offshore Structures (API, 1993a,b). The API guidelines were used as such, with the generic API design equations modified to reflect the site-specific soil conditions.

The design methods were developed with the intent of providing the soil parameters necessary for the assessment of pile performance under static and dynamic loading. Since the principal design consideration was pile performance rather than static capacity, strict adherence to design codes (which provide for methods to estimate capacity under static loading conditions) was not emphasized. It was recognized that, due to rate effects and cyclic degradation, direct comparisons between the nominal earthquake loads and the static axial capacities calculated to exist prior to the design event were not sufficient to evaluate adequate performance under seismic loading conditions. Hence, the most accurate prediction of the load-deformation behavior of the piles was emphasized.



The design methods used to produce the necessary soil parameters and the related soil-structure interaction analyses are briefly discussed in the following sections of the report. Evaluations of site-specific field test data and example calculations that model the complex soil-pile interaction behavior during an earthquake are contained in Appendix B.

4.3 ULTIMATE STATIC AXIAL PILE CAPACITY

The ultimate axial capacity of driven piles is generally calculated as the algebraic sum of the side shear (skin friction) acting on the outside surface of the embedded length of pile and the end-bearing pressure acting on the pile tip. For clay soils, the unit side shear transfer and the unit end-bearing pressures are calculated as functions of the undrained shear strength. For cohesionless soils (e.g., sands and silts), the unit side shear transfer and the unit end-bearing pressures are calculated as functions of the effective overburden pressure with limiting values given for both the side shear and the end bearing.

4.3.1 Side Shear (Skin Friction)

Cohesive Soils. The results of static pile load tests performed by Caltrans on piles supported in Young Bay Mud (Brittsan and Speer, 1993) were evaluated. Details of those evaluations are presented in Appendix B. As described in Appendix B, the ultimate side shear transfer in the pile load tests were estimated to be equal to the undrained shear strength. Hindcast analysis to match the observed static load-settlement behavior of the pile resulted in an estimate of the undrained strength ratio (c/p') of 0.31. Additionally, K_o Consolidated-Undrained Triaxial Tests were performed as a part of the marine site characterization procedures. The results of those tests also suggest a c/p' value on the order of 0.31 and are presented in the Final Marine Geotechnical Site Characterization report (Fugro-EM, 2001e).

Commentaries within API (1993a,b) recommend that pile capacity determination should be based on engineering judgement that takes into account site-specific soils information, available pile load test data, and industry experience in similar soils. The API design procedure (1993a,b) was adapted from an Offshore Technology Conference paper by Randolph and Murphy (1985) in which the unit side shear transfer is calculated using the relationship:

$$f = \alpha S_u$$

- where:
- α = $(c/p')^{1/2} (S_u / \sigma')^{-1/2}$
 - S_u = undrained shear strength at any depth
 - σ' = effective overburden stress at any depth
 - c/p' = ratio of the undrained shear strength to the vertical effective overburden pressure





The API adopted a lower-bound value of 0.25 for the c/p' ratio for Gulf of Mexico clays, resulting in a default value of 0.5 for the $(c/p')^{1/2}$ term in Eq. 6.4.2-2 of API RP 2A (1993a,b).

Based on available site-specific data, the design methods presented in API (1993a,b) were modified by increasing the value of the implicit c/p' ratio in API Sec. 6.4.2-2 from 0.25 to 0.31. The ultimate unit shear transfer in the clay strata was then calculated as:

$$\alpha = (0.31)^{1/2} \left(\frac{S_u}{\sigma'} \right)^{-1/2} \quad \text{for} \quad \frac{S_u}{\sigma'} \leq 1.0$$

$$\alpha = (0.31)^{1/2} \left(\frac{S_u}{\sigma'} \right)^{-1/4} \quad \text{for} \quad \frac{S_u}{\sigma'} > 1.0$$

$$f = \alpha S_u$$

- where: f = unit shear transfer
 S_u = undrained shear strength at any depth
 σ' = effective overburden stress at any depth
 α = adhesion factor

While these formulations give axial shear transfer capacities in clay approximately 11 percent greater than those given by the API, they are in much closer agreement with the lower bound of the experimental data. Since the formulations do not consider the additional shear transfer capacity available from deposits with non-zero shear strength intercepts at the mudline, the calculated capacities will retain an inherent degree of conservatism. However, the particular soil conditions under consideration render the magnitude of under-prediction of axial capacity acceptable, since only the axial capacities at shallow depths in the very soft to soft Young Bay Mud are affected.

Cohesionless Soil. The unit shear transfer in cohesionless strata was calculated using the API (1993a,b) procedure as:

$$f = k\sigma' \tan \delta \leq f_{\max}$$

- where: k = coefficient of lateral earth pressure (=0.8 for both tension and compression)
 σ' = effective overburden stress at any depth
 δ = friction angle between the pile and the soil
 f_{\max} = limiting unit shear transfer





4.3.2 End Bearing

To preliminarily evaluate the variation of pile compression capacity with penetration, estimates of end bearing were made along the full length of the pile. For piles end bearing in clay strata, the unit end bearing was calculated as:

$$q = N_c S_u$$

where: q = unit end bearing
 N_c = bearing capacity factor for clay (= 9.0)
 S_u = undrained shear strength at any depth

For piles end bearing in cohesionless soils, the unit end bearing was calculated by:

$$q = N_q \sigma'_v \leq q_{\max}$$

where: q = unit end bearing
 N_q = bearing capacity factor for cohesionless soils (a function of the soil friction angle ϕ)
 σ'_v = vertical effective stress at any depth
 q_{\max} = limiting unit end bearing

Equivalent Unit End Bearing. For the steel pipe piles, the end bearing was limited to the frictional resistance of a soil/concrete plug developed inside the pile. The total skin friction on the inside of the pile is assumed equal to the total skin friction on the outside of the pile. Any influence of the driving shoe on the internal skin friction was ignored along with the soil end bearing on the steel end area of the pile. The assumptions made in the analyses do not affect the unit end bearing below the point where the pile plugs (i.e., equivalent unit end bearing becomes equal to unit end bearing). Above this point, the frictional resistance of the soil plug limits the unit end bearing.

Evaluations of End-Bearing Resistance for Skyway Foundations. The Main Span-East Pier and Skyway piles are intended to tip in the primarily dense sand of the Lower Alameda Alluvial deposits. Although it is possible to estimate the elevation at which the top of the LAA-sand was encountered in the boring nearest each pier, the available data (see Plate 2.14) suggest that there will be variations within the relatively large area circumscribed by the pile tips at any pier. Additionally, as discussed in Section 2.0, the available data indicate that thin clay layers are pervasive (see Plate 2.15) within the LAA-sand, but are typically of limited thickness. Consequently, there is a fairly high probability that pile tips at any given pier may be tipped in either thick layers of sand or clay.



The elevation where LAA-sand was first encountered in a boring that was considered most representative of the conditions at each pier was selected as a reference datum for the selection of preliminary pile tip elevations. The objective was to reduce the potential for drivability concerns during construction, and the possibility of tipping piles in the somewhat thicker clay layers that are more prevalent at greater depth. Thus, the preliminary pile tip elevations were selected to be 4 meters below the top of the LAA-sand. At selected piers, additional penetrations were considered to provide for an axial capacity of approximately 80 MN in tension. In general, preliminary pile tip elevations typically ranged between El. -92 meters and El. -98 meters.

In order to develop estimates of end-bearing capacity, a statistical evaluation was performed to evaluate the probable presence of clay layers at the pile tip. Those evaluations were performed for all marine borings and also on a frame-by-frame basis. Fugro-EM's database of 1998 boring data was used to estimate the percent of borings with clay at: 1) a particular elevation, and 2) a particular depth below the top of LAA-sand in that boring. Those data are summarized for all marine borings on Plates 2.18 and 2.19. All borings considered in the analysis penetrated below the top of LAA-sand. As shown on Plate 2.18, between approximately 15 and 30 percent of the borings encountered clay layers between El. -92 and El. -98 meters. Similarly on Plate 2.19, the data suggest that typically between 10 and 35 percent of the borings encountered clay layers in the 5 meters (two pile diameters) below the pile tip elevation. Although Plate 2.19 suggests that little clay was encountered in the upper 4 meters below the top of LAA-sand, it should be noted that this particular presentation does not show variations in the elevation of the top of LAA-sand.

To account for the potential presence of clay layers, values for the end-bearing capacity were developed on a frame-by-frame basis using weighted averages based on the relative amounts and thicknesses of the interbedded clay layers expected to be encountered. On the basis of laboratory tests and in situ tests, a median value of 360 kPa was estimated for the undrained shear strength (S_u) of clay layers within the Lower Alameda Alluvial Formation. For the range of pile tip elevations being considered for the Main Span-East Pier and Skyway, the bearing capacity factors for both sand and clay have attained limiting values. The values adopted for design were an ultimate unit bearing pressure of 3.24 MPa for the clay layers and 11.97 MPa for the very dense, relatively coarse LAA-sand.

The value of the unit end-bearing pressure (q_u) for each frame was calculated as:

$$q_u = \frac{3.24X + 11.97Y}{100}$$

where: X = percentage of clay layers

Y = percentage of sand layers





Clay layer percentage values and the associated end-bearing values that were used for each frame in this analysis are summarized on the following table:

Frame	Percentage of Clay Layers (X)	End Bearing (MN)
1	20	50.2
2	35	43.7
3	30	45.9
4	25	48.1

4.4 AXIAL LOAD-DEFORMATION RELATIONSHIPS

Since the stresses developed in the bridge superstructure and the acceptability of its performance are sensitive to differential settlements between adjacent piers and among the piles at each pier, the load-settlement behavior of the piles is equal in importance to the total capacity. The performance of the piles under service and design loads thus warranted detailed consideration. The behavior of the piles under static and dynamic loading conditions was investigated using the DRIVE computer program (Matlock and Foo, 1979). In this program, the side shear (skin friction) is modeled by nonlinear support curves that describe the development of: a) side shear as a function of the local pile-soil displacement (*t-z* curves), and b) end bearing as a function of the local pile-soil displacement at the pile tip (*q-z* curves). The nonlinear curves representing the side shear were developed using methods proposed by Bogard and Matlock (1990), while the end-bearing curve shapes were taken from API RP 2A (API, 1993a,b).

4.4.1 *t-z* Curves

For sand, the reactions are elastic-plastic with yielding assumed to occur at a relative pile-soil displacement of 0.00254 meter. For clays, the curves are nonlinear with the values of displacement being proportional to the diameter. The recommended curve shapes are taken from Bogard and Matlock (1990). The curve is of the form:

$$\frac{t}{t_{\max}} = \frac{\left(\frac{z}{z_{\max}}\right)}{\left[0.3 + 0.7\left(\frac{z}{z_{\max}}\right)\right]}$$

- where:
- t* = the shear transfer
 - t*_{max} = the peak shear transfer
 - z* = the pile displacement
 - z*_{max} = the corresponding displacement taken as 0.01 times the diameter





For this study, the curve shape defined above was simplified to the following normalized relationship between the side shear reaction and the ratio of the pile displacement to the pile diameter:

Point	t/t_{max}	z/D
1	0.0	0.0
2	0.25	0.001
3	0.5	0.0024
4	0.75	0.0048
5	0.9	0.072
6	1.0	0.0100

A proprietary study performed by Fugro disclosed that this formulation yields very close agreement with the results of 17 pile load tests. Although similar in form, the curve shape recommended in the API RP 2A (1993a,b) gave less satisfactory agreement, particularly for pile head displacements near design load levels (one-half to two-thirds of the ultimate load).

4.4.2 q-z Curves

The curve shape for the pile end bearing-displacement curve is based on API RP 2A criteria (1993a,b) and is a cubic parabola of the form:

$$\frac{z}{D} = 0.10 \left(\frac{Q}{Q_u} \right)^3$$

- where:
- z = pile tip displacement
 - D = pile diameter
 - Q = end-bearing reaction corresponding to tip displacement, z
 - Q_u = ultimate end-bearing reaction

For this study, the curve shape defined above was simplified to the following normalized relationship between the end-bearing reaction and the ratio of the pile displacement to the pile diameter:

Point	Q/Q_u	z/D
1	0.0	0.0
2	0.25	0.0015
3	0.5	0.0125
4	0.75	0.0420
5	0.9	0.0730
6	1.0	0.1000



4.5 AXIAL PILE HEAD LOAD-DEFORMATION CURVES

Axial capacity versus displacement analyses were conducted using a single-pile model with pier-specific, depth-varying, nonlinear axial skin friction (t - z) and end-bearing (q - z) soil-support curves, specified pile lengths, and the preliminary pile section schedules provided by the designer. The DRIVE program was used for the axial pile analyses since the same input data can be used for static, quasi-static cyclic, or dynamic loading conditions. The computer program also accepts user-defined descriptions of the sensitivity of the soils to cyclic loading, thereby enabling the losses in resistance under cyclic loading to be estimated.

Since the soil-structure analysis program used for analysis of the SFOBB does not accept the large number of input curves provided for in the DRIVE program, and since the location of the input curves had to match the depths at which free-field ground motion had been estimated in the site response analyses (Fugro-EM, 2001b), additional analyses were performed to provide simplified profiles for the structural analysis. Preliminary analyses were performed using the detailed stratigraphy considered representative at each pier. Subsequent analyses were performed using a simplified profile. By comparing the results of the two solutions and adjusting the simplified profile, compatibility of the total axial capacity and the load-settlement behavior at each set of input support curves was obtained. Additional details and a typical example of the procedures followed are provided in Appendix B. The resulting nonlinear pile head load-deformation curves are provided on pier-specific Plates EX-YB.4 in Appendix A.

The load-deflection curves for the steel pipe piles indicate that the required vertical pile head-deflections to mobilize the full compression capacities are in excess of 0.3 meter. These relatively large deflections can be attributed to the relatively large displacements required to mobilize the end-bearing component of the pile resistance. Significantly less deflection is required to mobilize the full side shear component of resistance. The load deflection curves indicate that approximately 0.05 meter of deflection is required to mobilize approximately 65 to 70 percent of the ultimate compression capacity.

4.6 EARTHQUAKE LOADING EFFECTS

As discussed in Section 3.0, the two primary impacts of earthquake loads on soil-pile interaction are: 1) cyclic degradation of soil resistance, and 2) an increase in soil resistance (relative to static estimates) due to rate of loading effects. Those effects may occur simultaneously or independently, depending on the time-history of loading at the pile head.

4.6.1 Cyclic Degradation of Pile Capacity

Cyclic axial loading of long flexible piles may result in two detrimental effects: a) losses in capacity due to cyclic degradation of the side shear, and b) progressive settlement due to the



nonlinear and inelastic soil response (i.e., the pile tip does not rebound during upward loading phases to the same extent as it settles during downward loading phases at the pile head).

Since little experimental data was available to describe the progressive degradation in axial shear transfer capacity in the San Francisco Bay clays, preliminary analyses were performed by assuming that the cyclic degradation behavior is similar to that observed in the highly plastic Gulf of Mexico clays. In the Gulf of Mexico clays, the cyclic minimum shear transfer was experimentally determined to be approximately equal to the remolded shear strength. In detailed soil-pile interaction analyses (as can be done using the DRIVE program), the degradation of peak shear transfer (from the static value to that corresponding to the remolded shear strength of the soil) occurs progressively with each additional cycle of loading. Details relative to the degradation model used in such analyses are presented in Appendix B.

4.6.2 Strain Rate Effects

Earthquake ground motions result in horizontal and vertical forces on the piles that are applied quite rapidly. It was therefore necessary to develop methods to estimate the effects of loading rate on the magnitude of the shear transfer along the piles. A number of dynamic axial load tests were examined to evaluate the effects of loading rate expressed as a function of the relative pile-soil velocity. Details, results, and discussion of those tests are provided in the Final Marine Geotechnical Site Characterization report (Fugro-EM, 2001e). Additionally, rate of loading effects were evaluated (as described in Appendix B) from static load tests on piles.

The damping coefficients that were developed from those evaluations are of the form:

$$C_{eq} = \left(\frac{\beta}{V} \right) \text{Log} \left(\frac{V}{V_{ref}} \right)$$

where: C_{eq} = equivalent linear viscous damping coefficient
 β = site-specific strain rate parameter
 V = relative velocity of pile and soil
 V_{ref} = relative velocity of pile and soil corresponding to static loading

From dynamic direct simple shear (DSS) tests and hindcast estimates, β was determined to be 0.12. From axial load tests on a 30-inch-diameter pile in Gulf of Mexico clays, V_{ref} was determined to be 0.0254 millimeter per second (mm/sec). Viscous dashpots with a damping coefficient of C_{eq} can be used to model rate of loading effects on shear transfer along the piles. Additional details on the derivation of these values and examples of their application in dynamic soil-pile interaction analyses are provided in Appendix B.



4.6.3 Example Calculations of Earthquake Loading Effects

Example analyses of soil-pile interaction during earthquake loading were performed using the computer program DRIVE. Detailed descriptions of those analyses are provided in Appendix B and in Fugro-EM (1999). Those analyses were performed using preliminary pile head load-time histories provided by TY Lin/M&N for piles at Pier E10. DRIVE has an algorithm that models the progressive cyclic degradation of soil shear strength and allows for the use of viscous dashpots to model strain rate effects. Sensitivity analyses were performed using degrading soil properties, non-degraded soil properties, and reduced (but not degrading) t - z parameters.

In general, the total settlements predicted on those preliminary analyses for piles with degrading soil properties were similar to those for piles with no degradation as long as the piles could mobilize significant end bearing. This observation is attributed to the fact that the majority of the settlement appeared to be associated with the velocity/displacement pulse (referred to as the “fling”) that occurs at the start of the earthquake before significant degradation occurs.

For analyses with piles tipped in sand layers of the Lower Alameda Alluvium, the displacement appeared to stabilize after the initial “fling-induced” displacement. Sensitivity analyses performed for piles tipped in clay appeared to indicate progressive and larger settlement during the earthquake. However, it should be noted that the load time histories used in these analyses were generated for the stiffer pile response corresponding to sand end bearing. Somewhat reduced loads (and therefore smaller predicted settlements) would be anticipated for a softer pile with clay end bearing.

Although the analyses using degrading soil models indicated that side shear resistance of the pile could be reduced by up to 25 percent, there appears to be ample capacity remaining at the end of the earthquake to resist service loads. Most of the strength degradation appeared to be within the relatively soft Young Bay Mud layers. Over time, the pile will likely set up to its design static capacity.

The numerical models used by TY Lin/M&N generally are not able to model the degradation of soil resistance. However, the DRIVE program does not perfectly model the structural connectivity to the pile. Hence, the changes in pile-head load due to the pile response also are not modeled. Consequently, an iterative procedure would have been required to accurately model the earthquake performance of the piles. However, since the preliminary analyses suggested that the estimated pile settlements were similar in cases with and without degrading soil response, TY Lin/M&N elected not to model the cyclic degradation of soil resistance in their structural analyses.

The extent of cyclic degradation and pile performance is affected by the relative pile stiffness, the distribution of soil reactions with depth, and the magnitude of axial loads. Thus,



the observations from the example calculations may not be universally applicable to other piers with differing structural, foundation, and soil characteristics.

4.6.4 Recommendations for Design

As discussed in Section 3.0, the use of conventional safety factor-based analyses is not always meaningful in evaluating the performance of a structure during earthquake loading. The procedures used to estimate pile capacity frequently include some level of conservatism. The use of conservative soil properties, while appropriate for service load design, may not always be suitable for evaluating the seismic performance of the structure. In some cases, “conservatism” in pile support parameters and the consequent modeling of a relatively soft pile response can result in underprediction of stresses on the structure due to the earthquake. Therefore, it is recommended that structural design consider a range of soil support conditions to establish both the potential settlements at the piers and the stresses in the structure.

Load tests in San Francisco Bay soils (Brittsan and Speer, 1993) have shown that the unit side shear resistance on a pile can equal the undrained shear strength of the supporting soil, whereas the average skin friction values used in the static estimates generated using the modified API (1993a,b) methodology are typically on the order of 70 percent of the undrained shear strength of the surrounding soils. Those load tests therefore indicate that the available side shear resistance may be as much as 40 percent higher than that which would be used for design. Similarly, the API (1993a,b) procedures apply a limit to the end-bearing capacity that can be used for static design. Case histories document end-bearing resistances that are similar to those that would be calculated using bearing capacity factors that are commensurate with those predicted theoretically for the angle of internal friction of the soils at the pile tip. For the typical length of piles being considered for the Main Span East Pier and Skyway Structures, the removal of the API limiting end bearing produce end-bearing capacities that are on the order of 2.5 times larger than are recommended for the evaluation of service loads.

For earthquake analyses of the structure, it is recommended that the range of soil support conditions be established using:

1. The static pile design parameters presented in Appendix A for the service load performance evaluations; and
2. The t-z curves established by using a side shear capacity 1.4 times that used for static design and q-z curves established by using end-bearing capacities 2.5 times stiffer than those used for static design.

Additional sensitivity analyses should also be performed to evaluate the potential impacts on the structure due to at least some of the piles at a pier being tipped in clay interbeds in the LAA-sand. Those piles will likely exhibit a somewhat softer response under extreme seismic events due to reduced end bearing. Sensitivity analyses should also be performed to evaluate the stiffer response of the piles due to the stiff end-bearing spring where piles are to be tipped in bedrock at Piers E3 through E5.



**SECTION 5.0
PILE SETUP**

5.0 PILE SETUP

5.1 INTRODUCTION

Pile setup is a complex physical phenomenon. Although general mechanisms are understood, the specific behavior and results of the phenomenon are difficult to predict. During continuous driving in fine-grained soils, the soil near the pile tip and wall is sheared and remolded. This process generates large excess pore water pressures that reduce the effective stress and soil shear strength in the vicinity of the pile wall. Therefore, at the end of driving, the skin friction component of pile capacity in fine-grained soil will be significantly less than the static skin friction pile capacity used for design.

As the pore pressures generated during pile installation dissipate and the effective stresses in the vicinity of the pile wall increase, the pile capacity will increase. Field measurements from numerous projects and studies have shown that the time required for piles to achieve their ultimate geotechnical capacity in clay soils can be on the order of months to years. The reduced pile capacity at the end of driving and the subsequent rate and magnitude of pile setup should be considered in the scheduling of construction activities that will transmit load to the pile foundation.

5.2 PREDICTION OF PILE SETUP

Field measurements have shown that the rate of pile setup in clay soils differs between displacement and open-ended pipe piles. The rate of setup varies with pile diameter, pile wall thickness, and the horizontal coefficient of consolidation of the soil. The time rate phenomenon of setup is strongly influenced by the permeability of the zone immediately surrounding the pile. Since measurements of permeability and pore pressure dissipation rates are one of the least accurately predicted phenomena in geotechnical engineering, there is uncertainty associated with setup predictions. Consequently, in the absence of site-specific setup data, some conservatism is warranted in the predictions of setup.

Two methods have been used to predict setup. Initially, a procedure developed by Bogard and Matlock (1990) that was based on a lower bound of available empirical data from the Gulf of Mexico was used. Because there is an absence of site-specific setup measurements for large-diameter steel pipe piles, the estimated setup predictions were anticipated to be conservative. Subsequently, the procedure developed by Soderberg (1962) has since been incorporated to better utilize the available radial coefficient of consolidation data from this project. The applicability of the Soderberg procedure was later verified by data obtained from the Pile Installation Demonstration Project (PIDP).





5.2.1 Preliminary Predictions of Pile Setup in Clay

The Bogard and Matlock approach is based on a large number of experiments on Gulf of Mexico clays with instrumented probes and piles with various diameters and wall thicknesses. The empirical design procedures that were developed from those experiments include the effects of pile diameter, wall thickness, and plugging on the rate of consolidation and setup (Bogard and Matlock, 1990).

The procedure presented by Bogard and Matlock (1990) provide a single function describing the relationship between setup and time. This procedure implicitly assumes an initial setup factor of 5 and was developed as a lower bound of the experimental data. The experimental data presented in Bogard and Matlock (1990) also were used to derive an upper bound relationship, which assumes a setup factor of 3. The equations for the upper bound and lower bound estimates are as follows:

$$\text{Lower Bound: } Q(t) = Q_u[0.20 + 0.80U]$$

$$\text{Upper Bound: } Q(t) = Q_u[0.33 + 0.67U]$$

where: $Q(t)$ = axial capacity due to side shear at time, t
 Q_u = ultimate static axial capacity due to side shear
 U = percent consolidation (or setup) described by:

$$U = \frac{\frac{t}{t_{50}}}{1 + \frac{t}{t_{50}}}$$

where: t_{50} = time required for dissipation of 50 percent of the excess pore pressures and is described by the relationship presented by Soderberg (1962):

$$t_{50} = r^2/c_h$$

where: r = pile radius
 c_h = radial coefficient of consolidation ($c_h = 5.4$ square meters per year (m^2/yr))

The modified Bogard and Matlock (1990) curves presented on Plate 5.1 were based on experimental data from the Gulf of Mexico for piles with a pile diameter to pile wall thickness ratio (D/t) equal to 40, which is similar to the D/t ratio for the SFOBB piles. Although those relationships were known to be somewhat conservative, in the absence of site-specific data, they were recommended for preliminary design.



5.2.2 Revised Setup Predictions Based on Soderberg (1962)

The relationship for pile setup in clay developed by Soderberg (1962) also has been used. With this prediction method, the laboratory measurements of the radial coefficient of consolidation and the site-specific PIDP data can be incorporated in the predictions. Soderberg solved the radial consolidation problem with a finite difference approach. His solution is presented as a plot of percent pore pressure dissipation at the pile surface versus a dimensionless time factor (T) defined as:

$$T = (c_h t)/r_p^2$$

where: c_h = coefficient of radial consolidation
 t = time
 r_p = pile radius

Predictions of setup using the Soderberg (1962) relationship assume ultimate setup factors ranging from 3 to 5. A value of the horizontal coefficient of consolidation (c_h) was chosen for the Soderberg method based on available consolidation data in the Young and Old Bay Muds and a series of multiple orientation consolidation tests conducted as part of the Phase 2 marine site characterization (Fugro-EM, 2001e). The consolidation data show that a vertical coefficient of consolidation (c_v) of approximately 8 square meters per year [m^2/yr] is representative of approximately the lower one-third of the data. Based on available multi-oriented consolidation test data in the overconsolidated range of stresses, the ratio of c_h to c_v was estimated to be about 1.5. On the basis of that data, a c_h of 12 m^2/yr was used for the setup predictions using Soderberg (1962).

The assumed values of setup and c_h were validated by the data obtained from the PIDP. The Soderberg setup curves reasonably bounded the interpreted clay skin friction setup data from the PIDP (see Fugro-EM, 2001f). The interpretation of the PIDP data should be considered somewhat approximate since: 1) the data was interpreted from CAPWAP (Case Pile Wave Analysis Program) analyses with assumptions regarding the thickness and distribution of clay layers; 2) the longest setup period was only about 33 days, a relatively short time compared to the anticipated time required to reach the ultimate skin friction capacities; and 3) the PIDP tests were conducted at only two locations along the approximately 2.1-kilometer-long Skyway structure alignment.

5.2.3 Discussion of Prediction of Pile Setup in Clay

Upper- and lower-bound curves of predicted setup of skin friction in clay are provided on Plate 5.1 for both the Bogard and Matlock (1990) and Soderberg (1962) approaches. The Soderberg curves (using site-specific estimates of c_h) predict considerably faster setup during the first 3 to 4 months. Thereafter, the two sets of setup curves converge. The predictions using the



Soderberg relationship suggest that 50 percent of the ultimate skin friction capacity in clay is available in less than about 20 days. Predictions using the Bogard and Matlock relationship suggest that approximately 1 to 2 months are required to develop 50 percent of the ultimate skin friction capacity. The time required to reach approximately 80 percent of the ultimate skin friction capacity ranges from 9 to 10 months using the Soderberg relationship to 8 to 10 months using the Bogard and Matlock relationship.

5.2.4 Setup in Sand

Setup within the sand layers encountered along the N6 alignment is generally expected to occur relatively quickly compared to the setup of the fine-grained soils. The setup rate in sand depends on the amount and type of fines in the sand layer, the grain size distribution, the extent and thickness of the sand layer, the amount of smearing of adjacent clay layers into the sand, and other factors. The temporary degradation of pile resistance due to pile driving and subsequent setup of the pile capacity in sand layers has generally been ignored in these analyses.

5.3 IMPACT OF PILE SETUP ON CONSTRUCTION SCHEDULE

5.3.1 Preliminary Evaluations

TY Lin/M&N developed anticipated load-time histories during construction for the most heavily loaded piles at two Skyway piers (TY Lin/M&N, 2000c). Those time histories suggest that placement of the (cast-in-place) pile cap, pier, and pier cap generally do not transmit significant loads to the piles. Construction of the subsequent precast deck sections is anticipated to use unbalanced cantilever construction techniques, and the spans within a frame will be jacked to reduce potential shrinkage-induced loads. Those activities transmit large loads to the piles. The application of deck section loads to the piles will occur during the time frame when setup is expected to occur. Thus, the load capacity of the piles while the deck is being constructed will be less than the ultimate pile capacity. The load-deflection characteristics during this time period will be softer than the ultimate load-deformation behavior of the pile.

To help evaluate how the construction loading will affect the axial pile head load-deformation behavior, a series of preliminary analyses were performed using the computer program DRIVE. The analyses were performed for the "worst case" piers within each of the Skyway frames. The "worst case" piers were selected as those with the least number of sand inclusions above the pile tip elevation, which should correspond to the location where the setup will be slowest.

Load-deformation curves were then generated for compression and tension at different times after the end of continuous driving. For those analyses, the t-z curves at each time were reduced by the factor shown on the Bogard and Matlock (1990) setup curves presented on Plate 5.1. No reduction was applied to the end-bearing q-z curves or the t-z curves in sand layers. Ultimate end-bearing values were assumed to be the average values provided in Section 3.0 of



this report. The analysis results for each of the "worst case" piers were provided in a Fugro-EM project memorandum (2000).

The analyses were used to estimate the minimum time required before a particular construction activity could be conducted. Since little site-specific data were available to predict setup, the relatively conservative techniques presented by Bogard and Matlock (1990) were adopted in generating those estimates. The minimum time estimates before particular construction activities could occur were predicted for both capacity and load-deformation criteria. Those criteria were:

- The time required to achieve a factor of safety of 1.5 on side shear (skin friction) capacity alone (without consideration of the end-bearing capacity); and
- The time required to maintain axial pile-head displacement of less than 20 mm as predicted using the monotonic load-deformation curves for side shear.

From those analyses, the minimum required waiting periods (following the end of initial pile driving) before the initiation of a construction activity were estimated.

5.3.2 Findings From the Pile Installation Demonstration Project

Data from the PIDP generally indicate that pile setup at the PIDP locations occurred faster than the original (conservative) predictions using the Bogard and Matlock (1990) setup curves. The PIDP setup data therefore provides a basis for revising the previously recommended approach relative to construction waiting periods.

Estimated skin friction capacities (from CAPWAP analyses) calculated using data from a series of restrikes conducted on the PIDP piles are presented on Plate 5.2. The PIDP data suggests that 65 to 70 MN of skin friction capacity were available approximately 30 days after the end of initial driving at the PIDP Primary Test Location. The anticipated load-time history provided by TY Lin/M&N (2000c) for eastbound Pier E8 also is presented on Plate 5.2. A comparison of the anticipated loads with the available capacity suggests that the allowable pile capacity (based on skin friction capacity with a factor of safety of 1.5 [FS=1.5]) will exceed the maximum anticipated construction pile load (Pier 8 Jack Span 4, ~45 MN) after approximately 1 month. At these load levels, monotonic pile-head load-deformation analyses predict about 20 mm of axial pile-head deflection.

Predicted pile setup curves based on the Soderberg (1962) method also are provided on Plate 5.2. The predicted range of pile setup assumes:

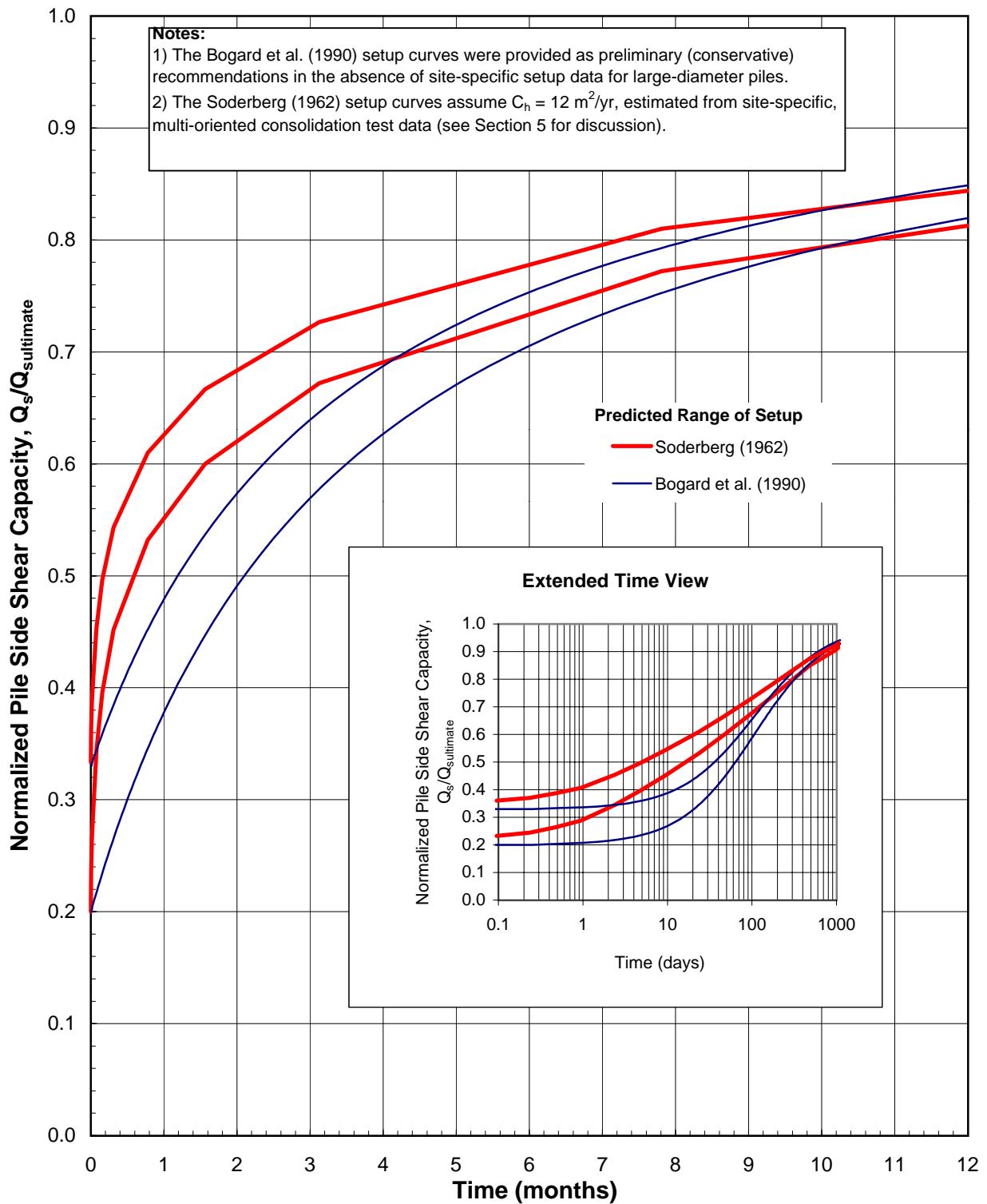
- Average clay sensitivity of 2.5 (a reasonable assumption based on available sensitivity data obtained during the field exploration program),



- 80 percent of the skin friction capacity from clay layers (based on static pile capacity calculations at the PIDP Primary Test Location), and
- Ultimate skin friction capacities ranging from 80 to 110 MN.

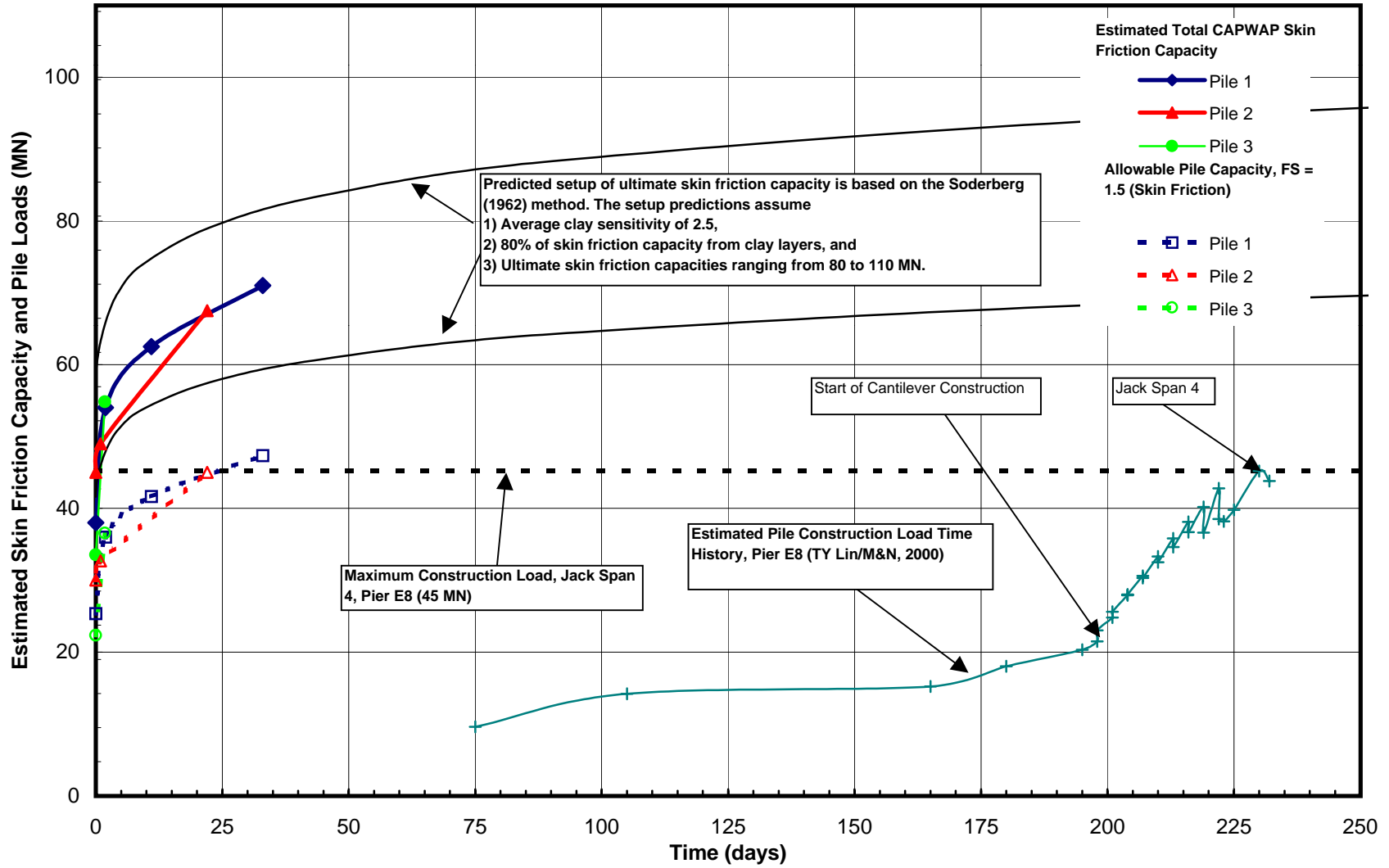
The assumed range of ultimate skin friction capacities considers the likelihood (based on the PIDP data) that the total skin friction capacity at the PIDP locations will meet or exceed the calculated API (1993a,b) design capacity (approximately 80 MN). The setup curves based on the above assumptions appear to bound the PIDP total skin friction capacity estimates.





PREDICTED SETUP OF SKIN FRICTION IN CLAY
2.5-Meter-Diameter Steel Pipe Piles
 SFOBB East Span Seismic Safety Project





ESTIMATED CAPWAP SKIN FRICTION CAPACITY AND ANTICIPATED CONSTRUCTION PILE LOADS
Pile Capacity from Pile Installation Demonstration Project
SFOBB East Span Seismic Safety Project

**SECTION 6.0
PILE DRIVABILITY CONSIDERATIONS**

6.0 PILE DRIVABILITY CONSIDERATIONS

6.1 INTRODUCTION

To evaluate the constructibility of the proposed pile foundations, preliminary pile drivability analyses were performed for the Main Span-East Pier and selected Skyway piers. The following sections summarize:

- Methodology and conditions considered in the preliminary drivability evaluations,
- Results of the preliminary drivability analyses, and
- Findings from the PIDP.

6.2 DRIVABILITY ANALYSES

6.2.1 Analytical Process

Drivability analyses are typically conducted to develop profiles of predicted blow counts and driving stresses versus pile penetration to evaluate the suitability of the proposed pile driving hammer system and to help highlight possible driving problems (e.g., early pile refusal or excessive driving stresses).

A schematic illustration of the processes involved in performing drivability analyses is presented on Plate 6.1. As shown on Plate 6.1, drivability analyses generally consist of three steps:

1. **Estimate Soil Resistance to Driving.** A soil resistance to driving (SRD) profile is developed for the anticipated soil profile. The SRD profiles are typically derived from the estimated static ultimate pile capacity profiles. The unit skin friction from the static pile capacity analyses may then be reduced (particularly in clays) to account for the degradation of soil resistance during driving. The methodologies used to calculate SRD for this project are presented in Section 6.2.2.
2. **Perform Wave Equation Analyses.** Wave equation analyses are conducted that model the particular pile–pile driving hammer system. The wave equation analyses establish the relationship between SRD and blow count (and driving stress) as presented in Section 6.2.3.
3. **Develop Profiles of Blow Counts and Driving Stresses.** The SRD profile and the results of the wave equation analysis are combined to develop a profile of pile penetration versus predicted blow count and/or driving stresses.



6.2.2 Soil Resistance to Driving

Computation of the soil resistance to pile driving is analogous to the computation of ultimate axial pile capacity by the static method. The resistance to driving is the sum of the shaft resistance and the toe resistance during driving. The shaft resistance is computed by multiplying the average unit skin friction during driving and the embedded surface area of the pile. The toe resistance is computed by multiplying the unit end bearing and the end-bearing area. Unlike static pile capacity computations, end bearing is not limited to the frictional resistance developed by the soil plug.

Stevens Method. Stevens et al. (1982) recommended computing lower-and upper-bound values of soil resistance to driving for both coring and plugged pile conditions. When a pile cores, relative movement between pile and soil occurs both on the outside and inside of the pile wall. Shaft resistance, therefore, may be developed on both the outside and inside pile wall. For the coring condition, the end-bearing area is equal to the cross-sectional area of steel at the driving shoe. When a pile plugs, the soil plug moves down with the pile during driving. For the plugged condition, shaft resistance is mobilized only on the outer wall, and the end-bearing area is the gross area of the pile.

Whether or not the advancing pile is coring, partially plugged, or plugged is determined by the soil conditions, pile diameter, pile roughness, and pile acceleration during driving. As discussed by Stevens (1988), the plugging of large-diameter pipe piles during continuous driving in predominantly cohesive soils is unlikely. The piles are assumed to initially plug, however, after each add-on is made. For a coring pile, a lower bound of SRD is computed assuming that the skin friction developed on the inside of the pile is negligible. An upper bound of the SRD is computed assuming the internal skin friction is equal to 50 percent of the external skin friction.

For a plugged pile, a lower bound is computed using unadjusted values of unit skin friction and unit end bearing. An upper bound plugged case for granular soils is computed by increasing the unit skin friction by 30 percent and the unit end bearing by 50 percent. A corresponding increase in limiting values for unit skin friction and unit end bearing is assumed. For cohesive soils, the unit skin friction is not increased and the unit end bearing is computed using a bearing capacity factor of 15, which is an increase of 67 percent.

For sand layers, a "smoothing" process is used to account for the effects of soil layering, which may reduce the calculated unit end-bearing (UEB) values. This process assumes that the full UEB in sand layers will not be mobilized until the pile penetrates at least three pile diameters into the sand layer. Similarly, it is assumed that the pile will not mobilize the full end bearing below a distance of three pile diameters above the bottom of the sand layer. The three pile-diameter transition zones at the top and bottom of the sand layers are based on project experience and results of model pile tests by Vesic (1977). The UEB reduction process to account for the



layering effect is typically carried out through a graphical procedure as outlined in McClelland Engineers (1981)

The lower- and upper-bound soil resistance curves represent experience gained from previous projects. Our experience with the drivability of large-diameter steel pipe piles into predominantly clay soils indicates that the soil resistance calculated for a "coring" pile will generally provide the best estimate of the field blow counts, provided the pile wall is of adequate thickness to effectively transmit the energy transmitted by an adequately sized pile driving hammer.

With the exception of clay skin friction, the unit skin friction and unit end-bearing values used in the drivability analyses are the same as those used to compute static pile capacity. For piles driven in cohesive soils, the unit skin friction during continuous driving is computed using the stress history approach presented by Semple and Gemeinhardt (1981). The unit skin friction for static loading is first computed by using the method recommended by the American Petroleum Institute (API RP 2A [API, 1986]). The unit skin friction for static loading is then adjusted incrementally by multiplying it by a pile capacity factor, such that:

$$f_{dr} = F_p f$$

where: f_{dr} = unit skin friction used in the drivability analyses
 F_p = an empirical pile capacity factor
 f = unit skin friction for static loading conditions

The pile capacity factor empirically determined from wave equation analyses performed for six sites is given by:

$$F_p = 0.5 (OCR)^{0.3}$$

The OCR may be estimated from: a) the measured undrained shear strength and Atterberg limit data, b) consolidation test results, and/or c) correlation with CPT tip resistance. When based on the measured undrained shear strength and Atterberg limit data OCR is estimated using the following equations.

$$\frac{S_u}{S_{unc}} = (OCR)^{0.85}$$

where: S_u = actual undrained shear strength of clay having a given plasticity index (PI)
 S_{unc} = undrained shear strength of the same clay if normally consolidated





According to a relationship developed by Skempton (1944):

$$S_{unc} = \sigma'_{vo} (0.11 + 0.0037 PI)$$

where: σ'_{vo} = effective overburden pressure

PI = plasticity index.

OCR is estimated from CPT tip resistances using the following equations:

$$\sigma'_p = 0.33 (q_c - \sigma'_{vo})$$

$$OCR = \sigma'_p / \sigma'_{vo}$$

where: σ'_{vo} = effective overburden pressure

σ'_p = preconsolidation stress

q_c = cone tip resistance

Sensitivity-Based Method. The sensitivity-based approach uses the same methodology as the Stevens et al. (1982) method, with the exceptions that: 1) the unit skin friction (f_s) for static loading is computed using the more recent API (1993a,b) recommendations with site-specific modifications in developing unit skin friction estimates; and 2) the clay SRD is calculated by reducing the calculated ultimate clay unit skin friction values by the measured clay sensitivity (the ratio of the undisturbed to remolded clay shear strengths). The sensitivity-based reduction of unit skin friction in clay for the development of SRD is similar to a model presented by Dutt et al. (1995) that predicts SRD for large-diameter pipe piles in normally consolidated clays. The measured clay sensitivities are typically determined from remolded undrained shear strength tests. As in the Stevens et al. (1982) method, the unit skin friction and unit end-bearing values for granular soils are the same as those used to compute static pile capacity (i.e., the sensitivity in granular soil is taken to be 1).

Example SRD Calculations. An illustrative example of the calculation of SRD for both the Stevens et al. (1982) and the sensitivity-based methods for the design soil profile at Pier E7 Eastbound (Boring 98-49) is presented on Plate 6.2. Shown on Plate 6.2 are:

- Soil stratigraphy
- Interpreted design submerged unit weight and shear strength profiles
- Unit skin friction profiles using the following methodologies:
 - API (1986), applicable to the Stevens et al. (1982) method
 - API (1993a,b) with site specific modifications applicable to the sensitivity-based method
- Unit end-bearing profile



- The skin friction reduction values:
 - The F_p factor for the Stevens et al. (1982) method
 - The inverse of the clay sensitivities for the sensitivity-based method
- Calculated upper- and lower-bound coring case SRD profiles for both the Stevens et al. (1982) and sensitivity-based methods.

The example calculations on Plate 6.2 demonstrate the relative differences in the unit skin friction and skin friction reduction values between the two methods used to calculate SRD. In addition, Plate 6.2 shows that the skin friction "reduction" value equals 1 in sand.

The example on Plate 6.2 also illustrates the differences between the two predicted SRD profiles. The sensitivity-based SRD is considerably lower than the Stevens-based SRD in the upper 30 to 40 meters of the soil profile. Below about 40 meters, the sensitivity-based profiles are typically 20 to 30 percent less than the Stevens-based SRD profiles. In the very dense sand layers of the Lower Alameda Alluvial sediments, the two SRD profile tend to converge.

6.2.3 Wave Equation Analyses

The GRLWEAP (GRL&A, 1997) computer program, originally coded as WEAP by Goble and Rausche (1976), was used for this study. Wave equation analysis of pile driving is based on the discrete element idealization of the hammer-pile-soil system formulated by Smith (1960). The parameters used in the wave equation analysis can be divided into three groups: 1) hammer parameters, 2) pile parameters, and 3) soil parameters. These parameters are discussed in the following paragraphs.

Hammer Parameters. Air/steam hammers are modeled by three segments: 1) the ram as a weight with infinite stiffness, 2) the cushion as a weightless spring with finite stiffness, and 3) the pile cap as a weight with infinite stiffness. For hydraulic hammers, such as were considered in this analysis, a cushion is not used and the ram impacts directly on the pile cap.

The pile driving hammer is described by the:

- Rated hammer energy,
- Efficiency of the hammer,
- Weight of the ram,
- Weight of the pile cap,
- Cushion stiffness, and
- Coefficients of restitution for the ram hitting the cushion and for the pile cap-pile contact.

The rated energy and the weight of the ram and pile cap are obtained from the manufacturer. The hammer efficiency and cushion properties are either the measured driving



system performance data (estimated from Fugro's proprietary database for 23 offshore hammers and 12 cushion configurations) or published values.

Pile Parameters. The pile is divided into an appropriate number of segments of approximately equal length. Each pile segment is modeled as a weight and a spring. The pile parameters consist of the diameter, the wall thickness schedule, modulus of elasticity of the pile material, unit weight of the pile material, free-standing length of pile, and penetration below the bay floor.

Soil Parameters. The soil resistance is distributed along the side of each embedded element and at the pile toe. During driving, the static component of resistance on each element is represented by an elastic spring with a friction block used to represent the ultimate static resistance. The dynamic component of resistance is modeled by a dashpot. There are essentially three soil parameters used in the wave equation analyses: 1) the quake (also referred to as the elastic ground compression) for the side and toe of the pile, 2) the damping coefficient for the side and toe of the pile, and 3) the percentage of the total resistance to driving along the shaft of the pile.

The soil quake and damping parameters recommended by Roussel (1979) were used in these wave equation analyses. Those parameters were determined from an analysis of the driving records of 58 large-diameter offshore piles at 15 offshore sites in the Gulf of Mexico. The side and toe quakes are assumed equal, with a magnitude of 0.25 centimeter (cm) for stiff to hard clay, silt, and sand. Side damping in clay decreases with increasing shear strength, which is in agreement with the laboratory test results of Coyle and Gibson (1970) and Heerema (1979). Toe damping of 0.49 second per meter (recommended for firm to hard clay, silt, and sand) was adopted in these analyses.

6.2.4 Evaluation of Pile Drivability

Preliminary evaluations of pile drivability were conducted for representative conditions underlying the Main Span-East Pier and each Skyway frame based on the subsurface conditions encountered in the 1998 marine borings. For each Skyway frame, a "best" case and a "worst" case pier were selected for analysis. The "worst case" pier was the location with the greatest thickness of relatively deep, dense sand layers above the anticipated pile tip elevation in the associated boring. Conversely, the "best case" pier was the location with the least thickness of deep, dense sand above the anticipated pile tip elevation in the associated boring. The selected "best" and "worst" case piers are tabulated below:



Location	"Best" Case	"Worst" Case
Main Span-East Pier	Pier E2 (Boring 98-26)	Pier E2 (Boring 98-25)
Frame 1	Pier E3-Eastbound (Boring 98-27)	Pier E6-Westbound (Boring 98-41)
Frame 2	Pier E10-Eastbound (Boring 98-33)	Pier E7-Eastbound (Boring 98-49) Pier E7-Westbound (Boring 98-30)
Frame 3	Pier E11-Westbound (Boring 98-34)	Pier E13-Eastbound (Boring 98-43)
Frame 4	Pier E14-Westbound (Boring 98-36)	Pier E15-Westbound (Boring 98-37)

The preliminary drivability analyses for the Main Span-East Pier and Skyway Frames 1 through 4 were for 2.5-meter, open-ended pipe piles. Three pile driving hammers (Menck MHU 500T, Menck MHU 1000, and Menck MHU 1700) were considered in the evaluation. The characteristics of those hammers are summarized on Plate 6.3. The evaluation was based on a preliminary wall thickness schedule provided by TY Lin/M&N. That wall thickness schedule is provided on Plate 6.4. The results of these drivability analyses are preliminary and should be reevaluated after the final pile wall thickness schedule and final driving system have been established.

Wave equation analyses were performed using the hammer, pile, and soil parameters given on Plates 6.3 and 6.4. The GRLWEAP (GRL&A, 1997) computer program was used to model the Menck MHU 500T, 1000, and 1700 hammers. For the purpose of those analyses, the Menck MHU 500T, 1000 and 1700 hammers were considered to be operating at a hammer efficiency of 95 percent. The coefficient of restitution for the ram impacting on the pile cap and the pile cap impacting on the pile were assumed to be 0.98 and 0.95, respectively.

6.3 RESULTS OF PRELIMINARY DRIVABILITY ANALYSES

Both the predicted blow count versus depth and the soil resistance to driving curves estimated from wave equation analyses for the piers considered in this study are discussed in the following sections and illustrated on the pier-specific plates in Appendix A. The estimated pile run and maximum predicted blow count from the analyses are summarized on Plate 6.5.

6.3.1 Computed Soil Resistance to Driving

The computed SRD for each of the piers considered in these preliminary pile drivability analyses is provided in the pier-specific plates in Appendix A at the end of this report. The soil resistance to driving was computed using the Stevens et al. (1982) method outlined in the preceding sections.

The SRD profiles indicate that within the primarily clay Young Bay Mud and Old Bay Mud/Upper Alameda Marine sequences, the coring and plugged soil resistances are relatively similar. In contrast, the SRD estimated for the plugged case is significantly greater than that



estimated for the coring case within the relatively thick and dense sand layers of the Upper Alameda Marine (UAM) Paleochannel Sand and LAA-sand. The UAM Paleochannel Sand is generally present in the vicinity of the Main Span-East Pier. The Skyway pile foundations are expected to be driven into or through the LAA-sand.

6.3.2 Pile Run

The term "pile run" is used to describe the penetration of the pile due to the self-weight of the pile and the weight of the hammer. Preliminary estimates of the pile-run due to self weight and the weight of the hammer were made by comparing an assumed weight of the first pile section and the hammer with the calculated Stevens et al. (1982) lower-bound soil resistance to driving. Those estimates are summarized for each hammer considered on Plate 6.5. As shown on Plate 6.5, the pile run ranges from 9 to 16 meters for the Menck MHU 500T hammer, from 12 to 18 meters for the Menck MHU 1000 hammer, and from 14 to 24 meters for the Menck MHU 1700 hammer. The estimates of pile run presented on Plate 6.5 are preliminary and should be reevaluated based upon the final pile wall thickness schedule, the number and length of pile sections, and the pile driving hammer system.

Use of the sensitivity-based SRD values to evaluate pile run would generally result in values of pile run that increase by up to approximately 70 percent over the values estimated using the Stevens et al. (1982) SRD profiles. The relatively large difference is attributed to the significantly lower SRD values predicted by the sensitivity-based method in the shallower portion of the stratigraphy.

6.3.3 Blow Counts

The predicted blow count profiles for each of the piers considered in these preliminary pile drivability analyses are provided in the pier-specific plates in Appendix A at the end of this report. The predicted blow count profiles in Appendix A are based on the Stevens et al. (1982) soil resistance to driving outlined in the preceding sections. For comparison, the coring case blow counts computed using the sensitivity-based and Stevens et al. (1982) SRD profiles for Pier E7 Eastbound are presented on Plate 6.6.

Young Bay Mud and Old Bay Mud/Upper Alameda Marine Clay Sediments. As described in Section 2.0, the Young Bay Mud (YBM) and Old Bay Mud/Upper Alameda Marine (OBM/UAM) sequences are comprised primarily of marine clay sediments. When driving through those sediments, our experience suggests that the coring cases are generally representative of conditions during continuous driving, while the plugged cases are representative of conditions subsequent to significant delays.

The initial pile section is expected to "run" through the majority of the Young Bay Mud (YBM) sediments under the weight of the pile and hammer. Blow counts in the YBM sediments



are expected to be relatively low, generally under 10 blows per 0.25 meter (bpqm) for the smaller Menck 500T hammer.

Within the clay sediments of the Old Bay Mud/Upper Alameda Marine (OBM/UAM) sequence, the drivability analyses suggest that the piles can be driven relatively easily with the three hammers investigated. The blow counts for the upper-bound coring case with the smaller Menck 500T hammer were less than 70 bpqm and typically less than 50 bpqm. The maximum blow count for the upper-bound plugged case in the clay sediments was typically less than 125 bpqm for the Menck 500T hammer. Those blow counts suggest that even with the smaller hammer, delays during driving in the clay sediments of the OBM/UAM sequence are unlikely to significantly impact the installation of the piles.

Upper Alameda Marine Paleochannel Sand. The Upper Alameda Marine (UAM) Paleochannel Sand is a relatively thick (10- to 20-meter) deposit of dense to very dense sand that underlies the western portion of the alignment. The interpreted lateral and vertical extent of the stratum are discussed in Section 2.0 of this report and shown on Plate 2.11a.

The UAM Paleochannel Sand is 12 to 15 meters thick under the Main Span-East Pier and is expected to significantly impact the pile driving at that location. To achieve 80 MN (tension capacity requirement specified by TY Lin/M&N during preliminary evaluations) of ultimate axial tension capacity at the Main Span-East Pier, will require the piles to be driven through the UAM Paleochannel Sand into the underlying LAA-sand. On the basis of the drivability analyses, the development of plugged conditions (such as during delays) within the UAM Paleochannel Sand could result in refusal even for the larger MHU 1700 hammer. If the pile foundations for the Main Span-East Pier are to be driven through the UAM Paleochannel Sand, supplementary installation techniques may be required. To reduce the potential for encountering refusal to driving within the UAM Paleochannel Sand, delays during driving through those layers should be avoided.

As shown on Plate 2.11a, the UAM Paleochannel Sand is also present beneath Pier E3. However, since this location is interpreted as being along the flank of the channel, the thickness of sequence is estimated to be about 3 to 4 meters. Because the UAM Paleochannel Sand stratum is relatively thin, refusal during driving is generally not expected at Pier E3.

Lower Alameda Alluvium (LAA). As discussed in Section 3.0 of this report, piles supporting Skyway Piers E6 through E16 are generally to be driven 4 meters below the estimated top of the LAA-sand. As shown on Plate 2.4, interpreted structural contours at the top of the LAA-sand range from approximately El. -85 to El. -95 meters. For the Skyway foundations, it is expected that the maximum blow counts during driving will typically occur at or a few meters above the specified tip elevation.





The maximum predicted blow counts at each pier chosen for drivability analysis are summarized on Plate 6.5 and below:

- Blow counts in excess of 250 bpqm may be encountered, even for the coring case, when using the smaller MHU 500T hammer.
- Blow counts above 80 bpqm are expected under coring conditions for the MHU 1000 hammer.
- Under plugged driving conditions, the MHU 500T is likely to meet refusal prior to reaching the specified tip elevations.
- The larger MHU 1700 is generally capable of driving to the specified tip elevations even when plugged. However, as indicated on Plate 6.5, refusal could be encountered at select piers with the MHU 1700 if the pile plugs.

The lower-bound coring case blow counts in the LAA clay cap probably are indicative of the lower-bound blow counts to be expected in the LAA-clay interbeds that may be present at the pile tip elevations. Lower-bound coring case blow counts within the LAA clay cap typically range from 30 to 35 bpqm for the MHU 500T, 20 to 28 bpqm for the MHU 1000, and 10 to 13 bpqm for the MHU 1700.

In general, the drivability analyses suggest that the MHU 500T hammer will be inadequate for driving piles into the LAA-sand. The data suggest that the MHU 1000 hammer has the minimum energy capable of driving the Skyway foundation piles at Piers E7 through E16 to the proposed tip elevations. However, that hammer is likely to encounter refusal above the proposed pile tip elevations at Piers E3 through E5 where the piles are to be tipped in rock or at a number of other pier locations if the pile plugs. With a few exceptions, it should generally be possible to restart driving within the LAA-sand with the Menck MHU 1700 hammer even if delays occur during driving within those intervals.

6.3.4 Driving Stresses

The pile drivability results also provide insight relative to the pile stresses during driving or due to the length of pile stickup. The maximum computed stresses in the piles during driving are listed in the following table. The results show that the maximum computed stresses in each of the pile sections are generally at least 20 percent below the yield stress of steel (approximately 344 MPa).

Pile Section	Menck MHU 500T (MPa)	Menck MHU 1000 (MPa)	Menck MHU 1700 (MPa)
P1	179	228	228
P2	193	262	262
P3	194	262	270
P4	186	248	255



6.4 ANALYSIS OF DRIVABILITY INTO THE FRANCISCAN FORMATION BEDROCK

6.4.1 Introduction

Analyses were performed to evaluate the potential for pile toe damage at Piers E3 through E5. At those piers, the recommended pile tip elevations are approximately 3 meters below the interpreted top of the Franciscan Formation bedrock.

Evaluation of "soil resistance to driving" in rock is difficult to reliably assess due to the large variations in the degree and thickness of weathering and nature of fracturing in the rock. Pile driving experience and wave equation analyses suggest that the ratio of end bearing to total resistance (percent end bearing) plays a significant role in the induced driving stresses. Typically, increases in percent end bearing produce increased driving stresses, with a concentration of stress occurring near the toe of the pile. Therefore, instead of attempting to evaluate SRD values for rock, analyses were conducted that investigated a range of SRD and percent end-bearing values to model the possible effects of driving piles into bedrock.

6.4.2 Analyses

The drivability assessment was performed for the soil profile and recommended tip elevation at Pier E3 Eastbound. Two hammers were considered in these analyses, the Menck MHU 1000 and MHU 1700. Hammer and soil properties used in the analyses are shown on Plate 6.3 and are the same as those used in the previously described preliminary drivability analyses. The pile wall thickness schedule taken from the 85-percent design submittal (TY Lin/M&N, 2000a) is shown in the table below:

Section Length (m)	Wall Thickness (mm)	Cross Sectional Area (mm ²)
0 - 35	68	519,544
35 - 50	57	437,470
50 - 108.5	51	392,382
108.5 - 110.0 (drive shoe)	57	437,470

Note: mm² = square millimeters

The analyses were run for SRD values ranging from 0 to 150 MN and a percent end bearing ranging from 10 to 90 percent.

6.4.3 Results and Discussion

Results of the analyses for the MHU 1700 hammer are presented on Plate 6.7, Figures A and B. Figure A on Plate 6.7 shows a profile of compressive stress in the pile for a range of percent end bearings at an assumed SRD of 105 MN, while Figure B is a plot of percent end bearing versus calculated maximum compressive stress in the pile. The SRD of 105 MN was estimated as an upper bound of the SRD that the MHU 1700 hammer is capable of mobilizing.

On Plate 6.7, Figure A shows the increasing trend of compressive stress with increasing percent end bearing. In addition, Figure A demonstrates the variation of pile stress along the length of the pile. Notable features of the stress profile include the relatively sharp changes (reduction) in stress at the changes in pile wall thickness and also the relatively large stresses computed near the toe of the pile. The profiles show that the maximum compressive driving stresses occur just above the pile driving shoe. Because the driving shoe is thicker than the bottom pile section, the stress in the driving shoe is less than the stress immediately above the shoe. The high stresses at the pile toe are attributed to the superposition of downward and upward (reflected) stress waves in hard driving conditions at the pile toe.

The plot on Figure B of Plate 6.7 indicates that the toe stresses increase relatively quickly when the percent end bearing exceeds about 70 percent for both MHU 1000 and MHU 1700 hammers. Since the MHU 1700 hammer is able to transfer greater energy to the toe of the pile, the predicted stresses exceed about 290 MPa when the percent end bearing exceeds approximately 80 percent.

Near the recommended pile tip elevations, the skin friction component of the lower-bound SRD estimates is approximately 30 to 35 MN. Since the MHU 1700 hammer may be capable of overcoming approximately 100 to 105 MN of soil resistance, the end-bearing component can be on the order of 70 percent if piles are driven into layers hard enough to cause refusal. For the MHU 1000 hammer, the percent end bearing for a lower bound skin friction estimate is only about 50 percent. Past experience has shown that for piles driven into very hard layers with a large hammer, the measured pile toe stresses may be larger than those predicted using drivability analyses. These differences may be due to uncertainties in the wave equation model including dynamic soil properties such as toe quake and damping. Furthermore, for piles driven into bedrock, relatively large toe stresses may develop relatively quickly prior to meeting the recommended refusal blow counts.

To reduce the potential for pile damage during driving as a result of hard driving conditions, the wall thickness of the driving shoe was increased from 57 to 76 mm in the 100-percent PS&E submittal. At Piers E3 through E5, it is recommended that driving (near the recommended tip elevation) be discontinued when dynamic monitoring data suggest that the pile toe stresses exceed $0.85 f_y$.



6.5 FINDINGS FROM THE PILE INSTALLATION DEMONSTRATION PROJECT

6.5.1 Introduction

Three piles were driven for the SFOBB East Span Seismic Safety Project PIDP between October 23 and December 13, 2000. Details of the installation of three 2.438-meter-diameter steel pipe piles and the subsequent interpretation and evaluation of results are provided in the Pile Installation Demonstration Project (PIDP) Geotechnical Report (Fugro-EM, 2001f). The following paragraphs present a summary of the program and findings relevant to pile drivability that were obtained from the PIPD program.

The piles were driven by Manson/Dutra (a joint venture of Manson Construction Co. and The Dutra Group) under contract to Caltrans. The piles were 2.438-meter-OD (outside diameter), steel pipe piles with a variable wall thickness. The piles measured approximately 108.5 meters in total length. Pile Nos. 2 and 3 were driven at a 1H:6V batter, and but Pile No. 1 was driven vertical. Each pile was installed in four sections (A through D, with the A section at the bottom) that varied in length from 26 to 30.5 meters. The pile sections were spliced in the field by welding.

The piles were installed at two locations approximately 50 and 90 meters north of the existing SFOBB East Span alignment. The Primary Test Location (where Pile Nos. 1 and 2 were installed) was approximately to the north of existing Bridge Pier E6, while the Pile No. 3 Test Location was north of existing Bridge Pier E8. Three restrikes were conducted on Pile No. 1, two restrikes on Pile No. 2, and one restrike on Pile No. 3. The PIDP test locations are shown on Plate 1.3.

The two hammers used to drive the piles, Menck MHU 500T and 1700, have rated energies (when used above water) of approximately 550 and 1,870 kilojoules (kJ), respectively. During initial driving and restrikes, Sections B through D of each pile were monitored by two Pile Driving Analyzer (PDA) units. CAPWAP analyses were conducted for at least one hammer blow from: 1) the initial driving of each pile's D section, and 2) each restrike.

6.5.2 Summary of Drivability-Related Findings

The PIDP provided significant insight into the drivability of the large-diameter pipe piles with large offshore hydraulic hammers into the soils near the proposed SFOBB East Span replacement bridge. Some general findings applicable to pile drivability along the proposed East Pier and Skyway structures include:

- Each of the three PIDP piles were successfully driven to the specified pile tip elevation (SPTE) without excessive blow counts or pile damage.



- Piles had little difficulty penetrating to the specified pile tip elevation, and sand layers/lenses located above the identified LAA-sand did not significantly impede driving.
- Piles were driven well into the LAA-sand at these two sites, and mostly likely can be driven into similar soils across the alignment if the same or similar large hammer (MHU 1700) is used.
- Piles cored through the soil during continuous driving, and the soil cores moved up within the pipe pile during penetration.

Soil Resistance to Driving. Estimates of SRD were computed from PDA data as the maximum Case Method capacity (RMX) using a damping coefficient (J) of 0.5. A comparison of RMX (with J=0.5) and CAPWAP capacities showed reasonable agreement, and validated the use of RMX capacities as SRD values.

Some general observations regarding the soil resistance to driving are:

- The PDA-measured SRD profiles for Pile Nos. 1 and 2 are very similar, which indicates that pile batter did not significantly affect SRD at the Primary Test Location.
- The SRD typically increased significantly during initial driving at penetrations below approximately 80 meters. This increase is likely due to increased tip resistance in the very dense, fine to coarse sands within the Lower Alameda Alluvial sediments.
- SRD increased by a factor of 2 to 3 during the 3- to 5-day welding delays between the driving of sections. This increase is attributed to a combination of skin friction setup and the tendency of the piles to initially drive "plugged" following the delays.

Predicted SRD profiles were generated for the Primary Test Location (Pile Nos. 1 and 2) and the Pile No. 3 Test Location. Two ranges of predicted SRD profiles were generated for each location. One range was based on the methodology presented by Stevens et al. (1982) and the other was calculated using the sensitivity-based method. Profiles of measured and predicted coring case SRDs for Pile No. 2 are provided as an example on Plate 6.8.

As shown on Plate 6.8, the upper- and lower-bound coring case SRD profiles based on both the Stevens and sensitivity-based methods predicted the SRD at the PIDP locations reasonably well. Therefore those predictive methodologies should provide reasonable estimates of SRD at other locations along the proposed SFOBB alignment.

Pile Run. Pile run was observed during the stabbing of Section A for all three piles. At the Primary Test Location (Pile Nos. 1 and 2) where the soft Young Bay Mud (YBM) was relatively thin (approximately 4 to 5 meters thick), the piles ran approximately 6 meters. At Pile No. 3 where the YBM is considerably thicker (approximately 20 meters), pile Section 3A ran



approximately 15 meters to the required cutoff elevation. After Section 3B was spliced onto the pile and the hammer imparted approximately 18 blows to the pile, the pile then ran to a total penetration of approximately 19 meters. Production piles are expected to run significant distances through the soft clays of the Young Bay Mud Formation, and particular attention will be required in placing and driving the first pile section at locations where the YBM is thick. Consideration should be given to using initial pile sections that are long enough to extend below the base of the YBM.

Blow Counts. The blow counts recorded during the initial driving of the three piles generally were similar for each pile and typically varied from 12 to 45 bpm. This relatively small range of blow counts is attributed to the fact that hammer energies were controlled to maintain relatively consistent blow counts during initial driving of all pile sections. The lower hammer energies used during the relatively easy driving in the upper soft sediments helped the contractor to: 1) maintain control of the hammer-pile system, 2) prevent the piles from running, and 3) maintain the pile alignment. By controlling the hammer energies during driving, there were no significant differences in the recorded blow counts between the two hammers or within the different geologic units underlying the Young Bay Mud.

Blow counts increased by factors of two to three times during the elapsed time between the driving of two sections. The increase in blow count is due to "setup" along the soil-pile interface (discussed in Section 5.0) as well as the tendency for the piles to act plugged at the very beginning of driving after a significant period of setup. After approximately 3 to 5 meters of driving, the blow counts typically returned to values similar to those observed at the end of initial driving of the previous section.

The PIDP also provided a means to validate the drivability model that has been adopted for this project. Wave equation analyses were run with the selected pile, hammer, and soil parameters (including SRD predicted from both the Stevens and sensitivity-based methods) at the measured hammer energies (from PDA data). Plate 6.9 presents a profile of observed and predicted blow count versus pile penetration for PIDP Pile No. 2.

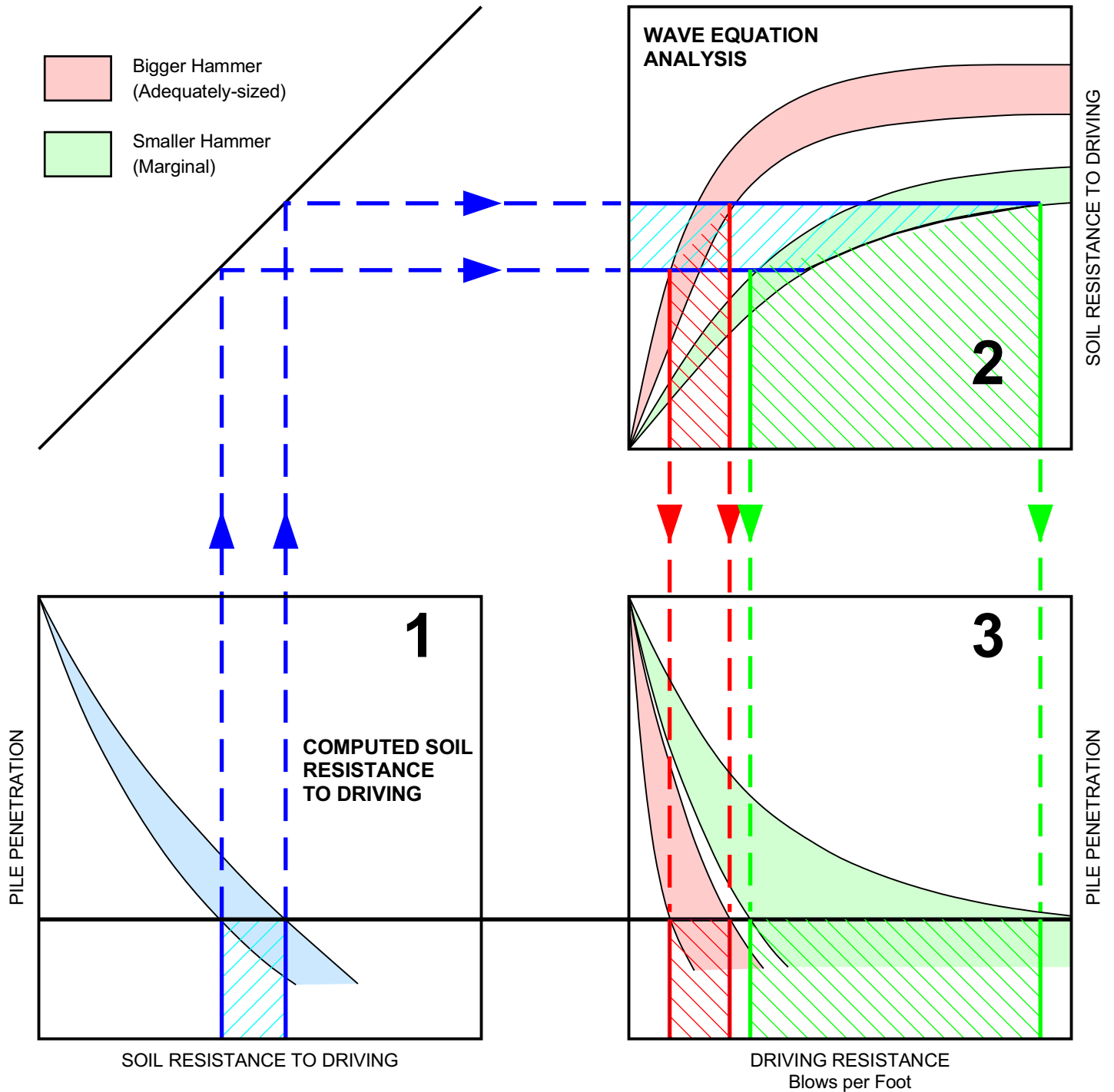
The observed blow counts tend to follow the lower bound of the blow counts estimated using SRD from the Stevens method and are generally bounded by the blow counts estimated using SRD from the sensitivity-based method. At penetrations above 40 meters, the predicted blow counts were typically higher than the observed blow counts. These discrepancies are likely due to the difficulties in accurately modeling pile driving behavior of large-diameter piles driven with a large pile driving hammer (operating at relatively low energy settings) into the relatively soft sediment encountered in the upper portions of the soil profile. Blow counts predicted using the sensitivity-based method SRD seem to better match the blow counts in the softer sediments in the upper 40 meters.

The predicted and observed blow counts also diverge at the beginning of driving of each pile section due to the setup that occurred between the driving of pile sections. The presented blow count predictions assume continuous driving conditions and do not account for pile setup (and associated increases in SRD) during driving delays such as those that occurred during the splicing/welding of pile sections. Typically after about 3 to 5 meters of driving, the setup is broken down and the predicted blow counts tend to reasonably approximate the observed blow counts.

Overall it appears that the method(s) used to estimate SRD and input parameters to the wave equation model were reasonable and can be used with added confidence to predict drivability of production piles.

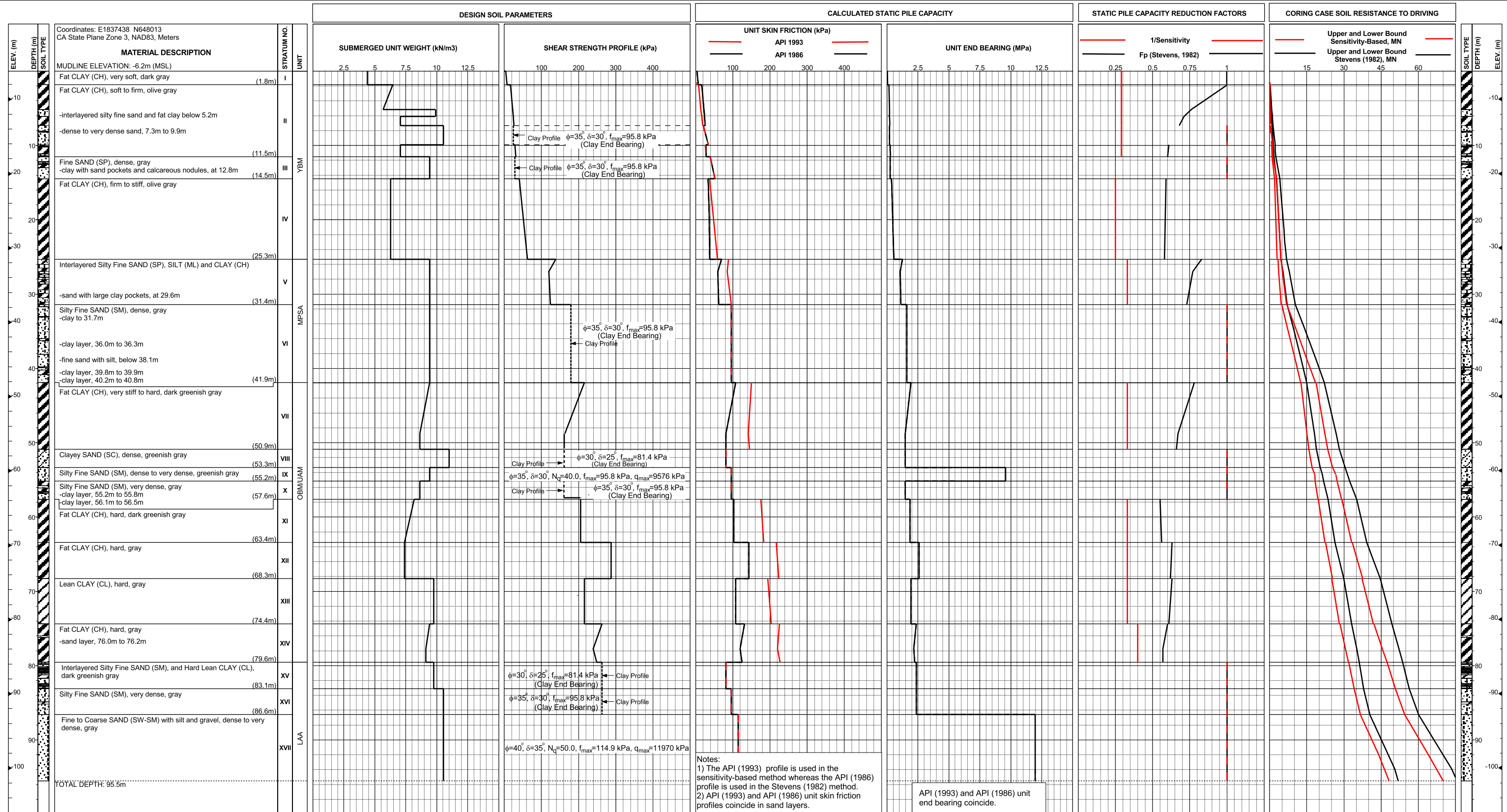
Driving Stresses. Maximum measured driving stresses in the piles typically occurred at the pile toe during the end of initial driving and restrikes. The compressive stresses were as high as approximately 330 MPa or 90 percent of the pile steel yield strength. Pile toe stresses should be closely monitored during production pile driving.





SCHEMATIC ILLUSTRATION OF PILE DRIVABILITY ANALYSIS
 SFOBB East Span Seismic Safety Project





COMPARISON OF CALCULATED SOIL RESISTANCE TO DRIVING PROFILES
Pier E7-Eastbound (Boring 98-49)
 SFOBB East Span Seismic Safety Project





HAMMER PROPERTIES

	Menck MHU 500T	Menck MHU 1000	Menck MHU 1700
Rated Energy, kN-m (kJ)	550	990	1,670
Hammer Efficiency, %	95	95	95
Weight of Ram, kN	295	565	924
Weight of Pile Cap, kN	256	276	373
Coefficient of Restitution			
Ram on Pile Cap	0.98	0.98	0.98
Pile Cap on Pile	0.95	0.95	0.95

PILE PROPERTIES

Diameter, m	2.5
Length, m	See Plate 6.4
Wall Thickness, mm	See Plate 6.4
Unit Weight, kN/m ³	77
Modulus, kN/m ²	2.1 x 10 ⁸

SOIL PROPERTIES

Quake, cm	
Side	0.254
Tip	0.254
Damping, sec/m	
Side	0.194 to 0.361
Tip	0.49
Tip Resistance, %	2 to 55

SUMMARY OF WAVE EQUATION PARAMETERS

SFOBB East Span Seismic Safety Project



Section	Section Length (m)	Wall Thickness (mm)	Yield Strength (MPa)
P-4	26.5	70	345
1.5-m Cut-Off Allowance			
P-3	8	70	345
	18	62	345
1.5-m Cut-Off Allowance			
P-2	13.5	62	345
	17	40	345
1.5-m Cut-Off Allowance			
P-1	29	40	345
	1.5	51	345

WALL THICKNESS SCHEDULE USED IN PRELIMINARY DRIVABILITY ANALYSES
2.5-Meter-Diameter Pipe Pile Composite Profile
 SFOBB East Span Seismic Safety Project





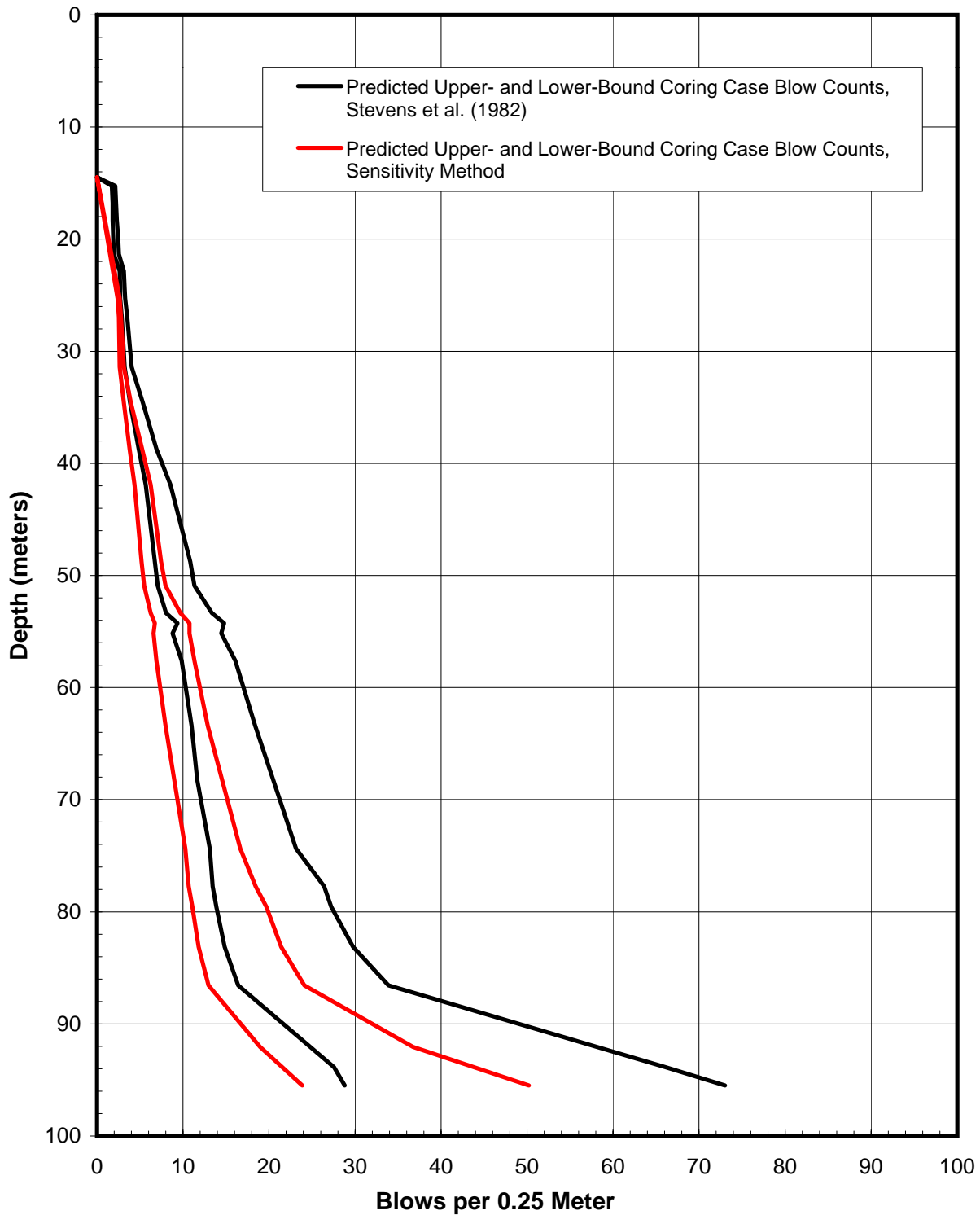
Pier/Boring	Tip Depth (m)	Maximum Blowcounts (blows per 0.25m)								
		Approx. Pile Run (m)			Coring			Plugged		
		500T	1000	1700	500T	1000	1700	500T	1000	1700
East Pier										
(98-26)*	82	15-17	16-19	17-21	34 - 55	24 - 40	13 - 22	>250 - R	218 - >250	97 - >250
(98-25)*	82	13-15	16-18	18-20	36 - 61	26 - 43	14 - 24	R - R	>250 - R	203 - R
Frame 1										
(E3-EB, 98-27)	87	11-Sep	13-15	14-15	55 - 138	40 - 82	20 - 40	R - R	R - R	>250 - R
(E6-WB, 98-41)	88	9-11	14-16	20-24	52 - 146	39 - 81	20 - 41	R - R	170 - R	76 - 354
Frame 2										
(E7-EB, 98-33)	87	12-14	14-15	18-20	42 - 103	31 - 64	17 - 32	R - R	R - R	>250 - >250
(E7-WB, 98-30)*	88	11-12	17-18	21-23	44 - 98	30 - 56	17 - 32	154 - >250	70 - 130	44 - 75
(E10-EB, 98-49)*	91	11-13	12-18	12-18	41 - 85	32 - 55	16 - 30	159 - >250	89 - 166	45 - 76
Frame 3										
(E11-WB, 98-34)*	91	9-10	12-14	14-17	42 - 89	29 - 52	16 - 30	233 - R	96 - 205	58 - 103
(E-13EB, 98-43)	88	11-12	14-17	17-19	55 - 156	40 - 84	21 - 42	R - R	R - R	>250 - R
Frame 4										
(E14-WB, 98-36)	92	12-15	15-17	18-22	50 - 150	35 - 74	20 - 38	R - R	R - R	162 - R
(E15-WB, 98-37)	90	10-12	12-16	12-16	66 - >250	46 - 120	25 - 56	R - R	>250 - R	133 - R

Notes:

1. * Denotes indicated max. blowcounts occurred above the pile tip
2. R denotes that the soil resistance exceeded the capacity of the hammer
3. Pile Run is the depth to which the pile is expected to penetrate under the weight of the hammer-pile system. Pile Run is estimated as the depth at which the Stevens et al. (1982) lower bound coring soil resistance to driving equals sum of pile plus hammer weight.

SUMMARY OF PRELIMINARY DRIVABILITY ANALYSES
SFOBB East Span Seismic Safety Project





**COMPARISON OF PREDICTED CORING CASE BLOW COUNTS
Pier E7-Eastbound (Boring 98-49)**

Menck MHU-1700, 2.5-Meter-Diameter Driven Pipe Piles
SFOBB East Span Seismic Safety Project



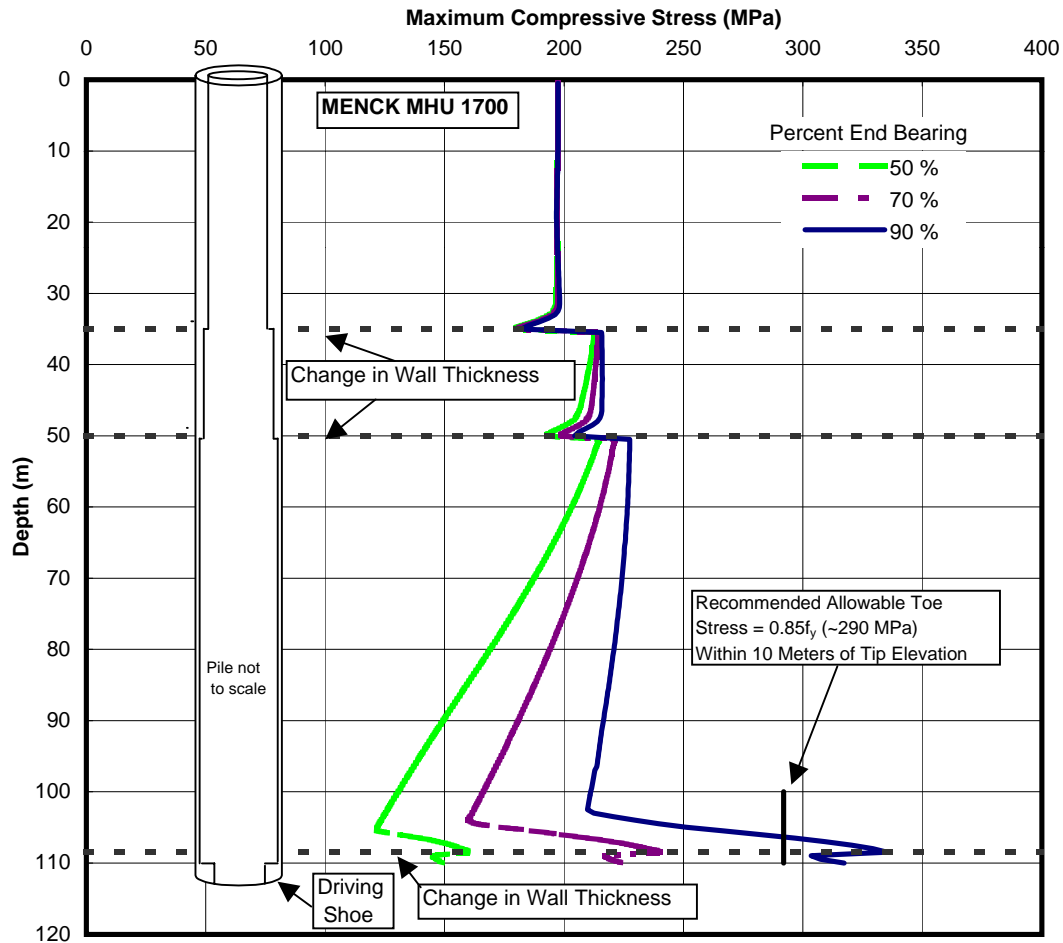


Figure A Profile of Compressive Stress, SRD = 105 MN

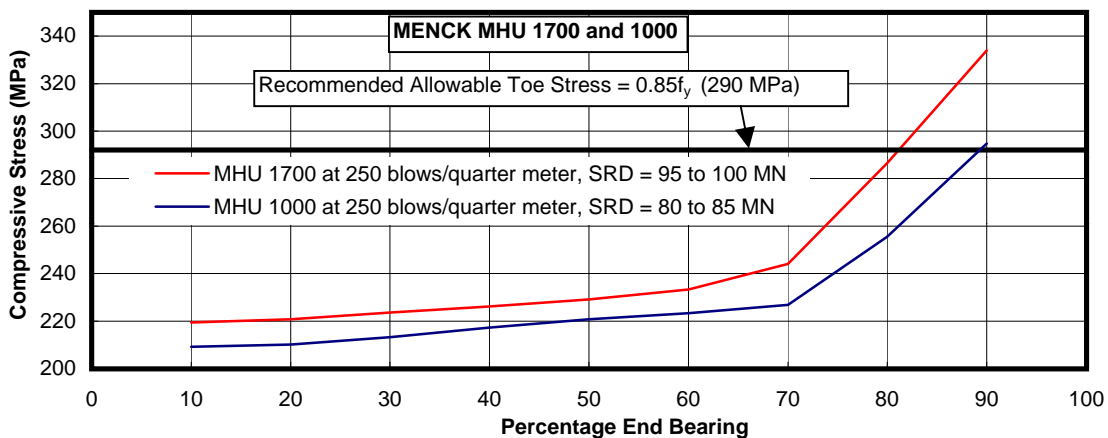
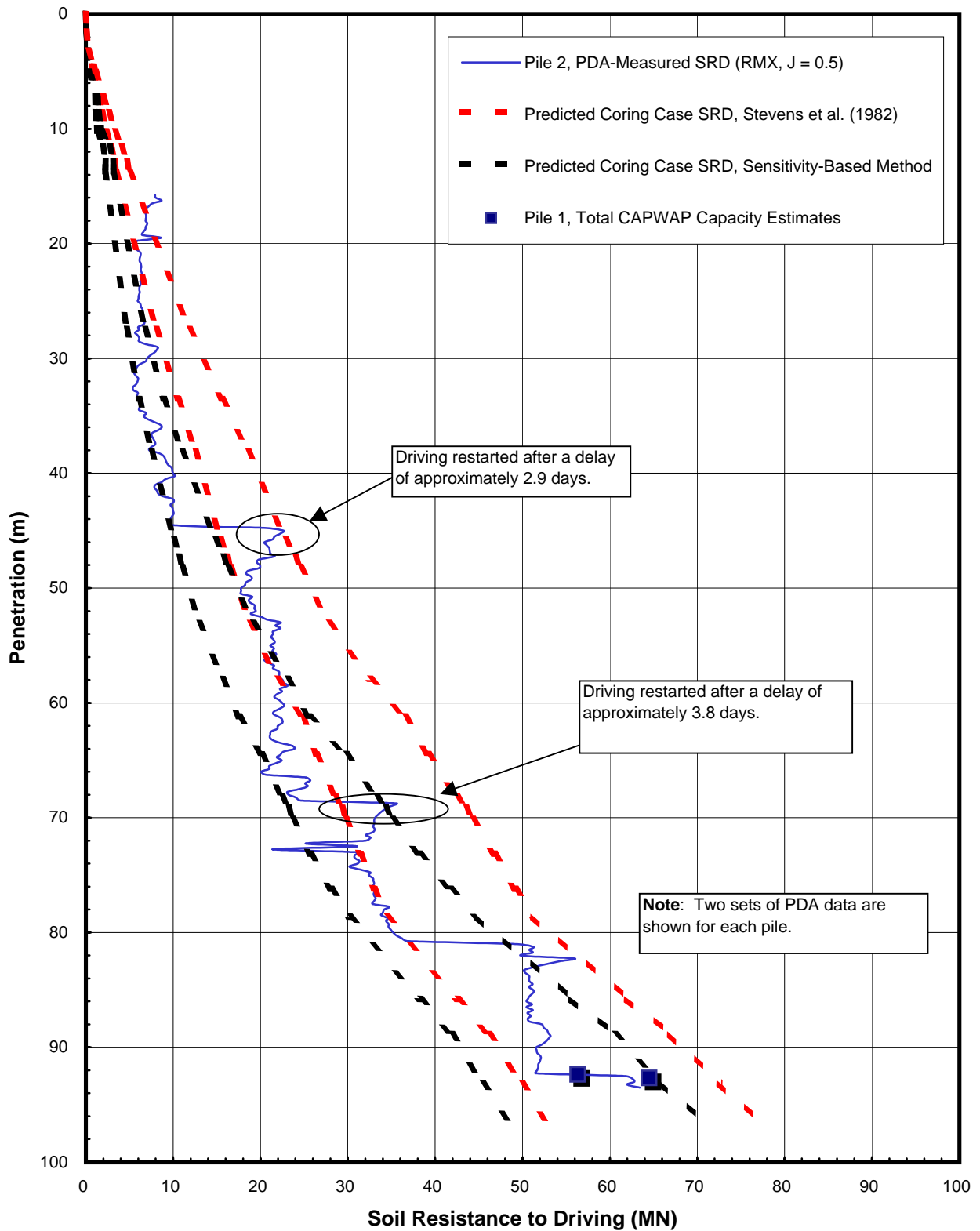


Figure B Effect of Percent End Bearing on Maximum Compressive Stress

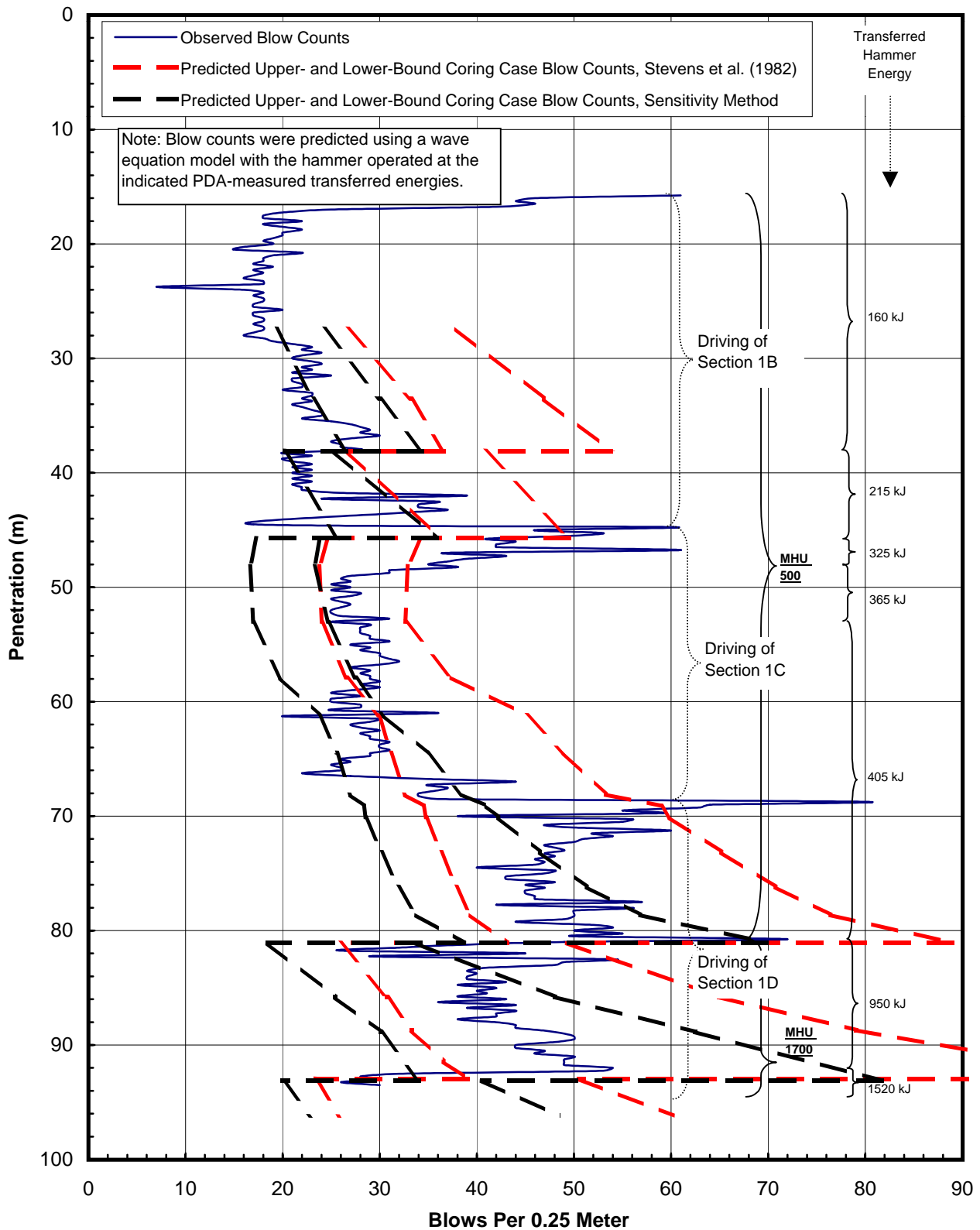
DRIVABILITY OF PILES TIPPED IN FRANCISCAN FORMATION BEDROCK
Piers E3 through E5 Eastbound and Westbound
 SFOBB East Span Seismic Safety Project





PDA-MEASURED AND PREDICTED SOIL RESISTANCE TO DRIVING, PILE NO. 2
Pile Installation Demonstration Project
SFOBB East Span Seismic Safety Project





OBSERVED AND PREDICTED BLOW COUNTS, PILE NO. 2
 Pile Installation Demonstration Project
 SFOBB East Span Seismic Safety Project



**SECTION 7.0
PILE INSTALLATION CONSIDERATIONS
AND RECOMMENDATIONS**

SECTION 7.0

7.0 PILE INSTALLATION CONSIDERATIONS AND RECOMMENDATIONS

7.1 INTRODUCTION

The installation of steel pipe piles for the Main Span-East Pier and Skyway structures will need to consider several site-specific and design issues. These include (but are not limited to):

- Soft near-surface soils that allow piles to penetrate significant distances under self-weight and the weight of the hammer,
- Possible local variations in soil conditions,
- Possible dense soils above the pile tip elevations that may result in hard driving,
- Soils that gain strength during delays in driving,
- Possible subsurface debris,
- Wind and wave excitation, and
- Tidal flow fluctuation.

For typical Caltrans projects, pile installation and pile acceptance are generally in accordance with Section 49-1 of Caltrans Standard Specifications (1995). In standard Caltrans practice, a minimum bearing criteria (as verified by the blow count during driving) is included in pile driving specifications to demonstrate that piles are capable of carrying the design loads. Pile foundations supporting the Main Span-East Pier and Skyway structures, however, derive much of their axial capacity from side shear resistance from clay soils. Therefore, the piles are anticipated to experience pile setup subsequent to initial driving. As described in Section 5.0, the time required to reach approximately 80 percent of the ultimate side shear capacity is anticipated to range from approximately 7 to 9 months for the 2.5-meter-diameter piles. Therefore, in view of the potential impact to construction cost and schedule, it is not considered advisable to follow the typical Caltrans acceptance criteria based on the Engineering News Record (ENR) formula.

7.2 DRIVING SYSTEM SUBMITTAL

Prior to installing driven piling, the contractor should provide a driving system submittal, including drivability analysis, in conformance with the provisions in Section 5-1.02, "Plans and Working Drawings," of the Caltrans Standard Specifications (1995). All proposed driving systems (i.e., each hammer that may be brought onto the site) should be included in the submittal. It is recommended that a minimum of 3 weeks be provided exclusively for review of the driving system submittal.



The driving system submittal should contain an analysis showing that the proposed driving systems will install piling to the specified tip elevation in accordance with the criteria described in the subsequent sections. Drivability studies included in the submittal should be based on a wave equation analysis done by using a computer program that has been approved by the engineer. The analysis should be performed for the pile schedule/details shown on the plans. Drivability studies should model the Contractor's proposed driving systems, including the hammers, hammer cushion, driving helmet, and any pile cushions and followers. The analyses should consider a range of total soil resistance to driving and associated percentage shaft resistance for plugged and unplugged cases. The range of soil resistance to driving and percentage shaft resistance should be determined for site conditions ranging from 10 meters above to 5 meters below the specified pile tip elevation shown on the plans. Separate analyses should be completed at elevations above the specified pile tip elevations where difficult driving or pile splices are anticipated. As a minimum, submittals should include the following:

- Complete description of soil parameters used, including soil quake and damping coefficients, skin friction distribution, percentage shaft resistance, and total soil resistance to driving;
- List of all hammer operation parameters assumed in the analysis, including rated energy, stroke limitations, and hammer efficiency;
- Completed "Pile and Driving Data Form";
- Results from drivability analyses should include plots of:
 - Maximum pile head and pile toe compressive stress versus blows per 250 mm
 - Soil resistance to driving versus blows per 250 mm;
- Estimated range of expected pile penetration due to self-weight and the weight of the hammer; and
- Copies of all test results from any previous pile load tests, dynamic monitoring, and all driving records used in the analyses.

When the drivability analyses indicate that steel shell penetration rates are less than 250 mm per 200 blows and that the driving stresses will exceed 80 percent of the specified yield strength of the steel shell that is more than 5 meters above the specified pile tip elevation, then the submittal should include assumptions and procedures for soil plug removal.

7.3 PILE TIP ELEVATIONS

Recommended pile tip elevations for the proposed 2.5-meter-diameter steel pipe piles planned for Piers E3 through E16 are provided on Plate 3.1. Two alternative pile tip elevations for the Main Span-East Pier are presented on Plate A-6 in Appendix A. For piles that have tip elevations within the Lower Alameda Alluvium (LAA), it is recommended that a minimum



5-meter underdrive allowance be included in the design of the pile wall thickness schedule. The results of preliminary drivability analyses performed for Pier E3 Eastbound are discussed in Section 6.0. Those analyses suggest that, if the pile were to plug, there would be a potential for refusal during driving within sand layers of the LAA (above bedrock). Additionally, the pile tip elevations at that location are specified to be 3 meters below the interpreted top of bedrock elevation. In view of the likely termination of driving above the specified tip elevation for those piers, it is recommended that a larger underdrive allowance be provided for Piers E3 through E5.

7.4 PILE SCHEDULE

Minimum Wall Thickness. It is recommended that pipe piles with a minimum wall thickness greater than that given in Sections 6.10.6 and 12.5.7b of API RP 2A (API, 1993a,b) be used to more fully utilize the driving capability of high-energy hammers and to reduce stresses in the pile during hard driving.

Driving Shoe. The use of a driving shoe at the pile tip is recommended to prevent damage from hard driving. The inside clearance provided by the driving shoe also acts to reduce skin friction on the inside of the pile, and may delay plugging by reducing lateral stresses developed in the soil plug. The driving shoe should be at least 1.5 meters long, have the same outside diameter as the pile, and have an inside clearance of at least 6 mm (i.e., the inside diameter should be 12 mm less than the bottom pile section).

7.5 DELAYS AND REDRIVING

During driving, it will be necessary to interrupt driving operations to change hammers or add pile sections for pipe piles. The interruption to driving operations may last over 24 hours. The required welding time increases with wall thickness. For example, in the offshore industry, typical welding times for 36-, 50-, and 75-mm wall thicknesses are approximately 4, 8, and 16 hours, respectively. Welding times from the PIDP indicate that delays during welding may be longer than those estimates. In addition, delays on the order of several days may result from bad weather or equipment breakdown.

During delays, clays will generally gain strength as excess pore pressures dissipate and the soil particles reorient themselves. This phenomenon is commonly referred to as setup. A similar phenomenon may also occur in fine-grained granular deposits. When piles are redriven after setup has occurred, increased blow counts should be expected for delays longer than about 2 hours. Interruptions in driving should be kept as short as possible and backup hammers should be available.

It is recommended that pile splices not be made at elevations where the pile tip will be within dense sand layers. The requirement for continuous driving through deep sand layers is particularly critical for Piers E2 through E5. At the Main Span-East Pier (E2), piles driven to the



Lower Alameda Alluvium will have to be driven through a thick Upper Alameda Marine Paleochannel Sand layer. Piers E3 through E5 are to be driven through sand layers of the Lower Alameda Alluvium to reach the specified tip elevation in bedrock. At both those locations, drivability analyses suggest that refusal may be encountered if the pile were to plug.

7.6 DYNAMIC MONITORING

We recommend that dynamic monitoring with a Case-Goble type PDA be performed when installing the last add-on of each pile for Piers E2 through E16 Eastbound/Westbound. Pile monitoring should be performed by Caltrans or its representatives using equipment provided by Caltrans or its representatives.

7.6.1 Preparation of Piles to be Monitored

The Special Provisions of the construction plans and specifications (P&S) should include allowances for the installation of dynamic monitoring instruments on the last add-on. Dynamic monitoring instrumentation is typically bolted onto opposite sides of the pile to cancel bending effects from eccentric hammer blows. During typical monitoring operations for large-diameter piles, three 5.6-mm- (1/32-inch-) diameter holes are drilled and tapped on opposite sides of the pile add-on at about two pile diameters from the top. To provide strain relief for the cable connecting the instrumentation to the data acquisition system, the cable is attached to an eyebolt located midway between the sensor locations. The holes are drilled about 25 mm into the pile wall. Typically, a three-man crew can drill and tap the holes in an average time of about 45 minutes per pile with the pile located on the materials barge, on the deck of the pile driving barge, or in the fabrication yard before loadout.

7.6.2 Mounting Instrumentation on the Pile

It is often possible for instrumentation to be bolted to the pile prior to lifting and stabbing. However, extreme care should be used during the lifting and positioning of the pile section to avoid damaging the instrumentation and associated cables. If it is decided that damage could occur during handling, the monitoring crew (working from a personnel basket) can attach the instrumentation in about 30 minutes. The Special Provisions should allow the engineer to determine if the contractor's handling operations are such that instrumentation may be damaged. Additionally, the contractor should be directed to halt operations, if needed, so that instrumentation can be mounted from a personnel basket after the last pile add-on has been made.

For piles driven with an underwater hammer, underwater strain transducers and accelerometers will need to be specially fabricated. Each sensor will have a 120-meter-long watertight cable. Fabrication of underwater instrumentation typically requires a lead time of at least 8 weeks. Similar to above-water instrumentation, the transducers can be bolted to the pile prior to lifting and stabbing. If it is decided that damage could occur during handling, the





instrumentation can be attached after the pile has been made. A personnel basket can be used while the instrument mounts are above water. However, divers will be required if the mounts are underwater. Since an operation using divers will take about 6 hours, it is recommended that instruments be mounted above water.

7.6.3 Removal of Instrumentation

The Special Provisions of the P&S should include guidance relative to the removal of instrumentation. The driving template should provide sufficient clearances for monitoring instruments such that piles can be driven to the specified tip elevation without damage to the monitoring instruments.

For overwater hammers, if instruments are accessible at the end of driving, personnel from the monitoring crew can walk out to the pile and remove the sensors. Alternatively, removal of instrumentation can be done from a personnel basket. Removal typically takes about 5 minutes.

For underwater hammers, the instruments can either be sacrificed or removed and re-used with the help of divers.

7.7 ACCEPTABLE HAMMER TYPES

The 2.5-meter-diameter steel pipe piles for Piers E2 through E16 should be installed with impact hammers that are approved in writing by the engineer. Impact hammers should be air/steam or hydraulic. Drop hammers and mechanical or hydraulic vibratory hammers will likely be inadequate relative to advancing the pile to the specified tip elevations. To assist with pile handling at shallow penetrations, vibratory hammers may be used. However, to reduce the potential for vibratory hammers to degrade soil side friction, it is recommended that vibratory hammers not be used below El. -35 meters.

The minimum hammer efficiency is dependent on the type of hammer selected. The hammer efficiency is defined as the ratio of the available ram kinetic energy at impact to the theoretical ram potential energy calculated at the equivalent hammer stroke. The system efficiency is defined as the ratio of the measured energy transmitted to the pile to the rated hammer energy. Adequate hammer performance should be defined by the system efficiency. Recommended minimum values of hammer and system efficiency are tabulated below:

Hammer Type	Recommended Minimum	
	Hammer Efficiency (%)	System Efficiency (%)
Air/Steam	65	50
Hydraulic	90	75



7.7.1 Primary Hammer

When performing satisfactorily, the contractor's primary hammer should be a hydraulic hammer capable of transmitting a minimum of 1,275 kJ of energy to the pile top. For example, if the system efficiency is 75 percent, the primary hammer should have a rated energy of at least 1,700 kJ. The contractor should demonstrate that the primary hammer is in good working order and capable of transmitting the specified minimum energy to the pile prior to the use of a smaller secondary hammer. Satisfactory performance of the primary hammer should be verified by dynamic monitoring during construction.

7.7.2 Secondary Hammers

In general, it is considered preferable for piles to be driven to the specified tip elevation with the primary hammer. However, the following recommendations are presented to assist with the evaluation of smaller secondary hammers that might be proposed by the contractor.

Preliminary drivability analyses suggest that it may be difficult to restart driving with the primary hammer if refusal occurs under coring conditions with a smaller secondary hammer. To reduce the potential for refusal under coring conditions, we recommend that secondary hammers: 1) be capable of transmitting a minimum of 375 kJ of energy to the pile top, and 2) transmit sufficient energy to drive piles to the specified tip elevation at a penetration rate of not less than 3 mm per blow count for continuous driving under coring conditions.

To reduce the potential for delays during driving within dense sand layers above the recommended pile tip elevation, it is recommended that secondary hammers not be used below El. -50 meters for Piers E2 through E5.

7.8 REFUSAL BLOW COUNT CRITERIA

The reasons for defining pile refusal as well as an example definition of pile refusal are given in Section 12.5.6 of API RP 2A (API, 1993a,b). As stated in API RP 2A, the definition of pile refusal is primarily for contractual purposes to define the point where pile driving with a particular hammer should be stopped and other methods instituted (e.g., drilling, jetting, or using a larger hammer). The definition of pile refusal is also meant to reduce the possibility of causing damage to the pile and hammer. The recommendations for defining pile refusal are based on the example definition provided in API (1993a,b).

It is recommended that pile refusal be defined as the point where pile driving resistance exceeds either 250 bpqm for six consecutive 0.25-meter increments, or 650 bpqm of penetration. If there has been a delay in pile driving operations for 1 hour or longer, the refusal criteria stated above should not apply until the pile has been advanced at least 0.25 meter following the



resumption of pile driving. However, in no case should the blow count exceed 650 blows for 0.12 meter.

7.9 ALLOWABLE DRIVING STRESS CRITERIA

Generally, the highest stress level in the life of a pile occurs during driving. For efficient utilization of both the pile driving hammer and pile material, it is desirable to stress the pile to the practical limit during driving. The high strain rate and temporary nature of the loading allow a substantially higher allowable stress during driving than for static loading.

Pile driving stresses for the last pile add-on should be monitored using dynamic monitoring equipment. It is recommend that driving generally be terminated when the maximum driving stress is greater than $0.9 f_y$, where f_y is the yield strength of the steel. The accuracy of the measured force and velocity signals is typically ± 5 percent.

Piles supporting Piers E3 through E5 are to be tipped in bedrock. Additionally, the Main Span-East Pier (Pier E2) is at a location where the Lower Alameda Alluvium onlaps the Franciscan Formation, and only a thin layer of Lower Alameda Alluvium is present. Since there is a relatively high probability that the piles (for Piers E3 through E5) will encounter bedrock above the recommended tip elevation, there is a potential for the pile toe to be damaged prior to the refusal criteria being met. Although less likely, a similar situation may develop at the Main Span-East Pier. Therefore, it is recommended that the driving stresses at the toe of the piles be closely monitored. To reduce the potential for damage to the tips of those piles, driving should be terminated when driving stresses at the toe of the piles for Piers E2 through E5 exceed $0.85 f_y$.

Driving stresses should be reduced to an acceptable level by proper selection of the pile driving hammer and hammer stroke. When driving stresses are excessive and hammer stroke cannot be reduced without encountering refusal, pile driving should be terminated before the refusal blow count (as defined above) is obtained.

7.10 MINIMUM BLOW COUNT CRITERIA (IF NEEDED)

In general, Fugro-Earth Mechanics joint venture believes that no minimum blow count criteria is required at the specified tip elevation for the large-diameter steel pipe piles proposed for Piers E17 through E22 Eastbound/Westbound of the Oakland Shore Approach. The specified tip elevations proposed for piles supporting those piers provide for a factor of safety of 2.0 against static axial loads from skin friction resistance alone.

The TY Lin/M&N joint venture, however, has requested guidance in developing a minimum blow count criteria for the Main Span-East Pier and Skyway structure piles. The following information is in response to that request and describes a technique that has been used for other projects involving the installation of large-diameter pile foundations in clay soils. This



information, even if not included in the Special Provisions of the P&S, should be provided to the project Resident Engineer during construction.

Minimum blow count criteria are typically included to reduce the potential for the foundation design to be impacted by variability in the pile bearing strata. In standard Caltrans practice, a minimum bearing criteria (as verified by the blow count during driving) is included in pile driving specifications to demonstrate that the piles are capable of carrying the design loads. However, in view of the relatively long setup periods predicted for the large-diameter steel pipe piles, demonstrating design pile capacity by pile restrike is likely to adversely impact construction cost and schedule. Thus, evaluating the design pile capacity at the end of driving requires modeling the degradation of soil resistance during pile driving. Stevens et al. (1982) suggest that a blow count that is representative of a lower-bound, degraded pile capacity is the predicted blow count for the lower-bound, coring case soil resistance to driving. That suggestion appears to be verified by observation during the PIDP (Fugro-EM, 20001f). Consequently, blow count values that are less than the lower-bound, coring case blow count may warrant additional evaluation prior to pile acceptance.

Predictions of soil degradation during driving involve some level of uncertainty. Sensitivity analyses performed by TY Lin/M&N suggest that pile performance is relatively insensitive to end bearing at the tip of the pile. The upper bound of predicted pier settlements (which may be excessive) is associated with cases that model piles tipped in clay layers above the LAA-sand. Therefore, as a minimum criterion, the blow count (during continuous driving) at the specified tip elevation should exceed the predicted lower-bound, coring case blow count that is interpreted within clay layers immediately above the interpreted top of the LAA-sand (i.e., within the LAA-clay cap) at that pier. That minimum blow count can be established from the driving system submittal for: 1) each hammer that the contractor intends to use, and 2) a range of hammer efficiencies. The estimated lower-bound, coring case blow counts within the LAA-clay cap for Menck MHU 500T, 1000, and 1700 hammers are summarized in Section 6.3.3. The estimated lower-bound coring cases in the LAA-clay cap range from 10 to 13 bpqm for an MHU 1700 hammer operating efficiently at full stroke.

7.11 PILE ACCEPTANCE CRITERIA

The recommended tip elevations for the Skyway structure piles supporting Piers E3 through E16 are provided on Plate 3.1. Alternative tip elevations for the Main Span-East Pier are provided in Appendix A (Plate A-6). Piles driven to the design tip elevation should be accepted.

Analyses to evaluate the performance of pile-supported piers that encounter refusal above the specified tip elevation were performed by TY Lin/M&N. TY Lin/M&N have indicated that: a) the performance of piers is satisfactory for piles encountering refusal up to 5 meters above the recommended tip elevation, and b) that the design pile wall thickness schedule provides for as



much as 10 meters of underdrive for Piers E3 through E5, and 5 meters of underdrive for the remaining Skyway structure piers. Therefore, piles also may be accepted if refusal or excessive driving stresses (as defined above) are encountered within 10 meters and 5 meters of the recommended tip elevation for Piers E3 through E5 and Piers E6 through E16, respectively. Pile acceptance should be contingent upon the satisfactory performance of the contractor's approved primary hammer. Similar recommendations are applicable to the Main Span-East Pier once the underdrive allowance has been established.

If refusal to driving is encountered above the recommended tip elevation with a secondary hammer that is smaller than the contractor's approved primary hammer, the contractor should be required to replace the smaller hammer with the primary hammer. Driving with the primary hammer should resume within 48 hours after the smaller hammer reaches refusal. When refusal is the result of unsatisfactory performance of the contractor's primary hammer, the problem should be corrected and the pile redriven.

If a pile reaches refusal more than 10 meters (Piers E3 through E5) or 5 meters (Piers E6 through E16) above the specified tip elevation when being driven with a satisfactorily performing primary hammer, remedial installation procedures should be undertaken if directed by the engineer. If the contractor is unable to restart driving after equipment breakdown within 5 meters of the specified tip elevation, the Special Provisions of the P&S should allow for a 24-hour evaluation period to determine whether the pile can be accepted. If the pile cannot be accepted, the contractor should be required to initiate remedial installation procedures as described below.

7.12 REMEDIAL INSTALLATION PROCEDURES

The computed ultimate pile capacities that were used for pile design were based on the assumption that piles will be driven to the desired penetration without supplemental drilling or jetting. Since pre-drilling may compromise the soil resistance on the pile, it is recommended that the procedure not be used for the installation of steel pipe piles.

In the event that a pile has met refusal to driving more than 5 meters above design penetration, jetting or drilling within the steel shell may be used to remove the soil plug with the approval of the engineer. Soil plug removal should not be allowed to disturb the soil in advance of the pile toe. In general, it is recommended that soil plug removal extend down to no more than 7 meters above the pile tip at that time.

Procedures for jetting or drilling should be submitted to the engineer for approval. If jetting or drilling is required, the contractor should be required to maintain standard logs and submit copies of these logs to the engineer.



7.13 PILE CLEAN OUT

7.13.1 Placement of Structural Concrete

After the required pile penetration has been reached, a portion of the soil plug will be removed as required by design for placement of the reinforcement cage and structural concrete. The project plans show that the Skyway piles should be cleaned out to elevations ranging from El. -63 meters to El. -71 meters. For piles driven to the recommended tip elevations shown on Plate 3.1, this will result in a soil plug that is approximately 21 to 35 meters thick. Within the limits of the Skyway structures, the clean out elevations generally fall within the Old Bay Mud/Upper Alameda Marine sediments. The available subsurface data suggest that those layers are composed primarily of very stiff to hard fine-grained materials with local dense sand layers. TY Lin/M&N have indicated that dewatering is required prior to placement of structural concrete. To reduce the potential for deterioration of the top of the soil plug, a seal course could be placed above the remaining soil plug prior to dewatering. A positive hydrostatic head should be maintained inside the pile during pile cleanout and during the placement and curing of the tremie seal.

7.13.2 Installation of Seismic Monitoring Instruments

Caltrans plans to install a Strong Motion Detection system for the planned replacement East Span of the San Francisco-Oakland Bay Bridge. The detection system is planned to include downhole sensors inside the southeast pile of Pier E6. The lowest sensor is planned to be approximately 7 meters above the recommended tip elevation for Pier E6. The soil plug in the pile is to be removed down to the elevation of the sensor in that pile.

To reduce the potential for pile cleanout to negatively impact the performance of the pile, the Special Provisions of the P&S should require very close scrutiny of the contractor's proposed cleanout procedures. The contractor's planned procedures should be submitted for the engineer's review to evaluate if cleanout can be performed in a controlled fashion. Further, the field operation should be closely monitored to ensure that the contractor's operations do not compromise the soil plug below the cleanout depth.

It is recommended that the casing for the sensor be grouted in place while maintaining a positive hydrostatic head inside the pile. Subsequently, the seal course concrete can be placed below the cleanout elevation required for the placement of structural concrete.

7.14 PILE SETUP AND CONSTRUCTION SCHEDULE

Installation of the piles for the Main Span-East Pier and Skyway structures is expected to remold the soil surrounding the pile, which will reduce the pile capacity at the end of driving. However, as discussed in Section 5.0, the capacity of the pile is expected to set up over time.



The reduced capacity of the pile at the end of initial driving and the subsequent setup of pile capacity should be considered by the contractor during construction. As discussed in Section 5.0, unbalanced cantilever construction techniques and subsequent jacking of the bridge spans are anticipated to cause relatively large loads on the piles during construction.

The contractor is responsible for the performance of the pier foundations during construction. Construction loads should be applied to the pile only when adequate pile stiffness and capacity are available. As a general guidance, the allowable capacity of the pile at any given time should be estimated as using a factor of safety of at least 1.5 on skin friction alone. Reliance on end-bearing pile capacity may result in excessive pile settlement under the applied construction loads.



**SECTION 8.0
REFERENCES**

8.0 REFERENCES

- American Petroleum Institute (1986), Recommended Practice for Planning, Designing, and Constructing Fixed Offshore Platforms, API RP-2A, 16th Ed., API, Washington, D.C.
- _____ (1993a), Recommended Practice for Planning, Designing, and Constructing Fixed Offshore Platform-Load and Resistance Factor Design, API Recommended Practice 2A-LRFD (RP 2A-LRFD), 1st Ed., API, Washington, DC.
- _____ (1993b), Recommended Practice for Planning, Designing, and Constructing Fixed Offshore Platforms-Working Stress Design, API Recommended Practice 2A-WSD (RP 2S-WSD), 20th Ed., API, Washington, D.C.
- Bogard, J.D., and Matlock, H. (1990), "Application of Model Pile Tests to Axial Pile Designs," in Proceedings, 22nd Annual Offshore Technology Conference, Houston, Texas, Vol. 3, pp. 271-278.
- Brittsan, D. and Speer, D. (1993), *Pile Load Test Results for Highway 280 Pile Uplift Test Site*, Caltrans Office of Geotechnical Engineering, Foundation Testing and Instrumentation Branch.
- California Department of Transportation (Caltrans) (1995), Standard Specifications State of California Business, Transportation and Housing Agency Department of Transportation, July.
- _____ (1997a), *Geologic Issues for the Proposed New East Span of the San Francisco-Oakland Bay Bridge*, August.
- _____ (1997b), Internal Caltrans Memorandum dated December 17 from SFOBB Investigations Section to Office of Structure Design, Subject: Addendum - Vertical Datum, Caltrans File Nos. 04-SF-80, 04-0434A1, C1, E1, F1, G1, Project Nos. 3, 4, 5, 6, 8, 21, Bridge No. 33-0025.
- Coyle, H.M. and Gibson, G.C. (1970), *Soil Damping Constants Related to Common Soil Properties in Sands and Clays*, Texas Transportation Institute, Research Report 125-1, Texas A&M University.
- Dutt, R.N., Doyle, E.H., Collins, J.T., and Ganguly, P. (1995), "A Simple Model to Predict Soil Resistance to Driving for Long Piles in Deepwater Normally Consolidated Clays," Proceedings, 27th Offshore Technology Conference, Houston, Vol. 1, pp. 257-269.



Fugro-Earth Mechanics (Fugro-EM) (1998), *Draft Preliminary Foundation Design Report, San Francisco-Oakland Bay Bridge East Span Seismic Safety Project*, FWI Job No. 98-42-0035, prepared for California Department of Transportation, August 31.

_____ (1999), "Dynamic t-z and p-y Method for Bay Bridge SSI Model for 2.5-Meter-Diameter Piles," project memorandum prepared for TY Lin/M&N Joint Venture, dated March 9.

_____ (2000), "Evaluation of Pile Setup and Impacts on Construction Schedule With Recommendations for Preparation of Special Provisions, SFOBB East Span Seismic Safety Project," FWI Job No. 98-42-0054, project memorandum prepared for Pile Installation-Skyway Implementation Team, dated June 13.

_____ (2001a), *Lateral Pile Design for Main Span-Pier E2 and Skyway Structure, San Francisco-Oakland Bay Bridge East Span Seismic Safety Project*, EMI Job No. 98-145, prepared for California Department of Transportation, February 28.

_____ (2001b), *Seismic Ground Motion Report, San Francisco-Oakland Bay Bridge East Span Seismic Safety Project*, EMI Job No. 97-146, prepared for California Department of Transportation, February 28.

_____ (2001c), *Analysis and Design Procedures for Pile Foundations Supporting Temporary Towers, Skyway Structures, San Francisco-Oakland Bay Bridge East Span Seismic Safety Project*, FWI Job No. 98-42-0054, prepared for California Department of Transportation, March 5.

_____ (2001d), *Final Marine Geophysical Survey, San Francisco-Oakland Bay Bridge East Span Seismic Safety Project*, FWI Job No. 98-42-0054, prepared for California Department of Transportation, March 5.

_____ (2001e), *Final Marine Geotechnical Site Characterization, San Francisco-Oakland Bay Bridge East Span Seismic Safety Project, Volumes 1A & 1B, Volumes 2A through 2H*, FWI Job No. 98-42-0054, prepared for California Department of Transportation, March 5.

_____ (2001f), *Pile Installation Demonstration Project (PIDP) Geotechnical Report, San Francisco-Oakland Bay Bridge East Span Seismic Safety Project*, FWI Job No. 98-42-0061, prepared for California Department of Transportation, March 5.

_____ (2001g), *Revised Final Oakland Shore Approach Geotechnical Site Characterization Report, San Francisco-Oakland Bay Bridge East Span Seismic Safety Project, Volumes 1 through 4*, FWI Job No. 98-42-0058, prepared for California Department of Transportation, March 5.



- _____ (2001h), *Subcontractor Reports, Final Geotechnical Site Characterization, San Francisco-Oakland Bay Bridge East Span Seismic Safety Project, Volumes 1 through 3*, FWI Job No. 98-42-0054, prepared for California Department of Transportation, March 5.
- Goble, G.G. and Rausche, F. (1976), Wave Equation Analysis of Pile Driving, WEAP Program, Vol. 1: Background, Vol. 2: User's Manual, Vol. 3: Program Documentation, U.S. Department of Transportation, Federal Highway Administration, Offices of Research and Development, Report No. FHWA-IP-76-14.1, 14.2, 14.3, and 14.4.
- Goble Rausche Likins and Associates (GRL&A) (1997), Wave Equation Analysis of Pile Foundations, GRLWEAP Version 1997-2 Program, U.S. Department of Transportation, Federal Highway Administration.
- Goldman, H.B. (1969), "Geology of San Francisco Bay", in Goldman, H.B., ed., *Geologic and Engineering Aspects of San Francisco Bay Fill: California Division of Mines and Geology Special Report 97*, p. 11-29.
- Heerema, E.P. (1979), "Relationships Between Wall Friction, Displacement Velocity, and Horizontal Stress in Clay and in Sand for Pile Driveability Analysis," *Ground Engineering*, Vol. 12, No. 1, pp. 55-56.
- Lee, C.H., and Praszker, M. (1969), "Bay Mud Developments and Related Structural Foundations" in Goldman, H.B., ed., *Geologic and Engineering Aspects of San Francisco Bay Fill: California Division of Mines and Geology Special Report 97*, p. 41-85.
- Matlock, H. and Foo, S.H.C. (1979), "Axial Analysis of Piles Using A Hysteretic and Degrading Soil Model," in *Proceedings, 1st International Conference on Numerical Methods in Offshore Piling*, London, England, May, pp. 127-133.
- McClelland Engineers (1981), *Engineering Department Guidelines, Design and Analysis Guideline 16C*.
- Randolph, M.F. and Murphy, B.S. (1985), "Shaft Capacity of Driven Piles in Clay," in *Proceedings, 17th Annual Offshore Technology Conference*, Houston, Texas, Vol. 1, pp. 371-378.
- Robertson, P.K., and Campanella, R.G. (1988), *Guidelines for Geotechnical Design Using PCPT and PCPTU*, The University of British Columbia, Soil Mechanics Series No. 120, Vancouver, B.C., Canada.





- Rogers, J.D., and Figures, S.H. (1991), Engineering Geologic Site Characterization of the Greater Oakland-Alameda Area, Alameda and San Francisco Counties, California: Final Report to National Science Foundation, Grant No. BCS-9003785,
- Roussel, H.J. (1979), "Pile Driving Analysis of Large-Diameter, High-Capacity Offshore Pipe Piles," Ph.D. Thesis, Department of Civil Engineering, Tulane University, New Orleans, Louisiana.
- Sample, R.M. and Gemeinhardt, J.P. (1981), "Stress History Approach to Analysis of Soil Resistance to Pile Driving," Proceedings, 13th Annual Offshore Technology Conference, Houston, Vol. 1, pp. 165-172.
- Skempton, A.W. (1944), "Notes on the Compressibility of Clays," Quarterly Journal, Geological Society, London, Vol. 100, pp. 199-235.
- Smith, E.A.L. (1960), "Pile Driving Analysis by the Wave Equation," Journal, Soil Mechanics and Foundations Division, ASCE, New York, Vol. 86, SM4, pp. 35-61.
- Soderberg, L.O. (1962), "Consolidation Theory Applied to Foundation Pile Time Effects," Geotechnique, Vol. 12, No. 3, pp. 217-225.
- Stevens, R.F. (1988), "The Effect of a Soil Plug on Pile Drivability in Clay," Proceedings, 3rd International Conference on the Application of Stress Wave Theory to Piles, Ottawa, pp. 861-868.
- Stevens, R.F., Wiltsie, E.A., and Turton, T.H. (1982), "Evaluating Pile Driveability for Hard Clay, Very Dense Sand, and Rock," in Proceedings, 14th Annual Offshore Technology Conference, Houston, Texas, Vol. 1, pp. 465-481.
- Trask, P.D., and Rolston, J.W. (1951), "Engineering Geology of the San Francisco Bay, California," in Bulletin of the Geological Society of America, Vol. 62, pp. 1079-1110.
- TY Lin/Moffatt & Nichol (TY Lin/M&N) (1999), *45% PS&E Submittal, Skyway Structures, The San Francisco-Oakland Bay Bridge East Span Seismic Safety Project*, dated January.
- _____ (2000a), *85% PS&E Submittal, Skyway Structures, The San Francisco-Oakland Bay Bridge East Span Seismic Safety Project*, dated February.
- _____ (2000b), *Draft 100% PS&E Submittal, Skyway Structures, The San Francisco-Oakland Bay Bridge East Span Seismic Safety Project*, dated November.
- _____ (2000c), table entitled "Pile Construction Load History", pages 4 and 8, provided by Rick Nutt of TY Lin/Moffatt & Nichol, received June 12.



_____ (2001a), E-Mail Transmittal of Microstation File "n6_r8.dgn", by Mr. Tom Ho of TY Lin, received January 26.

_____ (2001b), Unchecked Details, E2 Footing Layout, Main Span Suspension Bridge, Sheet T028, received February 28.

Vesic, A.S. (1977), Design of Pile Foundations, National Cooperative Highway Research Program, Synthesis of Highway Practice No. 42.



**APPENDIX A
PIER-SPECIFIC DESIGN PLATES**

APPENDIX A PIER-SPECIFIC DESIGN DATA

The axial pile design data are provided on a pier-specific basis for the Main Span-East Pier and each of the Skyway piers. For the Skyway alignment, data are provided for both the eastbound and westbound piers.

DESIGN DATA PRESENTATION

The pier-specific data are provided in a series of pier-specific groups of plates. Pier and boring location plans for the various Skyway frames are provided on Plates A-1 through A-3. A pier-boring correlation table is shown on Plate A-4.

For each pier, the axial design data are presented on a series of four illustrations within the appropriate pier-specific plate group. When drivability analyses were performed for a pier, three additional illustrations are included within the group. For example, the plates for Skyway Frame 1, Eastbound Pier 3 (of the East Span) are numbered as Plates E3-EB.1, E3-EB.2, E3-EB.3, etc. Similarly, the design data for Skyway Frame 1, Westbound Pier 3 are numbered Plates E3-WB.1, E3-WB.2, E3-WB.3, etc., and the design data for Skyway Frame 1, Eastbound Pier 4 are numbered Plates E4-EB.1, E4-EB.2, E4-EB.3, etc. An additional set of load-deformation analyses was performed for the borings located at the Main Span-East Pier (Borings 98-25 and 98-26). In these analyses, the load deformation-behavior was analyzed with the piles tipped in the middle of the Upper Alameda Marine Paleochannel Sand layer. These plates are numbered E2-WB.2b, E2-WB.3b, E2-WB.4b, E2-EB.2b, E2-EB.3b, and E2-EB.4b.

The pile design data provided for each pier are as follows:

- Axial Pile Design Parameters and Results, including:
soil stratigraphy, interpreted design strength and submerged
unit weight profiles, unit skin friction and end-bearing
curves, and static axial pile capacityPlate EX-YB.1
- Axial Pile Load Transfer-Displacement CurvesPlate EX-YB.2
- Tabulated Axial Pile Load Transfer DataPlate EX-YB.3
- Static Pile Head Load-Deformation Curves.....Plate EX-YB.4

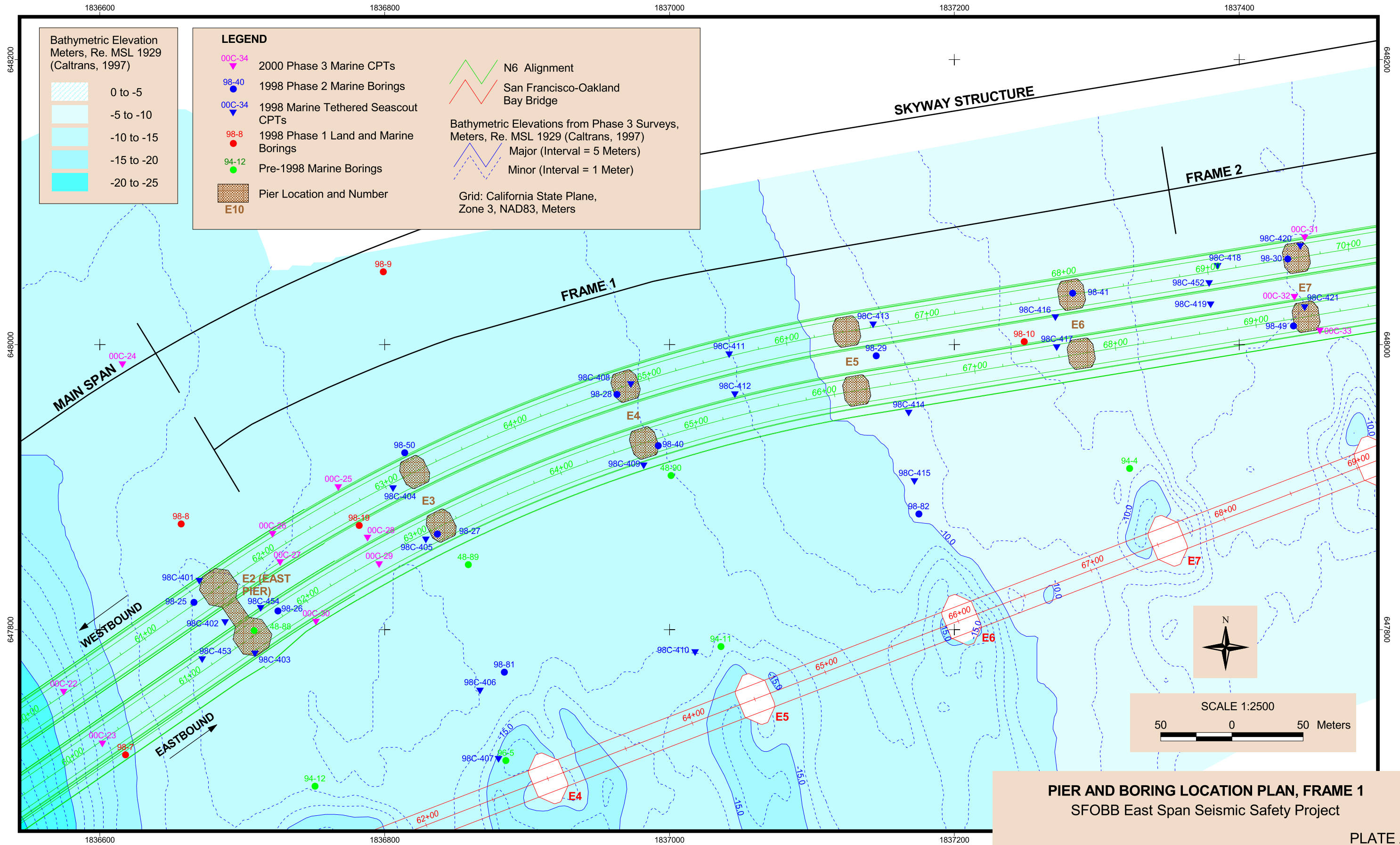
Plate A-5 provides a key to the legend for the Axial Pile Design Parameters and Results plates numbered as EX-YB.1. Plate A-6 shows the preliminary pile tip elevations used in the development of the load transfer data and load-deformation curves (Plates EX-YB.2, EX-YB.3, and EX-YB4).



When drivability analyses (based on the Stevens et al. [1982] method) were performed for a pier, the data provided also included:

- Soil Resistance to Driving.....Plate EX-YB.5
- Predicted Blow Counts, Menck MHU 500T.....Plate EX-YB.6a
- Predicted Blow Counts, Menck MHU 1000Plate EX-YB.6b
- Predicted Blow Counts, Menck MHU 1700Plate EX-YB.6c



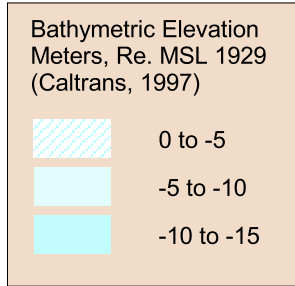


1837400

1837600

1837800

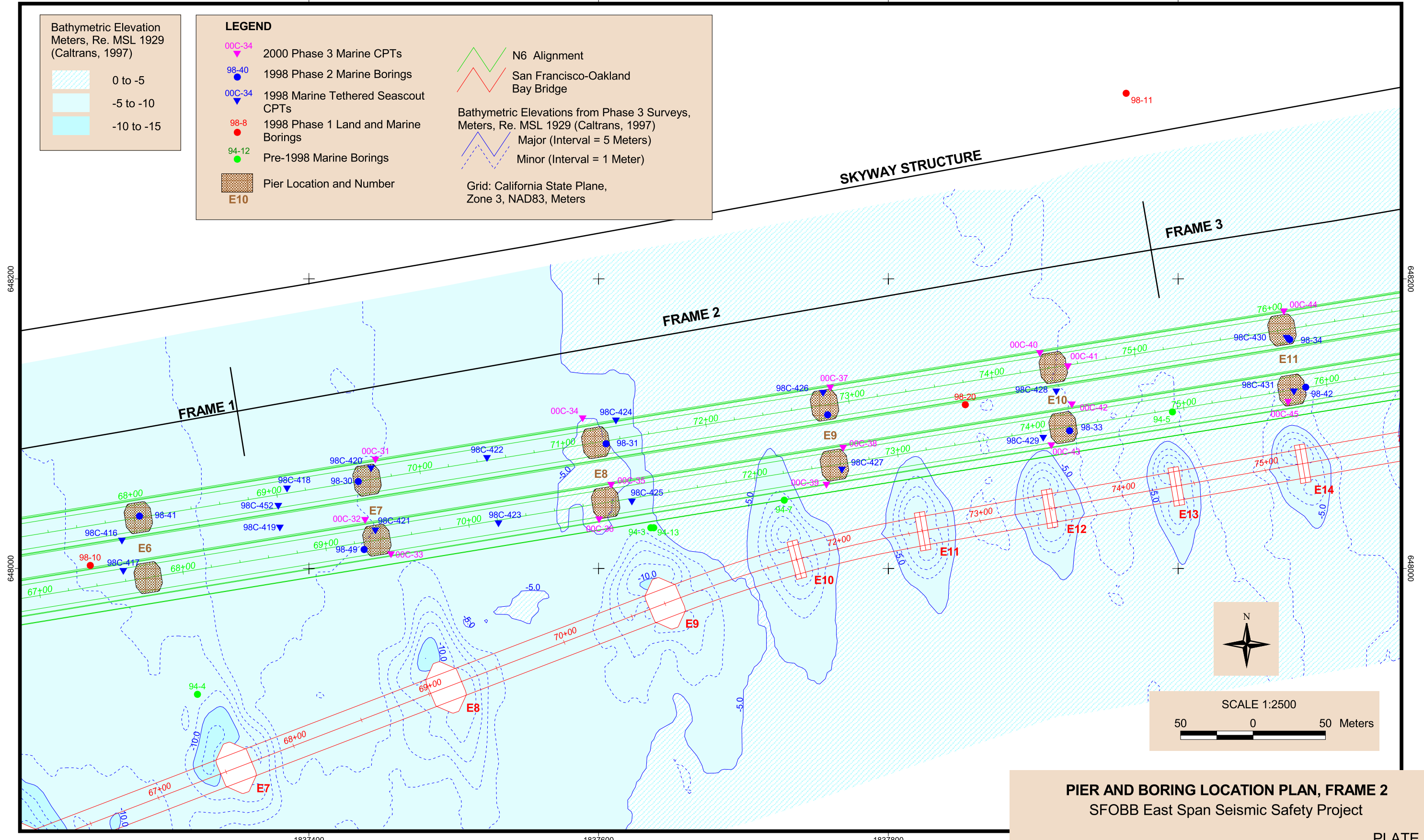
1838000



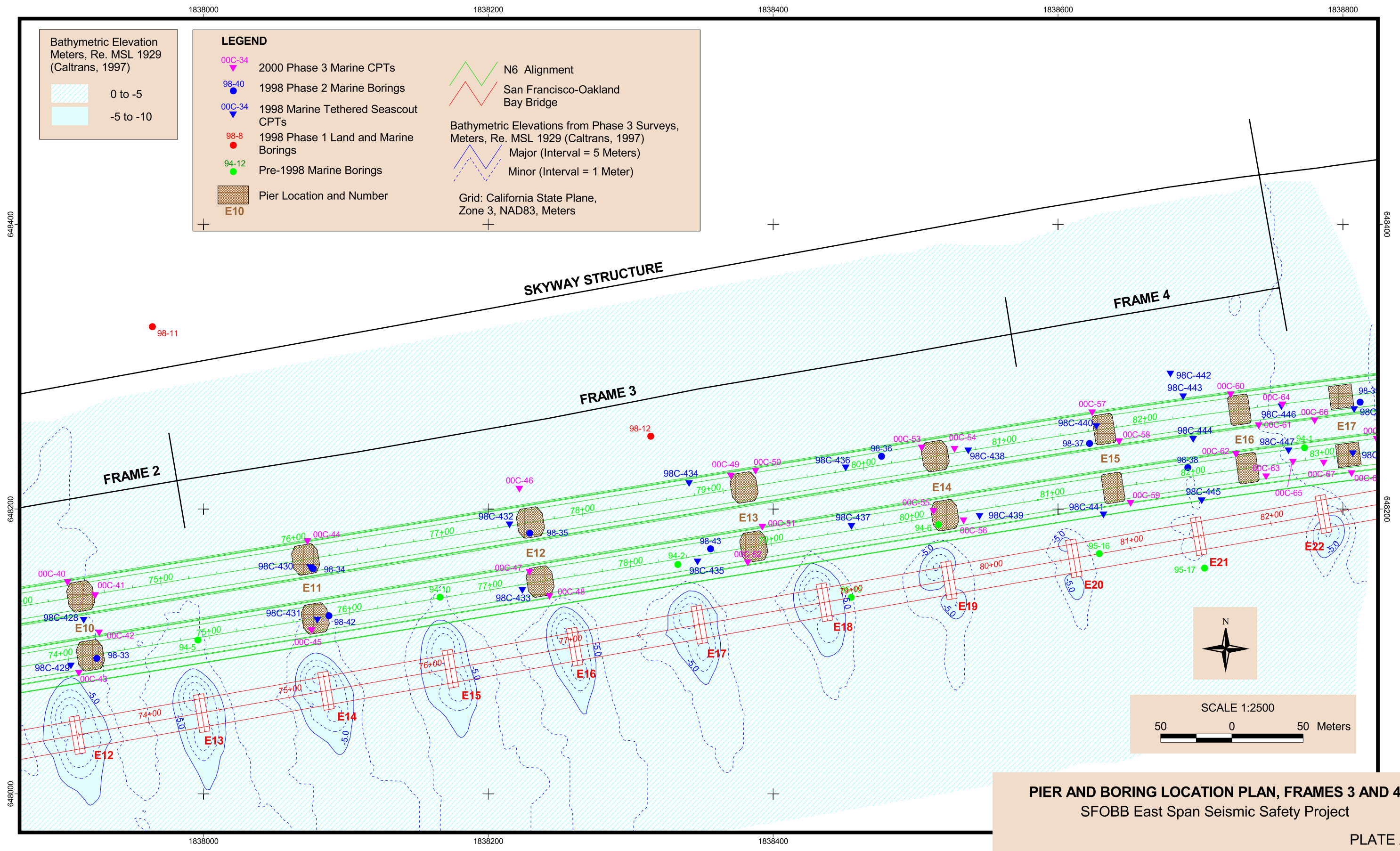
LEGEND

- 00C-34 2000 Phase 3 Marine CPTs
- 98-40 1998 Phase 2 Marine Borings
- 00C-34 1998 Marine Tethered Seascout CPTs
- 98-8 1998 Phase 1 Land and Marine Borings
- 94-12 Pre-1998 Marine Borings
- Pier Location and Number
E10
- N6 Alignment
- San Francisco-Oakland Bay Bridge
- Bathymetric Elevations from Phase 3 Surveys, Meters, Re. MSL 1929 (Caltrans, 1997)
Major (Interval = 5 Meters)
Minor (Interval = 1 Meter)

Grid: California State Plane, Zone 3, NAD83, Meters



PIER AND BORING LOCATION PLAN, FRAME 2
SFOBB East Span Seismic Safety Project
PLATE A-2



PIER AND BORING LOCATION PLAN, FRAMES 3 AND 4
SFOBB East Span Seismic Safety Project
PLATE A-3

j:\caltrans\reports\finalreports\finalaxpiledrive_book6\plates\oob-x\appendixa_pierspecific_design\plates11x17\updatedasoffeb\platea-3.oob_sdeshpande_03/01/2001

Pier	Centerline Station	Associated Boring(s)
Pier E2 Eastbound	61+54	98-26
Pier E2 Westbound	61+63	98-25
Pier E3 Eastbound	63+08	98-27
Pier E3 Westbound	63+23	98-50
Pier E4 Eastbound	64+62	98-40
Pier E4 Westbound	64+83	98-28
Pier E5 Eastbound	66+16	98-29
Pier E5 Westbound	66+43	98-29
Pier E6 Eastbound	67+76	98-10, 98-41
Pier E6 Westbound	68+03	98-41
Pier E7 Eastbound	69+36	98-49
Pier E7 Westbound	69+63	98-30
Pier E8 Eastbound	70+96	98-31
Pier E8 Westbound	71+23	98-31
Pier E9 Eastbound	72+56	98-32
Pier E9 Westbound	72+83	98-32
Pier E10 Eastbound	74+16	98-33
Pier E10 Westbound	74+43	98-31, 98-33
Pier E11 Eastbound	75+76	98-42
Pier E11 Westbound	76+03	98-34
Pier E12 Eastbound	77+36	98-35
Pier E12 Westbound	77+63	98-35
Pier E13 Eastbound	78+88	98-43
Pier E13 Westbound	79+15	98-43
Pier E14 Eastbound	80+24	98-36
Pier E14 Westbound	80+51	98-36
Pier E15 Eastbound	81+43	98-37
Pier E15 Westbound	81+71	98-37
Pier E16 Eastbound	82+39	98-38
Pier E16 Westbound	82+67	98-38

PIER-BORING CORRELATION TABLE
SFOBB East Span Seismic Safety Project



SOIL TYPES

	Well graded GRAVEL (GW)		Clayey SAND (SC)		Clayey silt (ML/CL)
	Poorly graded GRAVEL (GP)		Silty SAND (SM)		Highly plastic ORGANICS (OH)
	GRAVEL with sand (GP or GW)		SAND with silt (SP-SM)		Low plasticity ORGANICS (OL)
	GRAVEL with clay (GP or GW)		Fat CLAY(CH)		SANDSTONE (Rx)
	Clayey GRAVEL (GC)		Sandy fat CLAY (CH)		SILTSTONE (Rx)
	GRAVEL with silt (GP or GW)		Lean CLAY (CL)		CLAYSTONE (Rx)
	Silty GRAVEL (GM)		Sandy lean CLAY (CL)		Interbedded Rock Strata (Rx)
	Well graded SAND (SW)		Silty CLAY (CL-ML)		CONGLOMERATE (Rx)
	Poorly graded SAND (SP)		Elastic SILT (MH)		PAVEMENT
	SAND with gravel (SP or SW)		SILT (ML)		Rock Fragments (Rf)
	SAND with clay (SP-SC)		Sandy SILT (ML)		

GEOLOGIC UNITS

Af	Artificial Fill
YBM	Young Bay Mud
MPSA	Merritt-Posey-San Antonio Sequence
OBM/UAM	Old Bay Mud/ Upper Alameda Marine Formation
LAA	Lower Alameda Alluvial Formation
FF	Franciscan Formation

**KEY TO TERMS AND SYMBOLS USED ON
AXIAL PILE DESIGN PARAMETERS AND RESULTS**
SFOBB East Span Seismic Safety Project

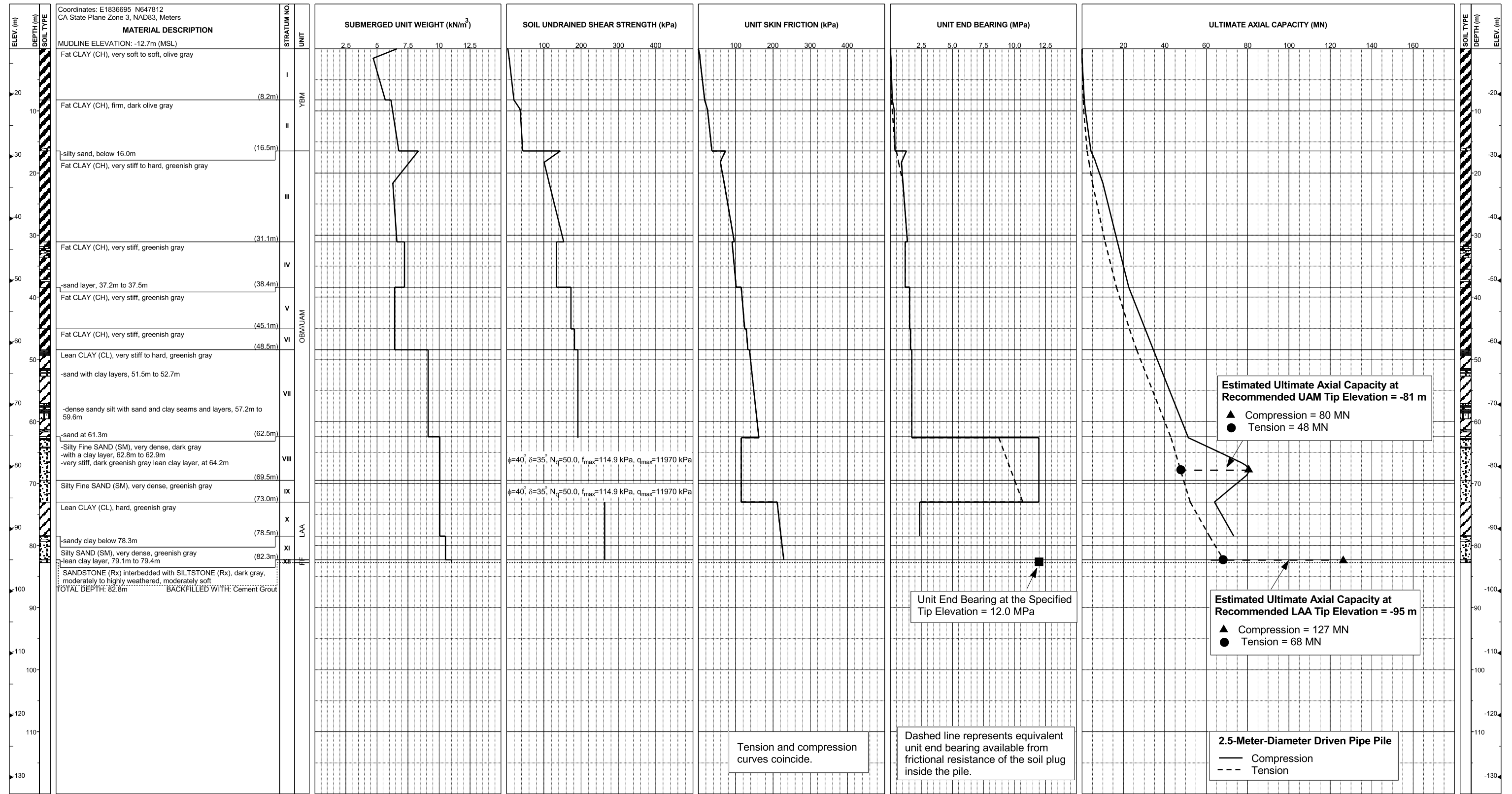
Pier	Bay Floor Elevation (m, re MSL)	Estimated Pile Tip Depth (m)	Estimated Pile Tip Elevation (m)	Ultimate Tension Capacity (MN)	Ultimate Compression Capacity (MN)
Pier E2 Eastbound - tipped in LAA	-13	82	-95	68	127
Pier E2 Eastbound - tipped in UAM	-13	69	-81	48	80
Pier E2 Westbound - tipped in LAA	-13	82	-95	64	123
Pier E2 Westbound - tipped in UAM	-13	69	-81	46	86
Pier E3 Eastbound	-13	87	-100	78	128
Pier E3 Westbound	-12	90	-102	78	129
Pier E4 Eastbound	-12	85	-97	77	127
Pier E4 Westbound	-11	83	-94	73	123
Pier E5 Eastbound	-10	88	-98	81	131
Pier E5 Westbound	-10	88	-98	80	130
Pier E6 Eastbound	-8	88	-96	80	130
Pier E6 Westbound	-8	88	-96	80	130
Pier E7 Eastbound	-6	87	-93	75	119
Pier E7 Westbound	-6	88	-94	77	121
Pier E8 Eastbound	-5	92	-97	83	126
Pier E8 Westbound	-5	91	-96	81	125
Pier E9 Eastbound	-4	90	-94	82	126
Pier E9 Westbound	-4	90	-94	82	126
Pier E10 Eastbound	-4	91	-95	88	131
Pier E10 Westbound	-4	94	-98	91	135
Pier E11 Eastbound	-4	91	-95	95	146
Pier E11 Westbound	-4	91	-95	92	138
Pier E12 Eastbound	-4	93	-97	92	138
Pier E12 Westbound	-4	93	-97	92	138
Pier E13 Eastbound	-3	88	-91	80	126
Pier E13 Westbound	-3	91	-94	86	132
Pier E14 Eastbound	-3	92	-95	98	146
Pier E14 Westbound	-3	92	-95	98	146
Pier E15 Eastbound	-3	90	-93	91	139
Pier E15 Westbound	-3	90	-93	91	139
Pier E16 Eastbound	-3	91	-94	93	141
Pier E16 Westbound	-3	91	-94	93	141

Note: Values in *Italics* have been superceded with those shown on Plate 3.1. However, these values were used for the preliminary axial load-deflection analyses presented in the pier-specific design plates.

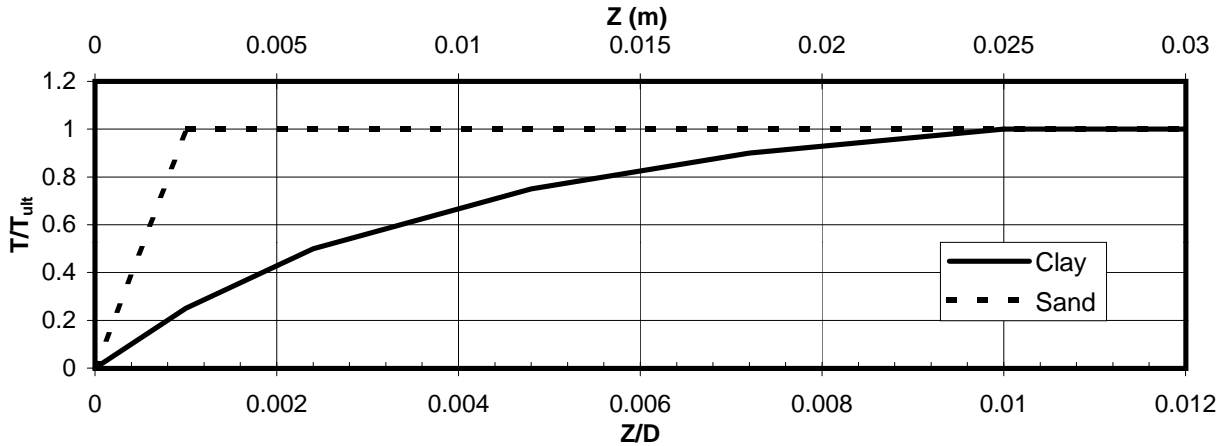
SUMMARY OF PRELIMINARY AXIAL PILE CAPACITY
Piers E2 through E16
SFOBB East Span Seismic Safety Project



**Pier E2-Eastbound (Boring 98-26)
Main Span East Pier**



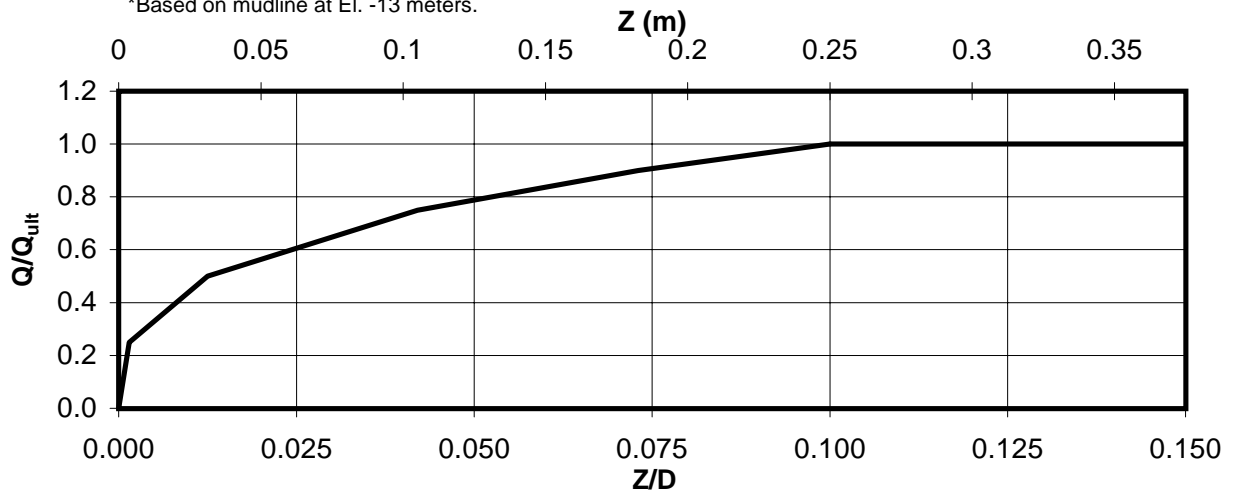
AXIAL PILE DESIGN PARAMETERS AND RESULTS
Pier E2-Eastbound (Boring 98-26)
SFOBB East Span Seismic Safety Project



Depth* (m)	Soil Type	T_{ult} (MN/m)
0-3	Clay	0.020
3-6	Clay	0.070
6-9	Clay	0.123
9-12	Clay	0.197
12-15	Clay	0.247
15-18	Clay	0.430
18-21	Clay	0.493
21-24	Clay	0.553
24-27	Clay	0.627
27-30	Clay	0.693
30-33	Clay	0.733
33-36	Clay	0.747

Depth* (m)	Soil Type	T_{ult} (MN/m)
36-39	Clay	0.783
39-42	Clay	0.920
42-45	Clay	0.967
45-51	Clay	1.053
51-57	Clay	1.160
57-63	Clay	1.218
63-69	Sand	0.907
69-75	Sand	1.125
75-81	Clay	1.739
81-82	Clay	1.750

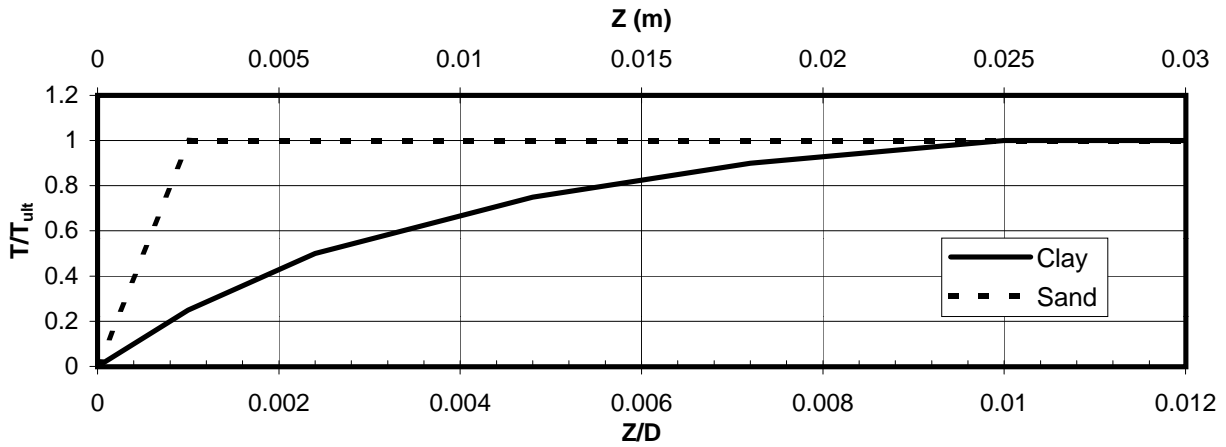
*Based on mudline at El. -13 meters.



Depth* (m)	Soil Type	Q_{ult} (MN)
82	Clay	58.8

AXIAL PILE LOAD TRANSFER-DISPLACEMENT CURVES
Pier E2-Eastbound (Boring 98-26)
 2.5-Meter-Diameter Pipe Piles (Pile Tip Elevation = -95 Meters)
 SFOBB East Span Seismic Safety Project

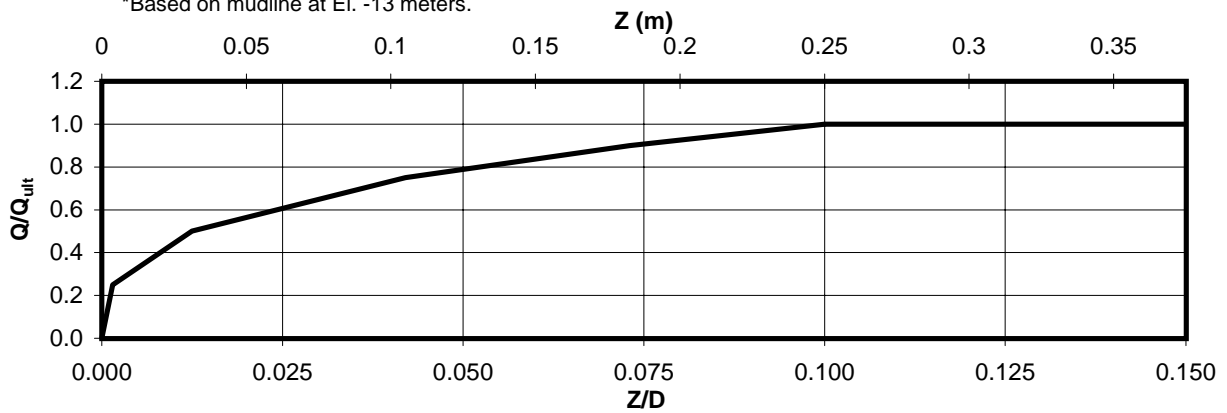




Depth* (m)	Soil Type	T_{ult} (MN/m)
0-3	Clay	0.017
3-6	Clay	0.073
6-9	Clay	0.123
9-12	Clay	0.197
12-15	Clay	0.247
15-18	Clay	0.430
18-21	Clay	0.497
21-24	Clay	0.553
24-27	Clay	0.623
27-30	Clay	0.697
30-33	Clay	0.733
33-36	Clay	0.743

Depth* (m)	Soil Type	T_{ult} (MN/m)
36-39	Clay	0.783
39-42	Clay	0.923
42-45	Clay	0.963
45-51	Clay	1.055
51-57	Clay	1.153
57-63	Clay	1.230
63-68	Sand	0.908

*Based on mudline at El. -13 meters.



Depth* (m)	Soil Type	Q_{ult} (MN)
68	Clay	32.5

AXIAL PILE LOAD TRANSFER-DISPLACEMENT CURVES
Pier E2-Eastbound (Boring 98-26)
 2.5-Meter-Diameter Pipe Piles (Pile Tip Elevation = -81 Meters)
 SFOBB East Span Seismic Safety Project



DEPTH (m)	t-z Data											
	t(1)	z(1)	t(2)	z(2)	t(3)	z(3)	t(4)	z(4)	t(5)	z(5)	t(6)	z(6)
0-3	0.0	0.0	0.005	0.003	0.010	0.006	0.015	0.012	0.018	0.018	0.020	0.025
3-6	0.0	0.0	0.018	0.003	0.035	0.006	0.053	0.012	0.063	0.018	0.070	0.025
6-9	0.0	0.0	0.031	0.003	0.062	0.006	0.092	0.012	0.111	0.018	0.123	0.025
9-12	0.0	0.0	0.049	0.003	0.098	0.006	0.148	0.012	0.177	0.018	0.197	0.025
12-15	0.0	0.0	0.062	0.003	0.123	0.006	0.185	0.012	0.222	0.018	0.247	0.025
15-18	0.0	0.0	0.108	0.003	0.215	0.006	0.323	0.012	0.387	0.018	0.430	0.025
18-21	0.0	0.0	0.123	0.003	0.247	0.006	0.370	0.012	0.444	0.018	0.493	0.025
21-24	0.0	0.0	0.138	0.003	0.277	0.006	0.415	0.012	0.498	0.018	0.553	0.025
24-27	0.0	0.0	0.157	0.003	0.313	0.006	0.470	0.012	0.564	0.018	0.627	0.025
27-30	0.0	0.0	0.173	0.003	0.347	0.006	0.520	0.012	0.624	0.018	0.693	0.025
30-33	0.0	0.0	0.183	0.003	0.367	0.006	0.550	0.012	0.660	0.018	0.733	0.025
33-36	0.0	0.0	0.187	0.003	0.373	0.006	0.560	0.012	0.672	0.018	0.747	0.025
36-39	0.0	0.0	0.196	0.003	0.392	0.006	0.587	0.012	0.705	0.018	0.783	0.025
39-42	0.0	0.0	0.230	0.003	0.460	0.006	0.690	0.012	0.828	0.018	0.920	0.025
42-45	0.0	0.0	0.242	0.003	0.483	0.006	0.725	0.012	0.870	0.018	0.967	0.025
45-51	0.0	0.0	0.263	0.003	0.527	0.006	0.790	0.012	0.948	0.018	1.053	0.025
51-57	0.0	0.0	0.290	0.003	0.580	0.006	0.870	0.012	1.044	0.018	1.160	0.025
57-63	0.0	0.0	0.305	0.003	0.609	0.006	0.914	0.012	1.096	0.018	1.218	0.025
63-69	0.0	0.0	0.907	0.003								
69-75	0.0	0.0	1.125	0.003								
75-81	0.0	0.0	0.435	0.003	0.870	0.006	1.304	0.012	1.565	0.018	1.739	0.025
81-82	0.0	0.0	0.438	0.003	0.875	0.006	1.313	0.012	1.575	0.018	1.750	0.025

Notes:

1. "t" is load (MN/m)
2. "z" is displacement (m)
3. Data for tension and compression coincide
4. Based on mudline at El. -13 meters

DEPTH (m)	Q-z Data											
	Q(1)	z(1)	Q(2)	z(2)	Q(3)	z(3)	Q(4)	z(4)	Q(5)	z(5)	Q(6)	z(6)
82	0.0	0.0	14.700	0.004	29.400	0.031	44.100	0.105	52.920	0.183	58.800	0.250

Notes:

1. "Q" is load in compression (MN)
2. "z" is displacement (m)

TABULATED AXIAL PILE LOAD TRANSFER DATA
Pier E2-Eastbound (Boring 98-26)
 2.5-Meter-Diameter Pipe Piles (Pile Tip Elevation = -95 Meters)
 SFOBB East Span Seismic Safety Project



DEPTH (m)	t-z Data											
	t(1)	z(1)	t(2)	z(2)	t(3)	z(3)	t(4)	z(4)	t(5)	z(5)	t(6)	z(6)
0-3	0.0	0.0	0.004	0.003	0.008	0.006	0.013	0.012	0.015	0.018	0.017	0.025
3-6	0.0	0.0	0.018	0.003	0.037	0.006	0.055	0.012	0.066	0.018	0.073	0.025
6-9	0.0	0.0	0.031	0.003	0.062	0.006	0.092	0.012	0.111	0.018	0.123	0.025
9-12	0.0	0.0	0.049	0.003	0.098	0.006	0.148	0.012	0.177	0.018	0.197	0.025
12-15	0.0	0.0	0.062	0.003	0.123	0.006	0.185	0.012	0.222	0.018	0.247	0.025
15-18	0.0	0.0	0.108	0.003	0.215	0.006	0.323	0.012	0.387	0.018	0.430	0.025
18-21	0.0	0.0	0.124	0.003	0.248	0.006	0.372	0.012	0.447	0.018	0.497	0.025
21-24	0.0	0.0	0.138	0.003	0.277	0.006	0.415	0.012	0.498	0.018	0.553	0.025
24-27	0.0	0.0	0.156	0.003	0.312	0.006	0.468	0.012	0.561	0.018	0.623	0.025
27-30	0.0	0.0	0.174	0.003	0.348	0.006	0.522	0.012	0.627	0.018	0.697	0.025
30-33	0.0	0.0	0.183	0.003	0.367	0.006	0.550	0.012	0.660	0.018	0.733	0.025
33-36	0.0	0.0	0.186	0.003	0.372	0.006	0.558	0.012	0.669	0.018	0.743	0.025
36-39	0.0	0.0	0.196	0.003	0.392	0.006	0.587	0.012	0.705	0.018	0.783	0.025
39-42	0.0	0.0	0.231	0.003	0.462	0.006	0.692	0.012	0.831	0.018	0.923	0.025
42-45	0.0	0.0	0.241	0.003	0.482	0.006	0.723	0.012	0.867	0.018	0.963	0.025
45-51	0.0	0.0	0.264	0.003	0.528	0.006	0.791	0.012	0.950	0.018	1.055	0.025
51-57	0.0	0.0	0.288	0.003	0.577	0.006	0.865	0.012	1.038	0.018	1.153	0.025
57-63	0.0	0.0	0.308	0.003	0.615	0.006	0.923	0.012	1.107	0.018	1.230	0.025
63-68	0.0	0.0	0.908	0.003								

Notes:

1. "t" is load (MN/m)
2. "z" is displacement (m)
3. Data for tension and compression coincide
4. Based on mudline at El. -13 meters

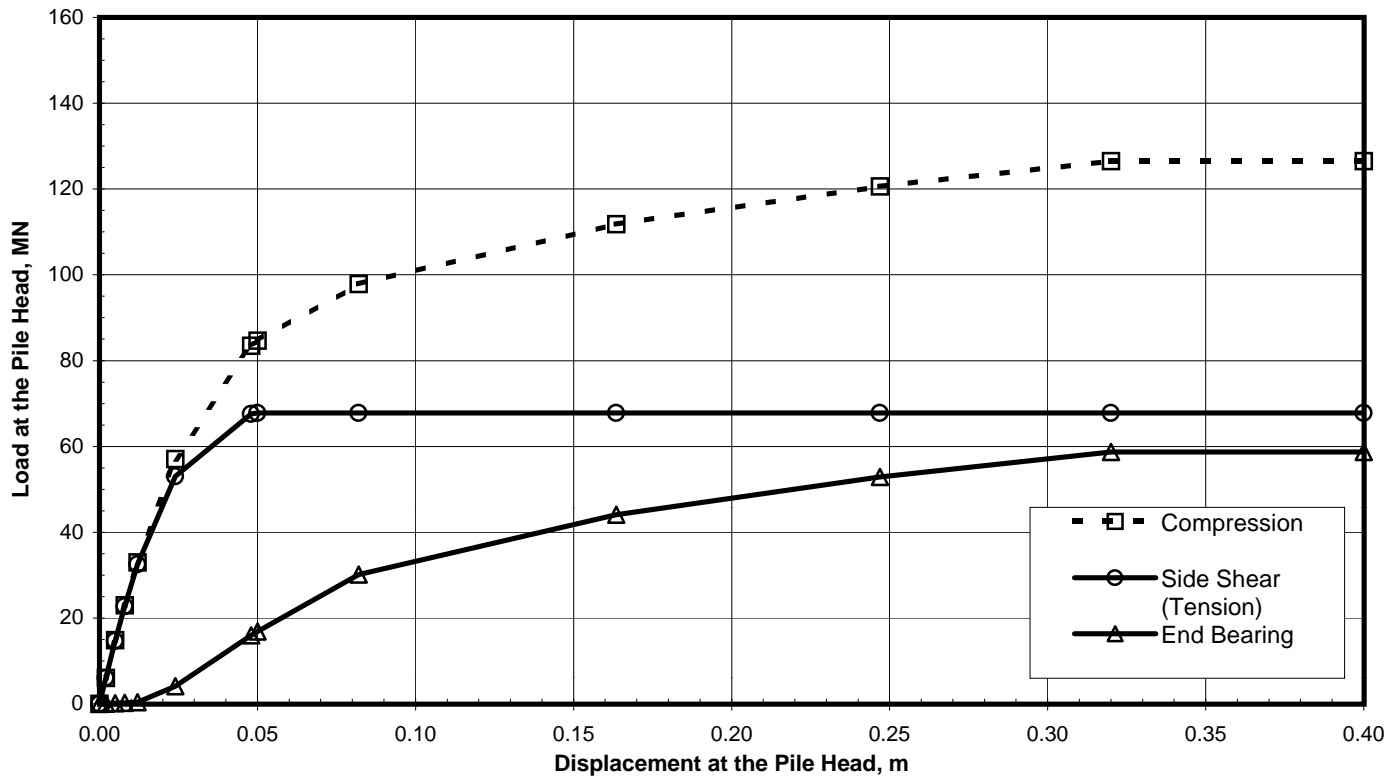
DEPTH (m)	Q-z Data											
	Q(1)	z(1)	Q(2)	z(2)	Q(3)	z(3)	Q(4)	z(4)	Q(5)	z(5)	Q(6)	z(6)
68	0.0	0.0	8.125	0.004	16.250	0.031	24.375	0.105	29.250	0.183	32.500	0.250

Notes:

1. "Q" is load in compression (MN)
2. "z" is displacement (m)

TABULATED AXIAL PILE LOAD TRANSFER DATA
Pier E2-Eastbound (Boring 98-26)
 2.5-Meter-Diameter Pipe Piles (Pile Tip Elevation = -81 Meters)
 SFOBB East Span Seismic Safety Project





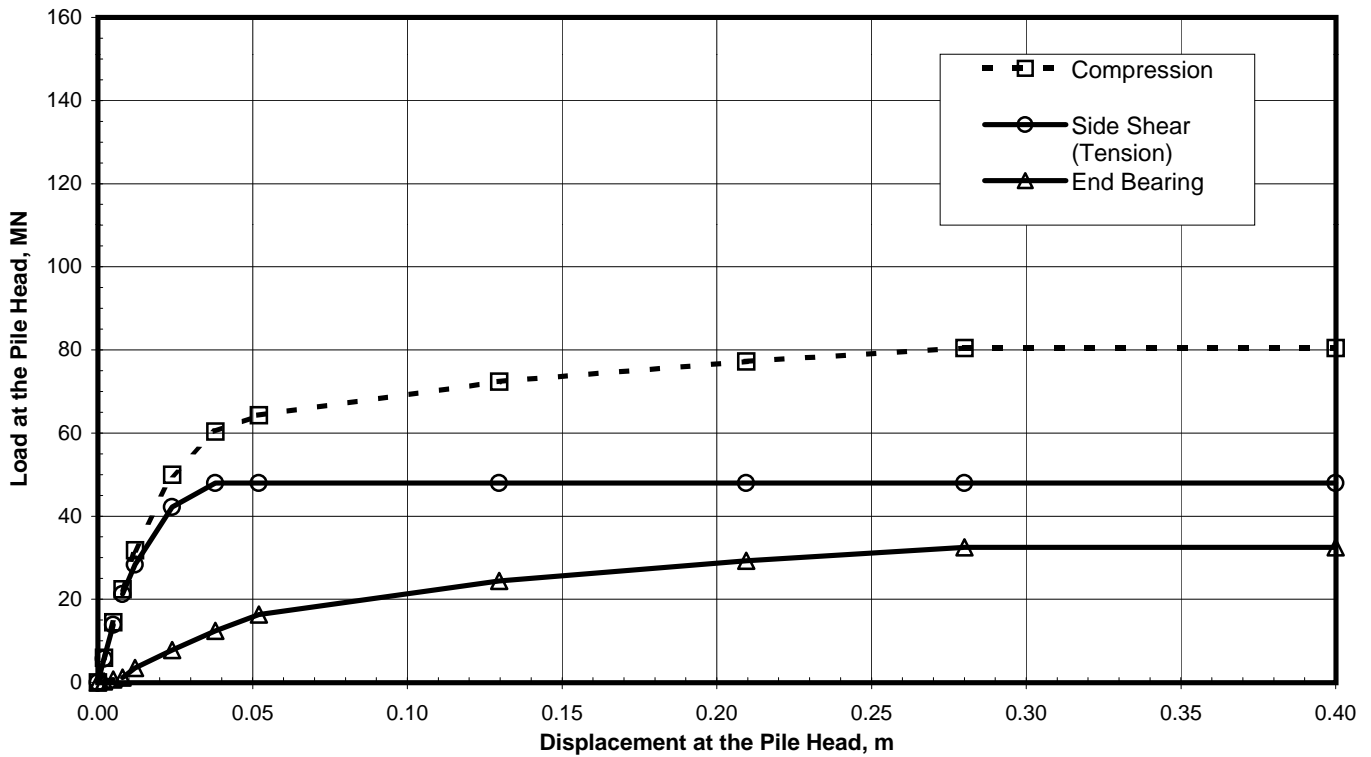
Pile Head Displacement (m)	Load at the Pile Head		End Bearing Component in Compression (MN)
	Compression (MN)	Tension (MN)	
0.000	0.00	0.00	0.00
0.002	6.06	6.01	0.05
0.005	14.84	14.71	0.13
0.008	23.00	22.77	0.23
0.012	32.96	32.55	0.41
0.024	57.08	53.01	4.07
0.048	83.49	67.56	15.93
0.050	84.66	67.77	16.89
0.082	97.89	67.77	30.12
0.163	111.82	67.77	44.05
0.247	120.63	67.77	52.86
0.320	126.50	67.77	58.73
0.400	126.50	67.77	58.73

Note:

Pile head load-displacement curves are based on the preliminary pile wall thickness schedule provided by TY Lin/M&N and static loading conditions.

STATIC PILE HEAD LOAD-DEFORMATION CURVES
Pier E2-Eastbound (Boring 98-26)
 2.5-Meter-Diameter Pipe Piles (Pile Tip Elevation = -95 Meters)
 SFOBB East Span Seismic Safety Project





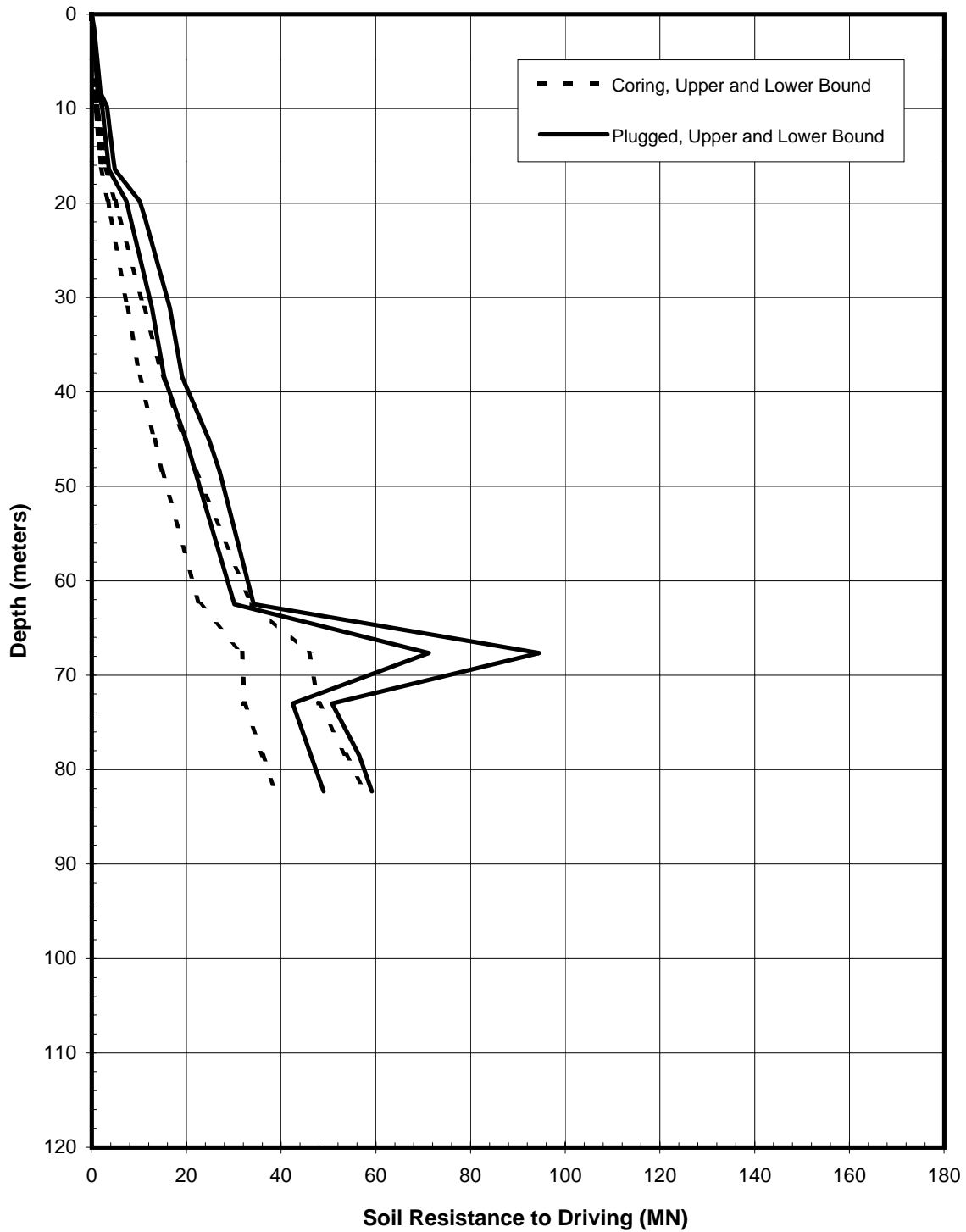
Pile Head Displacement (m)	Load at the Pile Head		End Bearing Component in Compression (MN)
	Compression (MN)	Tension (MN)	
0.000	0.00	0.00	0.00
0.002	5.94	5.70	0.24
0.005	14.50	13.84	0.66
0.008	22.41	21.23	1.18
0.012	31.80	28.32	3.48
0.024	49.96	42.22	7.74
0.038	60.38	47.97	12.41
0.052	64.27	47.97	16.30
0.130	72.35	47.97	24.38
0.210	77.22	47.97	29.25
0.280	80.47	47.97	32.50
0.400	80.47	47.97	32.50

Note:

Pile head load-displacement curves are based on the preliminary pile wall thickness schedule provided by TY Lin/M&N and static loading conditions.

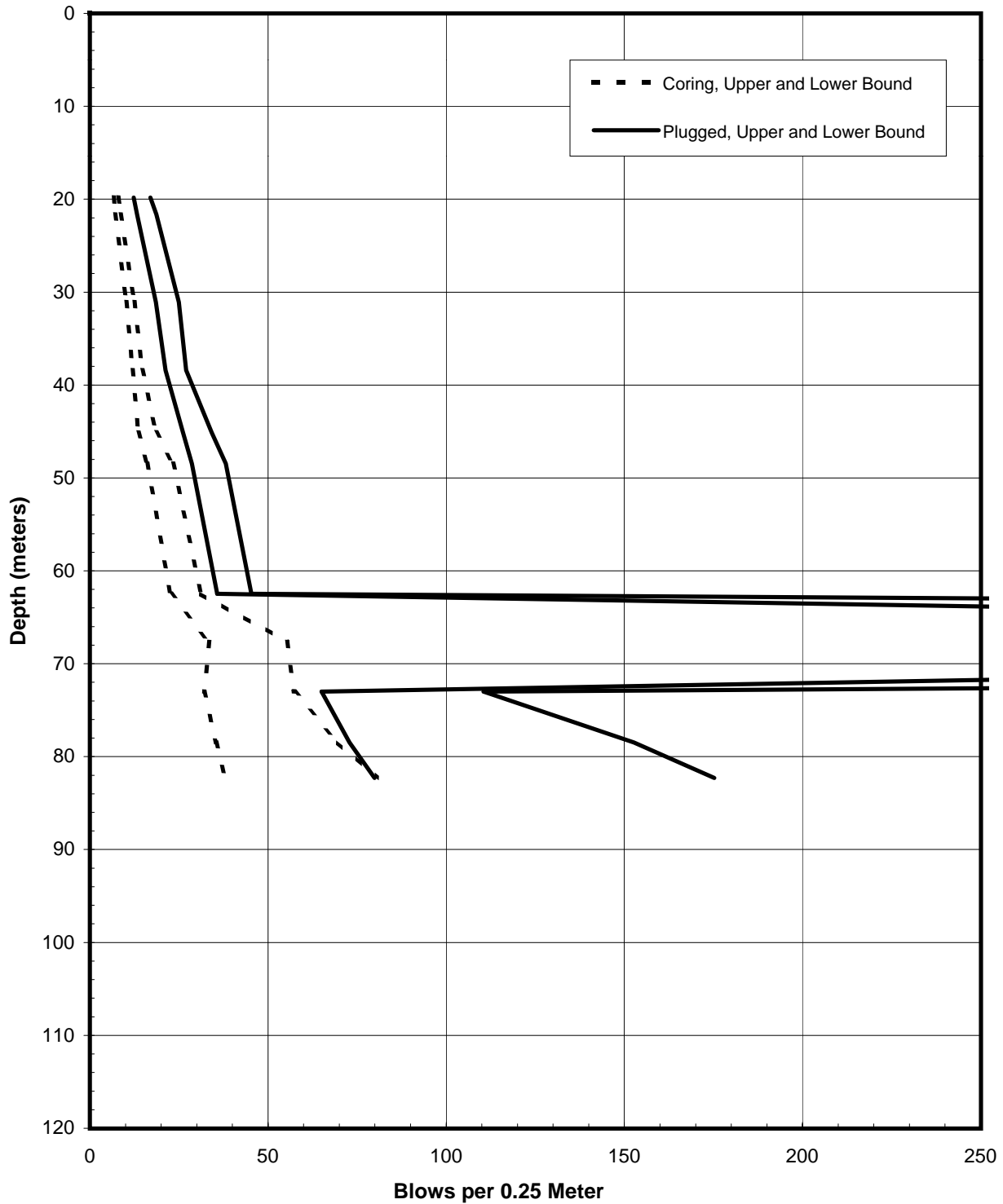
STATIC PILE HEAD LOAD-DEFORMATION CURVES
Pier E2-Eastbound (Boring 98-26)
 2.5-Meter-Diameter Pipe Piles (Pile Tip Elevation = -81 Meters)
 SFOBB East Span Seismic Safety Project





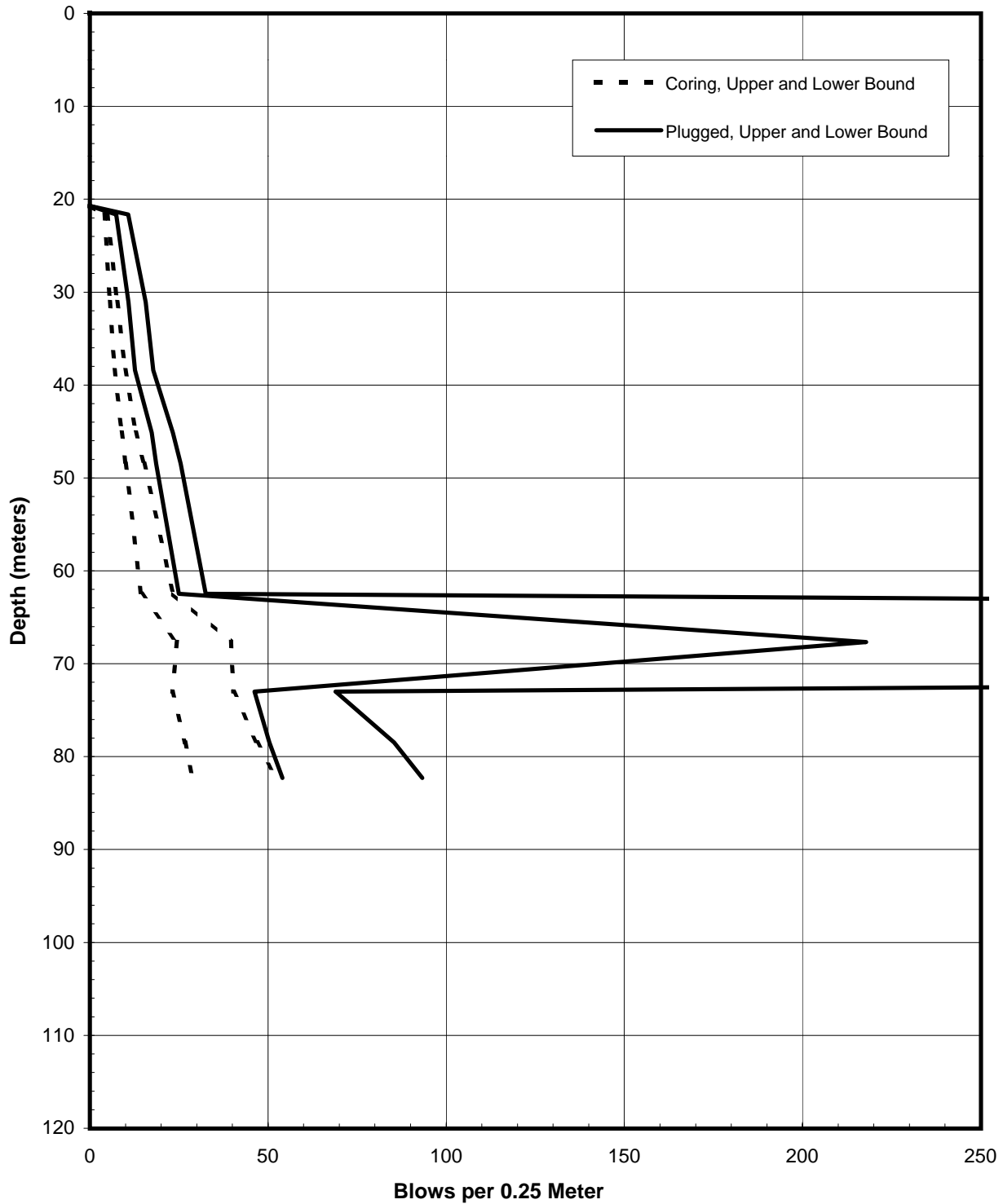
SOIL RESISTANCE TO DRIVING
Pier E2-Eastbound (Boring 98-26)
2.5-Meter-Diameter Driven Pipe Piles
SFOBB East Span Seismic Safety Project





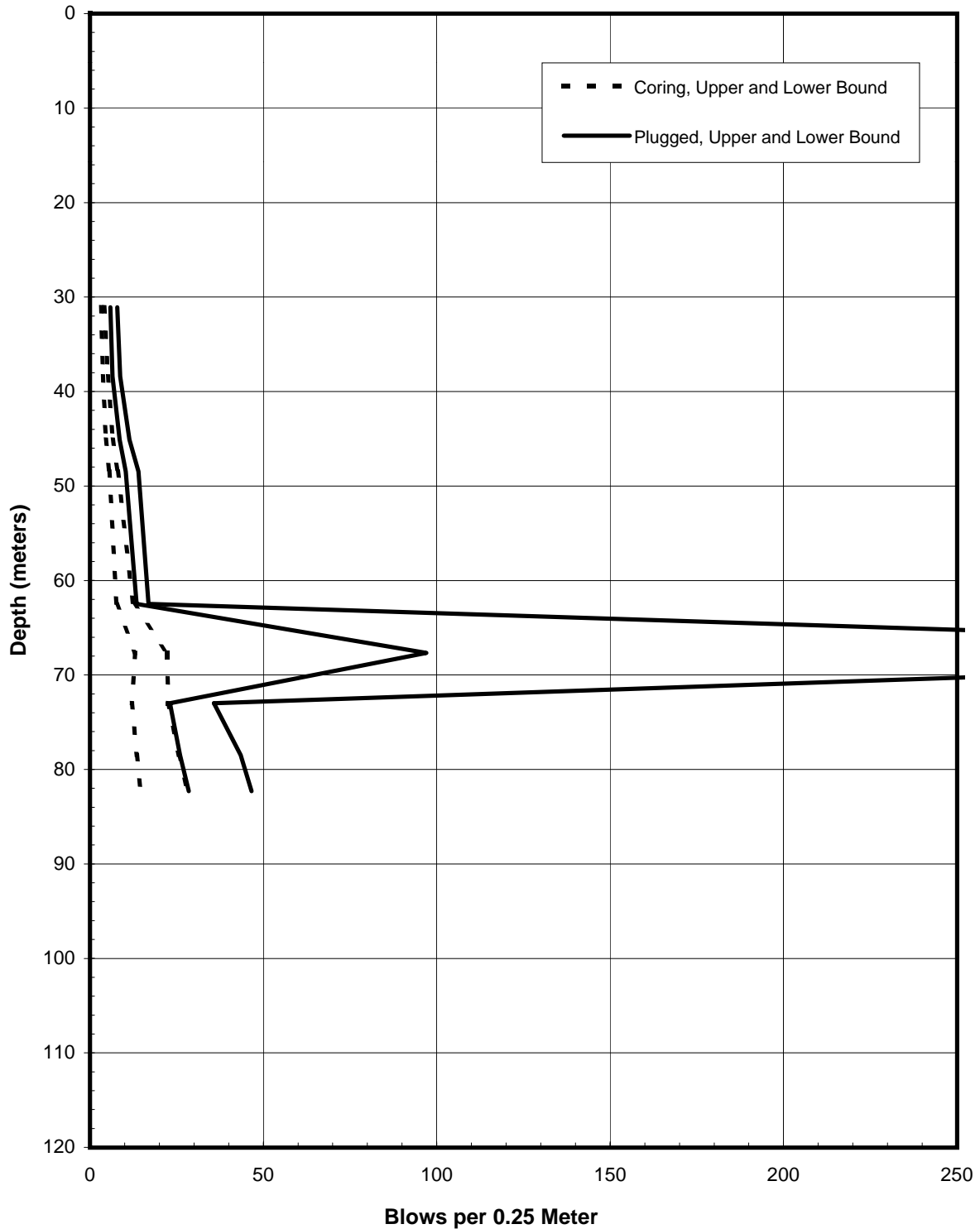
PREDICTED BLOW COUNTS
Pier E2-Eastbound (Boring 98-26)
Menck MHU-500T, 2.5-Meter-Diameter Driven Pipe Piles
SFOBB East Span Seismic Safety Project





PREDICTED BLOW COUNTS
Pier E2-Eastbound (Boring 98-26)
Menck MHU-1000, 2.5-Meter-Diameter Driven Pipe Piles
SFOBB East Span Seismic Safety Project

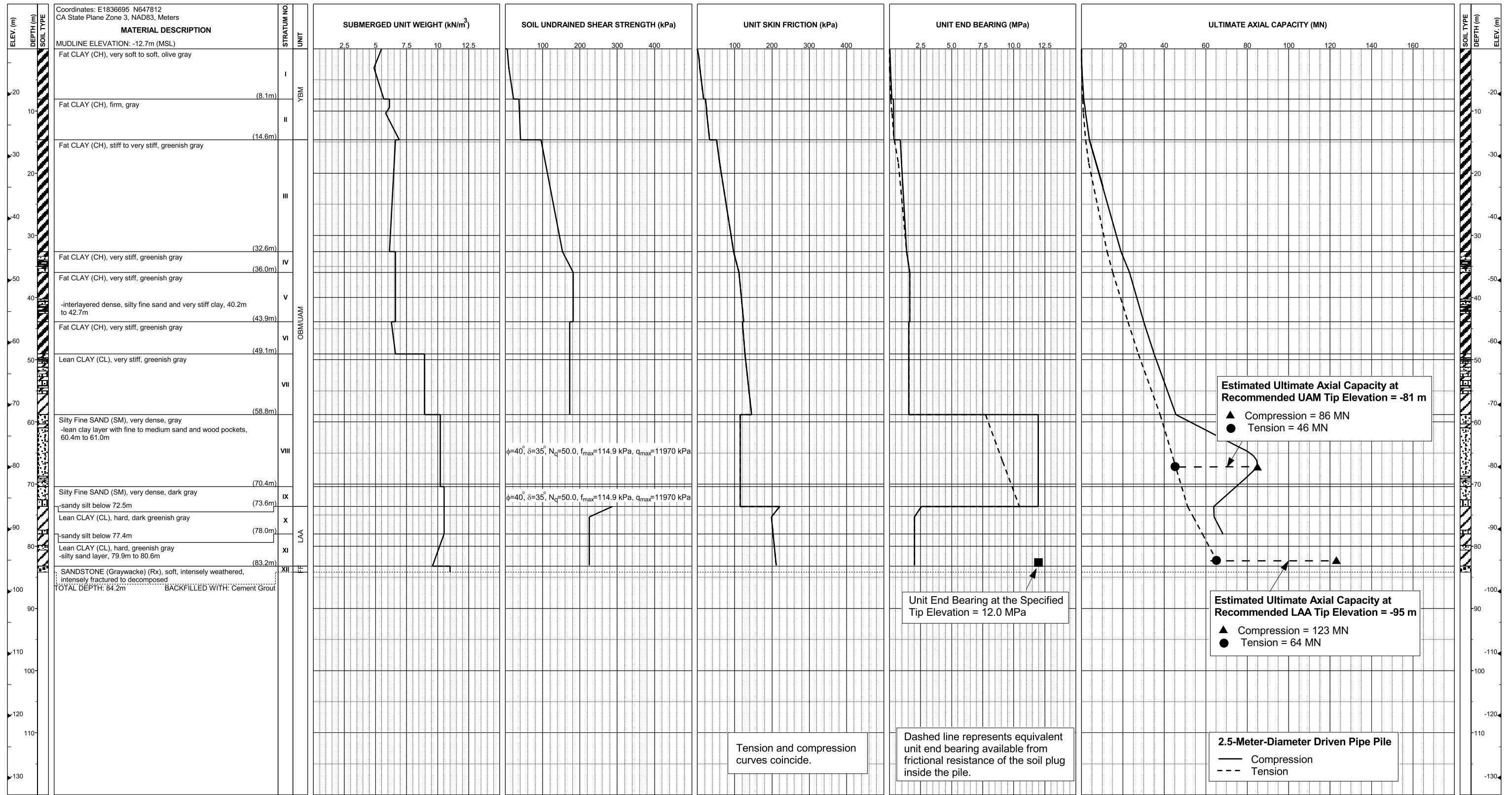




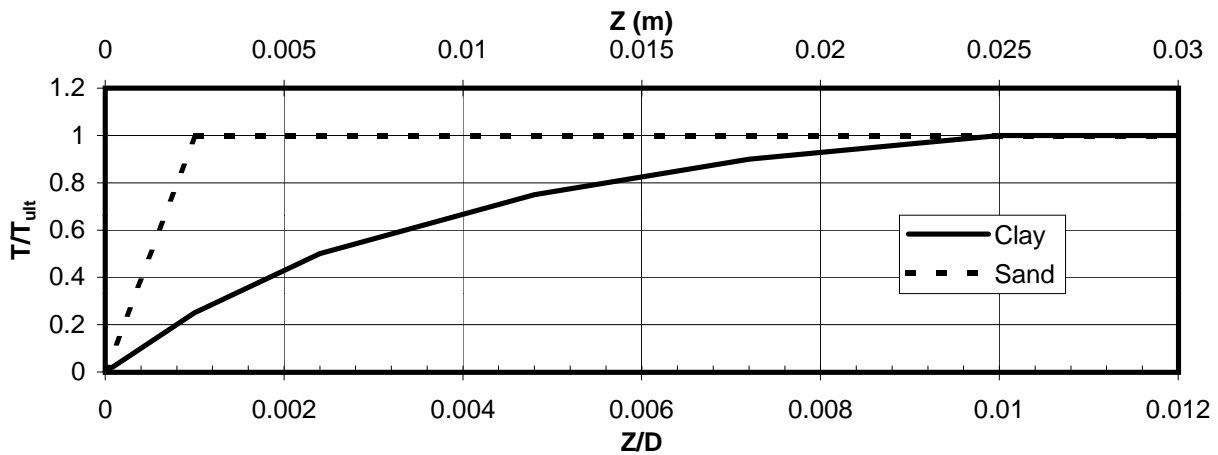
PREDICTED BLOW COUNTS
Pier E2-Eastbound (Boring 98-26)
Menck MHU-1700, 2.5-Meter-Diameter Driven Pipe Piles
SFOBB East Span Seismic Safety Project



**Pier E2-Westbound (Boring 98-25)
Main Span East Pier**



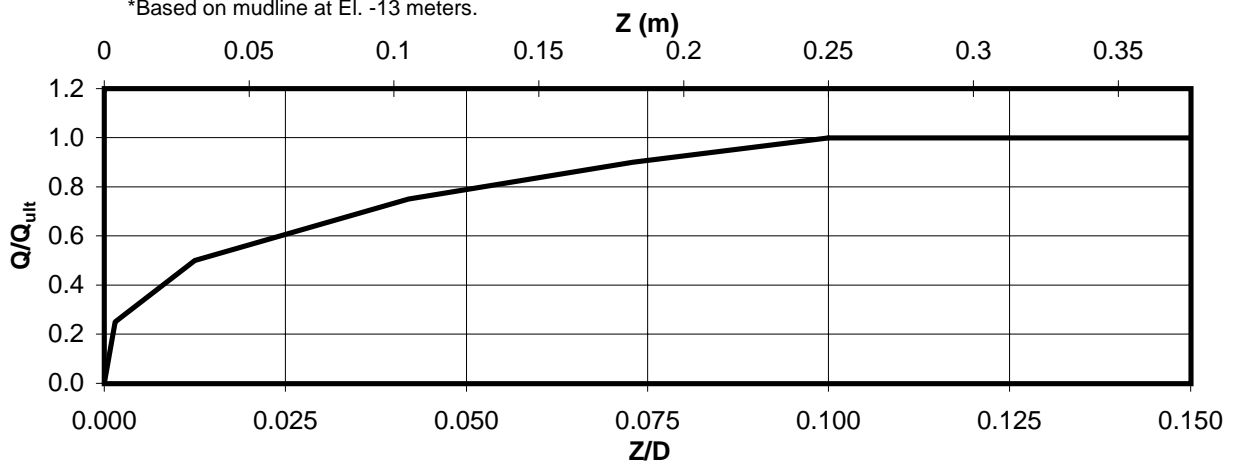
AXIAL PILE DESIGN PARAMETERS AND RESULTS
Pier E2-Westbound (Boring 98-25)
SFOBB East Span Seismic Safety Project



Depth* (m)	Soil Type	T _{ult} (MN/m)
0-3	Clay	0.023
3-6	Clay	0.077
6-9	Clay	0.133
9-12	Clay	0.210
12-15	Clay	0.237
15-18	Clay	0.437
18-21	Clay	0.500
21-24	Clay	0.557
24-27	Clay	0.613
27-30	Clay	0.673
30-33	Clay	0.733
33-36	Clay	0.810

Depth* (m)	Soil Type	T _{ult} (MN/m)
36-39	Clay	0.903
39-42	Clay	0.933
42-45	Clay	0.957
45-51	Clay	0.992
51-57	Clay	1.072
57-63	Sand	0.987
63-69	Sand	0.893
69-75	Sand	0.978
75-81	Clay	1.621
81-82	Clay	1.580

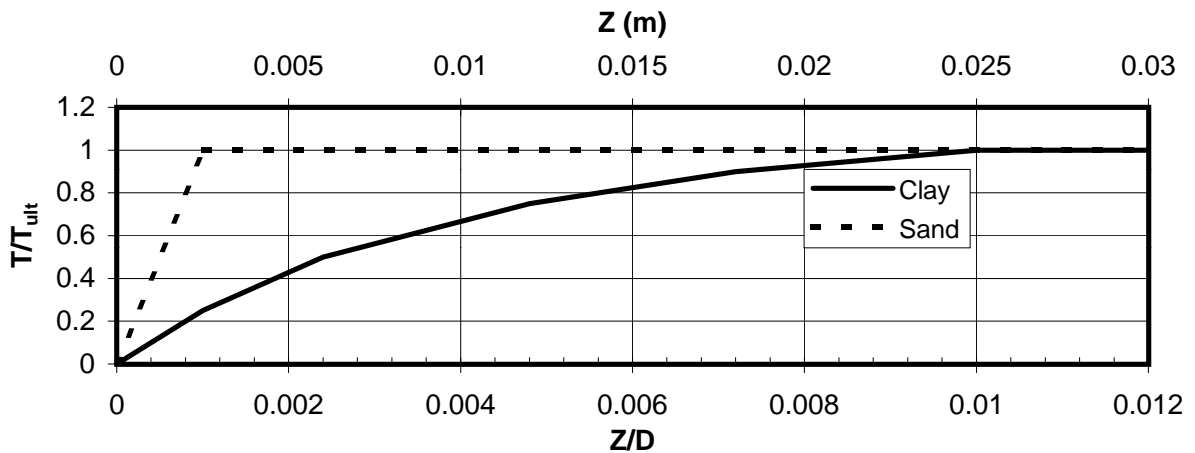
*Based on mudline at El. -13 meters.



Depth* (m)	Soil Type	Q _{ult} (MN)
82	Sand	58.8

AXIAL PILE LOAD TRANSFER-DISPLACEMENT CURVES
Pier E2-Westbound (Boring 98-25)
 2.5-Meter-Diameter Pipe Piles (Pile Tip Elevation = -95 Meters)
 SFOBB East Span Seismic Safety Project

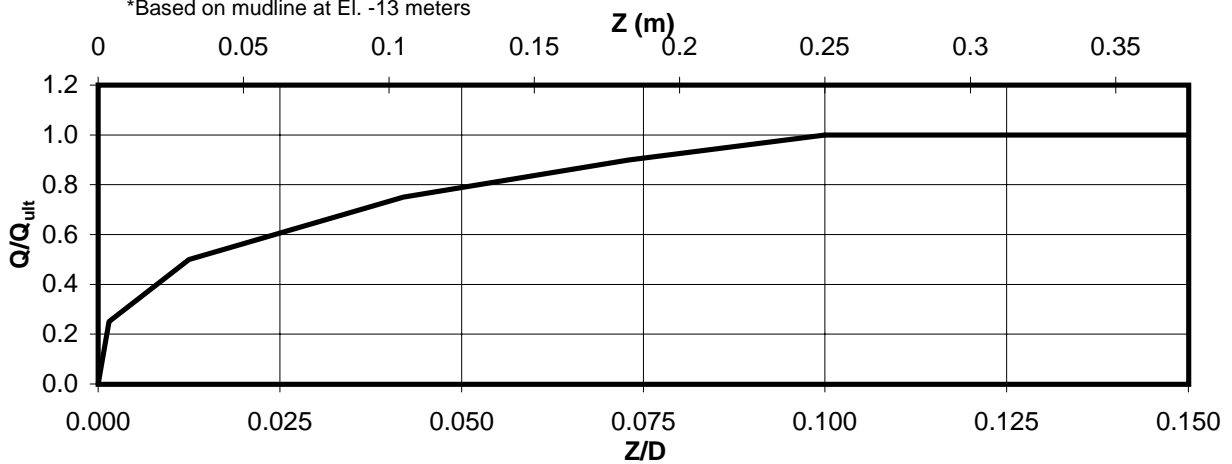




Depth* (m)	Soil Type	T_{ult} (MN/m)
0-3	Clay	0.020
3-6	Clay	0.080
6-9	Clay	0.133
9-12	Clay	0.210
12-15	Clay	0.237
15-18	Clay	0.437
18-21	Clay	0.500
21-24	Clay	0.557
24-27	Clay	0.613
27-30	Clay	0.673
30-33	Clay	0.730
33-36	Clay	0.813

Depth* (m)	Soil Type	T_{ult} (MN/m)
36-39	Clay	0.903
39-42	Clay	0.933
42-45	Clay	0.957
45-51	Clay	0.992
51-57	Clay	1.070
57-63	Sand	0.987
63-68	Sand	0.892

*Based on mudline at El. -13 meters



Depth* (m)	Soil Type	Q_{ult} (MN)
68	Sand	39.5

AXIAL PILE LOAD TRANSFER-DISPLACEMENT CURVES
Pier E2-Westbound (Boring 98-25)
 2.5-Meter-Diameter Pipe Piles (Pile Tip Elevation = -81 Meters)
 SFOBB East Span Seismic Safety Project



DEPTH (m)	t-z Data											
	t(1)	z(1)	t(2)	z(2)	t(3)	z(3)	t(4)	z(4)	t(5)	z(5)	t(6)	z(6)
0-3	0.0	0.0	0.006	0.003	0.012	0.006	0.017	0.012	0.021	0.018	0.023	0.025
3-6	0.0	0.0	0.019	0.003	0.038	0.006	0.058	0.012	0.069	0.018	0.077	0.025
6-9	0.0	0.0	0.033	0.003	0.067	0.006	0.100	0.012	0.120	0.018	0.133	0.025
9-12	0.0	0.0	0.053	0.003	0.105	0.006	0.158	0.012	0.189	0.018	0.210	0.025
12-15	0.0	0.0	0.059	0.003	0.118	0.006	0.178	0.012	0.213	0.018	0.237	0.025
15-18	0.0	0.0	0.109	0.003	0.218	0.006	0.328	0.012	0.393	0.018	0.437	0.025
18-21	0.0	0.0	0.125	0.003	0.250	0.006	0.375	0.012	0.450	0.018	0.500	0.025
21-24	0.0	0.0	0.139	0.003	0.278	0.006	0.418	0.012	0.501	0.018	0.557	0.025
24-27	0.0	0.0	0.153	0.003	0.307	0.006	0.460	0.012	0.552	0.018	0.613	0.025
27-30	0.0	0.0	0.168	0.003	0.337	0.006	0.505	0.012	0.606	0.018	0.673	0.025
30-33	0.0	0.0	0.183	0.003	0.367	0.006	0.550	0.012	0.660	0.018	0.733	0.025
33-36	0.0	0.0	0.203	0.003	0.405	0.006	0.608	0.012	0.729	0.018	0.810	0.025
36-39	0.0	0.0	0.226	0.003	0.452	0.006	0.677	0.012	0.813	0.018	0.903	0.025
39-42	0.0	0.0	0.233	0.003	0.467	0.006	0.700	0.012	0.840	0.018	0.933	0.025
42-45	0.0	0.0	0.239	0.003	0.478	0.006	0.718	0.012	0.861	0.018	0.957	0.025
45-51	0.0	0.0	0.248	0.003	0.496	0.006	0.744	0.012	0.893	0.018	0.992	0.025
51-57	0.0	0.0	0.268	0.003	0.536	0.006	0.804	0.012	0.965	0.018	1.072	0.025
57-63	0.0	0.0	0.987	0.003								
63-69	0.0	0.0	0.893	0.003								
69-75	0.0	0.0	0.978	0.003								
75-81	0.0	0.0	0.405	0.003	0.811	0.006	1.216	0.012	1.459	0.018	1.621	0.025
81-82	0.0	0.0	0.395	0.003	0.790	0.006	1.185	0.012	1.422	0.018	1.580	0.025

Notes:

1. "t" is load (MN/m)
2. "z" is displacement (m)
3. Data for tension and compression coincide
4. Based on mudline at El. -13 meters

DEPTH (m)	Q-z Data											
	Q(1)	z(1)	Q(2)	z(2)	Q(3)	z(3)	Q(4)	z(4)	Q(5)	z(5)	Q(6)	z(6)
82	0.0	0.0	14.700	0.004	29.400	0.031	44.100	0.105	52.920	0.183	58.800	0.250

Notes:

1. "Q" is load in compression (MN)
2. "z" is displacement (m)

TABULATED AXIAL PILE LOAD TRANSFER DATA
Pier E2-Westbound (Boring 98-25)
2.5-Meter-Diameter Pipe Piles (Pile Tip Elevation = -95 Meters)
SFOBB East Span Seismic Safety Project



DEPTH (m)	t-z Data											
	t(1)	z(1)	t(2)	z(2)	t(3)	z(3)	t(4)	z(4)	t(5)	z(5)	t(6)	z(6)
0-3	0.0	0.0	0.005	0.003	0.010	0.006	0.015	0.012	0.018	0.018	0.020	0.025
3-6	0.0	0.0	0.020	0.003	0.040	0.006	0.060	0.012	0.072	0.018	0.080	0.025
6-9	0.0	0.0	0.033	0.003	0.067	0.006	0.100	0.012	0.120	0.018	0.133	0.025
9-12	0.0	0.0	0.053	0.003	0.105	0.006	0.158	0.012	0.189	0.018	0.210	0.025
12-15	0.0	0.0	0.059	0.003	0.118	0.006	0.178	0.012	0.213	0.018	0.237	0.025
15-18	0.0	0.0	0.109	0.003	0.218	0.006	0.328	0.012	0.393	0.018	0.437	0.025
18-21	0.0	0.0	0.125	0.003	0.250	0.006	0.375	0.012	0.450	0.018	0.500	0.025
21-24	0.0	0.0	0.139	0.003	0.278	0.006	0.418	0.012	0.501	0.018	0.557	0.025
24-27	0.0	0.0	0.153	0.003	0.307	0.006	0.460	0.012	0.552	0.018	0.613	0.025
27-30	0.0	0.0	0.168	0.003	0.337	0.006	0.505	0.012	0.606	0.018	0.673	0.025
30-33	0.0	0.0	0.183	0.003	0.365	0.006	0.548	0.012	0.657	0.018	0.730	0.025
33-36	0.0	0.0	0.203	0.003	0.407	0.006	0.610	0.012	0.732	0.018	0.813	0.025
36-39	0.0	0.0	0.226	0.003	0.452	0.006	0.677	0.012	0.813	0.018	0.903	0.025
39-42	0.0	0.0	0.233	0.003	0.467	0.006	0.700	0.012	0.840	0.018	0.933	0.025
42-45	0.0	0.0	0.239	0.003	0.478	0.006	0.718	0.012	0.861	0.018	0.957	0.025
45-51	0.0	0.0	0.248	0.003	0.496	0.006	0.744	0.012	0.893	0.018	0.992	0.025
51-57	0.0	0.0	0.268	0.003	0.535	0.006	0.803	0.012	0.963	0.018	1.070	0.025
57-63	0.0	0.0	0.987	0.003								
63-68	0.0	0.0	0.892	0.003								

Notes:

1. "t" is load (MN/m)
2. "z" is displacement (m)
3. Data for tension and compression coincide
4. Based on mudline at El. -13 meters

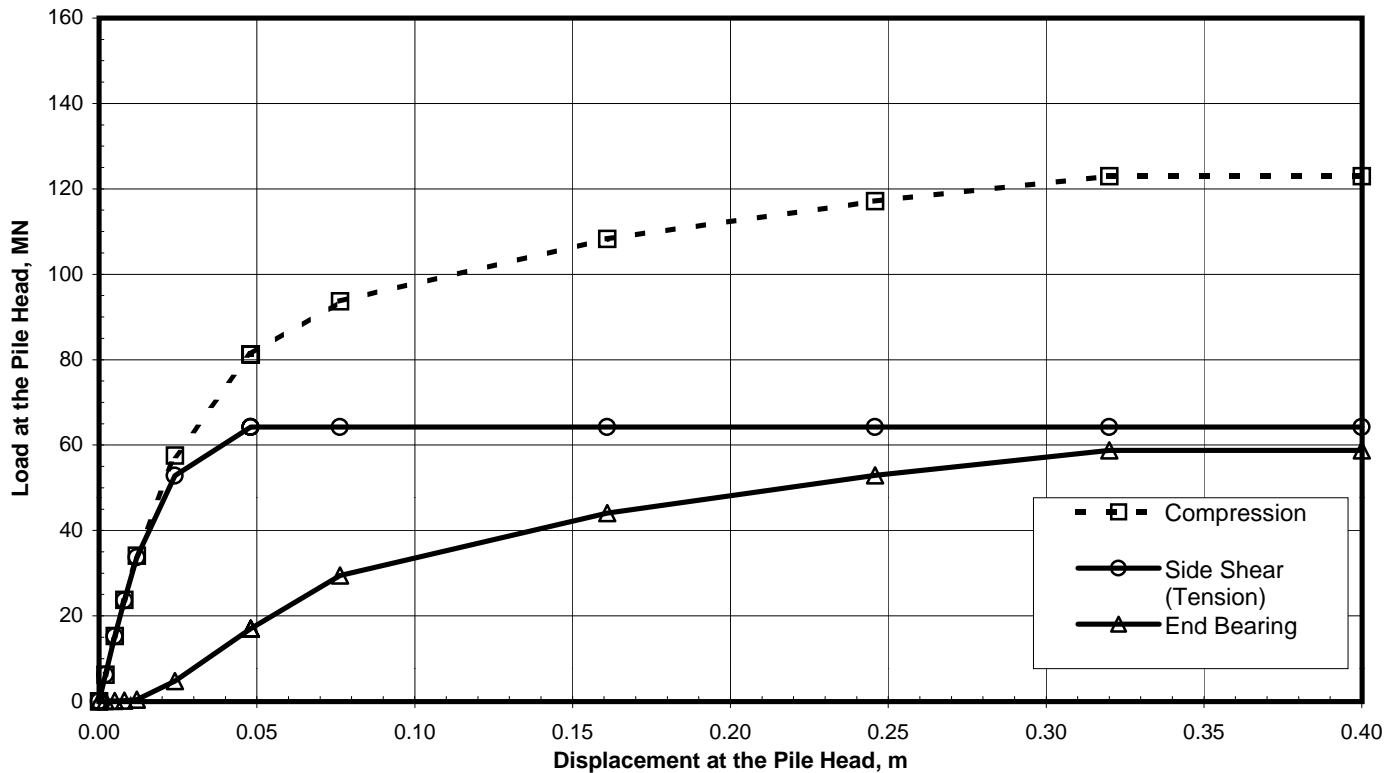
DEPTH (m)	Q-z Data											
	Q(1)	z(1)	Q(2)	z(2)	Q(3)	z(3)	Q(4)	z(4)	Q(5)	z(5)	Q(6)	z(6)
68	0.0	0.0	9.875	0.004	19.750	0.031	29.625	0.105	35.550	0.183	39.500	0.250

Notes:

1. "Q" is load in compression (MN)
2. "z" is displacement (m)

TABULATED AXIAL PILE LOAD TRANSFER DATA
Pier E2-Westbound (Boring 98-25)
 2.5-Meter-Diameter Pipe Piles (Pile Tip Elevation = -81 Meters)
 SFOBB East Span Seismic Safety Project



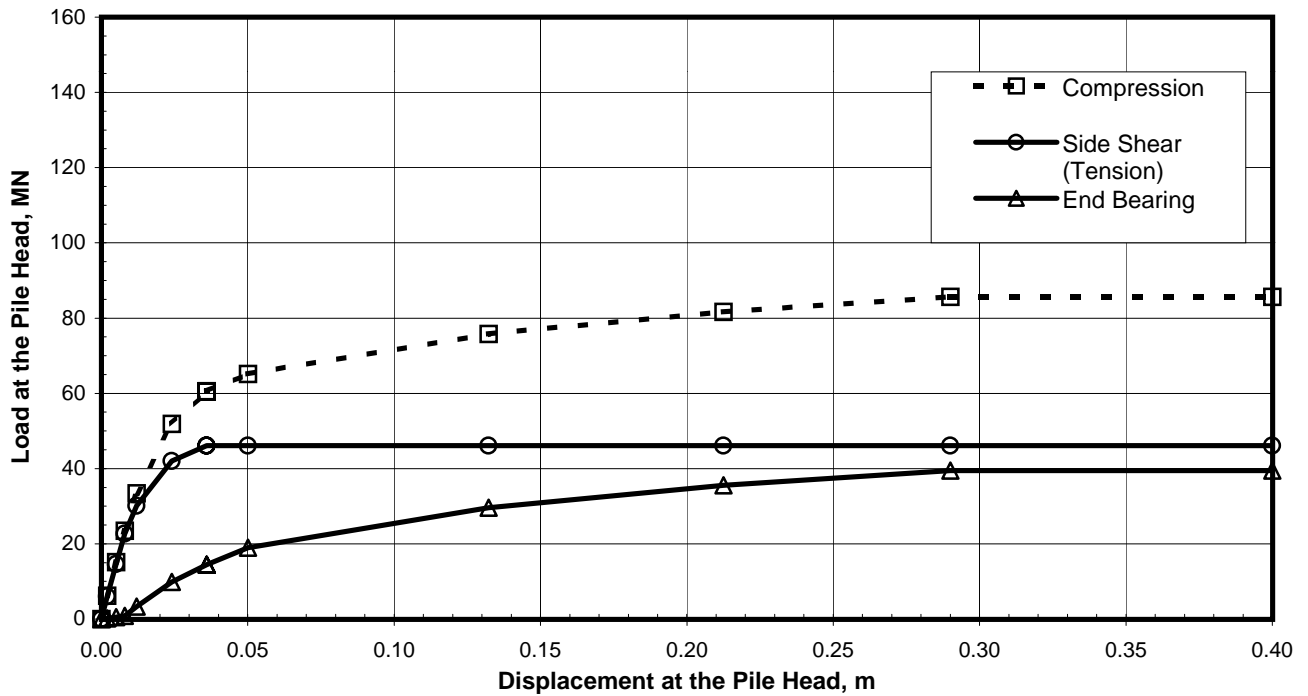


Pile Head Displacement (m)	Load at the Pile Head		End Bearing Component in Compression (MN)
	Compression (MN)	Tension (MN)	
0.000	0.00	0.00	0.00
0.002	6.24	6.20	0.04
0.005	15.29	15.20	0.10
0.008	23.78	23.60	0.18
0.012	34.07	33.69	0.38
0.024	57.53	52.83	4.70
0.048	81.23	64.23	17.00
0.076	93.68	64.23	29.45
0.161	108.31	64.23	44.08
0.246	117.12	64.23	52.89
0.320	123.00	64.23	58.77
0.400	123.00	64.23	58.77

Note:
 Pile head load-displacement curves are based on the preliminary pile wall thickness schedule provided by TY Lin/M&N and static loading conditions.

STATIC PILE HEAD LOAD-DEFORMATION CURVES
Pier E2-Westbound (Boring 98-25)
 2.5-Meter-Diameter Pipe Piles (Pile Tip Elevation = -95 Meters)
 SFOBB East Span Seismic Safety Project





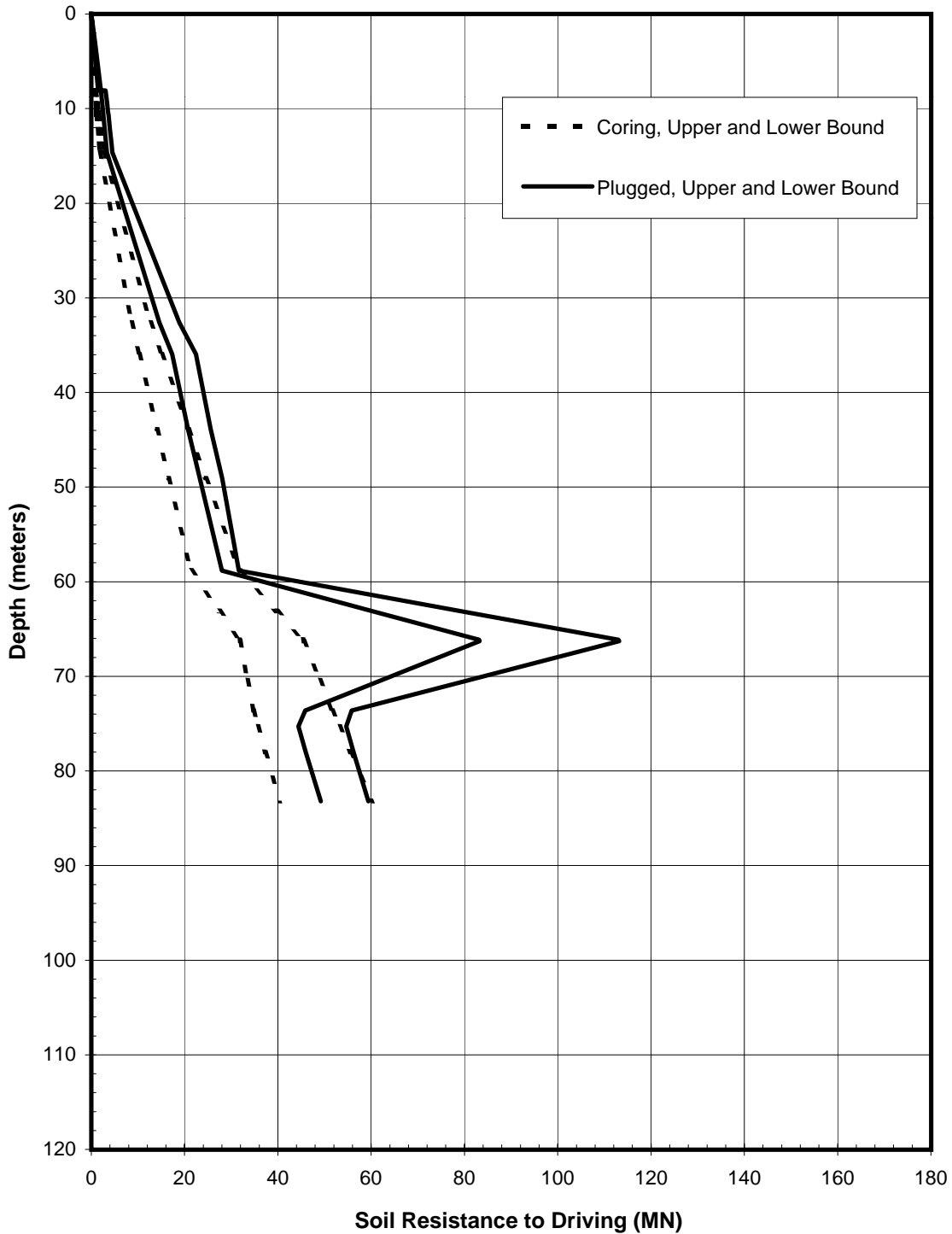
Pile Head Displacement (m)	Load at the Pile Head		End Bearing Component in Compression (MN)
	Compression (MN)	Tension (MN)	
0.000	0.00	0.00	0.00
0.002	6.18	6.01	0.18
0.005	15.14	14.67	0.47
0.008	23.51	22.69	0.82
0.012	33.47	30.15	3.32
0.024	51.86	41.98	9.88
0.036	60.56	46.14	14.42
0.050	65.14	46.14	19.00
0.132	75.77	46.14	29.63
0.213	81.69	46.14	35.55
0.290	85.64	46.14	39.50
0.400	85.64	46.14	39.50

Note:

Pile head load-displacement curves are based on the preliminary pile wall thickness schedule provided by TY Lin/M&N and static loading conditions.

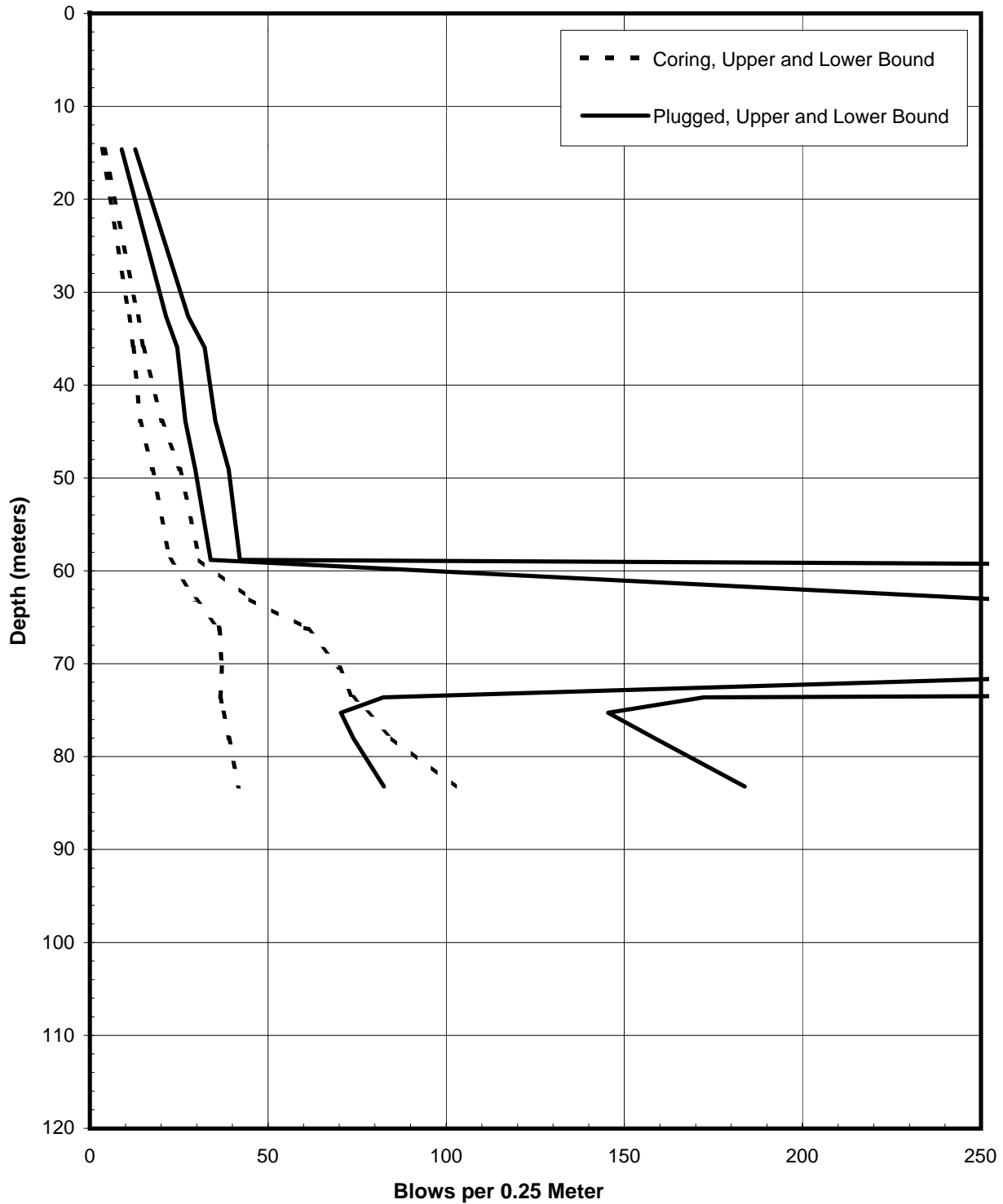
STATIC PILE HEAD LOAD-DEFORMATION CURVES
Pier E2-Westbound (Boring 98-25)
 2.5-Meter-Diameter Pipe Piles (Pile Tip Elevation = -81 Meters)
 SFOBB East Span Seismic Safety Project





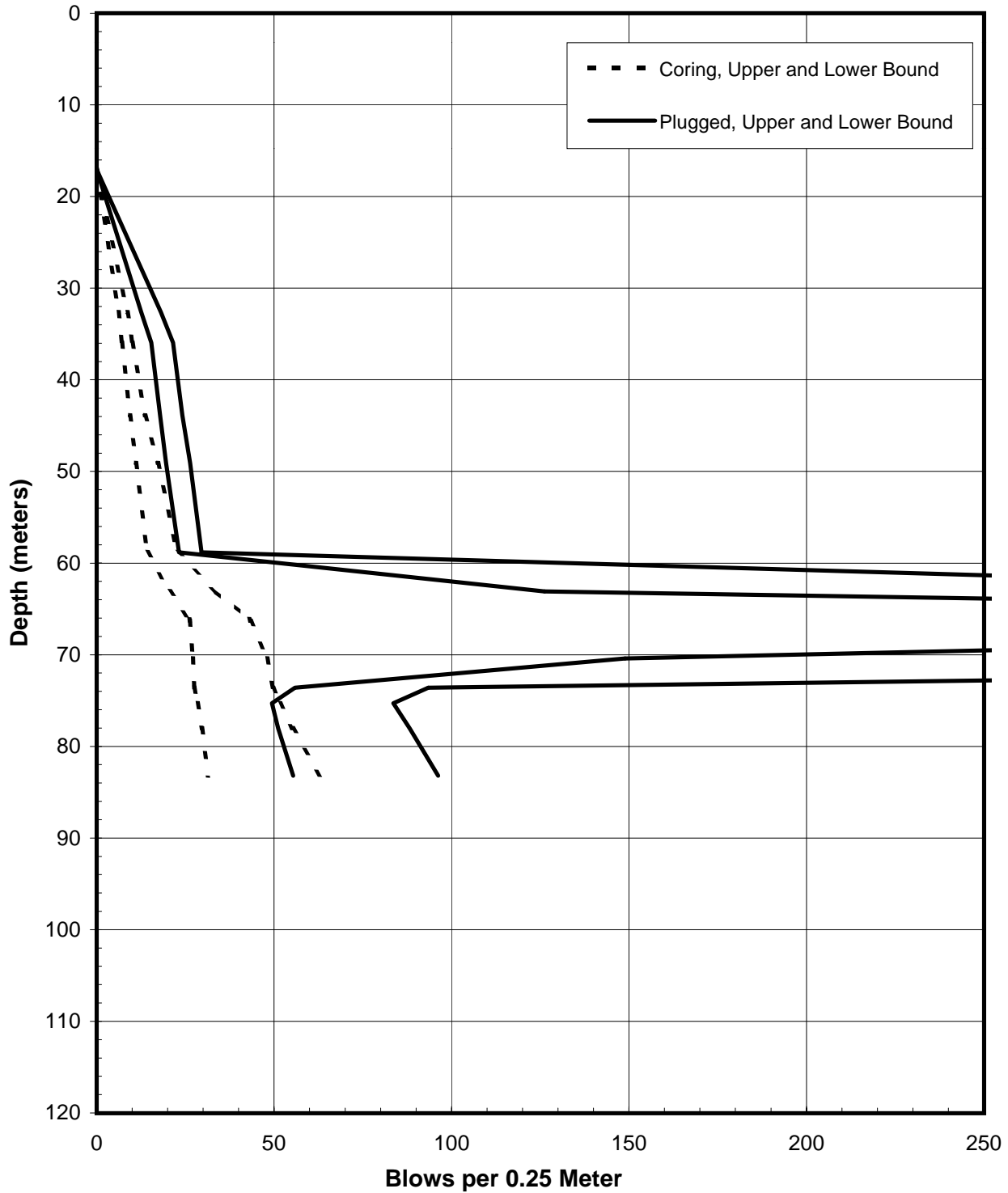
SOIL RESISTANCE TO DRIVING
Pier E2-Westbound (Boring 98-25)
2.5-Meter-Diameter Driven Pipe Piles
SFOBB East Span Seismic Safety Project





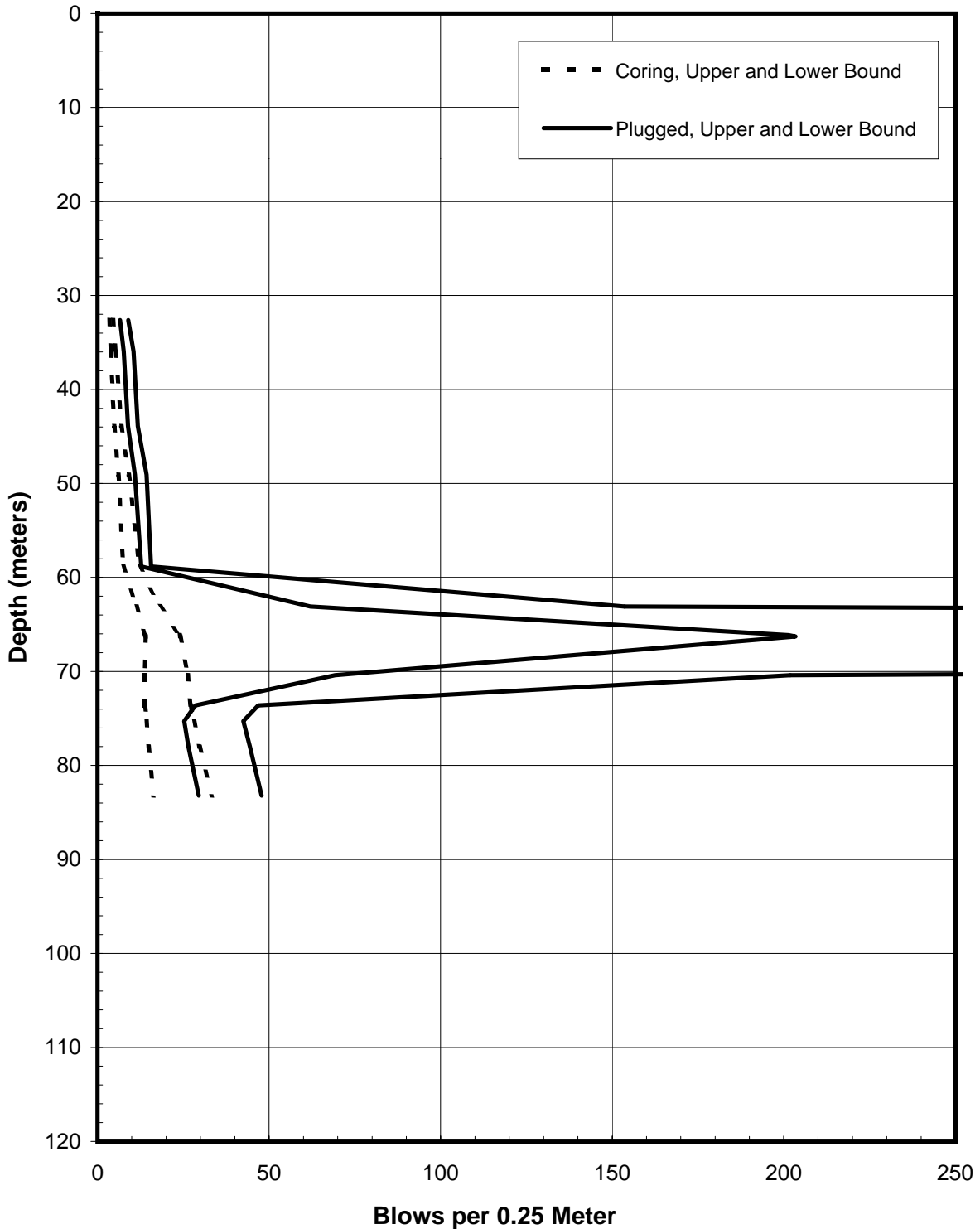
PREDICTED BLOW COUNTS
Pier E2-Westbound (Boring 98-25)
Menck MHU-500T, 2.5-Meter-Diameter Driven Pipe Piles
SFOBB East Span Seismic Safety Project





PREDICTED BLOW COUNTS
Pier E2-Westbound (Boring 98-25)
Menck MHU-1000, 2.5-Meter-Diameter Driven Pipe Piles
SFOBB East Span Seismic Safety Project

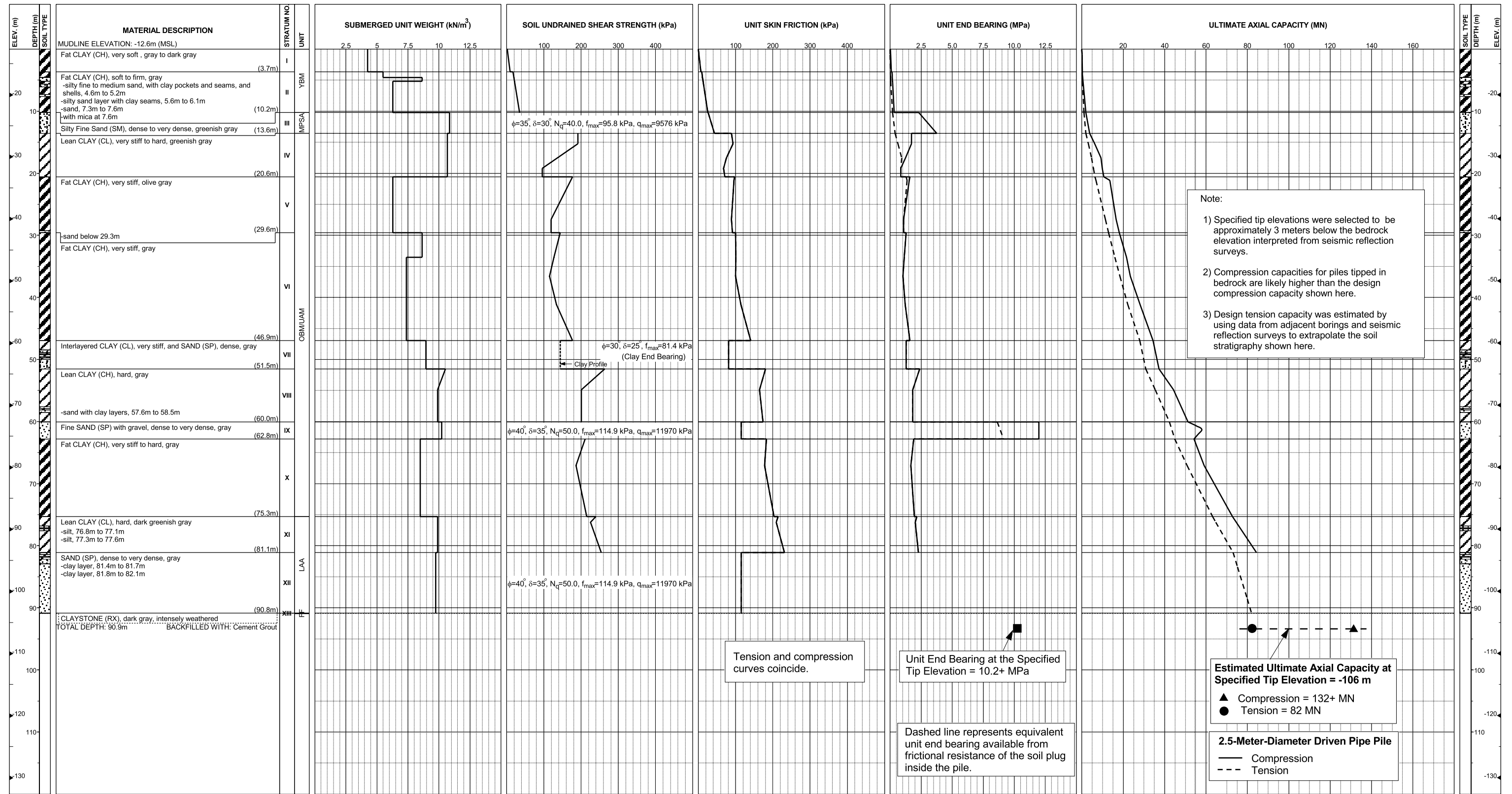




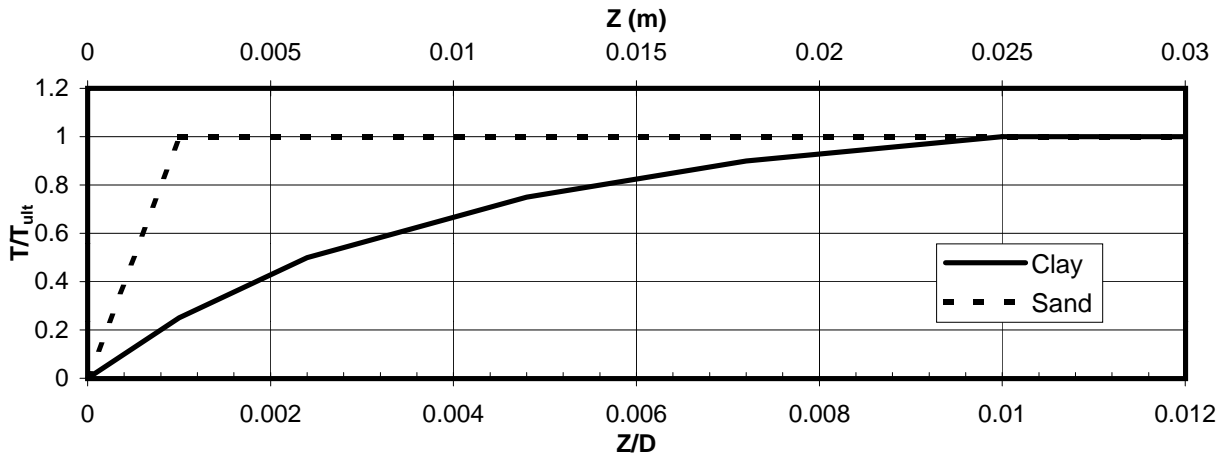
PREDICTED BLOW COUNTS
Pier E2-Westbound (Boring 98-25)
Menck MHU-1700, 2.5-Meter-Diameter Driven Pipe Piles
SFOBB East Span Seismic Safety Project



**Pier E3-Eastbound (Boring 98-27)
Skyway Frame 1**



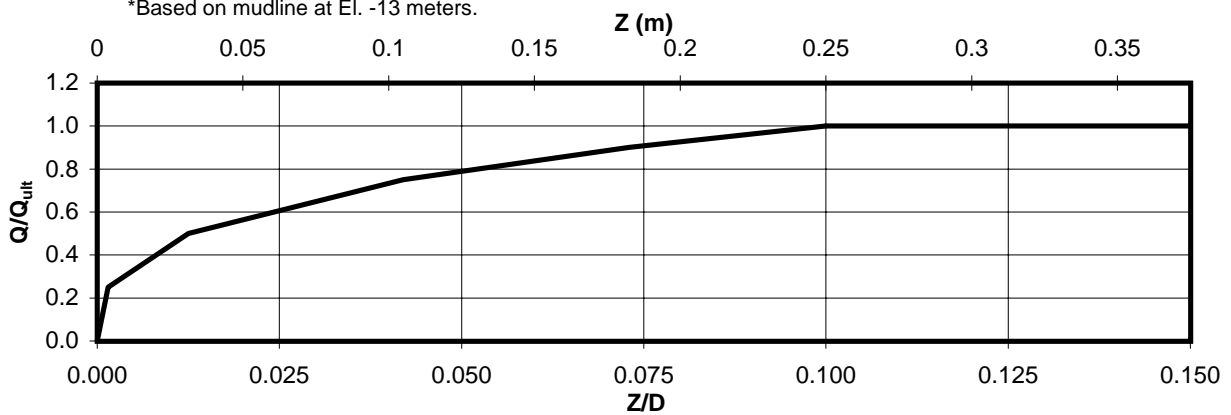
AXIAL PILE DESIGN PARAMETERS AND RESULTS
Pier E3-Eastbound (Boring 98-27)
SFOBB East Span Seismic Safety Project



Depth* (m)	Soil Type	T _{ult} (MN/m)
0-3	Clay	0.017
3-6	Clay	0.073
6-9	Clay	0.147
9-12	Sand	0.217
12-15	Sand	0.393
15-18	Clay	0.737
18-21	Clay	0.540
21-24	Clay	0.747
24-27	Clay	0.720
27-30	Clay	0.703
30-33	Clay	0.790
33-36	Clay	0.790

Depth* (m)	Soil Type	T _{ult} (MN/m)
36-39	Clay	0.800
39-42	Clay	0.887
42-45	Clay	0.983
45-51	Sand	0.800
51-57	Clay	1.188
57-63	Clay	1.158
63-69	Clay	1.391
69-75	Clay	1.520
75-81	Clay	1.714
81-87	Sand	0.909

*Based on mudline at El. -13 meters.



Depth* (m)	Soil Type	Q _{ult} (MN)
87	Sand	50.2

AXIAL PILE LOAD TRANSFER-DISPLACEMENT CURVES
Pier E3-Eastbound (Boring 98-27)
 2.5-Meter-Diameter Pipe Piles (Pile Tip Elevation = -100 Meters)
 SFOBB East Span Seismic Safety Project



DEPTH (m)	t-z Data											
	t(1)	z(1)	t(2)	z(2)	t(3)	z(3)	t(4)	z(4)	t(5)	z(5)	t(6)	z(6)
0-3	0.0	0.0	0.004	0.003	0.008	0.006	0.012	0.012	0.015	0.018	0.017	0.025
3-6	0.0	0.0	0.018	0.003	0.037	0.006	0.055	0.012	0.066	0.018	0.073	0.025
6-9	0.0	0.0	0.037	0.003	0.073	0.006	0.110	0.012	0.132	0.018	0.147	0.025
9-12	0.0	0.0	0.217	0.003								
12-15	0.0	0.0	0.393	0.003								
15-18	0.0	0.0	0.184	0.003	0.368	0.006	0.553	0.012	0.663	0.018	0.737	0.025
18-21	0.0	0.0	0.135	0.003	0.270	0.006	0.405	0.012	0.486	0.018	0.540	0.025
21-24	0.0	0.0	0.187	0.003	0.373	0.006	0.560	0.012	0.672	0.018	0.747	0.025
24-27	0.0	0.0	0.180	0.003	0.360	0.006	0.540	0.012	0.648	0.018	0.720	0.025
27-30	0.0	0.0	0.176	0.003	0.352	0.006	0.527	0.012	0.633	0.018	0.703	0.025
30-33	0.0	0.0	0.198	0.003	0.395	0.006	0.593	0.012	0.711	0.018	0.790	0.025
33-36	0.0	0.0	0.198	0.003	0.395	0.006	0.593	0.012	0.711	0.018	0.790	0.025
36-39	0.0	0.0	0.200	0.003	0.400	0.006	0.600	0.012	0.720	0.018	0.800	0.025
39-42	0.0	0.0	0.222	0.003	0.443	0.006	0.665	0.012	0.798	0.018	0.887	0.025
42-45	0.0	0.0	0.246	0.003	0.492	0.006	0.737	0.012	0.885	0.018	0.983	0.025
45-51	0.0	0.0	0.800	0.003								
51-57	0.0	0.0	0.297	0.003	0.594	0.006	0.891	0.012	1.069	0.018	1.188	0.025
57-63	0.0	0.0	0.290	0.003	0.579	0.006	0.869	0.012	1.042	0.018	1.158	0.025
63-69	0.0	0.0	0.348	0.003	0.696	0.006	1.043	0.012	1.252	0.018	1.391	0.025
69-75	0.0	0.0	0.380	0.003	0.760	0.006	1.140	0.012	1.368	0.018	1.520	0.025
75-81	0.0	0.0	0.429	0.003	0.857	0.006	1.286	0.012	1.543	0.018	1.714	0.025
81-87	0.0	0.0	0.909	0.003								

Notes:

1. "t" is load (MN/m)
2. "z" is displacement (m)
3. Data for tension and compression coincide
4. Based on mudline at El. -13 meters

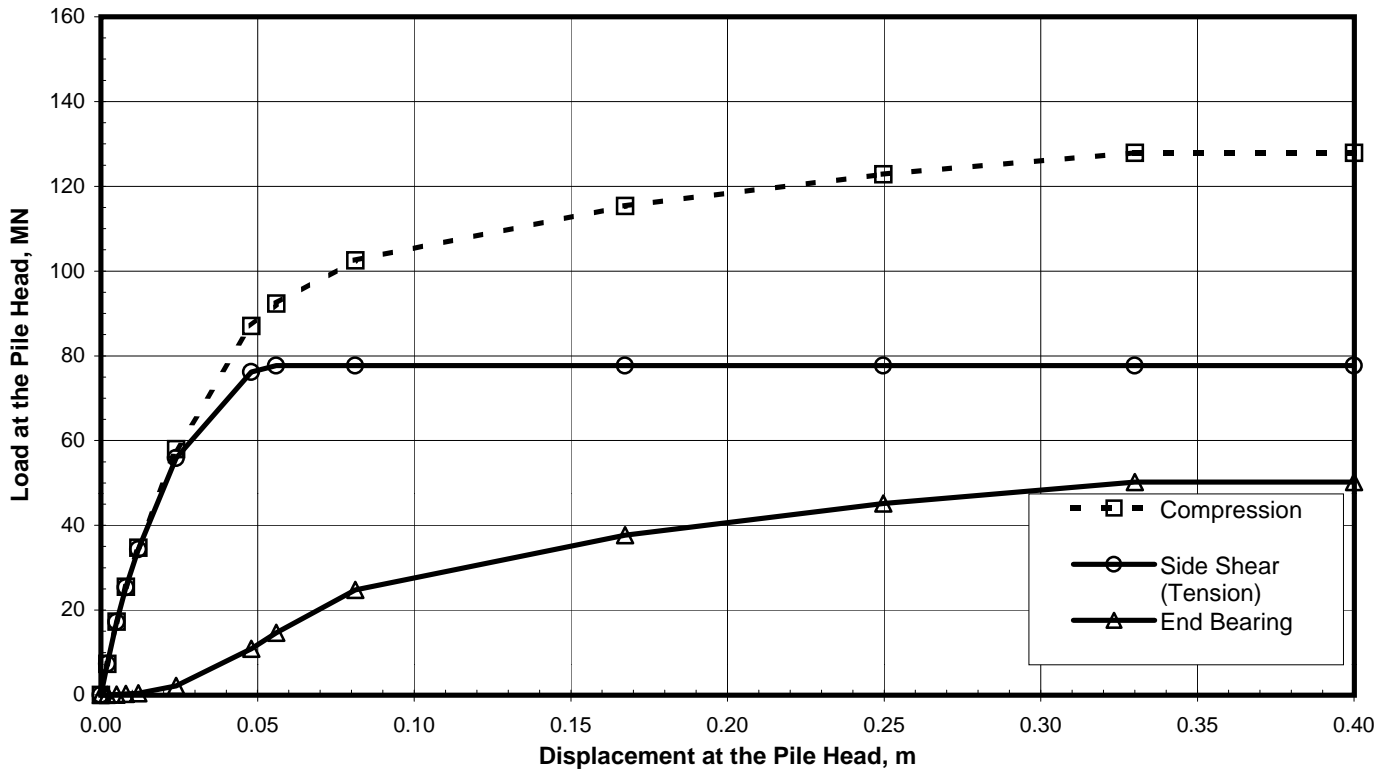
DEPTH (m)	Q-z Data											
	Q(1)	z(1)	Q(2)	z(2)	Q(3)	z(3)	Q(4)	z(4)	Q(5)	z(5)	Q(6)	z(6)
87	0.0	0.0	12.550	0.004	25.100	0.031	37.650	0.105	45.180	0.183	50.200	0.250

Notes:

1. "Q" is load in compression (MN)
2. "z" is displacement (m)

TABULATED AXIAL PILE LOAD TRANSFER DATA
Pier E3-Eastbound (Boring 98-27)
2.5-Meter-Diameter Pipe Piles (Pile Tip Elevation = -100 Meters)
SFOBB East Span Seismic Safety Project





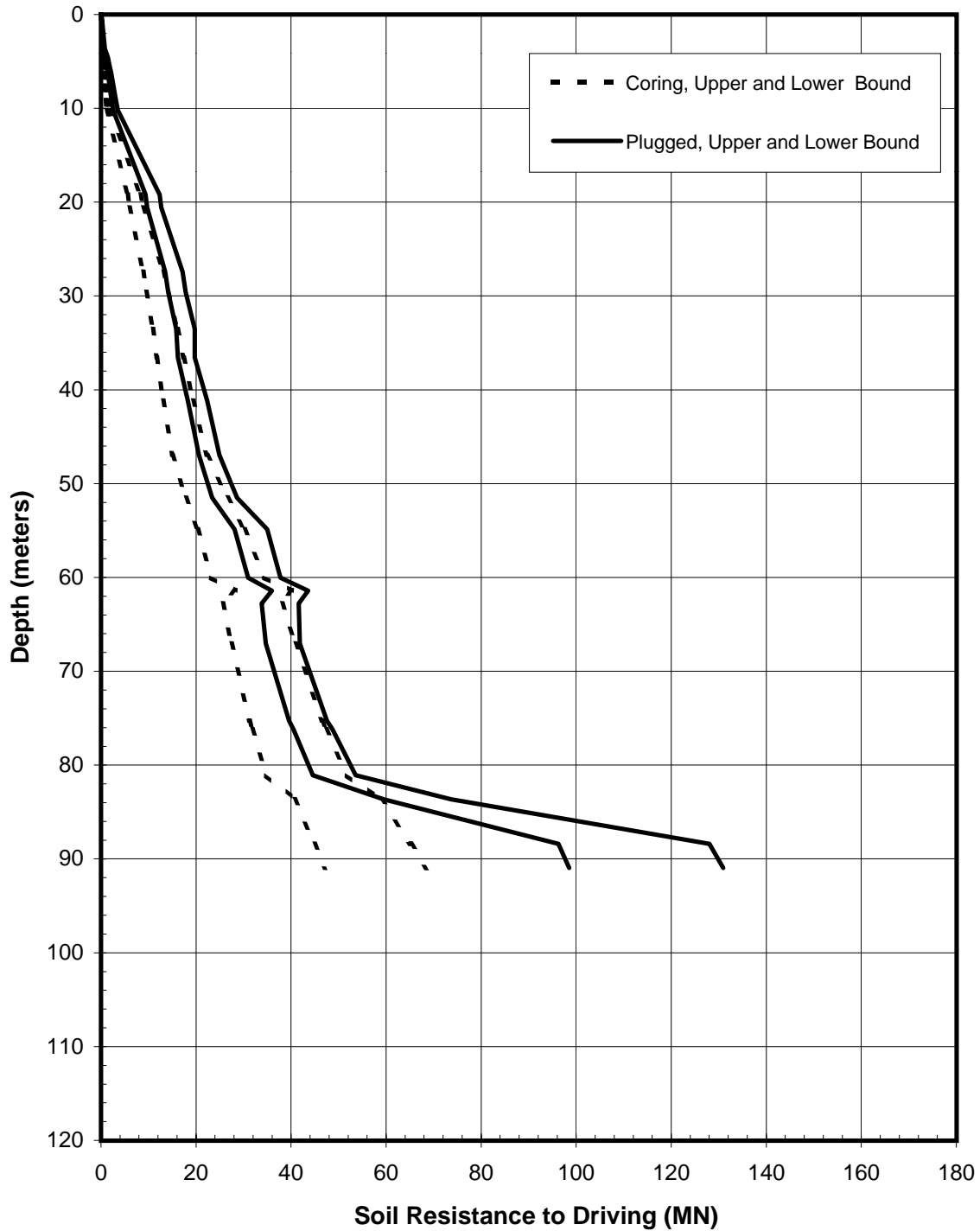
Pile Head Displacement (m)	Load at the Pile Head		End Bearing Component in Compression (MN)
	Compression (MN)	Tension (MN)	
0.000	0.00	0.00	0.00
0.002	7.36	7.32	0.03
0.005	17.32	17.23	0.08
0.008	25.55	25.36	0.19
0.012	34.73	34.37	0.36
0.024	57.99	55.88	2.11
0.048	87.06	76.17	10.89
0.056	92.35	77.71	14.64
0.081	102.51	77.71	24.80
0.167	115.35	77.71	37.64
0.250	122.88	77.71	45.17
0.330	127.90	77.71	50.19
0.400	127.90	77.71	50.19

Note:

Pile head load-displacement curves are based on the preliminary pile wall thickness schedule provided by TY Lin/M&N and static loading conditions.

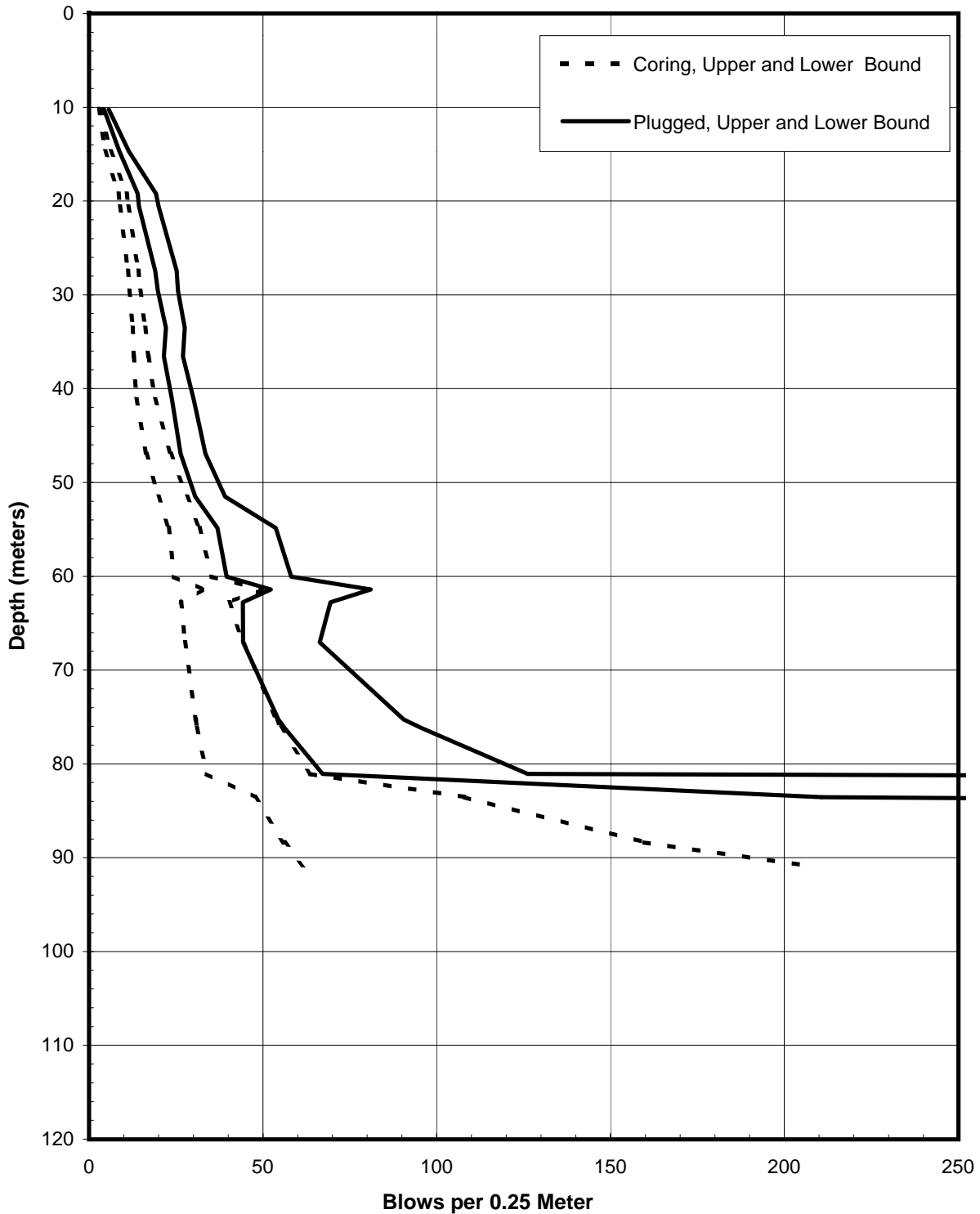
STATIC PILE HEAD LOAD-DEFORMATION CURVES
Pier E3-Eastbound (Boring 98-27)
 2.5-Meter-Diameter Pipe Piles (Pile Tip Elevation = -100 Meters)
 SFOBB East Span Seismic Safety Project





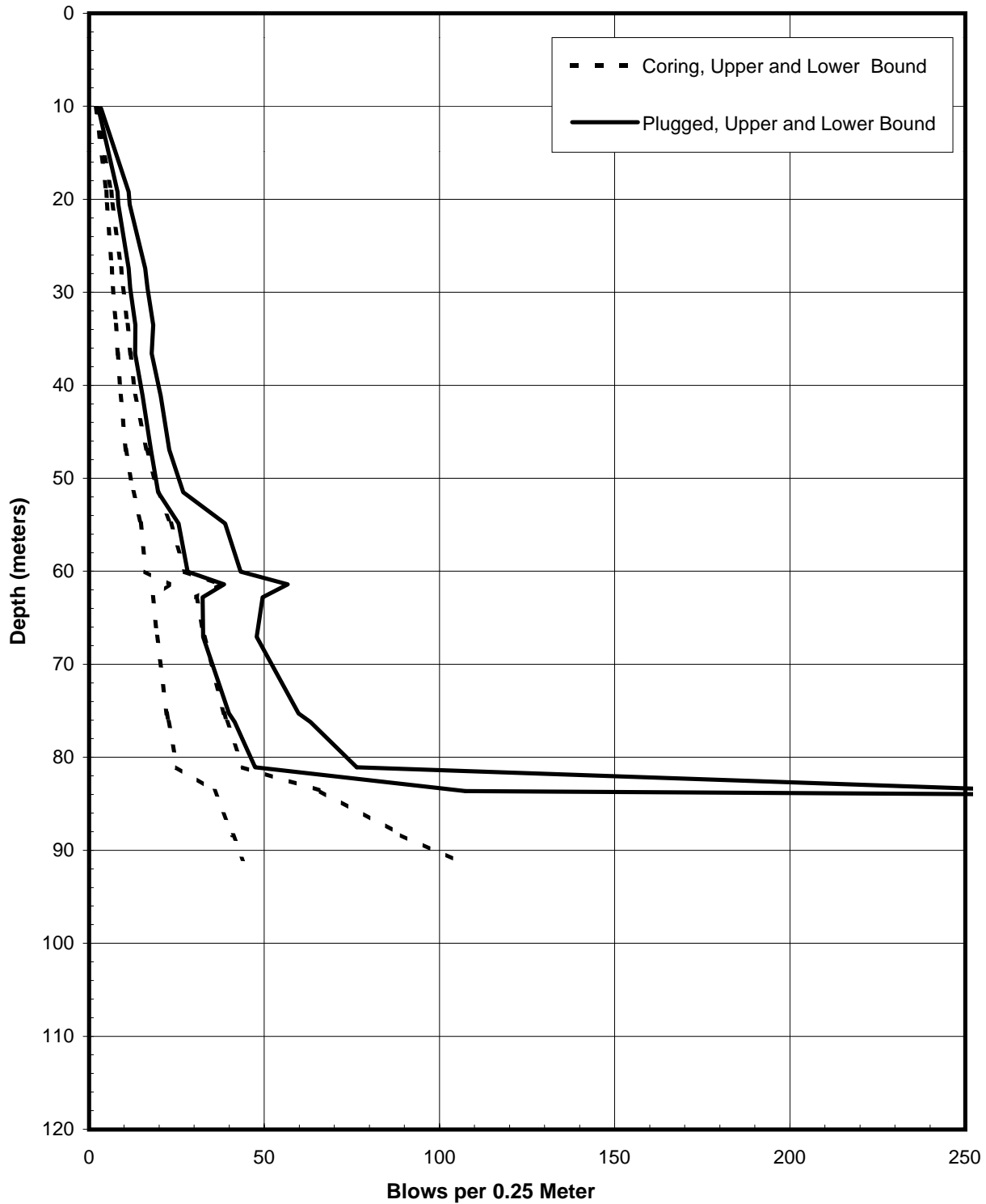
SOIL RESISTANCE TO DRIVING
Pier E3-Eastbound (Boring 98-27)
2.5-Meter-Diameter Driven Pipe Piles
SFOBB East Span Seismic Safety Project





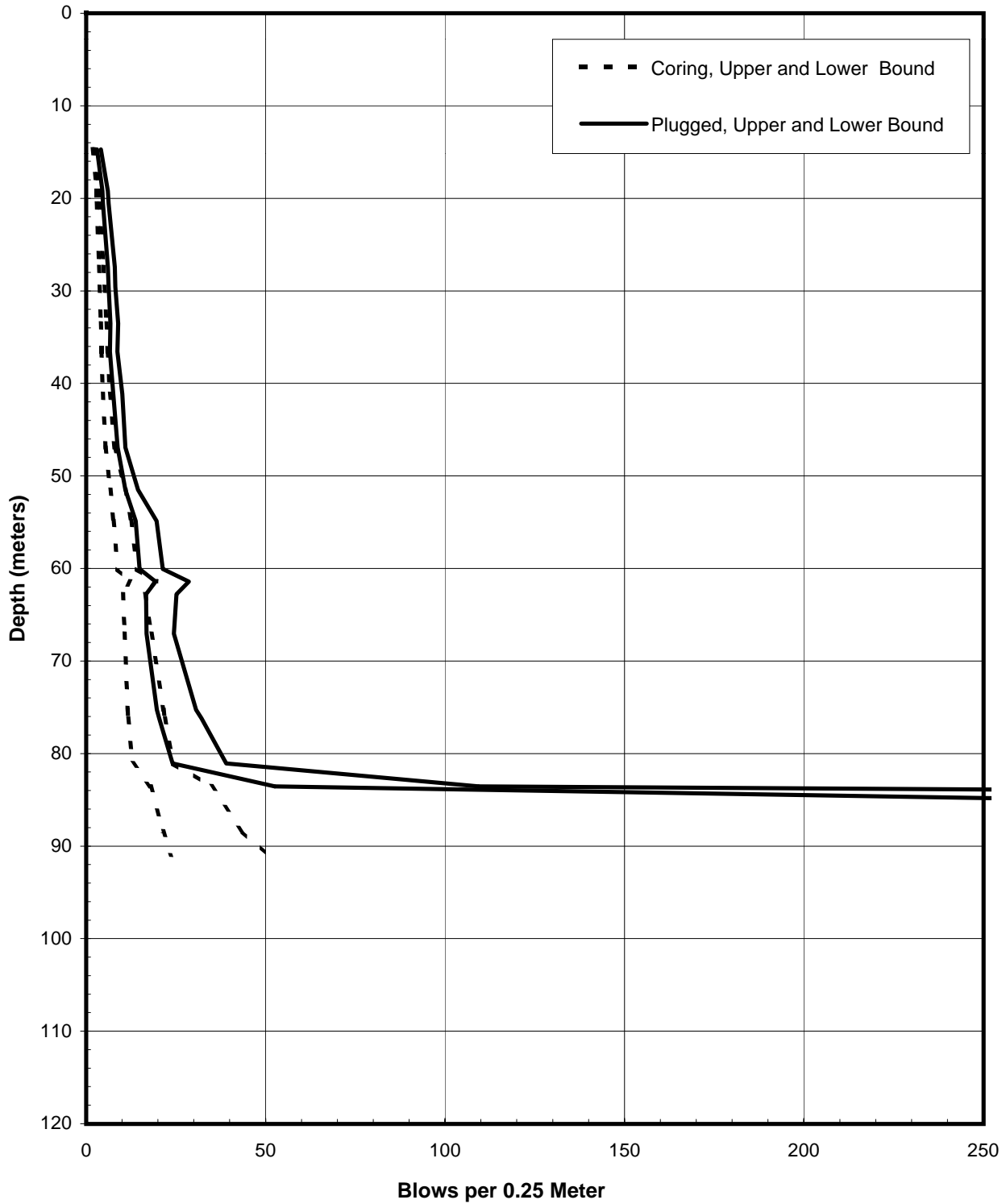
PREDICTED BLOW COUNTS
Pier E3-Eastbound (Boring 98-27)
Menck MHU-500T, 2.5-Meter-Diameter Driven Pipe Piles
SFOBB East Span Seismic Safety Project





PREDICTED BLOW COUNTS
Pier E3-Eastbound (Boring 98-27)
Menck MHU-1000, 2.5-Meter-Diameter Driven Pipe Piles
SFOBB East Span Seismic Safety Project

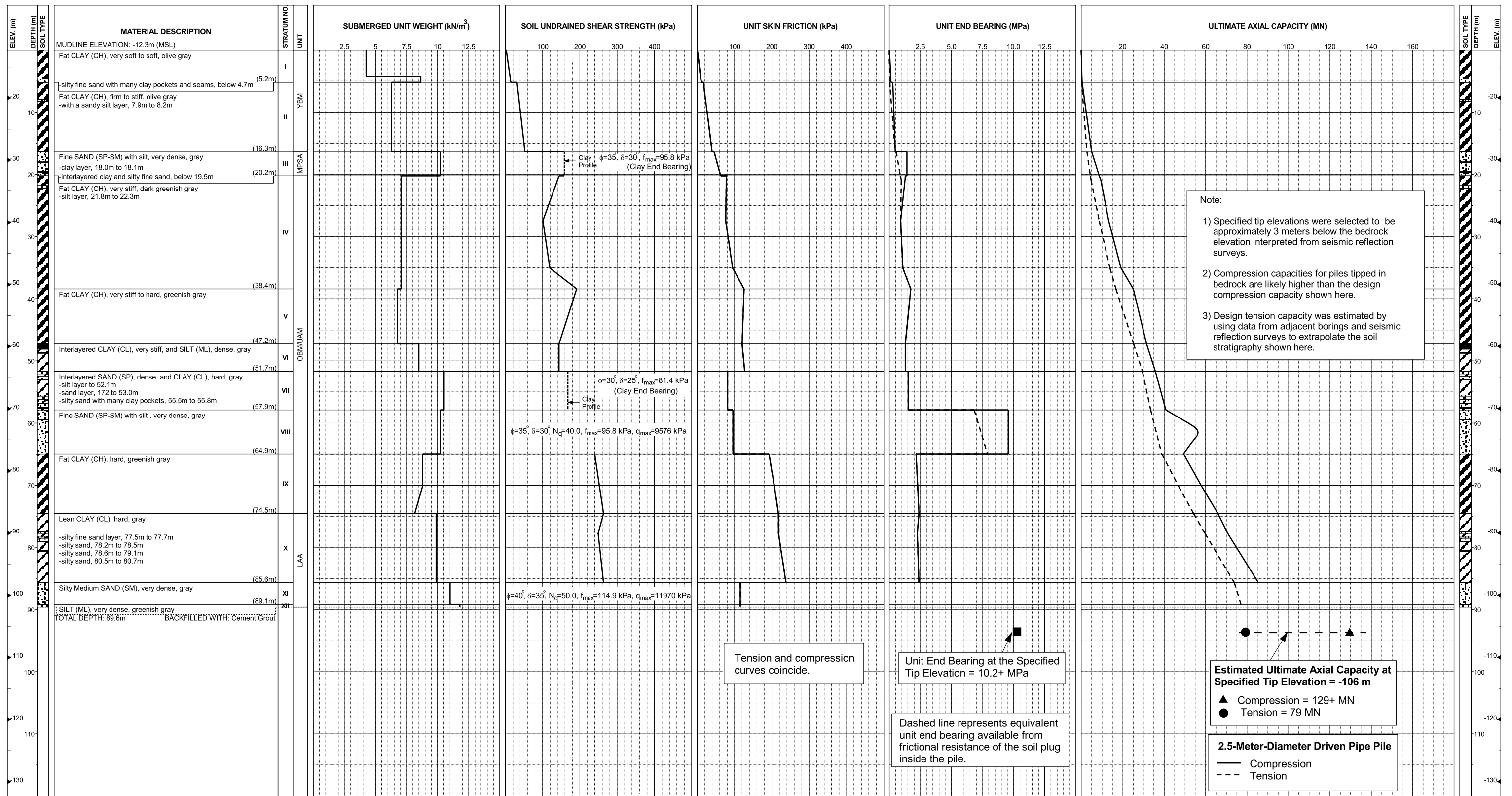




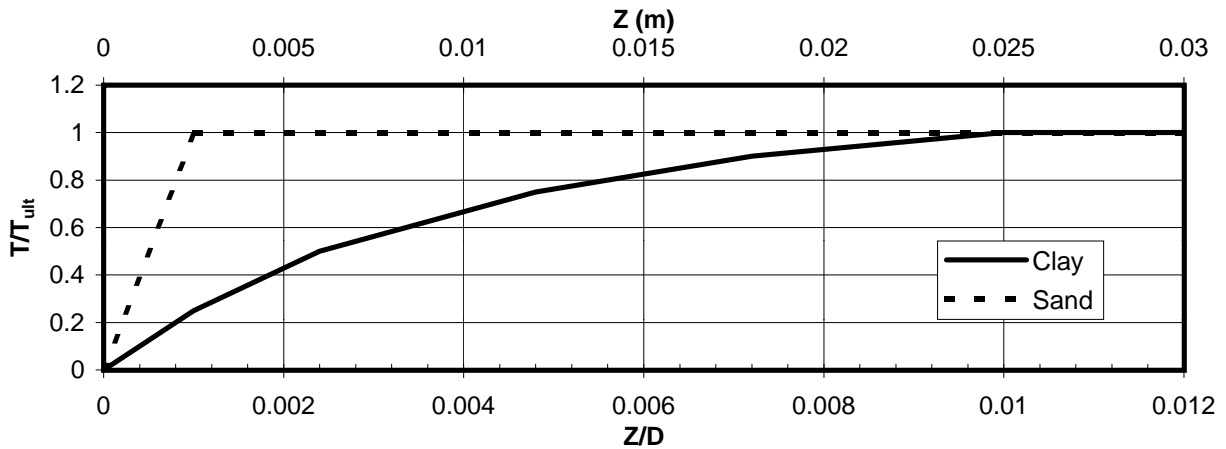
PREDICTED BLOW COUNTS
Pier E3-Eastbound (Boring 98-27)
Menck MHU-1700, 2.5-Meter-Diameter Driven Pipe Piles
SFOBB East Span Seismic Safety Project



**Pier E3-Westbound (Boring 98-50)
Skyway Frame 1**



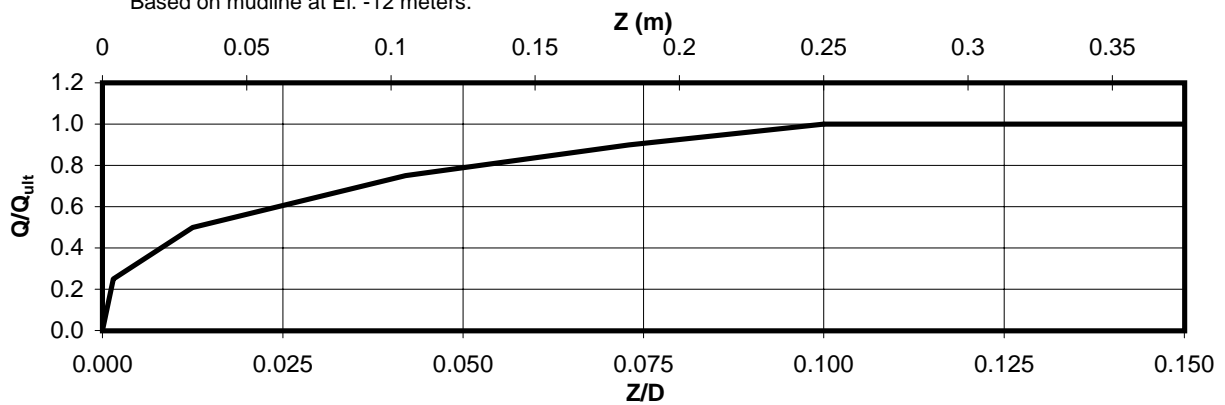
AXIAL PILE DESIGN PARAMETERS AND RESULTS
Pier E3-Westbound (Boring 98-50)
SFOBB East Span Seismic Safety Project



Depth* (m)	Soil Type	T_{ult} (MN/m)
0-3	Clay	0.020
3-6	Clay	0.087
6-9	Clay	0.183
9-12	Clay	0.223
12-15	Clay	0.273
15-18	Sand	0.347
18-21	Sand	0.507
21-24	Clay	0.637
24-27	Clay	0.597
27-30	Clay	0.620
30-33	Clay	0.680
33-36	Clay	0.737

Depth* (m)	Soil Type	T_{ult} (MN/m)
36-39	Clay	0.937
39-42	Clay	0.980
42-45	Clay	0.957
45-51	Clay	0.957
51-57	Clay	0.702
57-63	Sand	0.728
63-69	Clay	1.259
69-75	Clay	1.675
75-81	Clay	1.726
81-86	Clay	1.818
86-90	Sand	0.912

*Based on mudline at El. -12 meters.



Depth* (m)	Soil Type	Q_{ult} (MN)
90	Sand	50.2

AXIAL PILE LOAD TRANSFER-DISPLACEMENT CURVES
Pier E3-Westbound (Boring 98-50)
 2.5-Meter-Diameter Pipe Piles (Pile Tip Elevation = -102 Meters)
 SFOBB East Span Seismic Safety Project



DEPTH (m)	t-z Data											
	t(1)	z(1)	t(2)	z(2)	t(3)	z(3)	t(4)	z(4)	t(5)	z(5)	t(6)	z(6)
0-3	0.0	0.0	0.005	0.003	0.010	0.006	0.015	0.012	0.018	0.018	0.020	0.025
3-6	0.0	0.0	0.022	0.003	0.043	0.006	0.065	0.012	0.078	0.018	0.087	0.025
6-9	0.0	0.0	0.046	0.003	0.092	0.006	0.137	0.012	0.165	0.018	0.183	0.025
9-12	0.0	0.0	0.056	0.003	0.112	0.006	0.167	0.012	0.201	0.018	0.223	0.025
12-15	0.0	0.0	0.068	0.003	0.137	0.006	0.205	0.012	0.246	0.018	0.273	0.025
15-18	0.0	0.0	0.347	0.003								
18-21	0.0	0.0	0.507	0.003								
21-24	0.0	0.0	0.159	0.003	0.318	0.006	0.478	0.012	0.573	0.018	0.637	0.025
24-27	0.0	0.0	0.149	0.003	0.298	0.006	0.448	0.012	0.537	0.018	0.597	0.025
27-30	0.0	0.0	0.155	0.003	0.310	0.006	0.465	0.012	0.558	0.018	0.620	0.025
30-33	0.0	0.0	0.170	0.003	0.340	0.006	0.510	0.012	0.612	0.018	0.680	0.025
33-36	0.0	0.0	0.184	0.003	0.368	0.006	0.553	0.012	0.663	0.018	0.737	0.025
36-39	0.0	0.0	0.234	0.003	0.468	0.006	0.702	0.012	0.843	0.018	0.937	0.025
39-42	0.0	0.0	0.245	0.003	0.490	0.006	0.735	0.012	0.882	0.018	0.980	0.025
42-45	0.0	0.0	0.239	0.003	0.478	0.006	0.718	0.012	0.861	0.018	0.957	0.025
45-51	0.0	0.0	0.239	0.003	0.478	0.006	0.718	0.012	0.861	0.018	0.957	0.025
51-57	0.0	0.0	0.175	0.003	0.351	0.006	0.526	0.012	0.632	0.018	0.702	0.025
57-63	0.0	0.0	0.728	0.003								
63-69	0.0	0.0	0.315	0.003	0.629	0.006	0.944	0.012	1.133	0.018	1.259	0.025
69-75	0.0	0.0	0.419	0.003	0.838	0.006	1.256	0.012	1.508	0.018	1.675	0.025
75-81	0.0	0.0	0.431	0.003	0.863	0.006	1.294	0.012	1.553	0.018	1.726	0.025
81-86	0.0	0.0	0.455	0.003	0.909	0.006	1.364	0.012	1.637	0.018	1.818	0.025
86-90	0.0	0.0	0.912	0.003								

Notes:

1. "t" is load (MN/m)
2. "z" is displacement (m)
3. Data for tension and compression coincide
4. Based on mudline at El. -12 meters

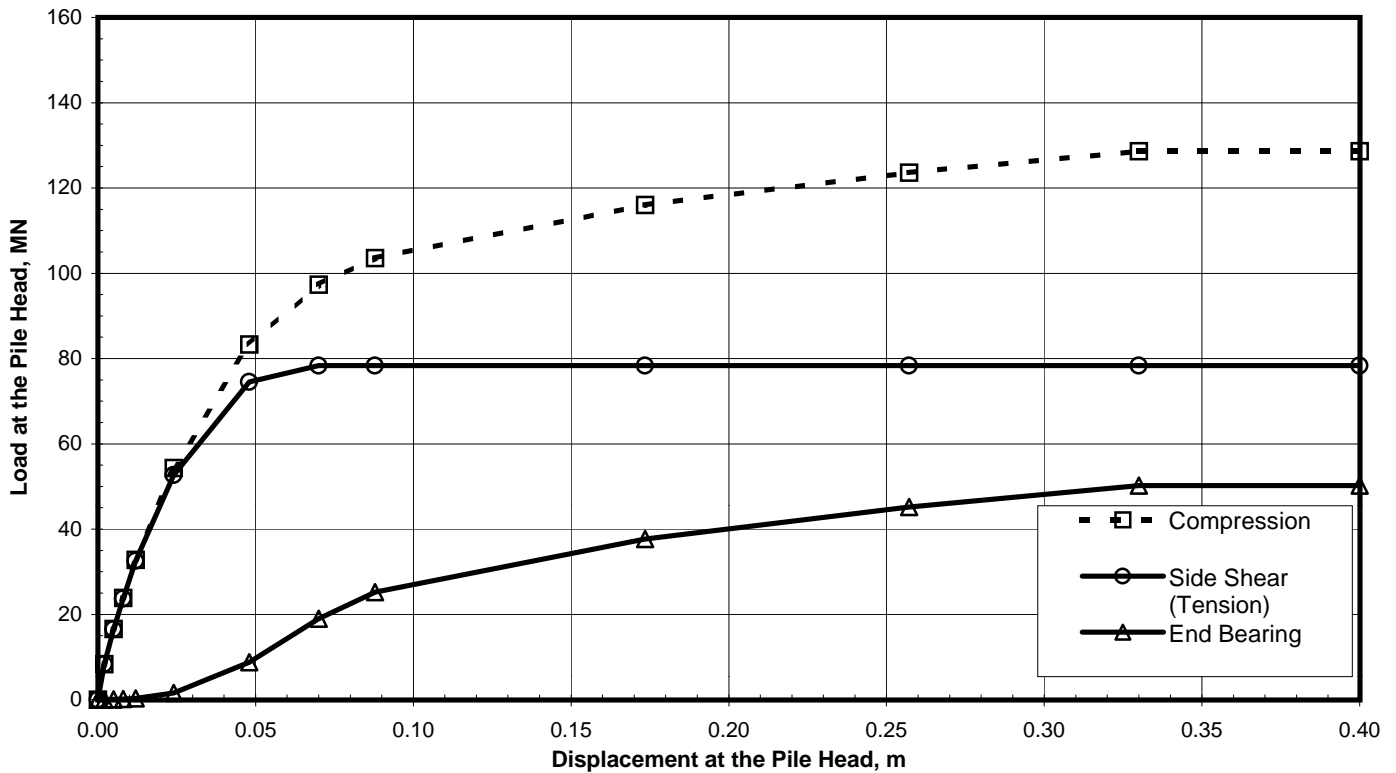
DEPTH (m)	Q-z Data											
	Q(1)	z(1)	Q(2)	z(2)	Q(3)	z(3)	Q(4)	z(4)	Q(5)	z(5)	Q(6)	z(6)
90	0.0	0.0	12.550	0.004	25.100	0.031	37.650	0.105	45.180	0.183	50.200	0.250

Notes:

1. "Q" is load in compression (MN)
2. "z" is displacement (m)

TABULATED AXIAL PILE LOAD TRANSFER DATA
Pier E3-Westbound (Boring 98-50)
 2.5-Meter-Diameter Pipe Piles (Pile Tip Elevation = -102 Meters)
 SFOBB East Span Seismic Safety Project





Pile Head Displacement (m)	Load at the Pile Head		End Bearing Component in Compression (MN)
	Compression (MN)	Tension (MN)	
0.000	0.00	0.00	0.00
0.002	8.33	8.30	0.03
0.005	16.62	16.53	0.09
0.008	23.84	23.68	0.16
0.012	32.83	32.54	0.29
0.024	54.30	52.69	1.61
0.048	83.32	74.55	8.77
0.070	97.34	78.37	18.97
0.088	103.57	78.37	25.20
0.173	116.04	78.37	37.67
0.257	123.58	78.37	45.21
0.330	128.60	78.37	50.23
0.400	128.60	78.37	50.23

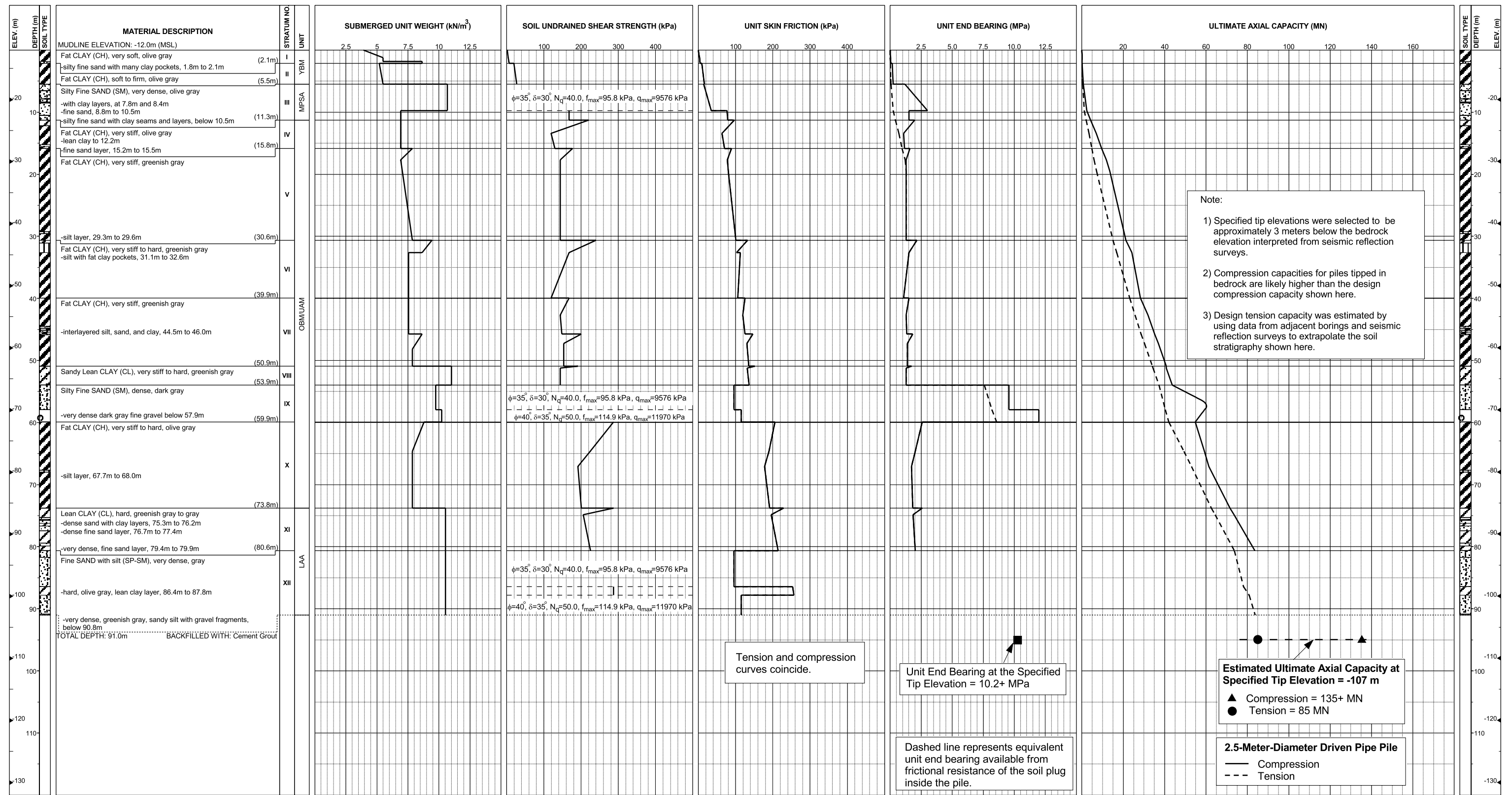
Note:

Pile head load-displacement curves are based on the preliminary pile wall thickness schedule provided by TY Lin/M&N and static loading conditions.

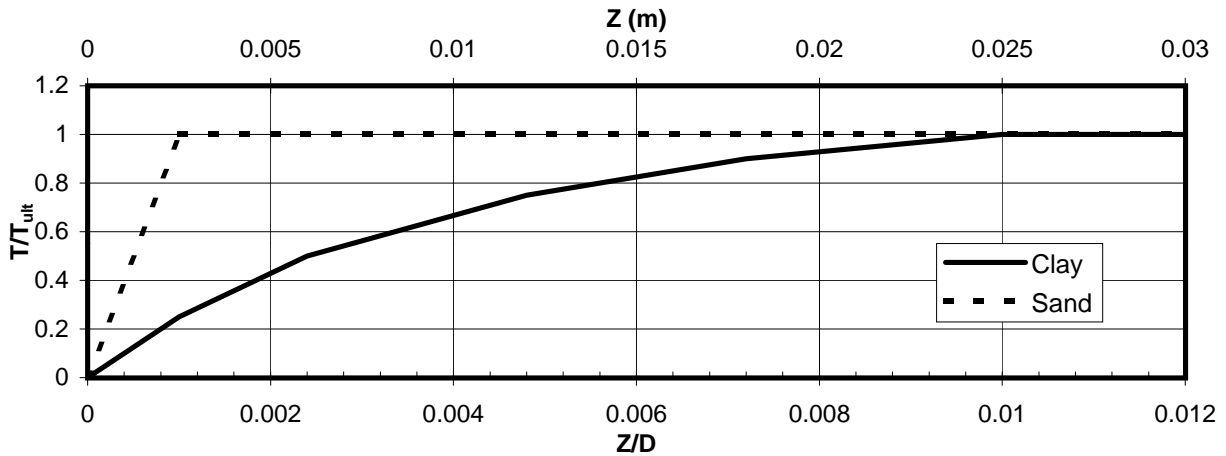
STATIC PILE HEAD LOAD-DEFORMATION CURVES
Pier E3-Westbound (Boring 98-50)
 2.5-Meter-Diameter Pipe Piles (Pile Tip Elevation = -102 Meters)
 SFOBB East Span Seismic Safety Project



**Pier E4-Eastbound (Boring 98-40)
Skyway Frame 1**



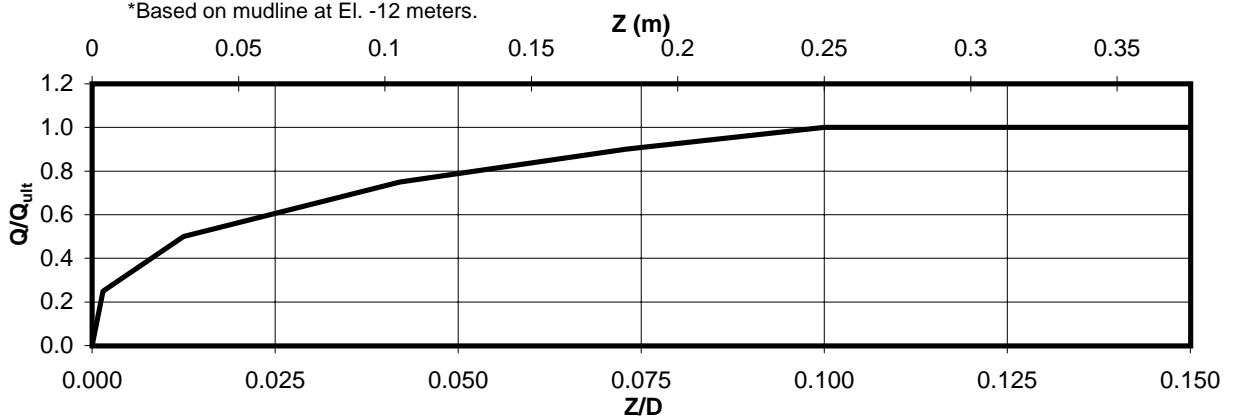
AXIAL PILE DESIGN PARAMETERS AND RESULTS
Pier E4-Eastbound (Boring 98-40)
SFOBB East Span Seismic Safety Project



Depth* (m)	Soil Type	T_{ult} (MN/m)
0-3	Clay	0.037
3-6	Clay	0.107
6-9	Sand	0.167
9-12	Sand	0.510
12-15	Clay	0.560
15-18	Clay	0.610
18-21	Clay	0.627
21-24	Clay	0.663
24-27	Clay	0.707
27-30	Clay	0.747
30-33	Clay	0.890
33-36	Clay	0.860

Depth* (m)	Soil Type	T_{ult} (MN/m)
36-39	Clay	0.853
39-42	Clay	0.910
42-45	Clay	0.953
45-51	Clay	1.037
51-57	Sand	0.928
57-63	Clay	1.172
63-69	Clay	1.490
69-75	Clay	1.488
75-81	Sand	1.612
81-85	Sand	0.765

*Based on mudline at El. -12 meters.



Depth* (m)	Soil Type	Q_{ult} (MN)
85	Sand	50.2

AXIAL PILE LOAD TRANSFER-DISPLACEMENT CURVES
Pier E4-Eastbound (Boring 98-40)
 2.5-Meter-Diameter Pipe Piles (Pile Tip Elevation = -97 Meters)
 SFOBB East Span Seismic Safety Project



DEPTH (m)	t-z Data											
	t(1)	z(1)	t(2)	z(2)	t(3)	z(3)	t(4)	z(4)	t(5)	z(5)	t(6)	z(6)
0-3	0.0	0.0	0.009	0.003	0.018	0.006	0.028	0.012	0.033	0.018	0.037	0.025
3-6	0.0	0.0	0.027	0.003	0.053	0.006	0.080	0.012	0.096	0.018	0.107	0.025
6-9	0.0	0.0	0.167	0.003								
9-12	0.0	0.0	0.510	0.003								
12-15	0.0	0.0	0.140	0.003	0.280	0.006	0.420	0.012	0.504	0.018	0.560	0.025
15-18	0.0	0.0	0.153	0.003	0.305	0.006	0.458	0.012	0.549	0.018	0.610	0.025
18-21	0.0	0.0	0.157	0.003	0.313	0.006	0.470	0.012	0.564	0.018	0.627	0.025
21-24	0.0	0.0	0.166	0.003	0.332	0.006	0.497	0.012	0.597	0.018	0.663	0.025
24-27	0.0	0.0	0.177	0.003	0.353	0.006	0.530	0.012	0.636	0.018	0.707	0.025
27-30	0.0	0.0	0.187	0.003	0.373	0.006	0.560	0.012	0.672	0.018	0.747	0.025
30-33	0.0	0.0	0.223	0.003	0.445	0.006	0.668	0.012	0.801	0.018	0.890	0.025
33-36	0.0	0.0	0.215	0.003	0.430	0.006	0.645	0.012	0.774	0.018	0.860	0.025
36-39	0.0	0.0	0.213	0.003	0.427	0.006	0.640	0.012	0.768	0.018	0.853	0.025
39-42	0.0	0.0	0.228	0.003	0.455	0.006	0.683	0.012	0.819	0.018	0.910	0.025
42-45	0.0	0.0	0.238	0.003	0.477	0.006	0.715	0.012	0.858	0.018	0.953	0.025
45-51	0.0	0.0	0.259	0.003	0.519	0.006	0.778	0.012	0.933	0.018	1.037	0.025
51-57	0.0	0.0	0.928	0.003								
57-63	0.0	0.0	0.293	0.003	0.586	0.006	0.879	0.012	1.055	0.018	1.172	0.025
63-69	0.0	0.0	0.373	0.003	0.745	0.006	1.118	0.012	1.341	0.018	1.490	0.025
69-75	0.0	0.0	0.372	0.003	0.744	0.006	1.116	0.012	1.339	0.018	1.488	0.025
75-81	0.0	0.0	1.612	0.003								
81-85	0.0	0.0	0.765	0.003								

Notes:

1. "t" is load (MN/m)
2. "z" is displacement (m)
3. Data for tension and compression coincide
4. Based on mudline at El. -12 meters

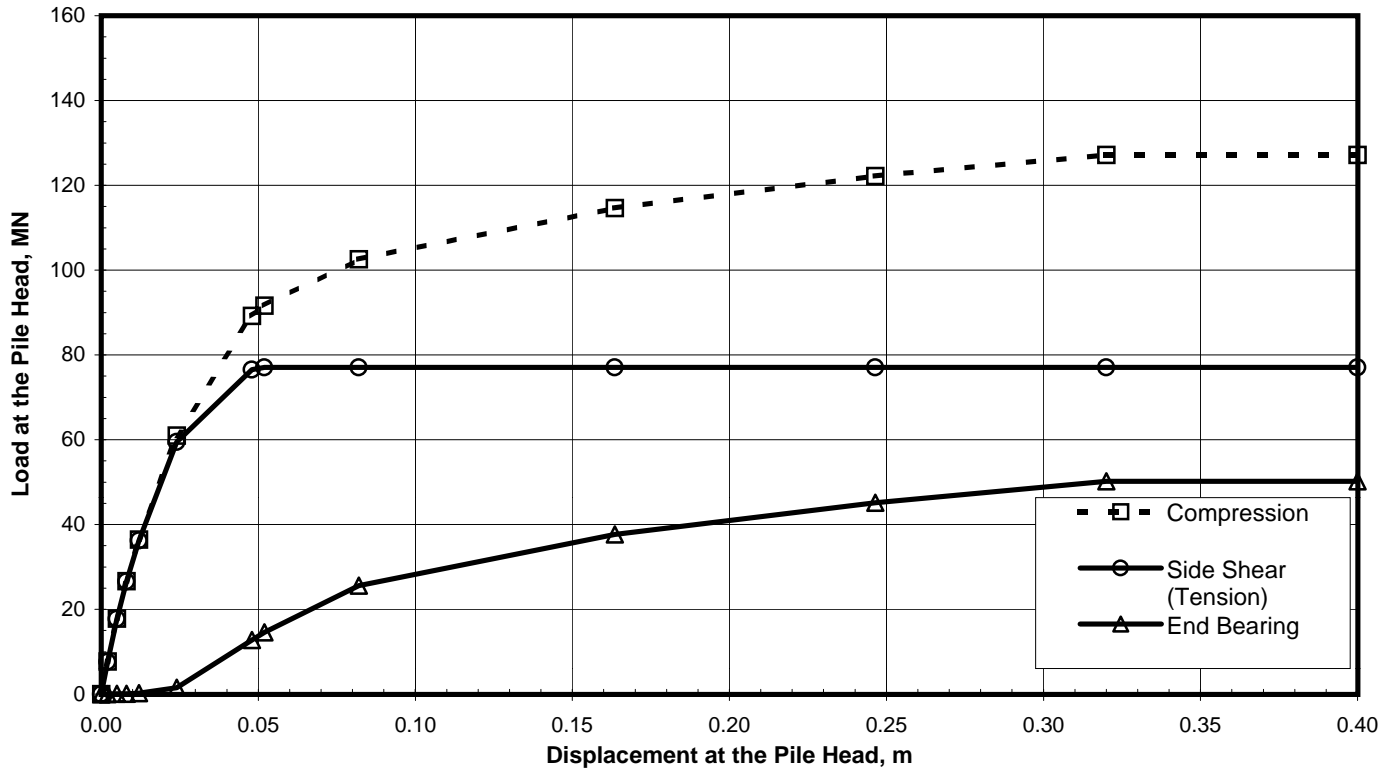
DEPTH (m)	Q-z Data											
	Q(1)	z(1)	Q(2)	z(2)	Q(3)	z(3)	Q(4)	z(4)	Q(5)	z(5)	Q(6)	z(6)
85	0.0	0.0	12.550	0.004	25.100	0.031	37.650	0.105	45.180	0.183	50.200	0.250

Notes:

1. "Q" is load in compression (MN)
2. "z" is displacement (m)

TABULATED AXIAL PILE LOAD TRANSFER DATA
Pier E4-Eastbound (Boring 98-40)
 2.5-Meter-Diameter Pipe Piles (Pile Tip Elevation = -97 Meters)
 SFOBB East Span Seismic Safety Project





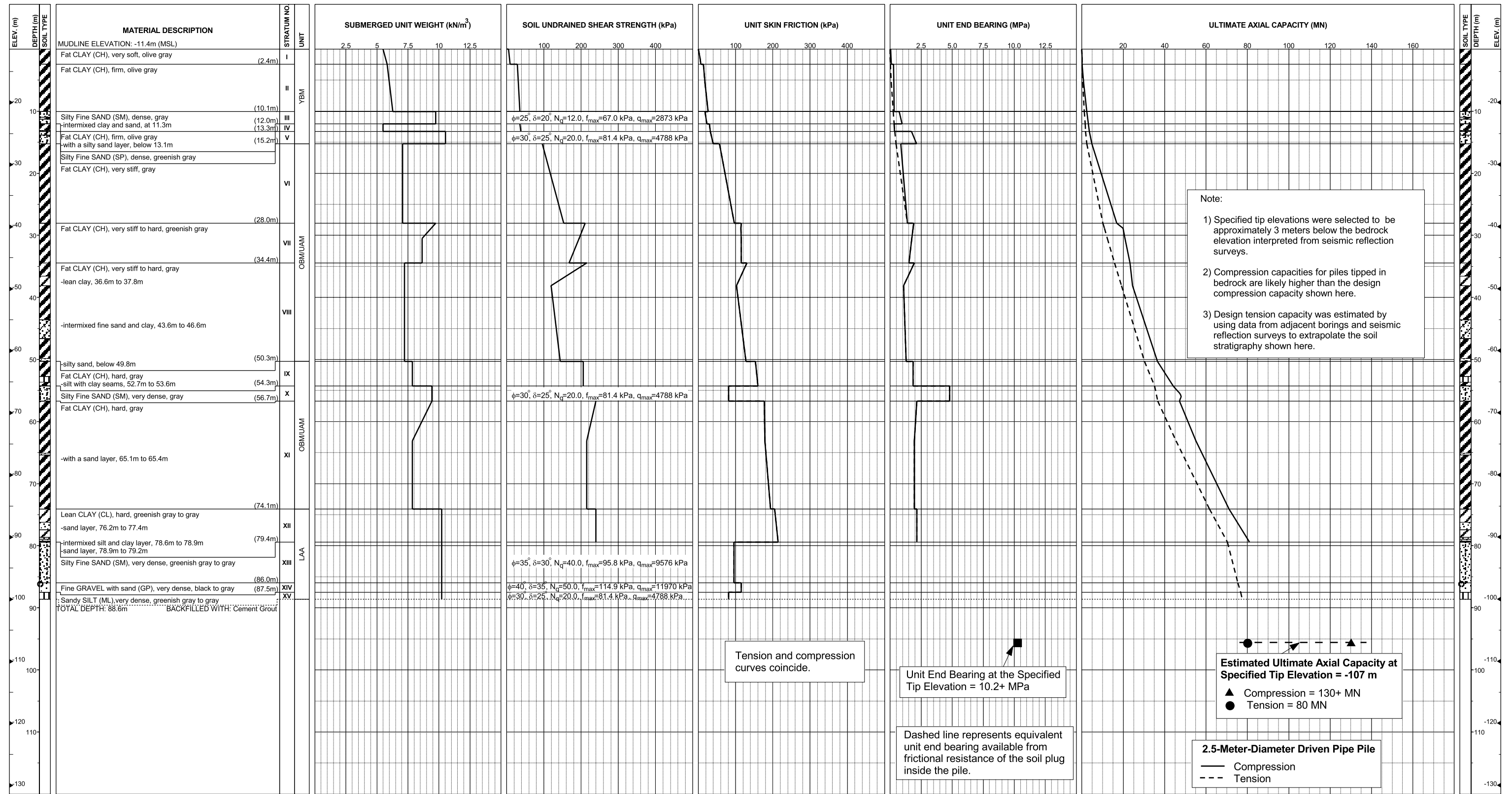
Pile Head Displacement (m)	Load at the Pile Head		End Bearing Component in Compression (MN)
	Compression (MN)	Tension (MN)	
0.000	0.00	0.00	0.00
0.002	7.66	7.65	0.02
0.005	17.79	17.73	0.06
0.008	26.65	26.55	0.10
0.012	36.45	36.23	0.22
0.024	60.98	59.50	1.48
0.048	89.22	76.50	12.72
0.052	91.61	77.02	14.59
0.082	102.60	77.02	25.58
0.164	114.66	77.02	37.64
0.246	122.18	77.02	45.16
0.320	127.20	77.02	50.18
0.400	127.20	77.02	50.18

Note:
 Pile head load-displacement curves are based on the preliminary pile wall thickness schedule provided by TY Lin/M&N and static loading conditions.

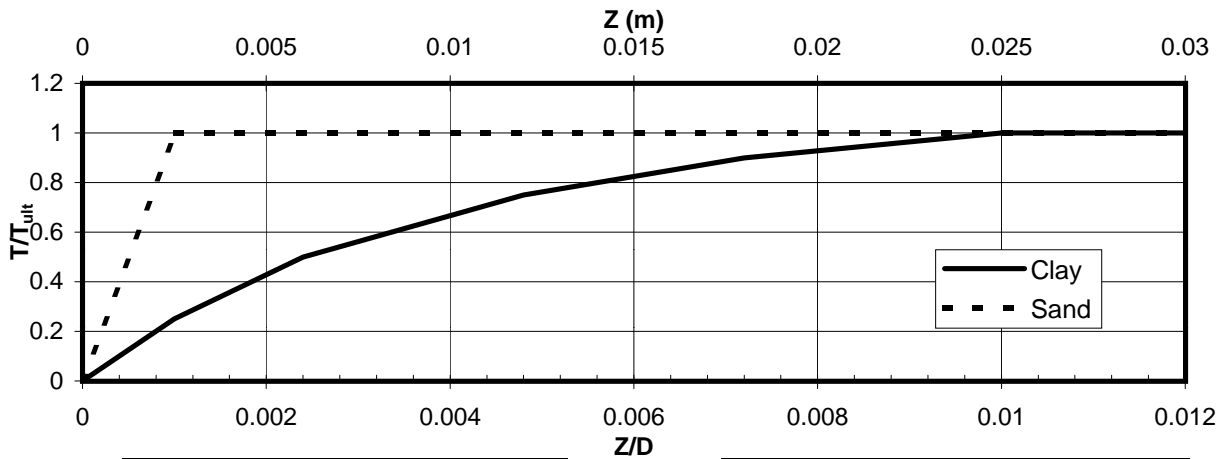
STATIC PILE HEAD LOAD-DEFORMATION CURVES
Pier E4-Eastbound (Boring 98-40)
 2.5-Meter-Diameter Pipe Piles (Pile Tip Elevation = -97 Meters)
 SFOBB East Span Seismic Safety Project



**Pier E4-Westbound (Boring 98-28)
Skyway Frame 1**



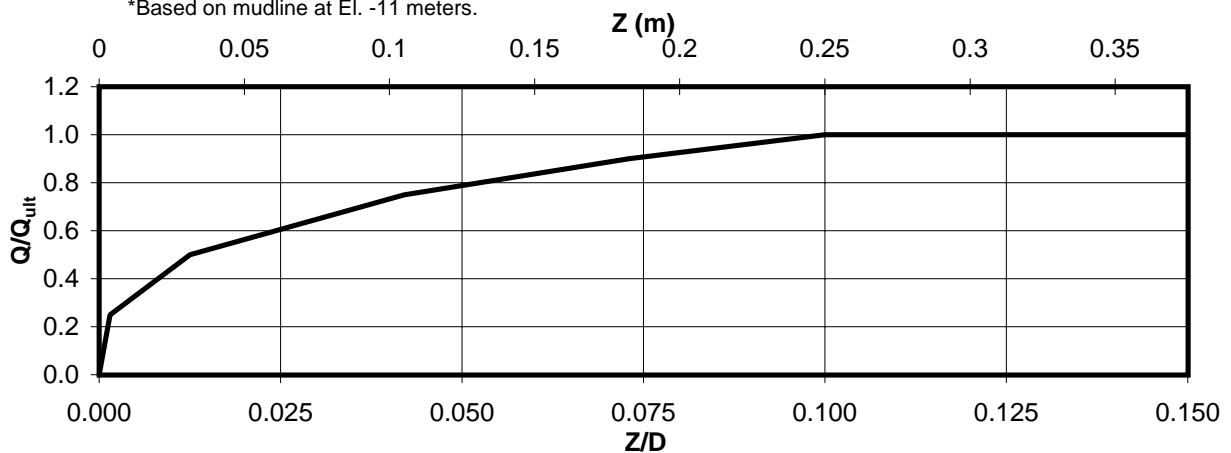
AXIAL PILE DESIGN PARAMETERS AND RESULTS
Pier E4-Westbound (Boring 98-28)
SFOBB East Span Seismic Safety Project



Depth* (m)	Soil Type	T_{ult} (MN/m)
0-3	Clay	0.033
3-6	Clay	0.147
6-9	Sand	0.170
9-12	Clay	0.173
12-15	Clay	0.263
15-18	Clay	0.480
18-21	Clay	0.550
21-24	Clay	0.627
24-27	Clay	0.697
27-30	Clay	0.850
30-33	Clay	0.913
33-36	Clay	0.950

Depth* (m)	Soil Type	T_{ult} (MN/m)
36-39	Clay	0.840
39-42	Clay	0.833
42-45	Clay	0.893
45-51	Clay	0.988
51-57	Clay	0.985
57-63	Clay	1.368
63-69	Clay	1.438
69-75	Clay	1.510
75-81	Clay	1.419
81-83	Sand	0.588

*Based on mudline at El. -11 meters.



Depth* (m)	Soil Type	Q_{ult} (MN)
83	Sand	50.2

AXIAL PILE LOAD TRANSFER-DISPLACEMENT CURVES
Pier E4-Westbound (Boring 98-28)
 2.5-Meter-Diameter Pipe Piles (Pile Tip Elevation = -94 Meters)
 SFOBB East Span Seismic Safety Project





DEPTH (m)	t-z Data											
	t(1)	z(1)	t(2)	z(2)	t(3)	z(3)	t(4)	z(4)	t(5)	z(5)	t(6)	z(6)
0-3	0.0	0.0	0.008	0.003	0.017	0.006	0.025	0.012	0.030	0.018	0.033	0.025
3-6	0.0	0.0	0.037	0.003	0.073	0.006	0.110	0.012	0.132	0.018	0.147	0.025
6-9	0.0	0.0	0.170	0.003								
9-12	0.0	0.0	0.043	0.003	0.087	0.006	0.130	0.012	0.156	0.018	0.173	0.025
12-15	0.0	0.0	0.066	0.003	0.132	0.006	0.197	0.012	0.237	0.018	0.263	0.025
15-18	0.0	0.0	0.120	0.003	0.240	0.006	0.360	0.012	0.432	0.018	0.480	0.025
18-21	0.0	0.0	0.138	0.003	0.275	0.006	0.413	0.012	0.495	0.018	0.550	0.025
21-24	0.0	0.0	0.157	0.003	0.313	0.006	0.470	0.012	0.564	0.018	0.627	0.025
24-27	0.0	0.0	0.174	0.003	0.348	0.006	0.523	0.012	0.627	0.018	0.697	0.025
27-30	0.0	0.0	0.213	0.003	0.425	0.006	0.638	0.012	0.765	0.018	0.850	0.025
30-33	0.0	0.0	0.228	0.003	0.457	0.006	0.685	0.012	0.822	0.018	0.913	0.025
33-36	0.0	0.0	0.238	0.003	0.475	0.006	0.713	0.012	0.855	0.018	0.950	0.025
36-39	0.0	0.0	0.210	0.003	0.420	0.006	0.630	0.012	0.756	0.018	0.840	0.025
39-42	0.0	0.0	0.208	0.003	0.417	0.006	0.625	0.012	0.750	0.018	0.833	0.025
42-45	0.0	0.0	0.223	0.003	0.447	0.006	0.670	0.012	0.804	0.018	0.893	0.025
45-51	0.0	0.0	0.247	0.003	0.494	0.006	0.741	0.012	0.889	0.018	0.988	0.025
51-57	0.0	0.0	0.246	0.003	0.493	0.006	0.739	0.012	0.887	0.018	0.985	0.025
57-63	0.0	0.0	0.342	0.003	0.684	0.006	1.026	0.012	1.231	0.018	1.368	0.025
63-69	0.0	0.0	0.360	0.003	0.719	0.006	1.079	0.012	1.294	0.018	1.438	0.025
69-75	0.0	0.0	0.378	0.003	0.755	0.006	1.133	0.012	1.359	0.018	1.510	0.025
75-81	0.0	0.0	0.355	0.003	0.710	0.006	1.064	0.012	1.277	0.018	1.419	0.025
81-83	0.0	0.0	0.588	0.003								

Notes:

1. "t" is load (MN/m)
2. "z" is displacement (m)
3. Data for tension and compression coincide
4. Based on mudline at El. -11 meters

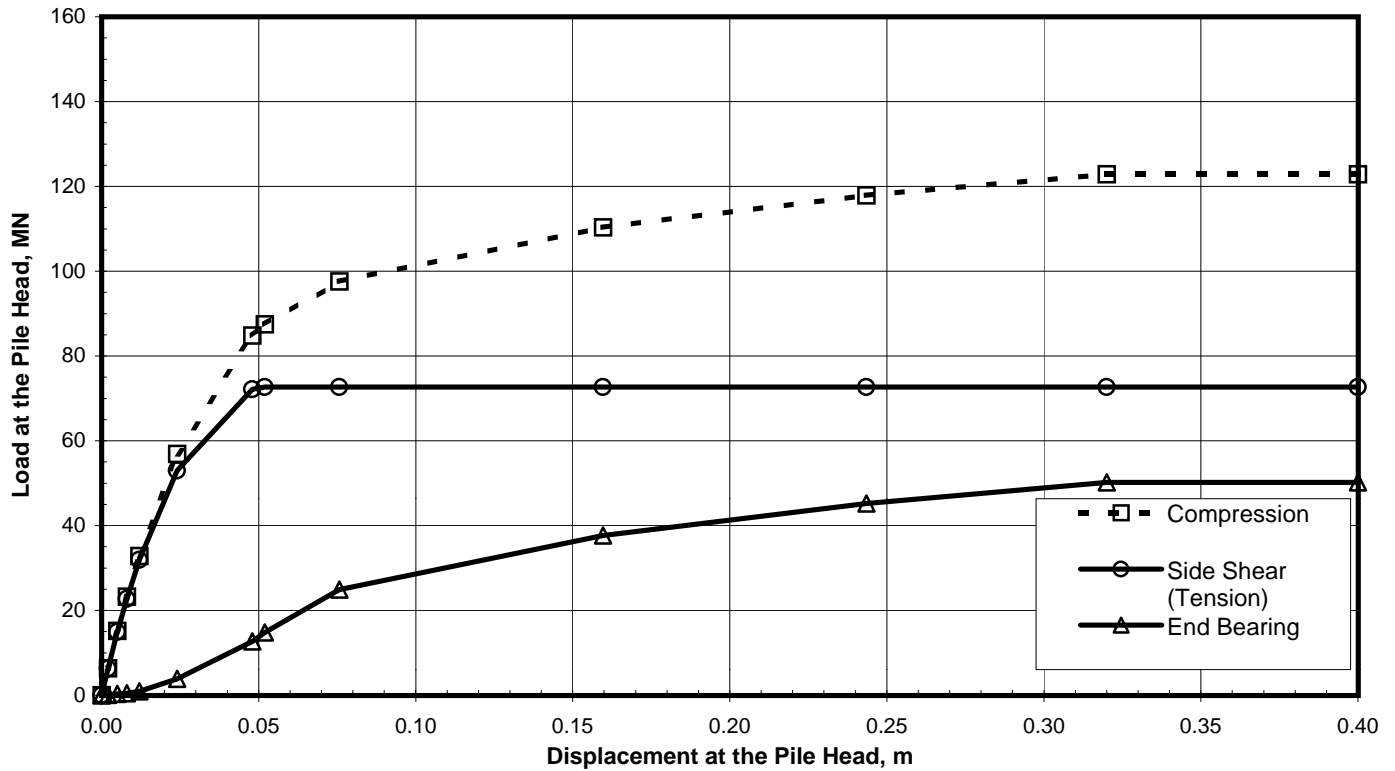
DEPTH (m)	Q-z Data											
	Q(1)	z(1)	Q(2)	z(2)	Q(3)	z(3)	Q(4)	z(4)	Q(5)	z(5)	Q(6)	z(6)
83	0.0	0.0	12.550	0.004	25.100	0.031	37.650	0.105	45.180	0.183	50.200	0.250

Notes:

1. "Q" is load in compression (MN)
2. "z" is displacement (m)

TABULATED AXIAL PILE LOAD TRANSFER DATA
Pier E4-Westbound (Boring 98-28)
2.5-Meter-Diameter Pipe Piles (Pile Tip Elevation = -94 Meters)
SFOBB East Span Seismic Safety Project





Pile Head Displacement (m)	Load at the Pile Head		End Bearing Component in Compression (MN)
	Compression (MN)	Tension (MN)	
0.000	0.00	0.00	0.00
0.002	6.34	6.24	0.10
0.005	15.19	14.92	0.27
0.008	23.21	22.72	0.49
0.012	32.80	31.89	0.91
0.024	56.89	53.01	3.88
0.048	84.85	72.16	12.69
0.052	87.50	72.68	14.82
0.076	97.58	72.68	24.90
0.160	110.35	72.68	37.67
0.243	117.88	72.68	45.20
0.320	122.90	72.68	50.22
0.400	122.90	72.68	50.22

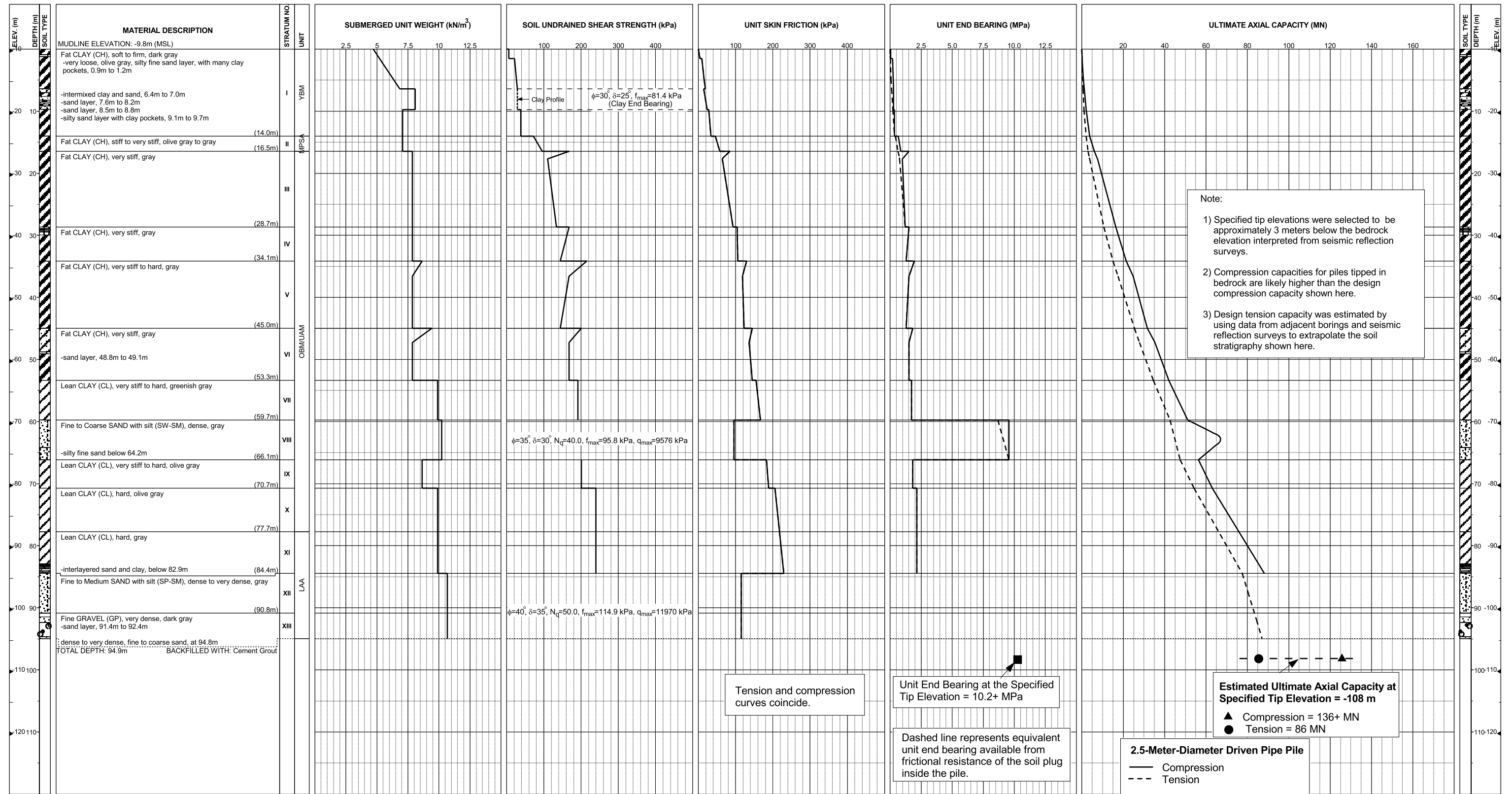
Note:

Pile head load-displacement curves are based on the preliminary pile wall thickness schedule provided by TY Lin/M&N and static loading conditions.

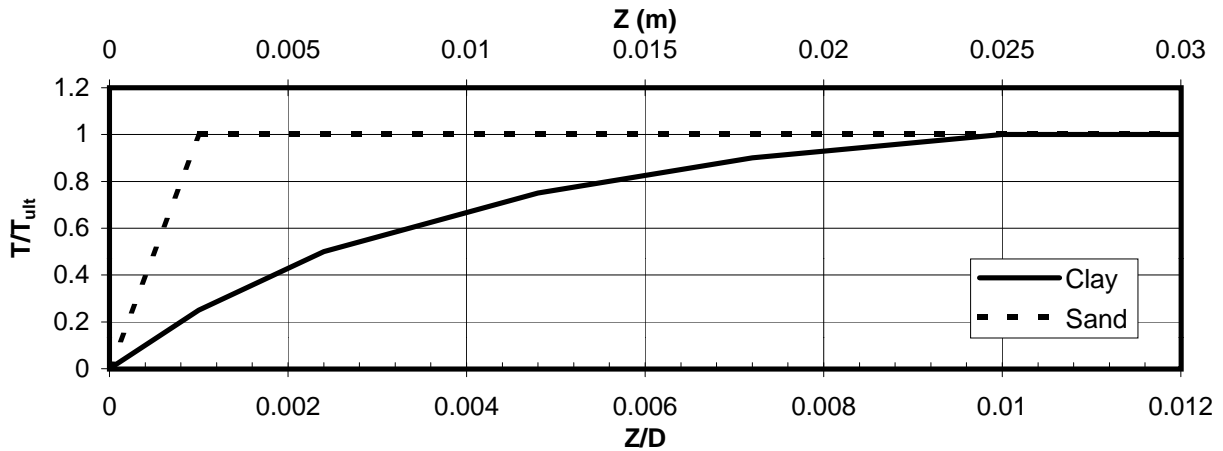
STATIC PILE HEAD LOAD-DEFORMATION CURVES
Pier E4-Westbound (Boring 98-28)
 2.5-Meter-Diameter Pipe Piles (Pile Tip Elevation = -94 Meters)
 SFOBB East Span Seismic Safety Project



**Pier E5-Eastbound (Boring 98-29)
Skyway Frame 1**



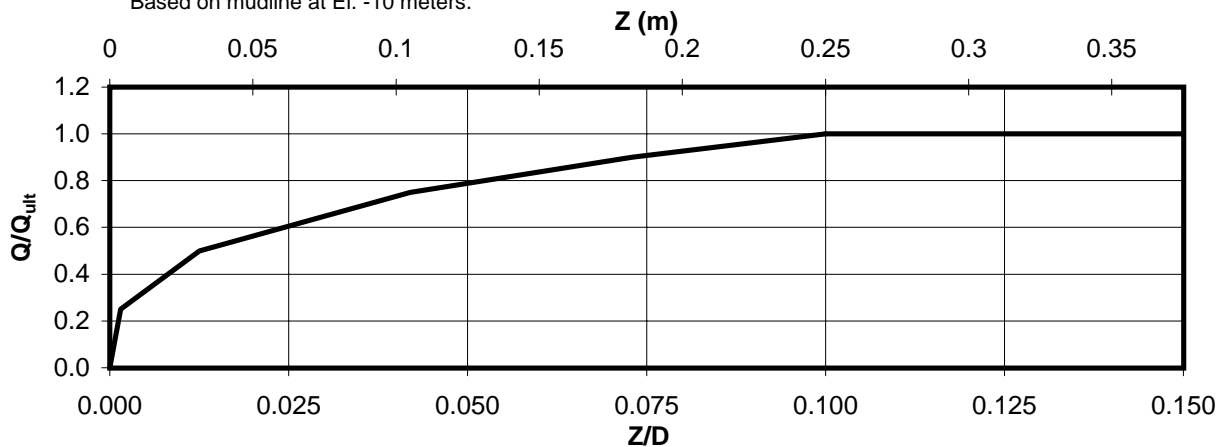
AXIAL PILE DESIGN PARAMETERS AND RESULTS
Pier E5-Eastbound (Boring 98-29)
SFOBB East Span Seismic Safety Project



Depth (m)	Soil Type	T_{ult} (MN/m)
0-3	Clay	0.023
3-6	Clay	0.123
6-9	Clay	0.140
9-12	Clay	0.213
12-15	Clay	0.277
15-18	Clay	0.493
18-21	Clay	0.530
21-24	Clay	0.597
24-27	Clay	0.657
27-30	Clay	0.737
30-33	Clay	0.840
33-36	Clay	0.930

Depth (m)	Soil Type	T_{ult} (MN/m)
36-39	Clay	0.943
39-42	Clay	0.943
42-45	Clay	0.957
45-51	Clay	1.093
51-57	Clay	1.202
57-63	Sand	1.053
63-69	Clay	1.040
69-75	Clay	1.618
75-81	Clay	1.717
81-84	Clay	1.782
84-88	Sand	0.903

*Based on mudline at El. -10 meters.



Depth (m)	Soil Type	Q_{ult} (MN)
88	Sand	50.2

AXIAL PILE LOAD TRANSFER-DISPLACEMENT CURVES
Pier E5-Eastbound (Boring 98-29)
 2.5-Meter-Diameter Pipe Piles (Pile Tip Elevation = -98 Meters)
 SFOBB East Span Seismic Safety Project



DEPTH (m)	t-z Data											
	t(1)	z(1)	t(2)	z(2)	t(3)	z(3)	t(4)	z(4)	t(5)	z(5)	t(6)	z(6)
0-3	0.0	0.0	0.006	0.003	0.012	0.006	0.017	0.012	0.021	0.018	0.023	0.025
3-6	0.0	0.0	0.031	0.003	0.062	0.006	0.092	0.012	0.111	0.018	0.123	0.025
6-9	0.0	0.0	0.035	0.003	0.070	0.006	0.105	0.012	0.126	0.018	0.140	0.025
9-12	0.0	0.0	0.053	0.003	0.107	0.006	0.160	0.012	0.192	0.018	0.213	0.025
12-15	0.0	0.0	0.069	0.003	0.138	0.006	0.208	0.012	0.249	0.018	0.277	0.025
15-18	0.0	0.0	0.123	0.003	0.247	0.006	0.370	0.012	0.444	0.018	0.493	0.025
18-21	0.0	0.0	0.133	0.0025	0.265	0.006	0.398	0.012	0.477	0.018	0.530	0.025
21-24	0.0	0.0	0.149	0.003	0.298	0.006	0.448	0.012	0.537	0.018	0.597	0.025
24-27	0.0	0.0	0.164	0.003	0.328	0.006	0.493	0.012	0.591	0.018	0.657	0.025
27-30	0.0	0.0	0.184	0.003	0.368	0.006	0.553	0.012	0.663	0.018	0.737	0.025
30-33	0.0	0.0	0.210	0.003	0.420	0.006	0.630	0.012	0.756	0.018	0.840	0.025
33-36	0.0	0.0	0.233	0.003	0.465	0.006	0.698	0.012	0.837	0.018	0.930	0.025
36-39	0.0	0.0	0.236	0.003	0.472	0.006	0.707	0.012	0.849	0.018	0.943	0.025
39-42	0.0	0.0	0.236	0.003	0.472	0.006	0.707	0.012	0.849	0.018	0.943	0.025
42-45	0.0	0.0	0.239	0.003	0.478	0.006	0.718	0.012	0.861	0.018	0.957	0.025
45-51	0.0	0.0	0.273	0.0025	0.547	0.006	0.820	0.012	0.984	0.018	1.093	0.025
51-57	0.0	0.0	0.301	0.003	0.601	0.006	0.902	0.012	1.082	0.018	1.202	0.025
57-63	0.0	0.0	1.053	0.003								
63-69	0.0	0.0	0.260	0.003	0.520	0.006	0.780	0.012	0.936	0.018	1.040	0.025
69-75	0.0	0.0	0.405	0.003	0.809	0.006	1.214	0.012	1.456	0.018	1.618	0.025
75-81	0.0	0.0	0.429	0.003	0.859	0.006	1.288	0.012	1.545	0.018	1.717	0.025
81-84	0.0	0.0	0.446	0.003	0.891	0.006	1.337	0.012	1.604	0.018	1.782	0.025
84-88	0.0	0.0	0.903	0.003								

Notes:

- "t" is load (MN/m)
- "z" is displacement (m)
- Data for tension and compression coincide
- Based on mudline at El. -10 meters

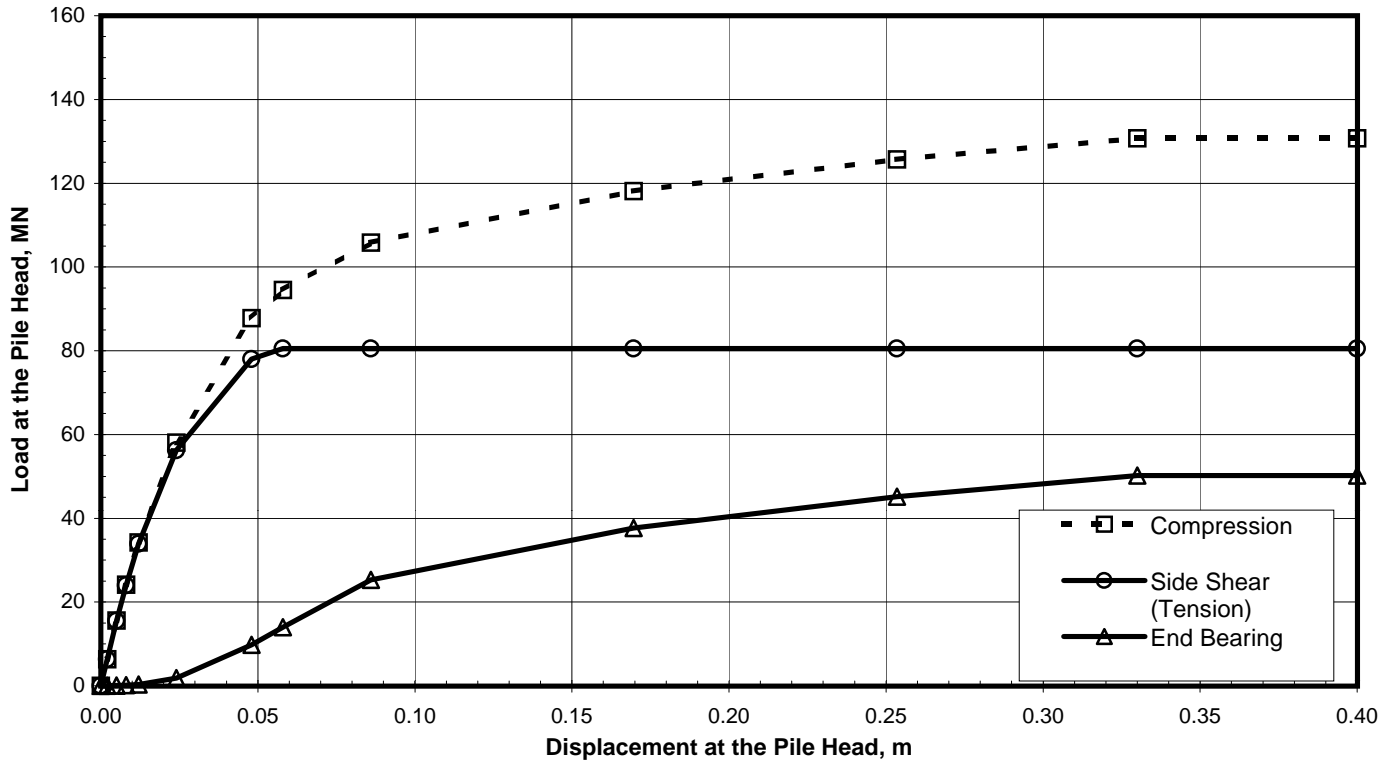
DEPTH (m)	Q-z Data											
	Q(1)	z(1)	Q(2)	z(2)	Q(3)	z(3)	Q(4)	z(4)	Q(5)	z(5)	Q(6)	z(6)
88	0.0	0.0	12.550	0.004	25.100	0.031	37.650	0.105	45.180	0.183	50.200	0.250

Notes:

- "Q" is load in compression (MN)
- "z" is displacement (m)

TABULATED AXIAL PILE LOAD TRANSFER DATA
Pier E5-Eastbound (Boring 98-29)
2.5-Meter-Diameter Pipe Piles (Pile Tip Elevation = -98 Meters)
SFOBB East Span Seismic Safety Project





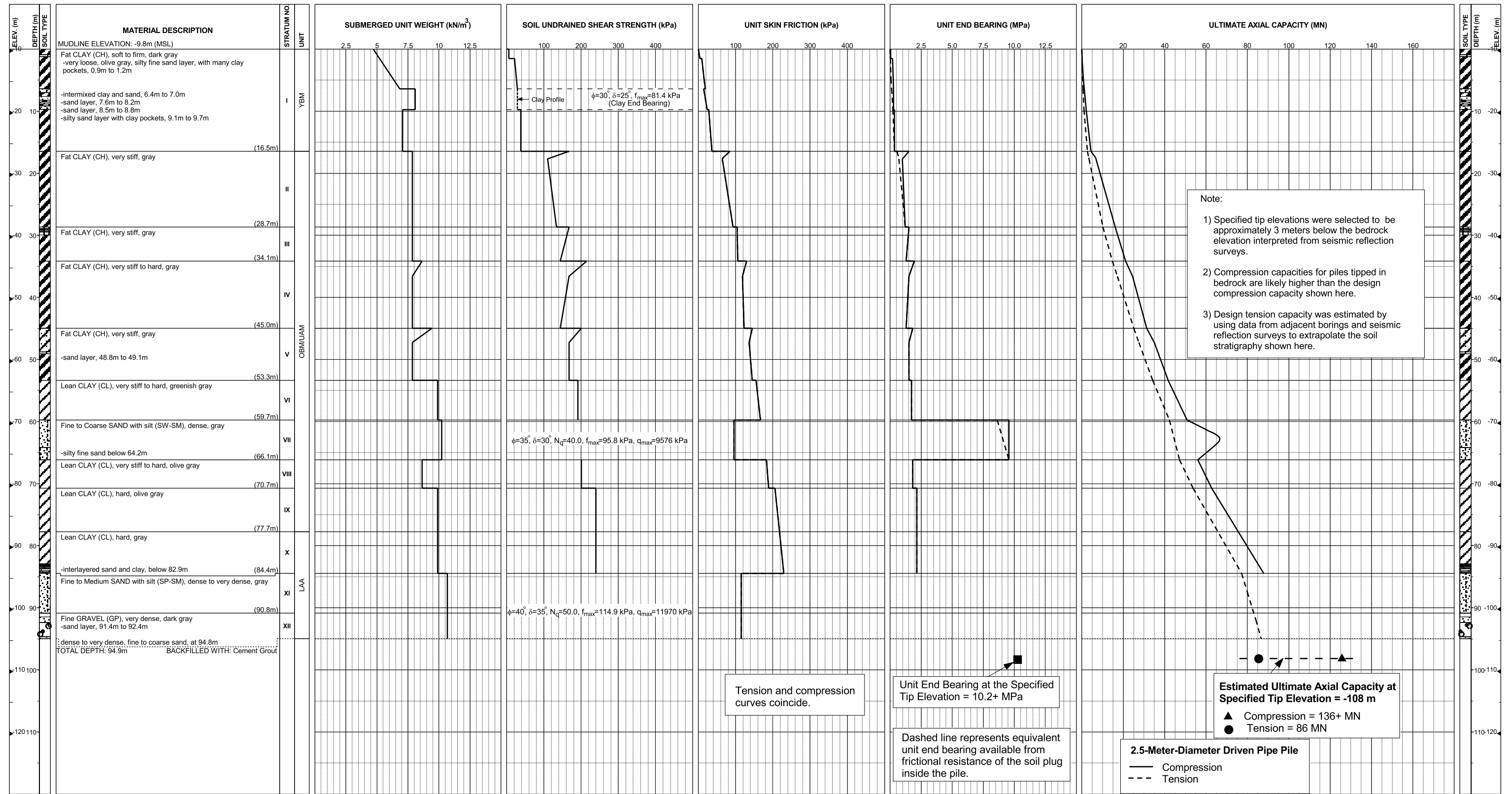
Pile Head Displacement (m)	Load at the Pile Head		End Bearing Component in Compression (MN)
	Compression (MN)	Tension (MN)	
0.000	0.00	0.00	0.00
0.002	6.36	6.33	0.03
0.005	15.56	15.48	0.08
0.008	24.13	24.00	0.13
0.012	34.26	33.93	0.33
0.024	58.07	56.27	1.80
0.048	87.78	77.99	9.79
0.058	94.53	80.51	14.02
0.086	105.80	80.51	25.29
0.170	118.15	80.51	37.64
0.254	125.68	80.51	45.17
0.330	130.70	80.51	50.19
0.400	130.70	80.51	50.19

Note:
 Pile head load-displacement curves are based on the preliminary pile wall thickness schedule provided by TY Lin/M&N and static loading conditions.

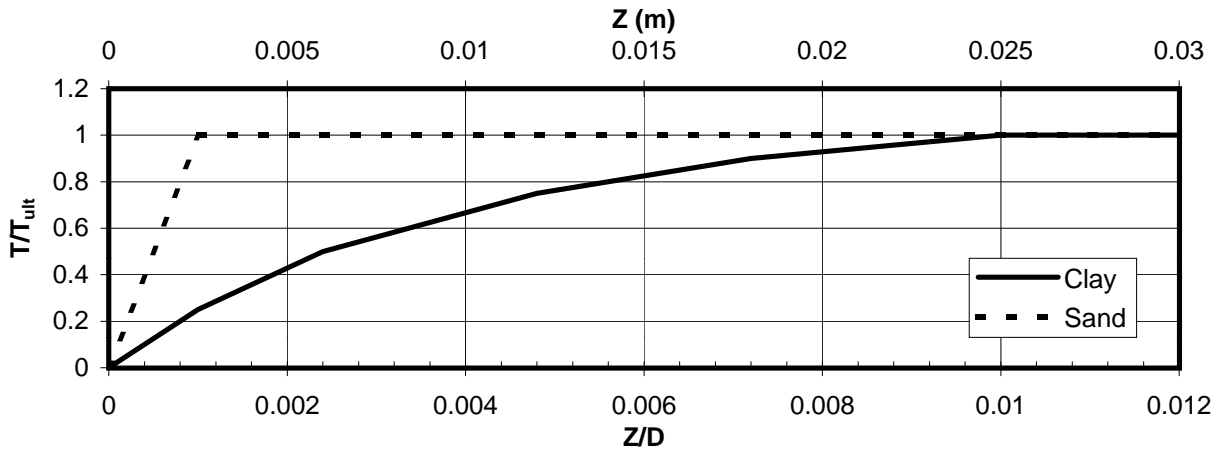
STATIC PILE HEAD LOAD-DEFORMATION CURVES
Pier E5-Eastbound (Boring 98-29)
 2.5-Meter-Diameter Pipe Piles (Pile Tip Elevation = -98 Meters)
 SFOBB East Span Seismic Safety Project



**Pier E5-Westbound (Boring 98-29-Modified)
Skyway Frame 1**



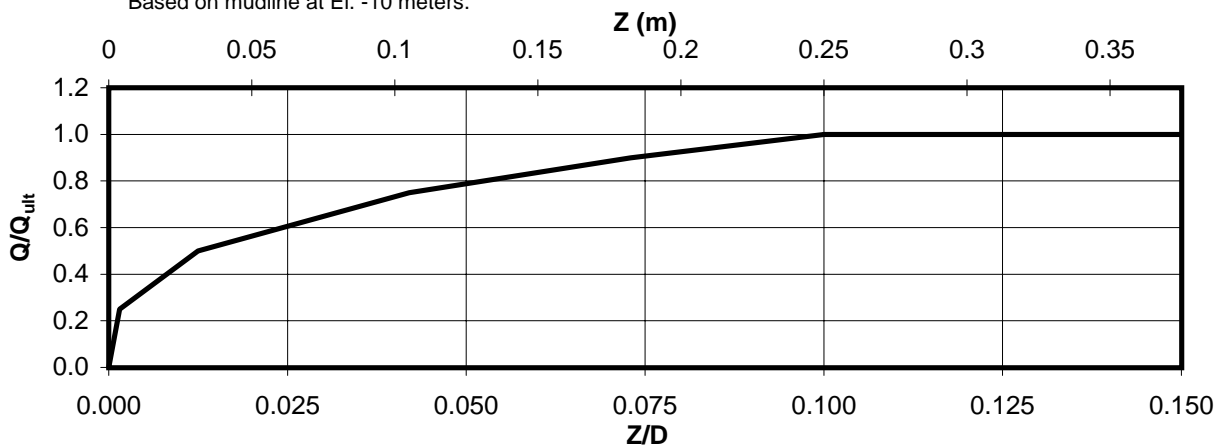
AXIAL PILE DESIGN PARAMETERS AND RESULTS
Pier E5-Westbound (Boring 98-29 Modified)
SFOBB East Span Seismic Safety Project



Depth (m)	Soil Type	T_{ult} (MN/m)
0-3	Clay	0.027
3-6	Clay	0.117
6-9	Clay	0.143
9-12	Clay	0.210
12-15	Clay	0.253
15-18	Clay	0.353
18-21	Clay	0.557
21-24	Clay	0.593
24-27	Clay	0.657
27-30	Clay	0.737
30-33	Clay	0.840
33-36	Clay	0.930

Depth (m)	Soil Type	T_{ult} (MN/m)
36-39	Clay	0.947
39-42	Clay	0.940
42-45	Clay	0.957
45-51	Clay	1.097
51-57	Clay	1.199
57-63	Clay	1.053
63-69	Sand	1.040
69-75	Clay	1.618
75-81	Clay	1.717
81-84	Clay	1.786
84-88	Sand	0.903

*Based on mudline at El. -10 meters.



Depth (m)	Soil Type	Q_{ult} (MN)
88	Sand	50.2

AXIAL PILE LOAD TRANSFER-DISPLACEMENT CURVES
Pier E5-Westbound (Boring 98-29 Modified)
 2.5-Meter-Diameter Pipe Piles (Pile Tip Elevation = -98 Meters)
 SFOBB East Span Seismic Safety Project



DEPTH (m)	t-z Data											
	t(1)	z(1)	t(2)	z(2)	t(3)	z(3)	t(4)	z(4)	t(5)	z(5)	t(6)	z(6)
0-3	0.0	0.0	0.007	0.003	0.013	0.006	0.020	0.012	0.024	0.018	0.027	0.025
3-6	0.0	0.0	0.029	0.003	0.058	0.006	0.087	0.012	0.105	0.018	0.117	0.025
6-9	0.0	0.0	0.036	0.003	0.072	0.006	0.108	0.012	0.129	0.018	0.143	0.025
9-12	0.0	0.0	0.053	0.003	0.105	0.006	0.158	0.012	0.189	0.018	0.210	0.025
12-15	0.0	0.0	0.063	0.003	0.127	0.006	0.190	0.012	0.228	0.018	0.253	0.025
15-18	0.0	0.0	0.088	0.003	0.177	0.006	0.265	0.012	0.318	0.018	0.353	0.025
18-21	0.0	0.0	0.139	0.0025	0.278	0.006	0.418	0.012	0.501	0.018	0.557	0.025
21-24	0.0	0.0	0.148	0.003	0.297	0.006	0.445	0.012	0.534	0.018	0.593	0.025
24-27	0.0	0.0	0.164	0.003	0.328	0.006	0.493	0.012	0.591	0.018	0.657	0.025
27-30	0.0	0.0	0.184	0.003	0.368	0.006	0.552	0.012	0.663	0.018	0.737	0.025
30-33	0.0	0.0	0.210	0.003	0.420	0.006	0.630	0.012	0.756	0.018	0.840	0.025
33-36	0.0	0.0	0.233	0.003	0.465	0.006	0.698	0.012	0.837	0.018	0.930	0.025
36-39	0.0	0.0	0.237	0.003	0.473	0.006	0.710	0.012	0.852	0.018	0.947	0.025
39-42	0.0	0.0	0.235	0.003	0.470	0.006	0.705	0.012	0.846	0.018	0.940	0.025
42-45	0.0	0.0	0.239	0.003	0.478	0.006	0.717	0.012	0.861	0.018	0.957	0.025
45-51	0.0	0.0	0.274	0.0025	0.549	0.006	0.823	0.012	0.987	0.018	1.097	0.025
51-57	0.0	0.0	0.300	0.003	0.600	0.006	0.899	0.012	1.079	0.018	1.199	0.025
57-63	0.0	0.0	0.263	0.003	0.527	0.006	0.790	0.012	0.948	0.018	1.053	0.025
63-69	0.0	0.0	1.040	0.003								
69-75	0.0	0.0	0.405	0.003	0.809	0.006	1.214	0.012	1.456	0.018	1.618	0.025
75-81	0.0	0.0	0.429	0.003	0.859	0.006	1.288	0.012	1.545	0.018	1.717	0.025
81-84	0.0	0.0	0.447	0.003	0.893	0.006	1.340	0.012	1.607	0.018	1.786	0.025
84-88	0.0	0.0	0.903	0.003								

Notes:

1. "t" is load (MN/m)
2. "z" is displacement (m)
3. Data for tension and compression coincide
4. Based on mudline at El. -10 meters

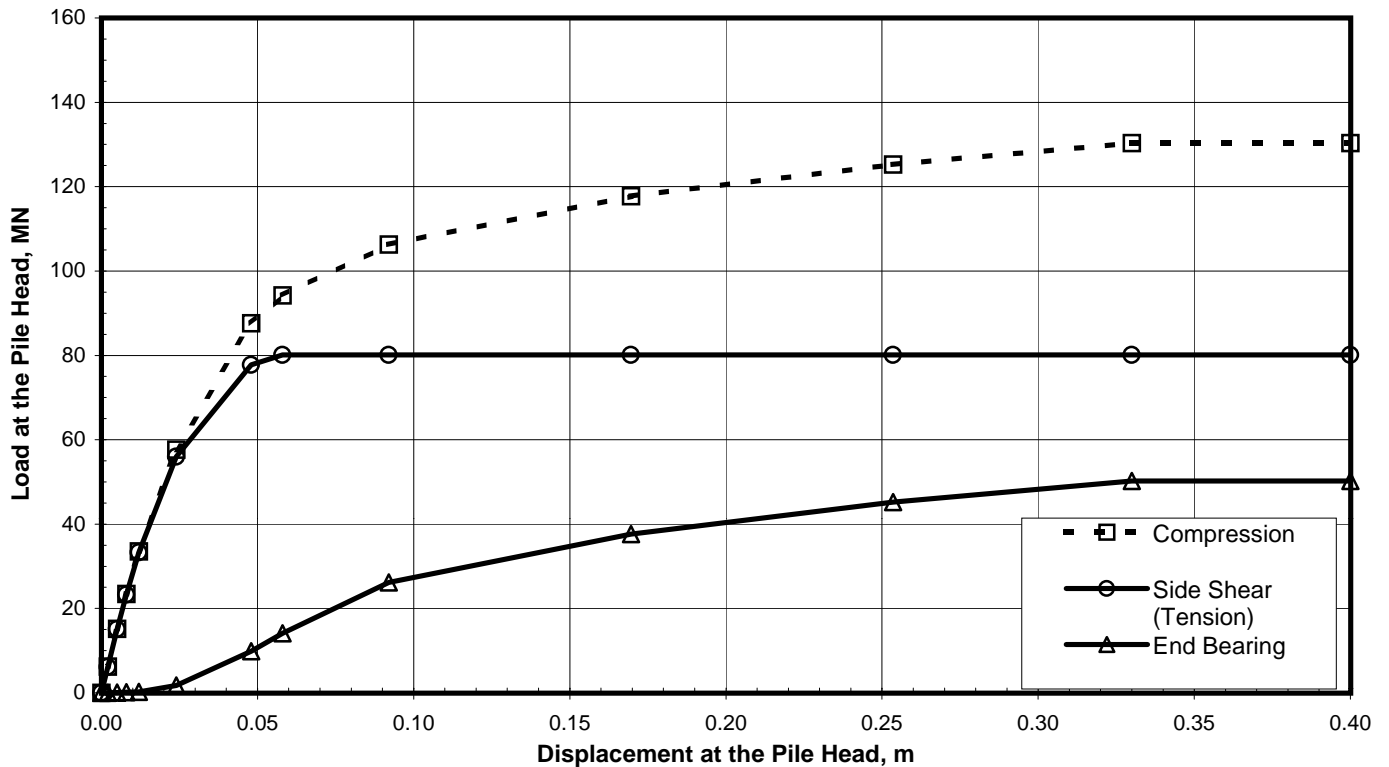
DEPTH (m)	Q-z Data											
	Q(1)	z(1)	Q(2)	z(2)	Q(3)	z(3)	Q(4)	z(4)	Q(5)	z(5)	Q(6)	z(6)
88	0.0	0.0	12.550	0.004	25.100	0.031	37.650	0.105	45.180	0.183	50.200	0.250

Notes:

1. "Q" is load in compression (MN)
2. "z" is displacement (m)

TABULATED AXIAL PILE LOAD TRANSFER DATA
Pier E5-Westbound (Boring 98-29 Modified)
 2.5-Meter-Diameter Pipe Piles (Pile Tip Elevation = -98 Meters)
 SFOBB East Span Seismic Safety Project





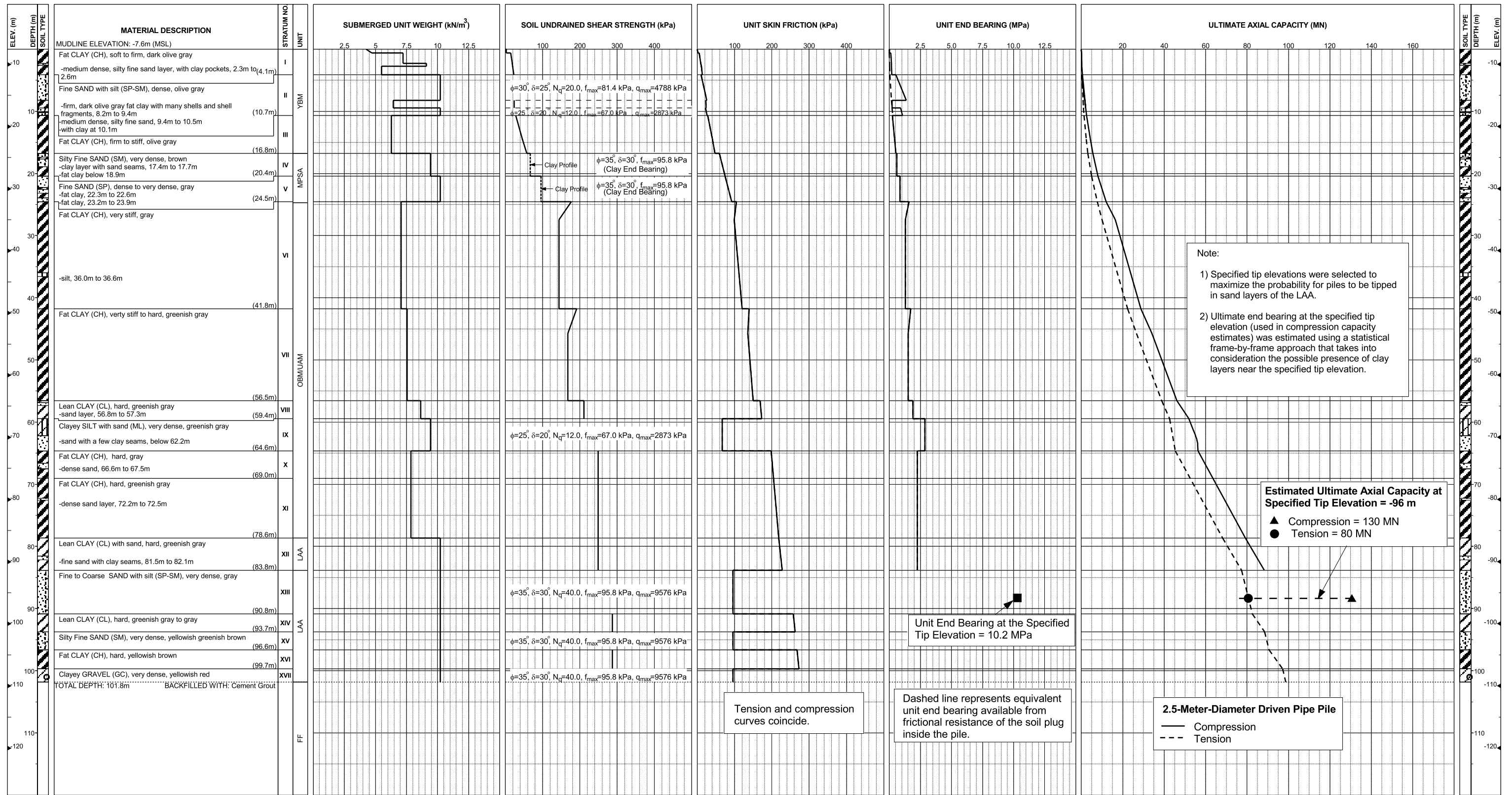
Pile Head Displacement (m)	Load at the Pile Head		End Bearing Component in Compression (MN)
	Compression (MN)	Tension (MN)	
0.000	0.00	0.00	0.00
0.002	6.19	6.17	0.03
0.005	15.14	15.07	0.07
0.008	23.44	23.32	0.12
0.012	33.53	33.30	0.23
0.024	57.67	55.96	1.71
0.048	87.63	77.76	9.87
0.058	94.19	80.10	14.09
0.092	106.30	80.10	26.20
0.170	117.75	80.10	37.65
0.254	125.28	80.10	45.18
0.330	130.30	80.10	50.20
0.400	130.30	80.10	50.20

Note:
 Pile head load-displacement curves are based on the preliminary pile wall thickness schedule provided by TY Lin/M&N and static loading conditions.

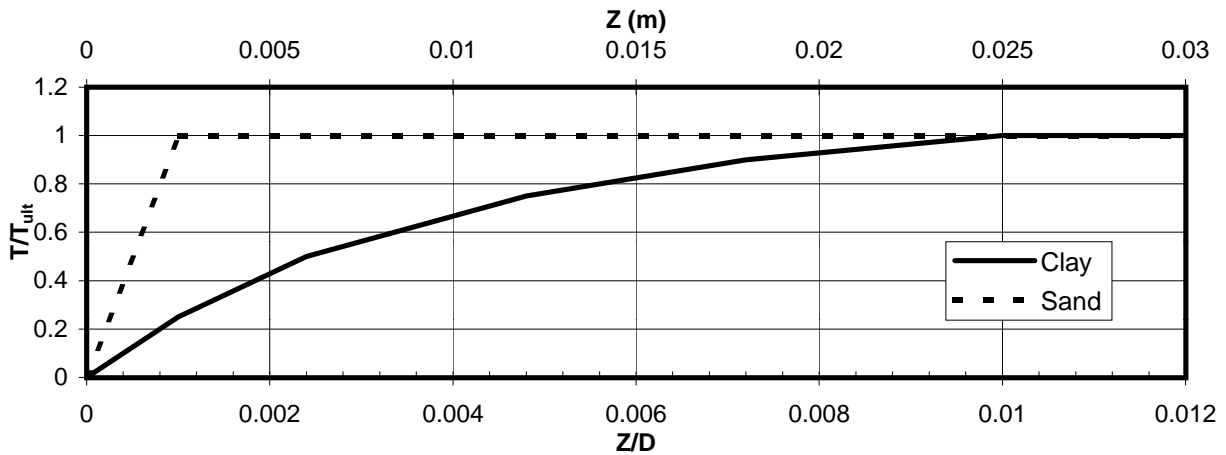
STATIC PILE HEAD LOAD-DEFORMATION CURVES
Pier E5-Westbound (Boring 98-29 Modified)
 2.5-Meter-Diameter Pipe Piles (Pile Tip Elevation = -98 Meters)
 SFOBB East Span Seismic Safety Project



**Pier E6-Eastbound (Boring 98-10 and 98-41)
Skyway Frame 1**



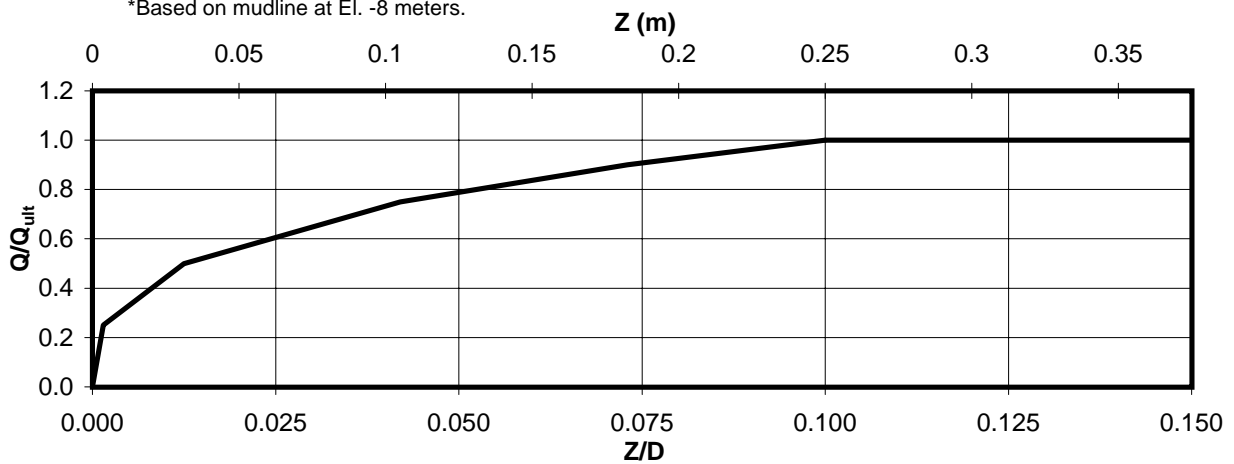
AXIAL PILE DESIGN PARAMETERS AND RESULTS
Pier E6-Eastbound (Borings 98-10 and 98-41)
SFOBB East Span Seismic Safety Project



Depth* (m)	Soil Type	T _{ult} (MN/m)
0-3	Clay	0.040
3-6	Clay	0.103
6-9	Sand	0.180
9-12	Sand	0.197
12-15	Clay	0.300
15-18	Clay	0.380
18-21	Sand	0.580
21-24	Sand	0.657
24-27	Clay	0.777
27-30	Clay	0.793
30-33	Clay	0.823
33-36	Clay	0.860

Depth* (m)	Soil Type	T _{ult} (MN/m)
36-39	Clay	0.893
39-42	Clay	0.923
42-45	Clay	1.083
45-51	Clay	1.078
51-57	Clay	1.147
57-63	Sand	0.825
63-69	Clay	1.163
69-75	Clay	1.672
75-81	Clay	1.700
81-84	Clay	1.768
84-88	Sand	0.755

*Based on mudline at El. -8 meters.



Depth* (m)	Soil Type	Q _{ult} (MN)
88	Sand	50.2

AXIAL PILE LOAD TRANSFER-DISPLACEMENT CURVES
Pier E6-Eastbound (Borings 98-10 and 98-41)
 2.5-Meter-Diameter Pipe Piles (Pile Tip Elevation = -96 Meters)
 SFOBB East Span Seismic Safety Project



DEPTH (m)	t-z Data											
	t(1)	z(1)	t(2)	z(2)	t(3)	z(3)	t(4)	z(4)	t(5)	z(5)	t(6)	z(6)
0-3	0.0	0.0	0.010	0.003	0.020	0.006	0.030	0.012	0.036	0.018	0.040	0.025
3-6	0.0	0.0	0.026	0.003	0.052	0.006	0.077	0.012	0.093	0.018	0.103	0.025
6-9	0.0	0.0	0.180	0.003								
9-12	0.0	0.0	0.197	0.003								
12-15	0.0	0.0	0.075	0.003	0.150	0.006	0.225	0.012	0.270	0.018	0.300	0.025
15-18	0.0	0.0	0.095	0.003	0.190	0.006	0.285	0.012	0.342	0.018	0.380	0.025
18-21	0.0	0.0	0.580	0.003								
21-24	0.0	0.0	0.657	0.003								
24-27	0.0	0.0	0.194	0.003	0.388	0.006	0.583	0.012	0.699	0.018	0.777	0.025
27-30	0.0	0.0	0.198	0.003	0.397	0.006	0.595	0.012	0.714	0.018	0.793	0.025
30-33	0.0	0.0	0.206	0.003	0.412	0.006	0.617	0.012	0.741	0.018	0.823	0.025
33-36	0.0	0.0	0.215	0.003	0.430	0.006	0.645	0.012	0.774	0.018	0.860	0.025
36-39	0.0	0.0	0.223	0.003	0.447	0.006	0.670	0.012	0.804	0.018	0.893	0.025
39-42	0.0	0.0	0.231	0.003	0.462	0.006	0.692	0.012	0.831	0.018	0.923	0.025
42-45	0.0	0.0	0.271	0.003	0.542	0.006	0.812	0.012	0.975	0.018	1.083	0.025
45-51	0.0	0.0	0.270	0.003	0.539	0.006	0.809	0.012	0.970	0.018	1.078	0.025
51-57	0.0	0.0	0.287	0.003	0.574	0.006	0.860	0.012	1.032	0.018	1.147	0.025
57-63	0.0	0.0	0.825	0.003								
63-69	0.0	0.0	0.291	0.003	0.582	0.006	0.872	0.012	1.047	0.018	1.163	0.025
69-75	0.0	0.0	0.418	0.003	0.836	0.006	1.254	0.012	1.505	0.018	1.672	0.025
75-81	0.0	0.0	0.425	0.003	0.850	0.006	1.275	0.012	1.530	0.018	1.700	0.025
81-84	0.0	0.0	0.442	0.003	0.884	0.006	1.326	0.012	1.591	0.018	1.768	0.025
84-88	0.0	0.0	0.755	0.003								

Notes:

1. "t" is load (MN/m)
2. "z" is displacement (m)
3. Data for tension and compression coincide
4. Based on mudline at El. -8 meters

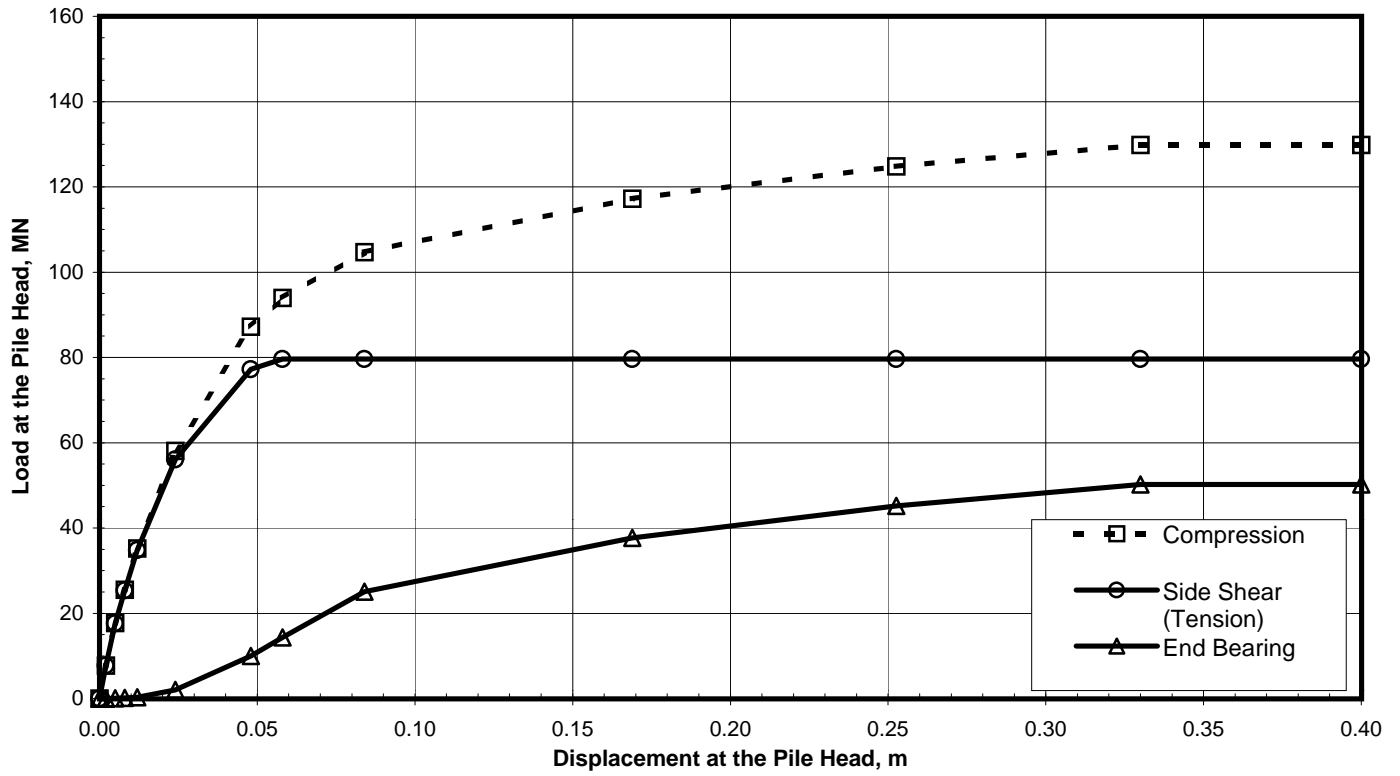
DEPTH (m)	Q-z Data											
	Q(1)	z(1)	Q(2)	z(2)	Q(3)	z(3)	Q(4)	z(4)	Q(5)	z(5)	Q(6)	z(6)
88	0.0	0.0	12.550	0.004	25.100	0.031	37.650	0.105	45.180	0.183	50.200	0.250

Notes:

1. "Q" is load in compression (MN)
2. "z" is displacement (m)

TABULATED AXIAL PILE LOAD TRANSFER DATA
Pier E6-Eastbound (Borings 98-10 and 98-41)
 2.5-Meter-Diameter Pipe Piles (Pile Tip Elevation = -96 Meters)
 SFOBB East Span Seismic Safety Project





Pile Head Displacement (m)	Load at the Pile Head		End Bearing Component in Compression (MN)
	Compression (MN)	Tension (MN)	
0.000	0.00	0.00	0.00
0.002	7.73	7.70	0.03
0.005	17.73	17.63	0.10
0.008	25.51	25.33	0.18
0.012	35.16	34.83	0.33
0.024	58.10	56.08	2.02
0.048	87.22	77.26	9.96
0.058	93.95	79.60	14.35
0.084	104.70	79.60	25.10
0.169	117.25	79.60	37.65
0.253	124.78	79.60	45.18
0.330	129.80	79.60	50.20
0.400	129.80	79.60	50.20

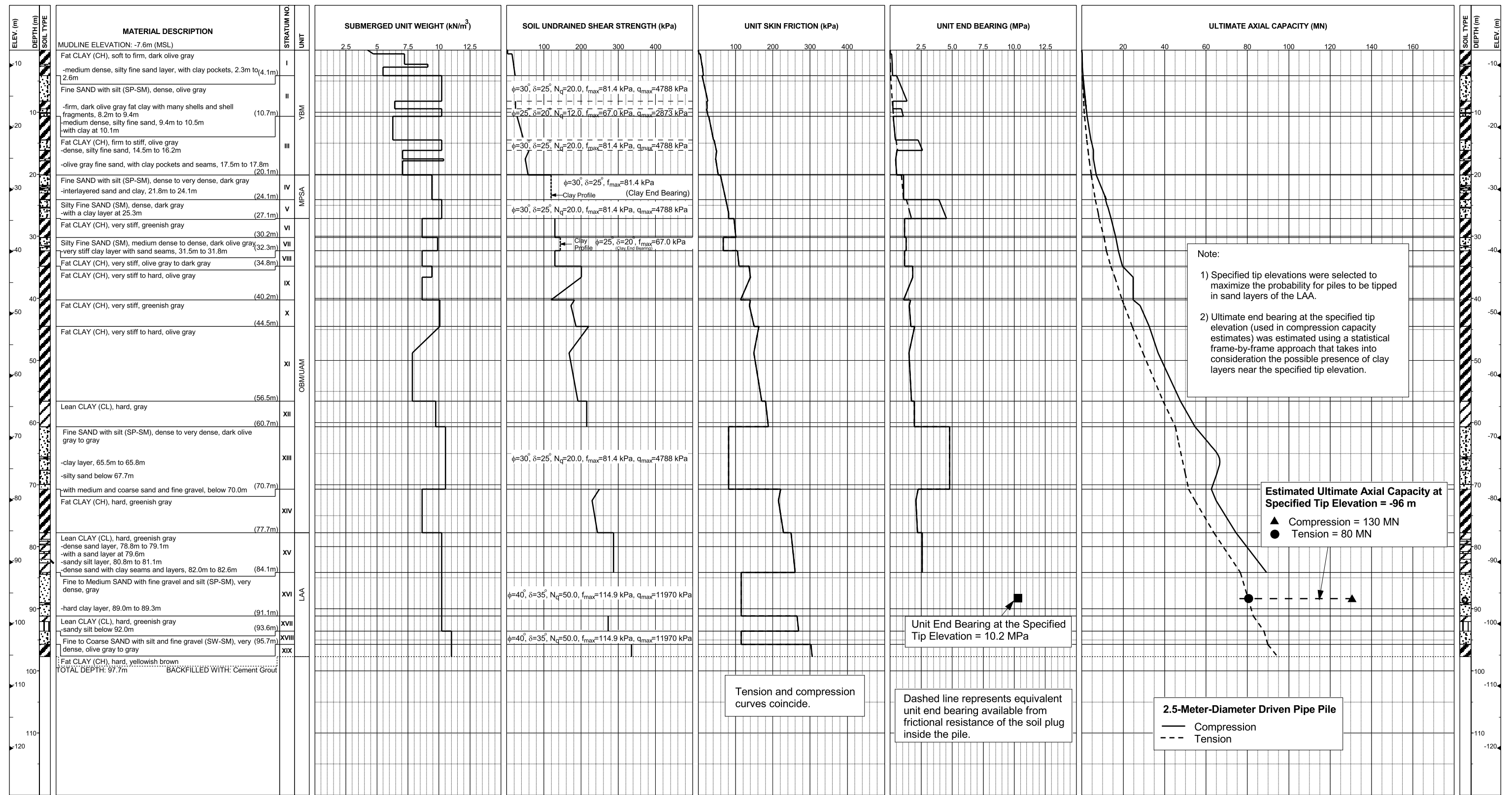
Note:

Pile head load-displacement curves are based on the preliminary pile wall thickness schedule provided by TY Lin/M&N and static loading conditions.

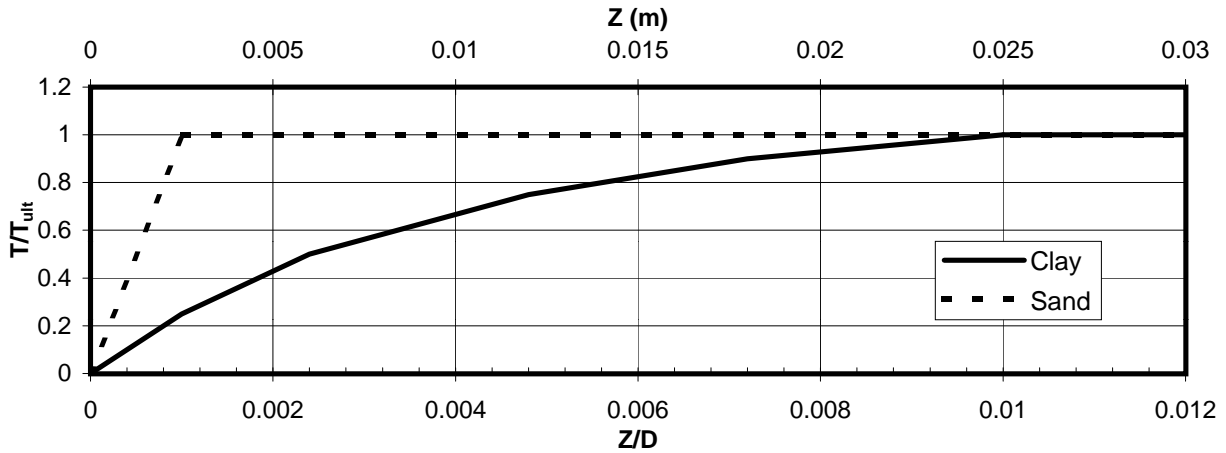
STATIC PILE HEAD LOAD-DEFORMATION CURVES
Pier E6-Eastbound (Borings 98-10 and 98-41)
 2.5-Meter-Diameter Pipe Piles (Pile Tip Elevation = -96 Meters)
 SFOBB East Span Seismic Safety Project



**Pier E6-Westbound (Boring 98-41)
Skyway Frame 1**



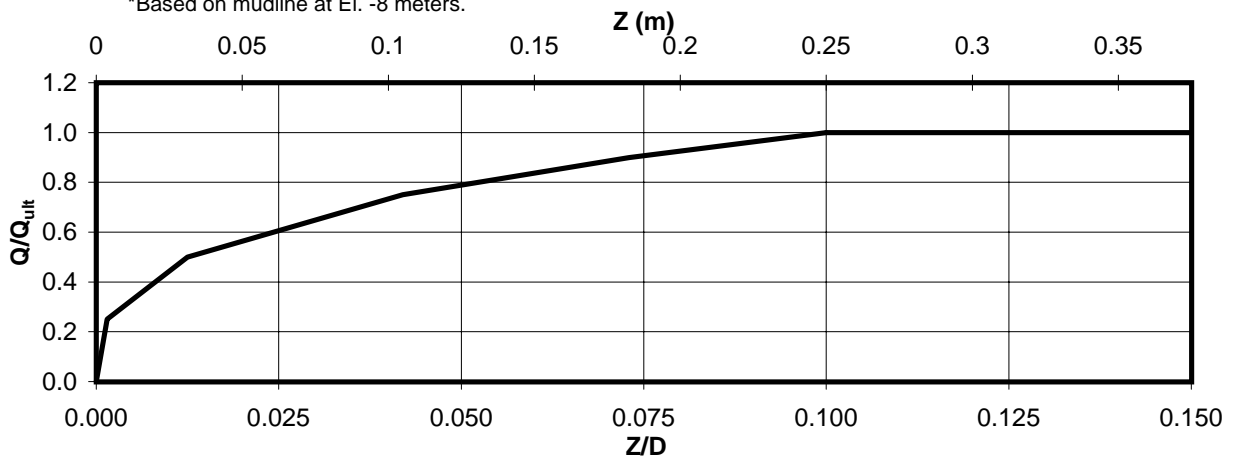
AXIAL PILE DESIGN PARAMETERS AND RESULTS
Pier E6-Westbound (Boring 98-41)
SFOBB East Span Seismic Safety Project



Depth* (m)	Soil Type	T_{ult} (MN/m)
0-3	Clay	0.040
3-6	Clay	0.107
6-9	Sand	0.183
9-12	Sand	0.193
12-15	Clay	0.283
15-18	Clay	0.373
18-21	Sand	0.407
21-24	Sand	0.543
24-27	Clay	0.623
27-30	Clay	0.767
30-33	Clay	0.590
33-36	Clay	0.937

Depth* (m)	Soil Type	T_{ult} (MN/m)
36-39	Clay	1.100
39-42	Clay	0.997
42-45	Clay	1.157
45-51	Clay	1.215
51-57	Clay	1.267
57-63	Sand	1.232
63-69	Clay	0.582
69-75	Clay	1.323
75-81	Clay	1.895
81-84	Clay	2.033
84-88	Sand	0.902

*Based on mudline at El. -8 meters.



Depth* (m)	Soil Type	Q_{ult} (MN)
88	Sand	50.2

AXIAL PILE LOAD TRANSFER-DISPLACEMENT CURVES
Pier E6-Westbound (Boring 98-41)
 2.5-Meter-Diameter Pipe Piles (Pile Tip Elevation = -96 Meters)
 SFOBB East Span Seismic Safety Project



DEPTH (m)	t-z Data											
	t(1)	z(1)	t(2)	z(2)	t(3)	z(3)	t(4)	z(4)	t(5)	z(5)	t(6)	z(6)
0-3	0.0	0.0	0.010	0.003	0.020	0.006	0.030	0.012	0.036	0.018	0.040	0.025
3-6	0.0	0.0	0.027	0.003	0.053	0.006	0.080	0.012	0.096	0.018	0.107	0.025
6-9	0.0	0.0	0.183	0.003								
9-12	0.0	0.0	0.193	0.003								
12-15	0.0	0.0	0.071	0.003	0.142	0.006	0.212	0.012	0.255	0.018	0.283	0.025
15-18	0.0	0.0	0.093	0.003	0.187	0.006	0.280	0.012	0.336	0.018	0.373	0.025
18-21	0.0	0.0	0.407	0.003								
21-24	0.0	0.0	0.543	0.003								
24-27	0.0	0.0	0.156	0.003	0.312	0.006	0.467	0.012	0.561	0.018	0.623	0.025
27-30	0.0	0.0	0.192	0.003	0.383	0.006	0.575	0.012	0.690	0.018	0.767	0.025
30-33	0.0	0.0	0.148	0.003	0.295	0.006	0.443	0.012	0.531	0.018	0.590	0.025
33-36	0.0	0.0	0.234	0.003	0.468	0.006	0.703	0.012	0.843	0.018	0.937	0.025
36-39	0.0	0.0	0.275	0.003	0.550	0.006	0.825	0.012	0.990	0.018	1.100	0.025
39-42	0.0	0.0	2.492	0.003	4.984	0.006	7.475	0.012	8.970	0.018	9.967	0.025
42-45	0.0	0.0	0.289	0.003	0.579	0.006	0.868	0.012	1.041	0.018	1.157	0.025
45-51	0.0	0.0	0.304	0.003	0.608	0.006	0.911	0.012	1.094	0.018	1.215	0.025
51-57	0.0	0.0	0.317	0.003	0.634	0.006	0.950	0.012	1.140	0.018	1.267	0.025
57-63	0.0	0.0	1.232	0.003								
63-69	0.0	0.0	0.145	0.003	0.291	0.006	0.436	0.012	0.524	0.018	0.582	0.025
69-75	0.0	0.0	0.331	0.003	0.662	0.006	0.992	0.012	1.191	0.018	1.323	0.025
75-81	0.0	0.0	0.474	0.003	0.948	0.006	1.421	0.012	1.706	0.018	1.895	0.025
81-84	0.0	0.0	0.508	0.003	1.017	0.006	1.525	0.012	1.830	0.018	2.033	0.025
84-88	0.0	0.0	0.902	0.003								

Notes:

1. "t" is load (MN/m)
2. "z" is displacement (m)
3. Data for tension and compression coincide
4. Based on mudline at El. -8 meters

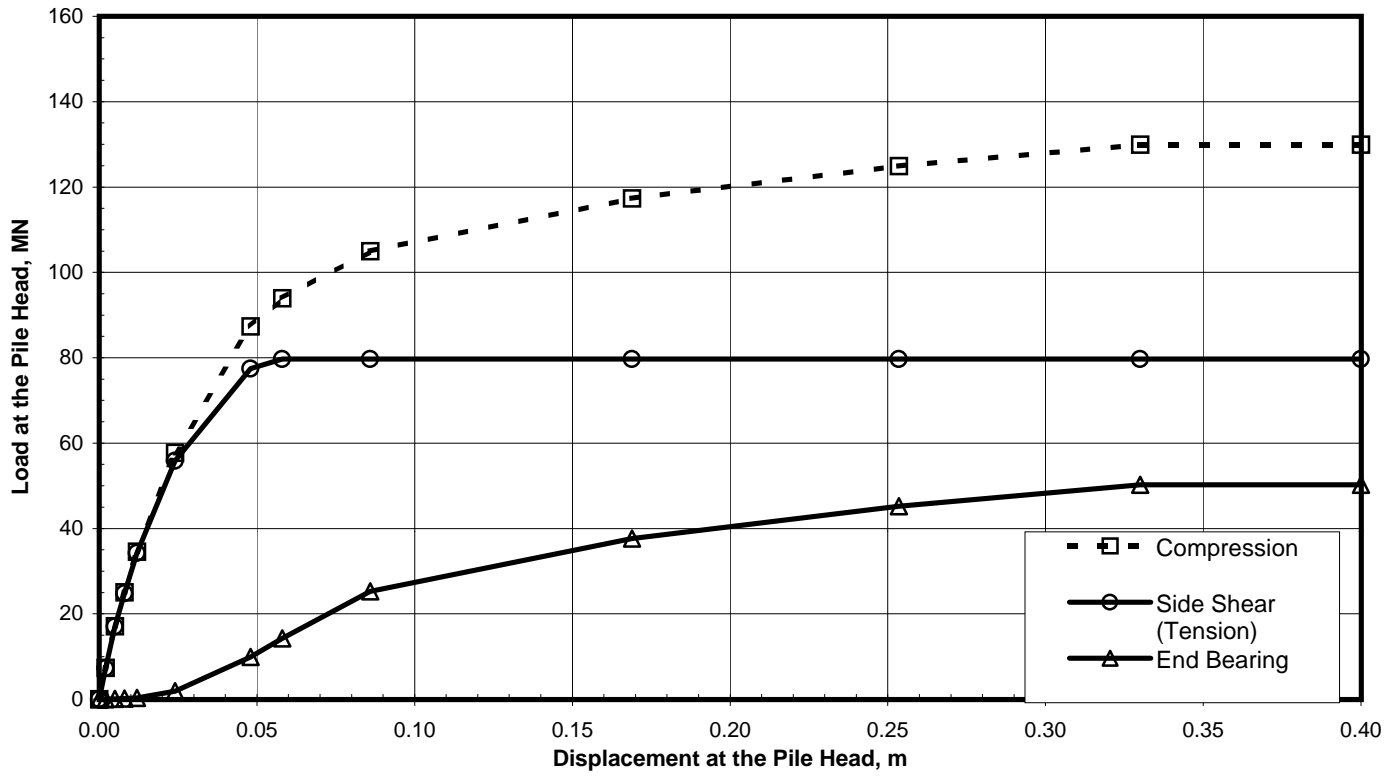
DEPTH (m)	Q-z Data											
	Q(1)	z(1)	Q(2)	z(2)	Q(3)	z(3)	Q(4)	z(4)	Q(5)	z(5)	Q(6)	z(6)
88	0.0	0.0	12.550	0.004	25.100	0.031	37.650	0.105	45.180	0.183	50.200	0.250

Notes:

1. "Q" is load in compression (MN)
2. "z" is displacement (m)

TABULATED AXIAL PILE LOAD TRANSFER DATA
Pier E6-Westbound (Boring 98-41)
2.5-Meter-Diameter Pipe Piles (Pile Tip Elevation = -96 Meters)
SFOBB East Span Seismic Safety Project





Pile Head Displacement (m)	Load at the Pile Head		End Bearing Component in Compression (MN)
	Compression (MN)	Tension (MN)	
0.000	0.00	0.00	0.00
0.002	7.32	7.30	0.03
0.005	17.10	17.02	0.08
0.008	25.01	24.85	0.16
0.012	34.54	34.23	0.31
0.024	57.72	55.85	1.87
0.048	87.37	77.45	9.92
0.058	93.91	79.69	14.22
0.086	104.99	79.69	25.30
0.169	117.35	79.69	37.66
0.253	124.88	79.69	45.19
0.330	129.90	79.69	50.21
0.400	129.90	79.69	50.21

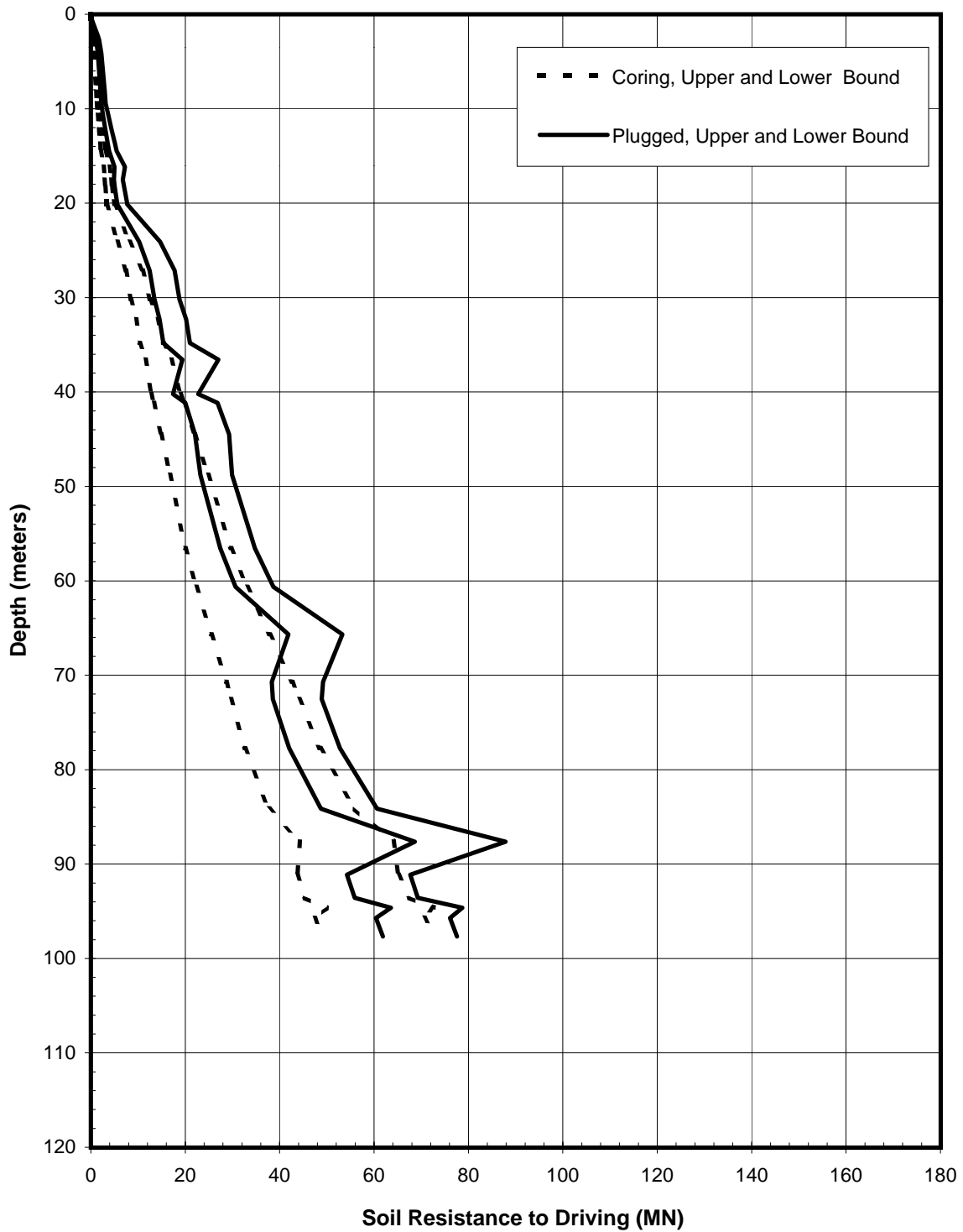
Note:

Pile head load-displacement curves are based on the preliminary pile wall thickness schedule provided by TY Lin/M&N and static loading conditions.

**STATIC PILE HEAD LOAD-DEFORMATION CURVES
 Pier E6-Westbound (Boring 98-41)**

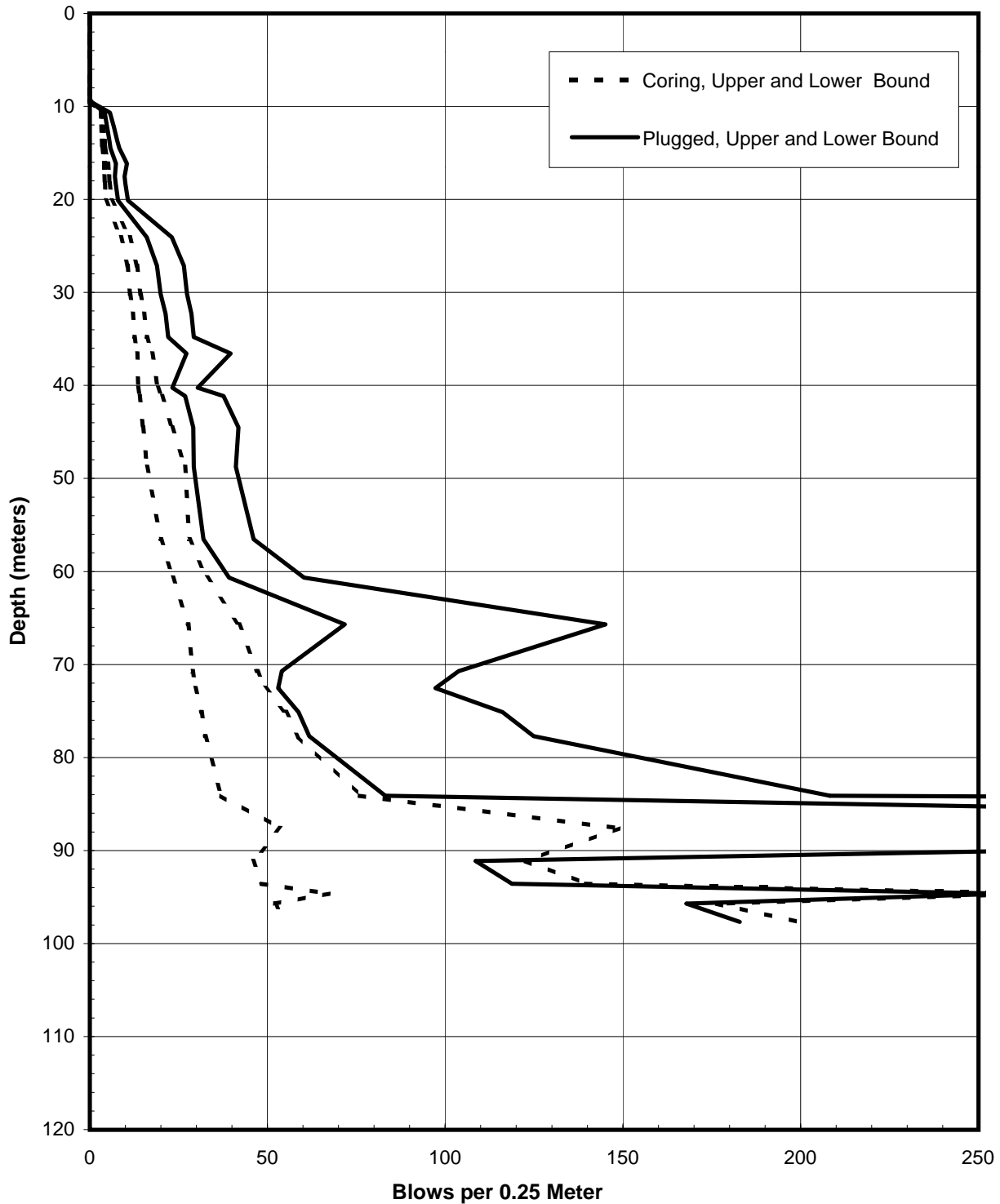
2.5-Meter-Diameter Pipe Piles (Pile Tip Elevation = -96 Meters)
 SFOBB East Span Seismic Safety Project





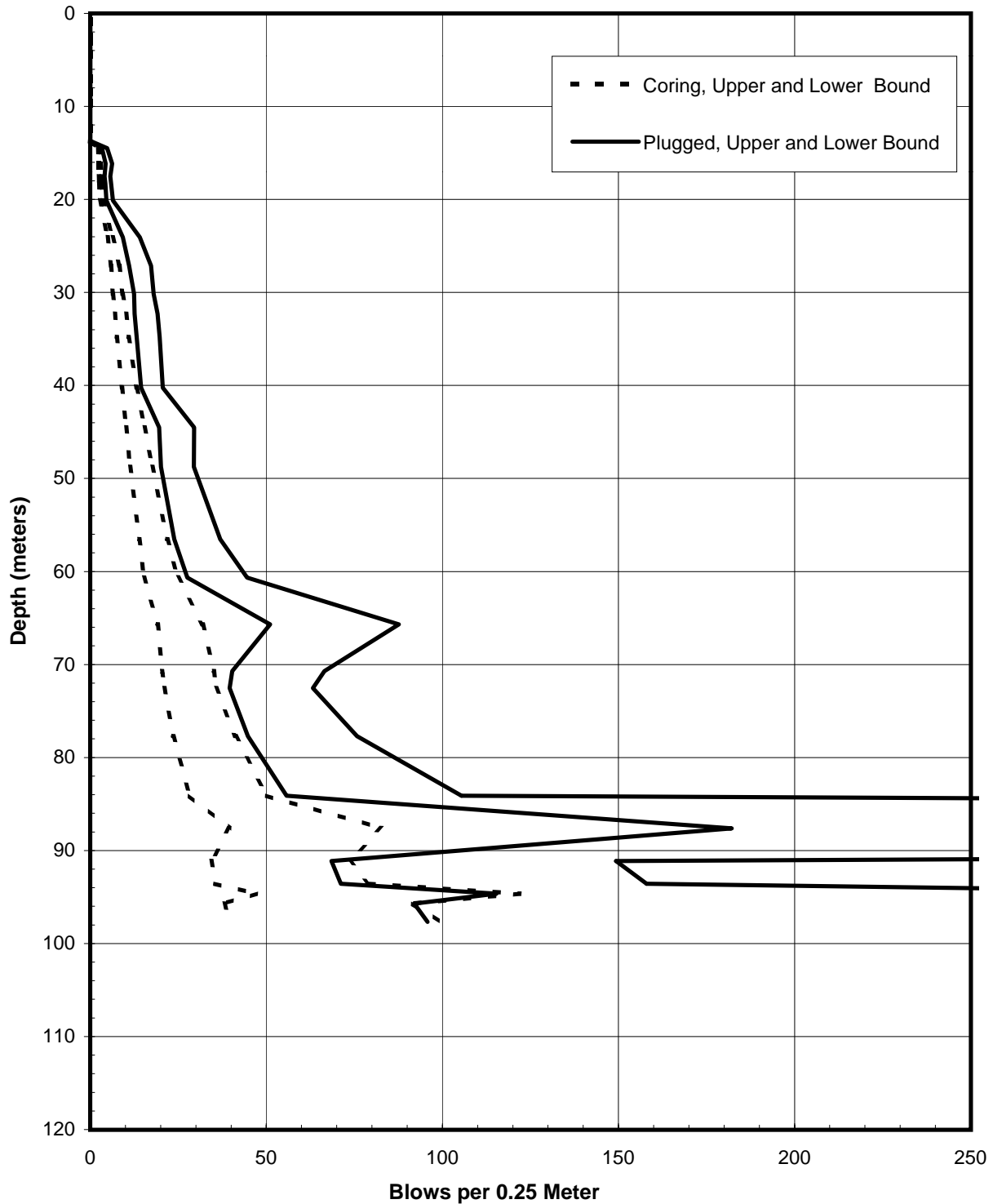
SOIL RESISTANCE TO DRIVING
Pier E6-Westbound (Boring 98-41)
2.5-Meter-Diameter Driven Pipe Piles
SFOBB East Span Seismic Safety Project





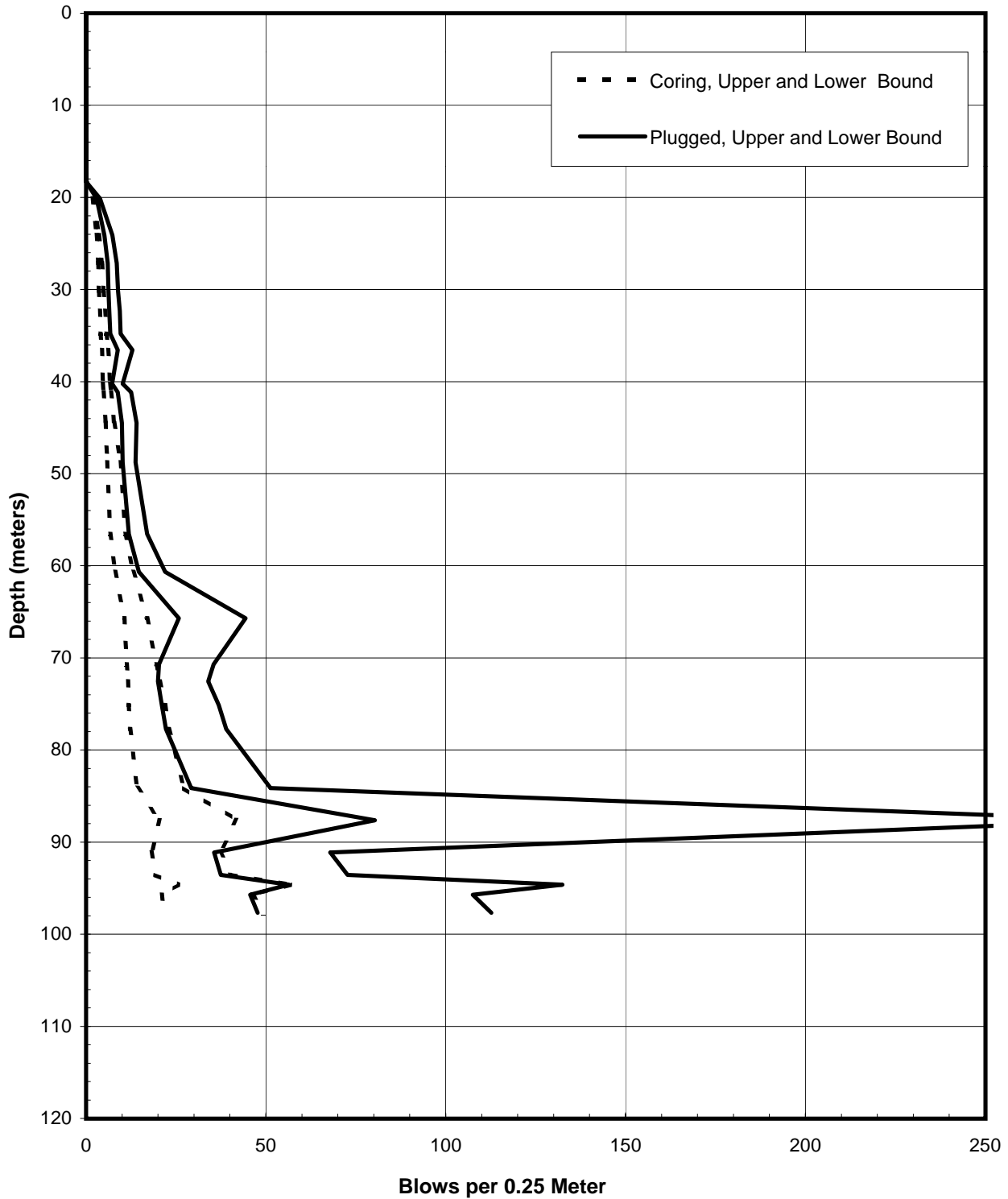
PREDICTED BLOW COUNTS
Pier E6-Westbound (Boring 98-41)
Menck MHU-500T, 2.5-Meter-Diameter Driven Pipe Piles
SFOBB East Span Seismic Safety Project





PREDICTED BLOW COUNTS
Pier E6-Westbound (Boring 98-41)
Menck MHU-1000, 2.5-Meter-Diameter Driven Pipe Piles
SFOBB East Span Seismic Safety Project

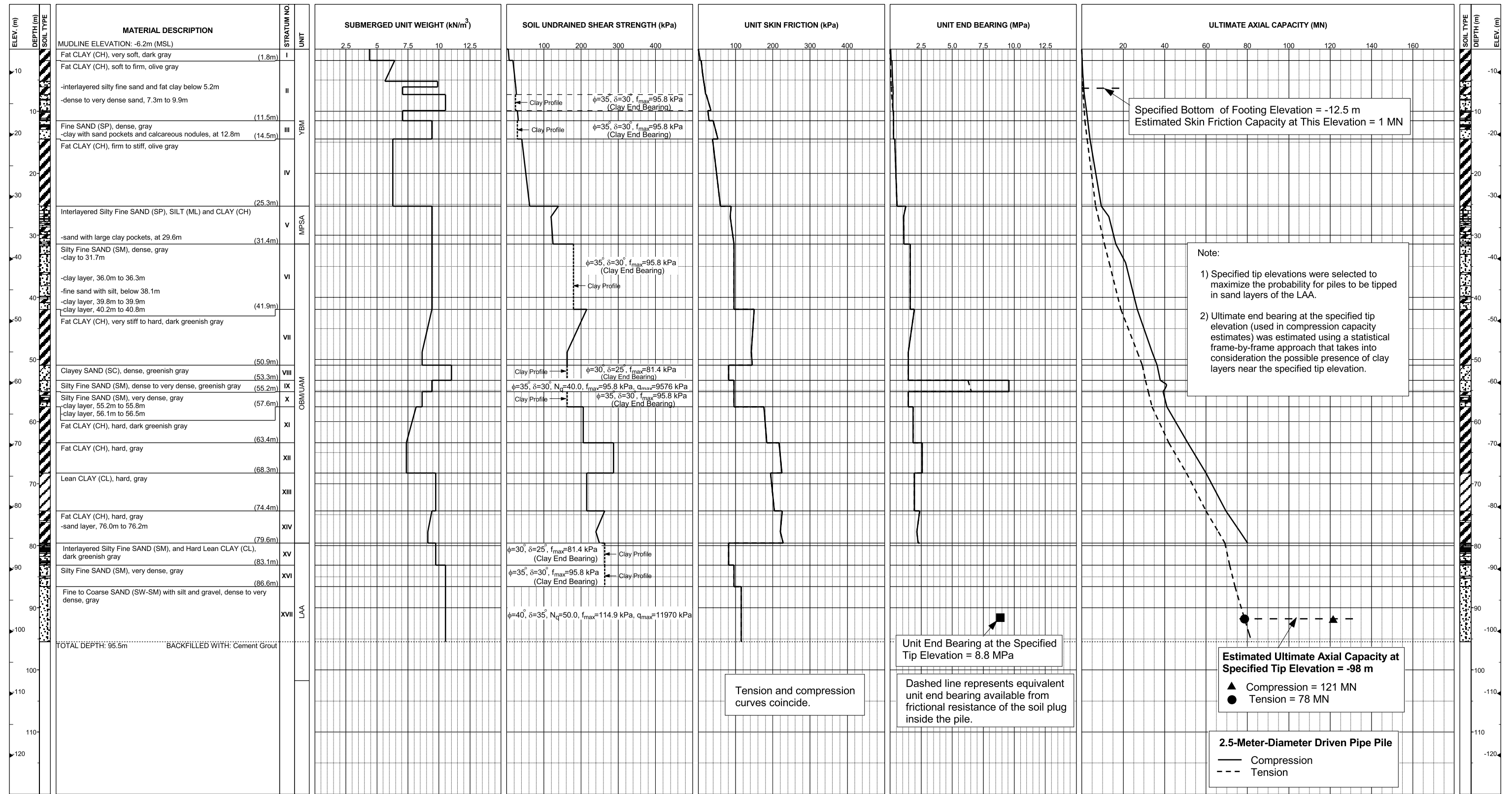




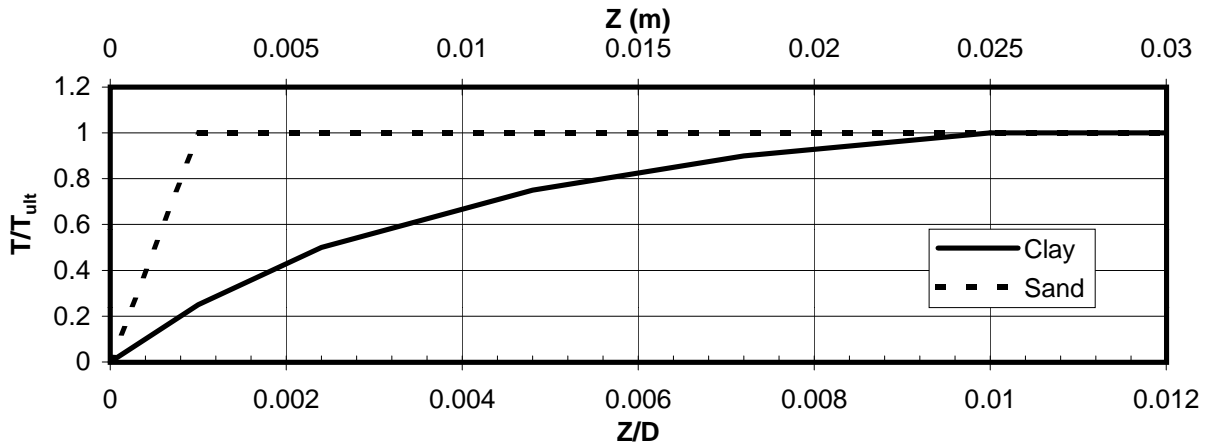
PREDICTED BLOW COUNTS
Pier E6-Westbound (Boring 98-41)
Menck MHU-1700, 2.5-Meter-Diameter Driven Pipe Piles
SFOBB East Span Seismic Safety Project



**Pier E7-Eastbound (Boring 98-49)
Skyway Frame 2**



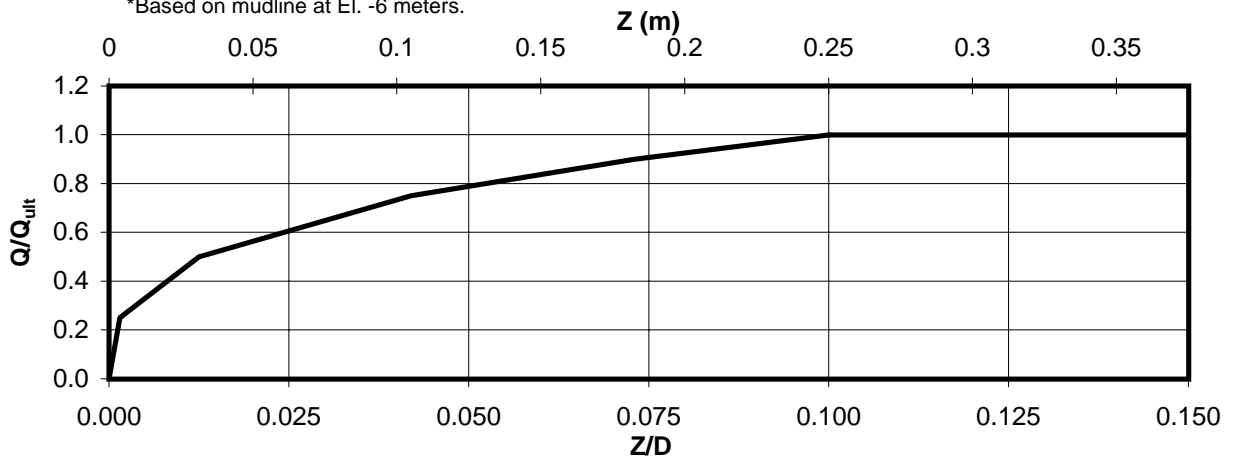
AXIAL PILE DESIGN PARAMETERS AND RESULTS
Pier E7-Eastbound (Boring 98-49)
 SFOBB East Span Seismic Safety Project



Depth* (m)	Soil Type	T_{ult} (MN/m)
0-3	Clay	0.017
3-6	Clay	0.110
6-9	Clay	0.173
9-12	Sand	0.244
12-15	Sand	0.340
15-18	Clay	0.337
18-21	Clay	0.367
21-24	Clay	0.423
24-27	Clay	0.600
27-30	Clay	0.700
30-33	Sand	0.761
33-36	Sand	0.754

Depth* (m)	Soil Type	T_{ult} (MN/m)
36-39	Sand	0.754
39-42	Sand	0.754
42-45	Clay	1.168
45-51	Clay	1.128
51-57	Sand	0.716
57-63	Clay	1.292
63-69	Clay	1.726
69-75	Clay	1.571
75-81	Clay	1.669
81-87	Sand	0.625

*Based on mudline at El. -6 meters.



Depth* (m)	Soil Type	Q_{ult} (MN)
87	Sand	43.7

AXIAL PILE LOAD TRANSFER-DISPLACEMENT CURVES
Pier E7-Eastbound (Boring 98-49)
 2.5-Meter-Diameter Pipe Piles (Pile Tip Elevation = -93 Meters)
 SFOBB East Span Seismic Safety Project



DEPTH (m)	t-z Data											
	t(1)	z(1)	t(2)	z(2)	t(3)	z(3)	t(4)	z(4)	t(5)	z(5)	t(6)	z(6)
0-3	0.0	0.0	0.004	0.003	0.008	0.006	0.013	0.012	0.015	0.018	0.017	0.025
3-6	0.0	0.0	0.028	0.003	0.055	0.006	0.083	0.012	0.099	0.018	0.110	0.025
6-9	0.0	0.0	0.043	0.003	0.087	0.006	0.130	0.012	0.156	0.018	0.173	0.025
9-12	0.0	0.0	0.244	0.003								
12-15	0.0	0.0	0.340	0.003								
15-18	0.0	0.0	0.084	0.003	0.168	0.006	0.252	0.012	0.303	0.018	0.337	0.025
18-21	0.0	0.0	0.092	0.003	0.183	0.006	0.275	0.012	0.330	0.018	0.367	0.025
21-24	0.0	0.0	0.106	0.003	0.212	0.006	0.317	0.012	0.381	0.018	0.423	0.025
24-27	0.0	0.0	0.150	0.003	0.300	0.006	0.450	0.012	0.540	0.018	0.600	0.025
27-30	0.0	0.0	0.175	0.003	0.350	0.006	0.525	0.012	0.630	0.018	0.700	0.025
30-33	0.0	0.0	0.761	0.003								
33-36	0.0	0.0	0.754	0.003								
36-39	0.0	0.0	0.754	0.003								
39-42	0.0	0.0	0.754	0.003								
42-45	0.0	0.0	0.292	0.003	0.584	0.006	0.876	0.012	1.051	0.018	1.168	0.025
45-51	0.0	0.0	0.282	0.003	0.564	0.006	0.846	0.012	1.015	0.018	1.128	0.025
51-57	0.0	0.0	7.157	0.003								
57-63	0.0	0.0	0.323	0.003	0.646	0.006	0.969	0.012	1.163	0.018	1.292	0.025
63-69	0.0	0.0	0.432	0.003	0.863	0.006	1.295	0.012	1.553	0.018	1.726	0.025
69-75	0.0	0.0	0.393	0.003	0.786	0.006	1.178	0.012	1.414	0.018	1.571	0.025
75-81	0.0	0.0	0.417	0.003	0.835	0.006	1.252	0.012	1.502	0.018	1.669	0.025
81-87	0.0	0.0	0.625	0.003								

Notes:

1. "t" is load (MN/m)
2. "z" is displacement (m)
3. Data for tension and compression coincide
4. Based on mudline at El. -6 meters

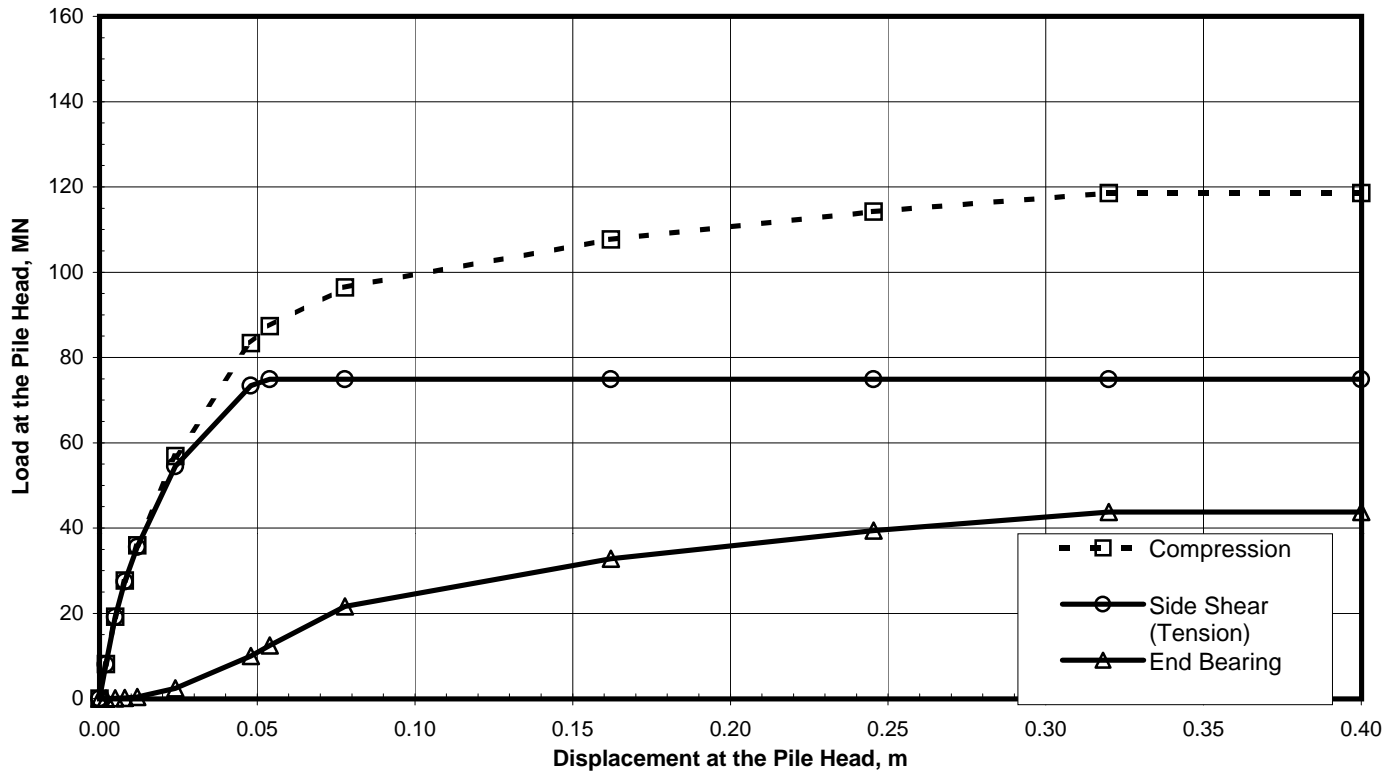
DEPTH (m)	Q-z Data											
	Q(1)	z(1)	Q(2)	z(2)	Q(3)	z(3)	Q(4)	z(4)	Q(5)	z(5)	Q(6)	z(6)
87	0.0	0.0	10.925	0.004	21.850	0.031	32.775	0.105	39.330	0.183	43.700	0.250

Notes:

1. "Q" is load in compression (MN)
2. "z" is displacement (m)

TABULATED AXIAL PILE LOAD TRANSFER DATA
Pier E7-Eastbound (Boring 98-49)
 2.5-Meter-Diameter Pipe Piles (Pile Tip Elevation = -93 Meters)
 SFOBB East Span Seismic Safety Project





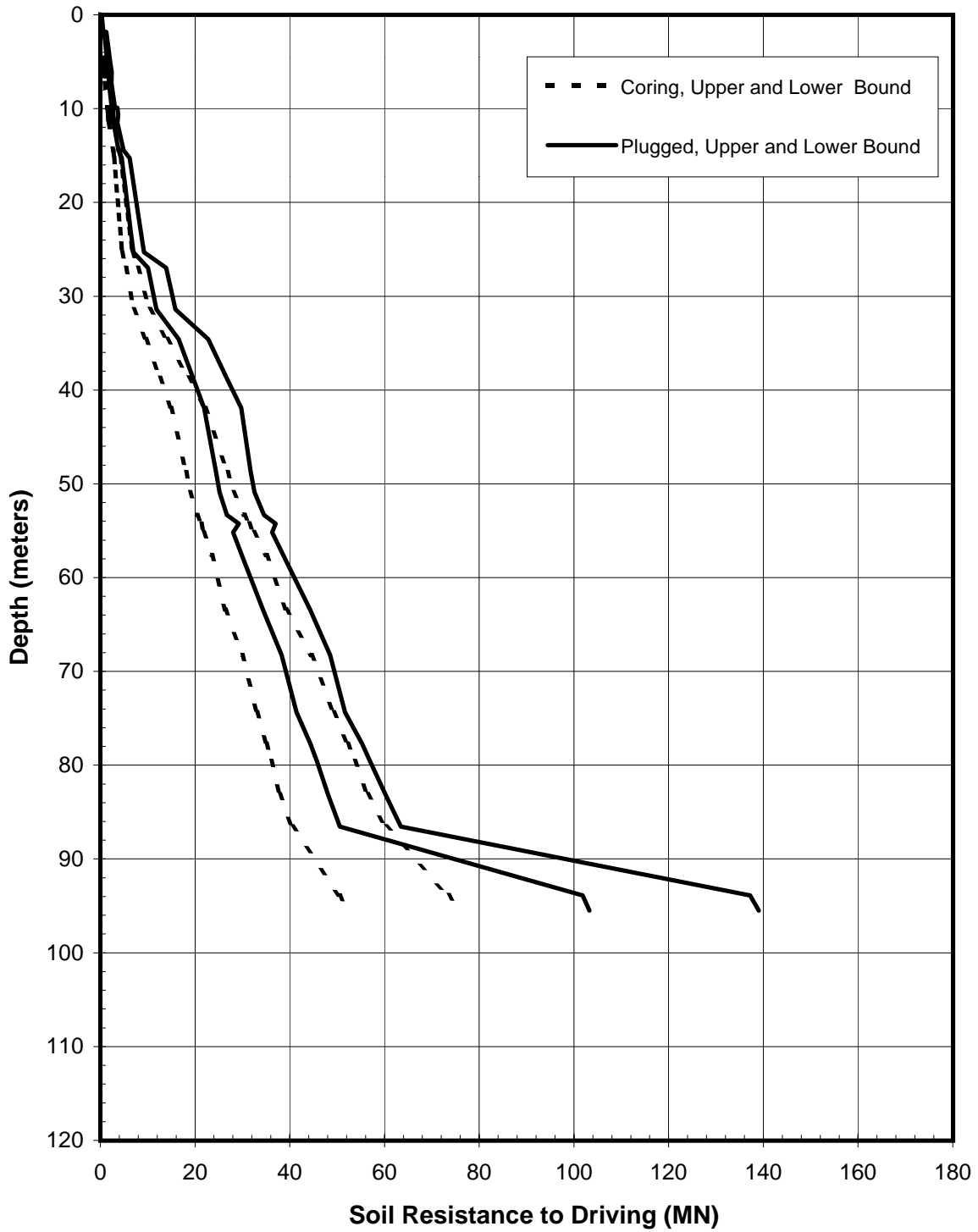
Pile Head Displacement (m)	Load at the Pile Head		End Bearing Component in Compression (MN)
	Compression (MN)	Tension (MN)	
0.000	0.00	0.00	0.00
0.002	8.07	8.05	0.02
0.005	19.20	19.13	0.07
0.008	27.67	27.50	0.17
0.012	35.97	35.58	0.39
0.024	56.88	54.49	2.39
0.048	83.39	73.43	9.96
0.054	87.32	74.86	12.46
0.078	96.46	74.86	21.60
0.162	107.67	74.86	32.81
0.245	114.23	74.86	39.37
0.320	118.60	74.86	43.74
0.400	118.60	74.86	43.74

Note:

Pile head load-displacement curves are based on the preliminary pile wall thickness schedule provided by TY Lin/M&N and static loading conditions.

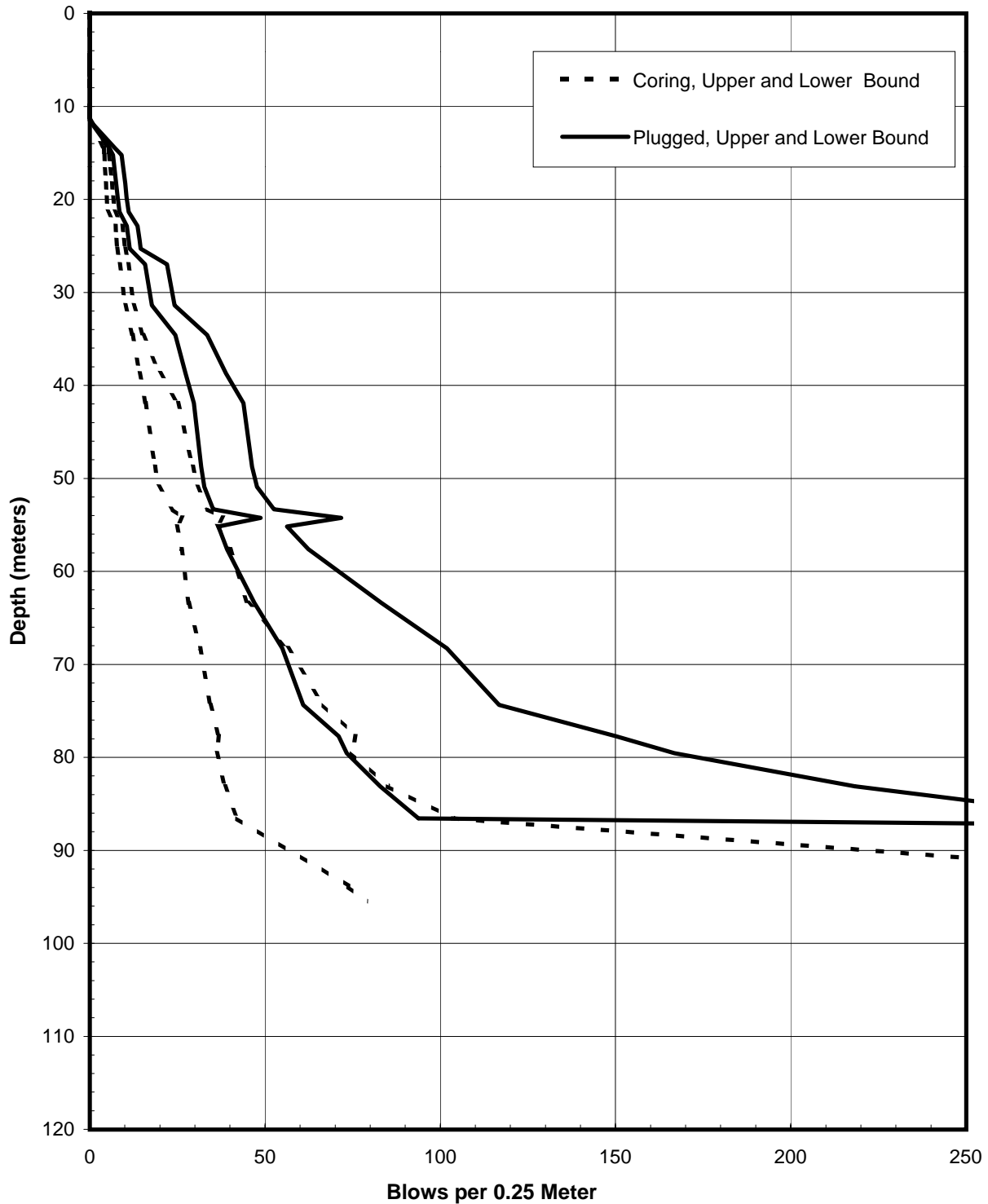
STATIC PILE HEAD LOAD-DEFORMATION CURVES
Pier E7-Eastbound (Boring 98-49)
 2.5-Meter-Diameter Pipe Piles (Pile Tip Elevation = -93 Meters)
 SFOBB East Span Seismic Safety Project





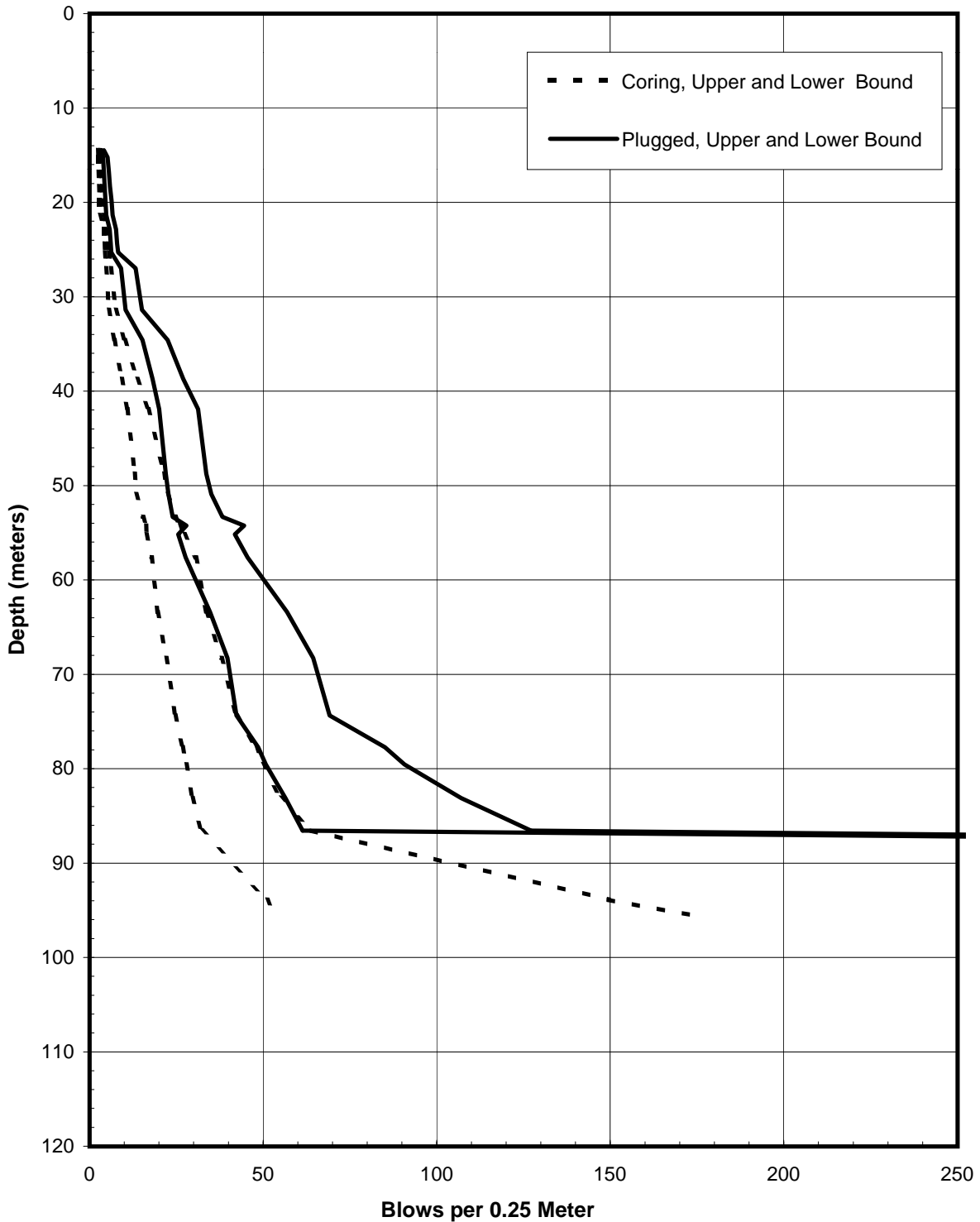
SOIL RESISTANCE TO DRIVING
Pier E7-Eastbound (Boring 98-49)
2.5-Meter-Diameter Driven Pipe Piles
SFOBB East Span Seismic Safety Project





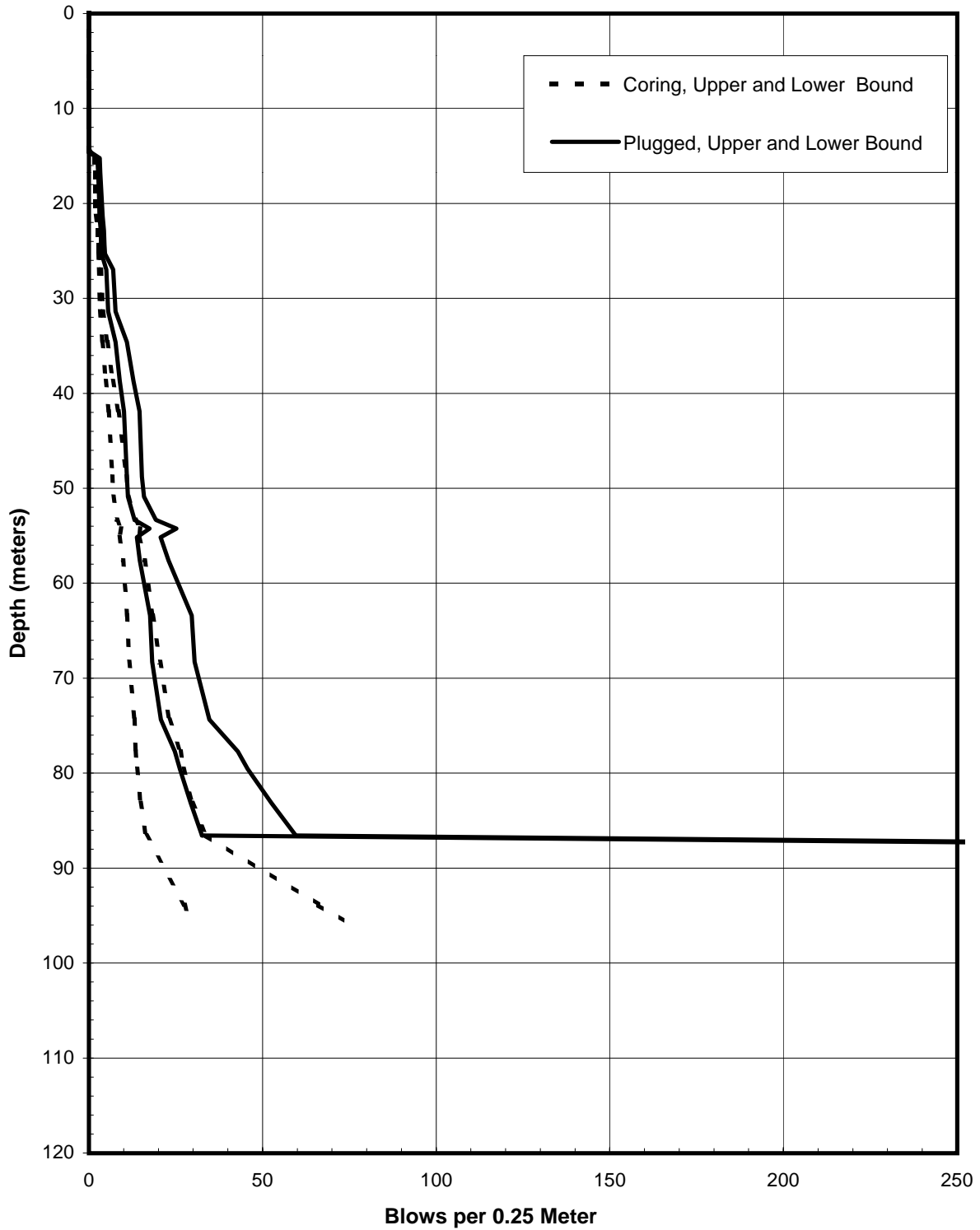
PREDICTED BLOW COUNTS
Pier E7-Eastbound (Boring 98-49)
Menck MHU-500T, 2.5-Meter-Diameter Driven Pipe Piles
SFOBB East Span Seismic Safety Project





PREDICTED BLOW COUNTS
Pier E7-Eastbound (Boring 98-49)
Menck MHU-1000, 2.5-Meter-Diameter Driven Pipe Piles
SFOBB East Span Seismic Safety Project

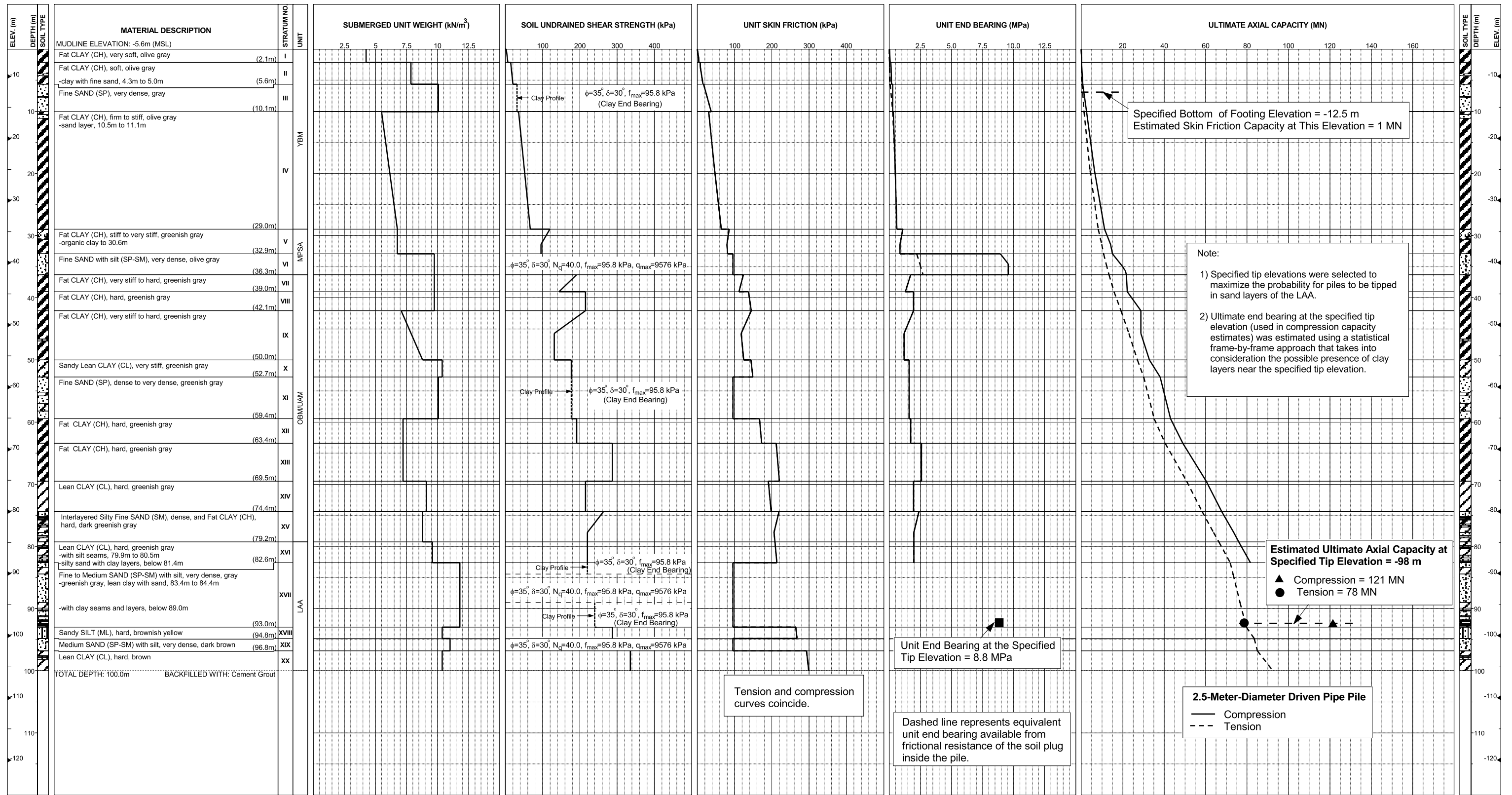




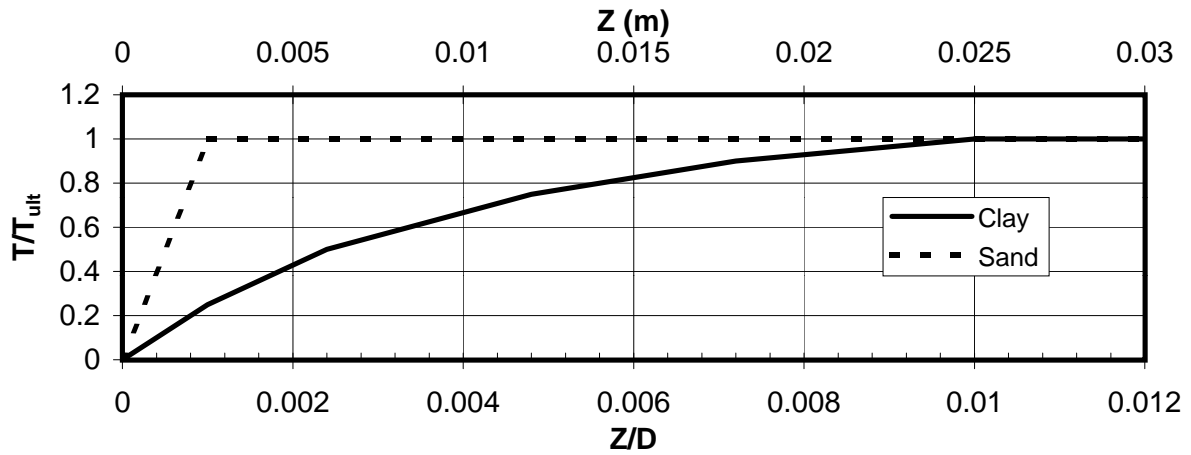
PREDICTED BLOW COUNTS
Pier E7-Eastbound (Boring 98-49)
Menck MHU-1700, 2.5-Meter-Diameter Driven Pipe Piles
SFOBB East Span Seismic Safety Project



**Pier E7-Westbound (Boring 98-30)
Skyway Frame 2**



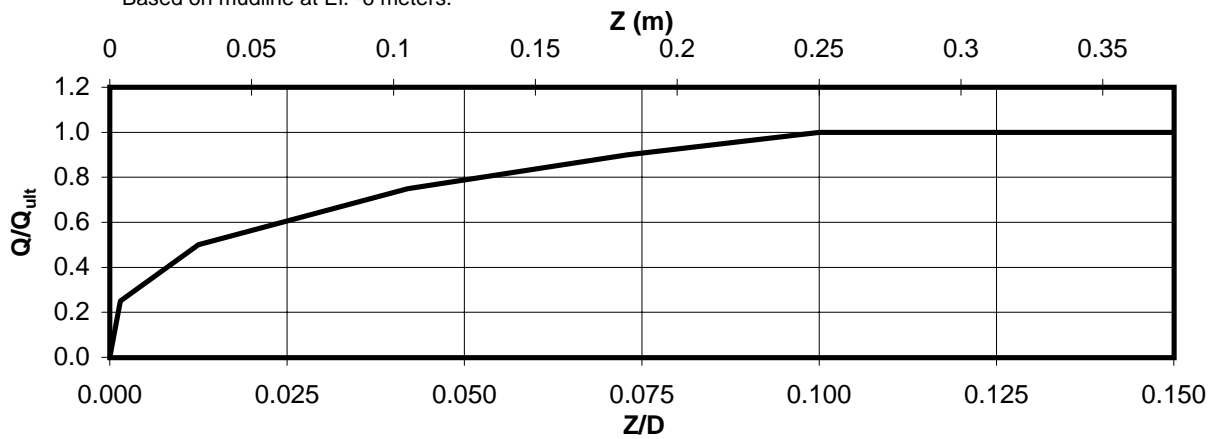
AXIAL PILE DESIGN PARAMETERS AND RESULTS
Pier E7-Westbound (Boring 98-30)
SFOBB East Span Seismic Safety Project



Depth* (m)	Soil Type	T_{ult} (MN/m)
0-3	Clay	0.026
3-6	Clay	0.099
6-9	Sand	0.177
9-12	Sand	0.269
12-15	Clay	0.281
15-18	Clay	0.313
18-21	Clay	0.385
21-24	Clay	0.408
24-27	Clay	0.457
27-30	Clay	0.526
30-33	Clay	0.650
33-36	Sand	0.768

Depth* (m)	Soil Type	T_{ult} (MN/m)
36-39	Clay	0.924
39-42	Clay	1.085
42-45	Clay	1.080
45-51	Clay	0.956
51-57	Sand	0.916
57-63	Sand	1.106
63-69	Clay	1.712
69-75	Clay	1.582
75-81	Clay	1.647
81-83	Clay	1.661
83-88	Sand	0.754

*Based on mudline at El. -6 meters.



Depth* (m)	Soil Type	Q_{ult} (MN)
88	Sand	43.7

AXIAL PILE LOAD TRANSFER-DISPLACEMENT CURVES
Pier E7-Westbound (Boring 98-30)
 2.5-Meter-Diameter Pipe Piles (Pile Tip Elevation = -94 Meters)
 SFOBB East Span Seismic Safety Project



DEPTH (m)	t-z Data											
	t(1)	z(1)	t(2)	z(2)	t(3)	z(3)	t(4)	z(4)	t(5)	z(5)	t(6)	z(6)
0-3	0.0	0.0	0.007	0.003	0.013	0.006	0.020	0.012	0.023	0.018	0.026	0.025
3-6	0.0	0.0	0.025	0.003	0.050	0.006	0.074	0.012	0.089	0.018	0.099	0.025
6-9	0.0	0.0	0.177	0.003								
9-12	0.0	0.0	0.269	0.003								
12-15	0.0	0.0	0.070	0.003	0.141	0.006	0.211	0.012	0.253	0.018	0.281	0.025
15-18	0.0	0.0	0.078	0.003	0.157	0.006	0.235	0.012	0.282	0.018	0.313	0.025
18-21	0.0	0.0	0.096	0.003	0.193	0.006	0.289	0.012	0.347	0.018	0.385	0.025
21-24	0.0	0.0	0.102	0.003	0.204	0.006	0.306	0.012	0.367	0.018	0.408	0.025
24-27	0.0	0.0	0.114	0.003	0.228	0.006	0.342	0.012	0.411	0.018	0.457	0.025
27-30	0.0	0.0	0.132	0.003	0.263	0.006	0.395	0.012	0.473	0.018	0.526	0.025
30-33	0.0	0.0	0.162	0.003	0.325	0.006	0.487	0.012	0.585	0.018	0.650	0.025
33-36	0.0	0.0	0.768	0.003								
36-39	0.0	0.0	0.231	0.003	0.462	0.006	0.693	0.012	0.831	0.018	0.924	0.025
39-42	0.0	0.0	0.271	0.003	0.543	0.006	0.814	0.012	0.977	0.018	1.085	0.025
42-45	0.0	0.0	0.270	0.003	0.540	0.006	0.810	0.012	0.972	0.018	1.080	0.025
45-51	0.0	0.0	2.391	0.003	4.782	0.006	7.173	0.012	8.608	0.018	9.564	0.025
51-57	0.0	0.0	9.158	0.003								
57-63	0.0	0.0	1.106	0.003								
63-69	0.0	0.0	0.428	0.003	0.856	0.006	1.284	0.012	1.541	0.018	1.712	0.025
69-75	0.0	0.0	0.396	0.003	0.791	0.006	1.187	0.012	1.424	0.018	1.582	0.025
75-81	0.0	0.0	0.412	0.003	0.824	0.006	1.235	0.012	1.482	0.018	1.647	0.025
81-83	0.0	0.0	0.415	0.003	0.831	0.006	1.246	0.012	1.495	0.018	1.661	0.025
83-88	0.0	0.0	0.754	0.003								

Notes:

1. "t" is load (MN/m)
2. "z" is displacement (m)
3. Data for tension and compression coincide
4. Based on mudline at El. -6 meters.

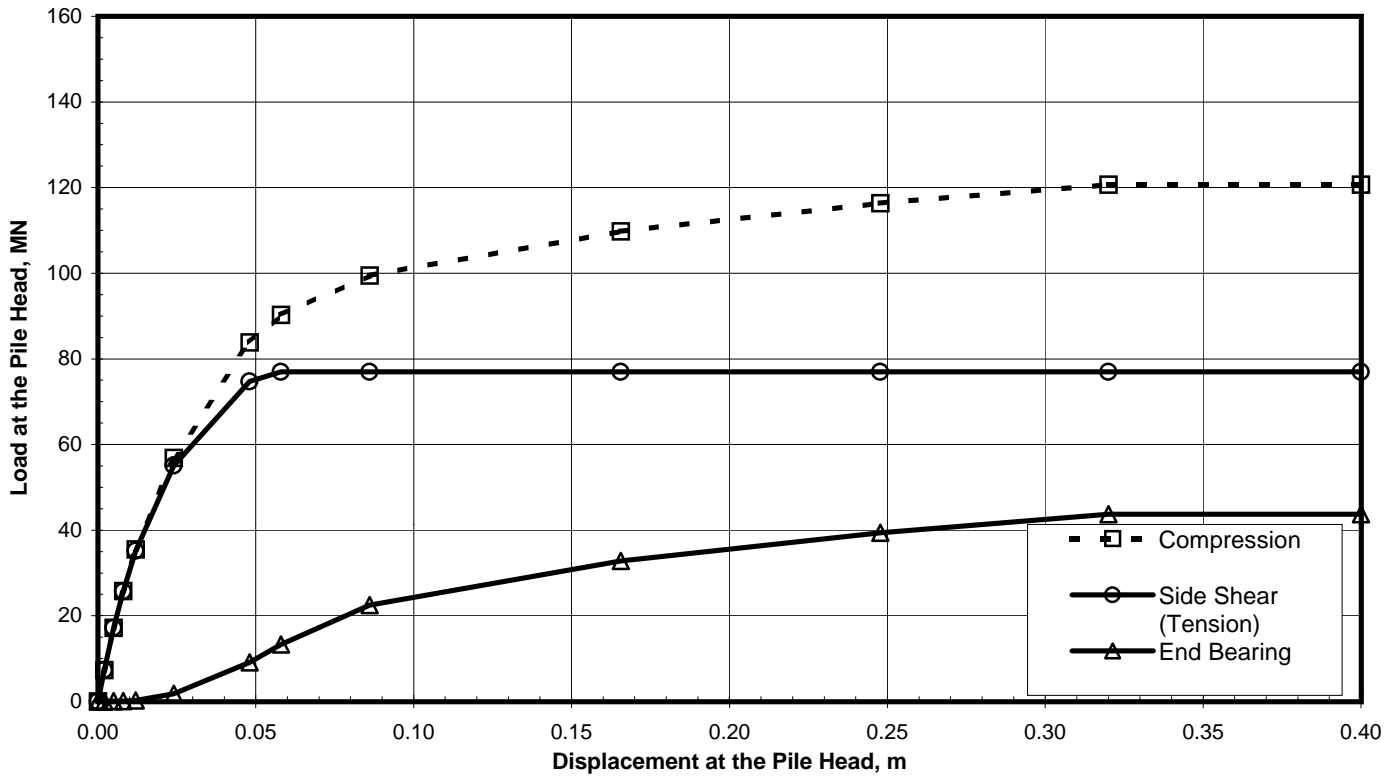
DEPTH (m)	Q-z Data											
	Q(1)	z(1)	Q(2)	z(2)	Q(3)	z(3)	Q(4)	z(4)	Q(5)	z(5)	Q(6)	z(6)
88	0.0	0.0	10.925	0.004	21.850	0.031	32.775	0.105	39.330	0.183	43.700	0.250

Notes:

1. "Q" is load in compression (MN)
2. "z" is displacement (m)

TABULATED AXIAL PILE LOAD TRANSFER DATA
Pier E7-Westbound (Boring 98-30)
 2.5-Meter-Diameter Pipe Piles (Pile Tip Elevation = -94 Meters)
 SFOBB East Span Seismic Safety Project





Pile Head Displacement (m)	Load at the Pile Head		End Bearing Component in Compression (MN)
	Compression (MN)	Tension (MN)	
0.000	0.00	0.00	0.00
0.002	7.30	7.29	0.02
0.005	17.22	17.18	0.04
0.008	25.81	25.73	0.08
0.012	35.47	35.23	0.24
0.024	56.89	55.11	1.78
0.048	83.86	74.71	9.15
0.058	90.24	76.95	13.29
0.086	99.45	76.95	22.50
0.166	109.76	76.95	32.81
0.248	116.33	76.95	39.38
0.320	120.70	76.95	43.75
0.400	120.70	76.95	43.75

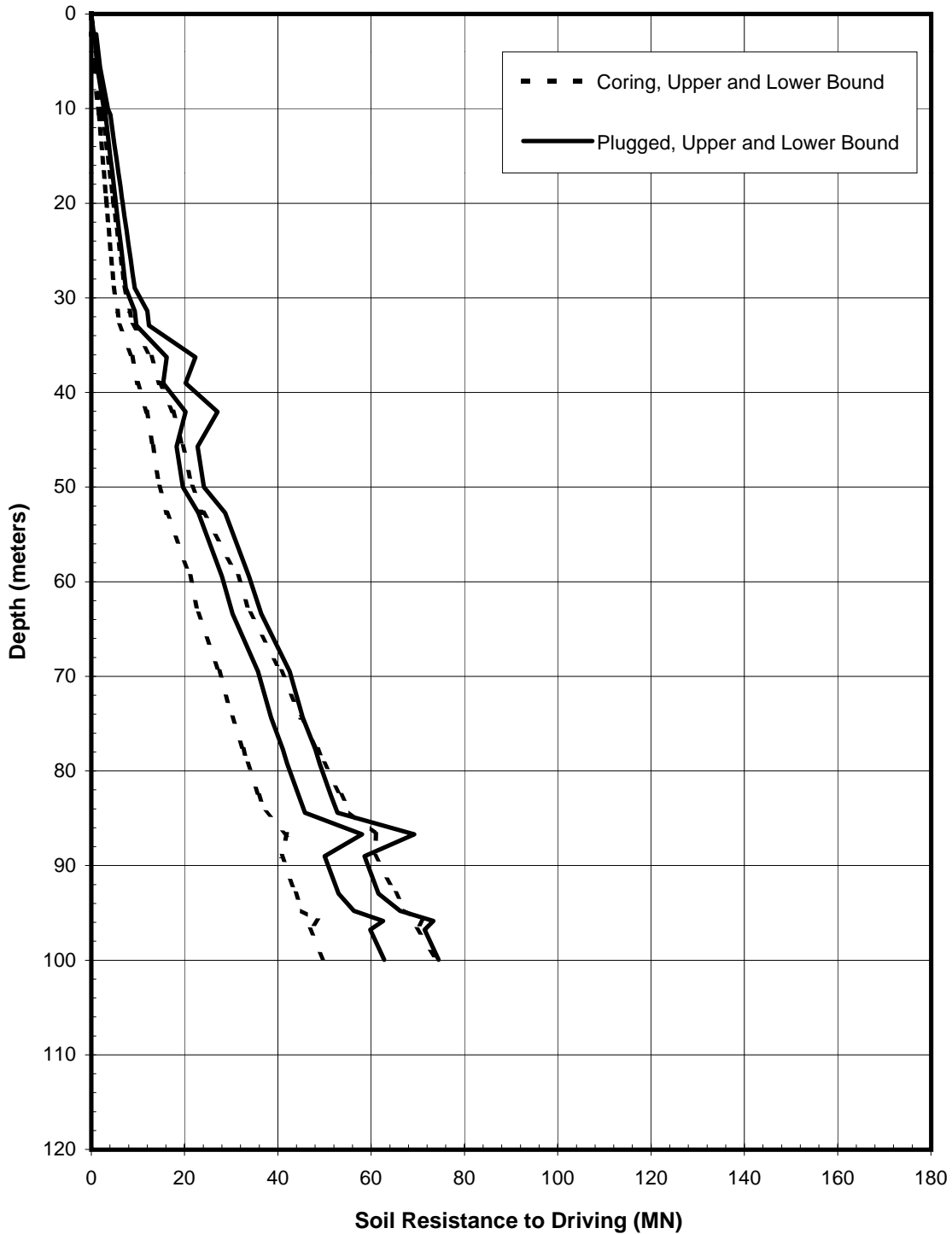
Note:

Pile head load-displacement curves are based on the preliminary pile wall thickness schedule provided by TY Lin/M&N and static loading conditions.

**STATIC PILE HEAD LOAD-DEFORMATION CURVES
 Pier E7-Westbound (Boring 98-30)**

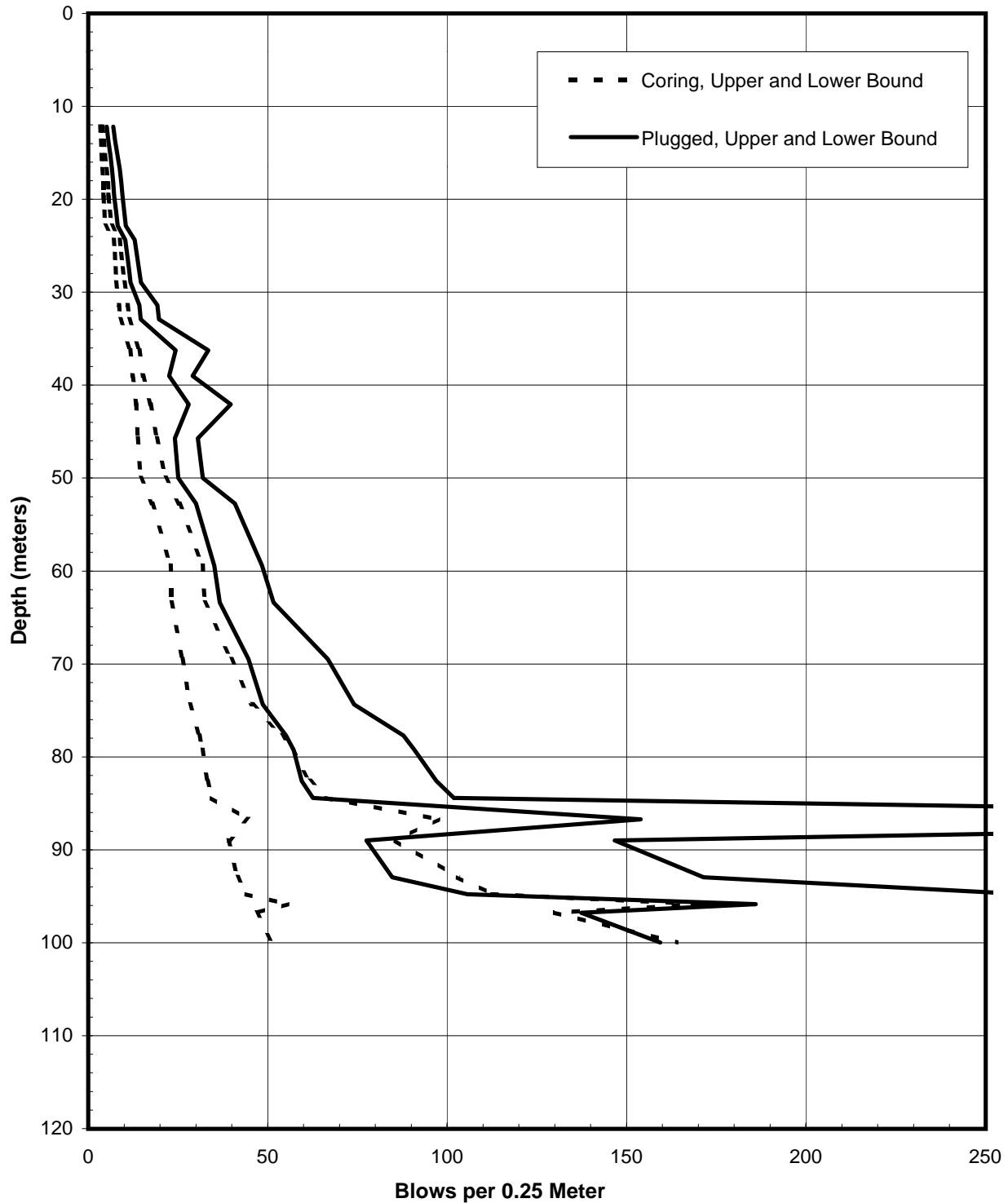
2.5-Meter-Diameter Pipe Piles (Pile Tip Elevation = -94 Meters)
 SFOBB East Span Seismic Safety Project





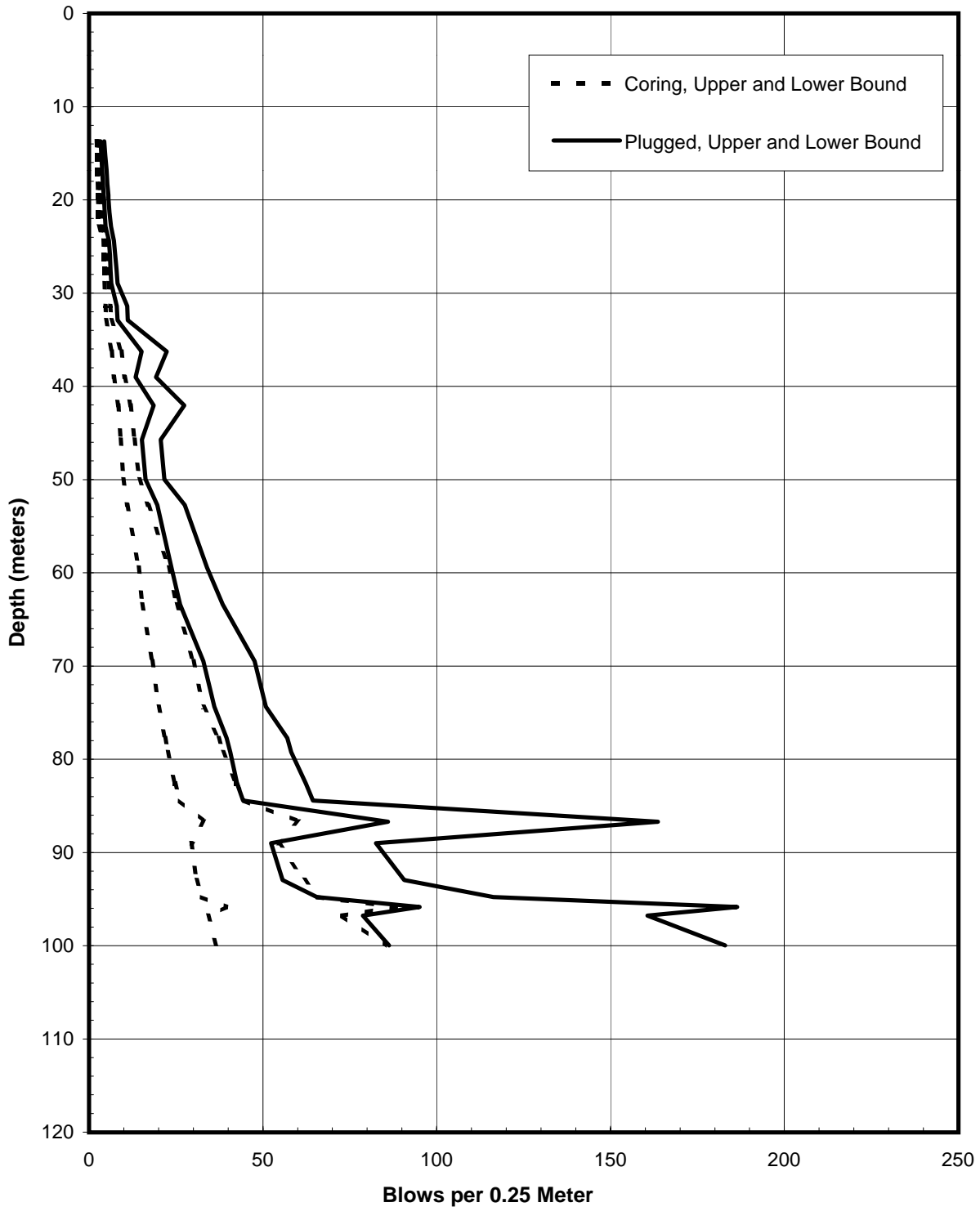
SOIL RESISTANCE TO DRIVING
Pier E7-Westbound (Boring 98-30)
2.5-Meter-Diameter Driven Pipe Piles
SFOBB East Span Seismic Safety Project





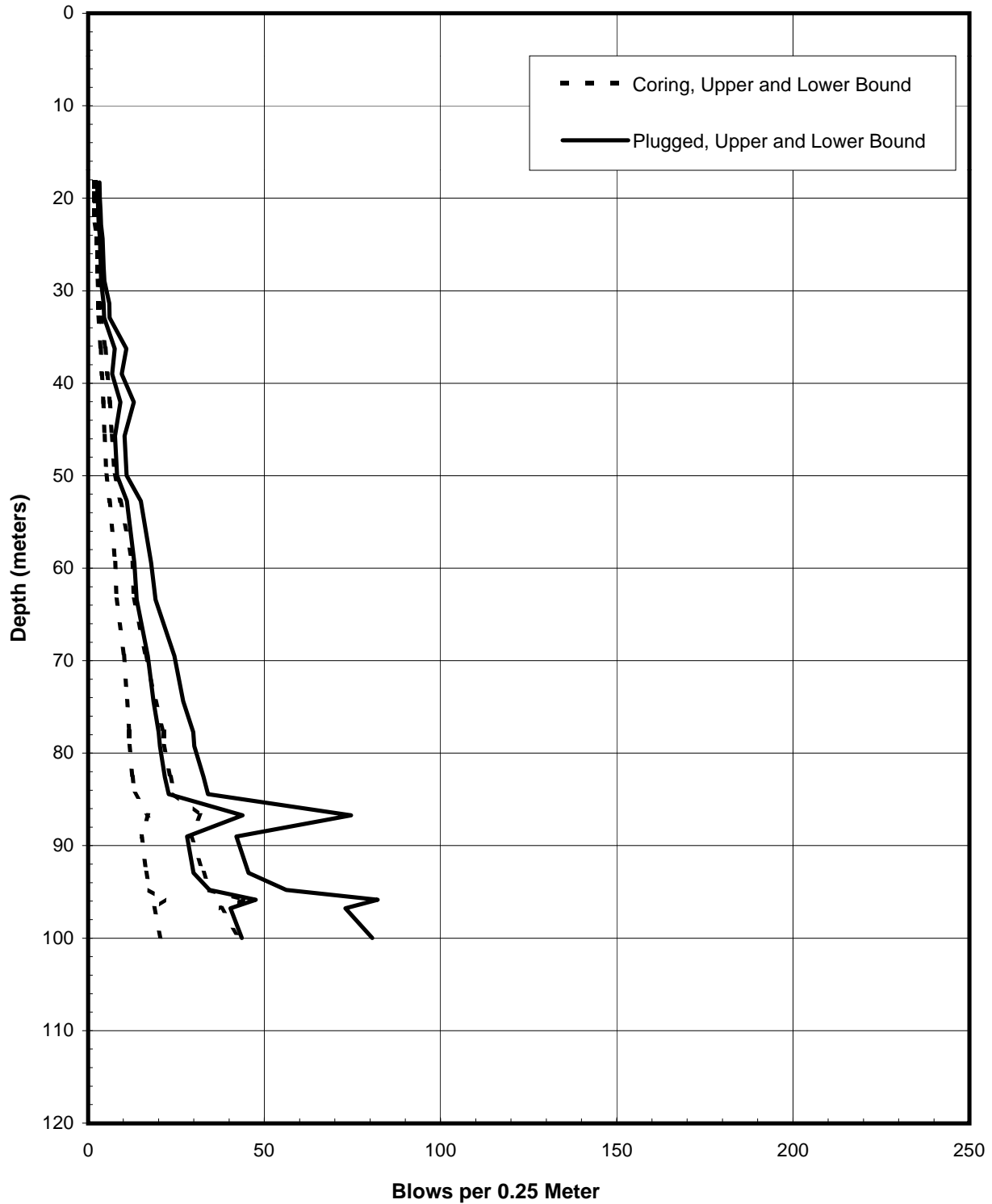
PREDICTED BLOW COUNTS
Pier E7-Westbound (Boring 98-30)
Menck MHU-500T, 2.5-Meter-Diameter Driven Pipe Piles
SFOBB East Span Seismic Safety Project





PREDICTED BLOW COUNTS
Pier E7-Westbound (Boring 98-30)
Menck MHU-1000, 2.5-Meter-Diameter Driven Pipe Piles
SFOBB East Span Seismic Safety Project

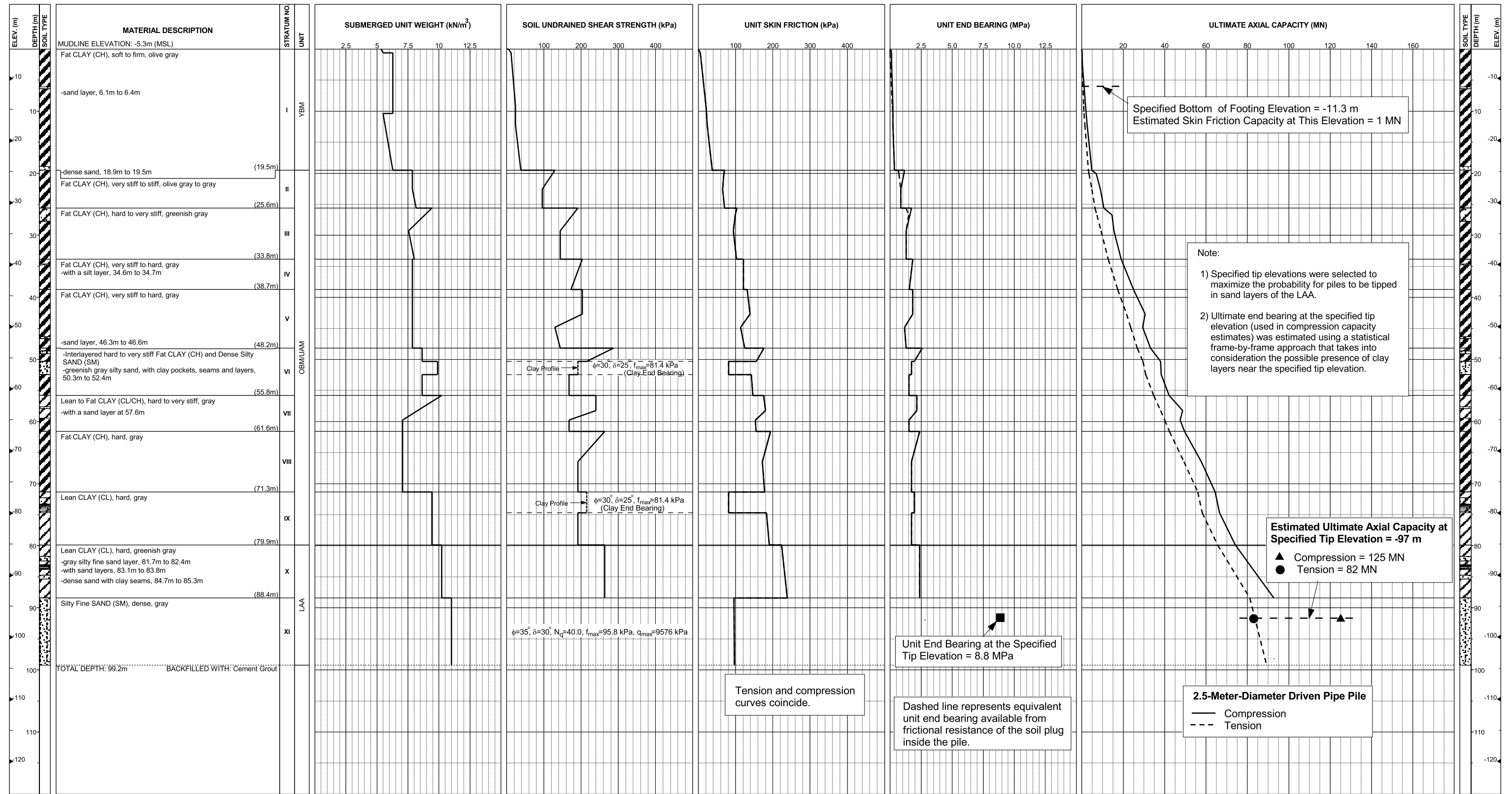




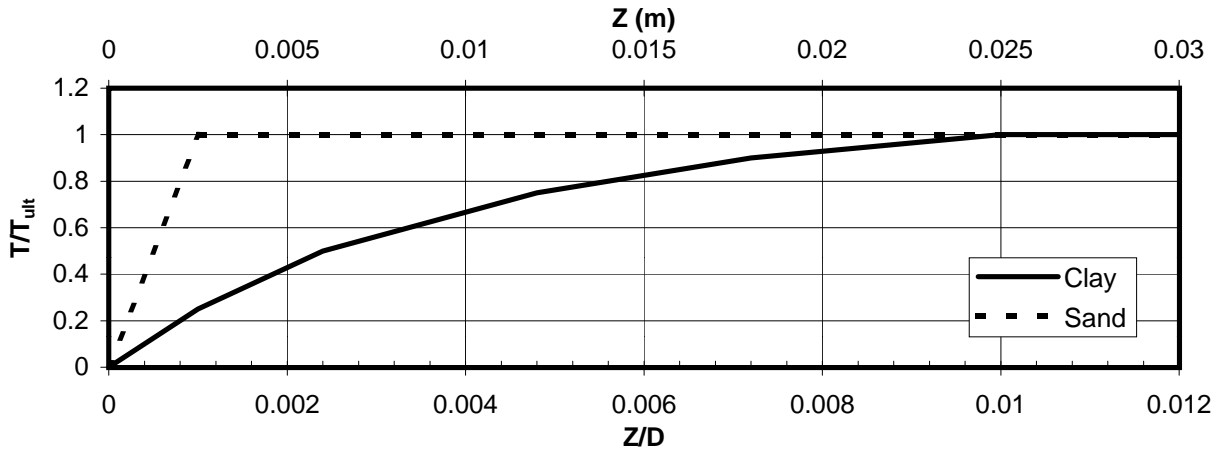
PREDICTED BLOW COUNTS
Pier E7-Westbound (Boring 98-30)
Menck MHU-1700, 2.5-Meter-Diameter Driven Pipe Piles
SFOBB East Span Seismic Safety Project



**Pier E8-Eastbound (Boring 98-31-Modified)
Skyway Frame 2**



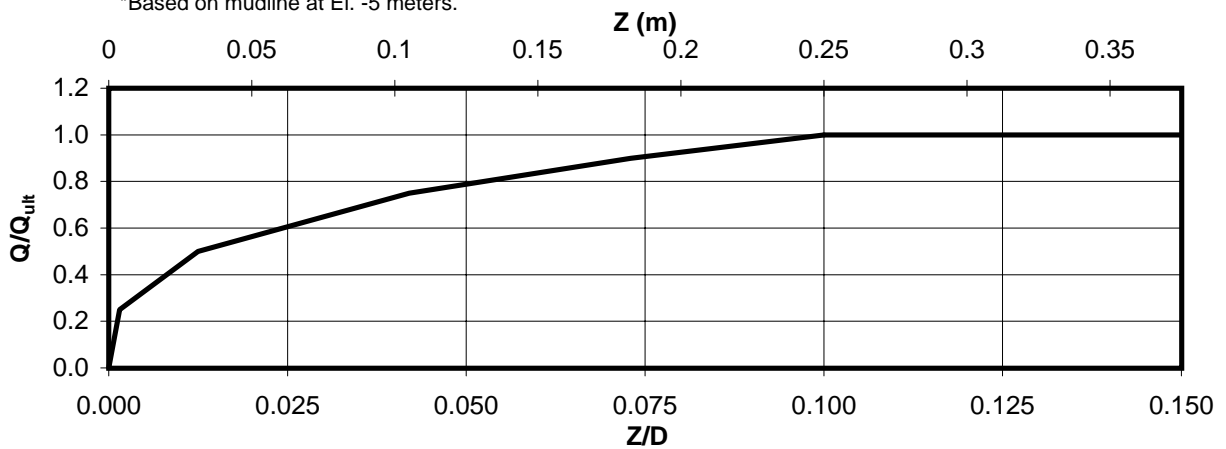
AXIAL PILE DESIGN PARAMETERS AND RESULTS
Pier E8-Eastbound (Boring 98-31 Modified)
SFOBB East Span Seismic Safety Project



Depth (m)	Soil Type	T_{ult} (MN/m)
0-3	Clay	0.025
3-6	Clay	0.094
6-9	Clay	0.132
9-12	Clay	0.167
12-15	Clay	0.219
15-18	Clay	0.251
18-21	Clay	0.340
21-24	Clay	0.557
24-27	Clay	0.590
27-30	Clay	0.805
30-33	Clay	0.750
33-36	Clay	0.888

Depth (m)	Soil Type	T_{ult} (MN/m)
36-39	Clay	0.959
39-42	Clay	1.042
42-45	Clay	1.050
45-51	Clay	1.024
51-57	Clay	1.032
57-63	Clay	1.339
63-69	Clay	1.405
69-75	Sand	0.910
75-81	Clay	1.458
81-88	Clay	1.847
88-92	Sand	0.754

*Based on mudline at El. -5 meters.



Depth (m)	Soil Type	Q_{ult} (MN)
92	Sand	43.7

AXIAL PILE LOAD TRANSFER-DISPLACEMENT CURVES
Pier E8-Eastbound (Boring 98-31 Modified)
 2.5-Meter-Diameter Pipe Piles (Pile Tip Elevation = -97 Meters)
 SFOBB East Span Seismic Safety Project



DEPTH (m)	t-z Data											
	t(1)	z(1)	t(2)	z(2)	t(3)	z(3)	t(4)	z(4)	t(5)	z(5)	t(6)	z(6)
0-3	0.0	0.0	0.006	0.003	0.013	0.006	0.019	0.012	0.023	0.018	0.025	0.025
3-6	0.0	0.0	0.023	0.003	0.047	0.006	0.070	0.012	0.084	0.018	0.094	0.025
6-9	0.0	0.0	0.033	0.003	0.066	0.006	0.099	0.012	0.118	0.018	0.132	0.025
9-12	0.0	0.0	0.042	0.003	0.084	0.006	0.125	0.012	0.150	0.018	0.167	0.025
12-15	0.0	0.0	0.055	0.003	0.109	0.006	0.164	0.012	0.197	0.018	0.219	0.025
15-18	0.0	0.0	0.063	0.003	0.125	0.006	0.188	0.012	0.226	0.018	0.251	0.025
18-21	0.0	0.0	0.085	0.0025	0.170	0.006	0.255	0.012	0.306	0.018	0.340	0.025
21-24	0.0	0.0	0.139	0.003	0.278	0.006	0.418	0.012	0.501	0.018	0.557	0.025
24-27	0.0	0.0	0.147	0.003	0.295	0.006	0.442	0.012	0.531	0.018	0.590	0.025
27-30	0.0	0.0	0.201	0.003	0.403	0.006	0.604	0.012	0.725	0.018	0.805	0.025
30-33	0.0	0.0	0.188	0.003	0.375	0.006	0.563	0.012	0.675	0.018	0.750	0.025
33-36	0.0	0.0	0.222	0.003	0.444	0.006	0.666	0.012	0.799	0.018	0.888	0.025
36-39	0.0	0.0	0.240	0.003	0.479	0.006	0.719	0.012	0.863	0.018	0.959	0.025
39-42	0.0	0.0	0.261	0.003	0.521	0.006	0.782	0.012	0.938	0.018	1.042	0.025
42-45	0.0	0.0	0.263	0.003	0.525	0.006	0.788	0.012	0.945	0.018	1.050	0.025
45-51	0.0	0.0	0.256	0.0025	0.512	0.006	0.768	0.012	0.922	0.018	1.024	0.025
51-57	0.0	0.0	0.258	0.003	0.516	0.006	0.774	0.012	0.929	0.018	1.032	0.025
57-63	0.0	0.0	0.335	0.003	0.670	0.006	1.004	0.012	1.205	0.018	1.339	0.025
63-69	0.0	0.0	0.351	0.003	0.703	0.006	1.054	0.012	1.265	0.018	1.405	0.025
69-75	0.0	0.0	0.910	0.003								
75-81	0.0	0.0	0.365	0.003	0.729	0.006	1.094	0.012	1.312	0.018	1.458	0.025
81-88	0.0	0.0	0.462	0.003	0.924	0.006	1.385	0.012	1.662	0.018	1.847	0.025
88-92	0.0	0.0	0.754	0.003								

Notes:

1. "t" is load (MN/m)
2. "z" is displacement (m)
3. Data for tension and compression coincide
4. Based on mudline at El. -5 meters

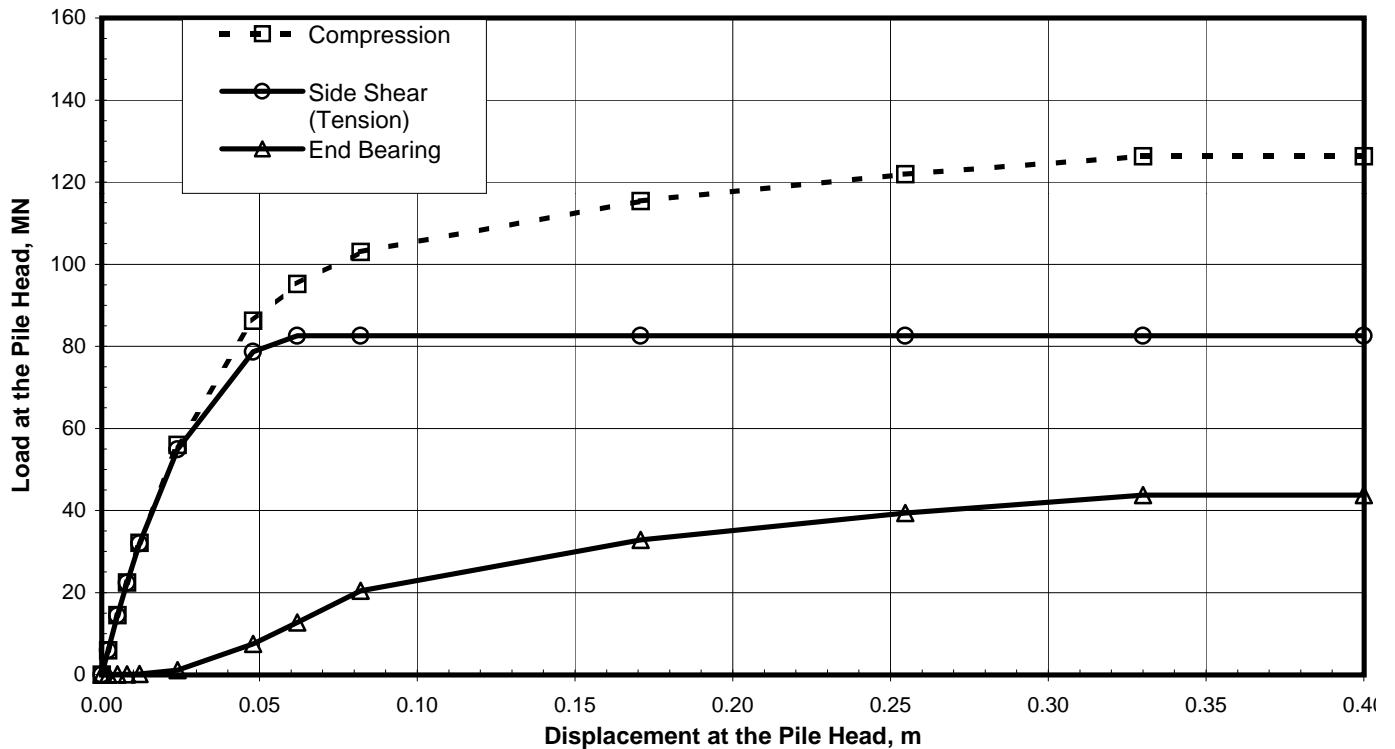
DEPTH (m)	Q-z Data											
	Q(1)	z(1)	Q(2)	z(2)	Q(3)	z(3)	Q(4)	z(4)	Q(5)	z(5)	Q(6)	z(6)
92	0.0	0.0	10.930	0.004	21.860	0.031	32.790	0.105	39.348	0.183	43.720	0.250

Notes:

1. "Q" is load in compression (MN)
2. "z" is displacement (m)

TABULATED AXIAL PILE LOAD TRANSFER DATA
Pier E8-Eastbound (Boring 98-31 Modified)
 2.5-Meter-Diameter Pipe Piles (Pile Tip Elevation = -97 Meters)
 SFOBB East Span Seismic Safety Project





Pile Head Displacement (m)	Load at the Pile Head		End Bearing Component in Compression (MN)
	Compression (MN)	Tension (MN)	
0.000	0.00	0.00	0.00
0.002	5.93	5.91	0.02
0.005	14.52	14.46	0.06
0.008	22.46	22.36	0.10
0.012	32.11	31.94	0.17
0.024	55.98	54.86	1.12
0.048	86.20	78.71	7.49
0.062	95.23	82.55	12.68
0.082	103.00	82.55	20.45
0.171	115.36	82.55	32.81
0.255	121.93	82.55	39.38
0.330	126.30	82.55	43.75
0.400	126.30	82.55	43.75

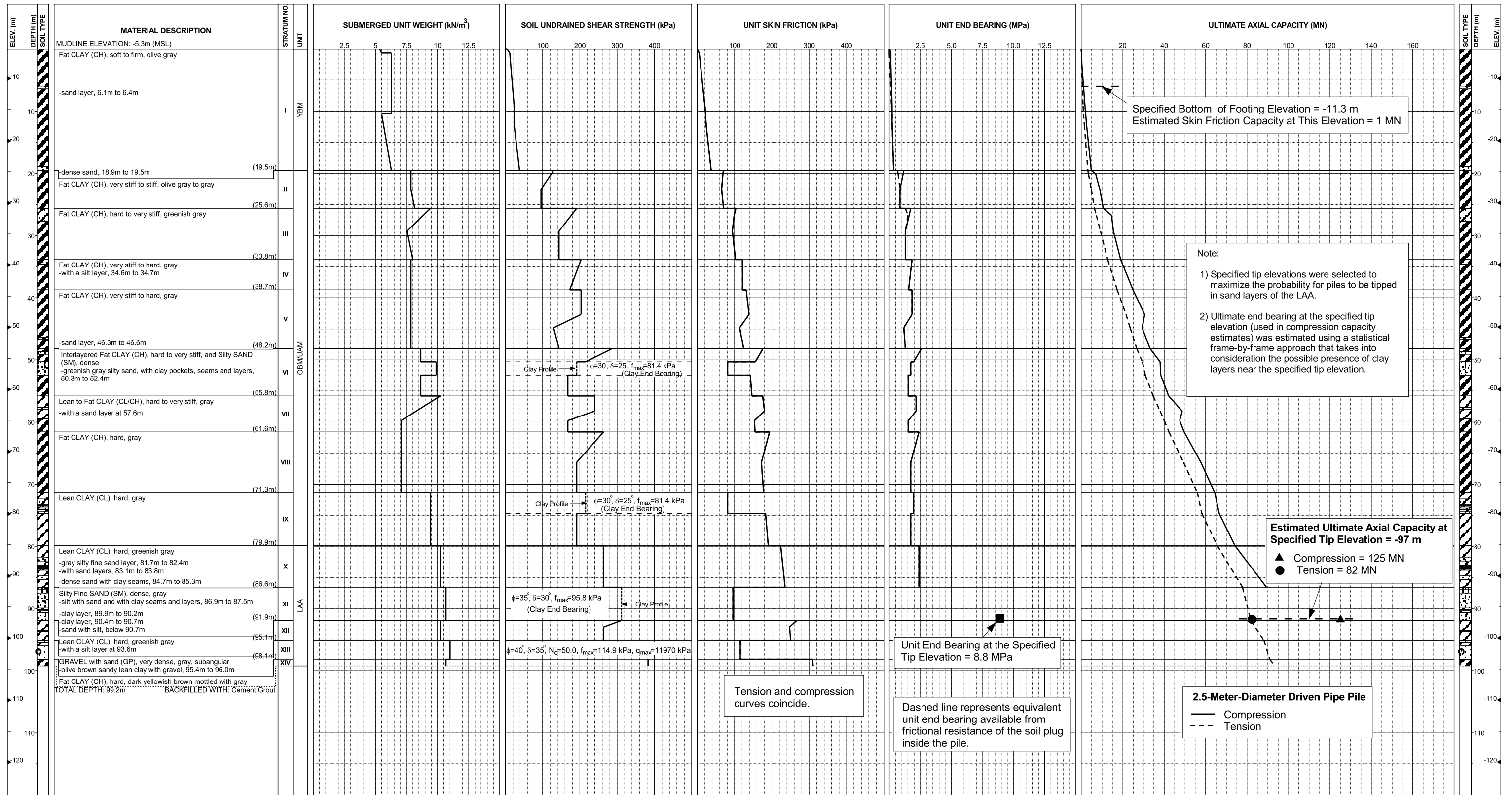
Note:

Pile head load-displacement curves are based on the preliminary pile wall thickness schedule provided by TY Lin/M&N and static loading conditions.

STATIC PILE HEAD LOAD-DEFORMATION CURVES
Pier E8-Eastbound (Boring 98-31 Modified)
 2.5-Meter-Diameter Pipe Piles (Pile Tip Elevation = -97 Meters)
 SFOBB East Span Seismic Safety Project

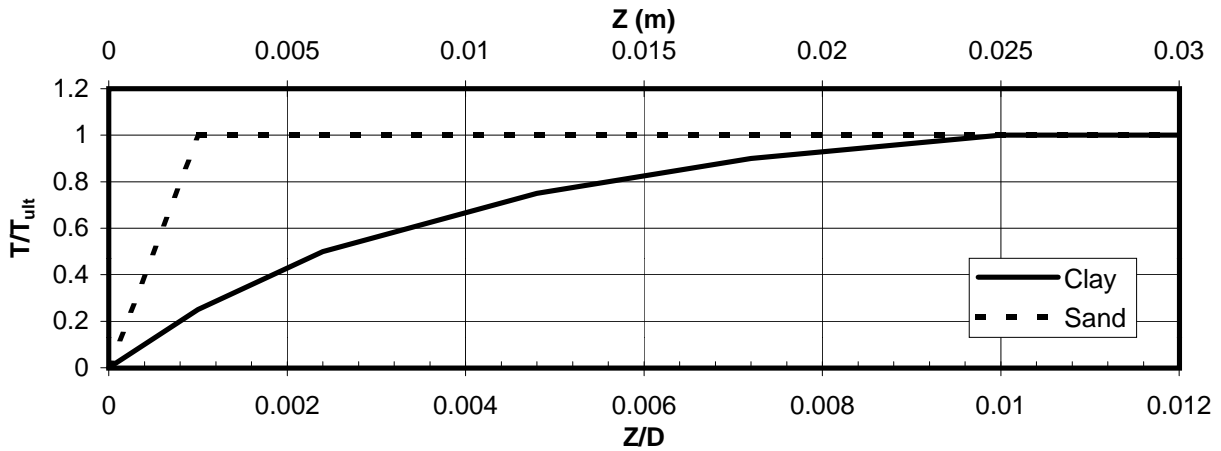


**Pier E8-Westbound (Boring 98-31)
Skyway Frame 2**



AXIAL PILE DESIGN PARAMETERS AND RESULTS
Pier E8-Westbound (Boring 98-31)
SFOBB East Span Seismic Safety Project

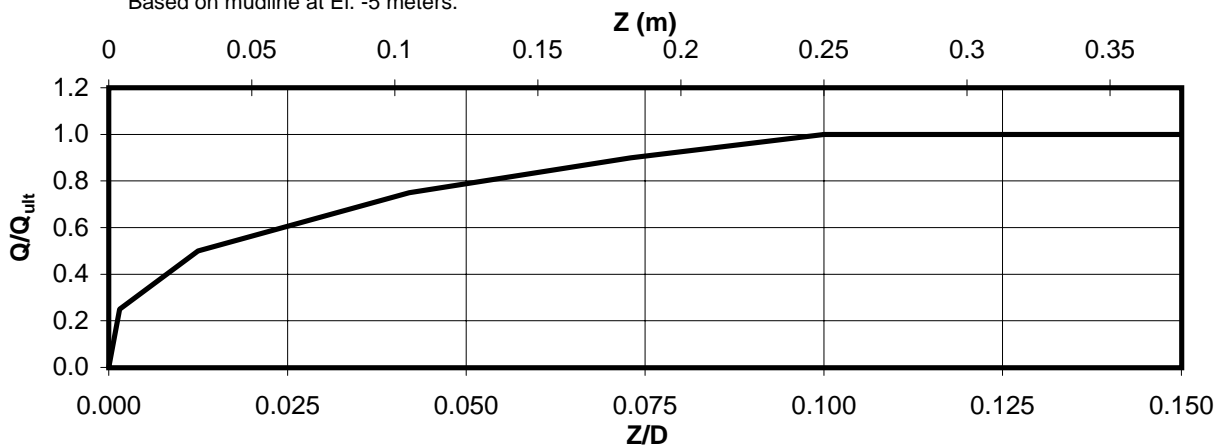




Depth (m)	Soil Type	T_{ult} (MN/m)
0-3	Clay	0.032
3-6	Clay	0.099
6-9	Clay	0.149
9-12	Clay	0.181
12-15	Clay	0.209
15-18	Clay	0.249
18-21	Clay	0.341
21-24	Clay	0.559
24-27	Clay	0.587
27-30	Clay	0.787
30-33	Clay	0.771
33-36	Clay	0.888

Depth (m)	Soil Type	T_{ult} (MN/m)
36-39	Clay	0.959
39-42	Clay	1.042
42-45	Clay	1.050
45-51	Clay	1.025
51-57	Clay	1.031
57-63	Clay	1.341
63-69	Clay	1.404
69-75	Sand	0.905
75-81	Clay	1.466
81-87	Clay	1.833
87-91	Sand	0.754

*Based on mudline at El. -5 meters.



Depth (m)	Soil Type	Q_{ult} (MN)
91	Sand	43.7

AXIAL PILE LOAD TRANSFER-DISPLACEMENT CURVES
Pier E8-Westbound (Boring 98-31)
 2.5-Meter-Diameter Pipe Piles (Pile Tip Elevation = -96 Meters)
 SFOBB East Span Seismic Safety Project



DEPTH (m)	t-z Data											
	t(1)	z(1)	t(2)	z(2)	t(3)	z(3)	t(4)	z(4)	t(5)	z(5)	t(6)	z(6)
0-3	0.0	0.0	0.008	0.003	0.016	0.006	0.024	0.012	0.029	0.018	0.032	0.025
3-6	0.0	0.0	0.025	0.003	0.050	0.006	0.074	0.012	0.089	0.018	0.099	0.025
6-9	0.0	0.0	0.037	0.003	0.075	0.006	0.112	0.012	0.134	0.018	0.149	0.025
9-12	0.0	0.0	0.045	0.003	0.091	0.006	0.136	0.012	0.163	0.018	0.181	0.025
12-15	0.0	0.0	0.052	0.003	0.105	0.006	0.157	0.012	0.188	0.018	0.209	0.025
15-18	0.0	0.0	0.062	0.003	0.125	0.006	0.187	0.012	0.224	0.018	0.249	0.025
18-21	0.0	0.0	0.085	0.0025	0.171	0.006	0.256	0.012	0.307	0.018	0.341	0.025
21-24	0.0	0.0	0.140	0.003	0.280	0.006	0.419	0.012	0.503	0.018	0.559	0.025
24-27	0.0	0.0	0.147	0.003	0.293	0.006	0.440	0.012	0.528	0.018	0.587	0.025
27-30	0.0	0.0	0.197	0.003	0.393	0.006	0.590	0.012	0.708	0.018	0.787	0.025
30-33	0.0	0.0	0.193	0.003	0.386	0.006	0.578	0.012	0.694	0.018	0.771	0.025
33-36	0.0	0.0	0.222	0.003	0.444	0.006	0.666	0.012	0.799	0.018	0.888	0.025
36-39	0.0	0.0	0.240	0.003	0.479	0.006	0.719	0.012	0.863	0.018	0.959	0.025
39-42	0.0	0.0	0.261	0.003	0.521	0.006	0.782	0.012	0.938	0.018	1.042	0.025
42-45	0.0	0.0	0.263	0.003	0.525	0.006	0.788	0.012	0.945	0.018	1.050	0.025
45-51	0.0	0.0	0.256	0.0025	0.513	0.006	0.769	0.012	0.923	0.018	1.025	0.025
51-57	0.0	0.0	0.258	0.003	0.516	0.006	0.773	0.012	0.928	0.018	1.031	0.025
57-63	0.0	0.0	0.335	0.003	0.671	0.006	1.006	0.012	1.207	0.018	1.341	0.025
63-69	0.0	0.0	0.351	0.003	0.702	0.006	1.053	0.012	1.264	0.018	1.404	0.025
69-75	0.0	0.0	0.905	0.003								
75-81	0.0	0.0	0.367	0.003	0.733	0.006	1.100	0.012	1.319	0.018	1.466	0.025
81-87	0.0	0.0	0.458	0.003	0.917	0.006	1.375	0.012	1.650	0.018	1.833	0.025
87-91	0.0	0.0	0.754	0.003								

Notes:

- "t" is load (MN/m)
- "z" is displacement (m)
- Data for tension and compression coincide
- Based on mudline at El. -5 meters.

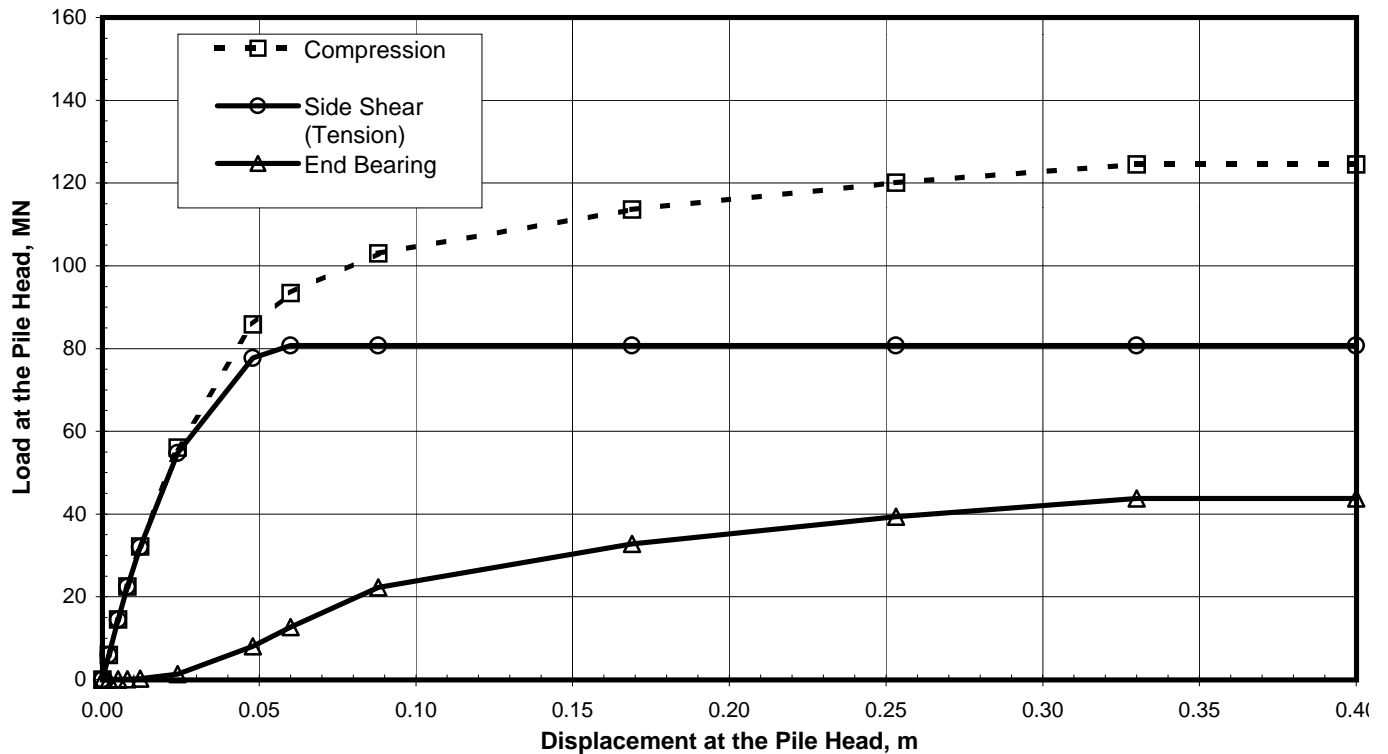
DEPTH (m)	Q-z Data											
	Q(1)	z(1)	Q(2)	z(2)	Q(3)	z(3)	Q(4)	z(4)	Q(5)	z(5)	Q(6)	z(6)
91	0.0	0.0	10.930	0.004	21.860	0.031	32.790	0.105	39.348	0.183	43.720	0.250

Notes:

- "Q" is load in compression (MN)
- "z" is displacement (m)

TABULATED AXIAL PILE LOAD TRANSFER DATA
Pier E8-Westbound (Boring 98-31)
 2.5-Meter-Diameter Pipe Piles (Pile Tip Elevation = -96 Meters)
 SFOBB East Span Seismic Safety Project





Pile Head Displacement (m)	Load at the Pile Head		End Bearing Component in Compression (MN)
	Compression (MN)	Tension (MN)	
0.000	0.00	0.00	0.00
0.002	5.95	5.93	0.02
0.005	14.56	14.49	0.06
0.008	22.51	22.40	0.11
0.012	32.18	31.98	0.20
0.024	56.07	54.75	1.32
0.048	85.81	77.74	8.07
0.060	93.42	80.75	12.67
0.088	103.00	80.75	22.25
0.169	113.56	80.75	32.81
0.253	120.13	80.75	39.38
0.330	124.50	80.75	43.75
0.400	124.50	80.75	43.75

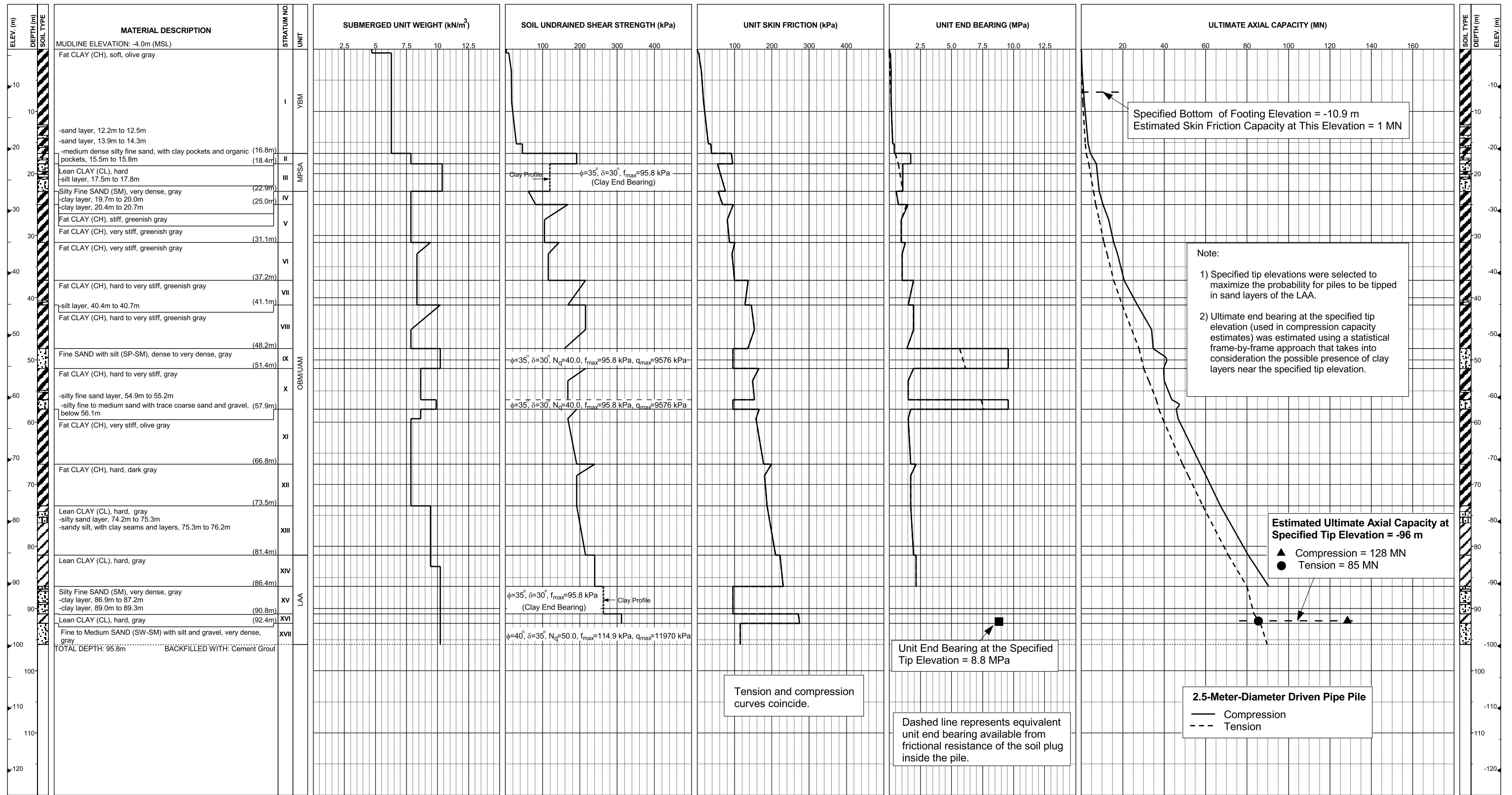
Note:

Pile head load-displacement curves are based on the preliminary pile wall thickness schedule provided by TY Lin/M&N and static loading conditions.

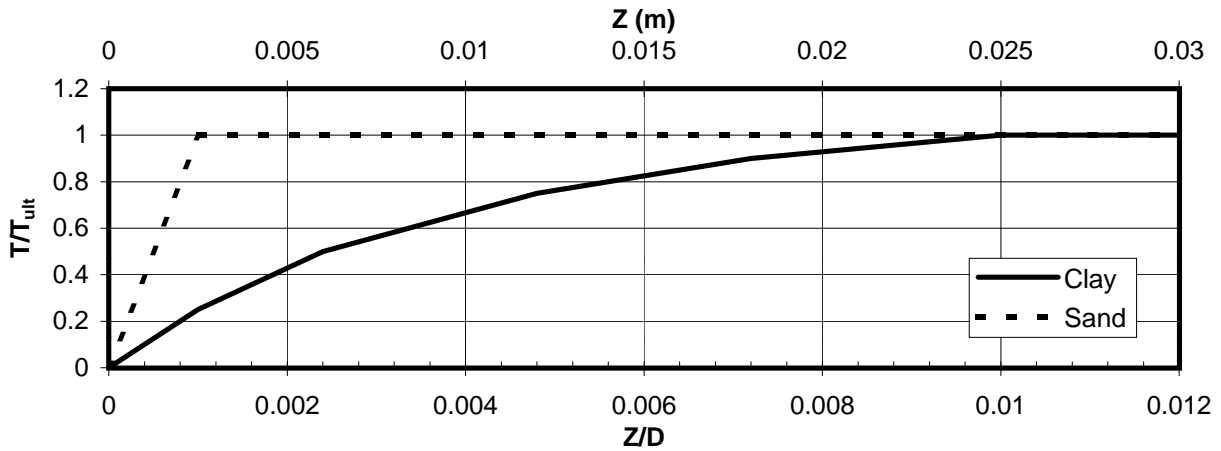
STATIC PILE HEAD LOAD-DEFORMATION CURVES
Pier E8-Westbound (Boring 98-31)
 2.5-Meter-Diameter Pipe Piles (Pile Tip Elevation = -96 Meters)
 SFOBB East Span Seismic Safety Project



**Pier E9-Eastbound and Westbound (Boring 98-32)
Skyway Frame 2**



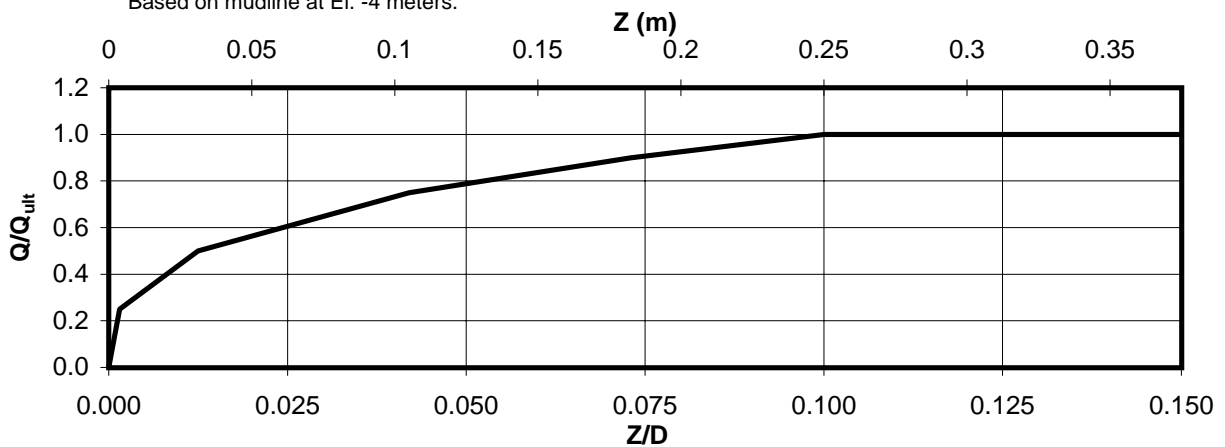
AXIAL PILE DESIGN PARAMETERS AND RESULTS
Piers E9-Eastbound and Westbound (Boring 98-32)
SFOBB East Span Seismic Safety Project



Depth (m)	Soil Type	T_{ult} (MN/m)
0-3	Clay	0.046
3-6	Clay	0.094
6-9	Clay	0.133
9-12	Clay	0.177
12-15	Clay	0.212
15-18	Clay	0.386
18-21	Sand	0.536
21-24	Clay	0.528
24-27	Clay	0.625
27-30	Clay	0.646
30-33	Clay	0.741
33-36	Clay	0.744

Depth (m)	Soil Type	T_{ult} (MN/m)
36-39	Clay	0.946
39-42	Clay	1.058
42-45	Clay	1.193
45-51	Sand	0.961
51-57	Clay	1.141
57-63	Clay	1.140
63-69	Clay	1.415
69-75	Clay	1.441
75-81	Clay	1.570
81-86	Clay	1.783
86-90	Sand	0.759

*Based on mudline at El. -4 meters.



Depth (m)	Soil Type	Q_{ult} (MN)
90	Sand	43.7

AXIAL PILE LOAD TRANSFER-DISPLACEMENT CURVES
Piers E9-Eastbound and Westbound (Boring 98-32)
 2.5-Meter-Diameter Pipe Piles (Pile Tip Elevation = -94 Meters)
 SFOBB East Span Seismic Safety Project



DEPTH (m)	t-z Data											
	t(1)	z(1)	t(2)	z(2)	t(3)	z(3)	t(4)	z(4)	t(5)	z(5)	t(6)	z(6)
0-3	0.0	0.0	0.012	0.003	0.023	0.006	0.035	0.012	0.042	0.018	0.046	0.025
3-6	0.0	0.0	0.024	0.003	0.047	0.006	0.071	0.012	0.085	0.018	0.094	0.025
6-9	0.0	0.0	0.033	0.003	0.067	0.006	0.100	0.012	0.120	0.018	0.133	0.025
9-12	0.0	0.0	0.044	0.003	0.089	0.006	0.133	0.012	0.160	0.018	0.177	0.025
12-15	0.0	0.0	0.053	0.003	0.106	0.006	0.159	0.012	0.191	0.018	0.212	0.025
15-18	0.0	0.0	0.096	0.003	0.193	0.006	0.289	0.012	0.347	0.018	0.386	0.025
18-21	0.0	0.0	0.536	0.0025								
21-24	0.0	0.0	0.132	0.003	0.264	0.006	0.396	0.012	0.475	0.018	0.528	0.025
24-27	0.0	0.0	0.156	0.003	0.313	0.006	0.469	0.012	0.563	0.018	0.625	0.025
27-30	0.0	0.0	0.162	0.003	0.323	0.006	0.485	0.012	0.581	0.018	0.646	0.025
30-33	0.0	0.0	0.185	0.003	0.370	0.006	0.555	0.012	0.667	0.018	0.741	0.025
33-36	0.0	0.0	0.186	0.003	0.372	0.006	0.558	0.012	0.670	0.018	0.744	0.025
36-39	0.0	0.0	0.237	0.003	0.473	0.006	0.710	0.012	0.851	0.018	0.946	0.025
39-42	0.0	0.0	0.265	0.003	0.529	0.006	0.794	0.012	0.952	0.018	1.058	0.025
42-45	0.0	0.0	0.298	0.003	0.597	0.006	0.895	0.012	1.074	0.018	1.193	0.025
45-51	0.0	0.0	0.961	0.0025								
51-57	0.0	0.0	0.285	0.003	0.571	0.006	0.856	0.012	1.027	0.018	1.141	0.025
57-63	0.0	0.0	0.285	0.003	0.570	0.006	0.855	0.012	1.026	0.018	1.140	0.025
63-69	0.0	0.0	0.354	0.003	0.708	0.006	1.061	0.012	1.274	0.018	1.415	0.025
69-75	0.0	0.0	0.360	0.003	0.721	0.006	1.081	0.012	1.297	0.018	1.441	0.025
75-81	0.0	0.0	0.393	0.003	0.785	0.006	1.178	0.012	1.413	0.018	1.570	0.025
81-86	0.0	0.0	0.446	0.003	0.892	0.006	1.337	0.012	1.605	0.018	1.783	0.025
86-90	0.0	0.0	0.759	0.003								

Notes:

1. "t" is load (MN/m)
2. "z" is displacement (m)
3. Data for tension and compression coincide
4. Based on mudline at El. -4 meters

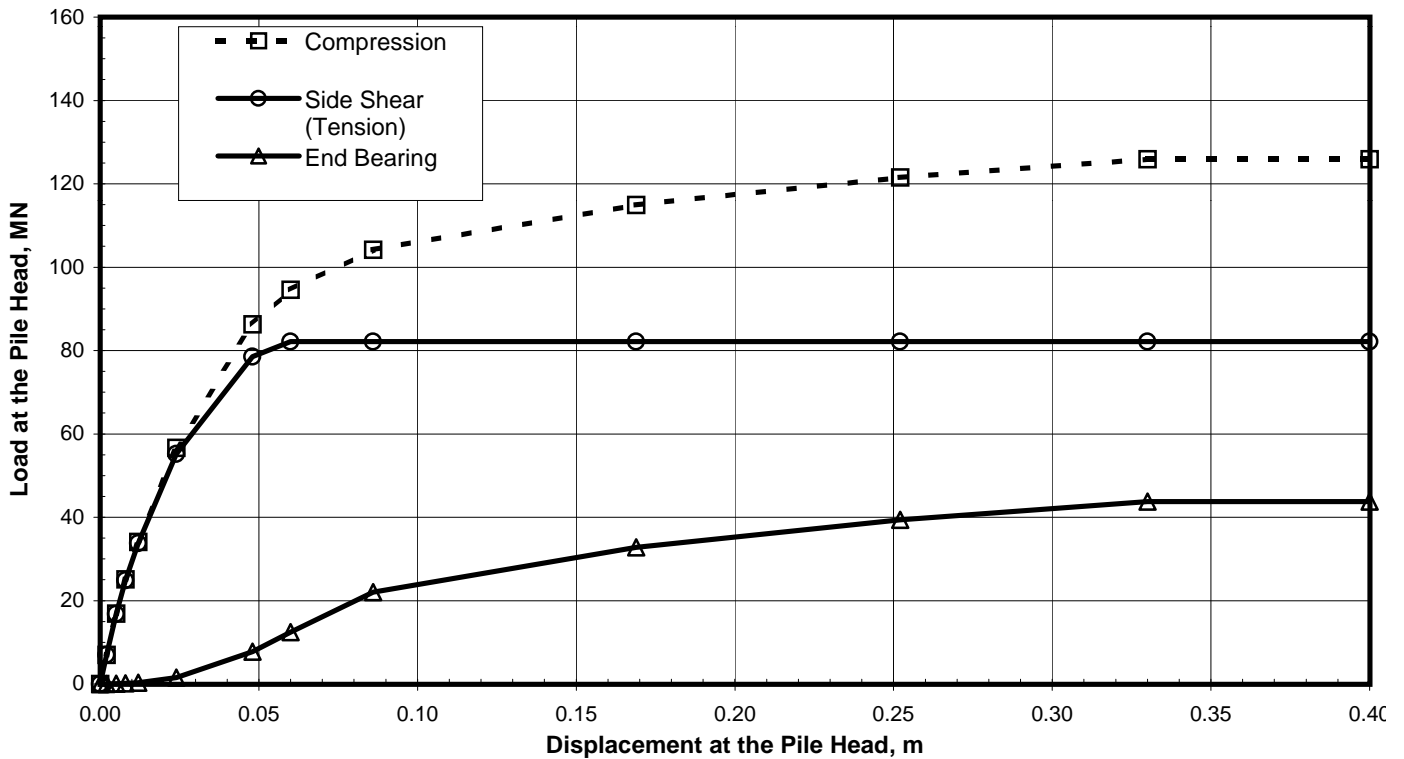
DEPTH (m)	Q-z Data											
	Q(1)	z(1)	Q(2)	z(2)	Q(3)	z(3)	Q(4)	z(4)	Q(5)	z(5)	Q(6)	z(6)
90	0.0	0.0	10.930	0.004	21.860	0.031	32.790	0.105	39.348	0.183	43.720	0.250

Notes:

1. "Q" is load in compression (MN)
2. "z" is displacement (m)

TABULATED AXIAL PILE LOAD TRANSFER DATA
Piers E9-Eastbound and Westbound (Boring 98-32)
 2.5-Meter-Diameter Pipe Piles (Pile Tip Elevation = -94 Meters)
 SFOBB East Span Seismic Safety Project





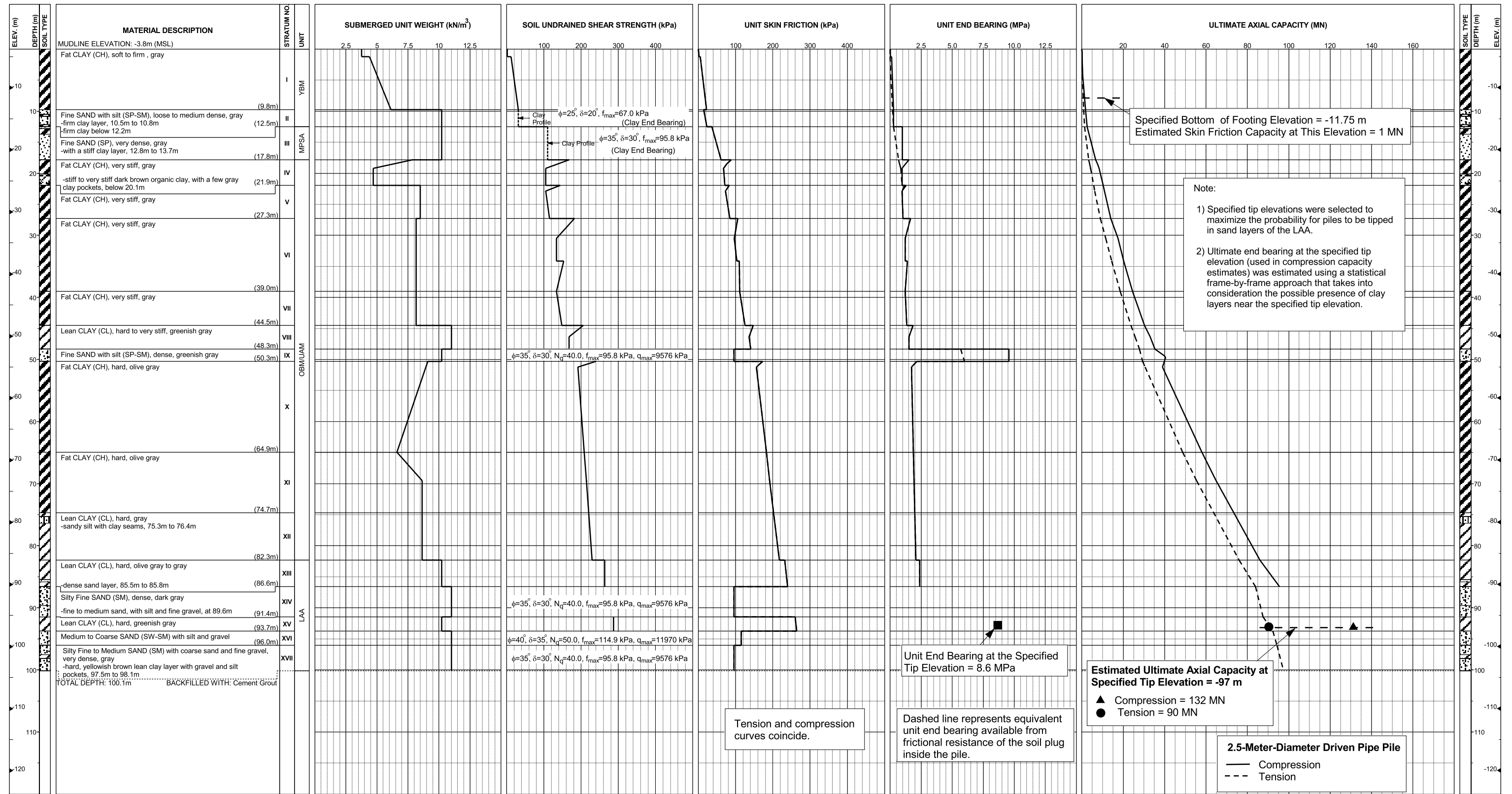
Pile Head Displacement (m)	Load at the Pile Head		End Bearing Component in Compression (MN)
	Compression (MN)	Tension (MN)	
0.000	0.00	0.00	0.00
0.002	7.00	6.98	0.02
0.005	16.88	16.82	0.07
0.008	25.07	24.91	0.16
0.012	34.08	33.76	0.32
0.024	56.68	55.17	1.51
0.048	86.28	78.52	7.76
0.060	94.56	82.16	12.40
0.086	104.20	82.16	22.04
0.169	114.97	82.16	32.81
0.252	121.53	82.16	39.37
0.330	125.90	82.16	43.74
0.400	125.90	82.16	43.74

Note:
 Pile head load-displacement curves are based on the preliminary pile wall thickness schedule provided by TY Lin/M&N and static loading conditions.

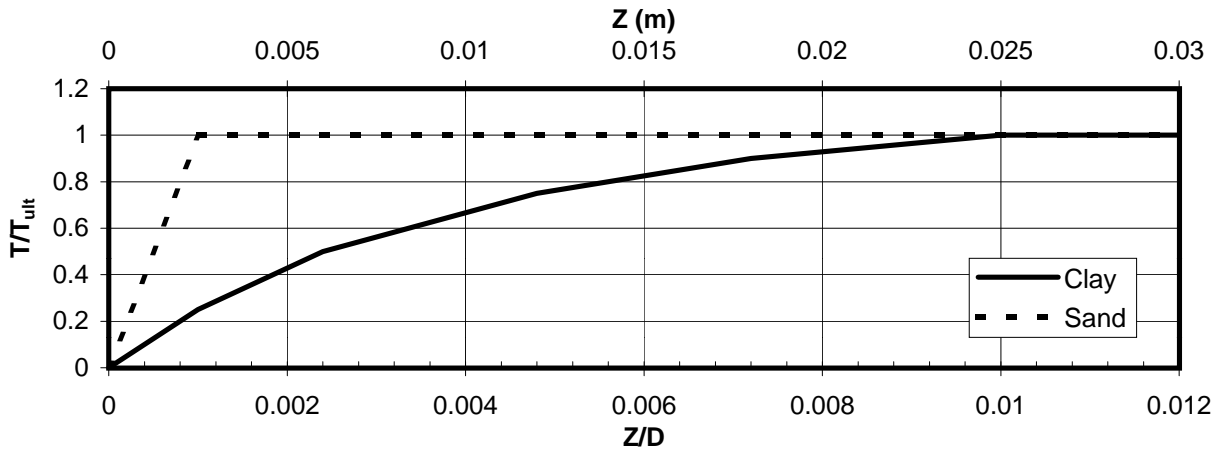
STATIC PILE HEAD LOAD-DEFORMATION CURVES
Piers E9-Eastbound and Westbound (Boring 98-32)
 2.5-Meter-Diameter Pipe Piles (Pile Tip Elevation = -94 Meters)
 SFOBB East Span Seismic Safety Project



**Pier E10-Eastbound (Boring 98-33)
Skyway Frame 2**



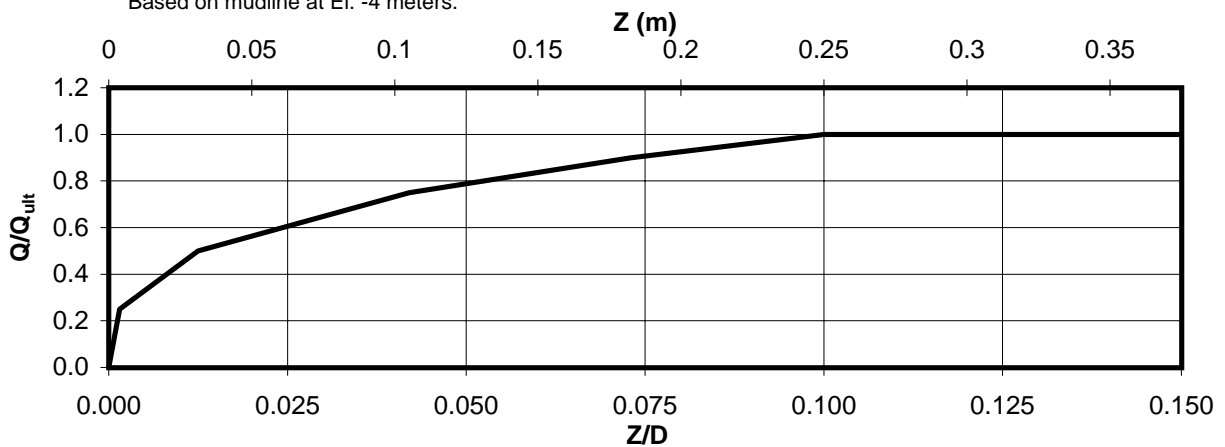
AXIAL PILE DESIGN PARAMETERS AND RESULTS
Pier E10-Eastbound (Boring 98-33)
SFOBB East Span Seismic Safety Project



Depth (m)	Soil Type	T_{ult} (MN/m)
0-3	Clay	0.017
3-6	Clay	0.079
6-9	Clay	0.133
9-12	Sand	0.147
12-15	Sand	0.252
15-18	Sand	0.434
18-21	Clay	0.580
21-24	Clay	0.563
24-27	Clay	0.613
27-30	Clay	0.823
30-33	Clay	0.763
33-36	Clay	0.845

Depth (m)	Soil Type	T_{ult} (MN/m)
36-39	Clay	0.875
39-42	Clay	0.890
42-45	Clay	0.958
45-51	Clay	0.998
51-57	Clay	1.290
57-63	Clay	1.360
63-69	Clay	1.459
69-75	Clay	1.549
75-81	Clay	1.641
81-87	Clay	1.816
87-91	Sand	0.763

*Based on mudline at El. -4 meters.



Depth (m)	Soil Type	Q_{ult} (MN)
91	Sand	43.7

AXIAL PILE LOAD TRANSFER-DISPLACEMENT CURVES
Pier E10-Eastbound (Boring 98-33)
 2.5-Meter-Diameter Pipe Piles (Pile Tip Elevation = -95 Meters)
 SFOBB East Span Seismic Safety Project



DEPTH (m)	t-z Data											
	t(1)	z(1)	t(2)	z(2)	t(3)	z(3)	t(4)	z(4)	t(5)	z(5)	t(6)	z(6)
0-3	0.0	0.0	0.004	0.003	0.009	0.006	0.013	0.012	0.015	0.018	0.017	0.025
3-6	0.0	0.0	0.020	0.003	0.040	0.006	0.059	0.012	0.071	0.018	0.079	0.025
6-9	0.0	0.0	0.033	0.003	0.066	0.006	0.100	0.012	0.119	0.018	0.133	0.025
9-12	0.0	0.0	0.147	0.003								
12-15	0.0	0.0	0.252	0.003								
15-18	0.0	0.0	0.434	0.003								
18-21	0.0	0.0	0.145	0.0025	0.290	0.006	0.435	0.012	0.522	0.018	0.580	0.025
21-24	0.0	0.0	0.141	0.003	0.282	0.006	0.422	0.012	0.507	0.018	0.563	0.025
24-27	0.0	0.0	0.153	0.003	0.307	0.006	0.460	0.012	0.552	0.018	0.613	0.025
27-30	0.0	0.0	0.206	0.003	0.411	0.006	0.617	0.012	0.740	0.018	0.823	0.025
30-33	0.0	0.0	0.191	0.003	0.381	0.006	0.572	0.012	0.687	0.018	0.763	0.025
33-36	0.0	0.0	0.211	0.003	0.423	0.006	0.634	0.012	0.761	0.018	0.845	0.025
36-39	0.0	0.0	0.219	0.003	0.438	0.006	0.656	0.012	0.788	0.018	0.875	0.025
39-42	0.0	0.0	0.223	0.003	0.445	0.006	0.668	0.012	0.801	0.018	0.890	0.025
42-45	0.0	0.0	0.240	0.003	0.479	0.006	0.719	0.012	0.863	0.018	0.958	0.025
45-51	0.0	0.0	0.249	0.0025	0.499	0.006	0.748	0.012	0.898	0.018	0.998	0.025
51-57	0.0	0.0	0.323	0.003	0.645	0.006	0.968	0.012	1.161	0.018	1.290	0.025
57-63	0.0	0.0	0.340	0.003	0.680	0.006	1.020	0.012	1.224	0.018	1.360	0.025
63-69	0.0	0.0	0.365	0.003	0.730	0.006	1.094	0.012	1.313	0.018	1.459	0.025
69-75	0.0	0.0	0.387	0.003	0.775	0.006	1.162	0.012	1.394	0.018	1.549	0.025
75-81	0.0	0.0	0.410	0.003	0.821	0.006	1.231	0.012	1.477	0.018	1.641	0.025
81-87	0.0	0.0	0.454	0.003	0.908	0.006	1.362	0.012	1.634	0.018	1.816	0.025
87-91	0.0	0.0	0.763	0.003								

Notes:

1. "t" is load (MN/m)
2. "z" is displacement (m)
3. Data for tension and compression coincide
4. Based on mudline at El. - 4 meters

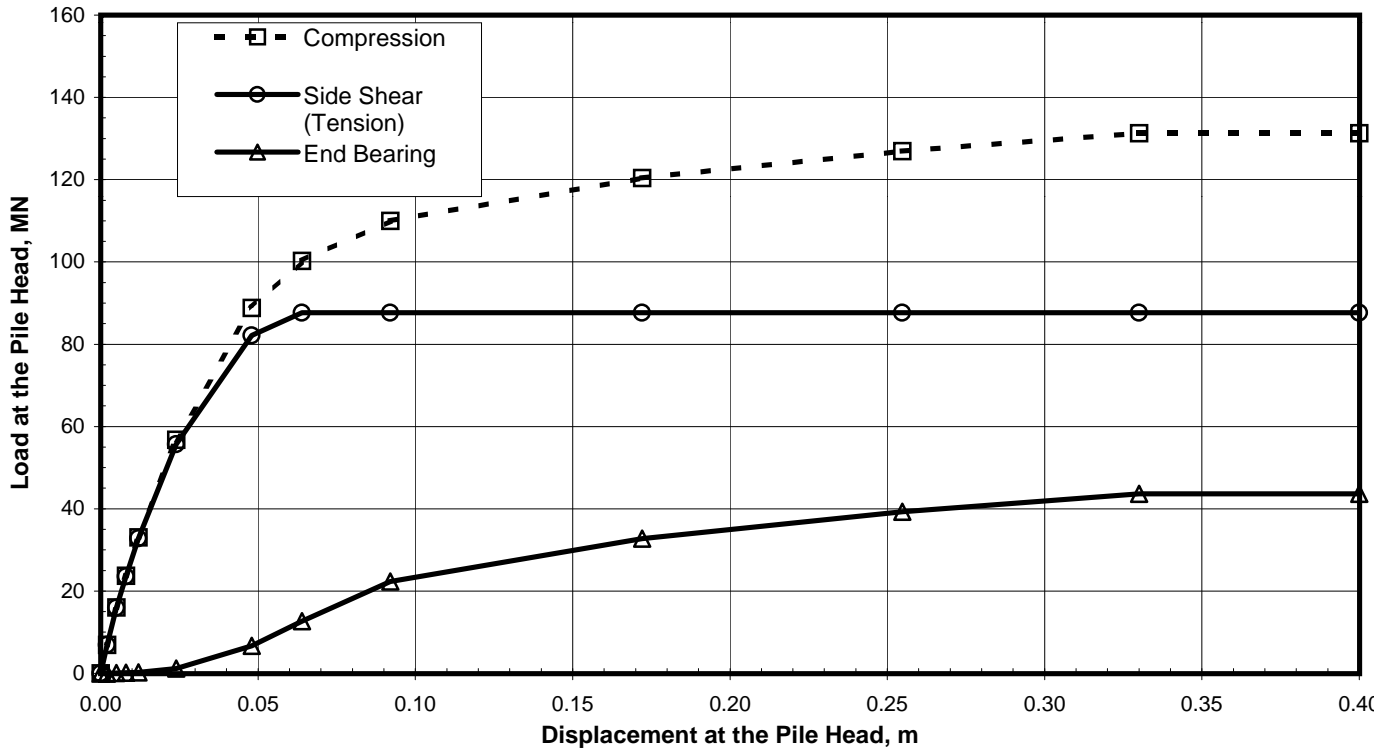
DEPTH (m)	Q-z Data											
	Q(1)	z(1)	Q(2)	z(2)	Q(3)	z(3)	Q(4)	z(4)	Q(5)	z(5)	Q(6)	z(6)
91	0.0	0.0	10.930	0.004	21.860	0.031	32.790	0.105	39.348	0.183	43.720	0.250

Notes:

1. "Q" is load in compression (MN)
2. "z" is displacement (m)

TABULATED AXIAL PILE LOAD TRANSFER DATA
Pier E10-Eastbound (Boring 98-33)
 2.5-Meter-Diameter Pipe Piles (Pile Tip Elevation = -95 Meters)
 SFOBB East Span Seismic Safety Project





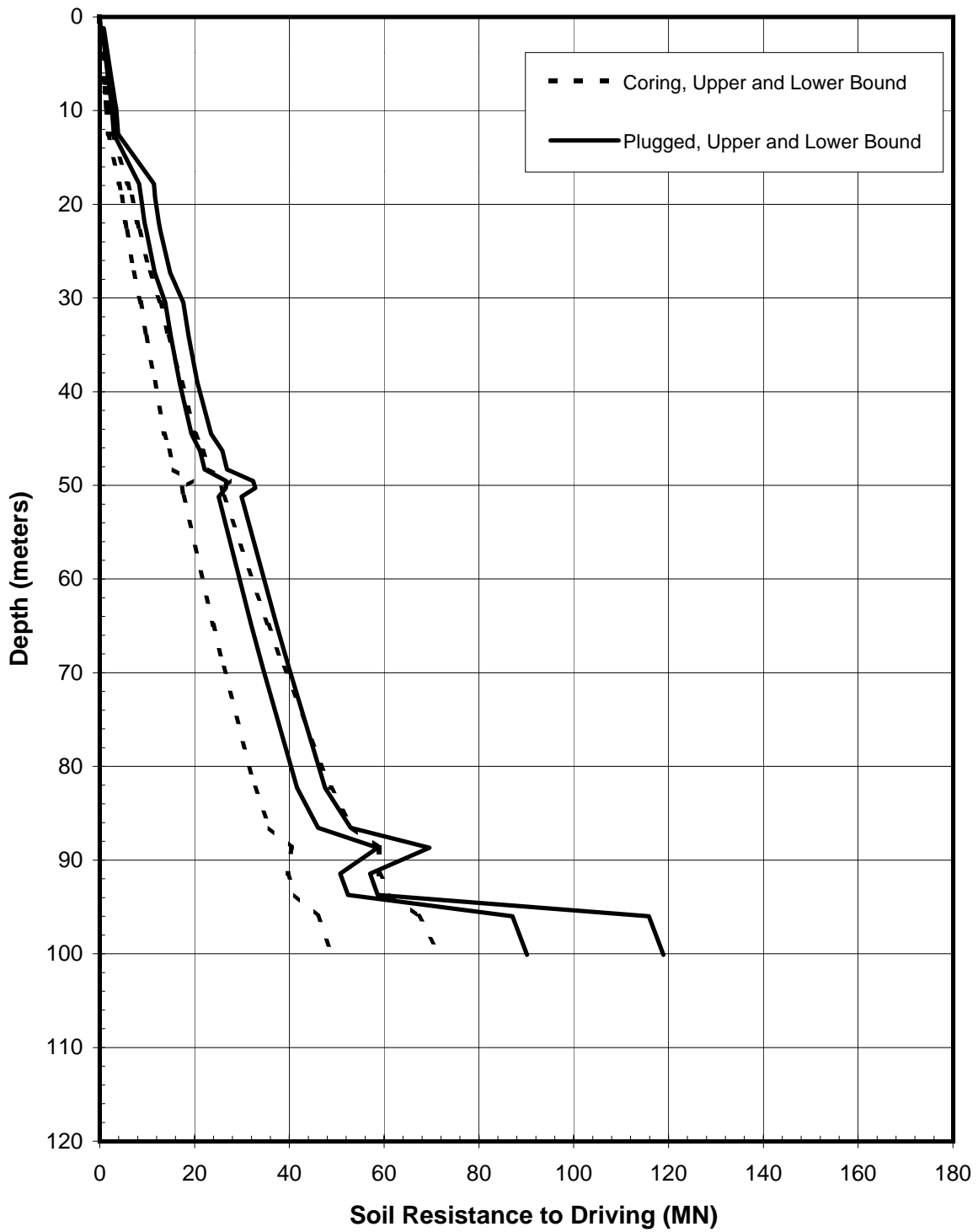
Pile Head Displacement (m)	Load at the Pile Head		End Bearing Component in Compression (MN)
	Compression (MN)	Tension (MN)	
0.000	0.00	0.00	0.00
0.002	6.92	6.89	0.03
0.005	16.02	15.94	0.08
0.008	23.71	23.57	0.14
0.012	33.08	32.81	0.27
0.024	56.80	55.66	1.14
0.048	88.82	82.12	6.70
0.064	100.30	87.65	12.65
0.092	110.00	87.65	22.35
0.172	120.39	87.65	32.74
0.255	126.94	87.65	39.29
0.330	131.30	87.65	43.65
0.400	131.30	87.65	43.65

Note:

Pile head load-displacement curves are based on the preliminary pile wall thickness schedule provided by TY Lin/M&N and static loading conditions.

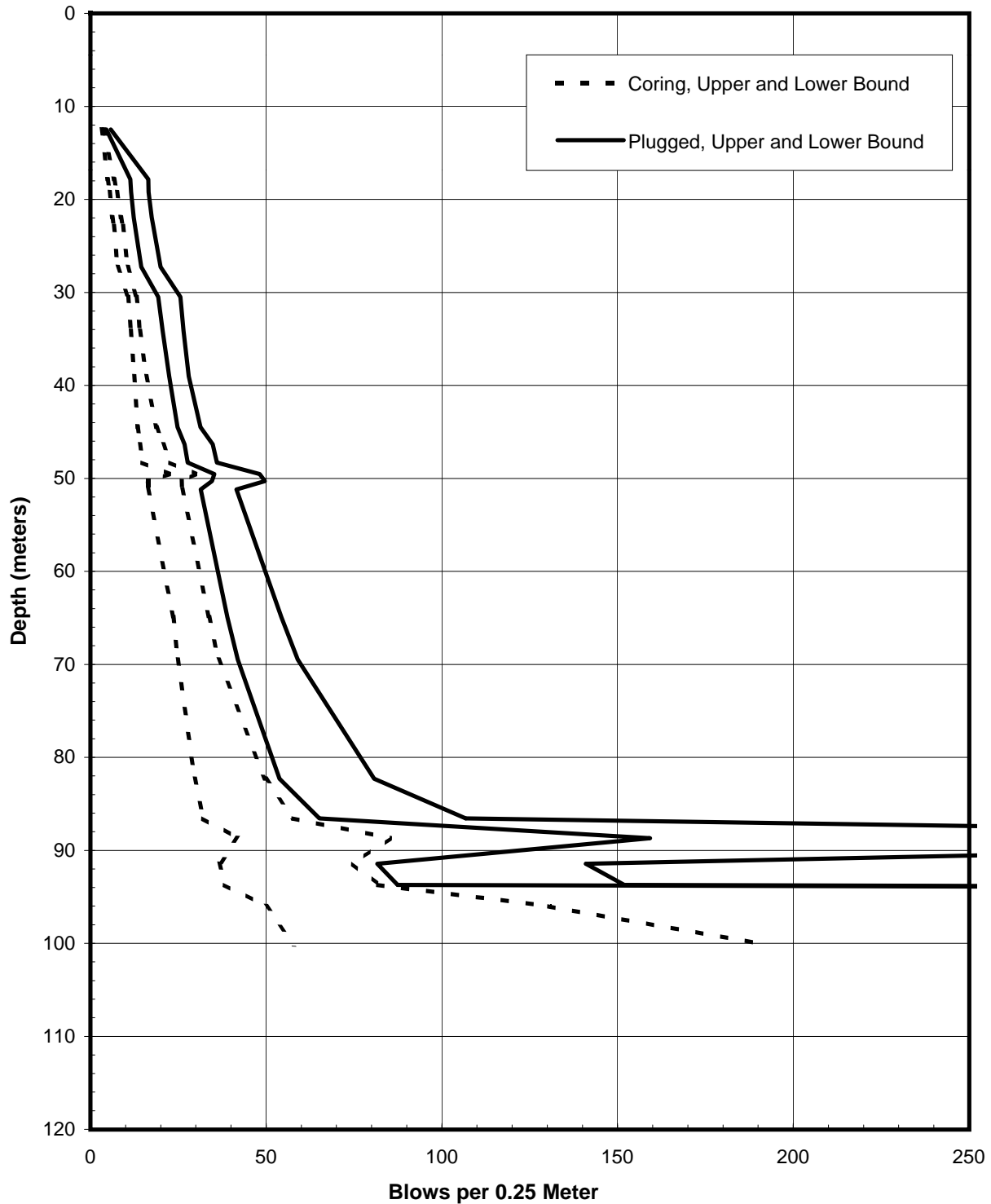
STATIC PILE HEAD LOAD-DEFORMATION CURVES
Pier E10-Eastbound (Boring 98-33)
 2.5-Meter-Diameter Pipe Piles (Pile Tip Elevation = -95 Meters)
 SFOBB East Span Seismic Safety Project





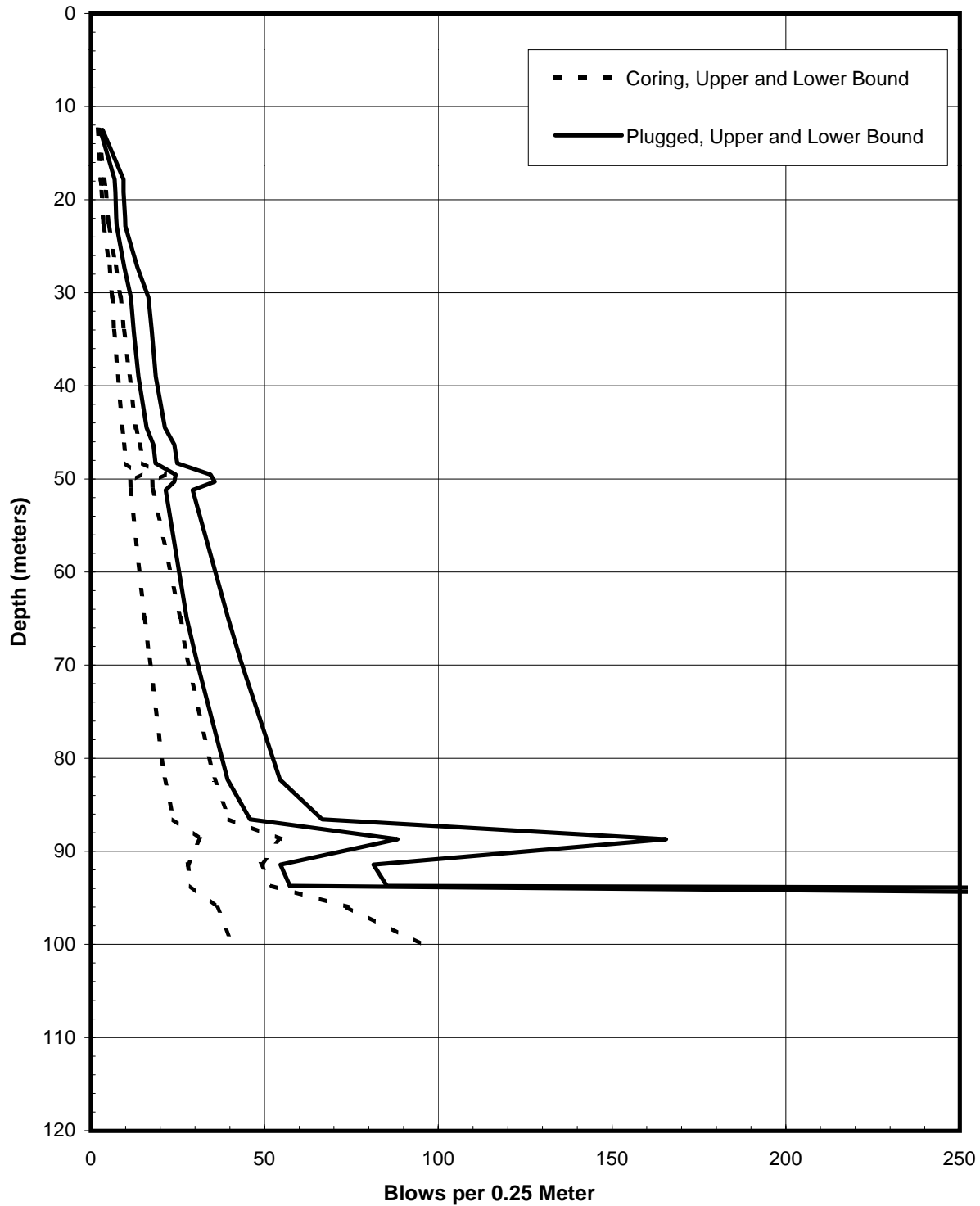
SOIL RESISTANCE TO DRIVING
Pier E10-Eastbound (Boring 98-33)
2.5-Meter-Diameter Driven Pipe Piles
SFOBB East Span Seismic Safety Project





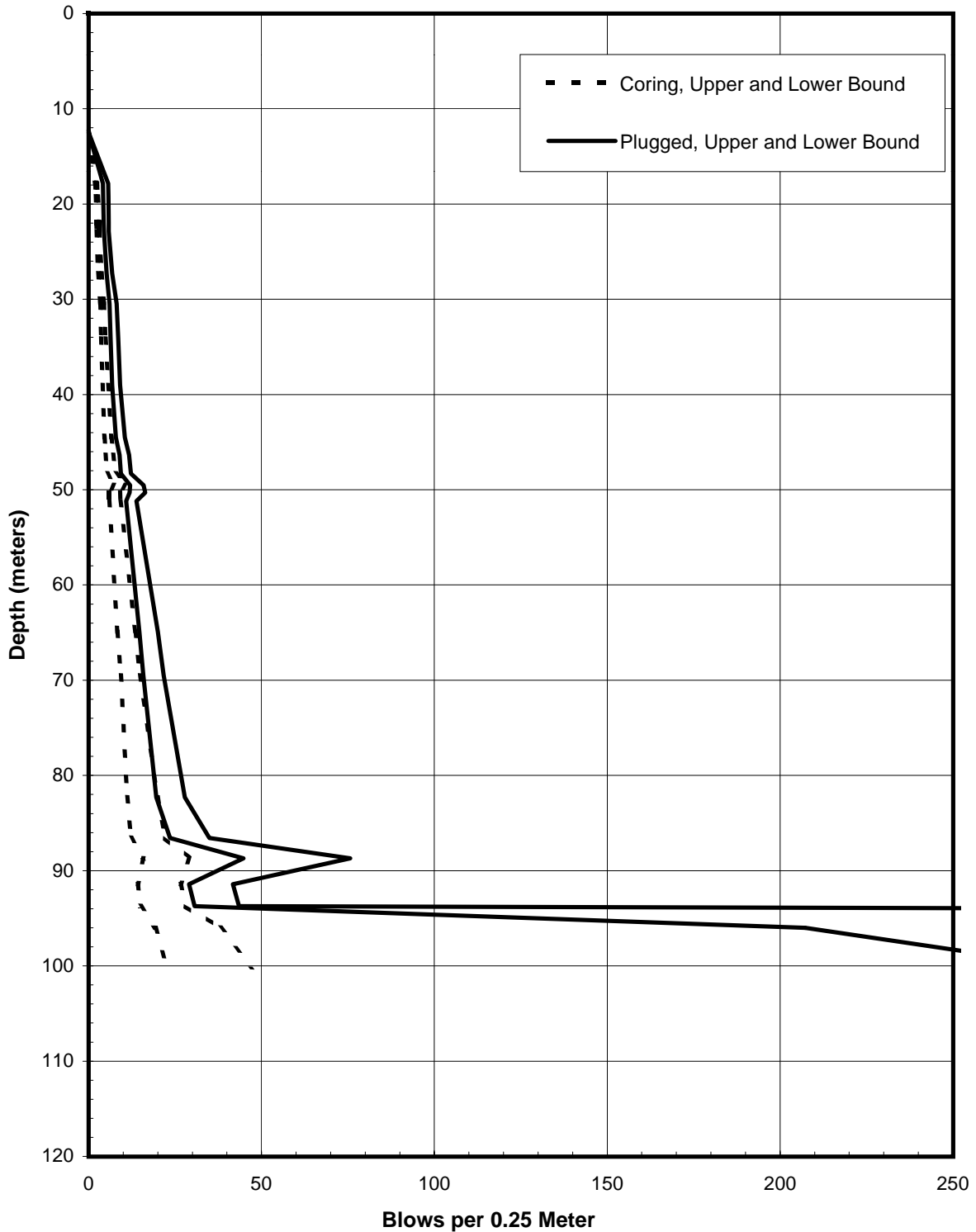
PREDICTED BLOW COUNTS
Pier E10-Eastbound (Boring 98-33)
Menck MHU-500T, 2.5-Meter-Diameter Driven Pipe Piles
SFOBB East Span Seismic Safety Project





PREDICTED BLOW COUNTS
Pier E10-Eastbound (Boring 98-33)
Menck MHU-1000, 2.5-Meter-Diameter Driven Pipe Piles
SFOBB East Span Seismic Safety Project

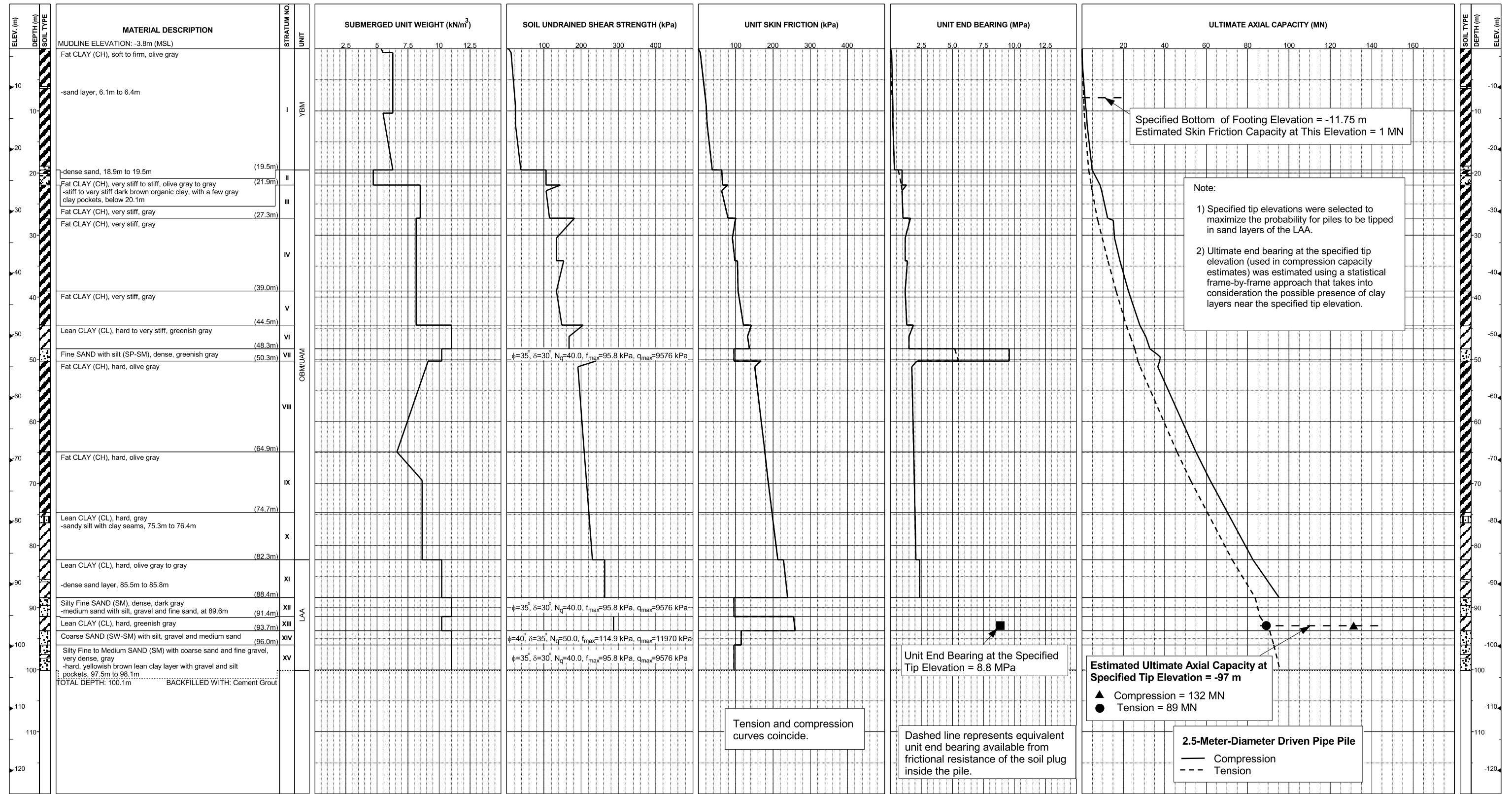




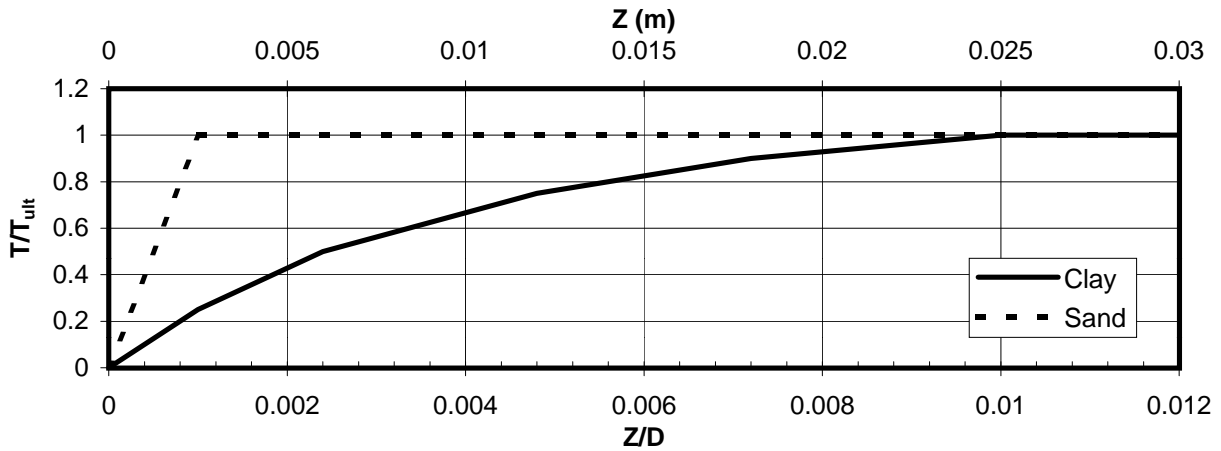
PREDICTED BLOW COUNTS
Pier E10-Eastbound (Boring 98-33)
Menck MHU-1700, 2.5-Meter-Diameter Driven Pipe Piles
SFOBB East Span Seismic Safety Project



**Pier E10-Westbound (Borings 98-31 and 98-33)
Skyway Frame 2**



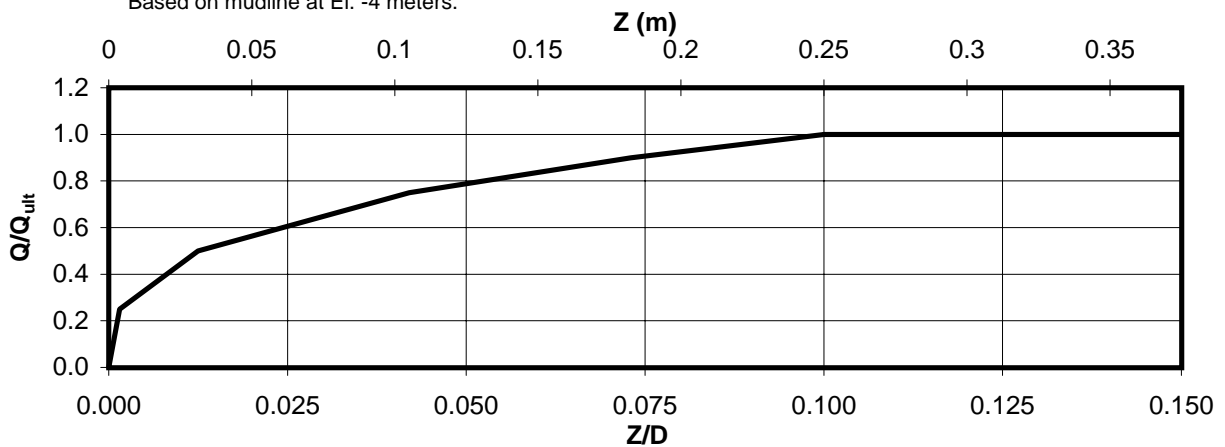
AXIAL PILE DESIGN PARAMETERS AND RESULTS
Pier E10-Westbound (Borings 98-31 and 98-33)
SFOBB East Span Seismic Safety Project



Depth (m)	Soil Type	T_{ult} (MN/m)
0-3	Clay	0.028
3-6	Clay	0.099
6-9	Clay	0.139
9-12	Clay	0.181
12-15	Clay	0.206
15-18	Clay	0.251
18-21	Clay	0.330
21-24	Clay	0.554
24-27	Clay	0.560
27-30	Clay	0.777
30-33	Clay	0.716
33-36	Clay	0.807

Depth (m)	Soil Type	T_{ult} (MN/m)
36-39	Clay	0.834
39-42	Clay	0.852
42-45	Clay	0.928
45-51	Clay	0.974
51-57	Clay	1.248
57-63	Clay	1.324
63-69	Clay	1.421
69-75	Clay	1.516
75-81	Clay	1.610
81-87	Clay	1.879
87-91	Sand	0.941
91-94	Clay	1.995

*Based on mudline at El. -4 meters.



Depth (m)	Soil Type	Q_{ult} (MN)
94	Sand	43.7

AXIAL PILE LOAD TRANSFER-DISPLACEMENT CURVES
Pier E10-Westbound (Borings 98-31 and 98-33)
 2.5-Meter-Diameter Pipe Piles (Pile Tip Elevation = -98 Meters)
 SFOBB East Span Seismic Safety Project



DEPTH (m)	t-z Data											
	t(1)	z(1)	t(2)	z(2)	t(3)	z(3)	t(4)	z(4)	t(5)	z(5)	t(6)	z(6)
0-3	0.0	0.0	0.007	0.003	0.014	0.006	0.021	0.012	0.025	0.018	0.028	0.025
3-6	0.0	0.0	0.025	0.003	0.049	0.006	0.074	0.012	0.089	0.018	0.099	0.025
6-9	0.0	0.0	0.035	0.003	0.070	0.006	0.104	0.012	0.125	0.018	0.139	0.025
9-12	0.0	0.0	0.045	0.003	0.090	0.006	0.135	0.012	0.163	0.018	0.181	0.025
12-15	0.0	0.0	0.052	0.003	0.103	0.006	0.155	0.012	0.185	0.018	0.206	0.025
15-18	0.0	0.0	0.063	0.003	0.125	0.006	0.188	0.012	0.225	0.018	0.251	0.025
18-21	0.0	0.0	0.082	0.0025	0.165	0.006	0.247	0.012	0.297	0.018	0.330	0.025
21-24	0.0	0.0	0.139	0.003	0.277	0.006	0.416	0.012	0.499	0.018	0.554	0.025
24-27	0.0	0.0	0.140	0.003	0.280	0.006	0.420	0.012	0.504	0.018	0.560	0.025
27-30	0.0	0.0	0.194	0.003	0.388	0.006	0.582	0.012	0.699	0.018	0.777	0.025
30-33	0.0	0.0	0.179	0.003	0.358	0.006	0.537	0.012	0.645	0.018	0.716	0.025
33-36	0.0	0.0	0.202	0.003	0.404	0.006	0.605	0.012	0.726	0.018	0.807	0.025
36-39	0.0	0.0	0.209	0.003	0.417	0.006	0.626	0.012	0.751	0.018	0.834	0.025
39-42	0.0	0.0	0.213	0.003	0.426	0.006	0.639	0.012	0.767	0.018	0.852	0.025
42-45	0.0	0.0	0.232	0.003	0.464	0.006	0.696	0.012	0.835	0.018	0.928	0.025
45-51	0.0	0.0	0.244	0.0025	0.487	0.006	0.731	0.012	0.877	0.018	0.974	0.025
51-57	0.0	0.0	0.312	0.003	0.624	0.006	0.936	0.012	1.123	0.018	1.248	0.025
57-63	0.0	0.0	0.331	0.003	0.662	0.006	0.993	0.012	1.192	0.018	1.324	0.025
63-69	0.0	0.0	0.355	0.003	0.711	0.006	1.066	0.012	1.279	0.018	1.421	0.025
69-75	0.0	0.0	0.379	0.003	0.758	0.006	1.137	0.012	1.364	0.018	1.516	0.025
75-81	0.0	0.0	0.403	0.003	0.805	0.006	1.208	0.012	1.449	0.018	1.610	0.025
81-87	0.0	0.0	0.470	0.003	0.940	0.006	1.409	0.012	1.691	0.018	1.879	0.025
87-91	0.0	0.0	0.941	0.003								
91-94	0.0	0.0	0.499	0.003	0.998	0.006	1.496	0.012	1.796	0.018	1.995	0.025

Notes:

1. "t" is load (MN/m)
2. "z" is displacement (m)
3. Data for tension and compression coincide
4. Based on mudline at El. -4 meters

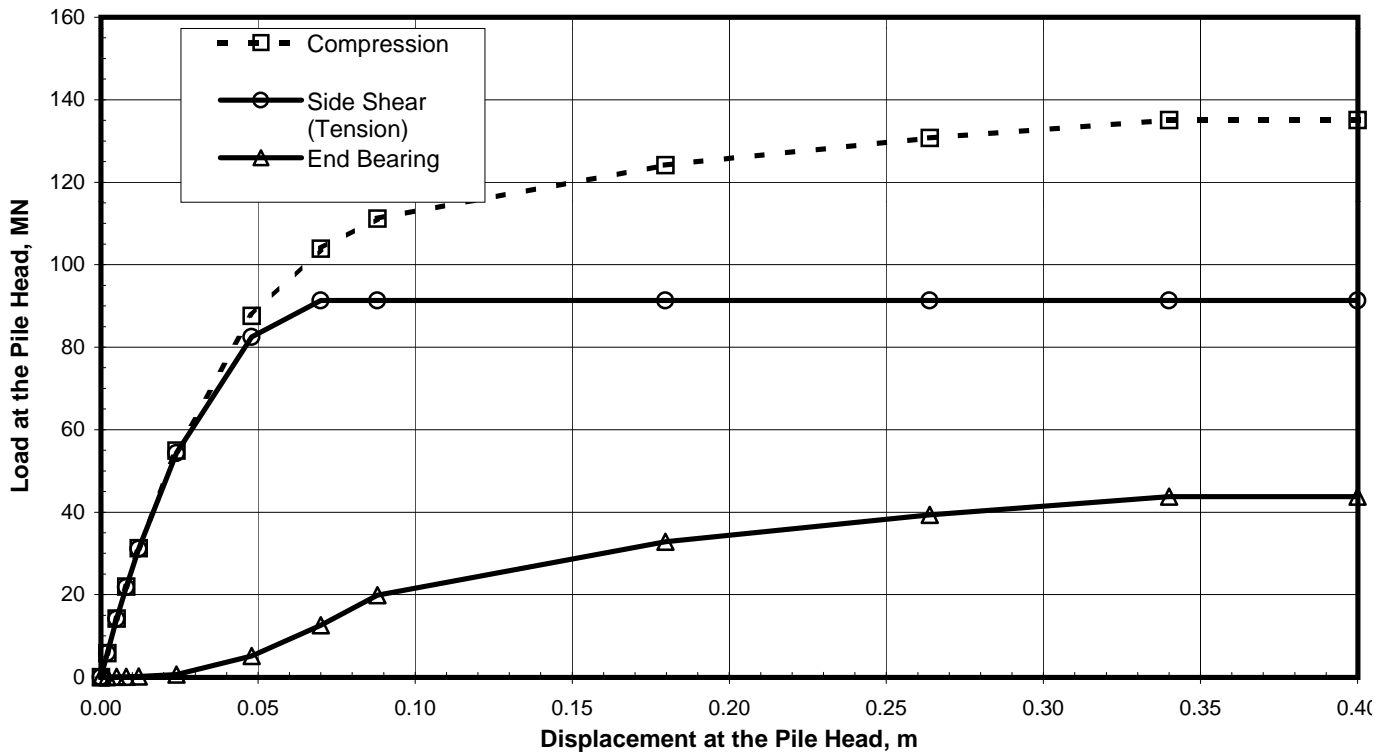
DEPTH (m)	Q-z Data											
	Q(1)	z(1)	Q(2)	z(2)	Q(3)	z(3)	Q(4)	z(4)	Q(5)	z(5)	Q(6)	z(6)
94	0.0	0.0	10.930	0.004	21.860	0.031	32.790	0.105	39.348	0.183	43.720	0.250

Notes:

1. "Q" is load in compression (MN)
2. "z" is displacement (m)

TABULATED AXIAL PILE LOAD TRANSFER DATA
Pier E10-Westbound (Borings 98-31 and 98-33)
 2.5-Meter-Diameter Pipe Piles (Pile Tip Elevation = -98 Meters)
 SFOBB East Span Seismic Safety Project





Pile Head Displacement (m)	Load at the Pile Head		End Bearing Component in Compression (MN)
	Compression (MN)	Tension (MN)	
0.000	0.00	0.00	0.00
0.002	5.81	5.79	0.02
0.005	14.19	14.13	0.06
0.008	21.93	21.84	0.09
0.012	31.28	31.10	0.18
0.024	54.95	54.30	0.65
0.048	87.62	82.49	5.13
0.070	103.89	91.36	12.53
0.088	111.20	91.36	19.84
0.180	124.17	91.36	32.81
0.264	130.73	91.36	39.37
0.340	135.10	91.36	43.74
0.400	135.10	91.36	43.74

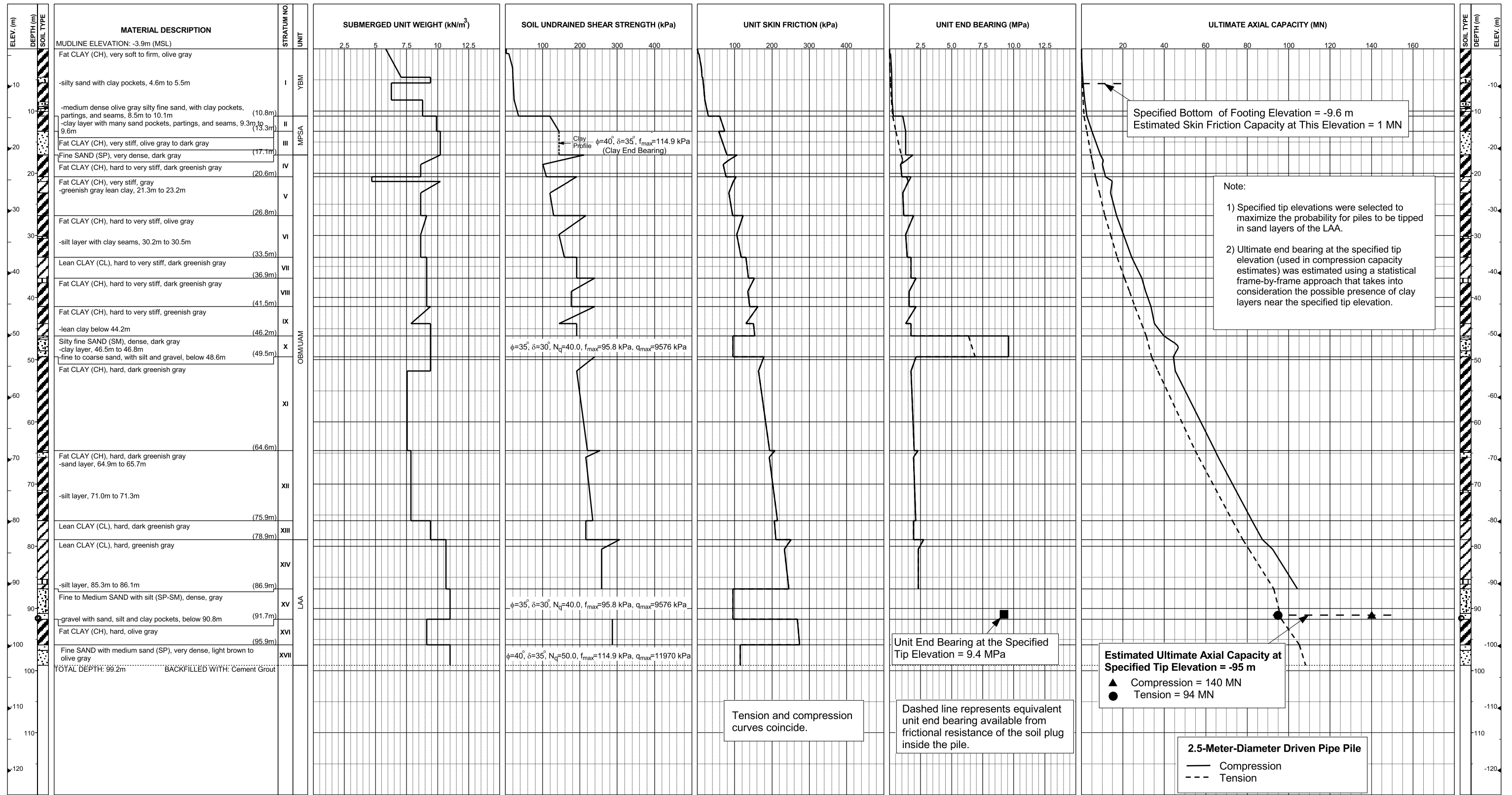
Note:

Pile head load-displacement curves are based on the preliminary pile wall thickness schedule provided by TY Lin/M&N and static loading conditions.

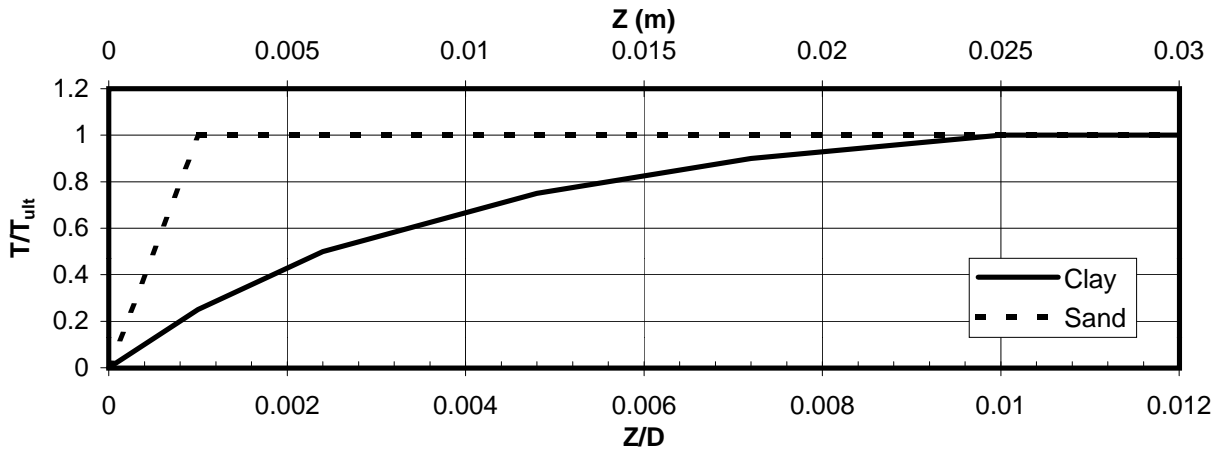
STATIC PILE HEAD LOAD-DEFORMATION CURVES
Pier E10-Westbound (Borings 98-31 and 98-33)
 2.5-Meter-Diameter Pipe Piles (Pile Tip Elevation = -98 Meters)
 SFOBB East Span Seismic Safety Project



**Pier E11-Eastbound (Boring 98-42)
Skyway Frame 3**



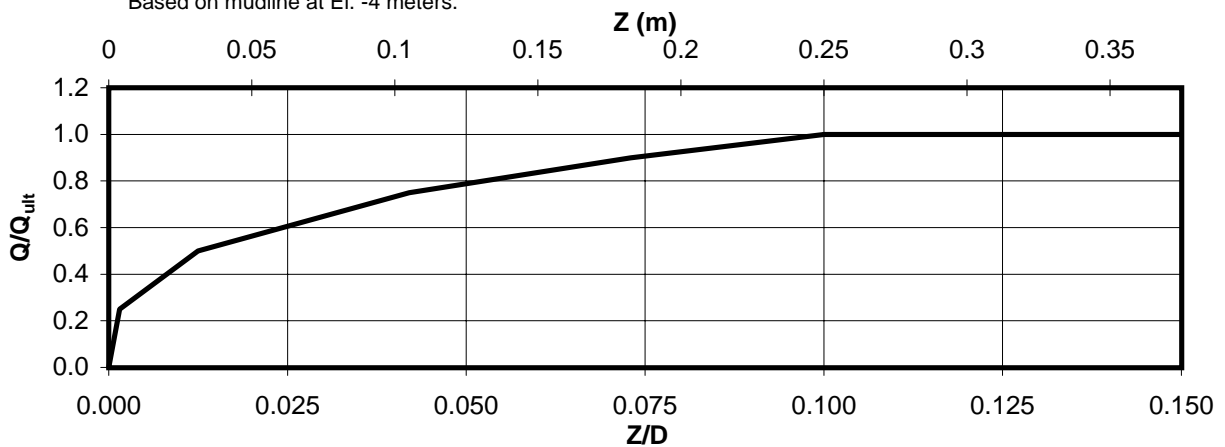
AXIAL PILE DESIGN PARAMETERS AND RESULTS
Pier E11-Eastbound (Boring 98-42)
SFOBB East Span Seismic Safety Project



Depth (m)	Soil Type	T_{ult} (MN/m)
0-3	Clay	0.037
3-6	Clay	0.100
6-9	Clay	0.150
9-12	Clay	0.267
12-15	Sand	0.557
15-18	Sand	0.627
18-21	Clay	0.587
21-24	Clay	0.733
24-27	Clay	0.697
27-30	Clay	0.920
30-33	Clay	0.840
33-36	Clay	0.997

Depth (m)	Soil Type	T_{ult} (MN/m)
36-39	Clay	1.137
39-42	Clay	1.103
42-45	Clay	1.137
45-51	Sand	0.897
51-57	Clay	1.367
57-63	Clay	1.425
63-69	Clay	1.535
69-75	Clay	1.617
75-81	Clay	1.717
81-87	Clay	1.893
87-91	Sand	0.758

*Based on mudline at El. -4 meters.



Depth (m)	Soil Type	Q_{ult} (MN)
91	Sand	45.9

AXIAL PILE LOAD TRANSFER-DISPLACEMENT CURVES
Pier E11-Eastbound (Boring 98-42)
 2.5-Meter-Diameter Pipe Piles (Pile Tip Elevation = -95 Meters)
 SFOBB East Span Seismic Safety Project



DEPTH (m)	t-z Data											
	t(1)	z(1)	t(2)	z(2)	t(3)	z(3)	t(4)	z(4)	t(5)	z(5)	t(6)	z(6)
0-3	0.0	0.0	0.009	0.003	0.018	0.006	0.028	0.012	0.033	0.018	0.037	0.025
3-6	0.0	0.0	0.025	0.003	0.050	0.006	0.075	0.012	0.090	0.018	0.100	0.025
6-9	0.0	0.0	0.038	0.003	0.075	0.006	0.113	0.012	0.135	0.018	0.150	0.025
9-12	0.0	0.0	0.067	0.003	0.133	0.006	0.200	0.012	0.240	0.018	0.267	0.025
12-15	0.0	0.0	0.557	0.003								
15-18	0.0	0.0	0.627	0.003								
18-21	0.0	0.0	0.147	0.0025	0.293	0.006	0.440	0.012	0.528	0.018	0.587	0.025
21-24	0.0	0.0	0.183	0.003	0.367	0.006	0.550	0.012	0.660	0.018	0.733	0.025
24-27	0.0	0.0	0.174	0.003	0.348	0.006	0.523	0.012	0.627	0.018	0.697	0.025
27-30	0.0	0.0	0.230	0.003	0.460	0.006	0.690	0.012	0.828	0.018	0.920	0.025
30-33	0.0	0.0	0.210	0.003	0.420	0.006	0.630	0.012	0.756	0.018	0.840	0.025
33-36	0.0	0.0	0.249	0.003	0.498	0.006	0.748	0.012	0.897	0.018	0.997	0.025
36-39	0.0	0.0	0.284	0.003	0.569	0.006	0.853	0.012	1.023	0.018	1.137	0.025
39-42	0.0	0.0	0.276	0.003	0.552	0.006	0.827	0.012	0.993	0.018	1.103	0.025
42-45	0.0	0.0	0.284	0.003	0.569	0.006	0.853	0.012	1.023	0.018	1.137	0.025
45-51	0.0	0.0	0.897	0.0025								
51-57	0.0	0.0	0.342	0.003	0.684	0.006	1.025	0.012	1.230	0.018	1.367	0.025
57-63	0.0	0.0	0.356	0.003	0.713	0.006	1.069	0.012	1.283	0.018	1.425	0.025
63-69	0.0	0.0	0.384	0.003	0.768	0.006	1.151	0.012	1.382	0.018	1.535	0.025
69-75	0.0	0.0	0.404	0.003	0.809	0.006	1.213	0.012	1.455	0.018	1.617	0.025
75-81	0.0	0.0	0.429	0.003	0.859	0.006	1.288	0.012	1.545	0.018	1.717	0.025
81-87	0.0	0.0	0.473	0.003	0.947	0.006	1.420	0.012	1.704	0.018	1.893	0.025
87-91	0.0	0.0	0.758	0.003								

Notes:

1. "t" is load (MN/m)
2. "z" is displacement (m)
3. Data for tension and compression coincide
4. Based on mudline at El. -4 meters

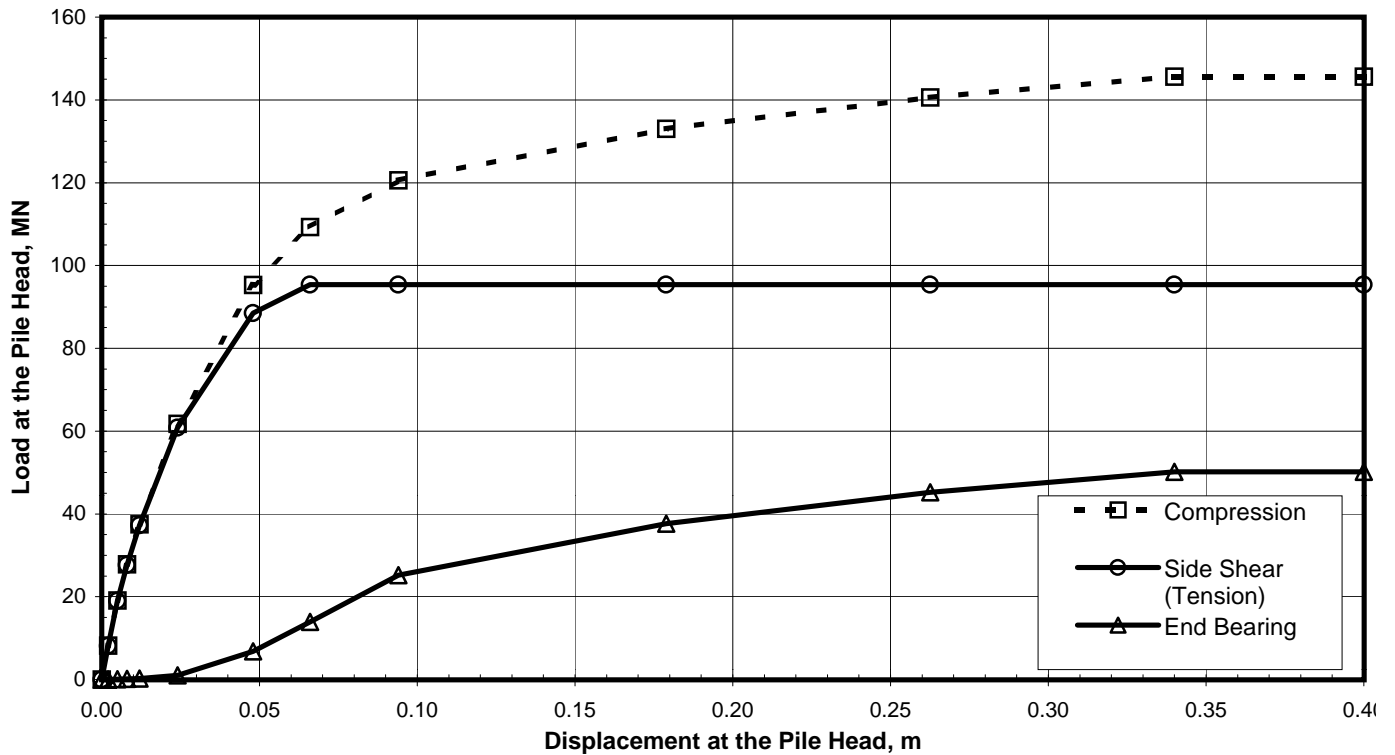
DEPTH (m)	Q-z Data											
	Q(1)	z(1)	Q(2)	z(2)	Q(3)	z(3)	Q(4)	z(4)	Q(5)	z(5)	Q(6)	z(6)
91	0.0	0.0	11.475	0.004	22.950	0.031	34.425	0.105	41.310	0.183	45.900	0.250

Notes:

1. "Q" is load in compression (MN)
2. "z" is displacement (m)

TABULATED AXIAL PILE LOAD TRANSFER DATA
Pier E11-Eastbound (Boring 98-42)
 2.5-Meter-Diameter Pipe Piles (Pile Tip Elevation = -95 Meters)
 SFOBB East Span Seismic Safety Project





Pile Head Displacement (m)	Load at the Pile Head		End Bearing Component in Compression (MN)
	Compression (MN)	Tension (MN)	
0.000	0.00	0.00	0.00
0.002	8.16	8.14	0.02
0.005	19.07	19.01	0.05
0.008	27.81	27.68	0.13
0.012	37.50	37.27	0.23
0.024	61.78	60.80	0.98
0.048	95.29	88.49	6.80
0.066	109.30	95.40	13.90
0.094	120.60	95.40	25.20
0.179	133.05	95.40	37.65
0.263	140.58	95.40	45.18
0.340	145.60	95.40	50.20
0.400	145.60	95.40	50.20

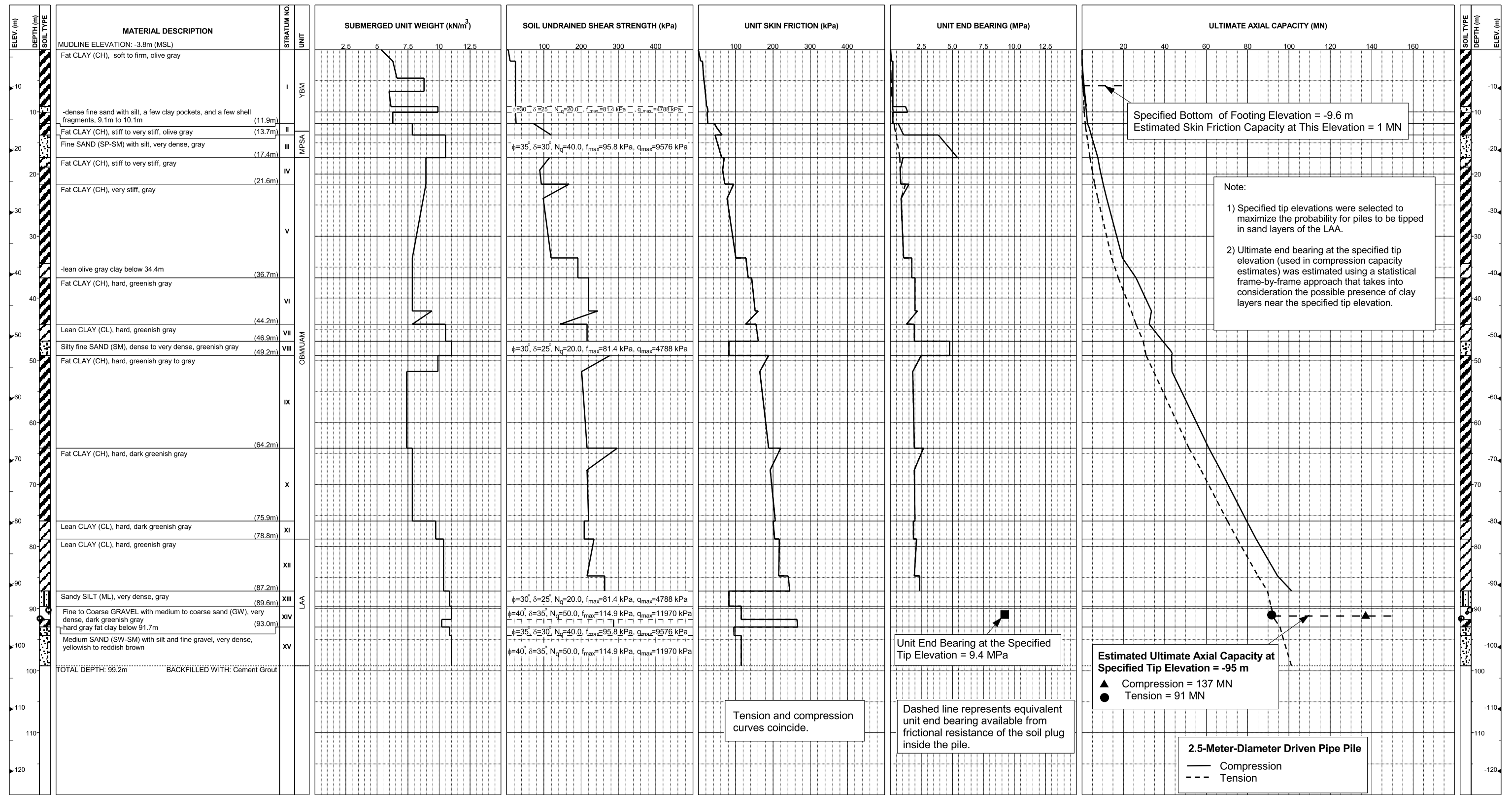
Note:

Pile head load-displacement curves are based on the preliminary pile wall thickness schedule provided by TY Lin/M&N and static loading conditions.

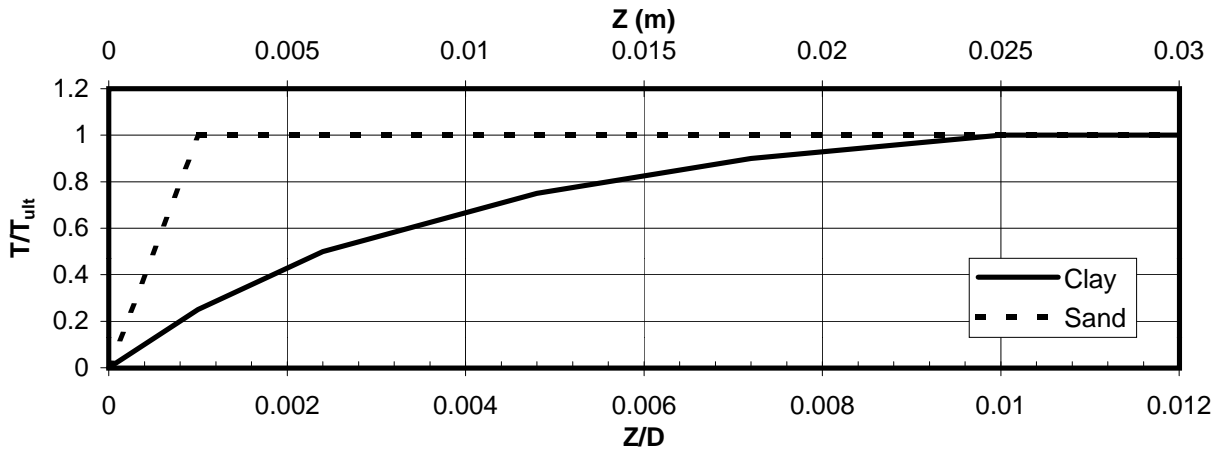
STATIC PILE HEAD LOAD-DEFORMATION CURVES
Pier E11-Eastbound (Boring 98-42)
2.5-Meter-Diameter Pipe Piles (Pile Tip Elevation = -95 Meters)
SFOBB East Span Seismic Safety Project



**Pier E11-Westbound (Borings 98-34)
Skyway Frame 3**



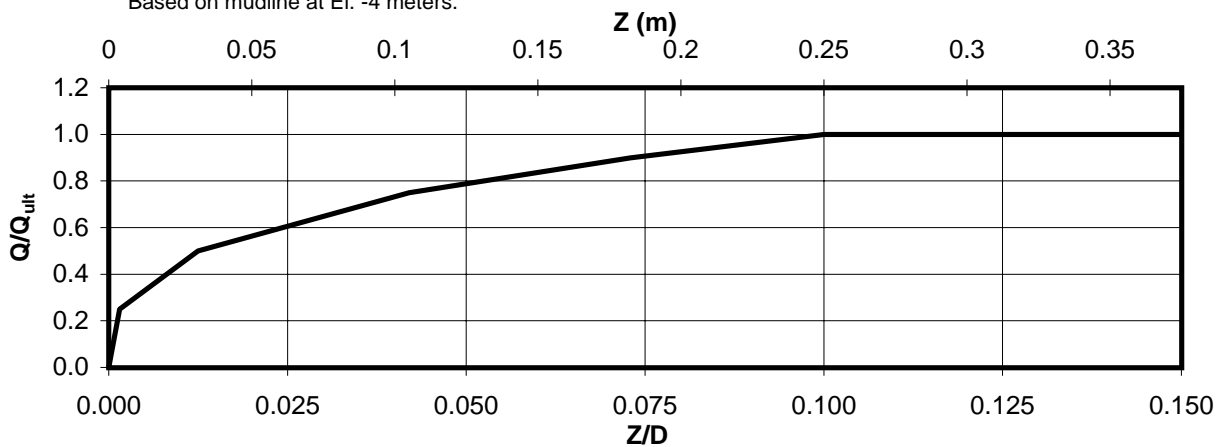
AXIAL PILE DESIGN PARAMETERS AND RESULTS
Pier E11-Westbound (Boring 98-34)
SFOBB East Span Seismic Safety Project



Depth (m)	Soil Type	T_{ult} (MN/m)
0-3	Clay	0.030
3-6	Clay	0.123
6-9	Clay	0.147
9-12	Clay	0.193
12-15	Clay	0.387
15-18	Sand	0.467
18-21	Clay	0.530
21-24	Clay	0.640
24-27	Clay	0.617
27-30	Clay	0.687
30-33	Clay	0.743
33-36	Clay	0.923

Depth (m)	Soil Type	T_{ult} (MN/m)
36-39	Clay	1.113
39-42	Clay	1.180
42-45	Clay	1.147
45-51	Clay	1.087
51-57	Clay	1.355
57-63	Clay	1.415
63-69	Clay	1.590
69-75	Clay	1.558
75-81	Clay	1.628
81-87	Clay	1.761
87-90	Sand	0.665
90-91	Sand	0.903

*Based on mudline at El. -4 meters.



Depth (m)	Soil Type	Q_{ult} (MN)
91	Sand	45.9

AXIAL PILE LOAD TRANSFER-DISPLACEMENT CURVES
Pier E11-Westbound (Boring 98-34)
 2.5-Meter-Diameter Pipe Piles (Pile Tip Elevation = -95 Meters)
 SFOBB East Span Seismic Safety Project





DEPTH (m)	t-z Data											
	t(1)	z(1)	t(2)	z(2)	t(3)	z(3)	t(4)	z(4)	t(5)	z(5)	t(6)	z(6)
0-3	0.0	0.0	0.008	0.003	0.015	0.006	0.023	0.012	0.027	0.018	0.030	0.025
3-6	0.0	0.0	0.031	0.003	0.062	0.006	0.092	0.012	0.111	0.018	0.123	0.025
6-9	0.0	0.0	0.037	0.003	0.073	0.006	0.110	0.012	0.132	0.018	0.147	0.025
9-12	0.0	0.0	0.048	0.003	0.097	0.006	0.145	0.012	0.174	0.018	0.193	0.025
12-15	0.0	0.0	0.097	0.003	0.193	0.006	0.290	0.012	0.348	0.018	0.387	0.025
15-18	0.0	0.0	0.467	0.003								
18-21	0.0	0.0	0.133	0.0025	0.265	0.006	0.398	0.012	0.477	0.018	0.530	0.025
21-24	0.0	0.0	0.160	0.003	0.320	0.006	0.480	0.012	0.576	0.018	0.640	0.025
24-27	0.0	0.0	0.154	0.003	0.308	0.006	0.463	0.012	0.555	0.018	0.617	0.025
27-30	0.0	0.0	0.172	0.003	0.343	0.006	0.515	0.012	0.618	0.018	0.687	0.025
30-33	0.0	0.0	0.186	0.003	0.372	0.006	0.557	0.012	0.669	0.018	0.743	0.025
33-36	0.0	0.0	0.231	0.003	0.462	0.006	0.692	0.012	0.831	0.018	0.923	0.025
36-39	0.0	0.0	0.278	0.003	0.557	0.006	0.835	0.012	1.002	0.018	1.113	0.025
39-42	0.0	0.0	0.295	0.003	0.590	0.006	0.885	0.012	1.062	0.018	1.180	0.025
42-45	0.0	0.0	0.287	0.003	0.574	0.006	0.860	0.012	1.032	0.018	1.147	0.025
45-51	0.0	0.0	0.272	0.0025	0.544	0.006	0.815	0.012	0.978	0.018	1.087	0.025
51-57	0.0	0.0	0.339	0.003	0.678	0.006	1.016	0.012	1.220	0.018	1.355	0.025
57-63	0.0	0.0	0.354	0.003	0.708	0.006	1.061	0.012	1.274	0.018	1.415	0.025
63-69	0.0	0.0	0.398	0.003	0.795	0.006	1.193	0.012	1.431	0.018	1.590	0.025
69-75	0.0	0.0	0.390	0.003	0.779	0.006	1.169	0.012	1.402	0.018	1.558	0.025
75-81	0.0	0.0	0.407	0.003	0.814	0.006	1.221	0.012	1.465	0.018	1.628	0.025
81-87	0.0	0.0	0.440	0.003	0.881	0.006	1.321	0.012	1.585	0.018	1.761	0.025
87-90	0.0	0.0	0.665	0.003								
90-91	0.0	0.0	0.903	0.003								

Notes:

- "t" is load (MN/m)
- "z" is displacement (m)
- Data for tension and compression coincide
- Based on mudline at El. -4 meters

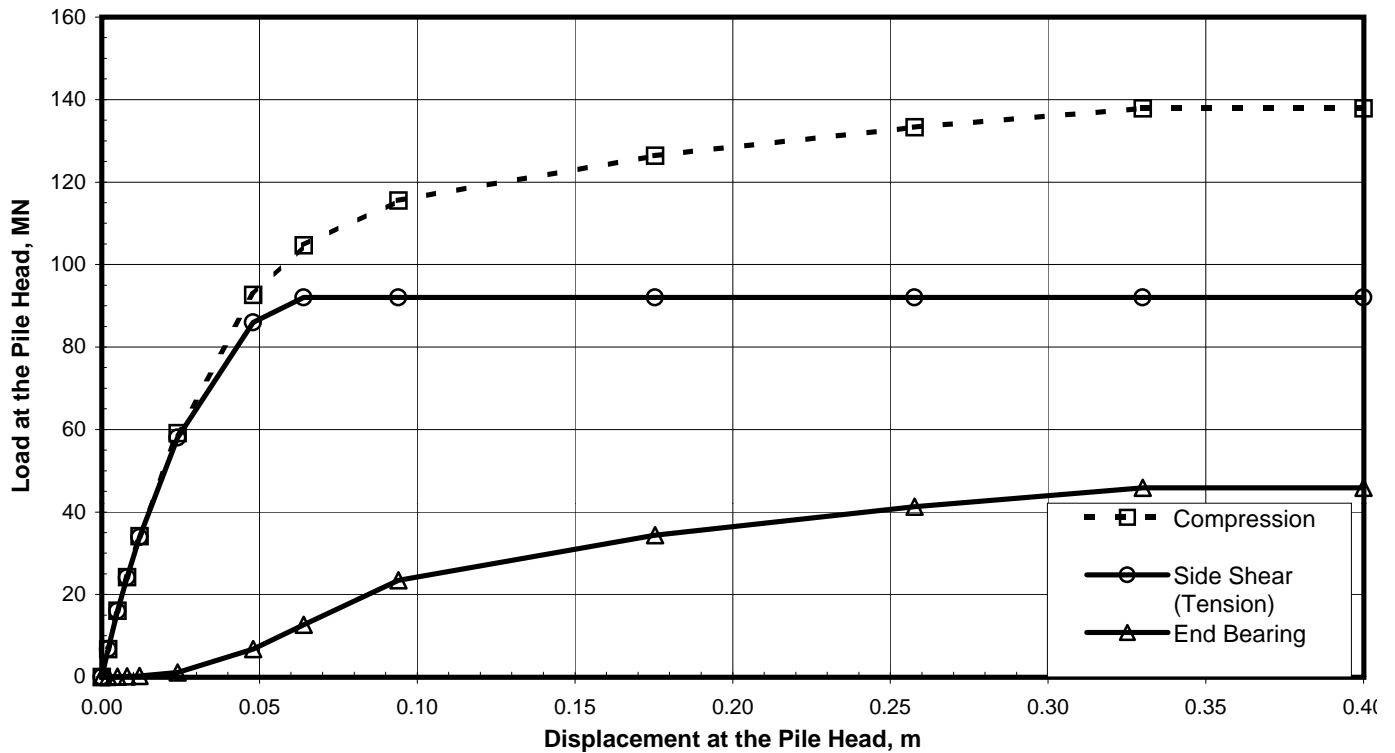
DEPTH (m)	Q-z Data											
	Q(1)	z(1)	Q(2)	z(2)	Q(3)	z(3)	Q(4)	z(4)	Q(5)	z(5)	Q(6)	z(6)
91	0.0	0.0	11.475	0.004	22.950	0.031	34.425	0.105	41.310	0.183	45.900	0.250

Notes:

- "Q" is load in compression (MN)
- "z" is displacement (m)

TABULATED AXIAL PILE LOAD TRANSFER DATA
Pier E11-Westbound (Boring 98-34)
 2.5-Meter-Diameter Pipe Piles (Pile Tip Elevation = -95 Meters)
 SFOBB East Span Seismic Safety Project





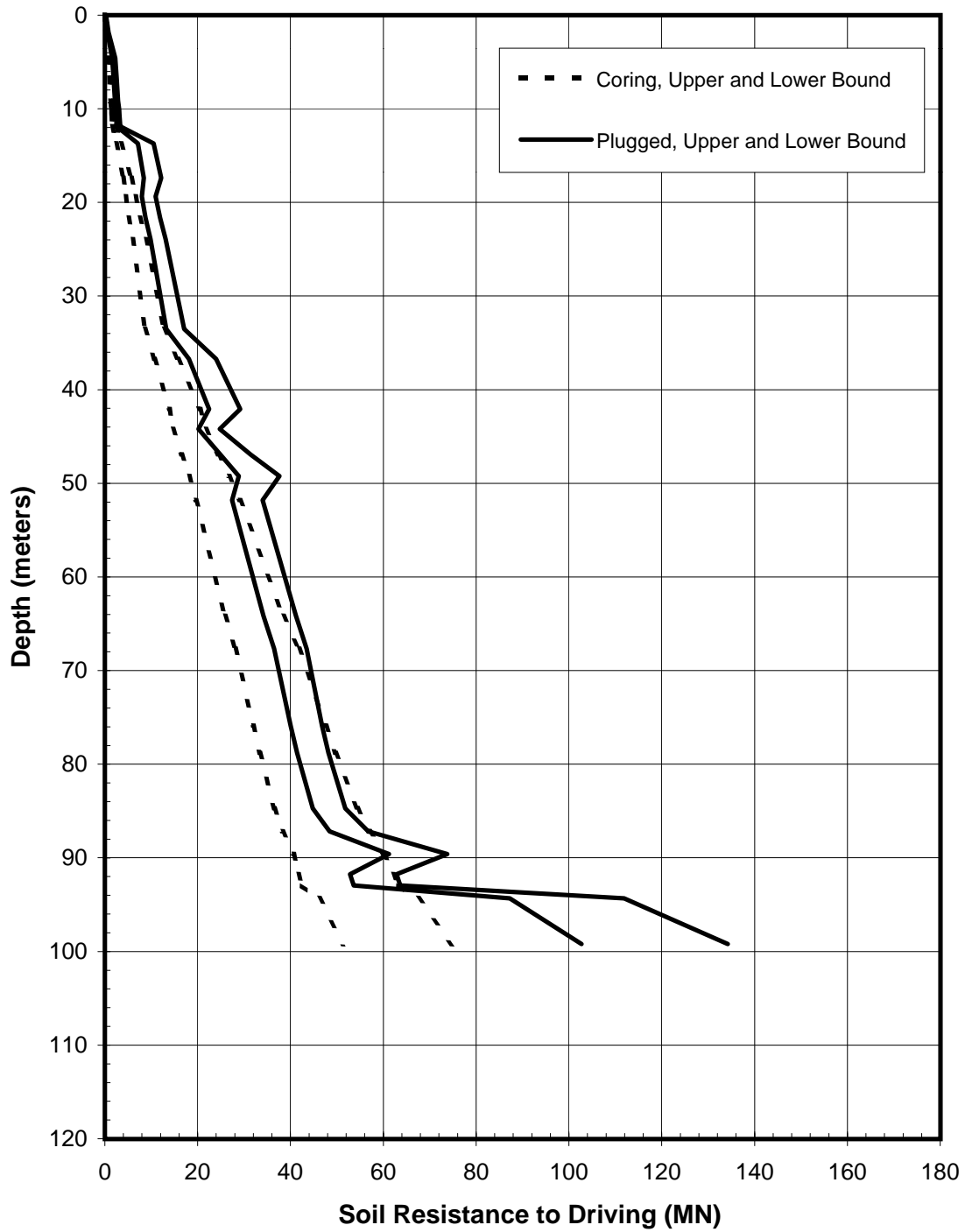
Pile Head Displacement (m)	Load at the Pile Head		End Bearing Component in Compression (MN)
	Compression (MN)	Tension (MN)	
0.000	0.00	0.00	0.00
0.002	6.75	6.72	0.03
0.005	16.06	15.98	0.08
0.008	24.24	24.10	0.14
0.012	34.18	33.92	0.26
0.024	59.14	58.06	1.08
0.048	92.68	85.96	6.72
0.064	104.70	92.04	12.66
0.094	115.50	92.04	23.46
0.175	126.44	92.04	34.40
0.258	133.31	92.04	41.27
0.330	137.90	92.04	45.86
0.400	137.90	92.04	45.86

Note:

Pile head load-displacement curves are based on the preliminary pile wall thickness schedule provided by TY Lin/M&N and static loading conditions.

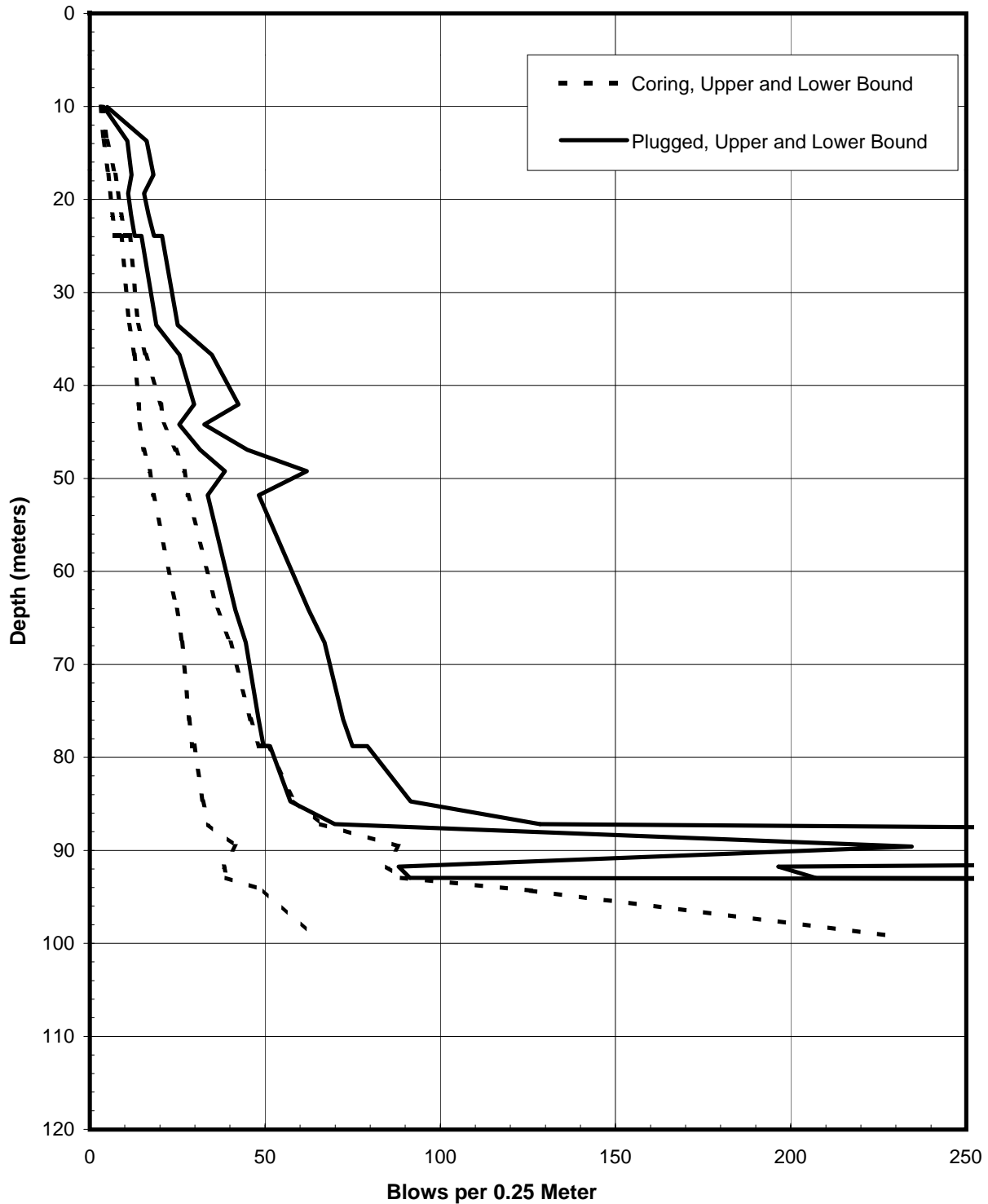
STATIC PILE HEAD LOAD-DEFORMATION CURVES
Pier E11-Westbound (Boring 98-34)
 2.5-Meter-Diameter Pipe Piles (Pile Tip Elevation = -95 Meters)
 SFOBB East Span Seismic Safety Project





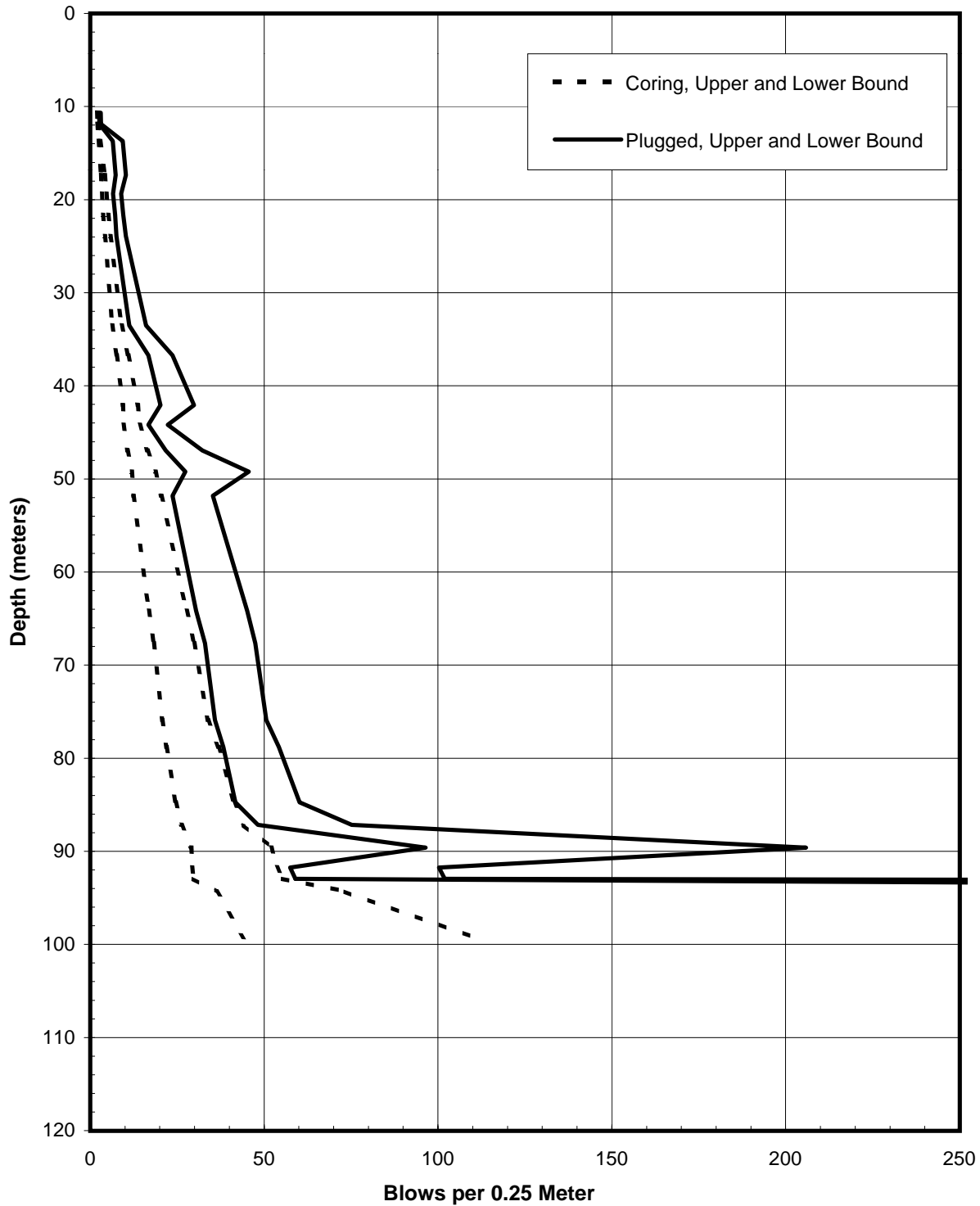
SOIL RESISTANCE TO DRIVING
Pier E11-Westbound (Boring 98-34)
2.5-Meter-Diameter Driven Pipe Piles
SFOBB East Span Seismic Safety Project





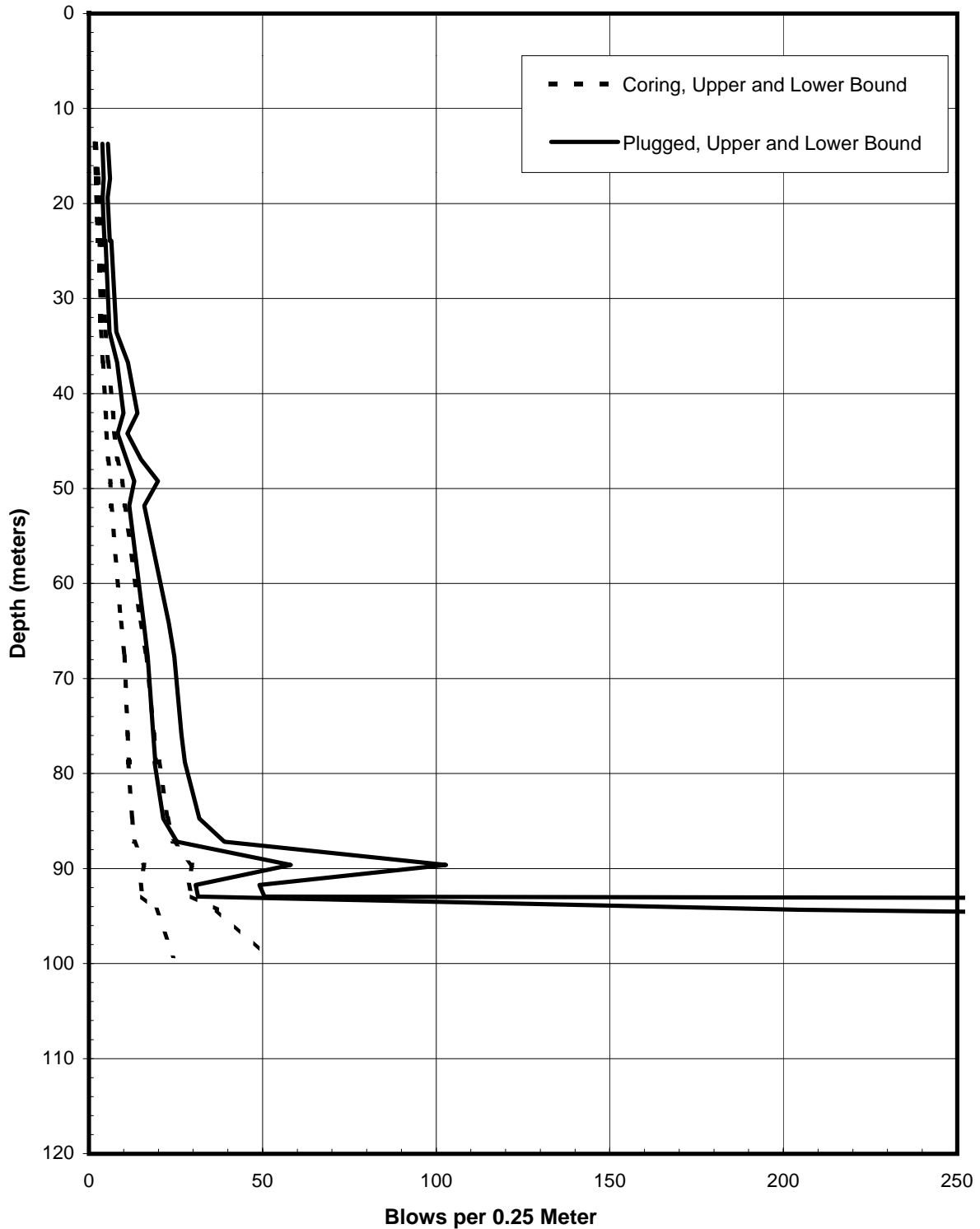
PREDICTED BLOW COUNTS
Pier E11-Westbound (Boring 98-34)
Menck MHU-500T, 2.5-Meter-Diameter Driven Pipe Piles
SFOBB East Span Seismic Safety Project





PREDICTED BLOW COUNTS
Pier E11-Westbound (Boring 98-34)
Menck MHU-1000, 2.5-Meter-Diameter Driven Pipe Piles
SFOBB East Span Seismic Safety Project

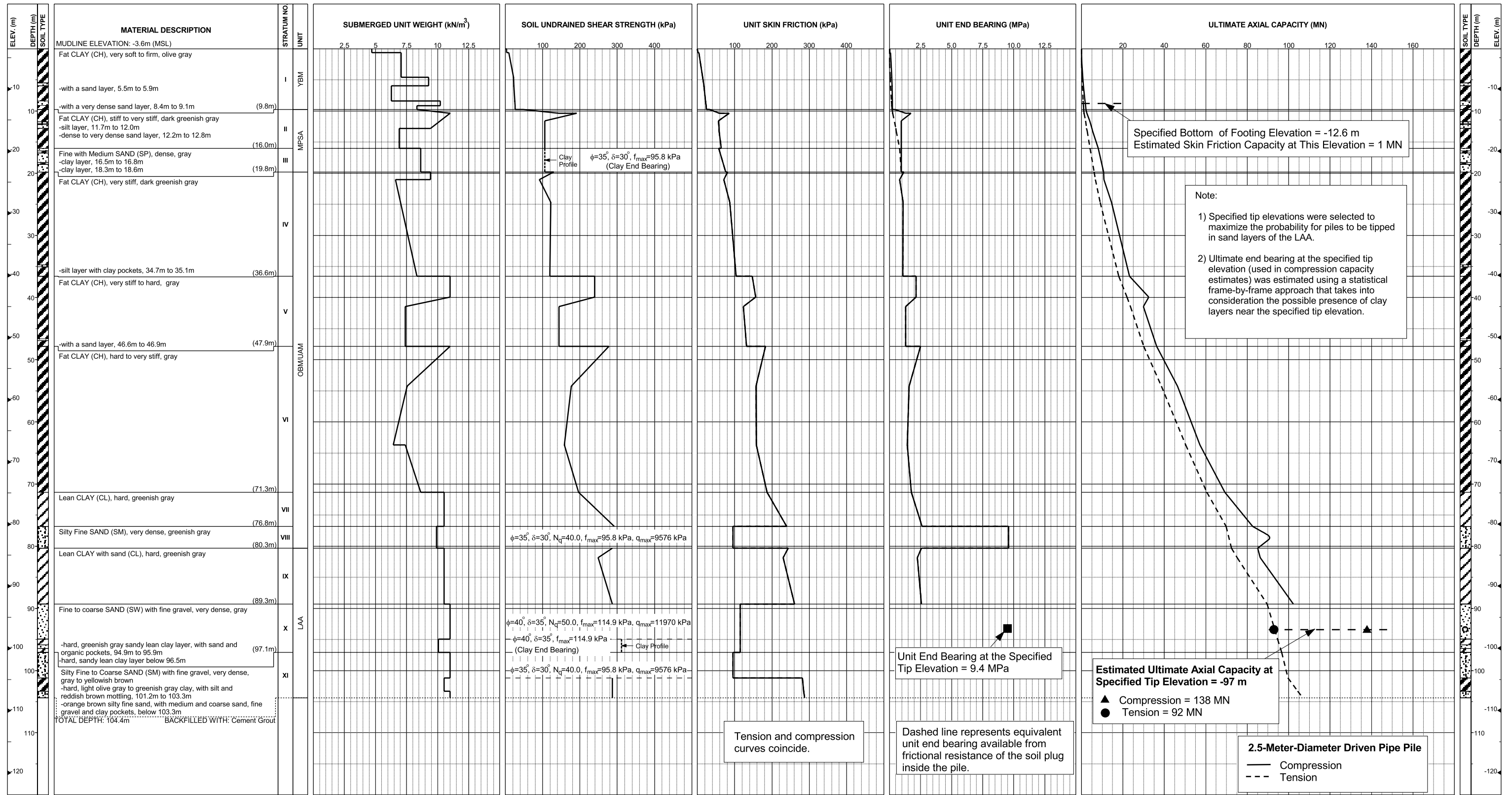




PREDICTED BLOW COUNTS
Pier E11-Westbound (Boring 98-34)
Menck MHU-1700, 2.5-Meter-Diameter Driven Pipe Piles
SFOBB East Span Seismic Safety Project

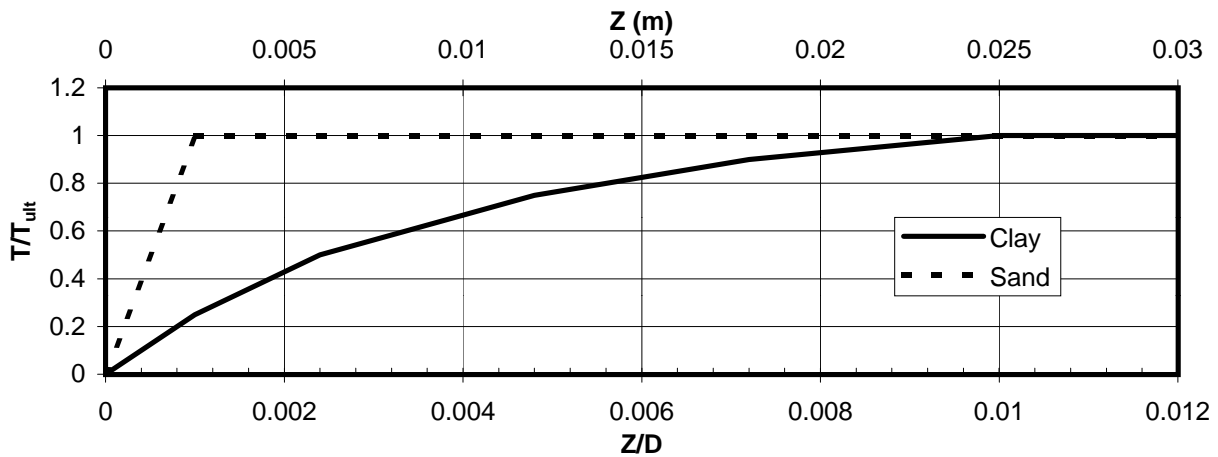


**Pier E12-Eastbound and Westbound (Boring 98-35)
Skyway Frame 3**



AXIAL PILE DESIGN PARAMETERS AND RESULTS
Piers E12-Eastbound and Westbound (Boring 98-35)
SFOBB East Span Seismic Safety Project

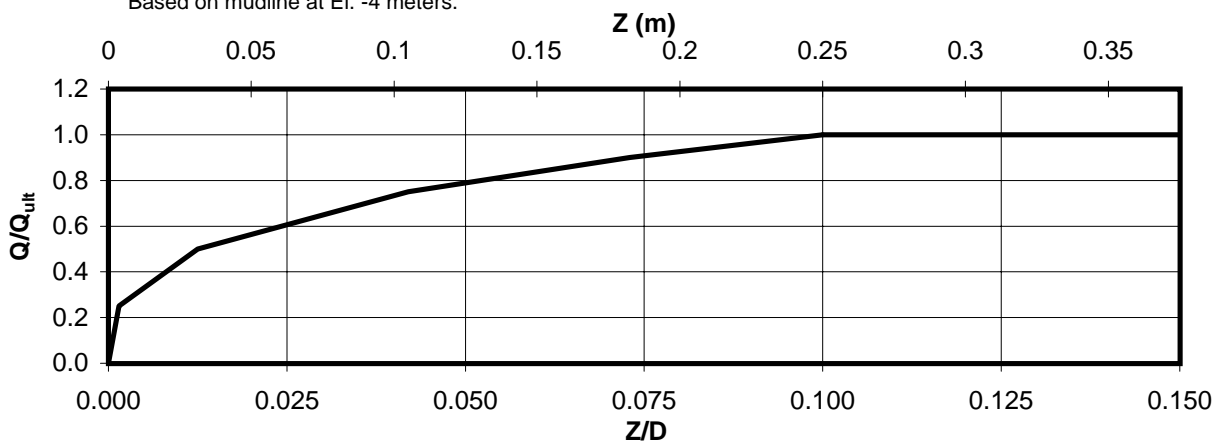




Depth* (m)	Soil Type	T _{ult} (MN/m)
0-3	Clay	0.030
3-6	Clay	0.127
6-9	Clay	0.056
9-12	Clay	0.363
12-15	Clay	0.477
15-18	Clay	0.483
18-21	Clay	0.580
21-24	Clay	0.587
24-27	Clay	0.693
27-30	Clay	0.723
30-33	Clay	0.753
33-36	Clay	0.790

Depth* (m)	Soil Type	T _{ult} (MN/m)
36-39	Clay	1.030
39-42	Clay	1.157
42-45	Clay	0.953
45-51	Clay	1.196
51-57	Clay	1.273
57-63	Clay	1.235
63-69	Clay	1.300
69-75	Clay	1.540
75-81	Clay	1.265
81-89	Clay	1.944
89-93	Sand	0.916

*Based on mudline at El. -4 meters.



Depth* (m)	Soil Type	Q _{ult} (MN)
93	Sand	45.9

AXIAL PILE LOAD TRANSFER-DISPLACEMENT CURVES
Piers E12-Eastbound and Westbound (Boring 98-35)
 2.5-Meter-Diameter Pipe Piles (Pile Tip Elevation = -97 Meters)
 SFOBB East Span Seismic Safety Project



DEPTH (m)	t-z Data											
	t(1)	z(1)	t(2)	z(2)	t(3)	z(3)	t(4)	z(4)	t(5)	z(5)	t(6)	z(6)
0-3	0.0	0.0	0.008	0.003	0.015	0.006	0.023	0.012	0.027	0.018	0.030	0.025
3-6	0.0	0.0	0.032	0.003	0.063	0.006	0.095	0.012	0.114	0.018	0.127	0.025
6-9	0.0	0.0	0.014	0.003	0.028	0.006	0.042	0.012	0.051	0.018	0.056	0.025
9-12	0.0	0.0	0.091	0.003	0.182	0.006	0.273	0.012	0.327	0.018	0.363	0.025
12-15	0.0	0.0	0.119	0.003	0.238	0.006	0.357	0.012	0.429	0.018	0.477	0.025
15-18	0.0	0.0	0.121	0.003	0.242	0.006	0.362	0.012	0.435	0.018	0.483	0.025
18-21	0.0	0.0	0.145	0.003	0.290	0.006	0.435	0.012	0.522	0.018	0.580	0.025
21-24	0.0	0.0	0.147	0.003	0.293	0.006	0.440	0.012	0.528	0.018	0.587	0.025
24-27	0.0	0.0	0.173	0.003	0.347	0.006	0.520	0.012	0.624	0.018	0.693	0.025
27-30	0.0	0.0	0.181	0.003	0.362	0.006	0.542	0.012	0.651	0.018	0.723	0.025
30-33	0.0	0.0	0.188	0.003	0.377	0.006	0.565	0.012	0.678	0.018	0.753	0.025
33-36	0.0	0.0	0.198	0.003	0.395	0.006	0.593	0.012	0.711	0.018	0.790	0.025
36-39	0.0	0.0	0.258	0.003	0.515	0.006	0.773	0.012	0.927	0.018	1.030	0.025
39-42	0.0	0.0	0.289	0.003	0.579	0.006	0.868	0.012	1.041	0.018	1.157	0.025
42-45	0.0	0.0	0.238	0.003	0.477	0.006	0.715	0.012	0.858	0.018	0.953	0.025
45-51	0.0	0.0	0.299	0.003	0.598	0.006	0.897	0.012	1.076	0.018	1.196	0.025
51-57	0.0	0.0	0.318	0.003	0.637	0.006	0.955	0.012	1.146	0.018	1.273	0.025
57-63	0.0	0.0	0.309	0.003	0.618	0.006	0.926	0.012	1.112	0.018	1.235	0.025
63-69	0.0	0.0	0.325	0.003	0.650	0.006	0.975	0.012	1.170	0.018	1.300	0.025
69-75	0.0	0.0	0.385	0.003	0.770	0.006	1.155	0.012	1.386	0.018	1.540	0.025
75-81	0.0	0.0	0.316	0.003	0.633	0.006	0.949	0.012	1.139	0.018	1.265	0.025
81-89	0.0	0.0	0.486	0.003	0.972	0.006	1.458	0.012	1.750	0.018	1.944	0.025
89-93	0.0	0.0	0.916	0.003								

Notes:

- "t" is load (MN/m)
- "z" is displacement (m)
- Data for tension and compression coincide
- Based on mudline at El. -4 meters

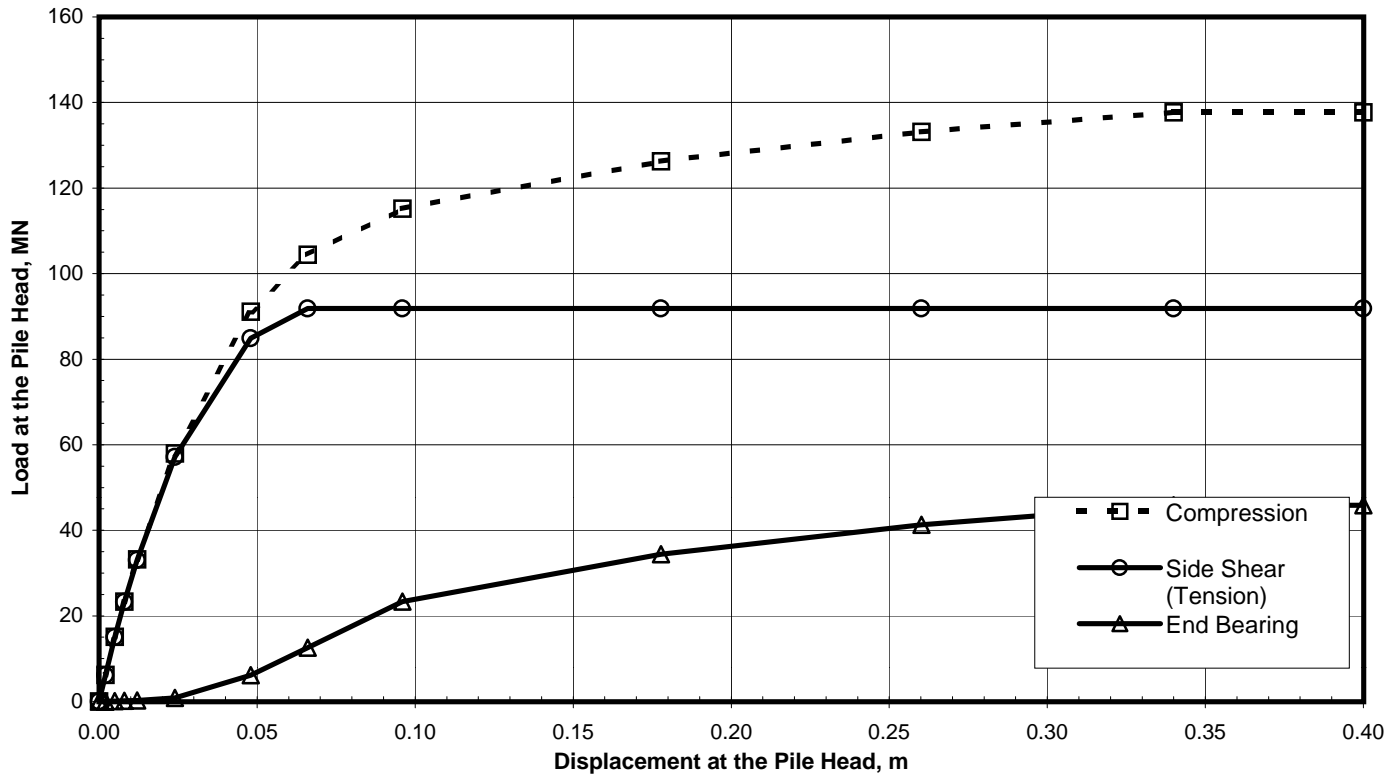
DEPTH (m)	Q-z Data											
	Q(1)	z(1)	Q(2)	z(2)	Q(3)	z(3)	Q(4)	z(4)	Q(5)	z(5)	Q(6)	z(6)
93	0.0	0.0	11.475	0.004	22.950	0.031	34.425	0.105	41.310	0.183	45.900	0.250

Notes:

- "Q" is load in compression (MN)
- "z" is displacement (m)

TABULATED AXIAL PILE LOAD TRANSFER DATA
Piers E12-Eastbound and Westbound (Boring 98-35)
 2.5-Meter-Diameter Pipe Piles (Pile Tip Elevation = -97 Meters)
 SFOBB East Span Seismic Safety Project





Pile Head Displacement (m)	Load at the Pile Head		End Bearing Component in Compression (MN)
	Compression (MN)	Tension (MN)	
0.000	0.00	0.00	0.00
0.002	6.19	6.17	0.02
0.005	15.12	15.06	0.06
0.008	23.36	23.24	0.12
0.012	33.23	33.03	0.20
0.024	57.98	57.18	0.80
0.048	91.09	84.93	6.16
0.066	104.40	91.84	12.56
0.096	115.20	91.84	23.36
0.178	126.24	91.84	34.40
0.260	133.11	91.84	41.27
0.340	137.70	91.84	45.86
0.400	137.70	91.84	45.86

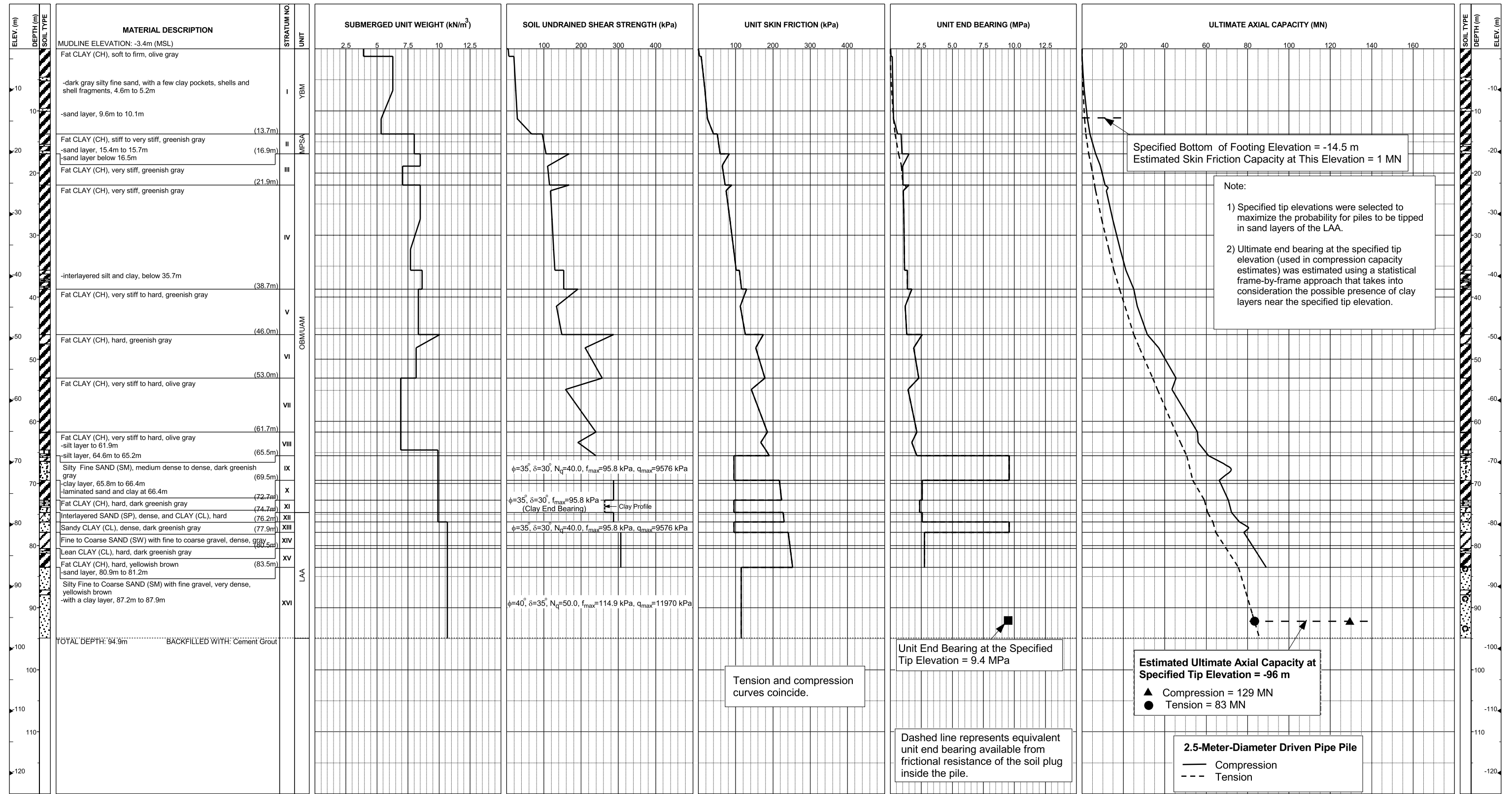
Note:

Pile head load-displacement curves are based on the preliminary pile wall thickness schedule provided by TY Lin/M&N and static loading conditions.

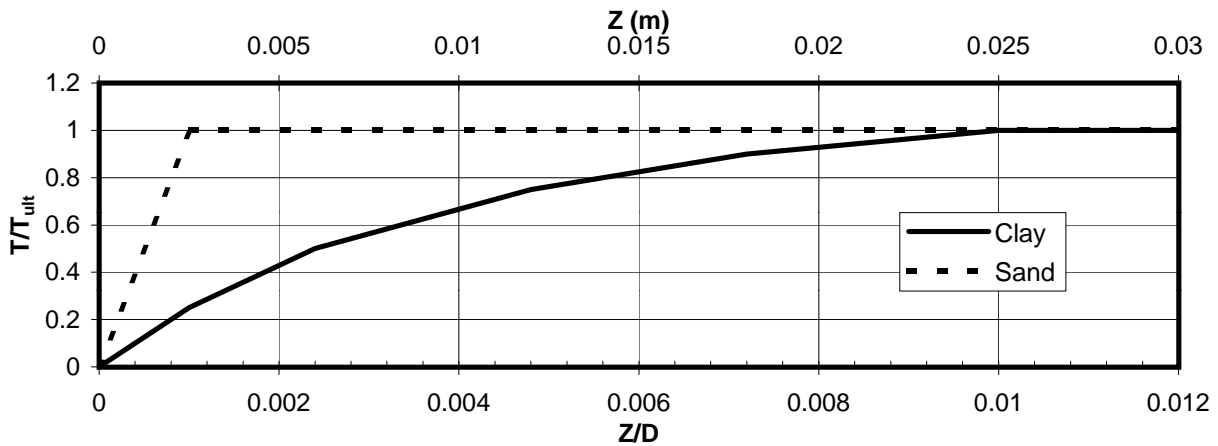
STATIC PILE HEAD LOAD-DEFORMATION CURVES
Piers E12-Eastbound and Westbound (Boring 98-35)
 2.5-Meter-Diameter Pipe Piles (Pile Tip Elevation = -97 Meters)
 SFOBB East Span Seismic Safety Project



**Pier E13-Eastbound (Boring 98-43)
Skyway Frame 3**



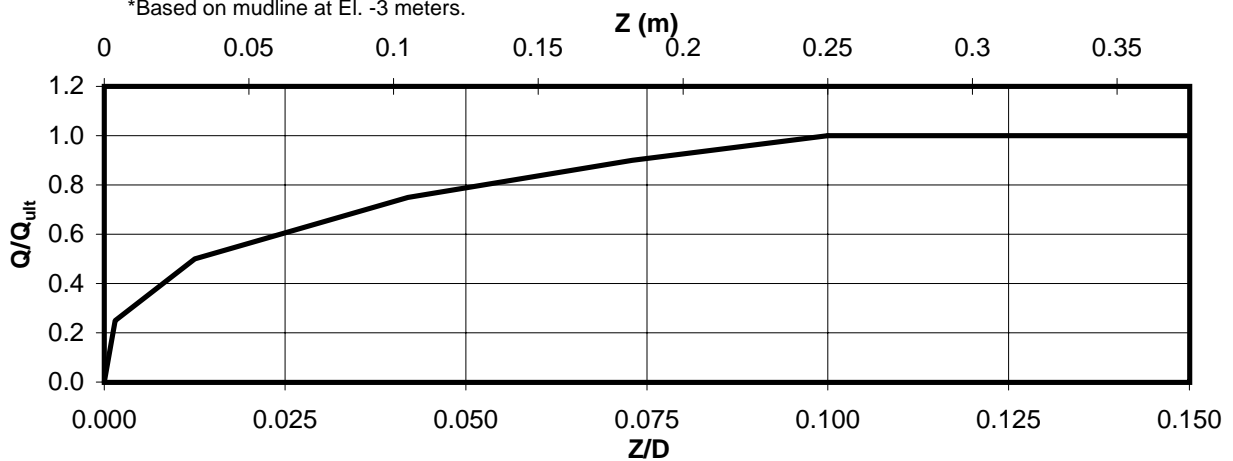
AXIAL PILE DESIGN PARAMETERS AND RESULTS
Pier E13-Eastbound (Boring 98-43)
SFOBB East Span Seismic Safety Project



Depth* (m)	Soil Type	T_{ult} (MN/m)
0-3	Clay	0.043
3-6	Clay	0.102
6-9	Clay	0.147
9-12	Clay	0.183
12-15	Clay	0.313
15-18	Clay	0.503
18-21	Clay	0.543
21-24	Clay	0.590
24-27	Clay	0.630
27-30	Clay	0.690
30-33	Clay	0.733
33-36	Clay	0.777

Depth* (m)	Soil Type	T_{ult} (MN/m)
36-39	Clay	0.890
39-42	Clay	0.937
42-45	Clay	0.920
45-51	Clay	1.218
51-57	Clay	1.278
57-63	Clay	1.337
63-69	Clay	1.102
69-75	Clay	1.433
75-81	Clay	1.408
81-88	Sand	1.395

*Based on mudline at El. -3 meters.



Depth* (m)	Soil Type	Q_{ult} (MN)
88	Sand	45.9

AXIAL PILE LOAD TRANSFER-DISPLACEMENT CURVES
Pier E13-Eastbound (Boring 98-43)
 2.5-Meter-Diameter Pipe Piles (Pile Tip Elevation = -91 Meters)
 SFOBB East Span Seismic Safety Project



DEPTH (m)	t-z Data											
	t(1)	z(1)	t(2)	z(2)	t(3)	z(3)	t(4)	z(4)	t(5)	z(5)	t(6)	z(6)
0-3	0.0	0.0	0.011	0.003	0.022	0.006	0.032	0.012	0.039	0.018	0.043	0.025
3-6	0.0	0.0	0.026	0.003	0.051	0.006	0.077	0.012	0.092	0.018	0.102	0.025
6-9	0.0	0.0	0.037	0.003	0.074	0.006	0.110	0.012	0.132	0.018	0.147	0.025
9-12	0.0	0.0	0.046	0.003	0.092	0.006	0.137	0.012	0.165	0.018	0.183	0.025
12-15	0.0	0.0	0.078	0.003	0.157	0.006	0.235	0.012	0.282	0.018	0.313	0.025
15-18	0.0	0.0	0.126	0.003	0.252	0.006	0.377	0.012	0.453	0.018	0.503	0.025
18-21	0.0	0.0	0.136	0.003	0.272	0.006	0.407	0.012	0.489	0.018	0.543	0.025
21-24	0.0	0.0	0.148	0.003	0.295	0.006	0.443	0.012	0.531	0.018	0.590	0.025
24-27	0.0	0.0	0.158	0.003	0.315	0.006	0.473	0.012	0.567	0.018	0.630	0.025
27-30	0.0	0.0	0.173	0.003	0.345	0.006	0.518	0.012	0.621	0.018	0.690	0.025
30-33	0.0	0.0	0.183	0.003	0.367	0.006	0.550	0.012	0.660	0.018	0.733	0.025
33-36	0.0	0.0	0.194	0.003	0.388	0.006	0.583	0.012	0.699	0.018	0.777	0.025
36-39	0.0	0.0	0.223	0.003	0.445	0.006	0.668	0.012	0.801	0.018	0.890	0.025
39-42	0.0	0.0	0.234	0.003	0.468	0.006	0.703	0.012	0.843	0.018	0.937	0.025
42-45	0.0	0.0	0.230	0.003	0.460	0.006	0.690	0.012	0.828	0.018	0.920	0.025
45-51	0.0	0.0	0.305	0.003	0.609	0.006	0.914	0.012	1.096	0.018	1.218	0.025
51-57	0.0	0.0	0.320	0.003	0.639	0.006	0.959	0.012	1.150	0.018	1.278	0.025
57-63	0.0	0.0	0.334	0.003	0.669	0.006	1.003	0.012	1.203	0.018	1.337	0.025
63-69	0.0	0.0	0.276	0.003	0.551	0.006	0.827	0.012	0.992	0.018	1.102	0.025
69-75	0.0	0.0	0.358	0.003	0.717	0.006	1.075	0.012	1.290	0.018	1.433	0.025
75-81	0.0	0.0	0.352	0.003	0.704	0.006	1.056	0.012	1.267	0.018	1.408	0.025
81-88	0.0	0.0	1.395	0.003								

Notes:

1. "t" is load (MN/m)
2. "z" is displacement (m)
3. Data for tension and compression coincide
4. Based on mudline at El. -3 meters

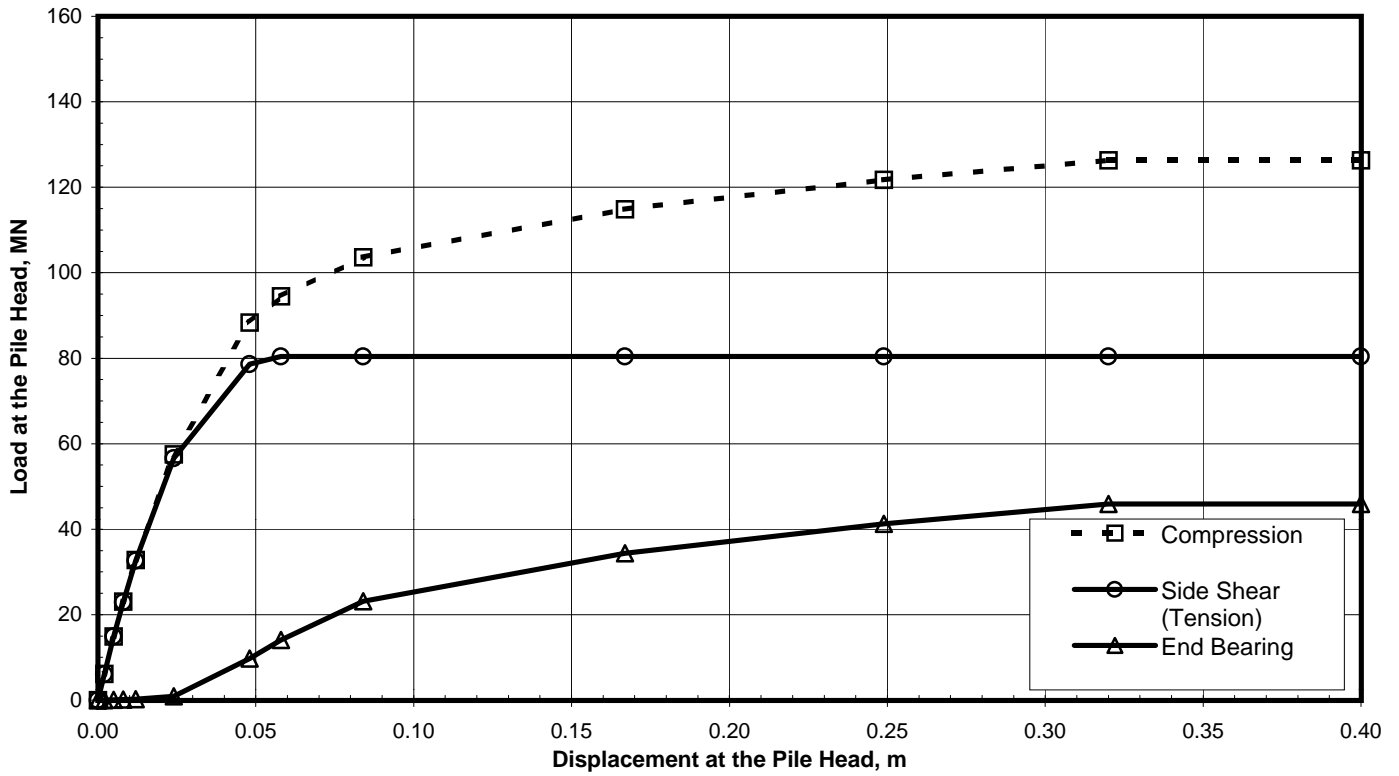
DEPTH (m)	Q-z Data											
	Q(1)	z(1)	Q(2)	z(2)	Q(3)	z(3)	Q(4)	z(4)	Q(5)	z(5)	Q(6)	z(6)
88	0.0	0.0	11.475	0.004	22.950	0.031	34.425	0.105	41.310	0.183	45.900	0.250

Notes:

1. "Q" is load in compression (MN)
2. "z" is displacement (m)

TABULATED AXIAL PILE LOAD TRANSFER DATA
Pier E13-Eastbound (Boring 98-43)
 2.5-Meter-Diameter Pipe Piles (Pile Tip Elevation = -91 Meters)
 SFOBB East Span Seismic Safety Project





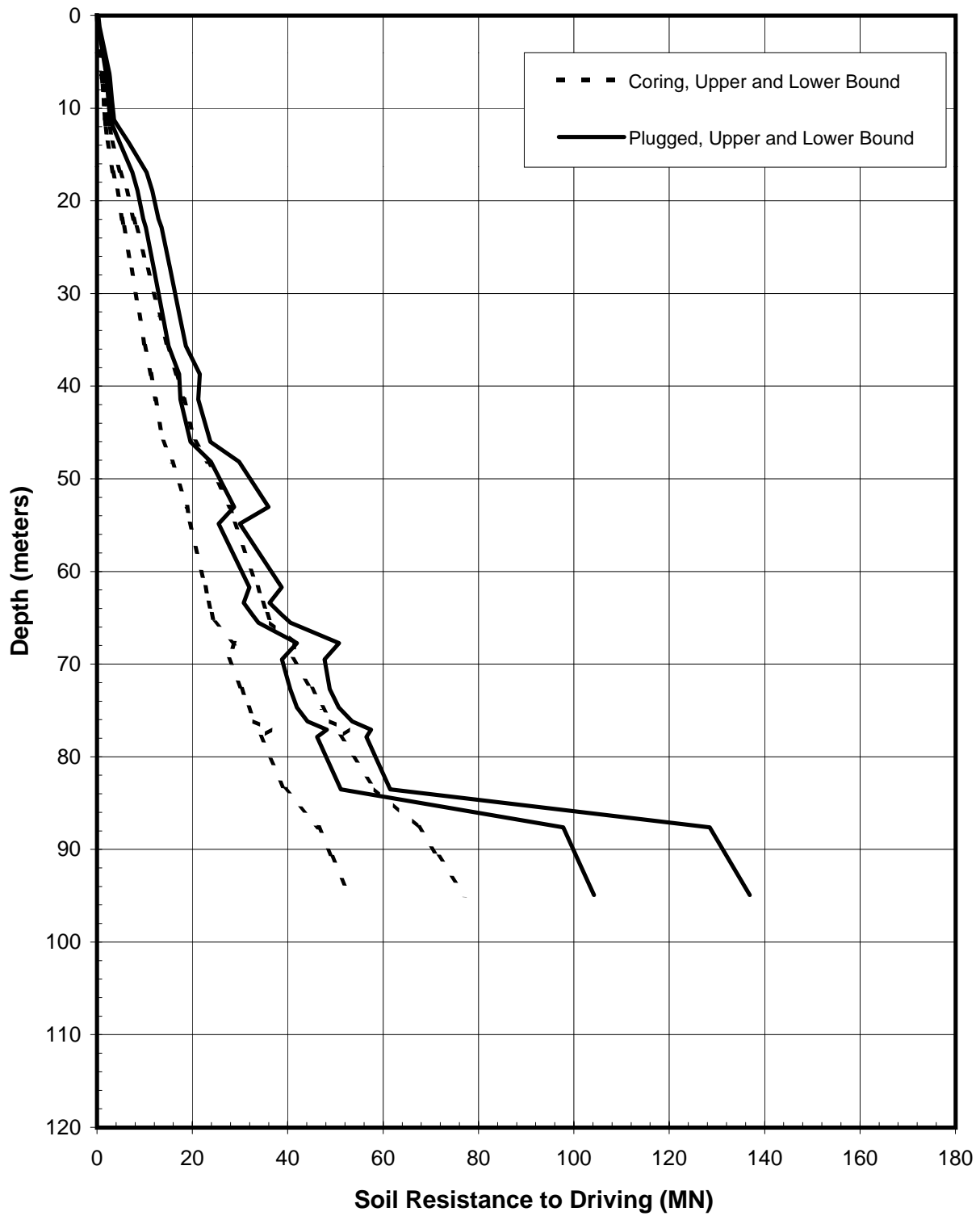
Pile Head Displacement (m)	Load at the Pile Head		End Bearing Component in Compression (MN)
	Compression (MN)	Tension (MN)	
0.000	0.00	0.00	0.00
0.002	6.12	6.09	0.02
0.005	14.93	14.87	0.07
0.008	23.06	22.94	0.12
0.012	32.83	32.62	0.21
0.024	57.51	56.60	0.91
0.048	88.35	78.65	9.70
0.058	94.47	80.43	14.04
0.084	103.60	80.43	23.17
0.167	114.83	80.43	34.40
0.249	121.71	80.43	41.28
0.320	126.30	80.43	45.87
0.400	126.30	80.43	45.87

Note:

Pile head load-displacement curves are based on the preliminary pile wall thickness schedule provided by TY Lin/M&N and static loading conditions.

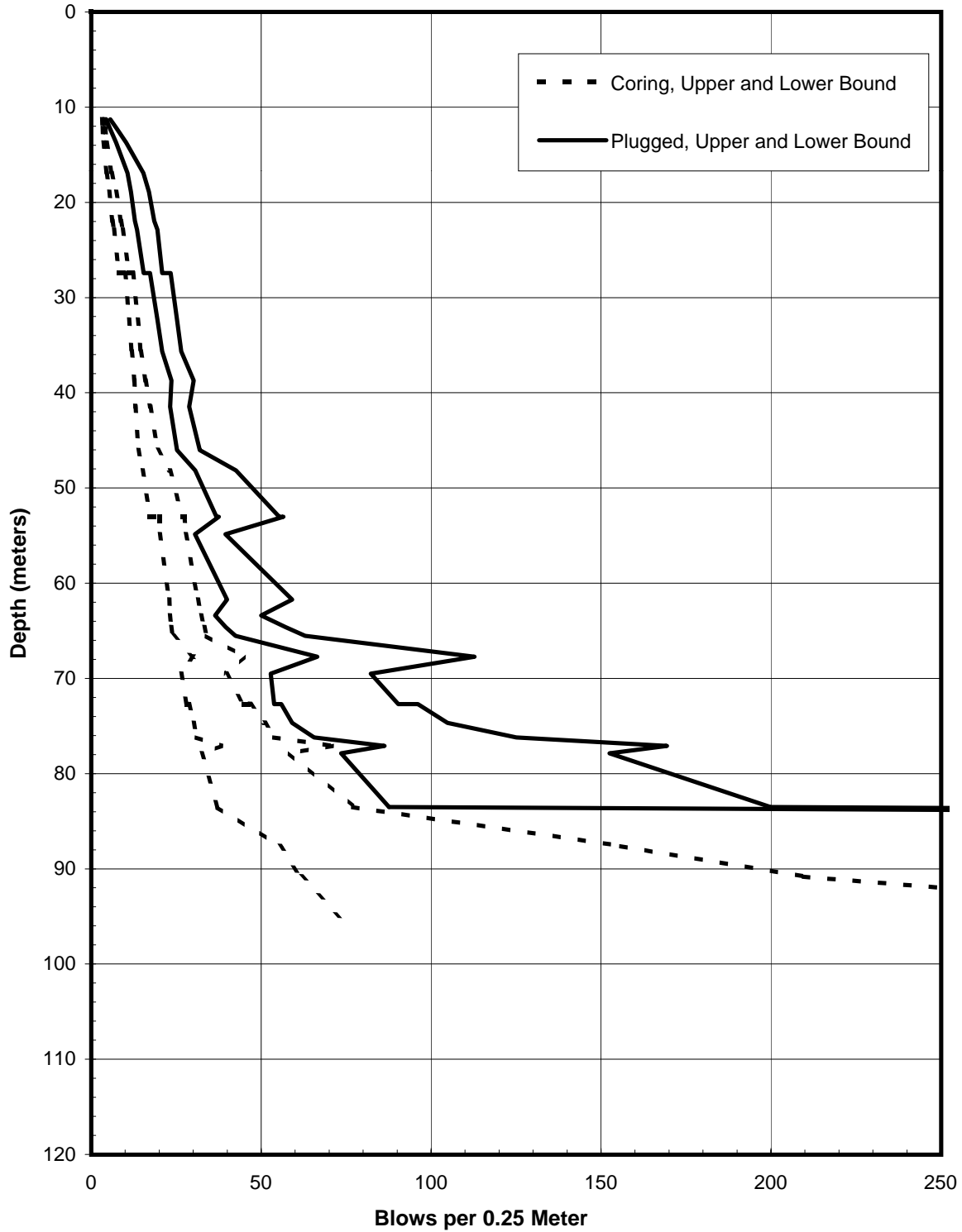
STATIC PILE HEAD LOAD-DEFORMATION CURVES
Pier E13-Eastbound (Boring 98-43)
 2.5-Meter-Diameter Pipe Piles (Pile Tip Elevation = -91 Meters)
 SFOBB East Span Seismic Safety Project





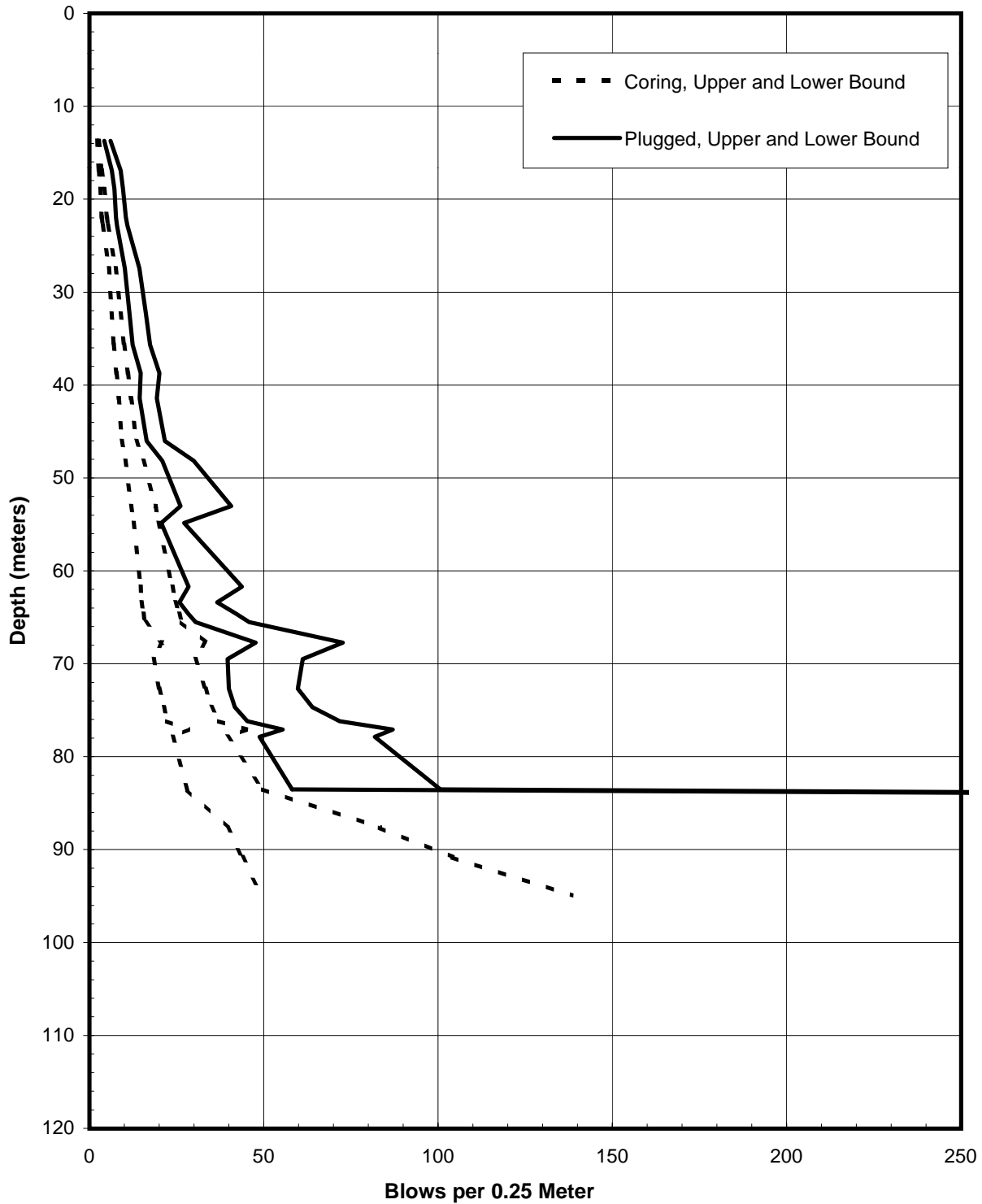
SOIL RESISTANCE TO DRIVING
Pier E13-Eastbound (Boring 98-43)
2.5-Meter-Diameter Driven Pipe Piles
SFOBB East Span Seismic Safety Project





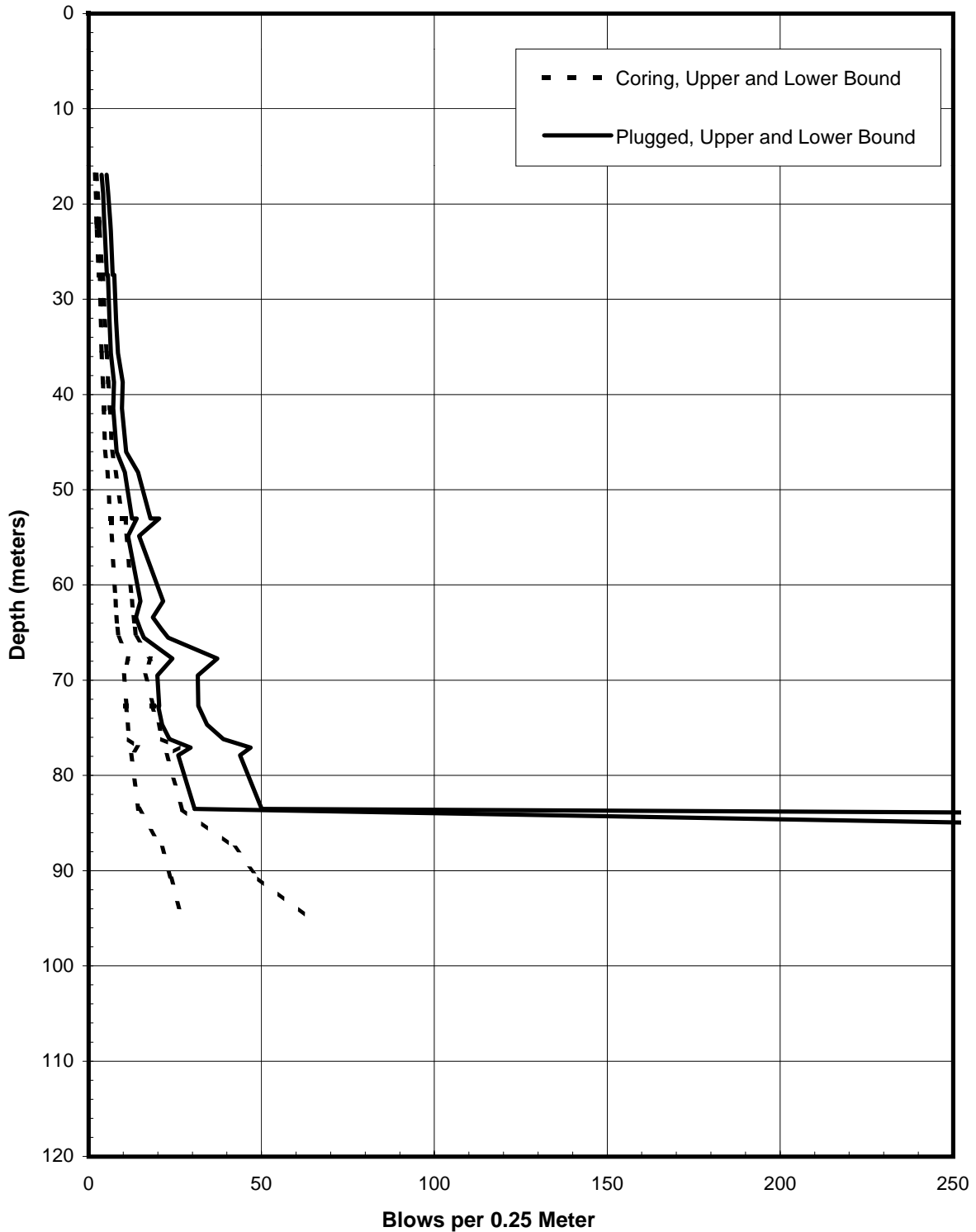
PREDICTED BLOW COUNTS
Pier E13-Eastbound (Boring 98-43)
Menck MHU-500T, 2.5-Meter-Diameter Driven Pipe Piles
SFOBB East Span Seismic Safety Project





PREDICTED BLOW COUNTS
Pier E13-Eastbound (Boring 98-43)
Menck MHU-1000, 2.5-Meter-Diameter Driven Pipe Piles
SFOBB East Span Seismic Safety Project

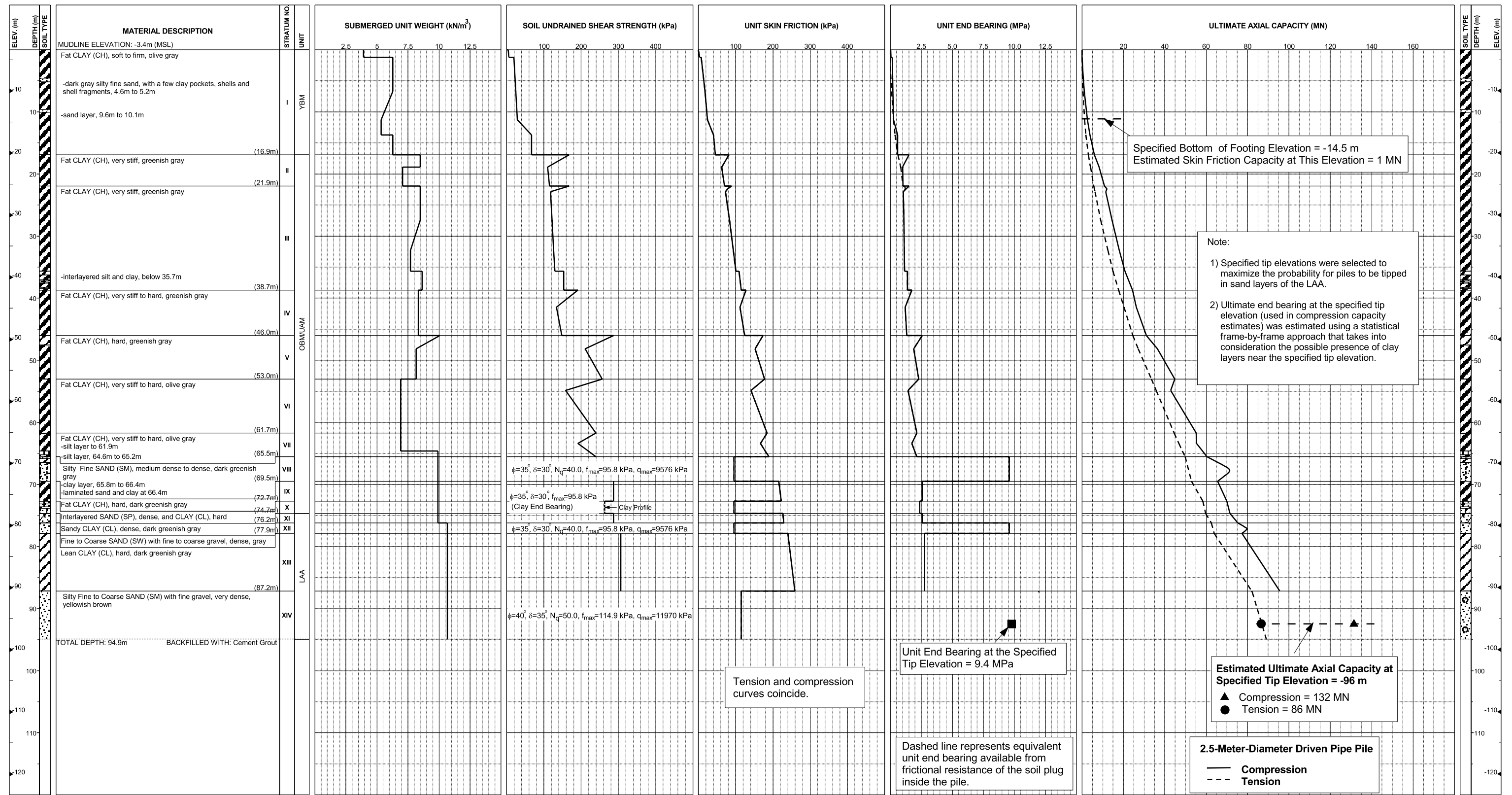




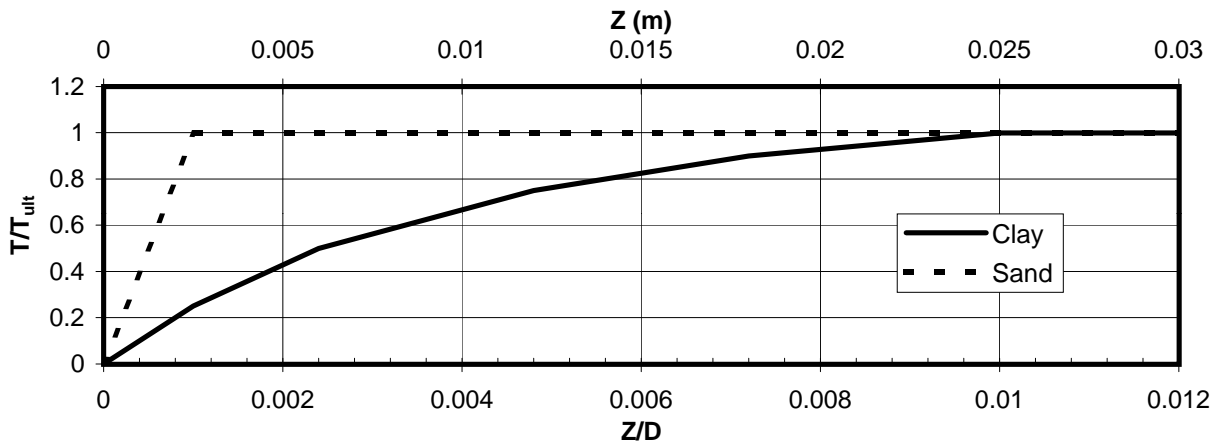
PREDICTED BLOW COUNTS
Pier E13-Eastbound (Boring 98-43)
Menck MHU-1700, 2.5-Meter-Diameter Driven Pipe Piles
SFOBB East Span Seismic Safety Project



**Pier E13-Westbound (Borings 98-43-Modified)
Skyway Frame 3**



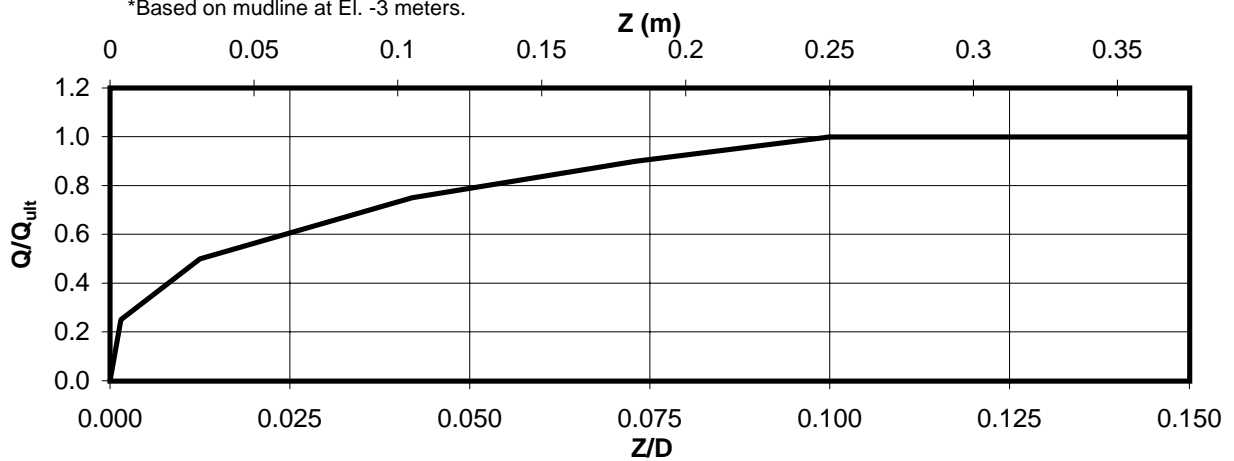
AXIAL PILE DESIGN PARAMETERS AND RESULTS
Pier E13-Westbound (Boring 98-43 Modified)
 SFOBB East Span Seismic Safety Project



Depth* (m)	Soil Type	T_{ult} (MN/m)
0-3	Clay	0.040
3-6	Clay	0.103
6-9	Clay	0.143
9-12	Clay	0.187
12-15	Clay	0.297
15-18	Clay	0.417
18-21	Clay	0.540
21-24	Clay	0.587
24-27	Clay	0.620
27-30	Clay	0.680
30-33	Clay	0.720
33-36	Clay	0.770

Depth* (m)	Soil Type	T_{ult} (MN/m)
36-39	Clay	0.877
39-42	Clay	0.933
42-45	Clay	0.913
45-51	Clay	1.208
51-57	Clay	1.267
57-63	Clay	1.330
63-69	Clay	1.098
69-75	Clay	1.423
75-81	Clay	1.407
81-87	Clay	2.031
87-91	Sand	0.899

*Based on mudline at El. -3 meters.



Depth* (m)	Soil Type	Q_{ult} (MN)
91	Sand	45.9

AXIAL PILE LOAD TRANSFER-DISPLACEMENT CURVES
Pier E13-Westbound (Boring 98-43 Modified)
 2.5-Meter-Diameter Pipe Piles (Pile Tip Elevation = -94 Meters)
 SFOBB East Span Seismic Safety Project





DEPTH (m)	t-z Data											
	t(1)	z(1)	t(2)	z(2)	t(3)	z(3)	t(4)	z(4)	t(5)	z(5)	t(6)	z(6)
0-3	0.0	0.0	0.010	0.003	0.020	0.006	0.030	0.012	0.036	0.018	0.040	0.025
3-6	0.0	0.0	0.026	0.003	0.052	0.006	0.077	0.012	0.093	0.018	0.103	0.025
6-9	0.0	0.0	0.036	0.003	0.072	0.006	0.107	0.012	0.129	0.018	0.143	0.025
9-12	0.0	0.0	0.047	0.003	0.093	0.006	0.140	0.012	0.168	0.018	0.187	0.025
12-15	0.0	0.0	0.074	0.003	0.148	0.006	0.223	0.012	0.267	0.018	0.297	0.025
15-18	0.0	0.0	0.104	0.003	0.208	0.006	0.313	0.012	0.375	0.018	0.417	0.025
18-21	0.0	0.0	0.135	0.003	0.270	0.006	0.405	0.012	0.486	0.018	0.540	0.025
21-24	0.0	0.0	0.147	0.003	0.293	0.006	0.440	0.012	0.528	0.018	0.587	0.025
24-27	0.0	0.0	0.155	0.003	0.310	0.006	0.465	0.012	0.558	0.018	0.620	0.025
27-30	0.0	0.0	0.170	0.003	0.340	0.006	0.510	0.012	0.612	0.018	0.680	0.025
30-33	0.0	0.0	0.180	0.003	0.360	0.006	0.540	0.012	0.648	0.018	0.720	0.025
33-36	0.0	0.0	0.193	0.003	0.385	0.006	0.578	0.012	0.693	0.018	0.770	0.025
36-39	0.0	0.0	0.219	0.003	0.438	0.006	0.658	0.012	0.789	0.018	0.877	0.025
39-42	0.0	0.0	0.233	0.003	0.467	0.006	0.700	0.012	0.840	0.018	0.933	0.025
42-45	0.0	0.0	0.228	0.003	0.457	0.006	0.685	0.012	0.822	0.018	0.913	0.025
45-51	0.0	0.0	0.302	0.003	0.604	0.006	0.906	0.012	1.087	0.018	1.208	0.025
51-57	0.0	0.0	0.317	0.003	0.634	0.006	0.950	0.012	1.140	0.018	1.267	0.025
57-63	0.0	0.0	0.333	0.003	0.665	0.006	0.998	0.012	1.197	0.018	1.330	0.025
63-69	0.0	0.0	0.275	0.003	0.549	0.006	0.824	0.012	0.988	0.018	1.098	0.025
69-75	0.0	0.0	0.356	0.003	0.712	0.006	1.067	0.012	1.281	0.018	1.423	0.025
75-81	0.0	0.0	0.352	0.003	0.704	0.006	1.055	0.012	1.266	0.018	1.407	0.025
81-87	0.0	0.0	0.508	0.003	1.016	0.006	1.523	0.012	1.828	0.018	2.031	0.025
87-91	0.0	0.0	0.899	0.003								

Notes:

1. "t" is load (MN/m)
2. "z" is displacement (m)
3. Data for tension and compression coincide
4. Based on mudline at El. -3 meters

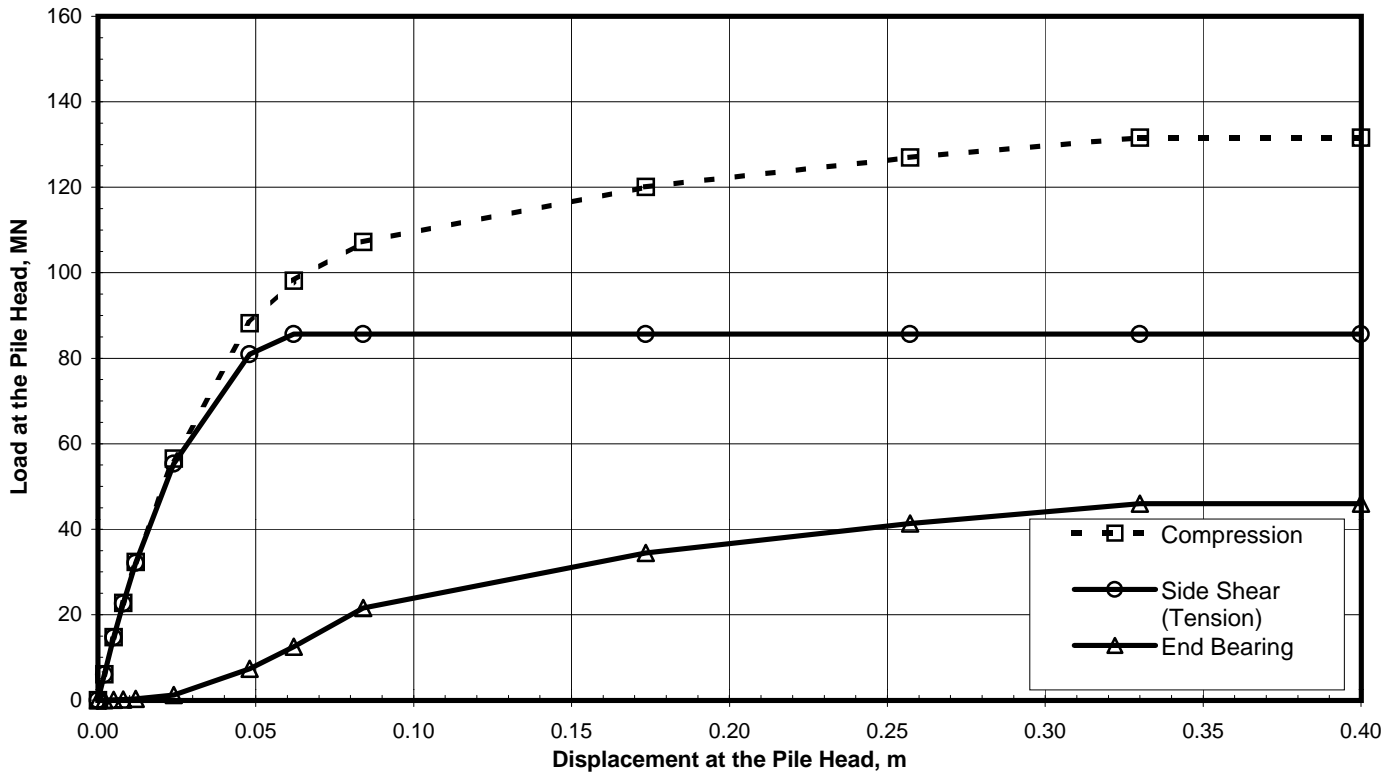
DEPTH (m)	Q-z Data											
	Q(1)	z(1)	Q(2)	z(2)	Q(3)	z(3)	Q(4)	z(4)	Q(5)	z(5)	Q(6)	z(6)
91	0.0	0.0	11.475	0.004	22.950	0.031	34.425	0.105	41.310	0.183	45.900	0.250

Notes:

1. "Q" is load in compression (MN)
2. "z" is displacement (m)

TABULATED AXIAL PILE LOAD TRANSFER DATA
Pier E13-Westbound (Boring 98-43 Modified)
 2.5-Meter-Diameter Pipe Piles (Pile Tip Elevation = -94 Meters)
 SFOBB East Span Seismic Safety Project





Pile Head Displacement (m)	Load at the Pile Head		End Bearing Component in Compression (MN)
	Compression (MN)	Tension (MN)	
0.000	0.00	0.00	0.00
0.002	6.04	6.01	0.03
0.005	14.74	14.65	0.09
0.008	22.75	22.60	0.15
0.012	32.37	32.10	0.27
0.024	56.53	55.33	1.20
0.048	88.20	80.90	7.30
0.062	98.18	85.66	12.52
0.084	107.20	85.66	21.54
0.174	120.12	85.66	34.46
0.257	127.01	85.66	41.35
0.330	131.60	85.66	45.94
0.400	131.60	85.66	45.94

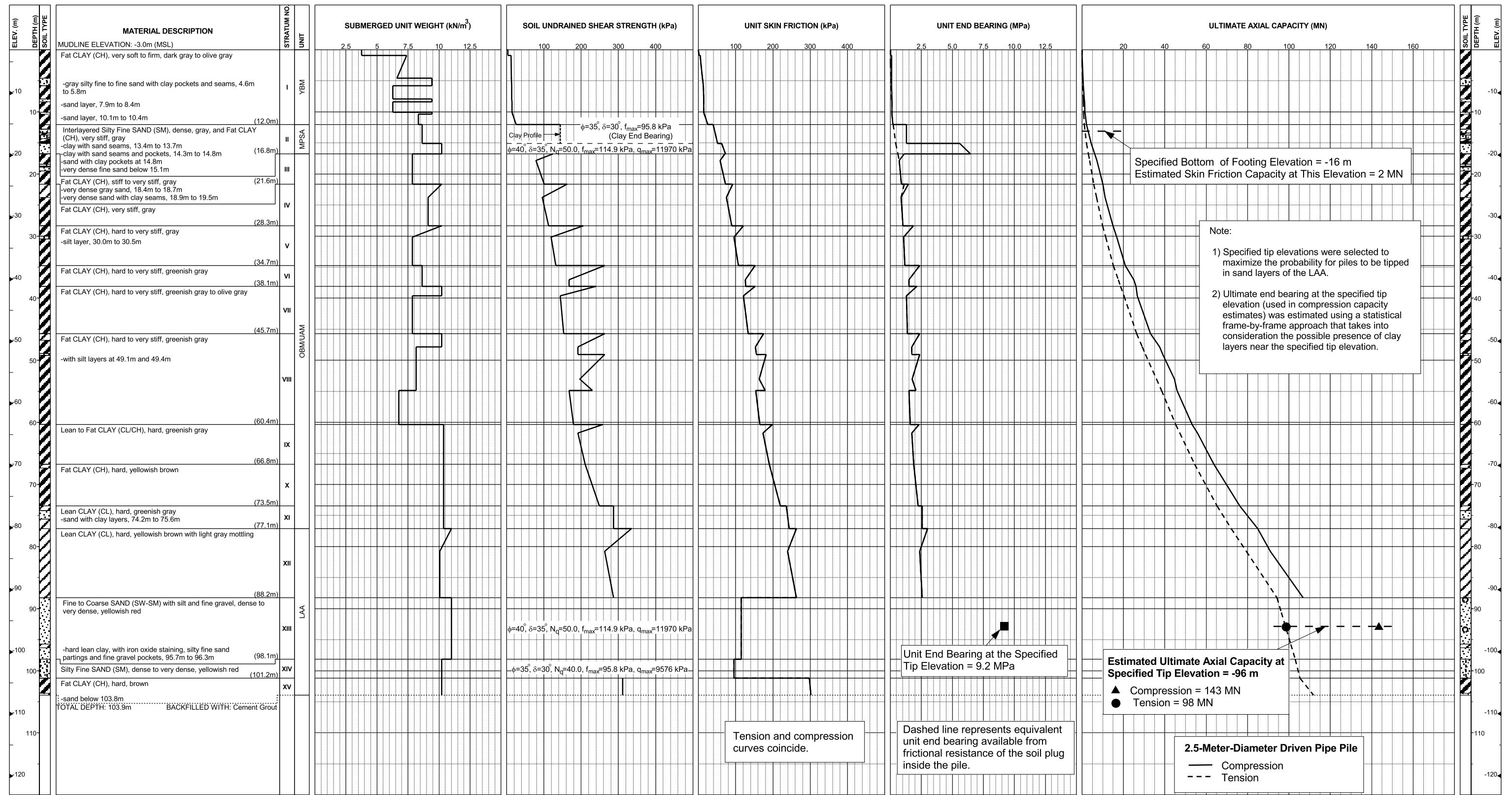
Note:

Pile head load-displacement curves are based on the preliminary pile wall thickness schedule provided by TY Lin/M&N and static loading conditions.

STATIC PILE HEAD LOAD-DEFORMATION CURVES
Pier E13-Westbound (Boring 98-43 Modified)
 2.5-Meter-Diameter Pipe Piles (Pile Tip Elevation = -94 Meters)
 SFOBB East Span Seismic Safety Project

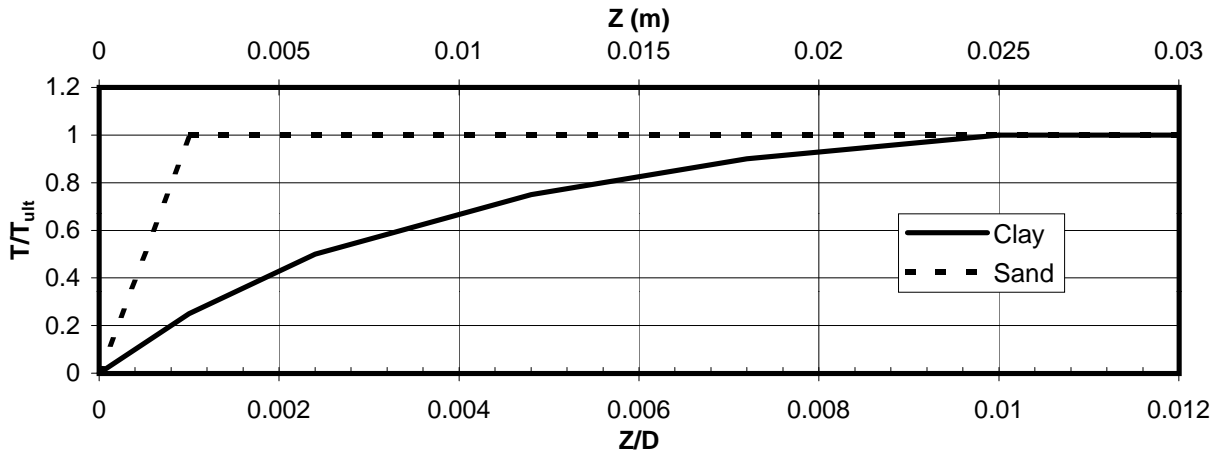


**Pier E14-Eastbound and Westbound (Boring 98-36)
Skyway Frame 4**



AXIAL PILE DESIGN PARAMETERS AND RESULTS
Piers E14-Eastbound and Westbound (Boring 98-36)
 SFOBB East Span Seismic Safety Project

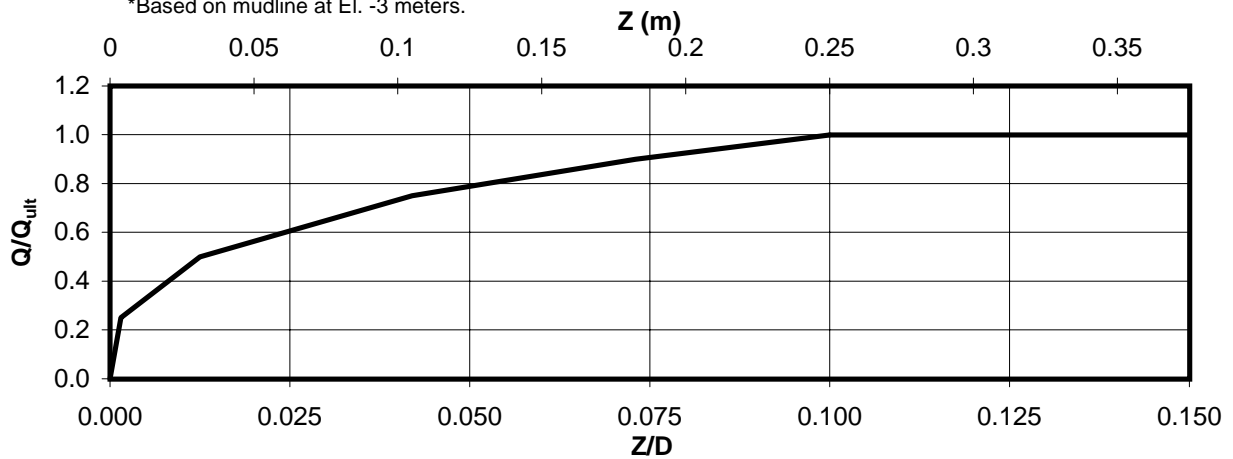




Depth* (m)	Soil Type	T _{ult} (MN/m)
0-3	Clay	0.030
3-6	Clay	0.080
6-9	Clay	0.113
9-12	Clay	0.137
12-15	Sand	0.360
15-18	Sand	0.547
18-21	Clay	0.470
21-24	Clay	0.640
24-27	Clay	0.613
27-30	Clay	0.817
30-33	Clay	0.766
33-36	Clay	0.907

Depth* (m)	Soil Type	T _{ult} (MN/m)
36-39	Clay	1.087
39-42	Clay	0.977
42-45	Clay	0.997
45-51	Clay	1.265
51-57	Clay	1.312
57-63	Clay	1.338
63-69	Clay	1.468
69-75	Clay	1.720
75-81	Clay	1.967
81-88	Clay	1.966
88-92	Sand	0.927

*Based on mudline at El. -3 meters.



Depth* (m)	Soil Type	Q _{ult} (MN)
92	Sand	48.1

AXIAL PILE LOAD TRANSFER-DISPLACEMENT CURVES
Piers E14-Eastbound and Westbound (Boring 98-36)
 2.5-Meter-Diameter Pipe Piles (Pile Tip Elevation = -95 Meters)
 SFOBB East Span Seismic Safety Project



DEPTH (m)	t-z Data											
	t(1)	z(1)	t(2)	z(2)	t(3)	z(3)	t(4)	z(4)	t(5)	z(5)	t(6)	z(6)
0-3	0.0	0.0	0.008	0.003	0.015	0.006	0.023	0.012	0.027	0.018	0.030	0.025
3-6	0.0	0.0	0.020	0.003	0.040	0.006	0.060	0.012	0.072	0.018	0.080	0.025
6-9	0.0	0.0	0.028	0.003	0.057	0.006	0.085	0.012	0.102	0.018	0.113	0.025
9-12	0.0	0.0	0.034	0.003	0.068	0.006	0.103	0.012	0.123	0.018	0.137	0.025
12-15	0.0	0.0	0.360	0.003								
15-18	0.0	0.0	0.547	0.003								
18-21	0.0	0.0	0.118	0.003	0.235	0.006	0.353	0.012	0.423	0.018	0.470	0.025
21-24	0.0	0.0	0.160	0.003	0.320	0.006	0.480	0.012	0.576	0.018	0.640	0.025
24-27	0.0	0.0	0.153	0.003	0.307	0.006	0.460	0.012	0.552	0.018	0.613	0.025
27-30	0.0	0.0	0.204	0.003	0.408	0.006	0.613	0.012	0.735	0.018	0.817	0.025
30-33	0.0	0.0	0.192	0.003	0.383	0.006	0.575	0.012	0.690	0.018	0.766	0.025
33-36	0.0	0.0	0.227	0.003	0.453	0.006	0.680	0.012	0.816	0.018	0.907	0.025
36-39	0.0	0.0	0.272	0.003	0.544	0.006	0.815	0.012	0.978	0.018	1.087	0.025
39-42	0.0	0.0	0.244	0.003	0.488	0.006	0.733	0.012	0.879	0.018	0.977	0.025
42-45	0.0	0.0	0.249	0.003	0.498	0.006	0.748	0.012	0.897	0.018	0.997	0.025
45-51	0.0	0.0	0.316	0.003	0.633	0.006	0.949	0.012	1.139	0.018	1.265	0.025
51-57	0.0	0.0	0.328	0.003	0.656	0.006	0.984	0.012	1.181	0.018	1.312	0.025
57-63	0.0	0.0	0.335	0.003	0.669	0.006	1.004	0.012	1.204	0.018	1.338	0.025
63-69	0.0	0.0	0.367	0.003	0.734	0.006	1.101	0.012	1.321	0.018	1.468	0.025
69-75	0.0	0.0	0.430	0.003	0.860	0.006	1.290	0.012	1.548	0.018	1.720	0.025
75-81	0.0	0.0	0.492	0.003	0.984	0.006	1.475	0.012	1.770	0.018	1.967	0.025
81-88	0.0	0.0	0.492	0.003	0.983	0.006	1.475	0.012	1.769	0.018	1.966	0.025
88-92	0.0	0.0	0.927	0.003								

Notes:

1. "t" is load (MN/m)
2. "z" is displacement (m)
3. Data for tension and compression coincide
4. Based on mudline at El. -3 meters

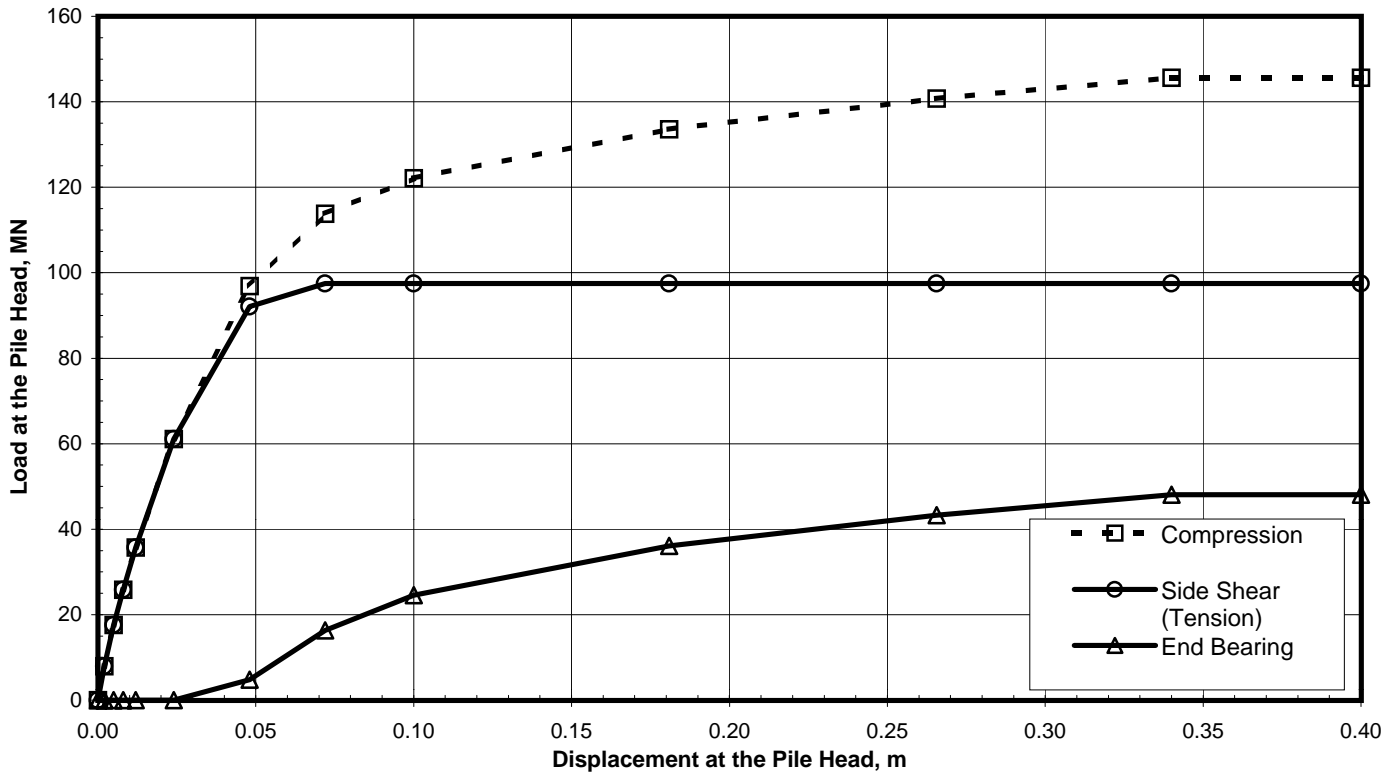
DEPTH (m)	Q-z Data											
	Q(1)	z(1)	Q(2)	z(2)	Q(3)	z(3)	Q(4)	z(4)	Q(5)	z(5)	Q(6)	z(6)
92	0.0	0.0	12.025	0.004	24.050	0.031	36.075	0.105	43.290	0.183	48.100	0.250

Notes:

1. "Q" is load in compression (MN)
2. "z" is displacement (m)

TABULATED AXIAL PILE LOAD TRANSFER DATA
Piers E14-Eastbound and Westbound (Boring 98-36)
 2.5-Meter-Diameter Pipe Piles (Pile Tip Elevation = -95 Meters)
 SFOBB East Span Seismic Safety Project



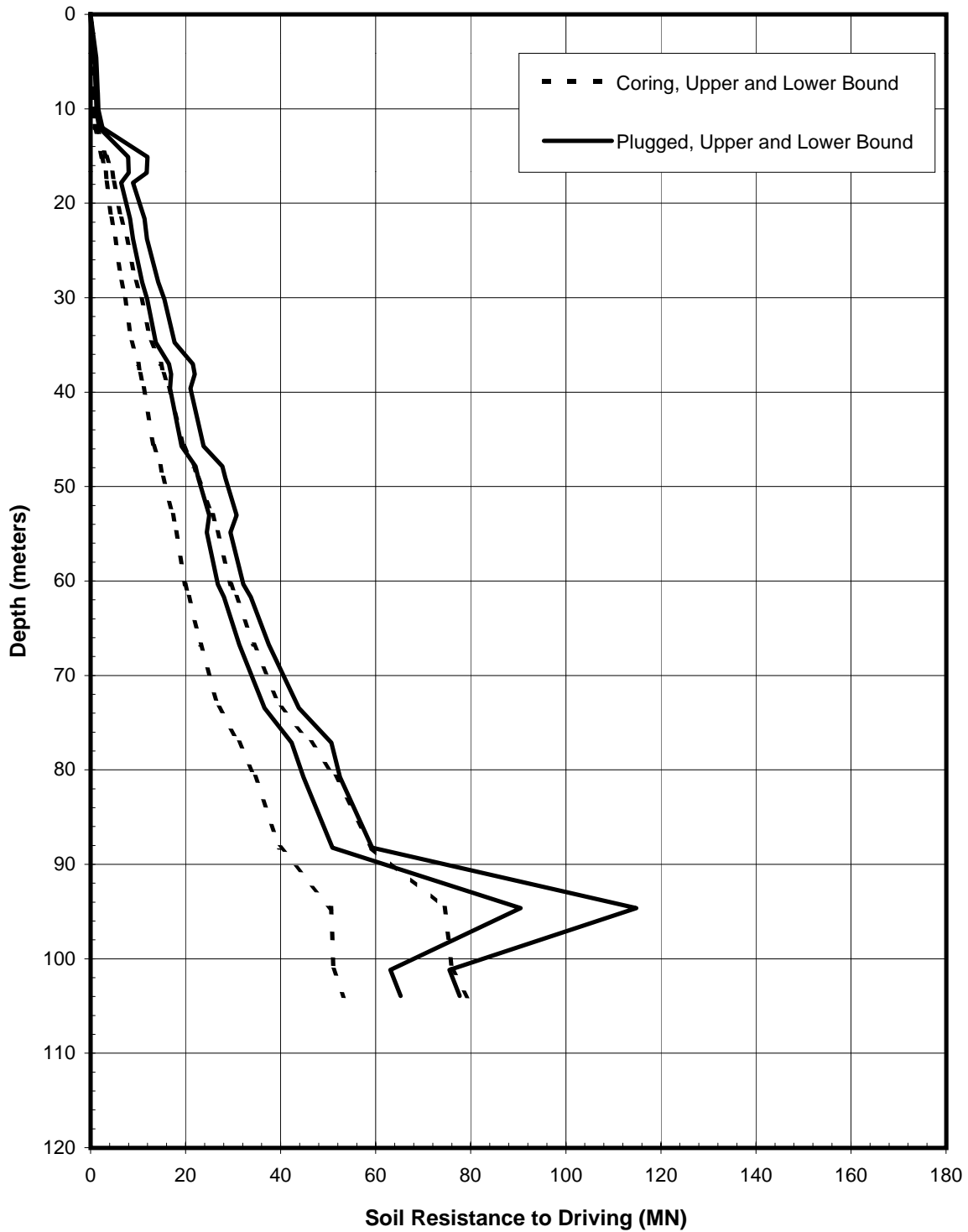


Pile Head Displacement (m)	Load at the Pile Head		End Bearing Component in Compression (MN)
	Compression (MN)	Tension (MN)	
0.000	0.00	0.00	0.00
0.002	7.92	7.92	0.00
0.005	17.63	17.63	0.00
0.008	25.81	25.81	0.00
0.012	35.69	35.69	0.00
0.024	61.12	61.11	0.01
0.048	96.85	92.09	4.76
0.072	113.80	97.51	16.29
0.100	122.10	97.51	24.59
0.181	133.58	97.51	36.07
0.266	140.79	97.51	43.28
0.340	145.60	97.51	48.09
0.400	145.60	97.51	48.09

Note:
 Pile head load-displacement curves are based on the preliminary pile wall thickness schedule provided by TY Lin/M&N and static loading conditions.

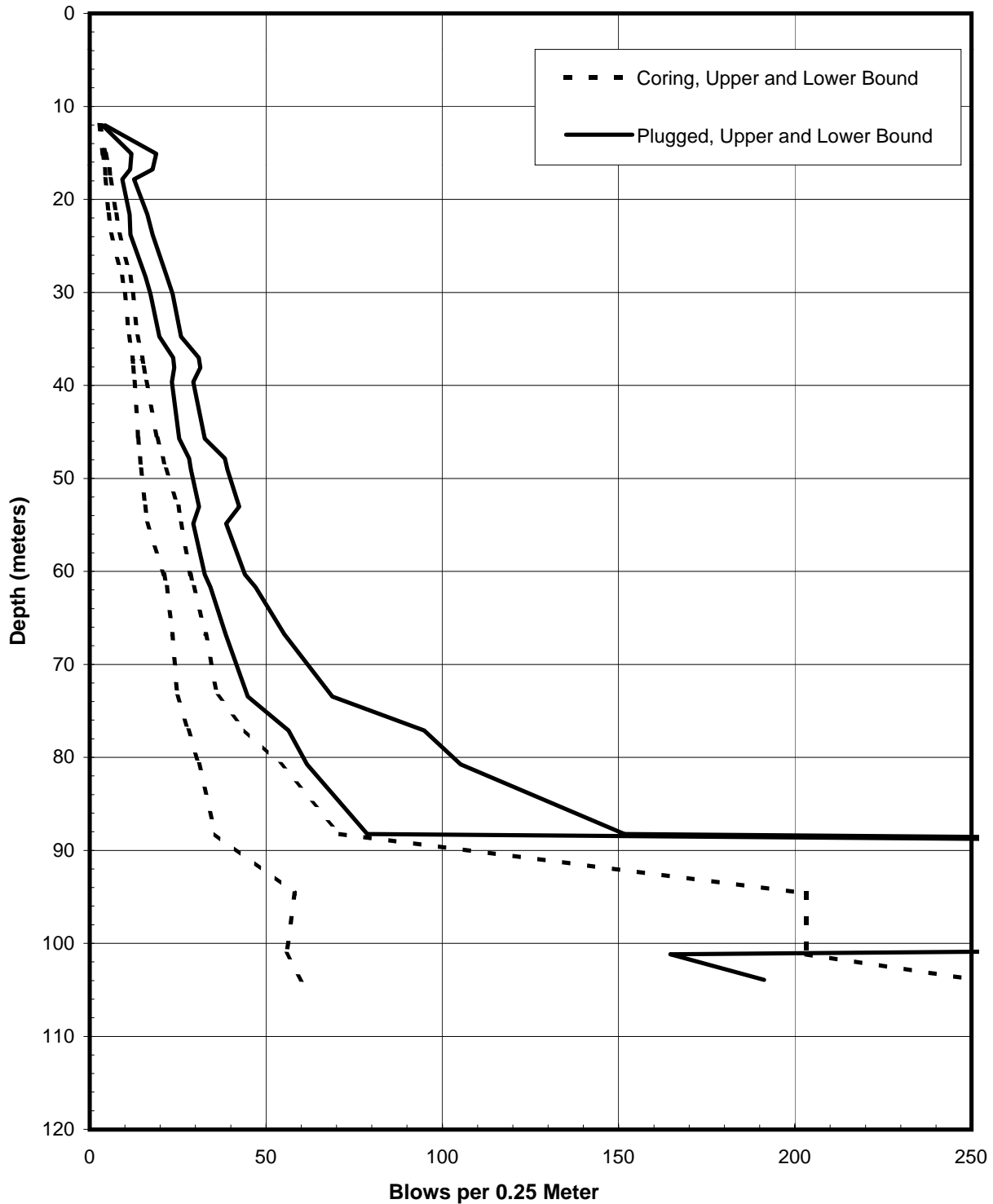
STATIC PILE HEAD LOAD-DEFORMATION CURVES
Piers E14-Eastbound and Westbound (Boring 98-36)
 2.5-Meter-Diameter Pipe Piles (Pile Tip Elevation = -95 Meters)
 SFOBB East Span Seismic Safety Project





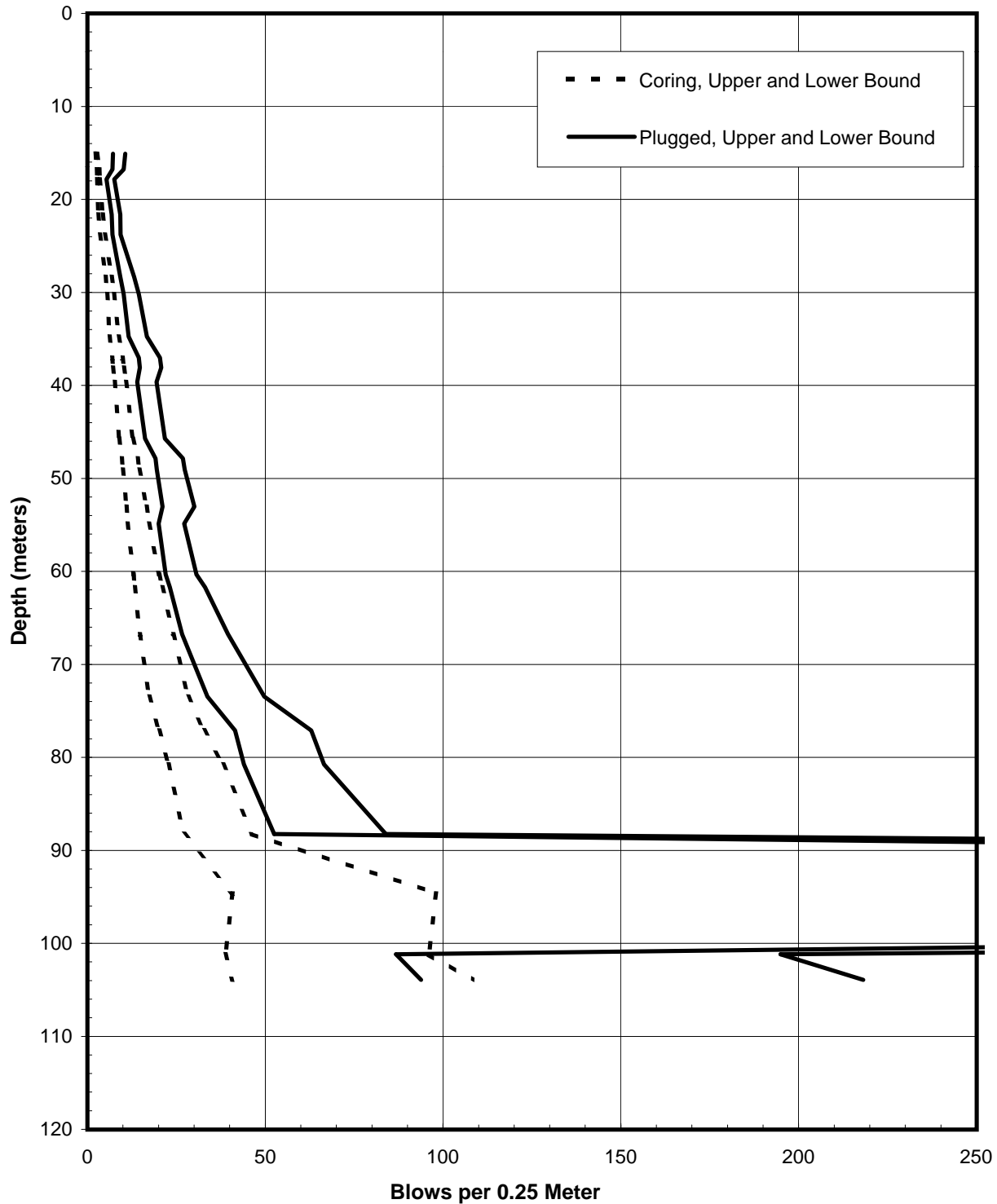
SOIL RESISTANCE TO DRIVING
Piers E14-Eastbound and Westbound (Boring 98-36)
2.5-Meter-Diameter Driven Pipe Piles
SFOBB East Span Seismic Safety Project





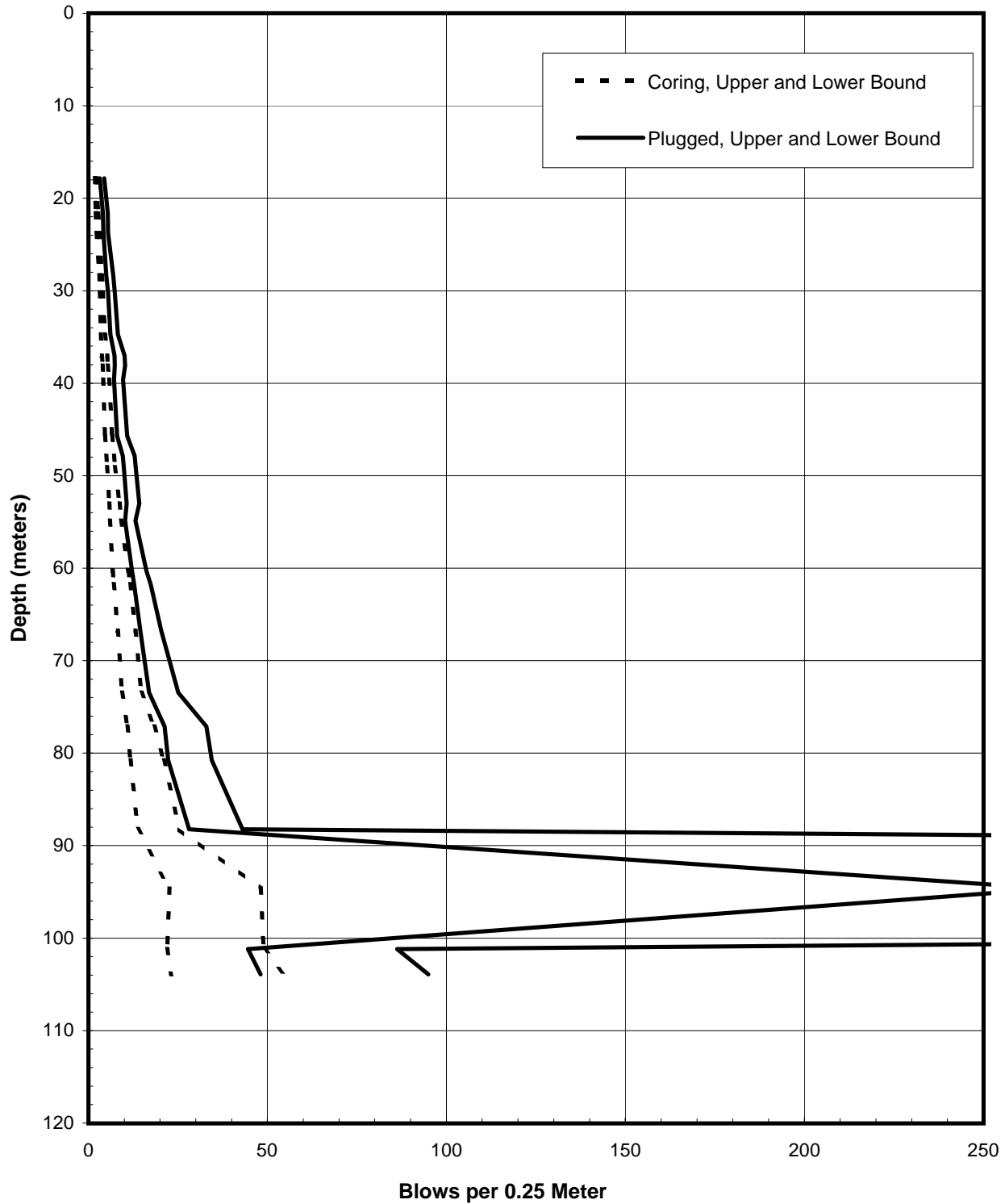
PREDICTED BLOW COUNTS
Piers E14-Eastbound and Westbound (Boring 98-36)
Menck MHU-500T, 2.5-Meter-Diameter Driven Pipe Piles
SFOBB East Span Seismic Safety Project





PREDICTED BLOW COUNTS
Piers E14-Eastbound and Westbound (Boring 98-36)
Menck MHU-1000, 2.5-Meter-Diameter Driven Pipe Piles
SFOBB East Span Seismic Safety Project

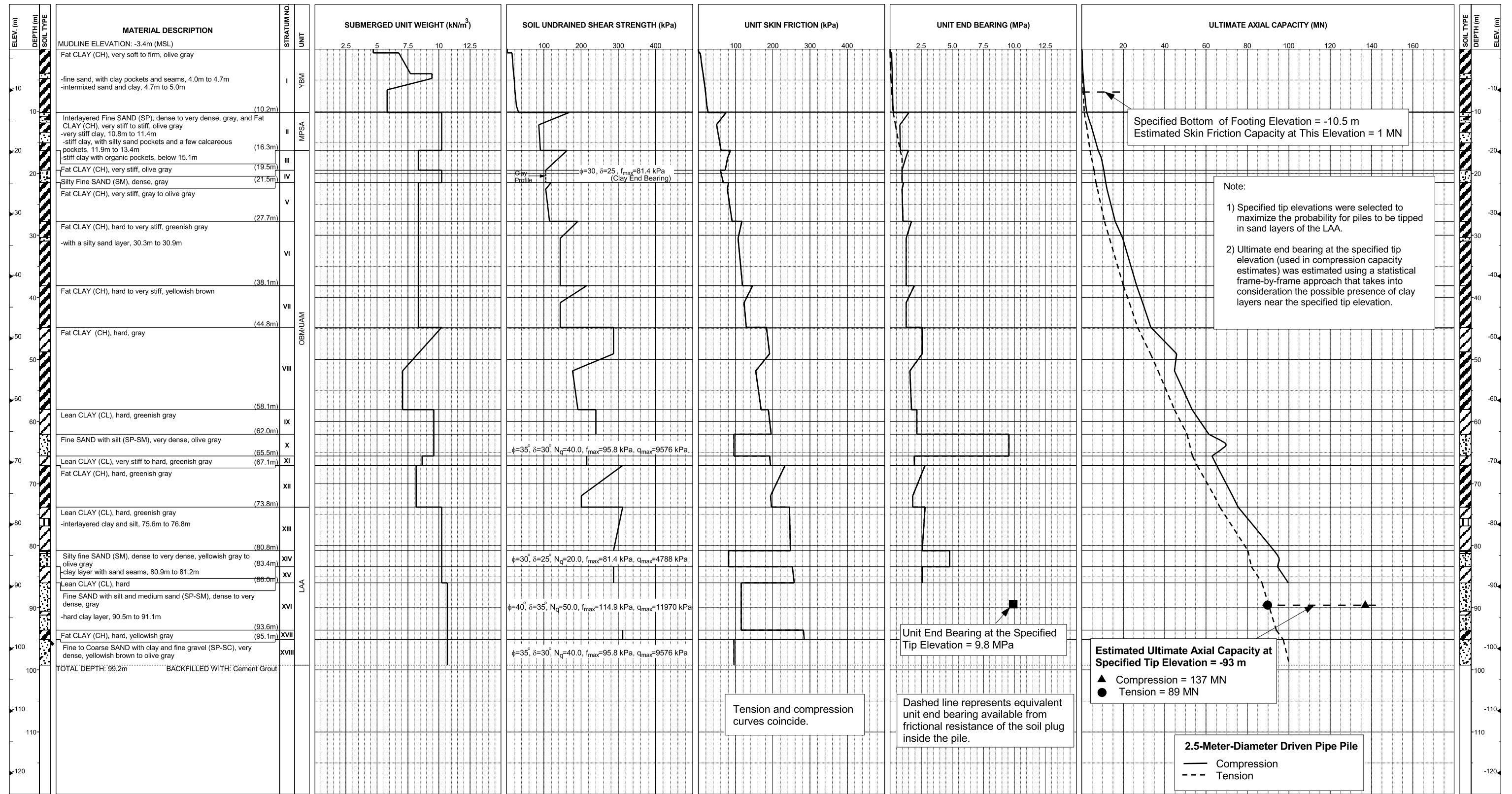




PREDICTED BLOW COUNTS
Piers E14-Eastbound and Westbound (Boring 98-36)
Menck MHU-1700, 2.5-Meter-Diameter Driven Pipe Piles
SFOBB East Span Seismic Safety Project

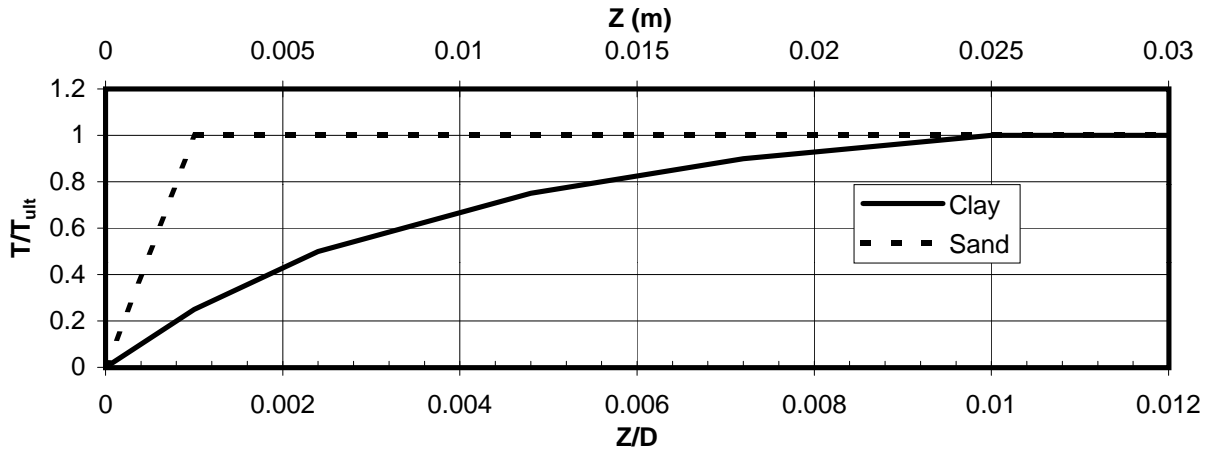


**Pier E15-Eastbound and Westbound (Boring 98-37)
Skyway Frame 4**



AXIAL PILE DESIGN PARAMETERS AND RESULTS
Piers E15-Eastbound and Westbound (Boring 98-37)
SFOBB East Span Seismic Safety Project

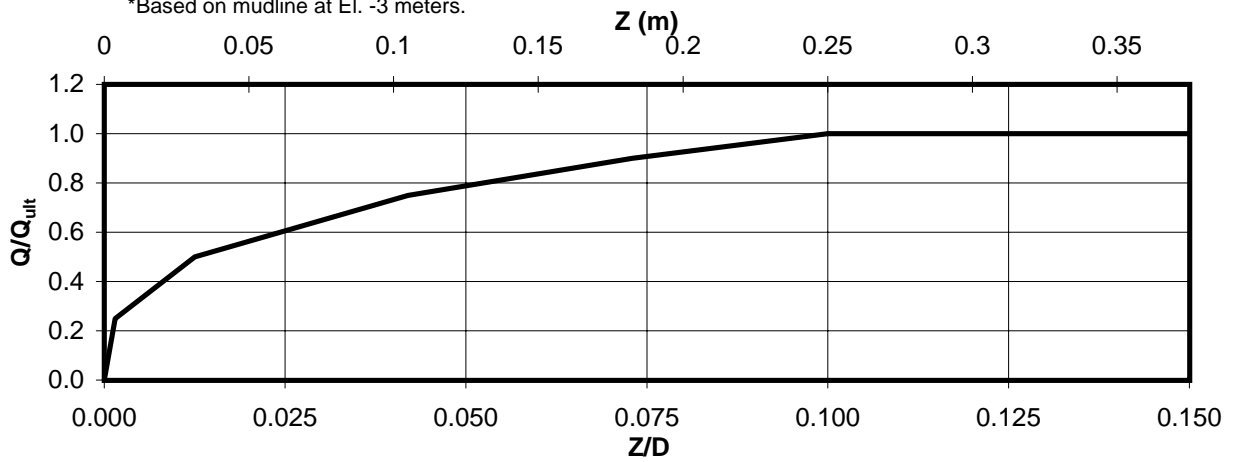




Depth* (m)	Soil Type	T _{ult} (MN/m)
0-3	Clay	0.027
3-6	Clay	0.110
6-9	Clay	0.150
9-12	Clay	0.387
12-15	Clay	0.420
15-18	Clay	0.573
18-21	Clay	0.570
21-24	Clay	0.613
24-27	Clay	0.660
27-30	Clay	0.817
30-33	Clay	0.857
33-36	Clay	0.890

Depth* (m)	Soil Type	T _{ult} (MN/m)
36-39	Clay	0.970
39-42	Clay	1.033
42-45	Clay	0.983
45-51	Clay	1.460
51-57	Clay	1.245
57-63	Clay	1.408
63-69	Clay	1.117
69-75	Clay	1.660
75-81	Clay	1.958
81-83	Sand	0.639
83-86	Clay	1.997
86-90	Sand	0.903

*Based on mudline at El. -3 meters.



Depth* (m)	Soil Type	Q _{ult} (MN)
90	Sand	48.1

AXIAL PILE LOAD TRANSFER-DISPLACEMENT CURVES
Piers E15-Eastbound and Westbound (Boring 98-37)
 2.5-Meter-Diameter Pipe Piles (Pile Tip Elevation = -93 Meters)
 SFOBB East Span Seismic Safety Project



DEPTH (m)	t-z Data											
	t(1)	z(1)	t(2)	z(2)	t(3)	z(3)	t(4)	z(4)	t(5)	z(5)	t(6)	z(6)
0-3	0.0	0.0	0.007	0.003	0.013	0.006	0.020	0.012	0.024	0.018	0.027	0.025
3-6	0.0	0.0	0.028	0.003	0.055	0.006	0.083	0.012	0.099	0.018	0.110	0.025
6-9	0.0	0.0	0.038	0.003	0.075	0.006	0.113	0.012	0.135	0.018	0.150	0.025
9-12	0.0	0.0	0.097	0.003	0.193	0.006	0.290	0.012	0.348	0.018	0.387	0.025
12-15	0.0	0.0	0.105	0.003	0.210	0.006	0.315	0.012	0.378	0.018	0.420	0.025
15-18	0.0	0.0	0.143	0.003	0.287	0.006	0.430	0.012	0.516	0.018	0.573	0.025
18-21	0.0	0.0	0.143	0.003	0.285	0.006	0.428	0.012	0.513	0.018	0.570	0.025
21-24	0.0	0.0	0.153	0.003	0.307	0.006	0.460	0.012	0.552	0.018	0.613	0.025
24-27	0.0	0.0	0.165	0.003	0.330	0.006	0.495	0.012	0.594	0.018	0.660	0.025
27-30	0.0	0.0	0.204	0.003	0.408	0.006	0.613	0.012	0.735	0.018	0.817	0.025
30-33	0.0	0.0	0.214	0.003	0.428	0.006	0.643	0.012	0.771	0.018	0.857	0.025
33-36	0.0	0.0	0.223	0.003	0.445	0.006	0.668	0.012	0.801	0.018	0.890	0.025
36-39	0.0	0.0	0.243	0.003	0.485	0.006	0.728	0.012	0.873	0.018	0.970	0.025
39-42	0.0	0.0	0.258	0.003	0.517	0.006	0.775	0.012	0.930	0.018	1.033	0.025
42-45	0.0	0.0	0.246	0.003	0.492	0.006	0.737	0.012	0.885	0.018	0.983	0.025
45-51	0.0	0.0	0.365	0.003	0.730	0.006	1.095	0.012	1.314	0.018	1.460	0.025
51-57	0.0	0.0	0.311	0.003	0.623	0.006	0.934	0.012	1.121	0.018	1.245	0.025
57-63	0.0	0.0	0.352	0.003	0.704	0.006	1.056	0.012	1.267	0.018	1.408	0.025
63-69	0.0	0.0	0.279	0.003	0.559	0.006	0.838	0.012	1.005	0.018	1.117	0.025
69-75	0.0	0.0	0.415	0.003	0.830	0.006	1.245	0.012	1.494	0.018	1.660	0.025
75-81	0.0	0.0	0.490	0.003	0.979	0.006	1.469	0.012	1.762	0.018	1.958	0.025
81-83	0.0	0.0	0.639	0.003								
83-86	0.0	0.0	0.499	0.003	0.999	0.006	1.498	0.012	1.797	0.018	1.997	0.025
86-90	0.0	0.0	0.903	0.003								

Notes:

1. "t" is load (MN/m)
2. "z" is displacement (m)
3. Data for tension and compression coincide
4. Based on mudline at El. -3 meters

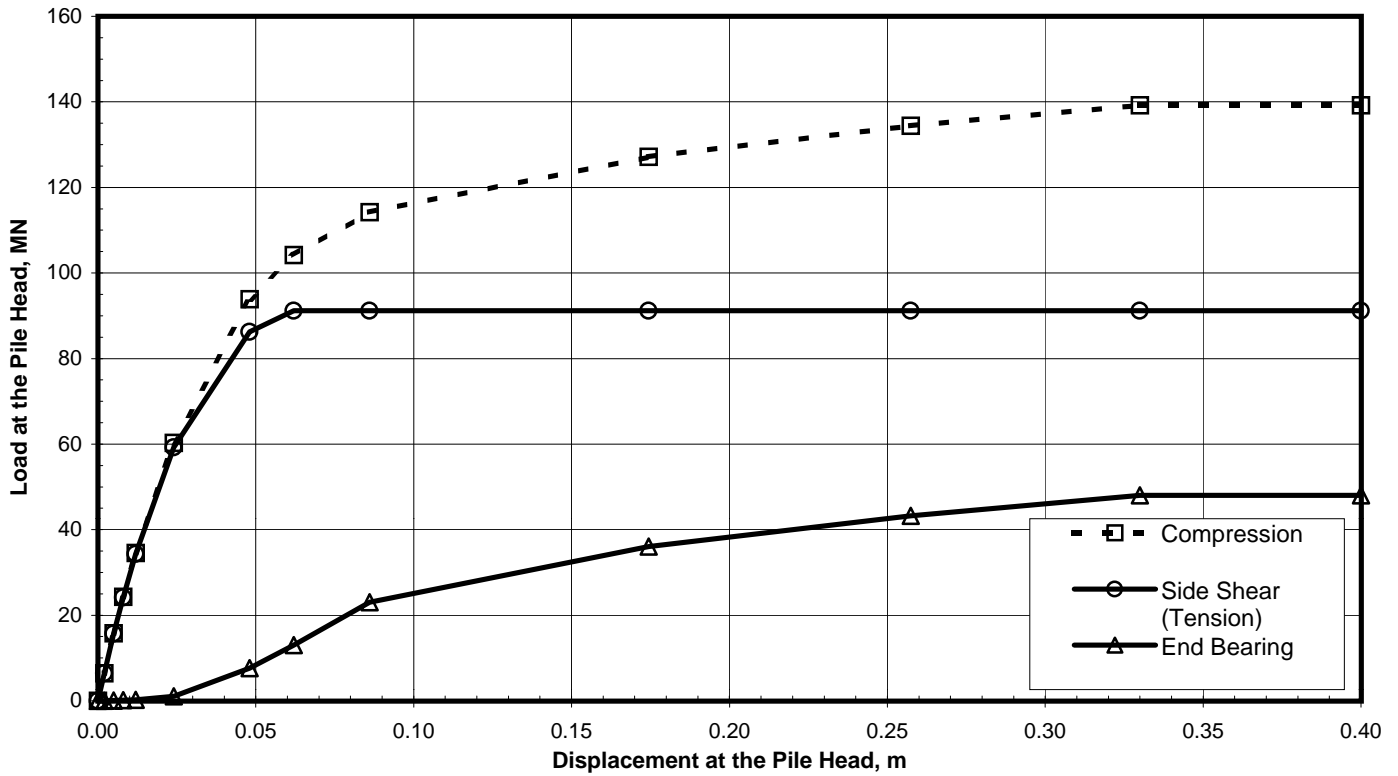
DEPTH (m)	Q-z Data											
	Q(1)	z(1)	Q(2)	z(2)	Q(3)	z(3)	Q(4)	z(4)	Q(5)	z(5)	Q(6)	z(6)
90	0.0	0.0	12.025	0.004	24.050	0.031	36.075	0.105	43.290	0.183	48.100	0.250

Notes:

1. "Q" is load in compression (MN)
2. "z" is displacement (m)

TABULATED AXIAL PILE LOAD TRANSFER DATA
Piers E15-Eastbound and Westbound (Boring 98-37)
 2.5-Meter-Diameter Pipe Piles (Pile Tip Elevation = -93 Meters)
 SFOBB East Span Seismic Safety Project



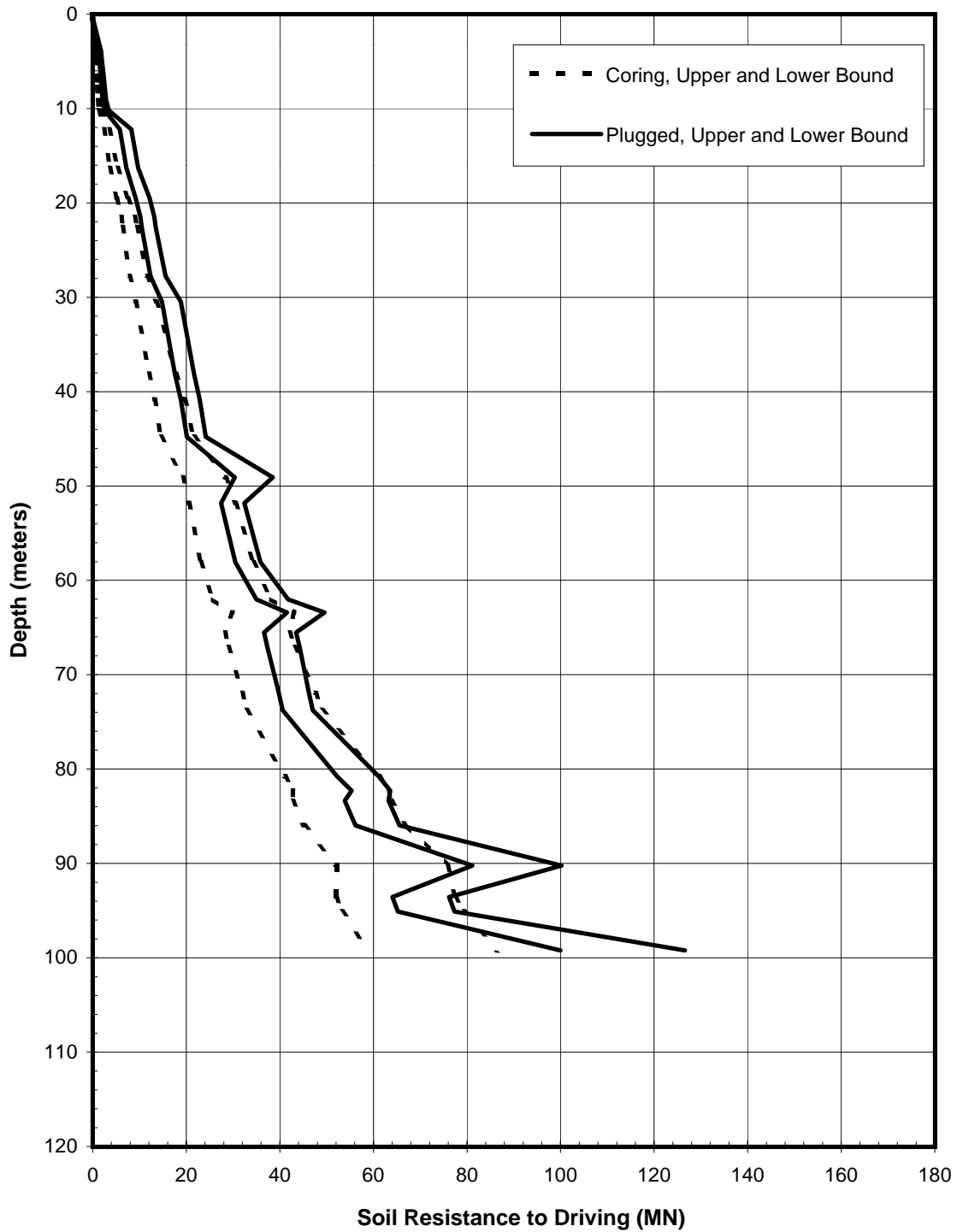


Pile Head Displacement (m)	Load at the Pile Head		End Bearing Component in Compression (MN)
	Compression (MN)	Tension (MN)	
0.000	0.00	0.00	0.00
0.002	6.46	6.43	0.03
0.005	15.75	15.68	0.08
0.008	24.31	24.18	0.13
0.012	34.57	34.34	0.23
0.024	60.29	59.24	1.05
0.048	93.86	86.25	7.61
0.062	104.20	91.15	13.05
0.086	114.20	91.15	23.05
0.174	127.19	91.15	36.04
0.257	134.40	91.15	43.25
0.330	139.20	91.15	48.05
0.400	139.20	91.15	48.05

Note:
 Pile head load-displacement curves are based on the preliminary pile wall thickness schedule provided by TY Lin/M&N and static loading conditions.

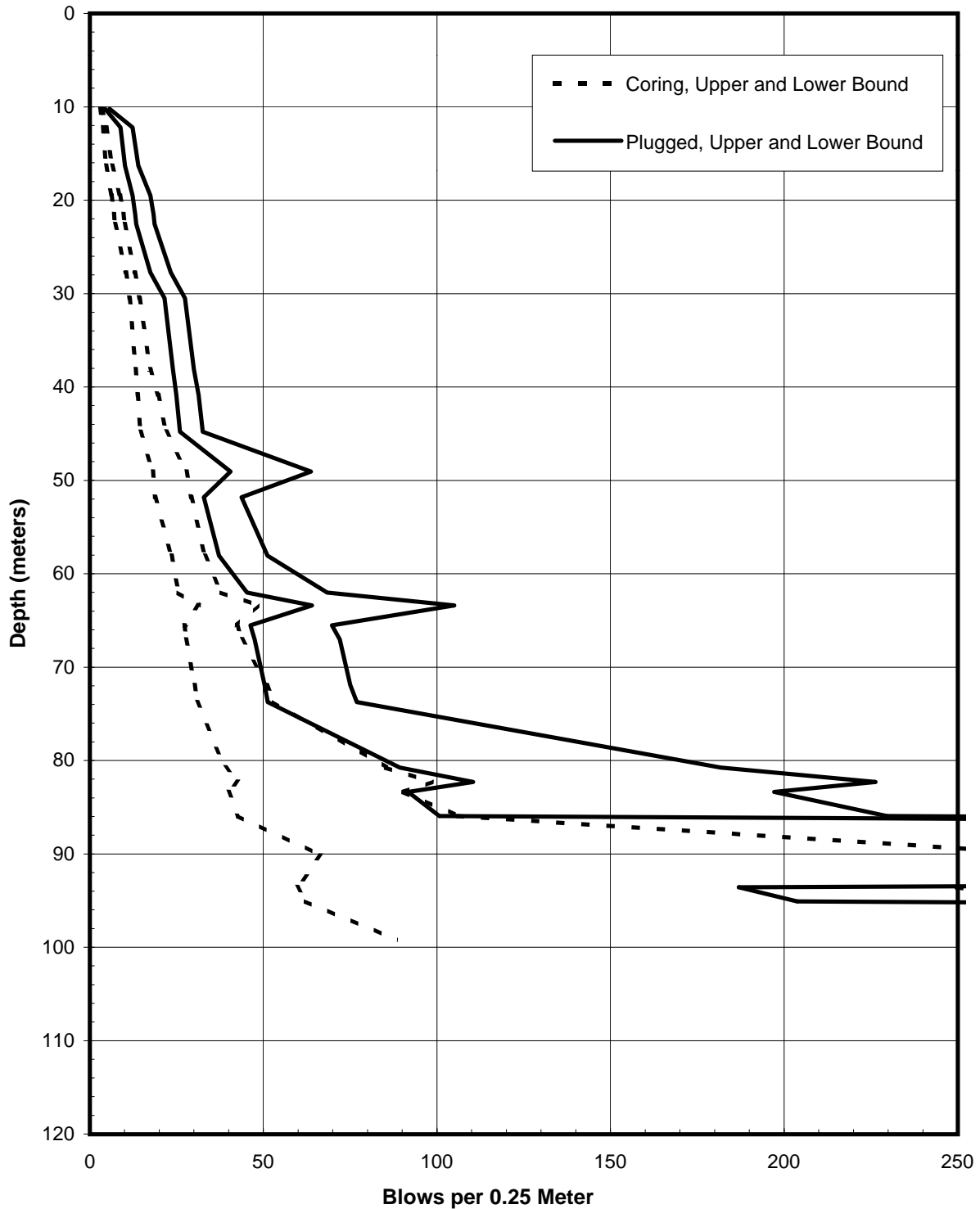
STATIC PILE HEAD LOAD-DEFORMATION CURVES
Piers E15-Eastbound and Westbound (Boring 98-37)
 2.5-Meter-Diameter Pipe Piles (Pile Tip Elevation = -93 Meters)
 SFOBB East Span Seismic Safety Project





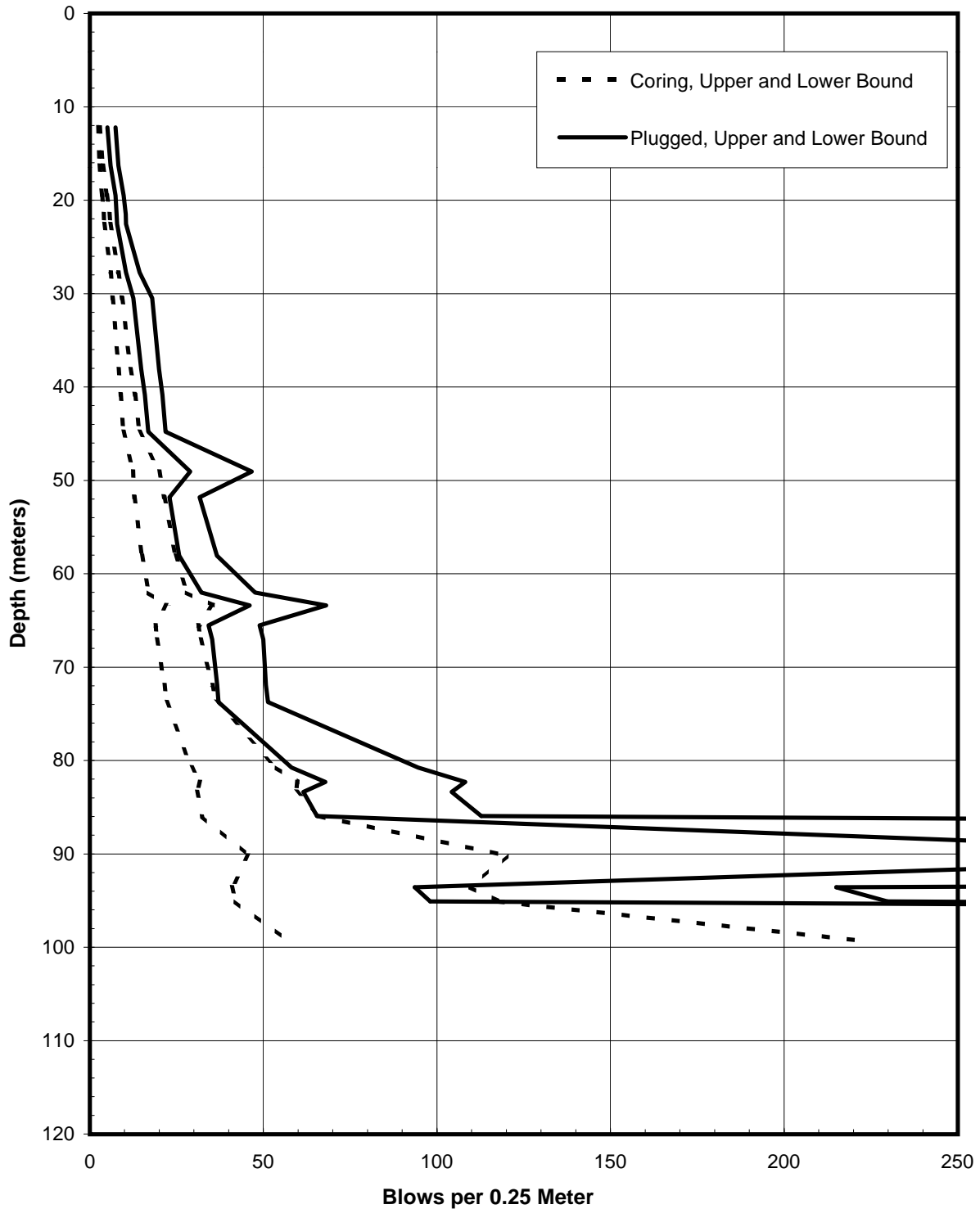
SOIL RESISTANCE TO DRIVING
Piers E15-Eastbound and Westbound (Boring 98-37)
2.5-Meter-Diameter Driven Pipe Piles
SFOBB East Span Seismic Safety Project





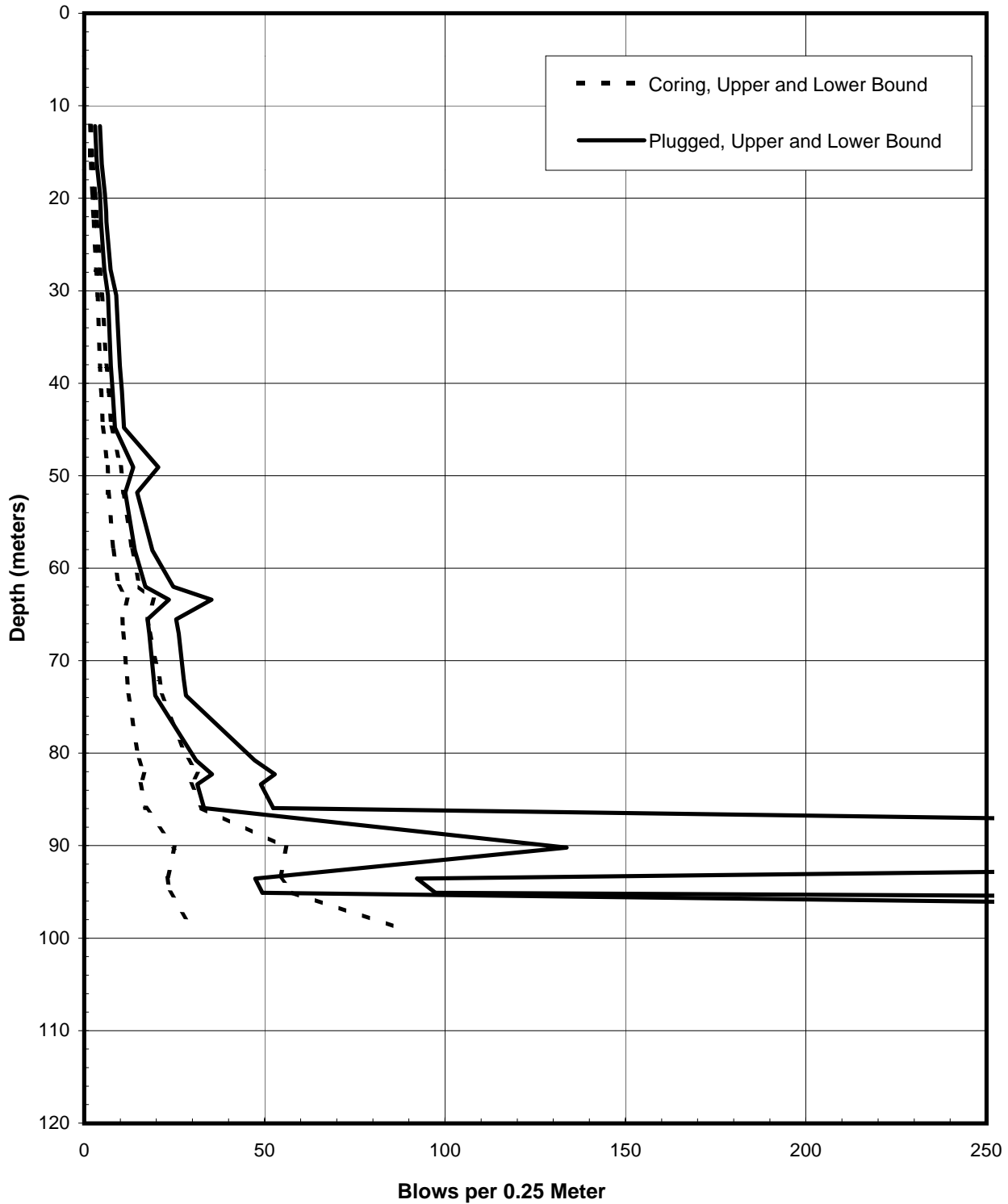
PREDICTED BLOW COUNTS
Piers E15-Eastbound and Westbound (Boring 98-37)
Menck MHU-500T, 2.5-Meter-Diameter Driven Pipe Piles
SFOBB East Span Seismic Safety Project





PREDICTED BLOW COUNTS
Piers E15-Eastbound and Westbound (Boring 98-37)
Menck MHU-1000, 2.5-Meter-Diameter Driven Pipe Piles
SFOBB East Span Seismic Safety Project

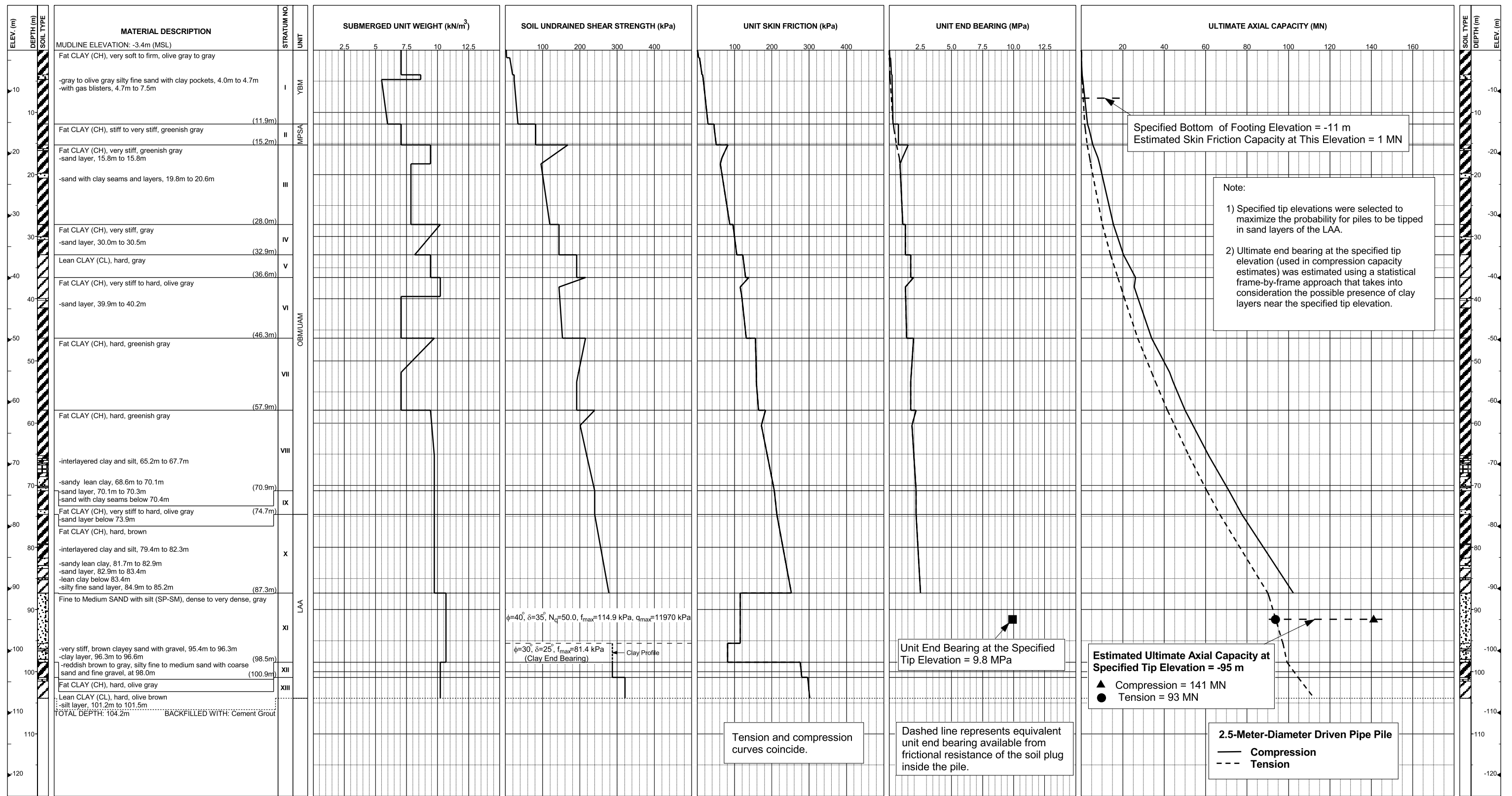




PREDICTED BLOW COUNTS
Piers E15-Eastbound and Westbound (Boring 98-37)
Menck MHU-1700, 2.5-Meter-Diameter Driven Pipe Piles
SFOBB East Span Seismic Safety Project

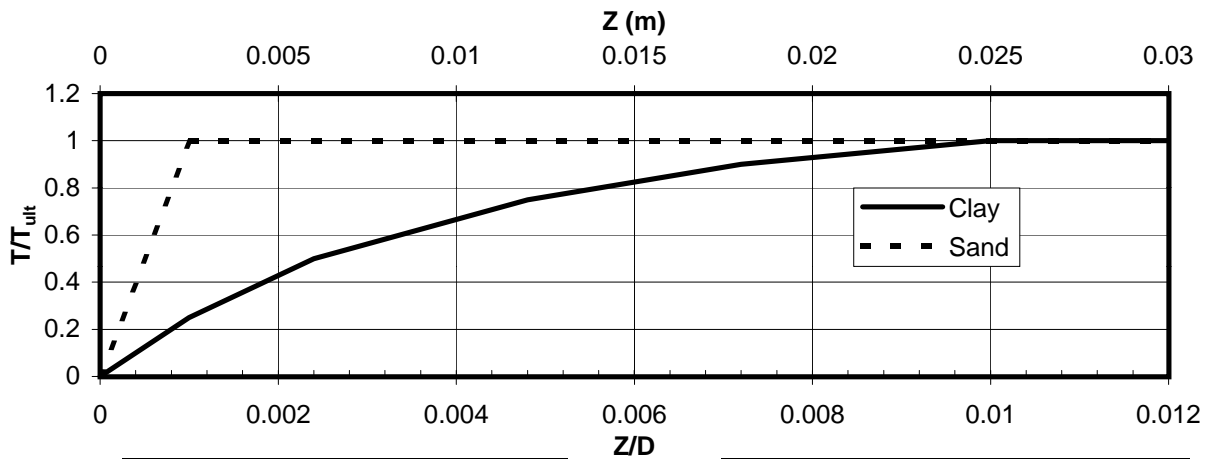


**Pier E16-Eastbound and Westbound (Boring 98-38)
Skyway Frame 4**



AXIAL PILE DESIGN PARAMETERS AND RESULTS
Piers E16-Eastbound and Westbound (Boring 98-38)
SFOBB East Span Seismic Safety Project

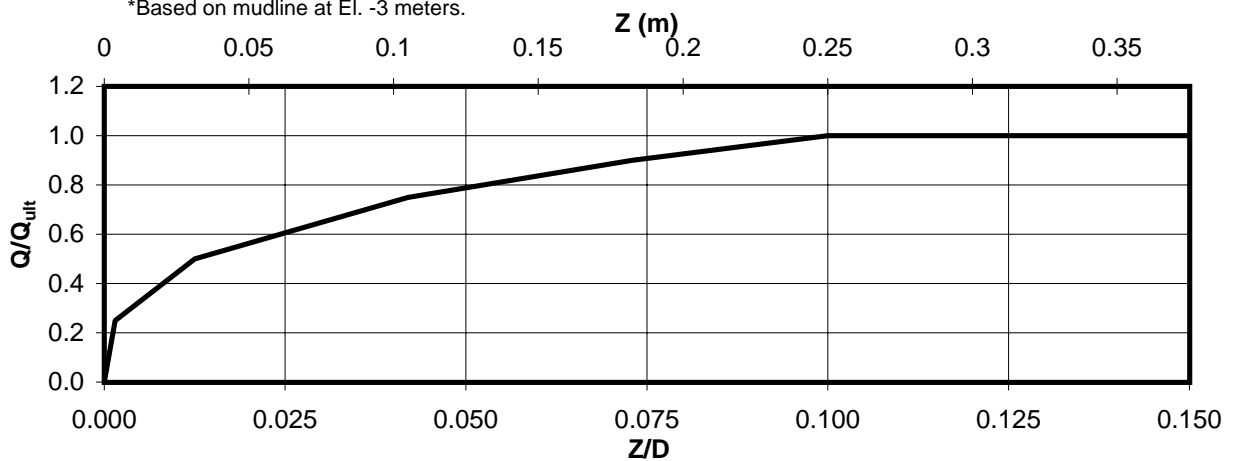




Depth* (m)	Soil Type	T_{ult} (MN/m)
0-3	Clay	0.033
3-6	Clay	0.113
6-9	Clay	0.163
9-12	Clay	0.200
12-15	Clay	0.363
15-18	Clay	0.573
18-21	Clay	0.497
21-24	Clay	0.580
24-27	Clay	0.630
27-30	Clay	0.733
30-33	Clay	0.807
33-36	Clay	0.977

Depth* (m)	Soil Type	T_{ult} (MN/m)
36-39	Clay	0.993
39-42	Clay	0.927
42-45	Clay	0.990
45-51	Clay	1.192
51-57	Clay	1.257
57-63	Clay	1.368
63-69	Clay	1.502
69-75	Clay	1.635
75-81	Clay	1.750
81-87	Clay	1.903
87-91	Sand	0.914

*Based on mudline at El. -3 meters.



Depth* (m)	Soil Type	Q_{ult} (MN)
91	Sand	48.1

AXIAL PILE LOAD TRANSFER-DISPLACEMENT CURVES
Piers E16-Eastbound and Westbound (Boring 98-38)
 2.5-Meter-Diameter Pipe Piles (Pile Tip Elevation = -94 Meters)
 SFOBB East Span Seismic Safety Project



DEPTH (m)	t-z Data											
	t(1)	z(1)	t(2)	z(2)	t(3)	z(3)	t(4)	z(4)	t(5)	z(5)	t(6)	z(6)
0-3	0.0	0.0	0.008	0.003	0.017	0.006	0.025	0.012	0.030	0.018	0.033	0.025
3-6	0.0	0.0	0.028	0.003	0.057	0.006	0.085	0.012	0.102	0.018	0.113	0.025
6-9	0.0	0.0	0.041	0.003	0.082	0.006	0.122	0.012	0.147	0.018	0.163	0.025
9-12	0.0	0.0	0.050	0.003	0.100	0.006	0.150	0.012	0.180	0.018	0.200	0.025
12-15	0.0	0.0	0.091	0.003	0.182	0.006	0.272	0.012	0.327	0.018	0.363	0.025
15-18	0.0	0.0	0.143	0.003	0.287	0.006	0.430	0.012	0.516	0.018	0.573	0.025
18-21	0.0	0.0	0.124	0.003	0.248	0.006	0.373	0.012	0.447	0.018	0.497	0.025
21-24	0.0	0.0	0.145	0.003	0.290	0.006	0.435	0.012	0.522	0.018	0.580	0.025
24-27	0.0	0.0	0.158	0.003	0.315	0.006	0.473	0.012	0.567	0.018	0.630	0.025
27-30	0.0	0.0	0.183	0.003	0.367	0.006	0.550	0.012	0.660	0.018	0.733	0.025
30-33	0.0	0.0	0.202	0.003	0.403	0.006	0.605	0.012	0.726	0.018	0.807	0.025
33-36	0.0	0.0	0.244	0.003	0.488	0.006	0.733	0.012	0.879	0.018	0.977	0.025
36-39	0.0	0.0	0.248	0.003	0.497	0.006	0.745	0.012	0.894	0.018	0.993	0.025
39-42	0.0	0.0	0.232	0.003	0.463	0.006	0.695	0.012	0.834	0.018	0.927	0.025
42-45	0.0	0.0	0.248	0.003	0.495	0.006	0.743	0.012	0.891	0.018	0.990	0.025
45-51	0.0	0.0	0.298	0.003	0.596	0.006	0.894	0.012	1.073	0.018	1.192	0.025
51-57	0.0	0.0	0.314	0.003	0.629	0.006	0.943	0.012	1.131	0.018	1.257	0.025
57-63	0.0	0.0	0.342	0.003	0.684	0.006	1.026	0.012	1.231	0.018	1.368	0.025
63-69	0.0	0.0	0.376	0.003	0.751	0.006	1.127	0.012	1.352	0.018	1.502	0.025
69-75	0.0	0.0	0.409	0.003	0.818	0.006	1.226	0.012	1.472	0.018	1.635	0.025
75-81	0.0	0.0	0.438	0.003	0.875	0.006	1.313	0.012	1.575	0.018	1.750	0.025
81-87	0.0	0.0	0.476	0.003	0.952	0.006	1.427	0.012	1.713	0.018	1.903	0.025
87-91	0.0	0.0	0.914	0.003								

Notes:

1. "t" is load (MN/m)
2. "z" is displacement (m)
3. Data for tension and compression coincide
4. Based on mudline at El. -3 meters

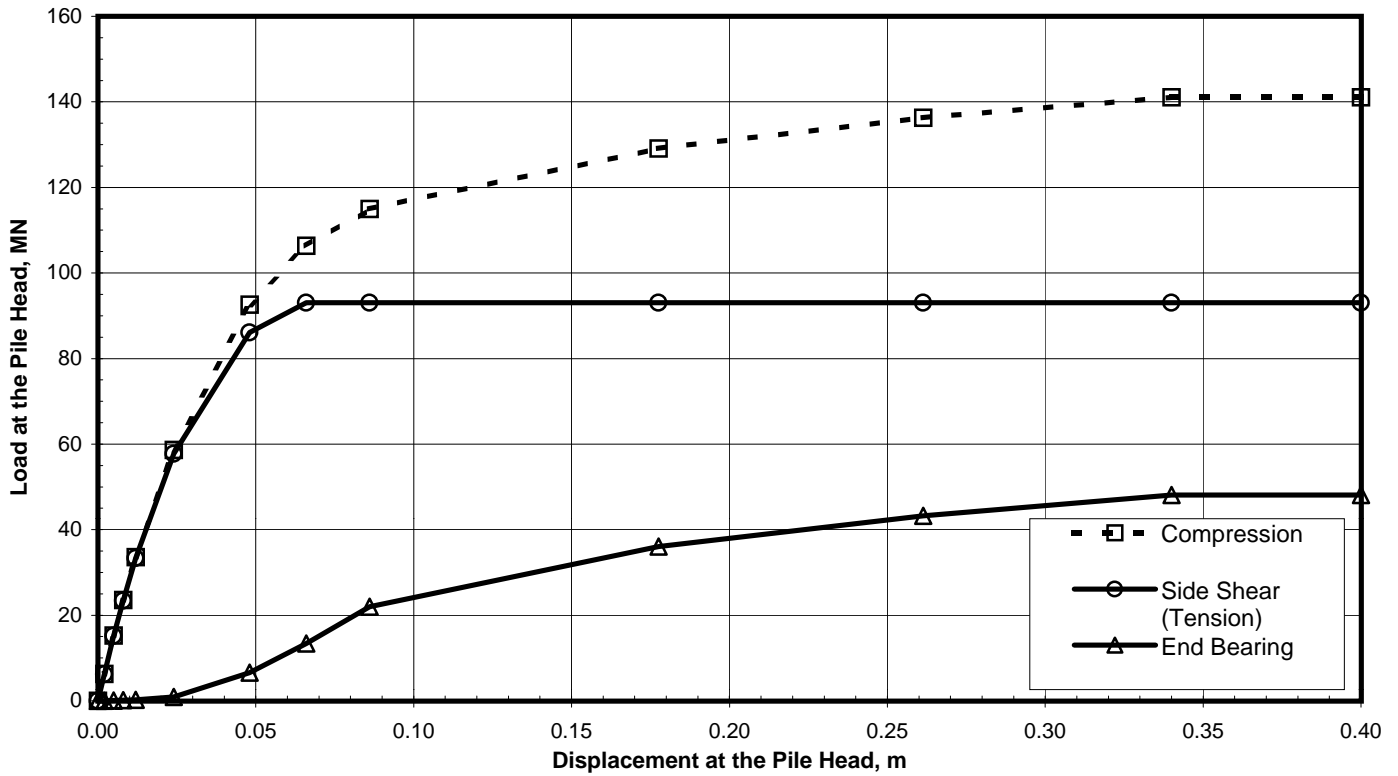
DEPTH (m)	Q-z Data											
	Q(1)	z(1)	Q(2)	z(2)	Q(3)	z(3)	Q(4)	z(4)	Q(5)	z(5)	Q(6)	z(6)
91	0.0	0.0	12.025	0.004	24.050	0.031	36.075	0.105	43.290	0.183	48.100	0.250

Notes:

1. "Q" is load in compression (MN)
2. "z" is displacement (m)

TABULATED AXIAL PILE LOAD TRANSFER DATA
Piers E16-Eastbound and Westbound (Boring 98-38)
 2.5-Meter-Diameter Pipe Piles (Pile Tip Elevation = -94 Meters)
 SFOBB East Span Seismic Safety Project





Pile Head Displacement (m)	Load at the Pile Head		End Bearing Component in Compression (MN)
	Compression (MN)	Tension (MN)	
0.000	0.00	0.00	0.00
0.002	6.25	6.23	0.03
0.005	15.26	15.19	0.07
0.008	23.57	23.44	0.13
0.012	33.56	33.33	0.23
0.024	58.67	57.77	0.90
0.048	92.62	86.07	6.55
0.066	106.40	93.04	13.36
0.086	115.00	93.04	21.96
0.178	129.09	93.04	36.05
0.261	136.29	93.04	43.25
0.340	141.10	93.04	48.06
0.400	141.10	93.04	48.06

Note:
 Pile head load-displacement curves are based on the preliminary pile wall thickness schedule provided by TY Lin/M&N and static loading conditions.

STATIC PILE HEAD LOAD-DEFORMATION CURVES
Piers E16-Eastbound and Westbound (Boring 98-38)
 2.5-Meter-Diameter Pipe Piles (Pile Tip Elevation = -94 Meters)
 SFOBB East Span Seismic Safety Project



**APPENDIX B
VERIFICATION OF AXIAL PILE DESIGN METHODS**

APPENDIX B VERIFICATION OF AXIAL PILE DESIGN METHODS

INTRODUCTION

Due to the economic importance of the San Francisco-Oakland Bay Bridge (SFOBB) and the consequences of catastrophic failure in both economic and human terms, the design and analysis of the pile foundations supporting the bridge explicitly consider a number of aspects of pile-soil behavior that are normally not considered. A description of the methods used to evaluate large-diameter pile foundations is presented in Section 4.0. This appendix documents several of the data sources and example analyses that were performed to verify the methods described in Section 4.0.

EVALUATION OF STATIC AXIAL LOAD TEST RESULTS IN SAN FRANCISCO BAY SOIL

The ultimate axial capacity of driven piles is generally calculated as the algebraic sum of the side shear acting on the outside surface of the embedded length of pile and the end-bearing pressure acting on the pile tip. For clay soils, the unit side shear transfer and the unit end-bearing pressures are calculated as functions of the undrained shear strength.

Since the foundation soils along the bridge right-of-way are predominantly clays, it was deemed appropriate to obtain examples of pile load test data from nearby sites in similar soils, and to use the results to improve the accuracy of the calculated axial pile capacities. The results of a number of pile load tests performed by Caltrans in conjunction with the construction of a bridge structure along I-280 in San Francisco were therefore examined to obtain factual data for improving the pile capacity calculations.

In the Caltrans study, two 400-millimeter- (mm-) diameter pipe piles were tested well after the piles were installed so that full setup had occurred. Since the piles supporting the Bay Bridge are also pipe piles, only the results of these two load tests were examined. Assuming that the differences in the measured tension and compression capacities were equal to twice the self-weight of the piles, the load tests were deduced to yield net axial capacities of 1,400 and 1,225 kilonewtons (kN). On the basis of the published load-settlement data, it was also deduced that the axial capacities were derived almost totally from shear transfer along the pile shaft. The corresponding average unit shear transfer (f) values over the embedded lengths of pipe were calculated to be 43 and 37 kilopascals (kPa).

The only soil parameter available for correlation was the total unit weight. On the basis of vertical overburden pressures (σ'_v) calculated from the total unit weights, the lower value of shear transfer corresponds to an equivalent β -value ($\beta = f / \sigma'_v$) of 0.31. Similarly, the higher



value of shear transfer corresponds to a β -value of 0.36. The Young Bay Mud at the site was assumed to be relatively normally consolidated. Published data suggest that the undrained shear strength ratio for Young Bay Mud is about 0.31. Since a β -value of 0.31 agrees well with published values of the undrained shear strength ratio for the Young Bay Mud, an undrained shear strength ratio value of 0.31 was considered appropriate for use (in lieu of the 0.25 inherently assumed by API [1993a,b]) with the Randolph and Murphy (1985) procedure (see Section 4.0) used to calculate side shear resistance on the pile.

VERIFICATION OF DAMPING FACTORS FOR BAY MUD

The design and analysis of pile foundations for earthquake loading requires that, in addition to normal static ultimate axial capacity design parameters, the characteristics defining the nonlinear resistance-deformation behavior under dynamic loading also be determined. To accomplish this purpose, dynamic laboratory tests on samples of Bay Mud were performed in Fugro's Houston laboratory. Those tests were performed to demonstrate methods by which the laboratory test results can be applied to the soil supporting the dynamically loaded foundation piles.

Experimental Investigation of Dynamic Pile Behavior

As part of a program of pile foundation design for a bridge along I-280, Caltrans previously conducted a comprehensive study of the behavior of various pile types in a deep deposit of Bay Mud (Brittsan and Speer, 1993). One of the piles was a 400-mm-diameter, 13-mm-wall steel pipe pile. This pile was subjected to both static and dynamic loading to failure about 8 months after driving. Since the mechanical properties for this pile are known, and since the pile-soil support characteristics should be similar to those for the steel pipe piles supporting the Bay Bridge, this pile was selected to demonstrate the reliability of the methods used to define the viscous damping characteristics of clay soils.

The results of the load tests are shown on Plates B-1 and B-2. Plate B-1 contains the results of a quasi-static loading to failure in compression performed on April 21, 1993. The results of a dynamic loading to failure (performed by Statnamics, Inc., on April 20, 1993) are given on Plate B-2.

Hindcast Estimates of Static and Dynamic Pile Behavior

The analyses of the pile load tests were performed sequentially, beginning with the static load tests in tension and compression, and then proceeding to the dynamic compression test. The static and dynamic pile solutions were performed using the DRIVE computer program, developed by Meyer and Foo at the University of Texas at Austin under the direction of Prof. Matlock (Meyer, 1976; Foo, 1978). The axial stiffness of Caltran's test pile was taken as $AE = 3.535 \times 10^6$ meganewtons (MN). The self-weight of the pile was calculated to be 1,315 kilonewtons per meter (kN/m) above and 2,024 kN/m below the mudline. These values



correspond to the weight of the steel cross section above the mudline and to the weight of the steel pile plus the internal soil plug below. The calculated self-weight was verified by the difference in the axial capacities measured in the static tension and compression tests.

By back-fitting the static load tests in tension and compression, the static soil reactions were found to vary linearly with depth at a rate equal to 0.31 times the effective overburden pressure, and to be equal in tension and compression. The shape of the axial support curve (t-z curve) was taken from Bogard and Matlock (1990). Comparison of the measured and calculated load-settlement behavior verified both the magnitude of the soil resistance and the shapes of the axial support curves used for static loading.

For the dynamic load test, an equivalent linear damping coefficient was calculated as:

$$C_{eq} = (\beta/V) \text{Log}_{10} (V/V_{ref})$$

where: C_{eq} = an equivalent linear damping coefficient
 β = the rate of increase in shearing resistance per log cycle of increase in strain rate
 V = the relative velocity of the pile with respect to the soil
 V_{ref} = a reference (static) velocity, experimentally determined to be 0.0254 millimeter per second (mm/sec)

On the basis of laboratory test results (Fugro-EM, 2001), the β coefficient for Bay Mud was determined to be 0.12. The velocity of the pile during the dynamic load test was calculated to be approximately 1.016 meters per second (m/sec), resulting in a damping coefficient of 0.00543 second per millimeter (sec/mm). The damping factor, C_{eq} , was then multiplied by the peak static soil reactions along the pile to define an equivalent linear damping coefficient.

The results of the analysis of the static compression test are shown on Plate B-3. A comparison of Plate B-3 with Plate B-1 indicates that the DRIVE solution closely matched the results of the pile load test. A similarly close agreement was obtained with the results of the static tension test.

Plates B-4 and B-5 contain the results of the simulation of the Statnamic load test. For the DRIVE analyses, the force-time data from Plate B-2 were used to develop an input load-time history, and the corresponding displacement-time history was calculated. The input force-time history and the resulting displacement-time history are shown on Plate B-4. On Plate B-5, the load and displacement data from Plate B-4 are compared with the static load-settlement data from Plate B-3. A comparison of Plates B-4 and B-5 with Plate B-2 indicates that the DRIVE results closely match the measured behavior.



The close agreement between the observed and calculated pile behavior under static and dynamic loading conditions implies that the method used for estimating the effects of load rate on the soil reactions is sufficiently accurate for use in the design of pile foundations for earthquake loading. It is expected that the earthquake loading will result in relative pile-soil velocities of about 100 to 200 mm/sec, which is within the range of velocities used to develop the damping coefficients.

EXAMPLE STATIC AND DYNAMIC SOIL-PILE INTERACTION ANALYSIS

To illustrate the static and dynamic axial load-deformation behavior of the piles planned for the Main Span-East Pier and Skyway piers, example analyses were performed for one of the piles supporting Pier E10.

Static Analyses

The surficial soils along the right-of-way exhibit a complex stratigraphy. Due to the complexity of the layering of the soil, a large number of soil support curves are required to describe the variation in the soil reactions with depth. In order to reduce the number of axial support curves along the pile, the stratigraphy must be simplified yet faithfully reflect the axial pile capacity and performance.

Initially, nonlinear axial support curves (t-z) are developed to describe the distribution with depth of the axial soil resistance that reflects the complexity of the soil profile. These support curves were then input into an axial pile-soil interaction program and the load-settlement behavior was calculated. The soil support curves representing the complex soil stratigraphy were then replaced with fewer curves that result in an identical load distribution along the pile, and the load-settlement behavior was again calculated. When the two sets of input support curves yield essentially identical load-settlement behavior, the simplification process is considered complete.

The results of the process are shown on Plates B-6 and B-7. Plate B-6 shows the distribution with depth of two distributions of peak shear transfer. The first contains the distribution from axial pile capacity calculations, while the second shows the simplified distribution. The initial distribution includes the variations due to layering and the calculation procedures. The second, a stepwise variation, depicts the simplified distribution. For the simplified distribution, the peak shear transfer was described as remaining constant within each soil layer used for the site response analysis. Since the layers were 3 meters thick above and 6 meters thick below 45-meter penetration, little error was introduced.

The DRIVE model used for the static and dynamic analyses of the pile consisted of 92 1-meter increments. The mudline was placed at Node 1 and the end-bearing support curve at Node 92 to represent a 91-meter penetration and 1-meter stickup. The axial stiffness of the pile was represented as: a) 9.752×10^4 meganewtons (MN) for the steel section between Node 0 and 60; b) 6.232×10^4 MN for the steel section between Node 60 and 92; and c) 1.160×10^5 MN for



the concrete between Node 0 and 55. For overlapping sequences, the stiffnesses are algebraically accumulated. The weight of the steel was taken as 0.03098 meganewtons per meter (MN/m) between Node 0 and 60, and 0.02017 MN/m between Node 60 and 92. The weight of the concrete plug was taken as 0.0568 MN/m with the soil plug assumed to weigh 0.03576 MN/m.

The load-settlement curves derived from the DRIVE solutions for a weightless pile using each load transfer distribution are shown on Plate B-7. As shown on Plate B-8, the pile-head behavior is virtually identical, since the axial capacities are not biased by the pile weight. For static (monotonic) loading, the pile can be replaced at each supported point on a structure by the nonlinear curves shown on Plate B-7. However, for cyclic or dynamic analyses, the curves shown on Plate B-7 cannot be used to describe the nonlinear, hysteretic response of a pile, particularly with regards to the effects of cyclic degradation, loading rate (damping), and residual load distributions.

To demonstrate such effects, the distributed weight of the steel pile, the internal concrete and soil plugs, and external damping coefficients were added and the analyses were repeated. The results of those analyses are shown on Plate B-8. In these analyses, a large time step (10^4 seconds) was used to minimize any contribution from mass and damping effects.

Dynamic Analyses

Cyclic axial loading of long flexible piles may result in two detrimental effects: 1) losses in capacity due to cyclic degradation of the side shear, and 2) progressive settlement due to the nonlinear and inelastic soil response. These effects may occur simultaneously or independently, depending on the axial stiffness of the pile and the time-history of loading at the pile head.

The DRIVE program contains a cyclic degradation algorithm that is based on experimental observations of the behavior of model and full-scale piles subjected to cyclic axial loading. The program also provides a time history of loads and displacements along the pile, and allows the investigation of the effects of biased cyclic loads on the progressive development of permanent settlements.

Since no experimental data were available to describe the progressive degradation in axial shear transfer capacity in the San Francisco Bay clays, the behavior was assumed to be similar to that observed in the high plasticity Gulf of Mexico clays. In the Gulf of Mexico clays, the cyclic minimum shear transfer was experimentally determined to be approximately equal to the remolded shear strength. The value of the cyclic minimum shear transfer in the Bay clays was therefore also taken to be equal to the remolded shear strengths.

The degradation model in the DRIVE program reduces the peak shear transfer on each cycle of reversal at a prescribed rate as $Q_{n+1} = (1 - \lambda)(Q_n - Q_{min}) + Q_{min}$, where Q_n is the resistance on cycle n and Q_{n+1} is the resistance on the next cycle, $n+1$. This formulation results



in the resistance Q asymptotically approaching the minimum value Q_{\min} at a rate prescribed by the constant λ .

The progressive loss of shear transfer capacity during seven cyclic axial load tests on instrumented piles in Gulf of Mexico clays are shown on Plate B-9. As shown on Plate B-9, the rate of loss of resistance per cycle is bounded by values of λ ranging from 0.25 to 0.40. For the Bay Bridge analysis, a λ value equal to 0.40 was selected.

Dynamic analyses were performed using a 51-second pile head force-time history provided by TY Lin/M&N for one of the piles supporting Pier E10. Initially, time steps of 0.01 and 0.001 second were used, which required 5,100 and 51,000 time steps, respectively. Since a comparison of the results showed them to be almost identical, the remaining analyses were performed using time steps of 0.01 second.

The input load-time history, which was applied at the mudline, is shown in Plate B-10. The load at the beginning and the end of the time history was 37 MN, implying that this value represents the static load on the pile. The resulting time history of displacement at the mudline is shown on Plate B-11, with the corresponding displacement history at the pile tip shown on Plate B-12. At the pile head, a change in the pile-head settlement of 0.017 meter was calculated. At the pile tip, 0.008 meter of settlement was calculated.

The source of the differential settlement can be found in a comparison of the residual loads and the corresponding elastic compression of the pile before and after the earthquake. The residual loads along the pile before and after the dynamic loading are shown on Plate B-13, with the deflected shapes corresponding to the two load distributions shown on Plate B-14. Due to the nonlinear and hysteretic nature of the soil reactions, the residual loads along the pile increased significantly. The effects of the increased residual loads on the pile displacements are shown in Plate B-14. Had the pile displacements been rigid body movement, the plastic slip at the pile head and the pile tip would have been equal. However, the pile head exhibited over twice the settlement of the pile tip. As shown on Plate B-14, the difference in the residual stress distribution accounts for the difference in the final displacements, with 0.009 meter due to elastic compression of the pile and only 0.008 meter due to plastic slip.

The results of the analyses shown on Plates B-11 through B-14 emphasize the need for modeling the pile/soil interaction with a program such as DRIVE. Had the pile-soil system been modeled solely by a lumped mass on nonlinear supports (even hysteretic supports), the calculated settlement would have been less than half that predicted with a model that includes the effects of residual stress along the pile.

The effects of cyclic degradation of the soil resistance along the pile are demonstrated on Plate B-15. The initial maximum load transfer and the cyclic minimum values are shown on Plate B-15 as the upper and lower bounds. The degraded values of load transfer at each node



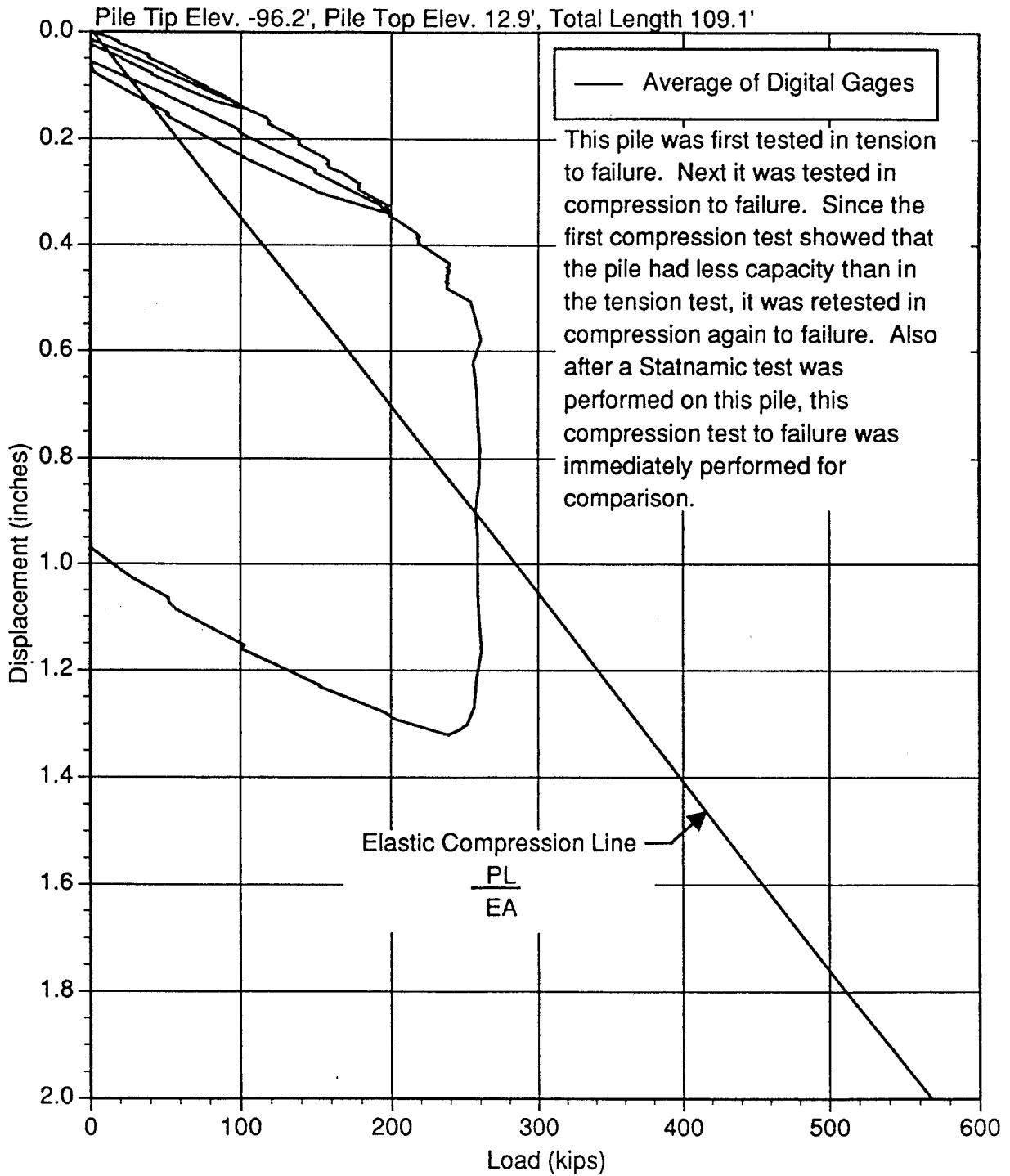
along the DRIVE model are identified. For this particular analysis, the effects of cyclic degradation are minor and are limited to a loss of about 10 percent of the side shear capacity along the upper portion of the pile. It should be noted, however, that the process of cyclic degradation is problem-dependent, being affected by the relative pile stiffness, the distribution with depth of the soil reactions, and the magnitudes of the differences in the axial load. The behavior predicted for the pile at this particular location under this single load-time history thus cannot be assumed to represent the behavior at other locations along the bridge where the soils, loads, and pile penetrations differ from those used for this example.



REFERENCES

- American Petroleum Institute (1993a), "Recommended Practice for Planning, Designing, and Constructing Fixed Offshore Platforms-Load and Resistance Factor Design," API Recommended Practice RP 2A-LRFD, (RP 2A-LRFD), 1st Ed., API, Washington, D. C.
- _____ (1993b), "Recommended Practice for Planning, Designing, and Constructing Fixed Offshore Platforms-Working Stress Design," API Recommended Practice RP 2A-WSD, (RP 2A-WSD), 20th Ed., API, Washington, D.C.
- Bogard, D. and Matlock, H. (1990), "Application of Model Pile Tests to Axial Pile Design," Proceedings, 1990 Offshore Technology Conference, Paper No. 6376, Houston, Texas, May.
- Brittsan, D. and Speer, D. (1993), "Pile Load Test Results for Highway 280 Pile Uplift Test Site."
- Foo, S.H.C. (1978), "Analysis of Driving of Foundation Piles," Master's Thesis, Civil Engineering Dept., The University of Texas at Austin, May.
- Fugro-Earth Mechanics (Fugro-EM) (2001), *Final Marine Geotechnical Site Characterization, San Francisco-Oakland Bay Bridge East Span Seismic Safety Project, Volumes 1A & 1B, Volumes 2A through 2H*, FWI Job No. 98-42-0054, prepared for California Department of Transportation, March 5.
- Meyer, P.L. (1976), "A Discrete-Element Method of Pile-Driving Analysis," Master's Thesis, Civil Engineering Dept., The University of Texas at Austin, August.
- Randolph, M.F. and Murphy, B.S. (1985), "Shaft Capacity of Driven Piles in Clay," Proceedings, 1985 Offshore Technology Conference, Paper No. 4883, Houston, Texas, May.





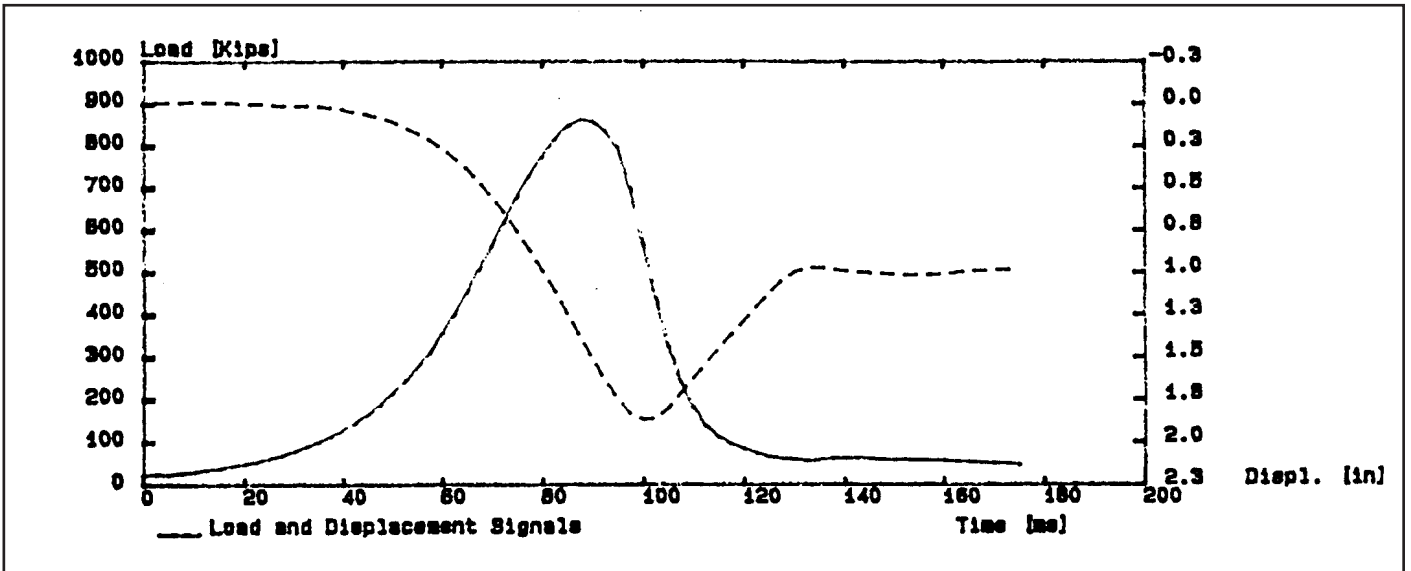
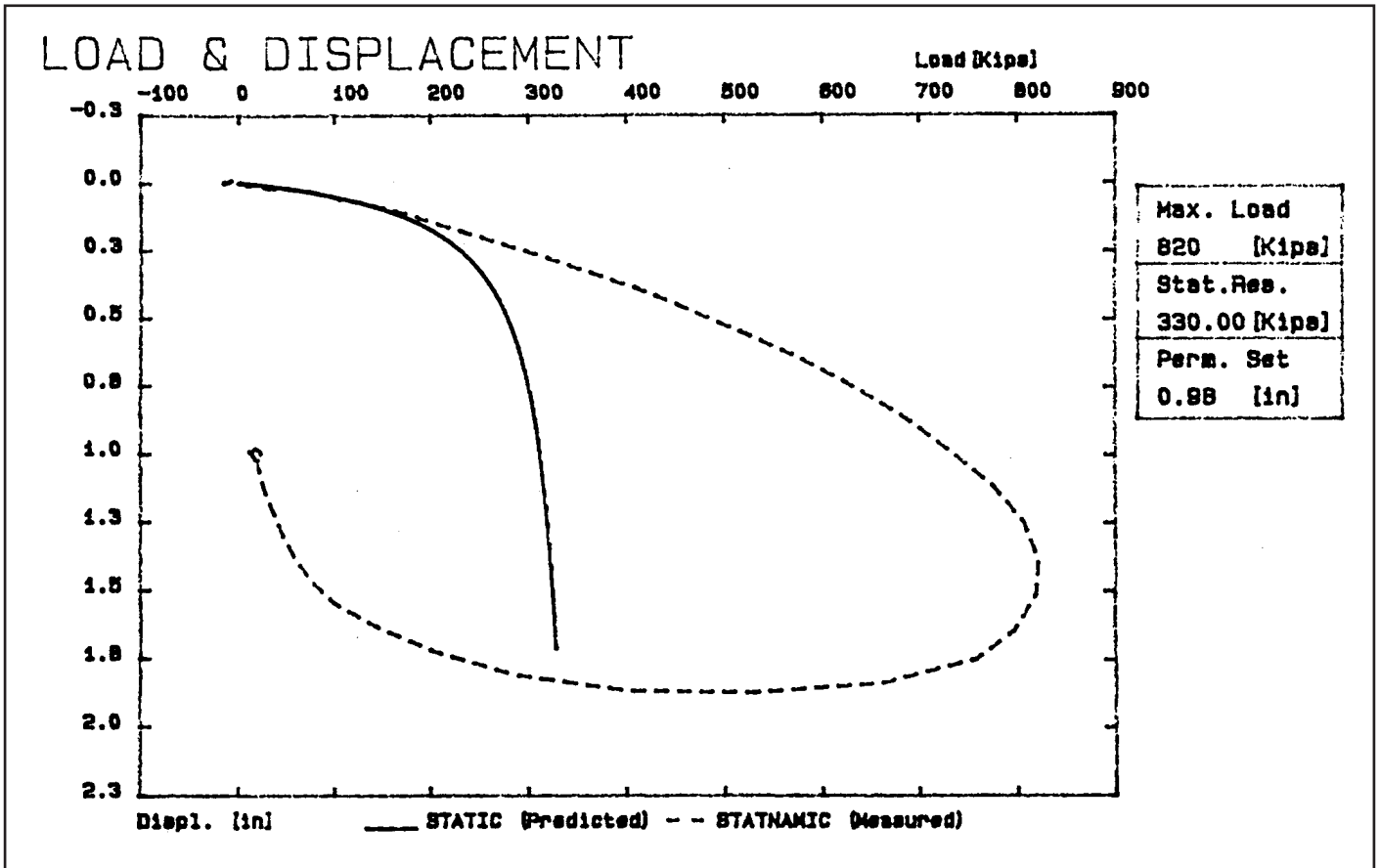
STATIC COMPRESSION LOAD TEST

Uplift Test Program, Bridge No. 34-46 (Test Date: 4/21/1993)

Pile 49-Open Ended Steel Pipe Pile 16" x 0.5"

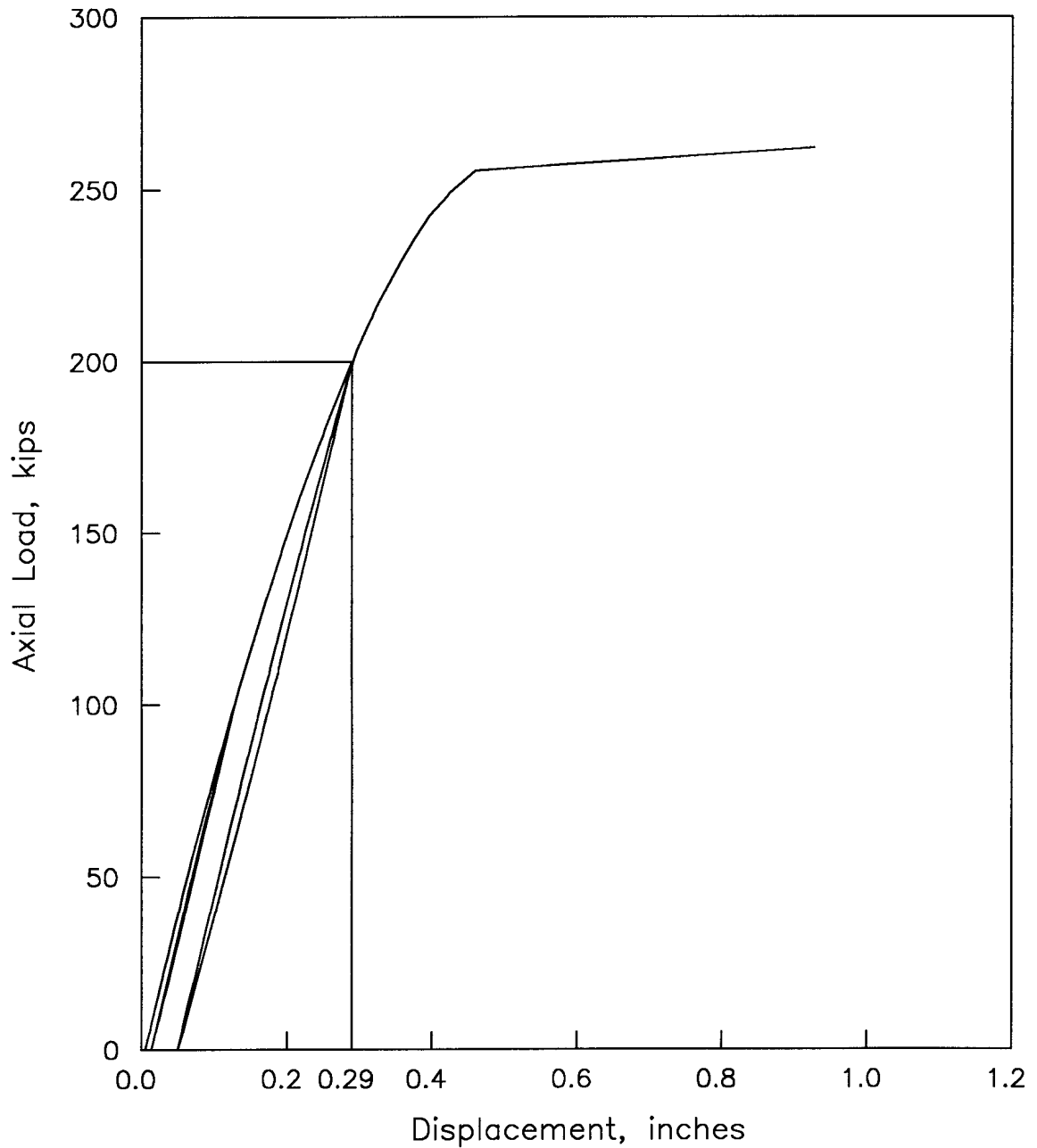
SFOBB East Span Seismic Safety Project





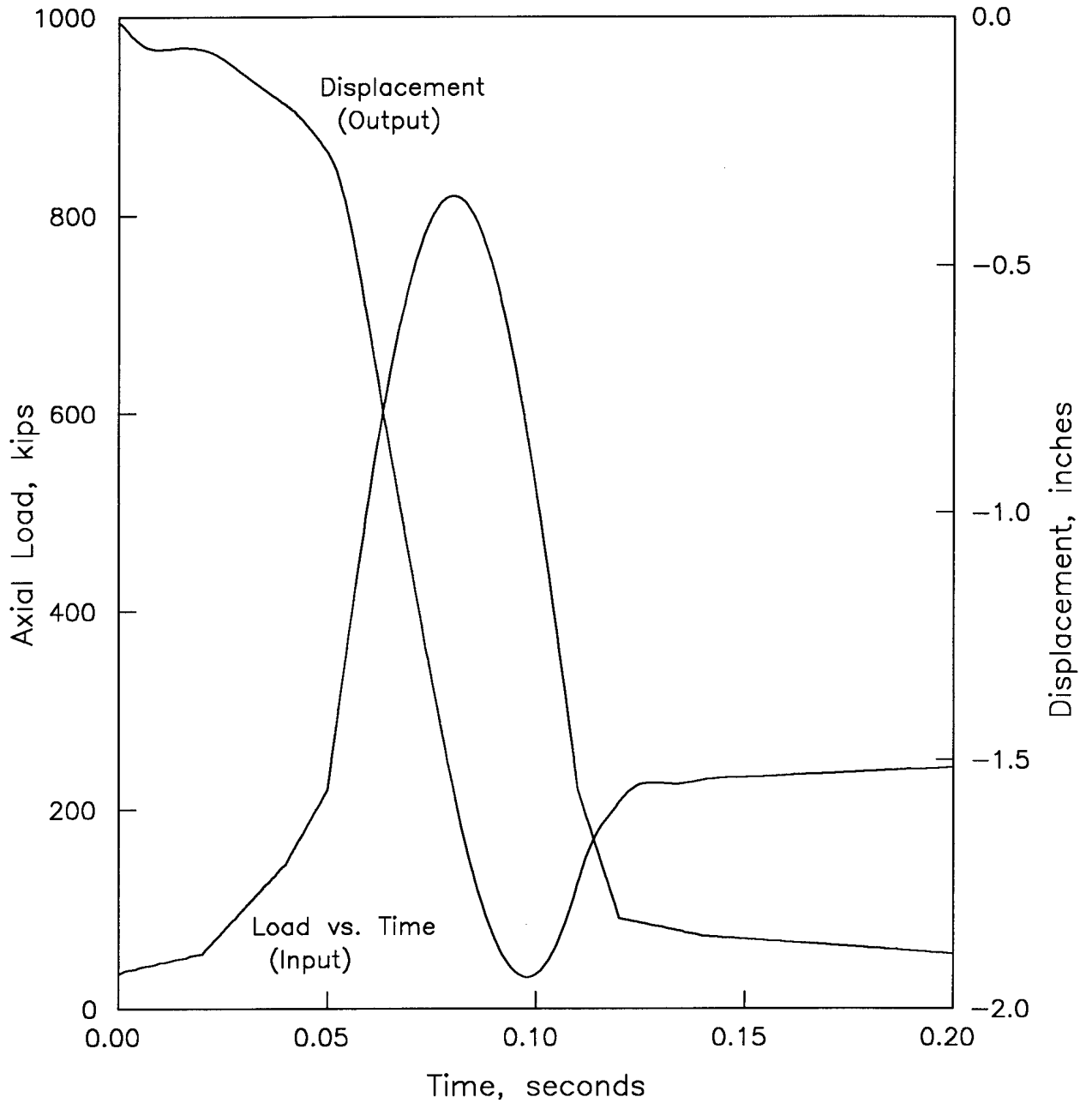
STATNOMIC TEST RESULTS
 Pile 48 (Test Date: 4/20/1973)
 SFOBB East Span Seismic Safety Project





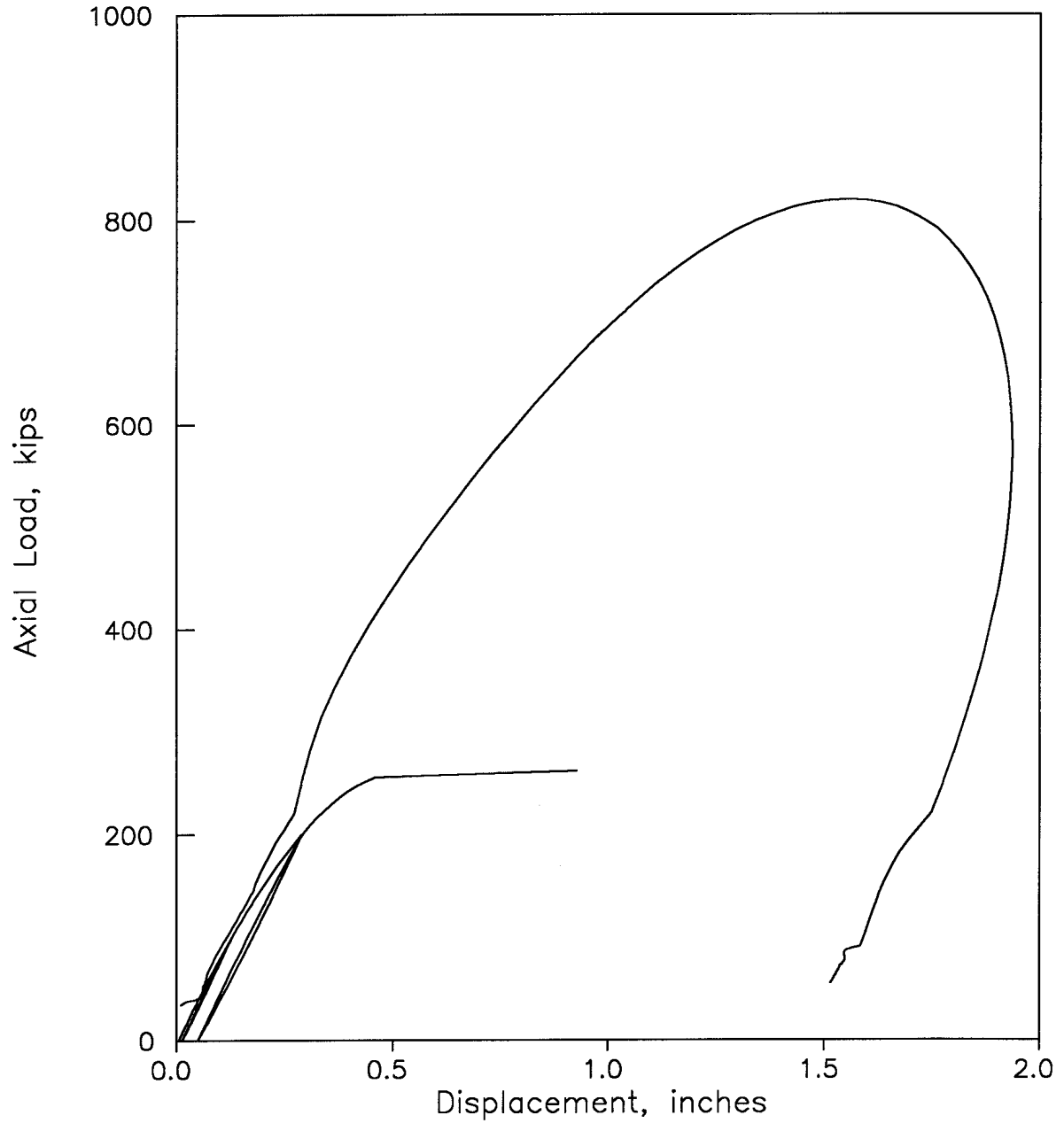
DRIVE SIMULATION OF COMPRESSION TEST
SFOBB East Span Seismic Safety Project





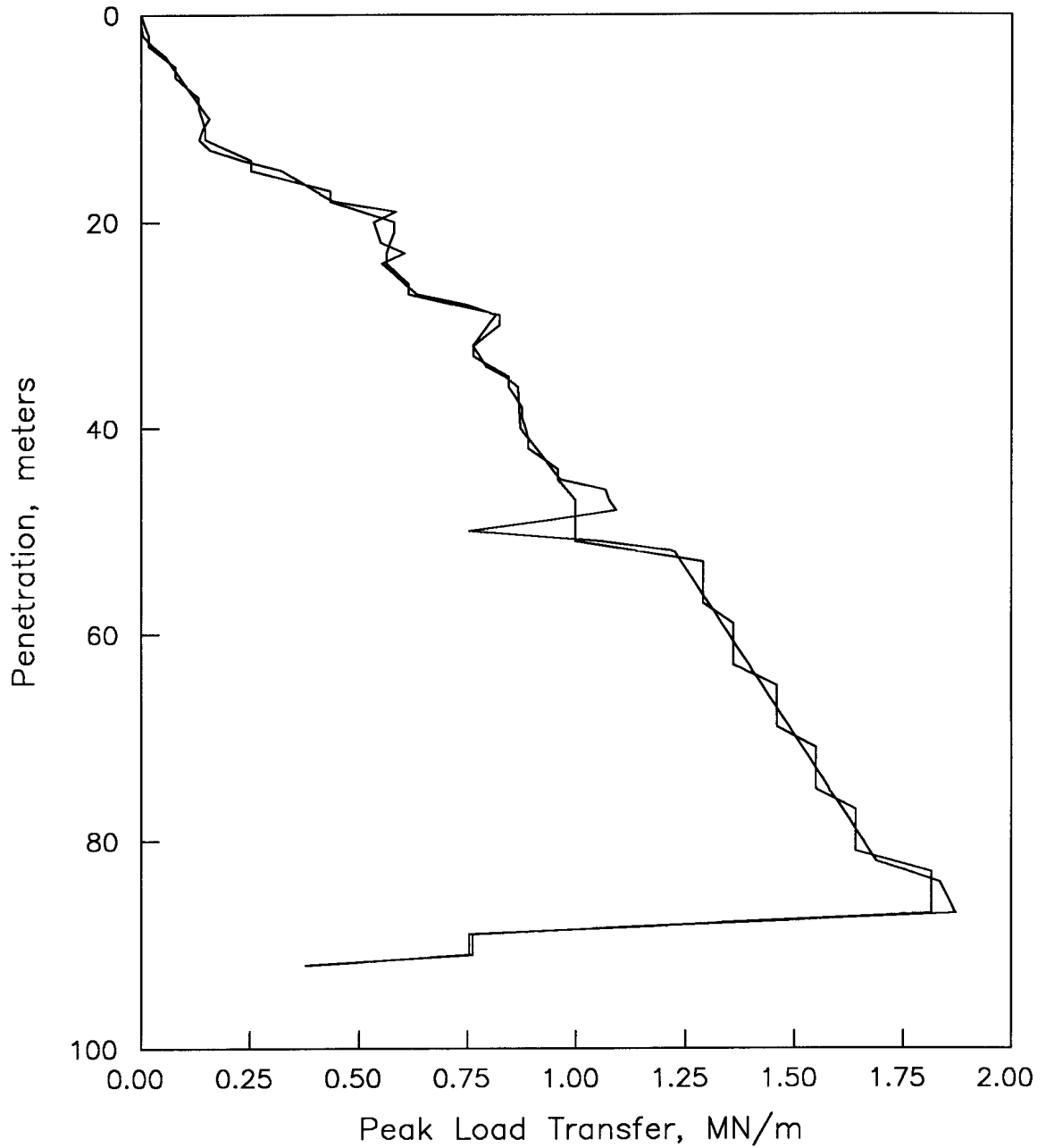
DRIVE SIMULATION OF STATNOMIC LOAD TEST
SFOBB East Span Seismic Safety Project





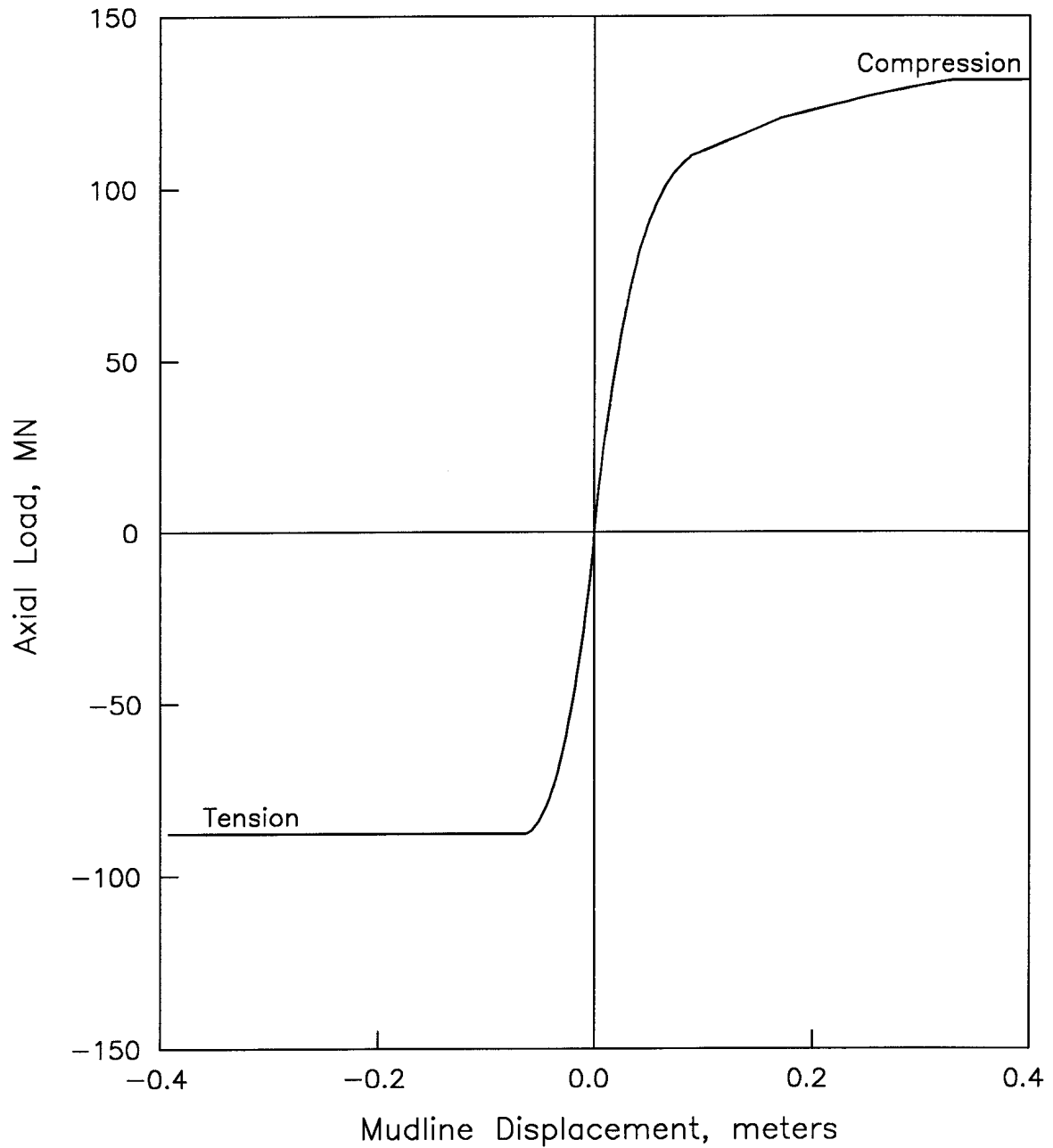
DRIVE SIMULATIONS OF LOAD TESTS
SFOBB East Span Seismic Safety Project





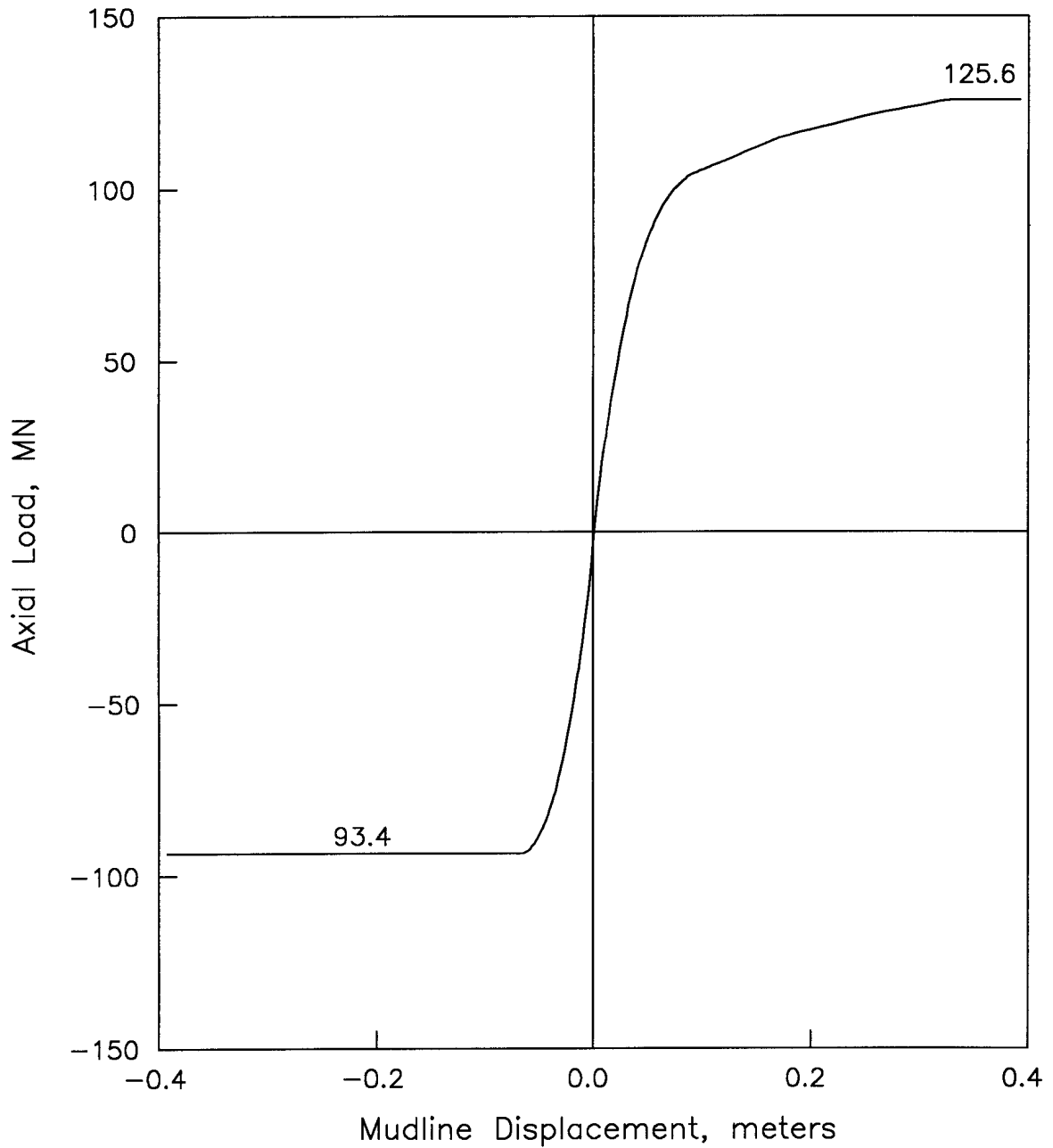
ORIGINAL AND SIMPLIFIED SOIL REACTIONS
SFOBB East Span Seismic Safety Project





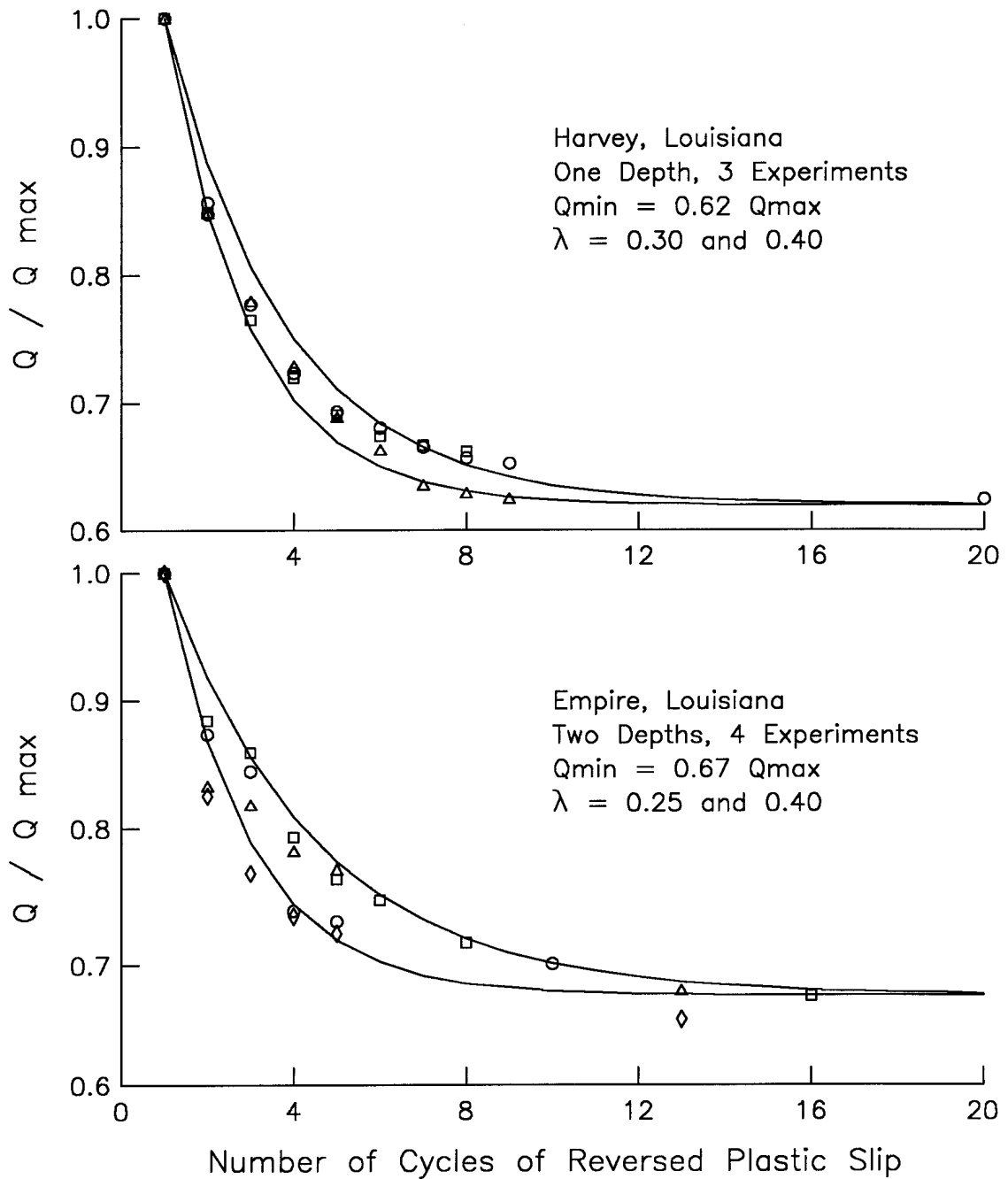
AXIAL PILE LOAD-SETTLEMENT BEHAVIOR
SFOBB East Span Seismic Safety Project

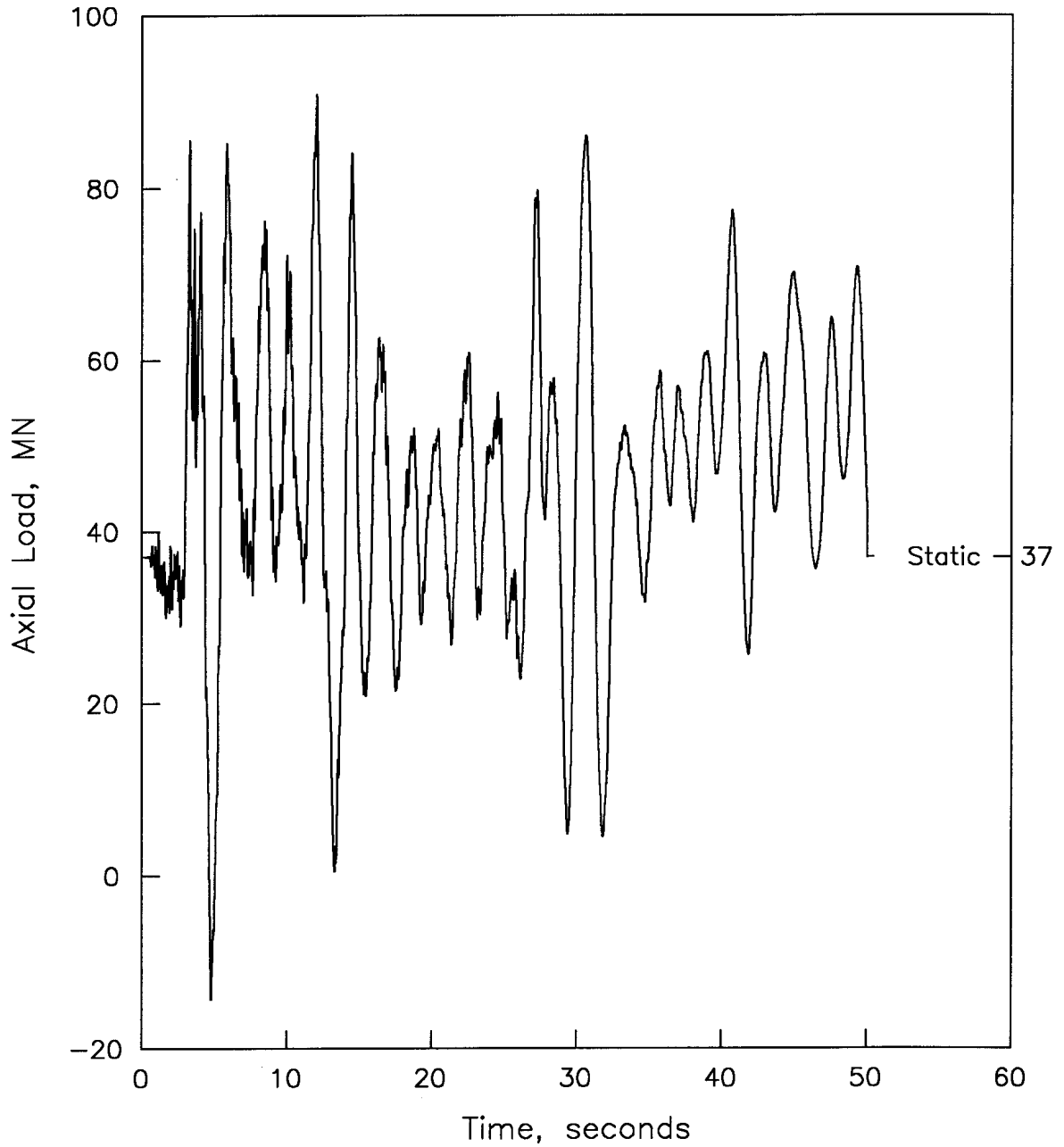




LOAD-SETTLEMENT BEHAVIOR WITH SELF-WEIGHT
SFOBB East Span Seismic Safety Project

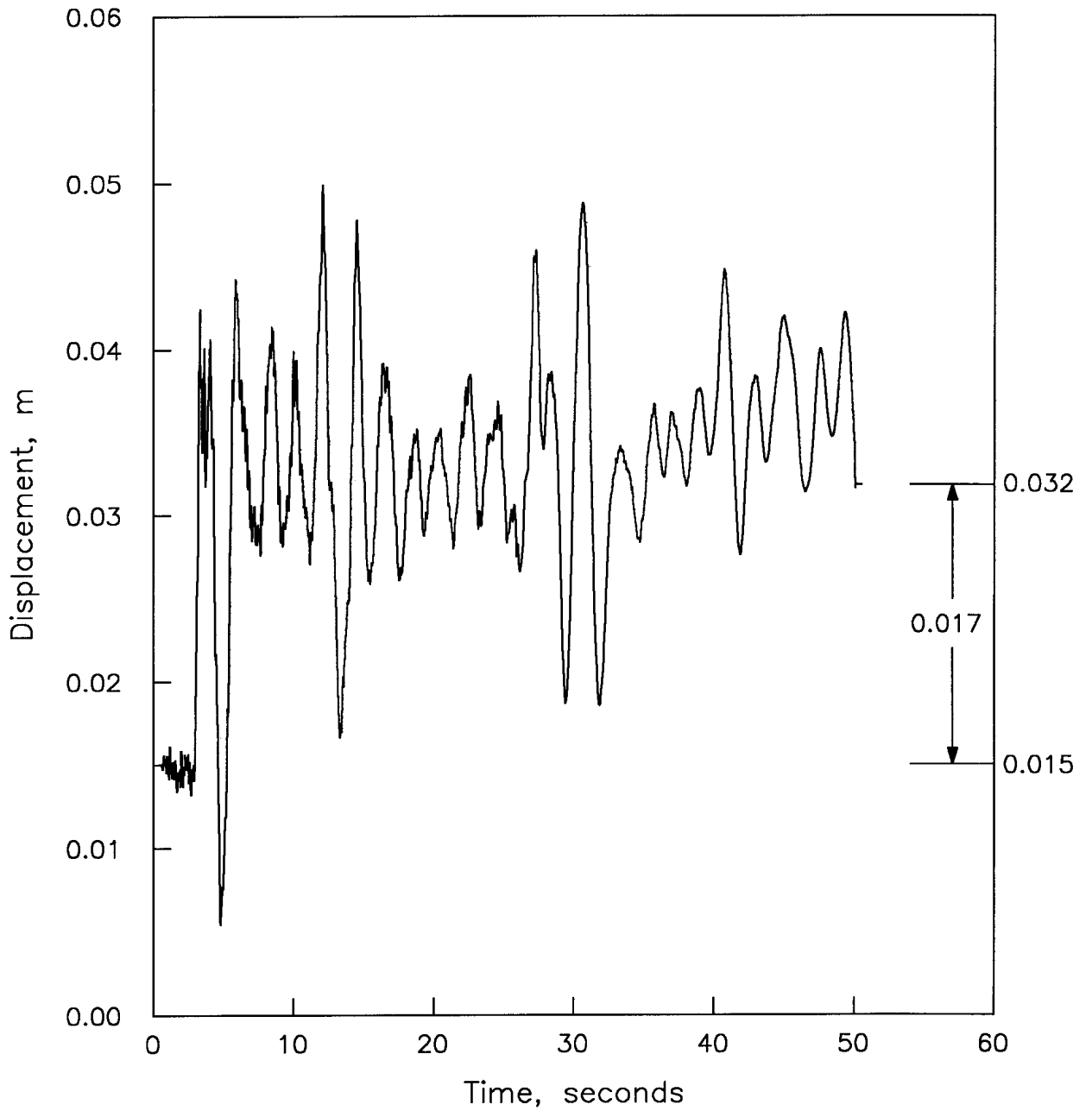






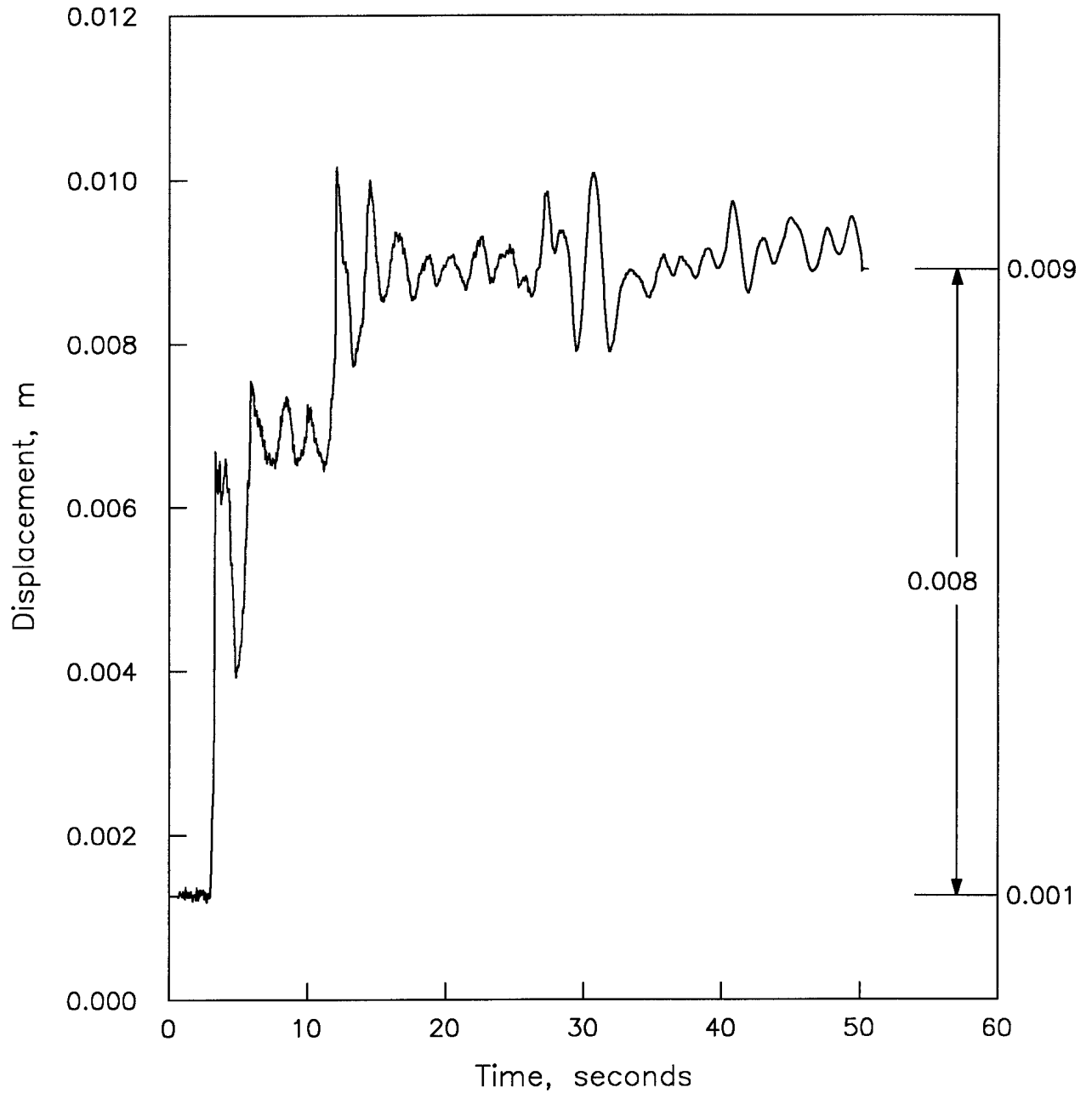
LOAD-TIME HISTORY AT THE MUDLINE
SFOBB East Span Seismic Safety Project





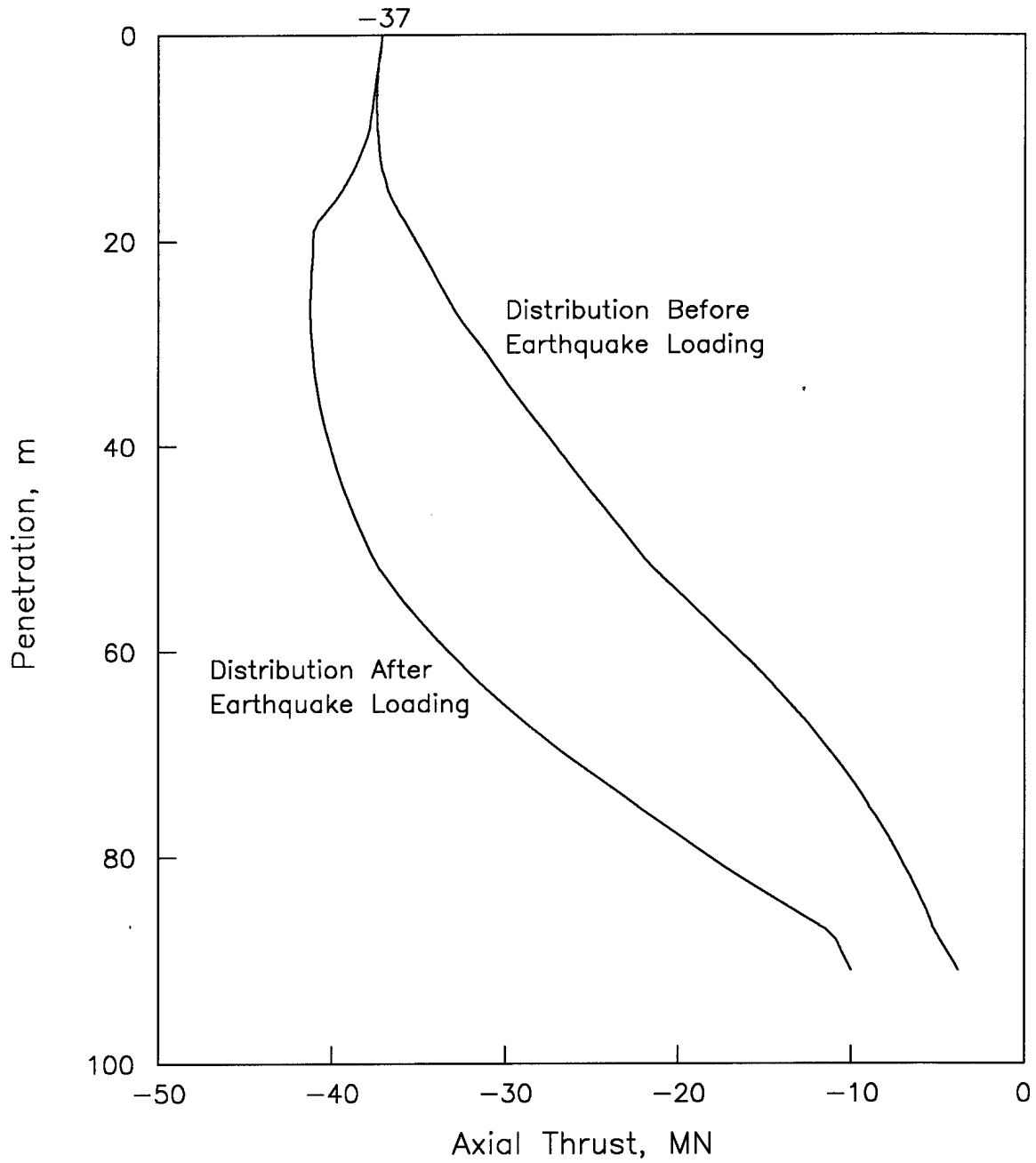
PILE HEAD DISPLACEMENT-TIME HISTORY
SFOBB East Span Seismic Safety Project





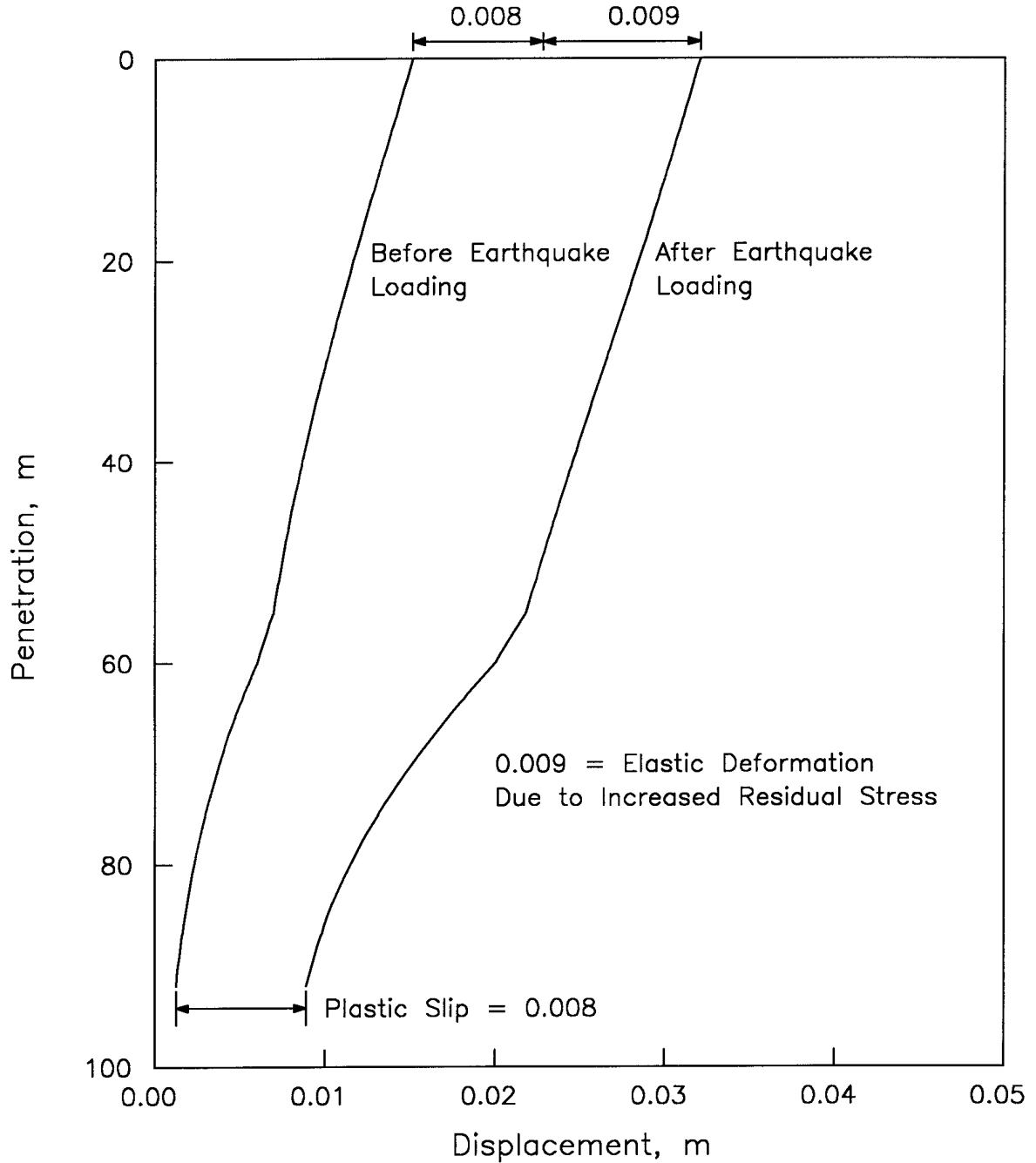
PILE TIP DISPLACEMENT-TIME HISTORY
SFOBB East Span Seismic Safety Project





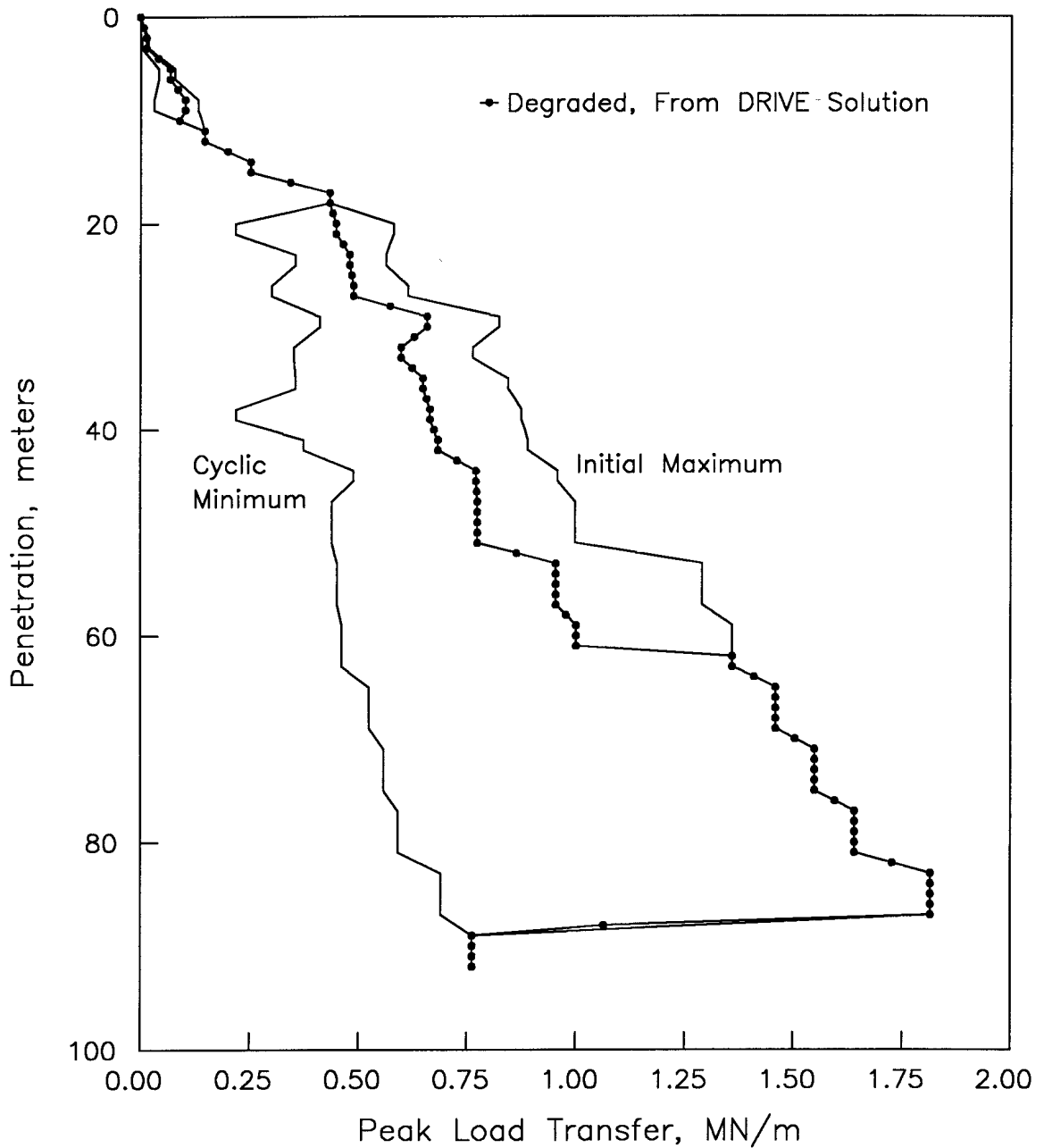
EFFECTS OF EARTHQUAKE ON RESIDUAL LOADS
SFOBB East Span Seismic Safety Project





EFFECTS OF EARTHQUAKE ON DISPLACEMENTS
SFOBB East Span Seismic Safety Project





STATIC AND DEGRADED SOIL REACTIONS
SFOBB East Span Seismic Safety Project

